U.S. Department
of Commerce

Volume 103
Number 1
January 2005

Fishery Bulletin

U.S. Department of Commerce
Donald L. Evans
Secretary

National Oceanic and Atmospheric Administration
Vice Admiral
Conrad C. Lautenbacher Jr., USN (ret.)
Under Secretary for Oceans and Atmosphere

National Marine Fisheries Service
William T. Hogarth
Assistant Administrator for Fisheries

The *Fishery Bulletin* (ISSN 0090-0656) is published quarterly by the Scientific Publications Office, National Marine Fisheries Service, NOAA, 7600 Sand Point Way NE, BIN C15700, Seattle, WA 98115-0070. Periodicals postage is paid at Seattle, WA, and at additional mailing offices. POSTMASTER: Send address changes for subscriptions to Fishery Bulletin, Superintendent of Documents, Attn.: Chief, Mail List Branch, Mail Stop SSOM, Washington, DC 20402-9373.

Although the contents of this publication have not been copyrighted and may be reprinted entirely, reference to source is appreciated.

The Secretary of Commerce has determined that the publication of this periodical is necessary according to law for the transaction of public business of this Department. Use of funds for printing of this periodical has been approved by the Director of the Office of Management and Budget.

For sale by the Superintendent of Documents, U.S. Government Printing Office, Washington, DC 20402. Subscription price per year: $55.00 domestic and $68.75 foreign. Cost per single issue: $28.00 domestic and $35.00 foreign. **See back for order form.**

Fishery Bulletin

Scientific Editor
Norman Bartoo, PhD

Associate Editor
Sarah Shoffler

National Marine Fisheries Service, NOAA
8604 La Jolla Shores Drive
La Jolla, California 92037

Managing Editor
Sharyn Matriotti

National Marine Fisheries Service
Scientific Publications Office
7600 Sand Point Way NE, BIN C15700
Seattle, Washington 98115-0070

Editorial Committee

Harlyn O. Halvorson, PhD	University of Massachusetts, Boston
Ronald W. Hardy, PhD	University of Idaho, Hagerman
Richard D. Methot, PhD	National Marine Fisheries Service
Theodore W. Pietsch, PhD	University of Washington, Seattle
Joseph E. Powers, PhD	National Marine Fisheries Service
Harald Rosenthal, PhD	Universität Kiel, Germany
Fredric M. Serchuk, PhD	National Marine Fisheries Service
George Watters, PhD	National Marine Fisheries Service

***Fishery Bulletin* web site: www.fishbull.noaa.gov**

The *Fishery Bulletin* carries original research reports and technical notes on investigations in fishery science, engineering, and economics. It began as the Bulletin of the United States Fish Commission in 1881; it became the Bulletin of the Bureau of Fisheries in 1904 and the *Fishery Bulletin* of the Fish and Wildlife Service in 1941. Separates were issued as documents through volume 46; the last document was No. 1103. Beginning with volume 47 in 1931 and continuing through volume 62 in 1963, each separate appeared as a numbered bulletin. A new system began in 1963 with volume 63 in which papers are bound together in a single issue of the bulletin. Beginning with volume 70, number 1, January 1972, the *Fishery Bulletin* became a periodical, issued quarterly. In this form, it is available by subscription from the Superintendent of Documents, U.S. Government Printing Office, Washington, DC 20402. It is also available free in limited numbers to libraries, research institutions, State and Federal agencies, and in exchange for other scientific publications.

U.S. Department of Commerce
Seattle, Washington

Volume 103
Number 1
January 2005

Fishery Bulletin

Contents

Articles

1–14 **Bochenek, Eleanor A., Eric N. Powell, Allison J. Bonner, and Sarah E. Banta**
An assessment of scup (*Stenotomus chrysops*) and black sea bass (*Centropristas striata*) discards in the directed otter trawl fisheries in the Mid-Atlantic Bight

15–22 **Cooper, Daniel W., Katherine E. Pearson, and Donald R. Gunderson**
Fecundity of shortspine thornyhead (*Sebastolobus alascanus*) and longspine thornyhead (*S. altivelis*) (Scorpaenidae) from the northeastern Pacific Ocean, determined by stereological and gravimetric techniques

23–33 **DeMartini, Edward E., Marti L. McCracken, Robert B. Moffitt, and Jerry A. Wetherall**
Relative pleopod length as an indicator of size at sexual maturity in slipper (*Scyllarides squammosus*) and spiny Hawaiian (*Panulirus marginatus*) lobsters

34–51 **Fisher, Joseph P., and William G. Pearcy**
Seasonal changes in growth of coho salmon (*Oncorhynchus kisutch*) off Oregon and Washington and concurrent changes in the spacing of scale circuli

52–62 **Groeneveld, Johan C., Jimmy P. Khanyile, and David S. Schoeman**
Escapement of the Cape rock lobster (*Jasus lalandii*) through the mesh and entrance of commercial traps

63–70 **Grusha, Donna S., and Mark R. Patterson**
Quantification of drag and lift imposed by pop-up satellite archival tags and estimation of the metabolic cost to cownose rays (*Rhinoptera bonasus*)

71–83 **Harvey, Chris J.**
Effects of El Niño events on energy demand and egg production of rockfish (Scorpaenidae: *Sebastes*): a bioenergetics approach

The conclusions and opinions expressed in *Fishery Bulletin* are solely those of the authors and do not represent the official position of the National Marine Fisheries Service (NOAA) or any other agency or institution.

The National Marine Fisheries Service (NMFS) does not approve, recommend, or endorse any proprietary product or proprietary material mentioned in this publication. No reference shall be made to NMFS, or to this publication furnished by NMFS, in any advertising or sales promotion which would indicate or imply that NMFS approves, recommends, or endorses any proprietary product or proprietary material mentioned herein, or which has as its purpose an intent to cause directly or indirectly the advertised product to be used or purchased because of this NMFS publication.

84–96 **Horodysky, Andrij Z., and John E. Graves**
Application of pop-up satellite archival tag technology to estimate postrelease survival of white marlin (*Tetrapturus albidus*) caught on circle and straight-shank ("J") hooks in the western North Atlantic recreational fishery

97–107 **Kerr, Lisa A., Allen H. Andrews, Kristen Munk, Kenneth H. Coale, Brian R. Frantz, Gregor M. Cailliet, and Thomas A. Brown**
Age validation of quillback (*Sebastes maliger*) using bomb radiocarbon

108–129 **Marancik, Katrin E., Lisa M. Clough, and Jonathan A. Hare**
Cross-shelf and seasonal variation in larval fish assemblages on the southeast United States continental shelf off the coast of Georgia

130–141 **O'Farrell, Michael R., and Ralph J. Larson**
Year-class formation in Pacific herring (*Clupea pallasi*) estimated from spawning-date distributions of juveniles in San Francisco Bay, California

142–152 **Parker, Denise M., William J. Cooke, and George H. Balazs**
Diet of oceanic loggerhead sea turtles (*Caretta caretta*) in the central North Pacific

153–160 **Roberson, Nancy E., Daniel K. Kimura, Donald R. Gunderson, and Allen M. Shimada**
Indirect validation of the age-reading method for Pacific cod (*Gadus macrocephalus*) using otoliths from marked and recaptured fish

161–168 **Sulikowski, James A., Jeff Kneebone, Scott Elzey, Joe Jurek, Patrick D. Danley, W. Huntting Howell, and Paul C. W. Tsang**
Age and growth estimates of the thorny skate (*Amblyraja radiata*) in the western Gulf of Maine

169–182 **Tracey, Sean R., and Jeremy M. Lyle**
Age validation, growth modeling, and mortality estimates for striped trumpeter (*Latris lineata*) from southeastern Australia: making the most of patchy data

183–194 **Trnski, Thomas, Amanda C. Hay, and D. Stewart Fielder**
Larval development of estuary perch (*Macquaria colonorum*) and Australian bass (*M. novemaculeata*) (Perciformes: Percichthyidae), and comments on their life history

195–206 **Venerus, Leonardo A., Laura Machinandiarena, Martin D. Ehrlich, and Ana M. Parma**
Early life history of the Argentine sandperch *Pseudopercis semifasciata* (Pinguipedidae) off northern Patagonia

207–218 **Wilson, Matthew T., Annette L. Brown, and Kathryn L. Mier**
Geographic variation among age-0 walleye pollock (*Theragra chalcogramma*): evidence of mesoscale variation in nursery quality?

Note

219–226 **Markaida, Unai, Joshua J. C. Rosenthal, and William F. Gilly**
Tagging studies on the jumbo squid (*Dosidicus gigas*) in the Gulf of California, Mexico

227 **Subscription form**

An assessment of scup (*Stenotomus chrysops*) and black sea bass (*Centropristas striata*) discards in the directed otter trawl fisheries in the Mid-Atlantic Bight

Eleanor A. Bochenek

Eric N. Powell

Allison J. Bonner

Sarah E. Banta

Haskin Shellfish Research Laboratory
Rutgers, The State University of New Jersey
6959 Miller Ave.
Port Norris, New Jersey 08349-3167
E-mail address (for E A. Bochenek); **bochenek@hsrl.rutgers.edu**

Abstract—This study was undertaken to re-assess the level of scup (*Stenotomus chrysops*) discards by weight and to evaluate the effect of various codend mesh sizes on the level of scup discards in the winter-trawl scup fishery. Scup discards were high in directed scup tows regardless of codend mesh—typically one to five times the weight of landings. The weight of scup discards in the present study did not differ significantly from that recorded in scup-targeted tows in the NMFS observer database. Most discards were required as such by the 22.86 cm TL (total length) fish-size limit for catches. Mesh sizes ≤12.7 cm, including the current legal mesh size (11.43 cm) did not adequately filter out scup smaller than 22.86 cm. The median length of scup discards was about 19.83 cm TL. Lowering the legal size for scup from 22.86 to 19.83 cm TL would greatly reduce discard mortality. Scup discards were a small fraction (0.4%) of black sea bass (*Centropristis striata*) landings in black-sea-bass–targeted tows. The black sea bass fishery is currently regulated under the small-mesh fishery gear-restricted area plan in which fishing is prohibited in some areas to reduce scup mortality. Our study found no evidence to support the efficacy of this management approach. The expectations that discarding would increase disproportionately as the trip limit (limit [in kilograms] on catch for a species) was reached towards the end of the trip and that discards would increase when the trip limit was reduced from 4536 kg to 454 kg at the end of the directed fishing season were not supported. Trip limits did not significantly affect discard mortality.

Manuscript submitted 6 January 2003 to the Scientific Editor's Office.

Manuscript approved for publication 7 September by the Scientific Editor.

Fish. Bull. 103:1–14 (2005).

Because of regulations, market factors, and other reasons, both commercial and recreational fishermen discard some of their catch. Discards are considered one of the principal sources of mortality for many fish species, including those of significant commercial and recreational fisheries (Howell and Langdon, 1987; Glass et al., 1999; Suuronen et al., 1996).

The Sustainable Fisheries Act (SFA), governing U.S. fisheries management in federal waters, states that "conservation and management measures shall minimize bycatch." Much has been written about the environmental impact of discarding (Mooney-Seus, 1999; Alverson, 1999; Kennelly, 1999). Discard mortality reduces population size by limiting the number of individuals that can reach maturity and spawn. Because EEZ (Exclusive Economic Zone) fisheries must be managed at B_{msy} (biomass at maximum sustainable yield) under SFA guidelines and discards must be included in estimates of the TAC (total allowable catch), discard mortality also reduces total allowable landings. Therefore, discarding is not just an environmental problem; it is a problem that affects all aspects of fisheries.

A recreational and commercial fishery for scup (*Stenotomus chrysops*) occurs in the Mid-Atlantic Bight (the portion of the U.S. Atlantic coast extending from Cape Hatteras to Cape Cod) and New England regions where scup are caught south and offshore in the winter and north and inshore in the summer (NEFSC[1]). In 1996, the legal size for commercially caught scup was raised to 22.86 cm total length (TL), more or less coincidently with the establishment of a legal codend mesh size of 11.43 cm to reduce discard mortality (MAFMC, 1996). Discarding is considered to be an important cause of mortality for this important commercial and recreational species (NEFSC[2]). Kennelly (1999) reported large amounts of scup

[1] NEFSC (Northeast Fisheries Science Center). 2002. SARC 35. 35th Northeast regional stock assessment workshop (35th SAW). Stock assessment review committee (SARC) consensus summary of assessments. Northeast Fisheries Science Center Reference Document 02-14, 259 p. Northeast Fisheries Science Center, NMFS, NOAA, 166 Water St., Woods Hole, MA 02543.

[2] NEFSC (Northeast Fisheries Science Center). 2000. SARC 31. 31st northeast regional stock assessment workshop (31stSAW). Stock assessment review committee (SARC) consensus summary of assessments. Northeast Fisheries Science Center Reference Document 00-15, 409 p. Northeast Fisheries Science Center, NMFS, NOAA, 166 Water St., Woods Hole, MA 02543.

discards from demersal trawlers operating in certain areas and depths in the Mid-Atlantic Bight. High numbers of scup discards occur in the directed scup fishery (Powell et al., 2004). It is generally believed that one of the keys to effective management of scup is to reduce discard mortality (NEFSC[2]; NEFSC[1]). Fisheries managers attempt to control discard mortality using a number of management measures, but principally through mesh regulations and time or area closures.

Analysis of NMFS observer data by Powell et al.[3] indicated that scup comprised 65% of the total catch in scup-targeted tows, but that the discards-to-landings ratio for scup in these tows was 1.05. Somewhat more than half of the scup taken in scup-targeted tows were subsequently discarded. However, this analysis was based on relatively few observations; many of the tows used codends with mesh sizes below the current legal mesh size of 11.43 cm. As a consequence, applicability of the NMFS observer data to the present-day scup fishery is unclear. The objective of the present study was to obtain additional observations in the directed scup fishery to re-assess the level of discards by weight and to evaluate the effect of simple variations in codend mesh size on the level of scup discards.

Data analysis focused on scup. However, we also analyzed black sea bass (*Centropristis striata*) catches using the same methods as those for scup. Black sea bass were included because one management option is to require a common codend mesh size for the two species. The present legal mesh size for black sea bass is 10.16 cm and the minimum size of black sea bass that can be harvested is 27.94 cm TL. Commonality would simplify fishing methods because the two species are often targeted on the same trip.

Methods

Description of data

This study was undertaken during the 2001 winter scup trawl fishery in the Mid-Atlantic Bight. The legal trip limit for scup was 4536 kg from 1 January through 24 January. After 24 January until the close of the season in late February, the legal trip limit for scup was lowered to 454 kg. An experimental fishing permit was obtained from NMFS 1) to allow the vessels to fish in the GRAs (gear-restricted areas), implemented to reduce scup discards in the *Loligo* squid, (*Loligo pealei*), silver hake (*Merluccius bilinearis*), and black sea bass fisheries, 2) to allow the use of codends with meshes less than the legal 11.43-cm mesh, and 3) to allow commercial vessels to retain an additional 1361 kg of scup per trip to help defray study costs.

The four vessels participating in this study used the following codends: 1) the legal-size (11.43-cm) mesh codend; 2) a composite codend with 30 meshes of 10.16-cm mesh at the very end of the bag followed by 45 meshes of 11.43-cm mesh; and 3) codends with some meshes ≥12.7 cm (including codends with or without a composite design). Two tows with codends of smaller mesh size (between 6.35 and 10.16 cm) were also observed and these tows were included in data tabulations for completeness. The composite codend was designed as a mechanism to reduce large catches of small scup when abundant scup are encountered but was also designed to retain black sea bass and scup when abundance was low. Captains usually had two of the codends onboard the vessel during a fishing trip and were asked to fish the codends in an ABBA sequence (i.e., first tow with codend A, second tow with codend B, third tow with codend B, next tow with codend A, and so forth). These tows typically lasted no longer than one hour. Otherwise, the captain operated his boat using normal fishing practices, including selecting where and when to fish.

The catch from each tow was sorted to species and weighed. Fork lengths (FL) were obtained for a minimum of fifty scup discarded followed by a minimum of fifty scup landed. If time permitted, length-frequency information was collected for black sea bass and discarded individuals were measured. Because some regulations use TL, FL was converted when necessary to TL with the following equation: $TL(\text{cm}) = 1.14FL(\text{cm}) - 0.44$ (Hamer[4] in MAFMC [1996]).

Catch data obtained from this study of the winter 2001 scup fishery were compared to scup-targeted tows from the NMFS observer database for 1997 through mid-2000 (Powell et al.[3]). NMFS observer program methodology is detailed in the Northeast Fisheries Science Center Fisheries Observer Program Manual (NEFSC[5]). Mesh size reported in the NMFS observer database included an array of small-mesh codends less than present-day legal size, as well as the legal mesh size of 11.43 cm.

A depth was assigned for each tow as the mean of the depths of net deployment and retrieval. Swept area of the tow could not be calculated directly because door or wing spread were not recorded by us, nor were these metrics available in NMFS observed tows. A surrogate for true swept area was obtained as "the average of the recorded headrope and sweep lengths" multiplied

[3] Powell, E. N., E. A. Bochenek, S. E. Banta, and A. J. Bonner. 2000. Scup bycatch in the small-mesh fisheries of the Mid-Atlantic. Final Report, National Fisheries Institute Scientific Monitoring Committee, 74 p. Haskin Shellfish Research Laboratory, Rutgers University, 6959 Miller Ave., Port Norris, NJ 08349.

[4] Hamer, P. E. 1979. Studies of the scup, *Stenotomus chrysops*, in the Middle Atlantic Bight. N.J. Div. Fish. Game and Shellfish, misc. rep. no. 5M, 14 p. New Jersey Department of Environmental Protection, New Jersey Division of Fish and Wildlife, Division of Marine Fisheries, Nacote Creek Research Station, PO Box 418, Port Republic, NJ 08241.

[5] NEFSC (Northeast Fisheries Science Center). 2001. Fisheries observer program manual, 217 p. Northeast Fisheries Science Center, NMFS, NOAA, 166 Water St., Woods Hole, MA 02583.

by "the recorded tow time and speed." CPUE was then calculated by using estimated swept area as the effort term. Scope was calculated as "tow wire out" divided by "average water depth." For geographic location, each tow was assigned to a 10-minute square area (10-minute latitude and longitude) (Powell et al.[3]).

For some analyses, data from the present study's winter 2001 fishery and the NMFS observer database were assigned to categories by codend mesh size: the legal codend with 11.43-cm mesh; a composite codend with 10.16-cm mesh followed by 11.43-cm mesh; codends with meshes less than 6.35 cm; codends with meshes between 6.35 cm and 10.16 cm; and codends having some meshes greater than or equal to 12.7 cm. Gear type was assigned to either a millionaire or large-mesh box net based on the net styles used in our study and interpretations of NMFS observer-recorded net descriptions by knowledgeable fishermen.

Statistical analysis

Catch was evaluated by using the ratio of scup discards to landings, total catch of all species, total discards of all species, total scup discards, total scup landings, and a comparison of whether the catch of scup per tow was above or below the median for all tows in the study. In addition, we examined the influence of fishing decisions on discards 1) by distinguishing tows where scup discards exceeded scup landings from tows where landings exceeded discards and 2) by distinguishing between the scup catch of tows taken in the first and last half of the trip. For the latter, we also analyzed tows by their fractional position in the trip (whether a tow occurred at the start of a trip, $^1/_4$, $^1/_2$, $^3/_4$, or at the end of the trip). This approach yielded results equivalent to the simpler assignment of tows to the first and last half of the trip. Only the results of the simpler analysis are presented. Finally, we evaluated the impact of fishing decisions on the length frequencies of scup caught. ANOVAs were run by using ranked raw variables with class variables that defined fishing practice (mesh size, gear, scope, effort), time, and catch. The variable time was used to allocate tows to three categories:

1 Those trips from the present study taken from 1 to 24 January 2001 with a legal trip limit of 4536 kg of scup;
2 Those trips from the present study taken after 24 January 2001, with a legal trip limit of 454 kg of scup; and
3 Those scup trips taken in 1997–2000 from the NMFS observer reports.

Length frequencies were analyzed by ANOVA by using the 25th, 50th, and 75th percentiles and the mean as descriptive variables. In initial analyses, the interaction terms between mesh size or time and the other independent variables were included. Interaction terms were not significant more frequently than expected by chance and, accordingly, were not included in our results. Significant differences identified by the ANOVA were further investigated by using Tukey's studentized range test and, for covariates, by Spearman's rank correlation.

Results

Catch statistics—scup

Ten trips were taken during our study and 62 tows were successfully completed; 39 tows targeted scup and 12 tows targeted black sea bass (Table 1). For the remaining tows, the captain targeted *Loligo* squid as part of the normal fishing process and used a much smaller codend mesh size. These *Loligo*-targeted tows were excluded from further analyses. However, frequent changes in target species emphasize the need for tow rather than trip-aggregated data in discard analyses (Powell et al., 2004) because multiple targets within trips commonly occur in Mid-Atlantic Bight fisheries.

The majority of tows were taken in NMFS statistical area 622. Scup-targeted tows occurred primarily during daylight and at depths ranging from about 73.2 to 137.2 m in our study and from 54.9 to 109.7 m in the NMFS observer data set. A few tows from both the NMFS observer database and our study were deleted from the analysis because the catch was released overboard rather than brought onboard. Bycatch estimates from these tows were assumed to be inaccurate in comparison to other tows. This phenomenon occurs sporadically in many fisheries (e.g., Roel et al., 2000). In our study, six scup-targeted tows were disregarded for this reason. All four participating boats had at least one trip where one tow was released overboard. Observers reported that the net was so full of fish, primarily scup, in these tows that it could not be brought on deck. The catch for one black-sea-bass–targeted tow was released overboard. In addition, tows in which no discards were recorded were not analyzed. Generally, such tows occurred when the observer was asleep or sea conditions were too dangerous to collect data from the tow. Such tows did not occur in our study but did occur sporadically in the NMFS observer database. Regardless of the reason, we assumed that any tow without recorded discards represented incomplete sampling and, consequently, we discarded that tow from further analysis (Powell et al.[3]). Differences in the tabulated number of observed tows and the number of observed tows analyzed reflect the number of tows excluded from the analyses for these two reasons.

Length frequency—scup

The length frequencies of landings and discards were consistently significantly different (often $P \leq 0.0001$) (Fig. 1). The mean size of discarded scup was 17.7 cm and ranged from 13.2 to 21.4 cm in our study. Fifty percent of the scup discarded fell between 16.8 cm (25th percentile) and 18.5 cm (75th percentile). In contrast, the average size of scup landed was 24.2 cm and ranged from 22.2 to 29.2 cm. Fifty percent of the scup landed

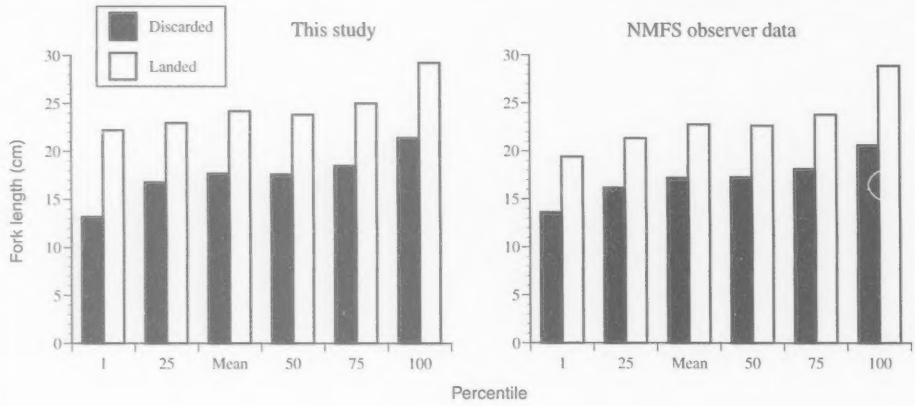

Figure 1

Mean length-frequency fractions for scup (*Stenotomus chrysops*) discarded and landed in our study and in the NMFS observer database. 1=smallest size. 100=largest size.

Table 1

Synopsis of scup and black-sea-bass–targeted tows by study, gear, and codend mesh size, including those tows where the catch was released overboard.

Scup-targeted tows

Study	Gear	6.35–10.16 cm mesh	11.43-cm mesh	10.16+11.43 cm composite	≥12.7 cm	Totals
This study	Millionaire net	2	3	0	0	5
	Large box net	0	14	19	7	40
Totals		2	17	19	7	45

Study	Gear	<6.35-cm mesh	6.35–10.16 cm mesh	11.43-cm mesh	Unknown	Totals
NMFS	Millionaire net	9	5	3	0	17
	Large box bet	5	4	2	7	18
Totals		14	9	5	7	35

Black-sea-bass–targeted tows

Study	Gear	6.35–10.16 cm mesh	11.43-cm mesh	10.16+11.43 cm composite	Totals
This study	Millionaire net	0	0	0	0
	Large box net	0	3	9	12
Totals		0	3	9	12

Study	Gear	<6.35-cm mesh	6.35–10.16 cm mesh	11.43-cm mesh	Unknown	Totals
NMFS	Millionaire net	0	0	0	0	0
	Large box net	0	6	0	0	6
Totals		0	6	0	0	6

fell between 22.9 cm (25th percentile) and 25.0 cm (75th percentile). For the NMFS observer data, the mean size of scup discards was 17.2 cm and ranged from 13.6 to 20.6 cm. Fifty percent of the scup discarded fell between 16.2 cm (25th percentile) and 18.2 cm (75th percentile). For scup landed, the mean size was 22.8 cm and ranged from 19.4 to 28.9 cm. Fifty percent of the scup landed fell between 21.3 cm (25th percentile) and 23.8 cm (75th percentile).

Codend and gear

Vessels participating in this study and in the NMFS observer program used either millionaire or box nets (Table 1). More tows were made with the box net in both data sets (Table 1). Most tows in our study were made with the composite and 11.43-cm codends because comparison of these two codends was one focus of our study. Most scup-targeted tows in the NMFS observer database were made with codends ≤10.16 cm mesh (Table 1).

Codend mesh size did not have a significant effect on catch length frequencies when data from our study and the NMFS observer data were analyzed separately or combined. We deleted codends with the smallest meshes (meshes ≤10.16 cm) and re-analyzed the data for the remaining larger codend meshes. Again, catch length frequencies were not significantly different for any of the codend mesh sizes. Finally, we considered the landed and discarded scup separately. For landings, codend mesh size had a moderately significant effect on median length (P=0.0220) and a stronger significant effect on mean length (P=0.0062). Codends with some meshes ≥12.7 cm caught more of the landed size fraction than the composite and slightly more than the 11.43-cm mesh codend; however, the actual difference in mean length between the three mesh-size groups was small, approximately one cm (Fig. 2).

The efficiency of the codend may change with the amount of fish caught such that selectivity declines with high catches. Accordingly, scup catches were divided into two groups: those above and those below the median catch for all tows. For catches above the median, codend mesh size had a significant effect (P=0.0441) on the 25th percentile of size for scup discarded in our study. The 25th percentile size was largest for codends with some meshes ≥12.7 cm and smallest for the composite codend. For landed scup, the 25th percentile sizes were about 22.0 cm regardless of codend mesh size. No significant differences existed between codend mesh sizes for scup length frequency in tows with catches below the median.

We examined the composition of the catch by weight. Codend mesh size had a limited effect on the ratio of scup discarded to landed, the total catch and total discards of all species, and total scup landed and discarded. Scup discards were greater with codends having some meshes ≥12.7 cm (P=0.0211). More scup were landed from these tows as well (P=0.0034) and therefore this codend style may contribute to a greater catch rate (Table 2). Very likely, this trend in increased catch is produced by the small number of tows (n=7) in this mesh size category rather than a real improvement in net performance.

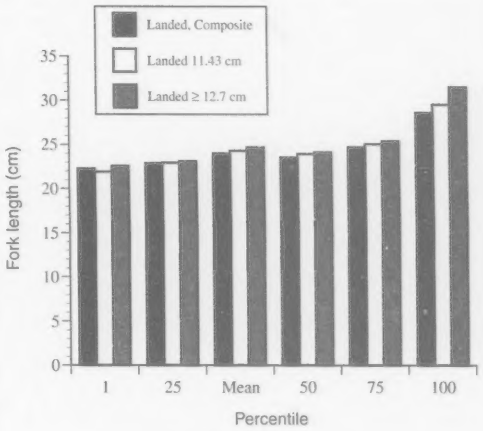

Figure 2

Mean scup (*Stenotomus chrysops*) length fractions for those tows with landed scup with a composite (10.16+11.43 cm) codend, 11.43-cm mesh codend, and a ≥12.7-cm mesh codend. 1=smallest size. 100=largest size.

No significant gear effects existed for any of the length-frequency fractions in the combined data set (our study and NMFS observer study). The only significant effect of scope (P=0.0175) was on total scup discarded in our study. This effect was not present in the NMFS observer data set.

Discards-to-landings ratio

Of the 62 tows completed in our study, 39 targeted scup. The NMFS observer program, from 1997–mid 2000, included 35 scup-targeted tows (Table 3). Overall, mean catch per tow for scup-targeted tows was 972.6 kg in our study and 945.3 kg for NMFS observed tows. In our study, the discards-to-landings ratio for all species combined ranged from 1.77 with the composite codend to 2.91 with a codend with some meshes ≥12.7 cm. In the NMFS observer data set, the discards-to-landings ratio for all species combined in scup-targeted tows ranged from 0.47 with codends having meshes of 6.35–10.16 cm to 3.43 with codends with meshes of 11.43 cm (Table 2). The mean discards-to-landings ratio for scup ranged from 1.1 for the NMFS database to 2.4 for our study (Table 3). Ratios varied from a low of 0.35 to a high of 5.72 among the various gear and mesh-size combinations (Table 4).

We analyzed cases where scup discards exceeded or were less than landings. When our data and the NMFS observer data were combined, the 25th (P=0.0219), 50th

Table 2

Mean weight (in kilograms) of scup discarded, scup landed, total discards of all species, total catch of all species, and total discards-to-landings ratio of all species per tow by codend mesh size for this study and the NMFS observer data.

Study	Codend	Scup discarded	Scup landed	Total discards	Total catch	Total discards-to-landings ratio	Total number of tows
This study	Composite	659.7	329.3	1078.1	1686.0	1.77	16
This study	11.43 cm	607.8	210.7	1060.2	1437.7	2.81	14
This study	≥12.70 cm	1020.7	404.9	1973.4	2652.8	2.91	7
NMFS	<6.35 cm	615.5	493.4	949.1	1530.1	1.63	14
NMFS	6.35–10.16 cm	230.5	510.5	321.1	999.2	0.47	9
NMFS	11.43 cm	535.2	260.0	1015.7	1311.6	3.43	5

Table 3

Mean catch and landings per tow for scup and black sea bass-targeted tows.

Scup

Study	Tow type	Total no. of tows	Mean catch (kg)	Mean landed (kg)	Mean discarded (kg)	Ratio of scup discards to landings
This study	Target	39	972.6	286.3	686.3	2.40
NMFS	Target	35	945.3	461.3	484.0	1.05

Black sea bass

Study	Tow type	Total no. of tows	Mean catch (kg)	Mean landed (kg)	Mean discarded (kg)	Ratio of black sea bass discards to landings
This study	Target	10	365.0	278.7	86.3	0.31
NMFS	Target	6	171.9	170.1	1.8	0.01

(P=0.0085), and 75th (P=0.0038) percentile sizes and the mean length (P=0.0001) were significantly lower for tows in which most scup were discarded (Fig. 3). When the data sets were analyzed separately, our study found that the 50th (P=0.0133) and 75th (P=0.0040) percentile sizes and the mean length (P=0.0338) were significantly lower for tows where discards exceeded landings. Not surprisingly, when fishermen caught larger scup, fewer scup were discarded. In the NMFS observer data set, no significant size effects were found for any of the percentile fractions.

When the discards and landings were analyzed separately, the lengths of fish discarded did not differ between tows for which discards exceeded landings and tows for which landings exceeded discards. However, for the landed fish, the 50th (P=0.0034) and 75th (P=0.0018) percentile sizes and the mean length (P=0.0033) were larger for tows where landings exceeded discards (Fig. 4). Discards decline when larger scup are proportionately more abundant in the catch.

We examined the influence of total catch (all species combined) on the length-frequencies of scup in tows where scup landings exceeded or did not exceed scup discards. For those tows with total catches below the median catch, a significant effect was noted for the median (P=0.0039), the 75th percentile (P=0.0006), and the mean (P=0.0288) length of scup. In those tows where total catch weight was relatively low, the median, mean, and 75th percentile lengths were larger in tows where scup landings exceeded discards. No significant effects on the length-frequency distribution of scup were observed for total catches that were above the median. The analysis identifies a strong trend towards the landing of larger-size scup in tows yielding total catches below the median for all tows.

Both landings and discards were affected in those tows in which total catch fell below the median. For landed scup, the median (P=0.0062), the 75th percentile (P=0.0051), and the mean (P=0.0113) length were higher in tows with total catches below the median when scup landings exceeded discards. For those scup that were discarded from tows with total catches below the median, a significant size effect was observed for the 75th percentile (P=0.0265). Discarded scup were larger in

Table 4

Synopsis of catch and landings data (kg) by study, gear, and codend mesh size for scup-targeted tows in our study and those in the NMFS observer database.

Gear	Mesh size	Total scup/tow	Scup landed	Scup discarded	Ratio of scup discards to landings	Number of tows
This study						
Large box	10.16+11.43 cm composite	1332.3	519.3	813.0	1.57	9
	11.43 cm	1572.8	431.6	1141.2	2.64	5
	≥12.70 cm	2609.7	624.1	1985.6	3.18	2
Millionaire	6.35–10.16 cm	32.7	16.3	16.3	1.00	1
	10.16+11.43 cm composite	547.5	85.0	462.5	5.44	7
	11.43 cm	399.5	88.1	311.5	3.54	9
	≥12.70 cm	951.9	317.2	634.8	2.00	5
Unknown		636.8	94.8	542.0	5.72	1
NMFS						
Large box	<6.35 cm	1076.7	196.0	880.8	4.49	5
	6.35–10.16 cm	20.8	3.4	17.4	5.12	4
	11.43 cm	176.9	131.5	45.4	0.35	2
Unknown		988.2	477.6	510.6	1.07	7
Millionaire	<6.35 cm	1126.6	658.6	468.1	0.71	9
	6.35–10.16cm	1317.1	916.2	401.0	0.44	5
	11.43 cm	1207.3	345.5	861.8	2.49	3

Table 5

Total discards and total catch of all fish species (in kg) and scup discarded and landed (in kg) for only those tows characterized by having more or less discards of scup than the median catch per tow.

Study	More or less discards	Scup discarded	Scup landed	Total discards	Total catch	Total number of tows
This study	Less	145.4	355.6	565.4	1027.5	11
This study	More	898.9	259.0	1451.6	1982.3	28
NMFS	Less	235.1	521.1	426.3	1058.3	20
NMFS	More	815.9	381.5	1242.8	1761.5	15

these tows, reflecting the overall larger size of the scup catch in tows where total catch was relatively low.

Finally, for tows in which scup discards exceeded landings, total catch of all species and total discards of all species were also high. This trend was significant for total catch (P=0.0273) and total discards (P=0.0038) in our study (Table 5) and for total discards (P=0.0017) and total catch (P=0.0112) in the NMFS observer data set (Table 5). Therefore, scup discards tended to increase with respect to landings as total catch increased.

Time and effort

For our study, effort significantly affected the 25th (P=0.0247) and 50th (P=0.0466) percentiles of the size-frequency distribution of discards. The size frequencies for landings were not similarly affected. In both former cases, the 25th and 50th percentile sizes were larger when effort was less (shorter tows). No significant effects were observed in the NMFS observer data set. Because the length frequency of the entire catch did not change significantly, this is likely an effect of processing onboard the boat.

Given trip limits, one might anticipate discards to increase in tows made at the end of the trip. We examined the amount of scup caught either in the first half of the tows or in the last half of the tows on each trip. For this study, more scup were landed (P=0.0008) and discarded (P=0.0001) in tows that occurred during the last half of the trip. Total catch and total discards were unaffected. For the NMFS observer data set, more scup were landed (P=0.0001) and discarded (P=0.0001)

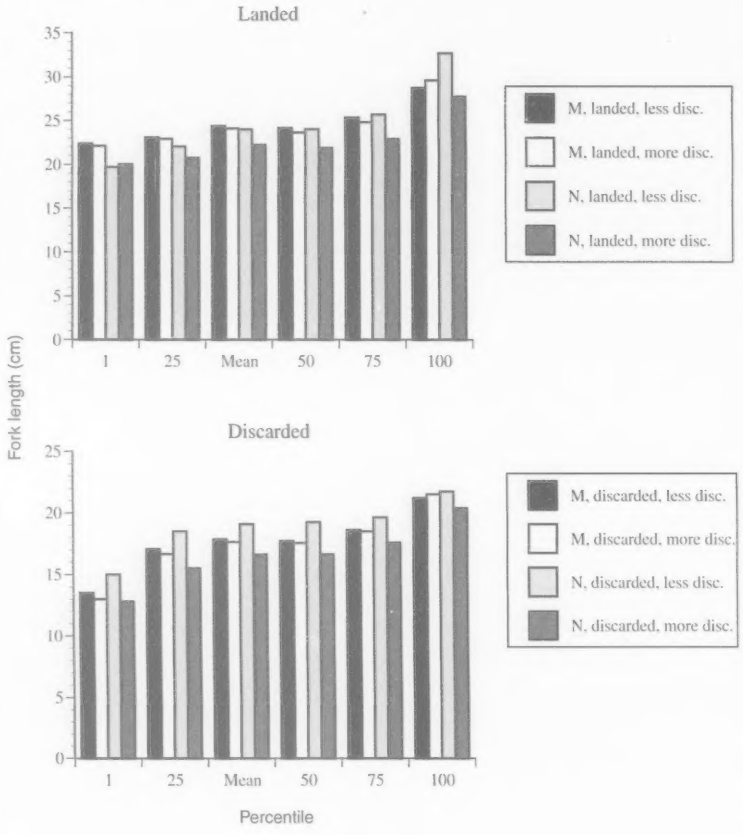

Figure 3

Percentiles of scup (*Stenotomus chrysops*) length frequency for those tows in which discards exceeded or failed to exceed landings for landed and discarded scup. "M" represents this study and "N" represents NMFS observer data. Landed, less disc. = for scup landed, tows with less discarded scup than landed scup. Discarded, less disc. = for scup discarded, tows with less discarded scup than landed scup. Landed, more disc. = for scup landed, tows with more discards of scup than landed scup. Discarded, more disc. = for scup discarded, tows with more discards of scup than landed scup. 1=smallest size. 100=largest size.

and the total catch of all species (P=0.0195) and total discards of all species (P=0.0004) were higher in tows taken during the last half of the trip (Table 6). More scup being landed and discarded in the last half of the trip indicates that captains learn where to fish for scup during the trip and CPUE rises as a consequence. No evidence exists that discards increased with respect to landings during the trip.

We anticipated that reduction of the trip limit from 4536 kg to 454 kg on 24 January would influence the total weight of discards. Time did influence total weight of scup discards (P=0.0056) in our study. More discards per tow occurred on trips taken prior to 24 January, likely because of the larger trip limit (weight limit per species for each trip) for the 1–24 January period. With a larger trip limit, more scup can be caught per tow and therefore more scup will be discarded. The discards-to-landings ratio, however, was not significantly affected—indicating that captains controlled total scup catch in proportion to the landing limit.

The present study versus the NMFS observer study

We compared trends in our data with those in the NMFS observer data. The subset of directed scup tows in the two data sets rarely disagreed, despite the disparity in codend mesh sizes reported (Table 1).

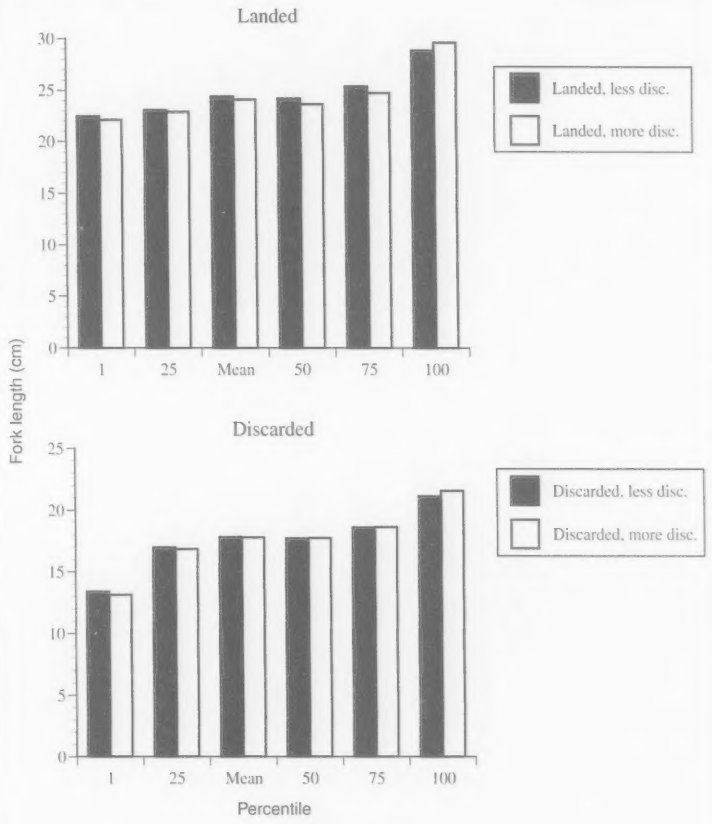

Figure 4

Percentiles of scup (*Stenotomus chrysops*) lengths (FL) for those tows in which discards exceeded or failed to exceed landings for landed and discarded scup. Codends included the composite (10.16+11.43 cm), 11.43 cm, and ≥12.7 cm meshes. Landed, less disc. = for scup landed, tows with less discarded scup than landed scup. Discarded, less disc. = for scup discarded, tows with less discarded scup than landed scup. Landed, more disc. = for scup landed, tows with more discards of scup than landed scup. Discard, more disc. = for scup discarded, tows with more discards of scup than landed scup. 1=smallest size. 100=largest size.

Table 6

Mean weight (in kg) of scup discarded and landed and the total of all fish species landed and discarded per tow for scup-targeted tows in the first half of the trip and the second half of the trip.

Study	First half or second half of trip	Scup discarded	Scup landed	Total discards	Total catch	Total number of tows
This study	First	253.3	125.2	970.2	1279.7	22
This study	Second	1246.8	494.7	1501.2	2273.8	17
NMFS	First	43.2	23.2	463.0	670.3	19
NMFS	Second	1007.5	981.5	1148.3	2178.3	16

Table 7

Mean weight (in kg) of black sea bass discarded, black sea bass landed, total discards of all species, total catch of all species, and total discards-to-landings ratio of all species per tow by codend mesh size and gear for this study and the NMFS observer data.

Study	Gear	Codend	Black sea bass discarded	Black sea bass landed	Total discards	Total catch	Total discards to landings	Ratio of Total number of tows
This study	Large box	10.16+11.43 cm composite	119.2	366.7	845.6	1306.9	1.83	7
This study	Large box	11.43 cm	5.0	25.9	1201.8	1250.3	24.78	2
This study	Millionaire	11.43 cm	18.6	168.3	368.1	683.8	1.17	1
NMFS	Large box	6.35–10.16 cm	1.8	170.1	23.7	224.2	0.12	6

Catch statistics—black sea bass

During the winter scup season, black sea bass are legally caught with 10.16-cm mesh codends in offshore waters. A boat captain often will target scup and black sea bass on the same trip, but will use different mesh codends. A total of 12 black-sea-bass–targeted tows were observed in our study and 6 black-sea-bass–targeted tows were documented in the NMFS observer data set (Table 1).

Length frequency—black sea bass

Black sea bass length-frequency distributions were highly significantly different (often $P=0.0001$) between those fish landed and those discarded. The mean size of discarded black sea bass from our study was 22.9 cm and ranged from 18.4 to 25.4 cm. Fifty percent of the black sea bass discarded fell between 22.1 cm (25^{th} percentile) and 24.3 cm (75^{th} percentile). In contrast, the mean size of landed black sea bass was 31.1 cm and ranged from 25.4 to 40.9 cm. For black sea bass landed, fifty percent of the fish were found between 28.6 cm (25^{th} percentile) and 33.3 cm (75^{th} percentile). For the NMFS observer data, the mean size of black sea bass discarded was 23.4 cm and ranged from 20.7 to 27.0 cm. Fifty percent of the black sea bass discarded fell between 22.3 cm (25^{th} percentile) and 24.7 cm (75^{th} percentile). The mean size of landed black sea bass was 28.5 cm and ranged from 24.5 to 34.0 cm. For landed black sea bass, fifty percent fell between 25.0 cm (25^{th} percentile) and 31.5 cm (75^{th} percentile).

Codend and gear

Nine tows were made with the composite codend and three tows were made with the 11.43-cm legal mesh codend in our study. For the NMFS observer data, all six targeted tows fell into the 6.35–10.16 cm mesh-size group that included the legal mesh size of 10.16 cm (Table 1).

We found no significant effects of codend mesh size on the percentile length-frequency fractions of black sea bass. We considered landed and discarded black sea bass separately for those tows with total catches above and below the median and, once again, no significant codend mesh-size effects were observed. The total number of tows, however, was small. A significant codend mesh-size effect ($P=0.0389$) was observed for black sea bass landed. Landings were higher with the larger mesh codends (composite 10.16+11.43 cm codend and the 11.43-cm codend) rather than with the ≤10.16-cm mesh codend (Table 7). The small number of total tows with the larger codend mesh sizes (10.16+11.43 cm and the 11.43 cm) is probably responsible for this difference in landings rather than differences in net performance. Gear effects (net types) were not determined because only the box net was used.

Discards-to-landings ratio

Total mean catch per tow was 365 kg and total mean landings per tow was 279 kg for the 10 tows in our study. For the six directed tows in the NMFS observer data, average total catch was 172 kg and average total landings were 170 kg (Table 3). In black-sea-bass–targeted tows, the black sea bass catch comprised 34.2% of the total catch. The discards-to-landings ratio for black sea bass was 0.230. Relatively few black sea bass were discarded. Scup comprised 0.9% of the total catch in black sea bass targeted tows. Less than one percent (0.4%) of the scup catch in black-sea-bass–targeted tows was discarded.

We analyzed cases where black sea bass discards exceeded or were less than landings in tows where total catch (all species combined) was above or below the median. For total catches above the median, a significant size effect was noted for the median length ($P=0.0040$), the 75^{th} percentile size ($P=0.0007$), and the mean length ($P=0.0026$). Larger fish were present in tows where discarding was lower (Fig. 5). No significant effects on the size distribution of black sea bass were observed in tows with total catches below the median. We further divided the catches above the median into discards and landings. For those black sea bass that were landed from tows with total catches above the median, a significant size effect was observed for the 25^{th} ($P=0.0199$), the

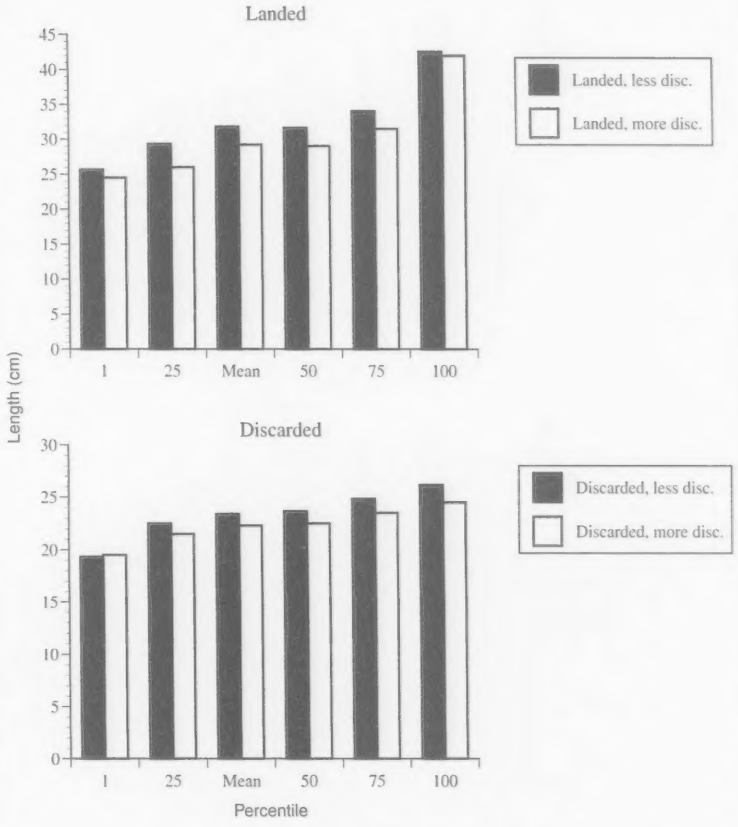

Figure 5

Percentiles of black sea bass (*Centropristas striata*) length frequencies for those tows in which discards of black sea bass exceeded or failed to exceed landings for landed or discarded black sea bass. Landed, less disc. = for black sea bass landed, tows with less discards of black sea bass than what was landed. Discarded, less disc. = for black sea bass discarded, tows with less discards of black sea bass than what was landed. Landed, more disc.: for black sea bass landed, tows with more discards of black sea bass than what was landed. Discarded, more disc. = for black sea bass discarded, tows with more discards of black sea bass than what was landed. 1=smallest size. 100=largest size.

50th (P=0.0280), and the 75th (P=0.0090) percentile size fractions and the mean length (P=0.0133). The size of landed black sea bass was larger in tows where discarding was low (Fig. 5).

Time and effort

Because of trip limits, discards could increase in tows taken near the end of a trip. Therefore, we compared the catch of black sea bass in the first and the last half of the tows. The quantity caught and the length-frequency percentiles were not significantly different between the first and last half of the tows. In contrast, for scup trips, discards and landings tended to be higher in tows made in the last half of the trip.

Effort significantly affected the 25th (P=0.0010), 50th (P=0.0003), and 75th percentile (P=0.0153) size fractions of black sea bass for the combined data sets (NMFS study and our study). In these cases, higher effort was associated with more smaller fish. When the two data sets were analyzed independently, most of the effort effects were no longer present.

Discussion

Scup

The type of net (gear) and the size of codend mesh had only a minor effect on the length frequencies of scup caught. Although variations in codend mesh size normally influence catch in other studies (Hastie, 1996; Petrakis and Stergiou, 1997; Stergiou et al., 1997; Broadhurst et al., 1999), a wide range in codend mesh sizes produced similar results for scup. Codends with some meshes ≥12.7 cm appeared to catch more of the size classes of fish chosen for landing than the composite codend and just slightly more than the legal 11.43-cm mesh codend; therefore the ≥12.7-cm mesh condend may reduce discards. The actual difference in scup lengths between the three codends was only about one cm. In terms of kilograms caught, more scup were caught in tows with the larger codend mesh. Landings increased, but so did discards, so that the discards-to-landings ratio remained unchanged. This finding indicates that the small upward bias in sizes caught did not significantly reduce total catch. In general, the smaller mesh codends (6.35–10.16 cm) and the composite codend (10.16+11.43 cm) performed similarly to the current legal mesh design (11.43 cm). Overall, discards of scup remained high regardless of the type of gear (nets) and codends used.

In our study, more larger scup were caught in longer tows. When a boat encounters a large school of scup, the mean length of the catch tended to be smaller. In addition, the larger-size scup tended to be caught more often in those tows with total catches below the median. This trend is probably a biological effect, but an effect of mesh size or gear cannot be excluded. Most populations contain relatively few larger fish and, therefore, more smaller individuals. Morse[6] (in Steimle et al., 1999) noted that scup schools are size-structured. When larger scup are less common in schools, then schools with these larger individuals most likely would be smaller and more effort would be required to achieve the same catch of these individuals. The same result would occur if larger scup tended to be on the outside or above smaller scup in schools. Little is known about scup behavior. However, any spatial size structure in the population could promote a direct relationship between effort and the mean length of fish caught and an inverse relationship between total catch (all species) and mean length of fish caught.

As an alternative explanation for the lower catch rate of larger individuals, clogging of the codend may occur when catch rates are high and, as a consequence, size-selectivity would decline. Different codend mesh sizes do not seem to affect the number of discarded scup as much as one might anticipate because codends clog during the interception of large schools. Accordingly, lower CPUE could produce greater size selectivity resulting in increased mean length when catches are relatively low. However, the trends observed in length frequency with effort and total catch were not significantly influenced by codend mesh size. Accordingly, the observed trend is likely a direct consequence of fishing on size-structured populations.

In general, more scup were landed and discarded in the last half of a trip. This finding indicates that the captain learns where to fish for scup by the second half of the trip and CPUE increases as a consequence. We had expected an increase in discards as the trip limit was reached towards the end of the trip. However, no effect of trip limits on the total weight of discards could be discerned in our data set or the NMFS observer data set.

More scup were discarded per tow in tows observed during the first half of the 2001 season, namely 1–24 January, than in the second half of the season, 25 January–February, but the discards-to-landings ratio did not vary for either half of the season. The fact that the ratio did not differ indicates that more scup are discarded per tow when fishermen are allowed a larger trip limit (4536 kg). The higher discards of scup per tow during the first half of the season are likely due to the increased total catch per tow that might be anticipated when allowable landings are higher. Accordingly, captains are able to reduce catch rate and, thus, discards when landing limits are low.

We compared the NMFS observer database to our observer data. Despite a substantial variation in the distribution of codend mesh sizes between the two data sets, the discards-to-landings ratio was not significantly different. Concerns raised by the high discards-to-landings ratio observed in the NMFS observer data were supported by our study. The discards-to-landings ratio for the directed scup fishery consistently exceeded 1.0.

In summary, the objective of our study was to evaluate the effect of codend mesh size on the amount of scup discards and to identify mechanisms to reduce scup discards. Although we observed a number of trends in discards in our study, neither the current legal mesh nor any of the experimental codends seem to adequately filter out scup smaller than 22.86 cm. Neither did trip limits seem to influence the total weight of scup discards. In fact, the only consistent trends produced by variations in effort and total catch seem most likely due to biological effects not easily controlled for by the captain of a fish vessel. Overall, the total weight of discards seems to be primarily a function of the regulated size limit, abetted by the tendency for smaller fish to be captured when encounter rates are high. The present study found that the length of the median discards was about 17.78 cm FL (19.83 cm TL based upon a conversion factor of Hamer[4] [in MAFMC, 1996]). O'Brien et al. (1993) and NEFSC (1993) reported that 50% of both male and female scup reach maturity at 15.49 cm FL (17.27 cm TL). Therefore, lowering the scup minimum size limit to 17.78 cm FL (19.83 cm TL) would greatly

[6] Morse, W. W. 1978. Biological and fisheries data on scup, *Stenotomus chrysops* (Linnaeus). NMFS, NEFSC, Sandy Hook Lab. tech. ser. rep. no. 12, 41 p. James J. Howard Marine Sciences Laboratory, Northeast Fisheries Science Center, 74 Magruder Rd., Sandy Hook, NJ 07732.

reduce scup discards, yet permit the majority of scup to attain sexual maturity. Kilograms discarded might be reduced by more than half. Fishermen would reach their trip limit sooner and thus stop fishing earlier. As a result, fishing mortality rate even on larger scup would be reduced. This single change would reduce discards more than any change in net or codend design tested to date and would not result in any increase in fishing-induced mortality for scup.

Black sea bass

Estimates of discards of black sea bass are low in the black-sea-bass–targeted fishery, based on the few observed tows in our study and data from the NMFS observer database. Regardless of which codends were used, the same size fractions of black sea bass were caught. The composite codend (10.16+11.43 cm mesh) caught more black sea bass than were landed. Discards was also higher. As with scup, mesh size and gear type had minor effects on the size frequency, the discards-to-landings ratio, and the kilograms of black sea bass caught. The majority of tows where black sea bass were caught had ratios of black sea bass discarded to landed of less than 0.3, indicating that few discards occur in this fishery. In contrast, most of the scup tows were characterized by discards-to-landings ratios greater than one. The differences in discards-to-landings ratios between black sea bass and scup may be due to a combination of biological factors controlling the average size of scup in the larger schools and to regulatory factors that do not match well with the size range of scup in schools.

Unlike scup, black sea bass size frequencies and total weight caught were similar in tows taken during the first and last half of the trip. Trip limits are in effect for both black sea bass and scup. The difference between the two species in the distribution of catch through the time course of the trip may be the result of biological effects in that the schooling of scup would tend to produce higher catches during the middle or latter part of the trip as the captain finds schools of fish.

Powell et al.[3] showed that black sea bass and scup are caught simultaneously more frequently than expected by chance in tows in the Atlantic mackerel (*Scomber scombrus*), *Loligo* squid, scup, and silver hake fisheries and suggested that they should be regulated together. Our analysis also showed this pattern in that the two species were frequently caught in the same tows (39 out of 40 scup-targeted tows and seven out of 10 black-sea-bass–targeted tows caught both scup and black sea bass). In addition, Shepherd and Terceiro (1994), Musick et al., (1985), and Musick and Mercer (1977) also found that both scup and black sea bass were caught in the same tow. Use of a common codend mesh size regulation for both fisheries may prove useful. The failure to find significant differences between mesh sizes suggests that the 10.16+11.43 cm composite bag might be a reasonable choice for both fisheries. However, scup discards were a small fraction of black sea bass landings in black-sea-bass–targeted tows (0.4%)—very small in comparison to the percentage in scup-targeted tows. This finding indicates that there is considerable discrimination between the two species at the level of the fishery. The black sea bass fishery is currently regulated under the small-mesh fishery GRA plan in which fishing is prohibited in some areas to reduce scup mortality. This investigation finds no evidence to support the efficacy of this management approach. Scup discards do not appear to be an important attribute of the black sea bass fishery.

Conclusions

Because fishermen catch both scup and black sea bass in the same tow and because the current regulations require fishermen to use an 11.43-cm mesh codend when targeting scup, and, a 10.16-cm mesh codend when targeting black sea bass, two different codend mesh sizes are used on the same trip. The composite codend was designed to retain the smaller black sea bass catches and some scup when catch rates are low but permits more scup to escape at higher catch rates. The composite codend (10.16+11.43 cm mesh) performed as well as the other codends used in our study, including the 11.43-cm legal-size codend. The composite codend with 10.16-cm mesh followed by the 11.43-cm or 12.7-cm mesh codends should be further evaluated on both black sea bass and scup-directed tows. If this composite codend works equally as well as the legal 11.43-cm mesh codend currently in place for scup (and the data presented here suggest that it does), consideration should be given to using this codend because it permits the retention of smaller black sea bass without negatively influencing scup. This change would eliminate the need to carry two codends onboard and thus would reduce overall trip costs without impacting the number of scup discards. However, neither codend successfully addresses the need to significantly reduce scup discarding in the scup-directed fishery.

Codends with some 12.7-cm meshes tended to reduce discards by reducing the catchability of smaller scup, but the trends were often not significant, possibly due to the small sample size, but possibly also because nets were clogged by schools of smaller-size scup. The data indicate that further studies with 12.7-cm or greater mesh composites may identify codend configurations that will produce fewer discards. DeAlteris and La Valley (1999) have documented that scup can survive capture in a trawl net and subsequent escapement. Therefore, optimizing codend mesh size could reduce discard mortality.

Larger scup were caught in tows where the total catch weight was low. Large catches tended to accompany the interception of scup schools. These large catches can clog the nets and thus reduce size selection even at larger mesh sizes. Alternatively, larger scup may not be associated with smaller scup in schools. We cannot discriminate between the two explanations. Regardless of the reason, the tendency of the largest catches to contain proportionately more smaller fish will likely minimize the positive influence of net management in

reducing scup discards. Rather, the tendency of the largest catches to contain proportionately more smaller fish suggests that fisheries managers may want to lower the legal-size limit for scup from 22.86 cm to 17.78 cm FL. The median size of scup discards in our study was 17.78 cm FL. Setting the size limit at 17.78 cm FL (19.83 cm TL) would greatly reduce discards and thus overall discard mortality. This management change would likely have a much greater effect in reducing scup discards than any other single management measure directed at gear modification or area closure and would not endanger the stock (most discarded scup fail to survive); thus, any approach significantly reducing discards must significantly increase overall survival of the population.

Acknowledgments

We would like to thank the National Fisheries Institute, Scientific Monitoring Committee, for providing support for this project. We also thank the captain and crew for the use of the four commercial fishing vessels from Cape May that cooperated in the project. Without their assistance, this project would not have been possible. We also thank NMFS-NEFSC for providing the NMFS observer data used in our analysis.

Literature cited

Alverson, D. L.
1999. Some observations on the science of bycatch. MTS (Marine Technology Society) Journal 33(2):6–12.

Broadhurst, M. K., S. J. Kennelly, and S. Eayrs.
1999. Flow-related effects in prawn-trawl codends: potential for increasing the escape of unwanted fish through square-mesh panels. Fish. Bull. 97:1–8.

DeAlteris, J., and K. J. La Valley.
1999. Physiological response of scup, *Stenotomus chrysops*, to a simulated trawl capture and escape event. MTS Journal 33(2):25–34.

Glass, C. W., B. Sano, H. O. Milliken, G. D. Morris, and H. A. Carr.
1999. Bycatch reduction in Massachusetts inshore squid (*Loligo pealei*) trawl fisheries. MTS Journal 33(2):35–41.

Hastie, L. C.
1996. Estimation of trawl codend selectivity for squid (*Loligo forbesi*), based on Scottish research vessel survey data. ICES J Mar Sci 53:741–744.

Howell, W. H., and R. Langdon.
1987. Commercial trawler discards of four flounder species in the Gulf of Maine. North Am. J. Fish Manag. 7:6–117.

Kennelly, S. J.
1999. Areas, depths and times of high discard rates of scup, *Stenotomus chrysops*, during demersal fish trawling off the northeastern United States. Fish. Bull. 97:185–192.

MAFMC (Mid-Atlantic Fishery Management Council).
1996. Amendment 8 to the summer flounder, scup, and black sea bass fishery management plan: fishery management plan and final environmental impact statement for the scup fishery. January 1996, 353 p. Mid-Atlantic Fishery Management Council, Dover, DE.

Mooney-Seus, M.
1999. Formula for bycatch reduction. MTS Journal 33(2):3–5.

Musick, J. A., J. A. Colvocoresses, and E. J. Foell.
1985. Seasonality and the distribution, availability and composition of fish assemblages in Chesapeake Bight. *In* Fish community ecology in estuaries and coastal lagoons: towards an ecosystem integration (A. Y. Arancibia, ed.), p. 451–474. OR(R) UNAM (Universidad Nacional Autonoma de Mexico) Press, Mexico. [ISBN 9688376183.]

Musick, J. A., and L. P. Mercer.
1977. Seasonal distribution of black sea bass, *Centropristis striata*, in the Mid-Atlantic Bight with comments on the ecology and fisheries of the species. Trans. Am. Fish. Soc. 106:12–25.

NEFSC (Northeast Fisheries Science Center).
1993. Status of the fishery resources off the Northeastern United States. NOAA Tech. Mem. NMFS-F/NEC-101, 140 p.

O'Brien, L., J. Burnett, and R. K. Mayo.
1993. Maturation of nineteen species of finfish off the northeast coast of the United States, 1985–1990. NOAA Tech. Rep. NMFS 113, 66 p.

Petrakis, G., and K. I. Stergiou.
1997. Size selectivity of diamond and square mesh codends for four commercial Mediterranean fish species. ICES J Mar Sci. 54:13–23.

Powell, E. N., A. J. Bonner, B. Muller, and E. A. Bochenek.
2004. Assessment of the effectiveness of scup bycatch-reduction regulations in the *Loligo* squid fishery. J. Environ. Manag. 71:155–167.

Roel, B. A., K. L. Cochrane, and J. J. Field.
2000. Investigation into the declining trend in Chokka squid *Loligo vulgaris reynaudii* catches made by South African trawlers. S. Afr. J. Mar. Sci. 22:212–135.

Shepherd, G. R., and M. Terceiro.
1994. The summer flounder, scup and black sea bass fishery of the Middle Atlantic Bight and southern New England waters. NOAA Tech. Rept NMFS 122, 13 p.

Steimle, F. W., C. A. Zetlin, P. L. Berrien, D. L. Johnson, and S. Chang.
1999. Essential fish habitat source document: scup, *Stenotomus chrysops*, life history and habitat characteristics. NOAA Tech. Mem. NMFS-NE-149, 48 p.

Stergiou, K. I., C-Y. Politou, E. D. Christou, and G. Petrakis.
1997. Selectivity experiments in the NE Mediterranean: the effect of trawl codend mesh size on species diversity and discards. ICES J Mar Sci 34:774–786.

Suuronen, P., J. A. Perez-Comas, L. Lehtonen, and V. Tschernij.
1996. Size-related mortality of herring (*Clupea harengus* L.) escaping through a rigid sorting grid and trawl codend meshes. ICES J Mar Sci 53:691–700.

Fecundity of shortspine thornyhead (*Sebastolobus alascanus*) and longspine thornyhead (*S. altivelis*) (Scorpaenidae) from the northeastern Pacific Ocean, determined by stereological and gravimetric techniques*

Daniel W. Cooper
Katherine E. Pearson
Donald R. Gunderson

School of Aquatic and Fishery Sciences
University of Washington
1122 NE Boat Street
Seattle, Washington 98105.

Present address (for D. W. Cooper, contact author): Alaska Fisheries Science Center, F/AKC2
7600 Sand Point Way NE
Seattle, Washington 98115-0700.

E-mail address (for D. W. Cooper): dan.cooper@noaa.gov

Abstract—Fecundity was estimated for shortspine thornyhead (*Sebastolobus alascanus*) and longspine thornyhead (*S. altivelis*) from the northeastern Pacific Ocean. Fecundity was not significantly different between shortspine thornyhead off Alaska and the West Coast of the United States and is described by $0.0544 \times FL^{3.978}$, where FL=fish fork length (cm). Fecundity was estimated for longspine thornyhead off the West Coast of the United States and is described by $0.8890 \times FL^{3.249}$. Contrary to expectations for batch spawners, fecundity estimates for each species were not lower for fish collected during the spawning season compared to those collected prior to the spawning season. Stereological and gravimetric fecundity estimation techniques for shortspine thornyhead provided similar results. The stereological method enabled the estimation of fecundity for samples collected earlier in ovarian development; however it could not be used for fecundity estimation in larger fish.

Manuscript submitted 15 July 2003 to the Scientific Editor's Office.

Manuscript approved for publication 20 September 2003 by the Scientific Editor.

Fish. Bull. 103:15–22 (2005).

Shortspine thornyhead (*Sebastolobus alascanus*) is distributed from the Bering Sea to Baja California (Orr et al., 2000). Longspine thornyhead (*S. altivelis*) is distributed from the Gulf of Alaska to Baja California (Orr et al., 2000), and a few specimens have recently been collected in the eastern Bering Sea (Hoff and Britt, 2003). Both species are commercially important (Piner and Methot, 2001; Gaichas and Ianelli, 2003) and inhabit deep waters over the continental shelf and slope. Both shortspine and longspine thornyhead are determinate spawners (Wakefield, 1990; Pearson and Gunderson, 2003), and spawn pelagic, gelatinous egg masses (Pearcy, 1962; Best, 1964; Wakefield, 1990; Wakefield and Smith, 1990). Shortspine thornyhead spawn between April and July in Alaska, and between December and May along the West Coast of the United States, whereas longspine spawn between January and April along the West Coast (Pearson and Gunderson, 2003).

Annual fecundity is used as a measure of reproductive output in fishery population models and life history studies. Accurate annual fecundity estimates require identifying oocytes to be spawned in the current spawning season. For iteroparous spawners, developing oocytes are often distinguished from reserve oocytes by diameter or yolk presence (Macer, 1974). Collection date for samples is important. If samples are collected too early in oocyte development, some developing oocytes will be indistinguishable from reserve oocytes, and fecundity will be underestimated.

In shortspine thornyhead, oocyte stages 4–8 are maturing to be spawned in the current spawning season, whereas oocyte stages 1–3 are reserve oocytes to be spawned in future spawning seasons (Pearson and Gunderson, 2003). Early vitellogenic oocytes (stage 4) overlap in size with late perinucleus (stage 3) reserve oocytes (Pearson and Gunderson, 2003). Late vitellogenic oocytes (stage 5) are easily distinguished from reserve oocytes. In whole oocytes, neither oocyte size nor appearance can be relied on to distinguish stage-3 and early stage-4 oocytes; however stage-3 and stage-4 oocytes can be visually distinguished from histological samples (Pearson and Gunderson, 2003). Emerson et al. (1990) developed a stereological method to estimate fecundity

* Contribution 929 from the Joint Institute for the Study of the Atmosphere and Ocean (JISAO), 4909 25th Ave NE, Seattle, WA.

from histological sections. Unlike gravimetric methods (e.g., Hunter et al., 1992) where whole oocytes are used to estimate fecundity, stereological methods do not rely on oocyte diameter or other proxies for vitellogenesis. A collection of shortspine thornyhead ovaries from Alaska contained few specimens considered suitable for a gravimetric fecundity method because too few of the specimens contained all developing oocytes in stage 5 or beyond. However, enough samples were suitable for the stereological method.

This study provides a fecundity estimate based on stereological and gravimetric techniques for shortspine thornyhead off Alaska. Benefits and limitations of the stereological method in this case are discussed. A gravimetric technique is also used to estimate fecundity for longspine thornyhead and shortspine thornyhead from samples off the West Coast of the United States. In addition, we examine the hypothesis that thornyheads are batch spawners, and that fecundity consequently declines over the course of the spawning season (Wakefield, 1990).

Materials and methods

Ovaries were collected from a large geographic area in Alaska, including the Gulf of Alaska, the Aleutian Islands, and the Bering Sea. National Marine Fisheries Service (NMFS) observers aboard commercial fishing vessels collected ovaries from April through June 2000. Length and somatic weight (ovaries and stomach contents removed) (±5 g) were recorded at sea. Ovaries were excised and placed in 10% formalin solution buffered with sodium bicarbonate.

Ovaries from shortspine thornyhead and longspine thornyhead were also collected during the 1999 NMFS West Coast trawl survey. Samples were collected between Northern California and Washington (34°57′N lat. 121°33′W long. to 48°04′ lat. 125°58′W long.). Length and somatic weight (±2 g) were recorded at sea.

Additional West Coast longspine and shortspine thornyhead ovaries were collected from commercial fishing vessels by the Oregon Department of Fish and Wildlife in Astoria. Ovaries were collected off Oregon and Washington from February through May 2000, during December 2000, and during January 2001. After shipment to the NMFS Alaska Fisheries Science Center in Seattle, length, somatic weight (±2 g), and ovary weight (±0.001 g) were recorded. Ovaries were excised and placed in 10% formalin buffered with sodium bicarbonate.

A cross section was removed from one ovarian lobe (middle or middle posterior region) for histological processing. When a whole cross section was too large to fit on a microscope slide, a wedge was cut from the cross section that included both the ovarian wall and the center of the ovary. Samples were processed through a dehydration series, embedded in paraffin, and sectioned at 4 µm. Slides were stained with hematoxylin and eosin.

Gravimetric fecundity estimation

Histological ovary sections were examined at 100× magnification to select samples for the gravimetric method. Oocytes were identified to one of eight developmental stages as described by Pearson and Gunderson (2003). To differentiate between oocytes to be spawned in the current year and reserve oocytes for future years, only ovaries with all maturing oocytes in stage-5 (late vitellogenesis) and beyond were used. By definition, yolk fills more than 50% of the cytoplasm within stage-5 oocytes, and the dark yolk made it easy to distinguish these oocytes. Stage-4 oocytes would also be spawned in the current year but overlapped significantly in size with nonmature stage-3 oocytes, and early stage-4 oocytes did not always have enough yolk (0–50%) to differentiate them from stage-3 oocytes with the gravimetric method. Specimens containing any stage-4 oocytes were omitted as a result. Ovaries with stage-8 oocytes were also omitted because the increased amount of gelatinous material which surrounds the oocytes in *Sebastolobus* could not be contained within the ovaries during subsampling.

Ovaries were weighed (±0.001 g) after they had been stored in formalin. Subsamples were cut from the ovaries and weighed (±0.001 g). For smaller ovaries, an entire cross section was taken. For larger ovaries, a pie-piece–shaped wedge was cut from the cross section to ensure a representative sample of outer ovarian wall. When cut correctly, a wedge starting at the center of the cross section would have the same weight ratio of ovarian wall to wedge subsample as the original cross section. Subsamples usually contained approximately 1000 oocytes (mean=1133), but this number varied according to stage of development and the amount of gelatinous material in the ovary (range: 108–3711).

Gelatinous material could not be subsampled by cutting at room temperature; therefore ovaries were briefly frozen before subsampling. This procedure enabled the gelatinous material to be cut, and also made it easier to obtain a representative sample of the ovarian wall. Initially, parts of three ovaries were frozen, and no effects of the freezing were detected with a light microscope. Only samples for gravimetric fecundity estimates were briefly frozen.

No difference in oocyte density was found among the different regions of the ovaries (see "Results" section); however, gravimetric subsamples were still taken randomly along the length of the ovaries to minimize potential bias from any location.

The oocytes in the subsamples were counted under a stereomicroscope, and fecundity was estimated by

$$Fec = \frac{W}{w} N,$$

where Fec = estimated fecundity;
W = total ovary weight;
w = subsample weight; and
n = number of oocytes in the subsample.

Stereological fecundity estimation

The majority of oocytes within an ovary were found to be at the same developmental stage; however development was not completely synchronous. Some ovaries containing stage-5 and -6 oocytes (late vitellogenesis to migratory nucleus) also contained a few stage-4 oocytes, which although unsuitable for fecundity estimation with the gravimetric method, could be used with the stereological method described by Emerson et al. (1990). Fecundity was estimated from ten of these samples by using the stereological method to complete the shortspine thornyhead collection from Alaska.

Fecundity was estimated per unit of volume and then multiplied by the volume of both ovaries. The formula used to estimate fecundity per unit of volume is

$$N_v = \frac{k}{\beta} \frac{N_a^{3/2}}{V_i^{3/2}},$$

where N_v = the number of oocytes per unit of volume;
k = an oocyte size correction coefficient;
β = an oocyte shape correction coefficient;
N_a = the average number of vitellogenic oocytes per unit of area; and
V_i = the average fractional volume of vitellogenic oocytes per unit of area.

The method for estimating the parameter k is given in Emerson et al. (1990) and the parameter k was estimated for six shortspine thornyhead samples. The resulting k values had a small range (1.0088–1.022), and a small standard deviation (0.0066), and a mean k value of 1.017 was used for all samples as a result. β was calculated by using the method given in Weibel and Gomez (1962). The β parameter was calculated from one shortspine thornyhead sample (53 oocytes) to be 1.565.

Exact volume of sample ovaries was impossible to determine because portions of the ovaries had already been removed for histological study (Pearson and Gunderson, 2003). Volume was estimated by dividing whole ovary weight by an average density of 1.052 g/mL. This was the average density from six samples (SD=0.0297) estimated by water displacement in a graduated cylinder.

Values for N_a and V_i were estimated by using a simplified Weibel grid for particulate structures (Weibel et al., 1966) instead of a Weibel multipurpose grid. A square containing 13 rows of 13 points was created and printed out on a clear acetate sheet. This overlay was taped to the front of a monitor. A video camera mounted to a stereomicroscope sent the image of the histology section to the computer monitor. The number of vitellogenic oocytes per grid and the number of points falling on vitellogenic oocytes were recorded and used to estimate N_a and V_i, respectively. The Weibel grid was used at 25× magnification, and 50× magnification was used to help distinguish borderline vitellogenic oocytes.

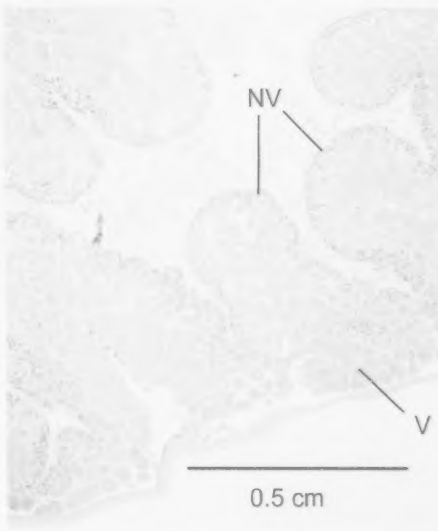

Figure 1
Partial cross section of shortspine thornyhead rockfish (*Sebastolobus alascanus*) ovary showing bands of vitellogenic (V) and nonvitellogenic (NV) oocytes.

A sampling grid was placed under the ovary histological section. The corner of the Weibel grid was aligned with corners of the sampling grid in order to systematically sample the ovary cross section. Two histological sections were sampled per ovary.

The number of Weibel grid counts per ovary depended on the size of the ovary cross section. An average of 55.9 (range: 29–103) Weibel grid counts were taken per ovary. This number was greater than the average number of Weibel grid counts used by Emerson et al. (1990), but the extra counts were made because shortspine thornyhead vitellogenic oocytes develop on peduncles (Erickson and Pikitch, 1993; Pearson and Gunderson 2003) and are distributed in a band around the central part of the ovary (Fig. 1). Because the vitellogenic oocytes are not uniformly distributed, the Weibel grid was applied systematically at more points across the entire ovary, and the counts were averaged. Because the whole cross section could not be systematically sampled and averaged, cross sections of larger fish were not used for stereological estimates.

Statistical methods

Length-fecundity relationships were estimated by using the following equation:

$$Fec = al^b,$$

Table 1

Fecundity estimates (number of oocytes) by ovary location and method.

	Stereological method				Gravimetric method			
	Sample location in ovary				Sample location in ovary			
Species	Mid	Posterior	Anterior	CV	Mid	Posterior	Anterior	CV
Shortspine	122,180	87,504	111,758	0.166	131,934	110,456	111,425	0.103
Shortspine	313,131	257,378	304,348	0.103	269,453	230,992	257,427	0.078
Shortspine	184,802	199,572	203,014	0.049				
Shortspine	474,432		458,877	0.024				
Longspine	38,061	26,179	28,424	0.204	38,968	33,207	33,653	0.091
Longspine	36,152	23,127	19,411	0.335				
			Mean CV	0.147			Mean CV	0.091

where Fec = estimated fecundity;
l = fork length; and
parameters a and b were estimated by nonlinear regression with SPSS software (version 11.0, SPSS Inc., Chicago, IL).

Weight-fecundity relationships were estimated by using the following equation

$$Fec = m(Wt_{somatic}) + b1,$$

where Fec = estimated fecundity;
$Wt_{somatic}$ = somatic weight; and
m and $b1$ were estimated by using linear regression in EXCEL (Microsoft, Redmond, WA).

Reduction in variance F tests (Quinn and Deriso, 1999) were used to compare fecundity relationships between areas, studies, and before and during spawning season.

Results

Ovary location differences

We tested for difference in oocyte density between middle, posterior, and anterior sections of six ovary pairs with the stereological method (ovaries from the migratory nucleus to late hydration phase) and did not find a significant difference in ovary location (two-way ANOVA, P=0.148) (Table 1).

Stereological method versus gravimetric method

The gravimetric method and the stereological method provided similar results. For shortspine thornyhead, the average ratio of gravimetric to stereological estimates for ten pairs of data was 0.993 (Table 2), and a plot of the gravimetric versus stereological estimates showed that they follow a 1:1 trend line (Fig. 2). The gravimetric method gave a somewhat lower coefficient of variation than the stereological method, based on multiple samples of the same ovaries (Table 1). An F test (Quinn and Deriso, 1999) did not show a significant difference (P=0.84) between the gravimetric (n=16) and stereological (n=10) methods in the length-fecundity relationships obtained for Alaskan shortspine thornyhead, and the data were therefore combined (Fig. 3).

Shortspine thornyhead

Shortspine thornyheads from Alaska (n=26) and the West Coast (n=30) had similar fecundity at length (Fig. 3). An F test did not indicate fecundity at length for the two areas was significantly different (P=0.53); therefore the data were combined to obtain the relationships (Figs. 3 and 4):

$$Fec = 0.0544\left(Fork\,Length(cm)\right)^{3.978} \quad (r^2=0.792,\ n=56)$$

$$Fec = 0.223\left(Wt_{somatic}(g)\right) - 63.079 \quad (r^2=0.781,\ n=53).$$

A majority of the shortspine thornyhead fecundity at length data points obtained in this study fell below the regression line reported by Miller (1985) (Fig. 3). The raw data from Miller (1985) were not published; therefore no statistical test was possible.

The data were also separated into months preceding the start of spawning and those after the start of spawning (Pearson and Gunderson, 2003) to look for evidence of batch spawning. Shortspine collected between October and November were grouped as specimens before the start of spawning. Shortspine collected from April through June in Alaska and from March through May off the West Coast were grouped as specimens after the start of spawning. Fish collected after spawning had begun (n=41) did not show a significant

Table 2

Paired fecundity estimates (number of oocytes) by method and by section of the ovary (middle, posterior, anterior) where oocyte samples were taken.

Specimen	Position in the ovary	Gravimetric	Stereological	Ratio of gravimetric to stereological
Shortspine 1	Middle	150,448	184,853	0.814
Shortspine 2	Middle	195,356	187,037	1.044
Shortspine 3	Middle	427,717	307,771	1.390
Shortspine 4	Middle	414,594	561,258	0.739
Shortspine 5	Middle	131,934	122,180	1.080
	Posterior	110,456	87,504	1.262
	Anterior	111,425	111,758	0.997
Shortspine 6	Middle	269,453	313,131	0.861
	Posterior	230,992	257,378	0.897
	Anterior	257,427	304,348	0.846
			Mean ratio	0.993

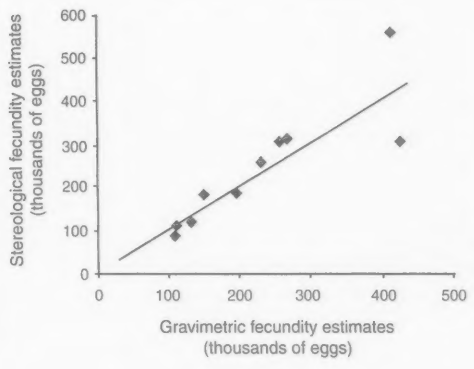

Figure 2

Plot of gravimetric versus stereological fecundity estimates for ten shortspine thornyhead rockfish (*Sebastolobus alascanus*) data pairs. Line = 1:1 ratio.

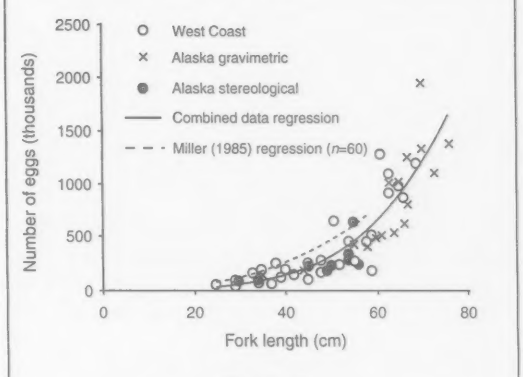

Figure 3

Shortspine thornyhead (*Sebastolobus alascanus*) fecundity-at-length estimates by location and method, and regression of combined data (our study) and by regression of data from Miller's study (1985).

decrease in fecundity at length when compared to fish collected before spawning had begun (n=11) (F test, P=0.71) (Fig. 5).

Longspine thornyhead

Longspine thornyhead fecundity data conformed more closely to a linear regression on somatic weight (Fig. 6):

$$Fec = 183.81\left(Wt_{somatic}(g)\right) - 4617 \qquad (r^2=0.536,\ n=29)$$

than to a nonlinear regression on length (Fig. 7):

$$Fec = 0.8890\left(Fork\ Length(cm)\right)^{3.249} \qquad (r^2=0.442,\ n=29).$$

A majority of the predicted fecundity values at somatic weight were higher than those derived from Wakefield's (1990) regression line on somatic weight (Fig. 6), but Wakefield's (1990) raw data were not published.

Wakefield (1990) estimated spawning to begin in February and created separate fecundity-at-weight relationships for fish collected in October–November and in February–March). He noted a decline in fecundity as the spawning season progressed but did not test this fecundity difference for statistical significance. Similar groupings (October–December, n=17; and February–March, n=11) in our study did show a statistically significant difference in fecundity as the spawning season progressed (F test, P=0.004) (Fig. 7); however, the

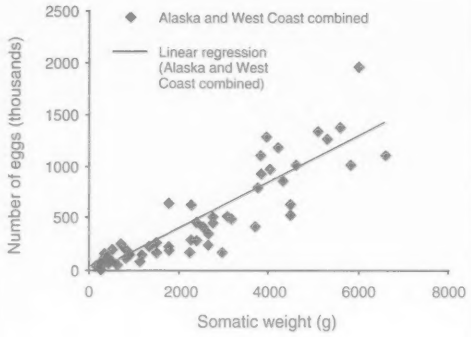

Figure 4

Fecundity at somatic weight for combined Alaska and West Coast shortspine thornyhead rockfish (*Sebastolobus alascanus*).

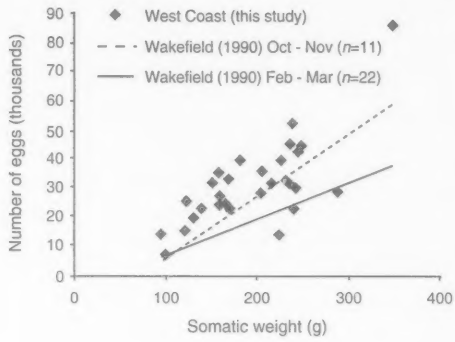

Figure 6

West Coast longspine thornyhead rockfish (*Sebastolobus altivelis*) fecundity data at somatic weight (our study), compared to fecundity data of Wakefield (1990).

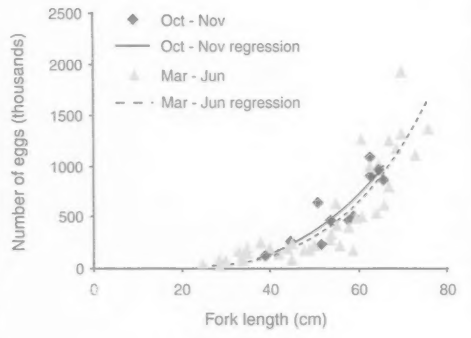

Figure 5

Shortspine thornyhead rockfish (*Sebastolobus alascanus*) fecundity at length separated by October–November and March–June collection dates.

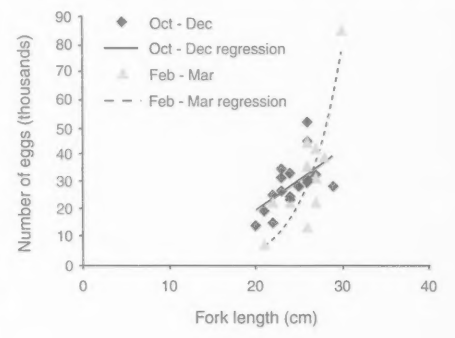

Figure 7

Longspine thornyhead rockfish (*Sebastolobus altivelis*) fecundity at length separated by October–December and February–March collection dates.

regression lines intersected, and the February–March group was not lower than the October–December group. The February–March group did have lower fecundity than the October–December group for lengths smaller than 27 cm; however the sample size was very small. No significant difference existed between the two groups when the single, large fecundity observation late in the spawning season was ignored (P=0.34).

Discussion

Emerson et al. (1990) cited the ability to distinguish borderline vitellogenic oocytes from nonvitellogenic oocytes as an advantage of the stereological method, and this was a clear benefit in our study. The stereological method allowed us to differentiate between vitellogenic and nonvitellogenic oocytes at an earlier stage of ovary development than was possible with the gravimetric method. However, the use of ovaries in earlier stages of development increases the potential magnitude of fecundity overestimates due to atresia. Atresia, or the resorption of oocytes, is a potential source of error for fecundity estimates (Hunter et al., 1992). Although atretic oocytes can be identified with the stereological method, oocytes that are destined for atresia will be counted, causing fecundity to be overestimated. The amount of atresia will determine the magnitude of this overestimate. Samples

collected at later ovarian development stages would avoid this potential error (Tuene et al., 2002).

Because of a nonrandom distribution of vitellogenic and nonvitellogenic oocytes in the ovary, it was necessary to average Weibel grid counts over an entire ovary cross section. Larger ovaries that did not fit on a single slide could not be used, so that fecundity of larger fish had to be determined with the gravimetric method. This was a major limitation because few fish greater than 60 cm had ovaries small enough to be suitable for the stereological method. This limitation, however, might not apply to fish species with vitellogenic oocytes randomly distributed throughout the ovary.

The number of Weibel grid counts required was larger in our study than in Emerson et al. (1990), and the extra counts increased the amount of time involved with computation of fecundity estimates. In addition to the time required to prepare histological sections, the time to obtain stereological estimates took approximately twice as long as those obtained with the gravimetric method. Our estimates of shortspine thornyhead fecundity at length (Fig. 3) appeared lower than the regression published by Miller (1985), but our longspine thornyhead fecundity estimates were higher than those published by Wakefield (1990) (Fig. 6). Several potential explanations exist for the differences. Temporal or geographic differences in fecundity could exist. Samples from different decades were used in the two studies, and Wakefield (1990) used longspine samples taken from off Point Sur, California, whereas we used samples collected off Oregon and Washington. However, the differences may also be explained by methodological differences between authors, including different criteria to include oocytes in fecundity estimates, and differences in the ovarian development of samples. Relatively small sample sizes from our study and from Wakefield (1990) may add uncertainty to these fecundity estimates. The length range of samples could also affect comparisons for shortspine thornyhead fecundity. The fecundity estimates from Miller (1985) did not include any fish greater than 60 cm, whereas we used fish approaching 80 cm.

Wakefield (1990) grouped fecundity data by date, that is to say before the start of spawning and after the start of spawning. His data indicated a decline in fecundity after spawning begins, which he attributed to batch spawning. Similar temporal groupings in our study did not necessarily show a decrease in fecundity that was indicative of batch spawning in longspine or shortspine thornyhead. An important caveat regarding these comparisons is that the combination of small sample sizes and high variability in fecundity at length would cause only large differences in fecundity to be detected. However, the sample sizes used for comparison before and during spawning season (shortspine thornyhead n=11, 41) (longspine thornyhead n=17,11) were close to the sample sizes Wakefield (1990) used as evidence for batch spawning (n=11,22). Larger sample sizes for both species would help answer the question of whether these are batch-spawning species. Pearson and Gunderson (2003) did not find any hydrated oocytes or postovulatory follicles co-occurring with vitellogenic oocytes in histological sections of either species used in our study. They concluded that batch spawning does not occur from off Northern California to Alaska for shortspine thornyhead, and from off Northern California to Washington for longspine thornyhead, and the results of the present study support this conclusion.

Ovaries are often opportunistically collected during commercial fishing seasons or scheduled fisheries surveys and may not provide oocyte samples from the optimum time of year for estimating fecundity with gravimetric techniques. Nevertheless, the stereological technique enabled us to make fecundity estimates for a greater number of the available samples. The technique could be used in similar instances where the logistics of sampling require collections to be made earlier than the optimal date for gravimetric estimates.

Acknowledgments

Dave Douglas of the Oregon Department of Fish and Wildlife collected many samples, as did numerous NMFS RACE and REFM division scientists and the following NMFS observers: C. Colway, A. Hayward, W. Mitchell, E. White, N. Spang, K. Redslob, M. Waters, and D. Tran. We thank Frank Morado, Lisa Appesland, and Dan Nichol of the NMFS Alaska Fisheries Science Center (AFSC) for use of equipment and equipment instruction. We also thank Marcus Duke of the UW SAFS for creating a Weibel grid. Jim Ianelli and Rebecca Reuter of the NMFS Alaska Fisheries Science Center provided quantitative assistance. Cathy Schwartz of the UW SAFS assisted with the figures and tables. We thank two anonymous reviewers for providing useful comments. This research was supported by the Joint Institute for the Study of the Atmosphere and Ocean (JISAO) under NOAA cooperative agreement no. NA17RJ1232.

Literature cited

Best, E. A.
1964. Spawning of longspine channel rockfish, *Sebastolobus altivelis* Gilbert. Calif. Fish Game 50:265–267.

Emerson L. S., M. G. Walker, and P. R. Witthames.
1990. A stereological method for estimating fish fecundity. J. Fish Biol. 36:721–730.

Erickson, D. L., and E. K. Pikitch.
1993. A histological description of shortspine thornyhead, *Sebastolobus alascanus*, ovaries: structures associated with the production of gelatinous egg masses. Environ. Biol. Fishes 36:273–282.

Gaichas, S., and J. N. Ianelli.
2003. Assessment of thornyheads (*Sebastolobus* spp.) in the Gulf of Alaska. *In* Stock assessment and fishery evaluation report for the groundfish resources of the Gulf of Alaska, p. 659–698. North Pacific Fishery Management Council, Anchorage, AK.

Hoff, G. R., and L. L. Britt.
2003. The 2002 eastern Bering Sea upper continental slope

survey of groundfish and invertebrate resources. NOAA Tech. Memo. NMFS-AFSC-141, 261 p.

Hunter, J. R., B. J. Macewicz, N. C. Lo, and C. A. Kimbrell.
1992. Fecundity, spawning, and maturity of female Dover sole, *Microstomus pacificus*, with an evaluation of assumptions and precision. Fish. Bull. 90:101–128.

Macer, C. T.
1974. The reproductive biology of the horse mackerel *Trachurus trachurus* (L.) in the North Sea and English Channel. J. Fish Biol. 6:415–438.

Miller, P. P.
1985. Life history study of the shortspine thornyhead, *Sebastolobus alascanus*, at Cape Ommaney, southeastern Alaska. M.S. thesis, 76 p. Univ. of Alaska, Juneau, AK.

Orr, J. W., M. A. Brown, and D. C. Baker.
2000. Guide to rockfishes (Scorpaenidae) of the genera *Sebastes*, *Sebastolobus*, and *Adelosebastes* of the Northeast Pacific Ocean, 2nd ed. NOAA Tech. Memo. NMFS-AFSC-117, 48 p.

Pearcy, W. G.
1962. Egg masses and early developmental stages of the scorpaenid fish, *Sebastolobus*. J. Fish. Res. Board Can. 19:1169–1173.

Pearson, K. E., and D. R. Gunderson.
2003. Reproductive biology and ecology of shortspine thornyhead rockfish, *Sebastolobus alascanus*, and longspine thornyhead rockfish, *S. altivelis*, from the northeastern Pacific Ocean. Environ. Biol. Fishes 67:11–136.

Piner, K., and R. Methot.
2001. Stock assessment and fishery evaluation report of shortspine thornyhead off the Pacific West Coast of the United States 2001. *In* Status of the Pacific coast groundfish fishery through 2001 and acceptable biological catches for 2002. Pacific Fishery Management Council. Portland, OR.

Quinn, T. J., and R. B. Deriso.
1999. Quantitative fish dynamics, 542 p. Oxford Univ. Press, New York, NY.

Tuene. S., A. C. Gundersen, W. Emblem, I. Fossen, J. Boje, P. Steingrund, and L. H. Ofstad.
2002. Maturation and occurrence of atresia in oocytes of Greenland halibut (*Reinhardtius hippoglossoides* W.) in the waters of East Greenland, Faroe Islands and Hatton Bank. *In* Reproduction of West-Nordic Greenland halibut: studies reflecting on maturity, fecundity, spawning, and TEP (A. C. Gundersen, ed.), p. 39–69. TemaNord 2002:519.

Wakefield, W. W.
1990. Patterns in the distribution of demersal fishes on the upper continental slope off central California with studies on the role of ontogenetic vertical migration in particle flux. Ph.D. diss., 281 p. Univ. California, San Diego, CA.

Wakefield, W. W., and K. L. Smith Jr.
1990. Ontogenetic vertical migration in *Sebastolobus altivelis* as a mechanism for transport of particulate organic matter at continental slope depths. Limnol. Oceanogr. 35:1314–1328.

Weibel, E. R., and D. M. Gomez.
1962. A principle for counting tissue structures on random sections. J. Appl. Physiol. 17:343–348.

Weibel, E. R., G. S. Kistler, and W. Scherle.
1966. Practical stereological methods for morphometric cytology. J. Cell Biol. 30:22–38.

Relative pleopod length as an indicator of size at sexual maturity in slipper (*Scyllarides squammosus*) and spiny Hawaiian (*Panulirus marginatus*) lobsters

Edward E. DeMartini
Marti L. McCracken
Robert B. Moffitt
Jerry A. Wetherall

Pacific Islands Fisheries Science Center
National Marine Fisheries Service, NOAA
2570 Dole Street
Honolulu, Hawaii 96822-2396

E-mail address (for E. E. DeMartini): edward.demartini@nooa.gov

Abstract — Body size at gonadal maturity is described for females of the slipper lobster *(Scyllarides squammosus)* (Scyllaridae) and the endemic Hawaiian spiny lobster *(Panulirus marginatus)* (Palinuridae) based on microscopic examination of histological preparations of ovaries. These data are used to validate several morphological metrics (relative exopodite length, ovigerous condition) of functional sexual maturity. Relative exopodite length ("pleopod length") produced consistent estimates of size at maturity when evaluated with a newly derived statistical application for estimating size at the morphometric maturation point (MMP) for the population, identified as the midpoint of a sigmoid function spanning the estimated boundaries of overlap between the largest immature and smallest adult animals. Estimates of the MMP were related to matched (same-year) characterizations of sexual maturity based on ovigerous condition — a more conventional measure of functional maturity previously used to characterize maturity for the two lobster species. Both measures of functional maturity were similar for the respective species and were within 5% and 2% of one another for slipper and spiny lobster, respectively. The precision observed for two shipboard collection series of pleopod-length data indicated that the method is reliable and not dependent on specialized expertise. Precision of maturity estimates for *S. squammosus* with the pleopod-length metric was similar to that for *P. marginatus* with any of the other measures (including conventional evidence of ovigerous condition) and greatly exceeded the precision of estimates for *S. squammosus* based on ovigerous condition alone. The two measures of functional maturity averaged within 8% of the estimated size at gonadal maturity for the respective species. Appendage-to-body size proportions, such as the pleopod length metric, hold great promise, particularly for species of slipper lobsters like *S. squammosus* for which there exist no other reliable conventional morphological measures of sexual maturity. Morphometric proportions also should be included among the factors evaluated when assessing size at sexual maturity in spiny lobster stocks; previously, these proportions have been obtained routinely only for brachyuran crabs within the Crustacea.

Manuscript submitted 2 September 2003 to the Scientific Editor's Office.

Manuscript approved for publication 26 August 2004 by the Scientific Editor.

Fish. Bull. 103:23–33 (2005).

Estimates of body size and age at sexual maturity provide key information for stock assessments and hence for managing sustainable fisheries. Characterizations of size at maturity are relatively straightforward in lobsters and most other crustaceans. One presently accepted standard is to regress percentage mature against classes of some body size metric and to fit a logistic model to predict the size class in which 50% of the population is mature. A necessary prerequisite is accurate data on the maturation state of individuals. In spiny lobsters of the family Palinuridae, female maturation is usually deduced from "berried" (ovigerous) condition (Groeneveld and Melville-Smith, 1994), the presence of external morphological indicators such as changes in the number of pleopod setae (Gregory and Labisky, 1981; Montgomery, 1992), relative lengths of abdominal and thoracic segments (Jayakody, 1989), or proportional lengths of segments of walking or egg-bearing appendages at the pubertal molt (George and Morgan, 1979; Grey, 1979; Juinio, 1987; Plaut, 1993; Evans et al., 1995; Hogarth and Barratt, 1996; Minagawa and Higuchi, 1997). A major complication arises, however, when the percentage mature within size classes cannot be accurately described. Such is the case for *Scyllarides squammosus*, a species of slipper lobster (family Scyllaridae) that prior to closure of the fishery in 2000 had become an increasingly important target of the Northwestern Hawaiian Island (NWHI) commercial trap fishery. In *S. squammosus*, unberried but mature females are indistinguishable, based on gross external morphology, from immature females. In this species, the additional variance introduced by combining falsely classified "immature" with truly immature females inflates requisite sample sizes enough (given the sampling effort feasible on annual research surveys) to prevent characterization of possible changes in size at maturity with data pooled from less than several surveys. Combining unberried adults with true immature individuals also introduces an overestimation bias (DeMartini et al., 2003).

To date only one study has provided a description of the use of a morphological measure of maturity in a slipper lobster (Hossain, 1978). Morphology-based maturity measures have been described for numerous spiny lobsters of the genus *Panulirus*, but such measures for the endemic Hawaiian spiny lobster (*Panulirus marginatus*) have not been fully described (Prescott, 1984).

Our objectives are to describe the development and use of an external body metric for accurately and precisely characterizing body size at morphological (functional) sexual maturity in female *Scyllarides squammosus*. We likewise use this external metric

to estimate size at maturity of females of the Hawaiian spiny lobster, for which functional maturity can be accurately described by using a combination of other, more apparent external features. We also estimate body size at gonadal maturity by microscopic examination of histological preparations of ovaries of each species and use these results to validate the functional maturity characterizations. We contrast the benefits of the different approaches for estimating functional maturity in these two lobsters and discuss the potential importance of applying efficient measures of maturation for managing the NWHI lobster fishery.

Materials and methods

Specimen collection

A research vessel was used to set and retrieve lobster traps. All specimens of spiny lobster used in this study were taken from Necker Bank surrounding Necker Island (23°34′N, 164°42′W), NWHI. All the slipper lobsters used were taken from Maro Bank, located about 600 km to the northwest of Necker at 25°25′N, 170°35′W. Lobsters were caught from bank terraces at median depths of 15 fm (slipper lobsters, Maro) and 17 fm (spiny lobsters, Necker) with molded plastic (Fathoms Plus®, San Diego, CA) traps baited with 1 kg of mackerel (*Scomber japonicus*) and left for a standard (overnight) soak.

Shipboard processing

All specimens were processed alive within minutes of trap retrieval. Tail width (TW), as defined for slipper lobster by DeMartini and Williams (2001) and for Hawaiian spiny lobster by DeMartini et al. (2003), was measured with 0.1 mm accuracy. Berried females were scored by egg-development stage with a gross visual proxy (brooded eggs noted as either orange or brown in color to the unaided eye). Female spiny lobsters were scored by the presence or absence and by condition ("smooth"=unused, "rough"=partly used) of spermatophoric (sperm) mass (Matthews, 1951; Berry and Heydorn, 1970) on the sternum. Female *S. squammosus* in almost all cases lack a sperm mass and the presence-absence of this feature provides no useful information. In 1998–2000, ovaries were dissected from a maximum of two living specimens for each 1-mm TW class of the two species and fixed in 10% (sea water buffered) formalin for subsequent histological analyses. Egg-bearing "tails" (abdominal segments) were flash-frozen at −20°C.

During 1997–99, pleopods of each species were measured aboard ship to evaluate measurement accuracy under field conditions. Maxima of 10 live individuals per 1-mm TW class of each species were measured as described below. Two independent measurements of each specimen were made by each of two measurers (one inexperienced and one experienced). In 2000–01, pleopods for a larger series of morphometrics were similarly measured aboard ship to evaluate production-scale numbers (500–1000 specimens per species on each cruise) based on a single measurement per specimen taken by one measurer.

Laboratory measurements

Beginning with specimens collected in 2000, the lengths of exopodites on first pleopods were measured for a representative sample of berried and unberried tails of each species, after the tails were thawed overnight in a refrigerator at 3°C. Preliminary observations indicated that the first pleopod was disproportionately large in berried females; measurements of the first pleopod of all (berried and unberried) females moreover were the most precise, i.e. the measurements were more likely to be obtained again—probably because the first pleopod was the easiest to measure. The straightline distance between base and tip of exopodite on the first pleopod (exopodite length=EL) was measured with dial calipers to 0.01 mm. An analogous measurement of exopodite width (EW) was taken perpendicular to the EL axis at the structure's widest point. The left exopodite in ventral aspect (Fig. 1) was routinely measured because the ventral aspect was easier to measure for live animals aboard ship. Measurements of the right exopodite (of the same specimen) in dorsal aspect were taken for a range of body sizes to evaluate the possible influence of aspect (dorsal vs. ventral) or body side (left vs. right) on the measurement that was taken. Replicate measurements (independent, with calipers reset to zero between measurements) were used to assess inter-measurer and inherent measurement error. Formalized ovaries were weighed (blotted damp-dry) to the nearest 0.01 g after fixation for at least a month.

Histological validation

Fixed ovary specimens of each species were dehydrated, imbedded, and sectioned by using standard techniques, and were stained with hematoxylin and counter-stained with eosin to differentiate protein and yolk materials within oocytes. Histological slides were viewed under a compound microscope at 150× magnification. For each specimen, the diameters (average of major and minor axis) were measured for 10 oocytes (randomly chosen) within the largest size class of oocytes present. The median diameter was used to characterize oocyte size for that specimen; the median diameter based on 10 measurements yielded CVs (100% × standard error/mean) <10% (DeMartini et al., 2003). Developmental staging followed Minagawa (1997) and Minagawa and Sano (1997): females were scored as mature 1) if unberried in developing or ripe ovarian stages II and III, respectively; 2) if berried in ripe and redeveloping stages IV and V, respectively; or 3) if recently spent (stage VI) with heavily setose pleopods (*P. marginatus* only). Inactive females in stage I were scored as immature. A gonad index, calculated as $GI = (OW \times 10^5 / TW^3)$, where OW = ovary weight in g, was used to complement his-

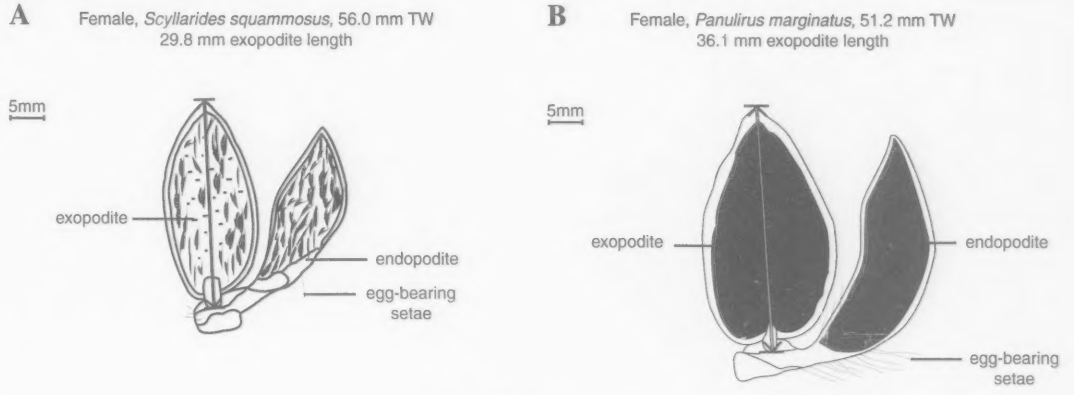

Figure 1

Schematic diagram of the left first exopodite (ventral aspect) of (**A**) slipper lobster (*Scyllarides squammosus*) and (**B**) the Hawaiian spiny lobster (*Panulirus marginatus*), showing axis of measurement. TW = tail width.

tological scores in assessing gonadal maturity (Minagawa and Sano, 1997). Gonadal maturity was used as a means of validating, as well as referencing, estimates of size at functional maturity (Ennis, 1984).

Statistical analyses

Data for EL and EW (as response variables) and TW (regressor) for the same specimen were first plotted for all specimens of each species. Preliminary evaluations of these data (both raw and log-transformed) with least-squares linear regression (REG procedure; SAS vers. 8, SAS Institute, Inc., Cary, NC) indicated allometric relationships for which double-log functions provided approximate fits. Identification of join points by iteration based on minimizing the total residual sums of squares of pairs of joined regression equations (Somerton, 1980), however, resulted in linear spline fits that, although significant, had obviously nonrandom residuals. Simple linear fits with log-log plots, however, were useful for selecting the most appropriate metric: the regressions of EW on TW, qualitatively similar to those for EL regressed on TW, had consistently lower r^2 values, likely because pleopod width was more difficult to measure than pleopod length. The EL metric was therefore chosen for all further analyses.

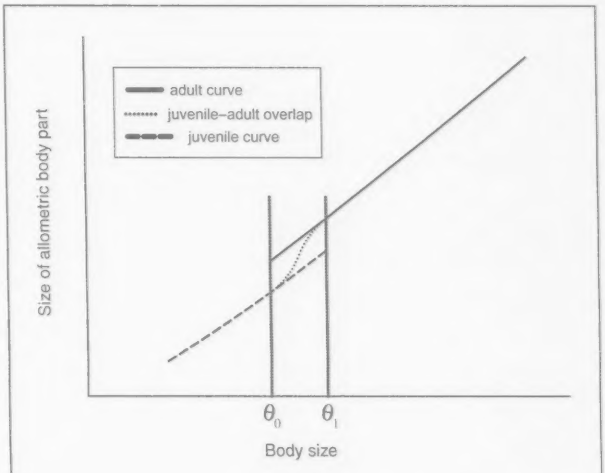

Figure 2

Conceptual model of the relationships between size of an allometric body part and body size in a population of organisms in which large immature individuals overlap in body size with small adults. Size overlap of immature individuals and adults is indicated by the distance between θ_0 and θ_1.

Because lobsters, like most biological populations, are composed of individuals that differ in the size at which first maturity occurs, we fitted a curve to the EL-TW relation that included a sigmoid segment bridging the region between the estimated sizes of the smallest adults (θ_0) and the largest immature individuals (θ_1) (Fig. 2). The curve was fitted by using iterative reweighted least squares (S-Plus 6 for Windows, Insightful Corporation, Seattle, WA; Ratkowsky, 1983) with appropriate weights to standardize the variance (Appendix). The morphometric maturation point, hereafter referred to as the MMP, was estimated at the inflection ($[\theta_0+\theta_1]/2$) of the sigmoid segment of the curve. This inflexion point represents the body size at which we expect 50% of the lobsters to become sexually mature (median size at attainment of

maturity). Confidence bounds on the MMP were estimated by using the studentized bootstrap method (Davison and Hinkley, 1997) with 1000 iterations.

In order to characterize median body size at gonadal maturity, the percentage mature per 5-mm TW class, deduced from viewing histological preparations of ovaries, was fitted to the conventional (2-parameter) logistic model,

$$P_x = 100 / \{1 + \exp[-a(TW - b)]\},$$

where P_x = percent mature at TW = x;
a and b are unknown constants; and
TW = tail width in mm.

To similarly estimate median size at maturity based on gross external characteristics, the percentage mature per 5-mm TW class was fitted to a 3-parameter logistic model for *Scyllarides squammosus* and to the conventional 2-parameter logistic for *Panulirus marginatus*. For *S. squammosus*, percentage maturity per 5-mm TW class was estimated by fitting the 3-parameter logistic equation,

$$P_x = 100a / \{1 + \exp[(4b / a)(c - TW)]\},$$

where a = the asymptotic proportion berried;
b = the slope of the logistic function at the inflection point; and
c = TW_{50} is the tail width at the inflection point (size at 50% of asymptote).

This function has been fully described for estimating percentage maturity based on incidence of ovigerous females in *S. squammosus*; the extra parameter is needed to fit an asymptote to the sigmoidal function at a value less than 100% (DeMartini et al., 2002). Parameters of the various models were estimated by using the maximum-likelihood nonlinear curve fitting procedure SAS NLIN; all nonlinear regressions were weighted by the square root of sample sizes.

The body size at which 50% of the population was estimated as mature (hereafter referred to as TW_{50}) was compared for 1) TW_{50} based on the relative incidence of berried individuals within the female population (both species), adjusted for the co-presence of a sperm mass (*P. marginatus* only), 2) TW_{50} estimated from histological evidence (both species), and 3) the MMP of the allometric EL-to-TW relation (both species). Estimates were compared graphically among methods for each species.

Analyses of pleopod-based maturity followed a series of evaluations of pleopod characteristics used to identify a standardized metric. Measurement aspect (dorsal, ventral) and side (right, left) were compared within individuals by using paired t-tests. A randomized complete block (RCB) ANOVA (SAS PROC ANOVA), with specimen as the blocking factor, was used to evaluate the effects of measurer and measurement venue (at sea versus ashore) on the mean measurement bias and precision (CVs) of pleopod measurements.

Results

Pleopod characteristics

Measurement error, and effect of side of lobster and aspect (ventral versus dorsal) on measurements Inherent measurement error averaged 0.23 mm and 0.16 mm (1.0% and 0.4%) for slipper and Hawaiian spiny lobster, respectively, based on two independent measurements by the same measurer. Exopodites of left-side pleopods averaged 3% and 2% shorter than exopodites of right-side pleopods for the two respective species (paired t-test; both $P<0.001$; Table 1). Exopodites of first left pleopods were 4% and 2% longer in ventral aspect for slipper and spiny lobster, respectively, (RCB ANOVA; both $P<0.001$; Table 1).

Measurement venue A matched (same-specimen) series of measurements made aboard ship versus in the laboratory (all by the same measurer) indicated a systematic difference in left pleopod length (ship > lab; RCB ANOVA; both $P=0.001$) for slipper lobster and spiny lobster (Table 1). For each species, however, the mean difference between venues was trivial (0.2–0.4 mm or 0.6–1.4%). Differences between ship and laboratory were detectable despite the consistently lower precision provided by shipboard measurements (shipboard CVs were 47% and 39% larger for slipper and spiny lobster, respectively; RCB ANOVA: both $P<0.001$; Table 1). Absolute differences between shipboard and lab CVs were small for the respective species (0.2% and 0.7%; Table 1).

Measurer effects An extensive series of shipboard intermeasurer comparisons between pleopod length measurements taken by one experienced (A) and a second inexperienced (B) measurer indicated trivial systematic differences between measurers (0.2%; RCB ANOVA; $P=0.25$). Precision also was unaffected by measurer ($P=0.31$; Table 1).

Standardized metric It follows from the above that the best measure available for use was the length (in ventral aspect) of the left first exopodite. This metric was used in all quantitative comparisons among maturity assessment methods and is recommended for future applications with these species.

Estimated sizes at functional maturity

Slipper lobster Pleopod-to-TW relations for *S. squammosus* did not differ meaningfully between 2000 and 2001 (ANCOVA; accept H_0: slopes equal, $P=0.11$; intercepts only 0.5% different) and both years' data were pooled for further analyses. The estimated MMP (95% CI) for the TW at which 50% of the female *S. squammosus* exhibit a disproportionately long first left exopodite was 47.6 mm (45.1–49.4 mm; Fig. 3). Estimated median body size at functional maturity based on presence or absence of berried eggs, using the same series of 2000–01 specimens, was 55.5 (52.7–58.3) mm TW (Fig. 4).

Table 1

Results of tests of potential effects of various criterion variables on the accuracy (bias of delta-bars) and precision (CVs of deltas) for measured lengths of first pleopod exopodites for slipper lobster (*Scyllarides squammosus*) and Hawaiian spiny lobster (*Panulirus marginatus*) caught from Necker Bank, Hawaii. Delta-bar = mean paired-difference; samples sizes are *n* paired observations.

Variable	Criterion	Test statistic	Delta-bar	*P*	*n*
Slipper lobster					
Body side (left vs. right)	accuracy	paired t=–4.0	0.9 mm	0.001	74
Measurement aspect (ventral vs. dorsal)	accuracy	RCB Anova			
		$F_{1, 62}$=202.7	0.9 mm	0.001	63
Measurement venue (shipboard vs. lab)	accuracy	RCB Anova			
		$F_{1, 62}$=23.6	0.4 mm	0.001	63
Measurement venue (shipboard vs. lab)	precision	RCB Anova			
		$F_{1, 62}$=21.6	0.7 %	0.001	63
Measurer (A vs. B)	accuracy	RCB Anova			
		$F_{1, 62}$=21.3	0.3 mm	0.001	63
Measurer (A vs. B)	precision	RCB Anova			
		$F_{1, 62}$=1.54	0.2 %	0.22	63
Spiny lobster					
Body side (left vs. right)	accuracy	paired t=–5.7	0.7 mm	0.001	135
Measurement aspect (ventral vs. dorsal)	accuracy	RCB Anova			
		$F_{1, 32}$=31.7	0.7 mm	0.001	33
Measurement venue (shipboard vs. lab)	accuracy	RCB Anova			
		$F_{1, 87}$=11.62	0.2 mm	0.001	88
Measurement venue (shipboard vs. lab)	precision	RCB Anova			
		$F_{1, 87}$=11.74	0.4 %	0.001	88
Measurer (A vs. B)	accuracy	RCB Anova			
		$F_{1, 87}$=1.37	<0.1 mm	0.25	88
Measurer (A vs. B)	precision	RCB Anova			
		$F_{1, 87}$=1.04	<0.2 %	0.31	88

Spiny lobster Year effects on pleopod-to-TW relations for *P. marginatus* were likewise insignificant (ANCOVA; accept H_0: slopes equal, P>0.67; intercepts only 0.2% different) and data for both years were pooled for further analyses. The MMP for the TW at which 50% of the *P. marginatus* females exhibit a disproportionately long pleopod was 36.4 mm (34.1–38.0 mm; Fig. 5). Figure 6 illustrates the corresponding estimate of median size at functional maturity, 35.4 (33.7–37.1) mm TW, based on the combined criteria of sperm mass and berried egg presence, for *P. marginatus*.

Estimated sizes at physiological maturity

Gonadal maturity determined from microscopic staging of histological ovary preparations indicated maturation stages ranging from oogonial to fully vitellogenic (Table 2; Minagawa and Sano, 1997) for the females of each species. For both species, gonad indices (GIs) and median oocyte diameters generally increased over the cycle of development even though berried specimens exhibited lower GIs and oocyte sizes than unberried adults of the respective species (Table 2). The ovaries of mature females contained a preponderance of fully yolked oocytes whose average minimum diameter (following dehydration and staining) was 0.24 mm and 0.30 mm for *S. squammosus* and *P. marginatus*, respectively. The maximum observed diameter of fully yolked oocytes was 0.60 mm (in *S. squammosus*) and 0.58 mm (*P. marginatus*).

The proportions of observed immature individuals ranged from 32% to 38% of total female specimens (depending on species) and were sufficient to construct logistic curves relating percentage gonadal maturity to body size for each species. Estimated median TWs at gonadal maturity were 51.1 (48.6–53.5) mm and 40.5 (37.9–43.1) mm TW for *S. squammosus* (Fig. 4) and *P. marginatus* (Fig. 6), respectively.

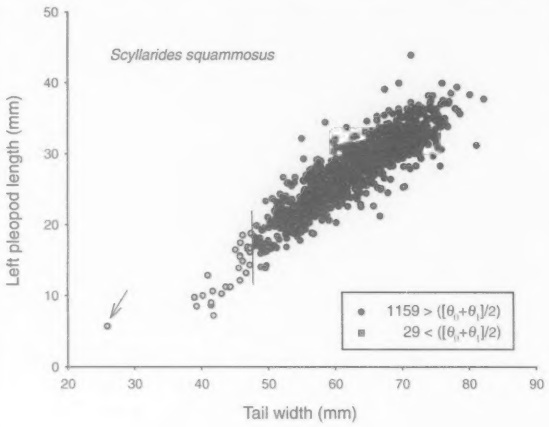

Figure 3

Scatterplots of the relation between exopodite length and tail width for slipper lobster (*Scyllarides squammosus*). The morphometric maturation point (MMP; indicated by the vertical line) represents the allometric threshold coincident with sexual maturity ($[\theta_0+\theta_1]/2$). The outlier indicated by an arrow was not used in estimating the MMP.

Table 2

Stages of ovarian development in 197 slipper lobster (*Scyllarides squammosus*) and 122 Hawaiian spiny lobster (*Panulirus marginatus*) caught from Necker Bank, Hawaii. There were no stage-VI *S. squammosus*.

Ovarian stage	Characteristics of ovaries and oocytes	Gonad index mean ±SD (range)	*n*	Most advanced oocyte substage (median diameter)
Slipper lobster	oogonia and previtellogenic oocytes conspicuous;	0.43 ±0.25	60	preyolk platelet
I (inactive)	ovary white	(0.02–1.08)		(0.18 mm)
II–III (developing and ripe)	unberried; developing moderately to fully vitellogenic oocytes; ovary pale orange to orange	1.63 ±1.45 (0.25–5.47)	75	prematuration or maturation (0.28 mm)
IV–V (ripe and redeveloping)	berried; developed fully yolked oocytes; ovary dark orange	1.12 ±0.66 (0.15–3.30)	62	maturation (0.26 mm)
Spiny lobster				
I (inactive)	oogonia and previtellogenic oocytes; ovary white	0.85 ±0.67 (0.16–2.59)	30	preyolk platelet (0.12)
II–III (developing and ripe)	unberried; developing moderately to fully vitellogenic oocytes; ovary pale orange to orange	14.03 ±4.46 (3.32–22.69)	42	prematuration or maturation (0.49)
IV–V (ripe and redeveloping)	berried; developed fully yolked oocytes; ovary dark orange	5.84 ±4.31 (0.56–17.06)	47	maturation (0.30)
VI (spent)	residual unspawned mature oocytes; ovulation traces	14.85 ±6.38 (7.5–18.9)	3	yolk platelet but atretic (0.48)

Discussion

Properties of the EL-TW model

In order to determine morphometric maturity, we first attempted to use a method developed by Watters and Hobday (1998). With this method splines were used to model the relationship between the morphometric character and body size; then the morphometric size at which the second derivative of the fitted curve is maximal is computed. At first this technique is alluring in that it makes no allometric or other assumption as to the shape of the relationship between the morphometric character and body size. It instead assumes that maturation corresponds to the maximum of the second derivative. This assumption is likely invalid even if we assume that the relationship between the morphometric character and body size changes abruptly at maturation for each individual (as at the pubertal molt in crustaceans) because individuals in the population mature at different sizes. When we applied the Watters and Hobday method, the resulting body size estimate appeared to characterize the minimum, not the median, size at attainment of sexual maturity in the population and was clearly inappropriate for our needs. Our method generated fitted splines that were comfortingly similar in shape to the parametric logistic (sigmoidal function) models that we used to estimate maturation with berried and histological criteria.

The magnitude of the difference between the sizes at maturity estimated by our and the Watters and Hobday (1998) model should vary in proportion to the magnitude of the difference between the minimum (θ_0) and median ($[\theta_0+\theta_1]/2$) body sizes at maturity and therefore be case-dependent. In our slipper lobster case, the θ_0 and θ_1 estimates differed by about 6.6 mm; hence, the two model estimates differed by about 6.6/2 = 3.3 mm or approximately 7% of the $[(\theta_0+\theta_1)/2]$ median. Because other cases certainly include those in which immature and adult sizes overlap even more greatly, we suggest that our more general and accurate model be adopted.

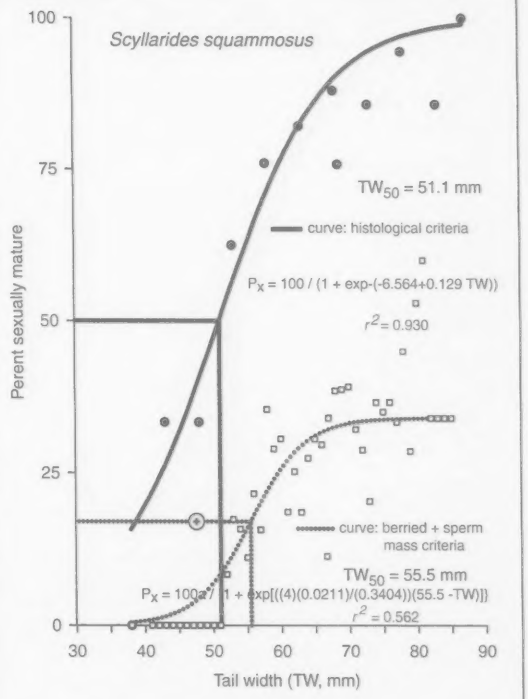

Figure 4

Scatterplots and fitted curves of the relations between body size (tail width, TW) and percent sexual maturity based on functional maturity gauged by presence-absence of berried condition (dotted curve), overlaid on gonadal maturation gauged by microscopic examination of ovaries (dark-line curve); the pleopod length-based morphometric maturation point (MMP) estimate of size at functional maturity is indicated by the large circle with cross-hairs (⊕), for slipper lobster (*Scyllarides squammosus*). A 3-parameter logistic equation was necessary to fit the dotted curve; a 2-parameter logistic was sufficient to fit the dark-line curve (see text).

Functional versus physiological measures of maturity

Morphological features can provide adequate if imperfect measures of functional sexual maturity, as can physiological evidence for gonadal maturity (Ennis, 1984). Morphological features such as ovigerous condition can underestimate the incidence of mature individuals, but the degree to which they do so depends on numerous factors including species and population. Physiological metrics in some cases can provide more accurate estimators of both body size and age at maturity because they reveal the reproductive readiness of individuals at the time of collection. Individual body size and age at maturity can be decoupled from functional maturity metrics in Crustacea, however. For example, some crustaceans like majid crabs exhibit determinate growth following a terminal, pubertal molt (Hartnoll, 1982). For such species, size at attainment of sexual maturity is synonymous with the median body size of adults. These two attributes are not synonymous for lobsters with indeterminate growth. It is further obvious that the pleopods and other allometric body parts of Crustacea like lobsters reflect an array of gonadal maturities ranging from developing immature to fully mature, which can be problematic because some or many females might abort and resorb developing gonadal eggs after the pubertal molt (Aiken and Waddy, 1980) or may not become inseminated (Heydorn, 1969). By attributing maturity to specimens that either have not matured physiologically or that will not reproduce although capable of doing so, appendage-to-body proportions can underestimate the age at maturity in Crustacea. The degree of underestimation should be proportional to the incidence of gonadal resorption during the intermolt period following the pubertal molt,

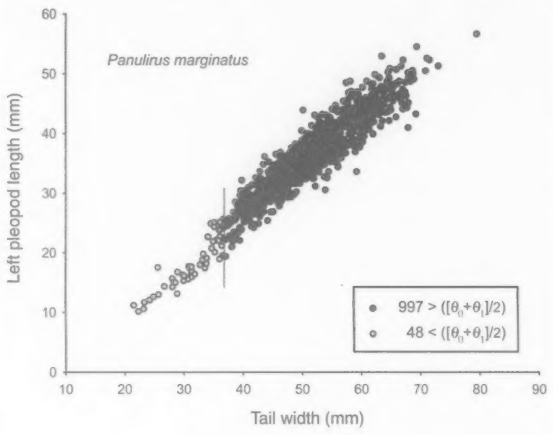

Figure 5

Scatterplots of the relation between pleopod length and tail width for the Hawaiian spiny lobster (*Panulirus marginatus*). The morphometric maturation point (MMP; indicated by a vertical line) represents the allometric threshold coincident with sexual maturity ($[\theta_0+\theta_1]/2$).

as well as the duration of the intermolt. These specific topics deserve future study.

The above caveats notwithstanding, it is helpful to compare estimates of body sizes at sexual maturity based on various morphological and physiological evidence and to ascertain the degree of agreement among the estimates (Fernandez-Vergaz et al., 2000). The estimate of MMP (47.6 mm) indicated by the pleopod length-to-TW relation for *S. squammosus*, for example, was about 16% smaller than the median size at maturity (55.5 [±1.35 SE] mm) estimated by using simple presence-absence of berried eggs for the same series of specimens. The latter estimate, however, is imprecise and an overestimate. The long-term mean TW at 50% maturity based on berried condition for the period from 1986 to 2001, indistinguishable among component years, was 50.0 ±0.83 mm, more precise than the single-year estimate although still biased high (DeMartini et al., 2002). If this 50.0 value is used for reference, the pleopod length-based estimate of the MMP falls within <5% of the long-term mean. For *P. marginatus*, the analogous MMP = 36.4 mm value was within 3% of the estimated median size at maturity (35.4 mm) based on the combined criteria of berried eggs and sperm mass presence. All the various estimates of functional maturity for the two species were within 2.0–12.6% (mean=7.9%) of the best respective estimate of gonadal maturity. These close similarities, despite the inherent biases of the two methods, indicate that maturity metrics such as relative pleopod length can provide highly satisfactory proxies of true functional maturity that are closely related to gonadal maturity in certain cases.

Pleopod length as a maturity metric

In some Crustacea (once again, not lobsters, as far as is known), allometries are not fixed at the pubertal molt; and, in a minority of these, allometric growth is seasonally cyclic and allometries disappear when mature instars molt during nonreproductive periods (Hartnoll, 1974, 1982). And body proportions may not be strong predictors of sexual maturity for clawed lobsters (Comeau and Savoie, 2002). In many, if not most, decapods such as spiny lobsters (e.g., George and Morgan, 1979; Groeneveld and Melville-Smith, 1994), however, relative appendage-to-body sizes, as well as obvious morphological criteria such as the presence of berried eggs and a sperm mass, indicate functional sexual maturity. Body part allometries in some cases can be better predictors of maturity than more obvious characters like berried eggs. An incomplete measure such as percentage berried, exemplified by the slipper lobster (*S. squammosus*) in the present study, can falsely fail to detect reproductively inactive adult females. Appendage-to-body size proportions thus have one major advantage over other morphometrics in that they permit reproductively inactive adult females to be correctly classified as mature. This advantage is relatively unimportant in other species like *P. marginatus* for which additional gross morphological indicators such as the presence-absence of a sperm mass complement the information provided by berried condition. Even so, proportional appendage lengths can be used in such cases as another fairly inexpensive and independent measure that could contribute to a multivariate assessment of maturity,

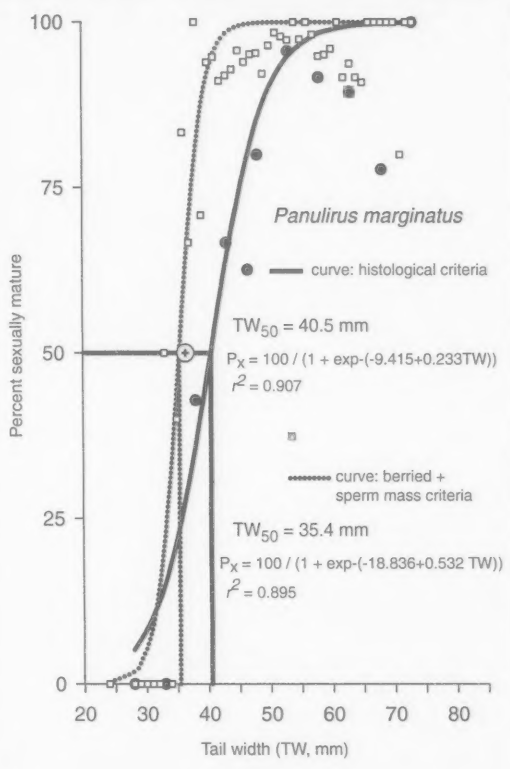

Figure 6

Scatterplots and fitted curves for the relations between body size (tail width, TW) and percent sexual maturity based on functional maturity gauged by presence-absence of sperm mass and berried condition (dotted curve), overlaid on gonadal maturation gauged by microscopic examination of ovaries (dark-line curve); the pleopod length-based morphometric maturation point (MMP) estimate of size at functional maturity is indicated by the large circle with cross-hairs (⊕), for Hawaiian spiny lobster (*Panulirus marginatus*). Two-parameter logistic equations were sufficient to fit both the dotted and dark-line curves.

unconstrained by a conspicuous but perhaps inaccurate feature like berried condition.

Management implications

Estimates of body size at sexual maturity can provide key information to various stock assessment models, but only if the estimates are accurate and sufficiently precise. For the slipper lobster (*S. squammosus*), DeMartini et al. (2002) have shown that estimates made by using percent berried as the lone maturity criterion, the only morphological metric previously available, are both inaccurate and imprecise. The inability to distinguish truly immature from mature, but reproductively inactive, females generates an inflated "immature" class, and the estimates of median size at sexual maturity thus obtained with logistic equation fits are biased high. Variances of median-size estimates based on sample sizes available on single research surveys are often so large that 3-parameter logistic applications (necessary to scale maturity to 100%) fail to converge, and reliable individual-year estimates are impossible (DeMartini et al., 2002). Unfortunately, the temporal dynamics of targeting species by fishermen in the NWHI trap fishery and the rapid phenotypic responses in fecundity and maturation size to harvesting, fluctuating natural productivity, and changing population densities that have been observed in *P. marginatus* (DeMartini et al., 2003), require that size at maturity be re-estimated at short (one-to-several-year) intervals for this species at least and possibly for *S. squammosus* as well.

The accurate and precise estimates of median body size at sexual maturity made possible by using the pleopod length metric enable such yearly re-evaluations for *S. squammosus* and provide a second reliable and independent estimator for *P. marginatus*. Our successful applications for a scyllarid as well as a palinurid, together with prior observations for numerous other spiny lobster species, indicate that easily measured appendage length-to-body size relations are generally suitable for assessing functional sexual maturity in lobsters and other decapods. We recommend that these relations be explored for other commercially exploited crustacean stocks and wherever possible routinely applied to provide cost-effective and timely information on size at maturity for stock assessments. Managers responsible for the assessment of lobster and other crustacean stocks will then have a more complete toolbox of methods generally available for assessing the size at maturity and harvestability of stocks, particularly for species like *S. squammosus* in which conventional morphological measures are inadequate.

Acknowledgments

We thank D. Yamaguchi for assistance with Figure 1 and G. DiNardo and J. Polovina for constructive criticisms of the manuscript.

Literature cited

Aiken, D. E., and S. L. Waddy.
1980. Reproductive biology. *In* The biology and management of lobsters, vol. I, physiology and behavior (J. S. Cobb and B. F. Phillips, eds.), p. 215–276. Academic Press, New York, NY.

Berry, P. F., and A. E. F. Heydorn.
1970. A comparison of the spermatophoric masses and mechanisms of fertilization in Southern African spiny lobsters (Palinuridae). S. Afr. Assoc. Mar. Biol. Res., Oceanogr. Res. Inst. Invest. Rep. 25, 18 p.

Comeau, M., and F. Savoie.
2002. Maturity and reproductive cycle of the female American lobster, *Homarus americanus*, in the southern Gulf of St. Lawrence, Canada. J. Crust. Biol. 22:762–774.

Davison, A. C., and D. V. Hinkley.
1997. Bootstrap methods and their application, 582 p. Cambridge University Press, New York, NY.

DeMartini, E. E., G. T. DiNardo, and H. A. Williams.
2003. Temporal changes in population density, fecundity and egg size of the Hawaiian spiny lobster, *Panulirus marginatus*, at Necker Bank, Northwestern Hawaiian Islands. Fish. Bull. 101:22–31.

DeMartini, E. E., P. Kleiber, and G. T. DiNardo.
2002. Comprehensive (1986–2001) characterization of size at sexual maturity for Hawaiian spiny lobster (*Panulirus marginatus*) and slipper lobster (*Scyllarides squammosus*) in the Northwestern Hawaiian Islands. NOAA Tech Memo NMFS-SWFSC-344, 12 p.

DeMartini, E. E., and H. A.Williams.
2001. Fecundity and egg size of *Scyllarides squammosus* (Decapoda: Scyllaridae) at Maro Reef, Northwestern Hawaiian Islands. J. Crust. Biol. 21:891–896.

Ennis, G. P.
1984. Comparison of physiological and functional size-at-maturity relationships in two Newfoundland populations of lobsters *Homarus americanus*. Fish. Bull. 82:244–249.

Evans, C. R., A. P. M. Lockwood, A. J. Evans, and E. Free.
1995. Field studies of the reproductive biology of the spiny lobster *Panulirus argus* (Latreille) and *P. guttatus* (Latreille) at Bermuda. J. Shellfish Res. 14:371–381.

Fernandez-Vergaz, V., L. J. Lopez Abellan, and E. Balguerias.
2000. Morphometric, functional and sexual maturity of the deep-sea red crab *Chaceon affinis* inhabiting Canary Island waters: chronology of maturation. Mar. Ecol. Prog. Ser. 204:169–178.

George, R. W., and G. R. Morgan.
1979. Linear growth stages in the rock lobster (*Panulirus versicolor*) as a method for determining size at first physical maturity. Rap. P.-V. Reun. Cons. Int. Explor. Mer 175:182–185.

Gregory, D. R. Jr, and R. F. Labisky.
1981. Ovigerous setae as an indicator of reproductive maturity in the spiny lobster, *Panulirus argus* (Latreille). Northeast Gulf Sci. 4:109–113.

Grey, K. A.
1979. Estimates of the size at first maturity of the western rock lobster, *Panulirus cygnus*, using secondary sexual characteristics. Aust. J. Mar. Freshw. Res. 30:785–791.

Groeneveld, J. C., and R. Melville-Smith.
1994. Size at onset of sexual maturity in the south coast rock lobster, *Panulirus gilchristi* (Decapoda: Palinuridae). S. Afr. J. Mar. Sci. 14:219–233.

Hartnoll, R. G.
1974. Variation in growth pattern between some secondary sexual characters in crabs (Decapoda: Brachyura). Crustaceana 27:131–136.
1982. Growth. *In* The biology of Crustacea, vol. I, embryology, morphology, and genetics (D. E. Bliss, ed.), p. 111–196. Academic Press, London.

Heydorn, A. E. F.
1969. The rock lobster of the South African west coast *Jasus lalandii* (H. Milne-Edwards). 2. Population studies, behavior, reproduction, moulting, growth and migration. S. Afr. Div. Sea Fish. Invest. Rep. 7:1–52.

Hogarth, P. J., and L. A. Barratt.
1996. Size distribution, maturity and fecundity of the spiny lobster *Panulirus penicillatus* (Oliver 1791) in the Red Sea. Trop. Zool. 9:399–408.

Hossain, M. A.
1978. Appearance and development of sexual characters of sand lobster *Thenus orientalis* (Lund) (Decapoda: Scyllaridae) from the Bay of Bengal. Bangladesh. J. Zool. 6:31–42.

Jayakody, D. S.
1989. Size at onset of sexual maturity and onset of spawning in female *Panulirus homarus* (Crustacea: Decapoda: Palinuridae) in Sri Lanka. Mar. Ecol. Prog. Ser. 57:83–87.

Juinio, M. A. R.
1987. Some aspects of the reproduction of *Panulirus penicillatus* (Decapoda: Palinuridae). Bull. Mar. Sci. 41:242–252.

Matthews, D. C.
1951. The origin, development, and nature of the spermatophoric mass of the spiny lobster, *Panulirus penicillatus* (Oliver). Pac. Sci. 5:359–371.

Minagawa, M.
1997. Reproductive cycle and size-dependent spawning of female spiny lobsters (*Panulirus japonicus*) off Oshima Island, Tokyo, Japan. Mar. Freshw. Res. 48:869–874.

Minagawa, M., and S. Higuchi.
1997. Analysis of size, gonadal maturation, and functional maturity in the spiny lobster *Panulirus japonicus* (Decapoda: Palinuridae). J. Crust. Biol. 17:70–80.

Minagawa, M., and M. Sano.
1997. Oogenesis and ovarian development cycle of the spiny lobster *Panulirus japonicus* (Decapoda: Palinuridae). Mar. Freshw. Res. 48:875–887.

Montgomery, S. S.
1992. Sizes at first maturity and at onset of breeding in female *Jasus verreauxi* (Decapoda: Palinuridae) from New South Wales waters, Australia. Aust. J. Mar. Freshw. Res. 43:1373–1379.

Plaut, I.
1993. Sexual maturity, reproductive season and fecundity of the spiny lobster *Panulirus penicillatus* from the Gulf of Eilat (Aqaba), Red Sea. Aust. J. Mar. Freshw. Res. 44:527–535.

Prescott, J. H.
1984. Determination of size at maturity in the Hawaiian spiny lobster *Panulirus marginatus*, from changes in relative growth. Proc. Res. Inv. NWHI. UNIHI-SEA GRANT-MR-84-01, p. 345. Univ. Hawaii, Honolulu, HI.

Ratkowsky, D. A.
1983. Nonlinear regression modeling: a unified practical approach, 276 p. Marcel Dekker, New York, NY.

Somerton, D. A.
1980. A computer technique for estimating the size of sexual maturity in crabs. Can. J. Fish. Aquat. Sci. 37:1488–1494.

Watters, G., and A. J. Hobday.
1998. A new method for estimating the morphometric size at maturity of crabs. Can. J. Fish. Aquat. Sci. 55:704–714.

Appendix

Method for estimation of maturation with pleopod metrics

To model the allometry we used the power function $Y=\delta X^{\beta}$ and assumed multiplicative error. The logarithmic transformation of this function leads to a linear regression model. Specifically, we defined $\ln(Y)= f_1(X)+\varepsilon_1$, where $f_1(X)=\alpha_1+\beta_1\ln(X)$ and $\alpha_1 =\ln(\delta_1)$, as the allometric relationship for juvenile lobsters and $\ln(Y)= f_2(X)+\varepsilon_2$, where $f_2(X)=\alpha_2+\beta_2\ln(X)$ and $\alpha_2 =\ln(\delta_2)$, as the allometric relationship for adult lobsters. The errors, ε_1 and ε_2, were assumed to be independent and normally distributed with mean 0 and variance ${\sigma_1}^2$ and ${\sigma_2}^2$, respectively. We assumed that maturation occurred over a range of tail widths. Dividing the domain of x into four intervals, we defined the probability that a lobster with observed tail width x was mature (m) as

$$P(m|x)=\begin{cases} 0 & x<\theta_0 \\ \dfrac{x-\theta_0}{\theta_1-\theta_0}\exp\left(-\gamma\left(\dfrac{\theta_0+\theta_1-2x}{\theta_1-\theta_0}\right)\right) & \theta_0\le x<\dfrac{\theta_0+\theta_1}{2} \\ 1-\dfrac{\theta_1-x}{\theta_1-\theta_0}\exp\left(-\gamma\left(\dfrac{2x-(\theta_0+\theta_1)}{\theta_1-\theta_0}\right)\right) & \dfrac{\theta_0+\theta_1}{2}\le x<\theta_1 \\ 1 & x\ge\theta_1 \end{cases} \quad (1)$$

When $\gamma=0$, $P(m|x)$ increases linearly from 0 to 1 over the interval $[\theta_0, \theta_1]$. For $\gamma>0$, the curves are sigmoidal, symmetrical, and the rate that the probability changes with respect to tail width is bell shaped (the sigmoidal curve first accelerates, then decelerates). The point of inflection, $(\theta_0+\theta_1)/2$, is the tail width at which 50% of the lobsters are expected to be mature. For both species, we assumed that $\gamma\ge0$.

Defining the allometry model and the probability of maturity as above, we expressed the model relating pleopod length to tail width as $\ln(Y)=f_1(X)(1-P(m|x))+f_2(X)P(m|x)+\varepsilon$, where ε are independent normal variates with mean 0 and covariance V_m.

Assuming (x_i,y_i) $i=1, \ldots, n$ independent paired observations and ${\sigma^2}={\sigma_1}^2={\sigma_2}^2$, $V_m=I\sigma^2+M$, where I is the $(n \times n)$ identity matrix, M is the diagonal matrix $M_{ii}=\Delta^2(x_i)P(m_i|x_i)(1-P(m_i|x_i))$, and $\Delta(x_i)=f_2(x_i)-f_1(x_i)$. Hence, we have a weighted least squares problem with weights

$$w_i=\begin{cases} 1 & \text{if } x_i\le\theta_0 \text{ or } x_i\ge\theta_1 \\ \dfrac{\sigma^2}{(\sigma^2+M_{ii})} & \text{if } \theta_0<x_i<\theta_1. \end{cases} \quad (2)$$

To fit the model, we defined $\alpha_3=\alpha_2-\alpha_1$ and $\beta_3=\beta_2-\beta_1$ and expressed the model as $\ln(Y)=f_3(X)P(m|x)+f_1(X)+\varepsilon$, where $f_3(X)=\alpha_3+\beta_3\ln(X)$. To ensure that the curve in the transition range was monotonically increasing (if $\beta_3>0$), θ_0 was bounded such that $\theta_0\ge\exp(-\alpha_3/\beta_3)$, and if $\beta_3<0$, θ_1 was bounded such that $\theta_1\le\exp(-\alpha_3/\beta_3)$. The curve was fitted by using iteratively reweighted least squares. The weights were recomputed at each iteration.

While fitting the lobster data to the specified model, we observed that one or more of the parameters involved in defining the sigmoidal curve departed from linear behavior. Under these circumstances, the confidence interval derived by assuming the asymptotic properties of maximum likelihood estimates may be invalid (Ratkowsky, 1983). Therefore, we computed approximate 95% confidence intervals for the point of inflection using the bootstrap method. Specifically, we used case resampling with 1000 bootstrap replications. Confidence intervals were derived by using the studentized bootstrap confidence limits (Davison and Hinkley, 1997).

Seasonal changes in growth of coho salmon (*Oncorhynchus kisutch*) off Oregon and Washington and concurrent changes in the spacing of scale circuli

Joseph P. Fisher

William G. Pearcy

College of Oceanic and Atmospheric Sciences
Oregon State University
104 Ocean Admin. Building
Corvallis, Oregon 97331-5503
E-mail address (for J. P. Fisher): jfisher@coas.oregonstate.edu

Abstract—In this study we present new information on seasonal variation in absolute growth rate in length of coho salmon (*Oncorhynchus kisutch*) in the ocean off Oregon and Washington, and relate these changes in growth rate to concurrent changes in the spacing of scale circuli. Average spacing of scale circuli and average rate of circulus formation were significantly and positively correlated with average growth rate among groups of juvenile and maturing coho salmon and thus could provide estimates of growth between age groups and seasons. Regression analyses indicated that the spacing of circuli was proportional to the scale growth rate raised to the 0.4–0.6 power. Seasonal changes in the spacing of scale circuli reflected seasonal changes in apparent growth rates of fish. Spacing of circuli at the scale margin was greatest during the spring and early summer, decreased during the summer, and was lowest in winter or early spring. Changes over time in length of fish caught during research cruises indicated that the average growth rate of juvenile coho salmon between June and September was about 1.3 mm/d and then decreased during the fall and winter to about 0.6 mm/d. Average growth rate of maturing fish was about 2 mm/d between May and June, then decreased to about 1 mm/d between June and September. Average apparent growth rates of groups of maturing coded-wire–tagged coho salmon caught in the ocean hook-and-line fisheries also decreased between June and September. Our results indicate that seasonal change in the spacing of scale circuli is a useful indicator of seasonal change in growth rate of coho salmon in the ocean.

Manuscript submitted 20 September 2003 to the Scientific Editor.

Manuscript approved for publication 8 September 2004 by the Scientific Editor

Fish. Bull. 34–51 (2005).

Large interannual and decadal variations occur in the abundance and productivity of North Pacific salmonids. These fluctuations, which affect harvestable biomass, are influenced by survival rates, ages at maturity, and somatic growth (Beamish and Bouillon, 1993; Mantua et al., 1997; Hare et al. 1999; Pyper et al., 1999; Hobday and Boehlert, 2001).

The growth of smolts after ocean entry—growth that is critical to production—is also thought to be an important determinant of their survival. As for juvenile and larval fishes in general, size-selective mortality may occur (Miller et al., 1988; Bailey and Houde, 1989; Litvak and Leggett, 1992; Sogard, 1997) with the result that faster growing salmonids experience less mortality from predators than slower growing salmonids (Parker, 1971; Bax, 1983; Fisher and Pearcy, 1988; Holtby et al., 1990; Jaenicke et al., 1994; Willette, 1996, 2001). This size-selective mortality may explain much of the interannual variability in survival of juvenile salmonids and the subsequent abundance of different year classes. However, other investigators have not found a strong relationship between growth of juvenile salmon and mortality (Fisher and Pearcy, 1988; Mathews and Ishida, 1989; Blackbourn, 1990).

Intercirculus spacing of scales has been used to estimate early ocean growth rate of juvenile salmon and has been linked to differential survival rates. For example, Healey (1982) used the spacing of the first five circuli to demonstrate intensive size-selective mortality in juvenile chum salmon (*Oncorhynchus keta)* as they migrated offshore. Holtby et al. (1990) correlated early ocean growth, based on intercirculus spacing, with marine survival of age 1+ coho (*O. kisutch*) smolts. The spacing of early ocean circuli from the scales of maturing Atlantic salmon (*Salmo salar*) has been used to estimate juvenile growth rates, which are correlated with survival and age at maturity, and to identify stocks (Friedland et al., 1993; Friedland and Haas, 1996; Friedland and Reddin, 2000; Friedland et al., 2000).

Correlation between circulus spacing and growth rate was reported by Fisher and Pearcy (1990) for age 0.0 coho smolts reared for 60 days in salt water tanks. In addition, positive correlations between the spacing of scale circuli and fish growth rate have been observed for rainbow trout (*O. mykiss*) (Bhatia, 1932), and sockeye salmon (*O. nerka*) (Fukuwaka and Kaeriyama, 1997), and between the spacing of circuli and feeding ration and growth for sockeye salmon (Bilton and Robins, 1971; Bilton, 1975). Bigelow and White (1996) were able to manipulate the spacing of scale circuli of cutthroat trout (*O. clarkii*)

Table 1

Main sources of coho salmon data used in this study.

Source	Numbers of fish	Scale samples
CWT maturing fish caught in the Oregon ocean sport and troll fisheries 1982–92 (see Table 2)	687	687
Maturing coho salmon caught in the ocean during research cruises		
1981–85	1391	352
1998–2002	714	236
Juvenile fish caught in the ocean during research cruises		
1981–85		1798
1998–2002	3684	1052
CWT maturing coho salmon caught in the sport and troll ocean fisheries (all catch areas) and released between northern Oregon and northern Washington[1]	149,718	—

[1] FL data in the Pacific States Marine Fisheries Commission, Regional Mark Information System online CWT database http://www.rmis.org/. [Accessed 1 April 2003.]

in the hatchery by varying the feeding levels: the group that was fed the most also grew the most and had the most widely spaced scale circuli. Positive correlations between circulus spacing and growth also have been observed for nonsalmonid fishes including *Tilapia* (Doyle et al., 1987; Matricia et. al., 1989; Talbot and Doyle, 1992), and walleye (*Stizostedion vitreum*) (Glenn and Mathias, 1985).

Circulus spacing is potentially useful for comparing ocean growth rates of salmon in the ocean. Spacing of the first few ocean scale circuli may indicate relative growth rates of juvenile fish immediately after ocean entry. However, in order for spacing of scale circuli to be a practical indicator of fish growth rate, the relationship between the two must be consistent and significant. The relationship between circulus spacing and fish or scale growth rate is determined by the relative rates of growth and circulus formation. If circuli (like tree rings) are formed at a constant rate, then there would be a directly proportional relationship between spacing and growth rate (e.g., a doubling of growth rate would result in a doubling of spacing). Conversely, if the rates at which circuli are formed are directly proportional to growth rates (e.g., a doubling of growth rate would result in a doubling of circulus formation rate), then the spacing of circuli would be constant. Our earlier study of growth rate, circulus formation, and circulus spacing among 82 individually marked juvenile coho salmon growing for a period of 63 days in saltwater tanks indicated that neither of these two extremes is the case, but that both circulus formation rate and circulus spacing are positively correlated with fish growth rate (Fisher and Pearcy, 1990).

Our main objectives in this study are to further assess the reliability of circulus spacing as an indicator of growth rate in FL of coho salmon in the ocean, to investigate how growth of coho salmon changes seasonally, and to compare any seasonal changes in growth rate with seasonal changes in the spacing of scale circuli. If circulus spacing is a reliable indicator of growth rate, then seasonal changes in growth rate should be tracked by changes in the spacing of circuli laid down at the scale margin. We investigated relationships between scale growth rate, fish growth rate, circulus spacing, and circulus formation rate for coded-wire–tagged (CWT) adult coho salmon collected in the ocean fisheries in years when ocean growth varied widely, including year classes affected by the 1982–83 El Niño, and for juvenile and maturing coho salmon caught in the ocean off Oregon and Washington in research cruises 1981–85 and 1998–2002.

Materials and methods

Scale and FL data

Fish fork length (FL) and scale data from a variety of sources were used in this study (Table 1). During research cruises on the Oregon and Washington coastal shelf we collected juvenile and maturing coho salmon in the upper 20–40 m of the water column with purse seines from 1981–85 (Pearcy and Fisher, 1988, 1990) and with a rope trawl from 1998–2002 (Emmett and Brodeur, 2000). Scales samples were removed from the fish from an area equivalent to area "A" described in Scarnnechia (1979). When scales were not available from area "A," we took scales from between areas "A" and "B" in Scarnnechia (1979). (See also Clutter and Whitesel, 1956). We also examined scales from the same area from 687 maturing CWT Columbia River and northern coastal Oregon coho salmon caught in the Oregon ocean fisheries between 1982 and 1992.

Changes over time in FLs of maturing coho salmon caught in research nets and of CWT hatchery coho salmon originating between northern Oregon and northern Washington and caught in the ocean fisheries be-

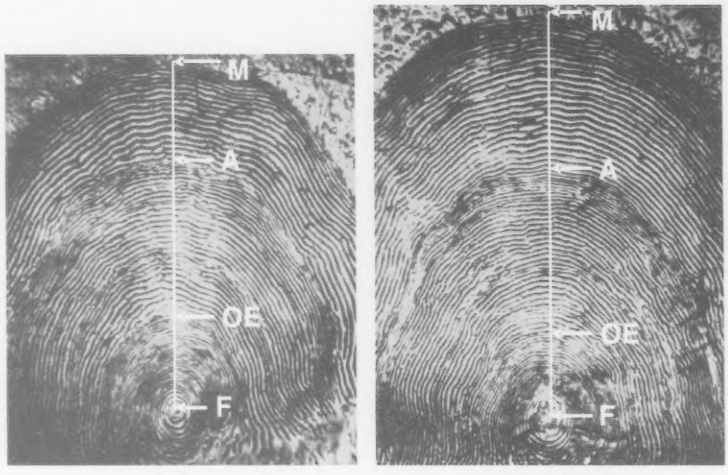

Figure 1

Scales from the 1982–83 and 1983–84 (smolt year through adult year) year classes of coho salmon (*Oncorhynchus kisutch*) showing the axis of measurement, the scale focus (F), ocean entry (OE), the annulus (A) at the end of the annual ring and the scale margin (M).

tween 1975 and 2002 were used to estimate growth rates of maturing fish (Table 1).

Scale measurements

We measured the distances (mm) along the anterior–posterior scale axis from the focus (F) to the last circulus of the freshwater zone (ocean entry, OE), to the outside edge of the winter annual ring (the "winter annulus," A) when present, and to the margin (M), and also determined the total numbers and average spacing of circuli in the ocean growth zone (Fig. 1). For certain scale samples we also determined the spacing of every circulus in the ocean growth zone of the scales or of the last few circuli at the scale margin.

Measurements of scales from juvenile fish caught during research cruises 1981–85 were taken from images projected by a microfiche reader at a magnification of about 88× and measurements of scales from all other fish were acquired with image analysis software (Optimas, vers. 5.1, Optimas, Inc., Seattle, WA, and Image-Pro Discovery, vers. 4.5, Media Cybernetics, Silver Spring, MD) by using a CCD camera coupled to a Leica compound microscope. All measurements were calibrated from images of a stage micrometer.

Circulus spacing and formation rate versus growth rate

We used correlation and regression analyses to relate average circulus spacing and formation rate to average scale and fish growth rate among year classes of juvenile coho salmon during their first four or five months in the ocean and among groups of maturing CWT coho salmon during their entire ocean life (Table 2). We described the relationships between the scale characteristics and growth rate as power functions by using natural log (ln) transformed variables in linear regressions. Geometric mean (GM) regression (Ricker, 1973, 1992; Sokal and Rohlf, 1995) was used to relate the ln-transformed variables because they were subject to both natural variability and measurement error and because our purpose in the present study was to describe the functional relationships between the variables and not to predict one from the other.

For each fish, rates of scale growth, fish growth, and circulus formation in the ocean were estimated as $(SR-SR_{OE})/\Delta d$, $(FL-FL_{OE})/\Delta d$, and $CIRC/\Delta d$, respectively, where SR=scale radius at capture, SR_{OE}= scale radius at ocean entry (F to OE in Fig. 1), FL= fork length at capture, FL_{OE}=estimated fork length at ocean entry, $CIRC$=the total number of circuli in the ocean growth zone of the scale, and Δd = estimated days between ocean entry and capture. Average spacing of circuli was calculated as $(SR_{LAST}-SR_{OE})/CIRC$, where SR_{LAST}=the scale radius to the last circulus before the scale margin.

For juvenile fish, FL_{OE} was estimated by using the Fraser-Lee back-calculation method (Ricker, 1992) and the intercept from the FL–SR regression for ocean-caught juvenile fish (34.16 mm, Fig. 2). However, be-

cause of allometry in the FL-SR relationships of juvenile and maturing fish (Fig. 2), which a ln-ln transformation of the data failed adequately to correct, the Fraser-Lee method was not used to estimate FL_{OE} of the maturing fish caught in the ocean. Instead, FL_{OE} of maturing fish was estimated by direct substitution of (SR_{OE}) into the *GM* regression relationship between *FL* and *SR* for juvenile coho salmon caught in the ocean 1981–85 and 1998–2001 (gray regression line, Fig. 2).

For juvenile fish caught in August or September, Δd was estimated as the capture date minus 25 May, a date near the peak of coho salmon smolt migration in the Columbia River estuary (Dawley et al., 1985a). Because we used a single date of ocean entry for all fish, errors in estimated growth rates of some individual juvenile coho salmon probably were quite large; the timing of ocean entry of fish can vary by as much as two months. However, for the correlation and regression analyses we used growth rates averaged by year class, which were probably quite accurate, if the average date of ocean entry of the fish in the samples is assumed to be similar across years. In the Columbia River, the major source of juvenile coho salmon on the Oregon and Washington coasts, ocean entry was concentrated between late April and early June and the timing of ocean entry varied little between years (Dawley et al., 1985a).

Dates of ocean entry of the maturing CWT Sandy and Cowlitz hatchery coho salmon (Table 2) were estimated from the hatchery release dates and the rates of downstream migrations of these fish observed during extensive sampling of migrating smolts at rkm 75 in the upper Columbia River estuary (Dawley et al., 1985b). To estimate dates of ocean entry of the Fall Creek hatchery fish, for which data on downstream migration were lacking, we assumed that smolts migrated to the ocean from the different release sites at the same average rate of downstream migration as that of Cowlitz Hatchery fish released in late April (5.7 km/d).

Potential errors in estimated growth rates of maturing CWT coho salmon caused by inaccurately estimating size of fish at ocean entry, or date of ocean entry, were proportionally very small when compared to the total amount or duration of ocean growth. At a typical SR_{OE} of around 0.7 mm, the 95% prediction limits for *FL* from the SR-FL regression of juvenile fish (Fig. 2) are about ±31mm. An error in size at OE of 15–30 mm would only be 2–10% of the estimated total growth in *FL* in the ocean of the maturing fish (320 mm–610 mm). Similarly, an error in estimated date of ocean entry of 30 days would equal only about 6–10% of the total time that the fish was in the ocean (336–535 d). Errors for the group-averaged data used in our correlation and regression analyses were probably much lower.

Table 2

Nine year classes of juvenile coho salmon caught in research nets in August or September and 17 groups of CWT maturing coho salmon caught in the Oregon ocean fisheries used in the correlation and regression analyses of scale characteristics and growth rate. CWT maturing fish were from three hatcheries (Fall Creek "F" on the northern Oregon coast and Sandy "S" and Cowlitz "C" in the lower Columbia River basin) and were released from hatcheries during three periods.

Capture year	Hatcheries	Numbers of fish
CWT maturing fish released late April or early May (days 119–127)		
1982	F, S	11, 15
1983	F, S, C	34, 17, 51
1984	S, C	52, 35
1985	S, C	12, 26
1986	S	67
1987	S	94
1989	S	57
1990	S	18
CWT maturing fish released in March (days 74–76)		
1984	F	31
1985	F	21
CWT maturing fish released in late May or early June(days 151–157)		
1991	S	30
1992	S	77
Juvenile fish		
1981	—	99
1982	—	95
1983	—	81
1984	—	88
1998	—	13
1999	—	60
2000	—	75
2001	—	67
2002	—	123

Seasonal changes in spacing of circuli

To investigate whether circulus spacing and growth rate were correlated seasonally, we first described the patterns of seasonally changing circulus spacing of juvenile and maturing coho salmon in the ocean and then compared these patterns of changing circulus spacing to changing fish growth rates. Because the widths of the pre-annulus and postannulus scale zones and the numbers of circuli in each zone varied greatly among individual fish and among groups of fish, we described circulus spacing in each of 25 equally spaced intervals between *OE* and the annulus and in each of 25 equally spaced intervals between the annulus and the scale margin, rather than on a circulus by circulus basis. Specifically, the pre-annulus and postannulus ocean zones of scales were each divided into 25 equal intervals, and the radial distance from OE to the upper bounds of each of the intervals was determined. Next, the numbers of ocean circuli between OE and the upper bounds of each of the 50 intervals were interpolated. For example, if a boundary fell 25% of the distance

between the 38th and 39th ocean circulus, the circulus number 38.25 was assigned to that boundary. We calculated the circulus spacing in each interval as Δmm/Δcirc, where Δmm = the width in mm of the interval, and Δcirc = the difference between the interpolated circulus numbers at the upper and lower bounds of the interval. The circulus spacing in each of the 50 intervals was averaged across all the scales from the fish in a group. This produced a profile of the average spacing of circuli at 50 different positions in relation to *OE* (lower bound of interval 1), the annulus (upper bound of interval 25) and the scale margin (upper bound of interval 50). Finally, the group-average circulus spacing in each of the 50 intervals was plotted against the group-average radial distance from *OE* to the upper bounds of each of the 50 intervals. For juvenile fish caught in trawls in September 1999–2002, circulus spacing was described at 25 intervals in relation to *OE* (lower bound of interval 1) and the scale margin (upper bound of interval 25).

Seasonal changes in the spacing of circuli at the growing edge of the scale may reflect similar seasonal changes in the growth rate of the juvenile and maturing coho salmon. To investigate this possible correlation, we measured the spacing of the last two circulus pairs at the scale margin of juvenile fish caught in early and late summer in 1982 and 1999 through 2002 and of maturing fish caught in research nets 1981–83 and 2000–2002 and in the ocean fisheries 1982–92 (Table 1). Mean spacing of the last two circulus pairs was summarized by cruise for the fish caught in research nets, and by 10-day catch intervals for the fish caught in the ocean fisheries. The seasonal trends in spacing at the scale margin were then compared with the seasonal trend in apparent growth rates of fish.

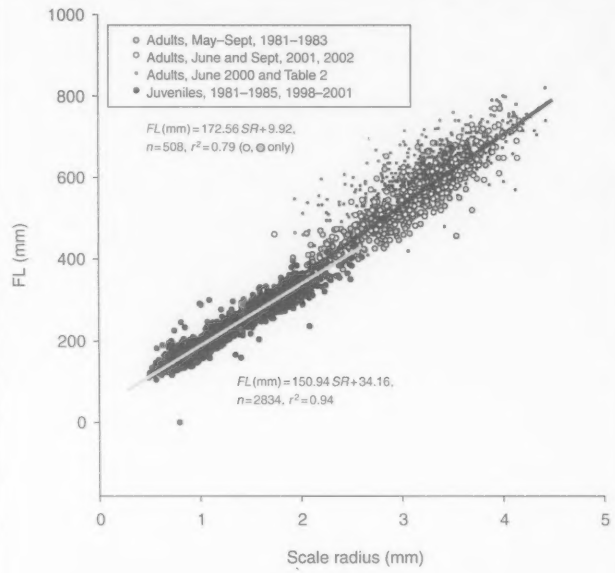

Figure 2

Fork length (FL) versus scale radius (SR) for juvenile and maturing coho salmon (*O. kisutch*) caught in research trawls and GM regressions of FL versus SR fitted to juvenile and adult fish separately. Note the allometry in the FL-SR relationship of juvenile and adult fish.

Seasonal changes in fish growth rate

Seasonal trends in growth rates of juvenile and maturing coho salmon caught in research cruises 1981–83 and 1998–2002 were estimated from the changes between cruises in average FL. We also estimated average growth rates (pooled across years) of juvenile and adult coho salmon during different seasons by fitting regressions to the FL versus catch date data.

Changing stock composition of the juvenile (Teel et al., 2003) or maturing coho salmon caught in research nets over the course of the summer could potentially have a strong effect, independent of growth, on the size distributions of fish caught at different times. Therefore, changes over time in average FLs of mixed stocks of fish, such as in our research collections, may not accurately indicate actual fish growth rates.

Because of the potential for error when inferring seasonal changes in growth rate from changes over time in average FLs of mixed stocks of fish, we also examined temporal changes in FL of maturing CWT coho salmon of known origin caught in the ocean hook-and-line fisheries (sport and troll fisheries). Using data available from the Pacific States Marine Fisheries Commission[1] we investigated changes over the summer in FLs of maturing CWT coho salmon originating from six areas (north Oregon coast, lower Columbia River basin–Oregon, lower Columbia River basin–Washington, Willapa Bay basin, Grays Harbor basin, and the northwest Washington coast). Because the date that a smolt is released from a hatchery (e.g., March vs. June) could affect its size the following year, we also grouped the fish by release periods of 25–46 days duration. Data were available on FLs of maturing CWT fish from 1975–2002. For each group in each year we calculated the average FL of CWT fish at 10-day intervals in the hook-and-line fisheries (sport and troll fisheries) pooled for all catch areas between California and Alaska. Data were discarded when there were fewer than 5 fish mea-

1 Regional Mark Information System CWT database (http://www.rmis.org). [Accessed on: 1 April 2003.]

Table 3

Summary statistics of average estimated fish growth rate, average estimated scale growth rate, average estimated rate of circulus formation, and average circulus spacing between ocean entry and late summer for nine year classes of juvenile coho salmon and during the entire ocean growth period for the 17 groups of CWT maturing coho salmon (see Table 2).

Statistic	Average fish growth rate (mm/d)	Average scale growth rate (mm/d)	Average circulus formation rate (circuli/d)	Average circulus spacing (mm)
Juvenile fish, n=9				
Grand average	1.33	0.0087	0.188	0.0460
Minimum	1.18	0.0080	0.175	0.0428
Maximum	1.52	0.0101	0.202	0.0494
SD	0.10	0.0007	0.008	0.0023
CV	7.6%	8.3%	4.1%	4.9%
Maturing fish, n=17				
Grand average	1.11	0.0060	0.131	0.0463
Minumum	0.94	0.0048	0.110	0.0426
Maximum	1.23	0.0066	0.144	0.0511
SD	0.07	0.0005	0.009	0.0020
CV	6.7%	8.1%	6.8%	4.4%

sured in any 10-day catch period. The average FLs were averaged across all years of data, yielding grand-average FLs for each 10-day catch period. The grand average FL for each 10-day catch interval comprised 1–27 years of data, but those periods with fewer than 5 years of data were discarded. In all, FLs from 149,718 fish were used in the analysis. Grand average FLs and the apparent growth rates in FL between each 10-day catch period were plotted against date and compared with the seasonal changes in circulus spacing at the scale margin of the fish in our scale sample.

Results

Growth and scale statistics for juvenile and maturing fish

Average growth rates and circulus formation rates were greater for juvenile fish during their first ocean summer than for maturing fish during their entire ocean life probably because maturing fish experience slow growth in the winter (Table 3). During their first summer in the ocean, juvenile fish grew an average of 1.33 mm/d and formed circuli at the rate of 0.188/d (one every 5.3 days): whereas, during their entire ocean life maturing fish grew an average of 1.11 mm/d and formed circuli at the rate of 0.131/d (one every 7.6 days). The highest average growth rate (1.52 mm/d) among the eight year classes of juvenile coho salmon was about 28% higher than the lowest average growth rate (1.18 mm/d). The percentage range in growth rate of maturing fish was similar (31%). Average spacing of circuli was similar for both juvenile and maturing coho salmon (0.0460 mm vs. 0.0463 mm), probably because scales from the maturing fish contained both more narrowly spaced circuli formed during the winter and more widely spaced circuli formed during the second ocean summer (see below). The variation among groups in average circulus spacing (CV=4.9% and 4.4%) was lower than the variation in fish or scale growth rates (CV=6.7% to 8.3%), although estimation error may have increased the coefficients of variation of the growth rates.

Correlations between scale characteristics and growth rate

Circulus spacing was strongly correlated (r=0.89 and 0.82, respectively) with scale and fish growth rates among the nine year classes of juvenile coho salmon (Table 4). Circulus spacing was also significantly correlated with scale and fish growth rates among the 17 groups of maturing fish, but the correlations were weaker (r=0.57 and 0.55, respectively) than those for the juvenile fish. Conversely, correlations between the rate of circulus formation and the scale and fish growth rates were slightly higher for the maturing fish (r=0.85 and 0.75, respectively) than for the juvenile fish (r=0.76 and 0.81, respectively). These results suggest that when growth is averaged over several seasons, during which growth rate varies greatly and may even cease for varying periods of time, differences in growth among year classes or groups may be reflected more clearly by differences in the numbers of circuli laid down on the scale than by differences in the average spacing of circuli.

Although the average spacing of circuli and the average rate at which circuli form were both correlated with scale and fish growth rates, they were not correlated with each other (Table 4). This finding indicates that

circulus spacing and circulus formation rate are independent indicators of growth rate—both tending to increase with increasing growth rate but not necessarily together in the same fish or in the same group or year class. At least when averaged over periods of months or more than a year, differences in average growth rate may be expressed by differences in average spacing of circuli, differences in average rate of circulus formation, or differences in both.

Regressions of circulus spacing and formation rate on growth rate

We expressed average spacing of circuli and rates of circulus formation as power functions of the scale growth rates, equivalent to linear regressions of ln-ln transformed data. These regressions are shown in Figures 3 and 4 for year classes of juvenile fish and groups of maturing fish, respectively. Because scale growth rate and fish growth rate were very strongly correlated (Table 4), we show only the regressions with scale growth rate.

Change in average spacing of circuli and in average rate at which circuli form was proportionally smaller than the change in average scale growth rate. Average spacing of circuli was proportional to the average scale growth rate raised to the 0.6 power (juvenile fish, Fig. 3A) or the 0.5 power (maturing fish, Fig. 4A). If these relationships hold over a wider range of scale growth rate and circulus spacing, then a doubling of scale growth rate would be associated with only a 1.5-fold ($2^{0.6}$) or 1.4-fold ($2^{0.5}$) increase in circulus spacing. Similarly, average rate of circulus formation was proportional to the average scale growth rate raised to the 0.5 power (juvenile fish, Fig. 3B) or the 0.8 power (maturing fish, Fig. 4B).

Seasonal changes in circulus spacing and fish growth rate

Seasonal changes in average circulus spacing were consistent among the different year classes and release times of CWT coho salmon (Fig. 5, A–E). During the first year in the ocean, average spacing of scale circuli increased rapidly after OE (usually in May) to average peak values of about 0.050 mm–0.055 mm, then gradually decreased to average minimum values of about 0.031 mm–0.040 mm in the annual ring. By late September 1999–2002, spacing at the margin of scales from juvenile fish had decreased from peak values (Fig. 5E), indicating that the gradual decrease in spacing of circuli which forms the annual ring begins as early as the late summer of the first ocean year. For some year classes (e.g., 82–83, 85–86, 90–91, 91–92) the annual ring was a distinct narrow zone of very closely spaced circuli (Fig. 5, A and C), whereas in other years the annual ring was broad and subtle, with more widely spaced circuli (e.g., 83–84, 86–87, and 84–85 for the March released fish; Fig. 5, A and B).

After the annulus (black dots, Fig. 5), the spacing of circuli increased sharply to peak values of about 0.055 mm–0.060 mm and remained high for a variable distance. Compared to the peak spacing, spacing of circuli at the scale margin was relatively high for maturing fish caught in late June or July 1982, 1984, 1985, 1986, 1987, 1991, and 2000, whereas, spacing at the scale margin was quite low compared to the peak spacing for fish caught in July 1983, 1989, 1990, and 1992 (Fig. 5, A, C, and D). Spacing at the scale margin was very low among unmarked maturing fish caught in late September 2001 (Fig. 5D).

Compared to the large interseasonal variation in spacing of circuli in the pre- and postannulus zones, from about 0.03 mm in the annual ring to about 0.06 mm for the most widely spaced circuli, interannual variation the peak and minimum spacing of circuli was quite small. The peak spacing of circuli was similar among year classes, even when total growth differed greatly (e.g., the 82–83 vs. the 81–82 and 83–84 year classes, Fig 5A). The unusually small postannulus scale growth of fish caught during a strong El Niño in July 1983 (Fig. 5A) was characterized by a much narrower region of widely spaced circuli and more closely spaced circuli at the scale margin than in other years.

In general, pre-annulus scale growth was greatest for the fish released in March (Fig. 5B), was slightly less for the fish released in late April or early May (Fig. 5A), and was smallest for the fish released in late May or early June (Fig. 5C). These data indicate that date of release may strongly affect the amount of growth at-

Table 4

Correlations (r) between average circulus spacing (mm), average estimated scale growth rate (mm/d), average estimated fish growth rate (mm/d), and average estimated circulus formation rate (circuli/d) between ocean entry and late summer for nine year classes of juvenile coho salmon and during the entire ocean growth period for 17 groups of CWT maturing coho salmon (see Table 2). All correlations were significant ($P<0.05$), except were noted ("n.s").

Comparison	Juvenile fish r	Maturing fish r
Circulus spacing vs. scale growth rate	0.89	0.57
Circulus spacing vs. fish growth rate	0.82	0.55
Circulus spacing vs. circulus formation rate	0.38, n.s.	0.05, n.s.
Scale growth rate vs. fish growth rate	0.97	0.91
Scale growth rate vs. circulus formation rate	0.76	0.85
Fish growth rate vs. circulus formation rate	0.81	0.75

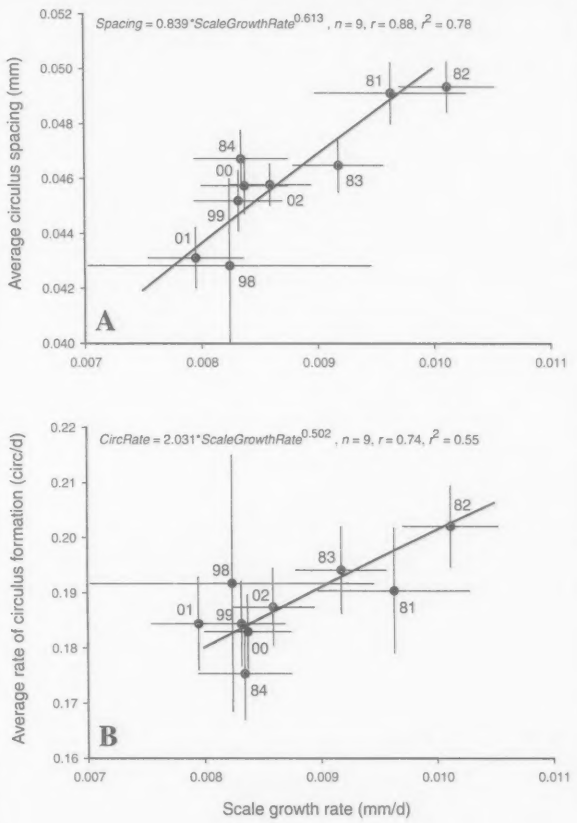

Figure 3

Estimated average scale growth rate versus (**A**) average spacing of ocean circuli and (**B**) estimated average rate of circulus formation for nine year classes (see Table 2) of juvenile coho salmon (*O. kisutch*) caught in the ocean in research nets in August (1981) or September (1982–84 and 1998–2002; black symbols, ±2 SE). Regressions are GM linear regressions of ln-transformed variables (presented in their power function form).

tained by juvenile coho salmon during their first summer, fall, and winter in the ocean.

Do the seasonal changes in circulus spacing in the ocean growth zones of scales coincide with similar seasonal changes in growth rates of juvenile and maturing coho salmon? In Figure 6 we plotted the average lengths of juvenile and maturing coho salmon from all research cruises 1981–2002 and the average apparent growth rates of coho salmon during different seasons (dashed lines). Apparent average growth rate of juvenile coho salmon between June and September was 1.30 mm/d, about twice the apparent growth rate of 0.64 mm/d between September and the following May. Apparent growth rates of maturing fish between late May and late June was very rapid (2.11 mm/d), about twice as great as the apparent growth rate of maturing fish later between June and September (1.01 mm/d).

In a general sense, this pattern of changing apparent growth rate over time in the ocean corresponds well to the pattern of changing circulus spacing seen in Figure 5, A–E. The rapid growth of juvenile coho salmon between June and September occurs during a period when the spacing of circuli generally is high (Fig. 5E). When maturing fish were caught in the ocean fisheries in late June and in July and August a zone of widely spaced circuli already was present on the scales (Fig. 5,

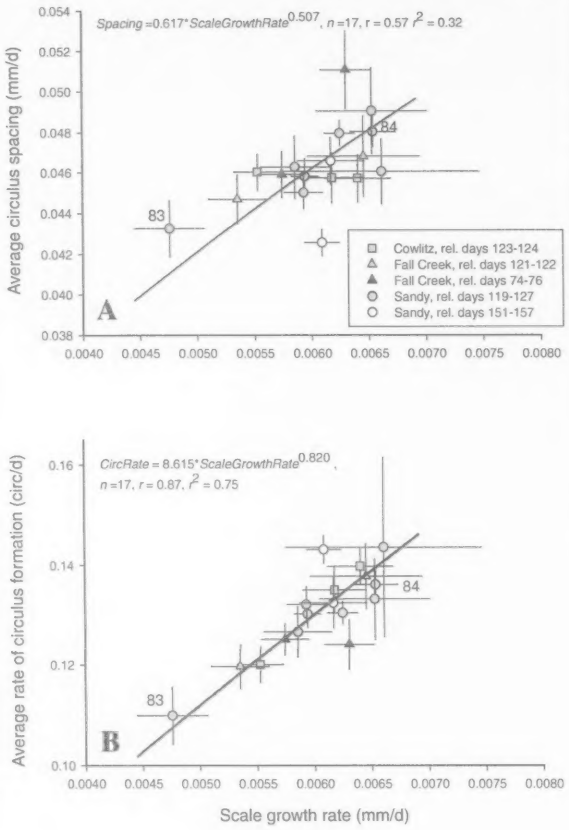

Figure 4

Estimated average scale growth rate versus (**A**) average spacing of ocean circuli and (**B**) estimated average rate of circulus formation for 17 groups (see Table 2) of maturing coho salmon (*O. kisutch*) caught in the Oregon ocean fisheries (±2 SE). Regressions are GM linear regressions of ln-transformed variables (presented in their power function form). Data for Sandy Hatchery fish caught in 1983 and 1984 are labeled as examples of year when average growth rates were extremely different.

A–C), indicating that these widely spaced circuli were produced earlier during the period of apparently rapid growth in the spring and early summer (Fig. 6). Circulus spacing at the scale margin was already declining in July among maturing fish in some years (Fig. 5A), and was clearly lower among maturing fish caught in August or September (Fig. 5, B and D) indicating that these more narrowly spaced circuli were produced sometime during the apparently slower growth of maturing fish between late June and September (Fig. 6). Finally, the low spacing of circuli in the annual ring occurs sometime between late September of the first year and mid-May of the second year, which was also the period of lowest apparent growth rate (Fig. 6).

The pattern of changing circulus spacing at the scale margin is most clearly seen when average spacing of the outer two circulus pairs is plotted against the average julian day of capture (Fig. 7, A and B). Among juvenile fish caught in research nets, the average spacing of the circuli at the scale margin was narrower in September than in June (Fig. 7A, see also Fig. 5E). We lack sufficient FL data from mid and late summer to determine whether or not a decrease in the average growth rate of juvenile fish was associated with the observed

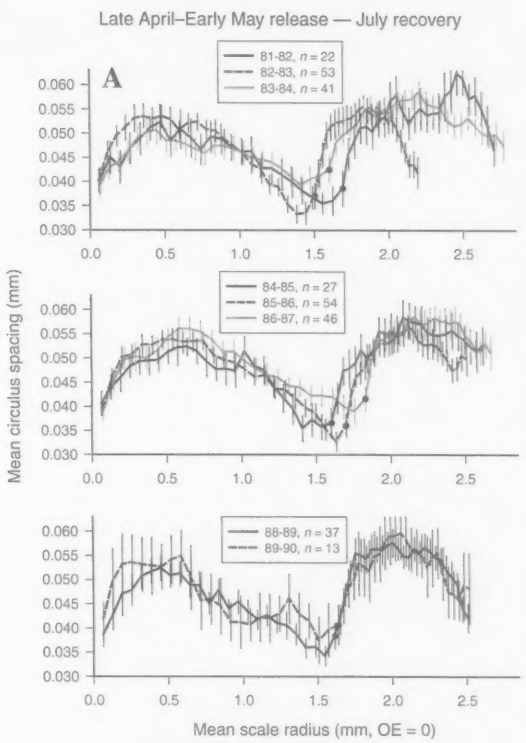
Late April–Early May release — July recovery
A
81-82, n = 22
82-83, n = 53
83-84, n = 41
84-85, n = 27
85-86, n = 54
86-87, n = 46
88-89, n = 37
89-90, n = 13
Mean circulus spacing (mm)
Mean scale radius (mm, OE = 0)

Figure 5

Profiles of changing average circulus spacing (±2 SE) versus average scale radius at 50 intervals along the axis of measurement (see "Methods and Materials" section) for maturing coho salmon (*O. kisutch*) caught in the ocean fisheries and (**A**) released as smolts from hatcheries in late April or early May and caught in July, (**B**) released in March, (**C**) released in late May or early June and caught late June to late July, (**D**) unmarked maturing fish caught in research nets in June 2000 and September 2001, and (**E**) juvenile fish caught September 1999–2002. For clarity, error bars for the average scale radius at each interval are not shown.

decrease in spacing of circuli at the scale margin in September.

Among maturing fish, average spacing of the last two circulus pairs at the scale margin decreased greatly between the spring through early summer period and early fall (Fig. 7B). The decrease in circulus spacing at the scale margin during the summer occurred for both maturing fish of mixed stocks caught in research nets (gray and white symbols) and for CWT fish of known stocks caught in the ocean sport and troll fisheries (black symbols). The decrease also was very consistent among year classes; 11 of the 12 year-class groups (grouped by release period and pooled across hatcheries) of Table 2 showed significant negative correlations between spacing at the margin and date of capture ($P<0.05$, $r=-0.40$ to -0.59). In September the average circulus spacing at the scale margin was about as low as the average circulus spacing in the annual ring (about 0.035 mm).

The decrease in spacing of circuli at the scale margin over the summer mirrors a similar decrease over the summer in apparent growth rates in FL of maturing fish caught in research nets (Fig. 7C). The apparent growth rates of maturing coho salmon were usually

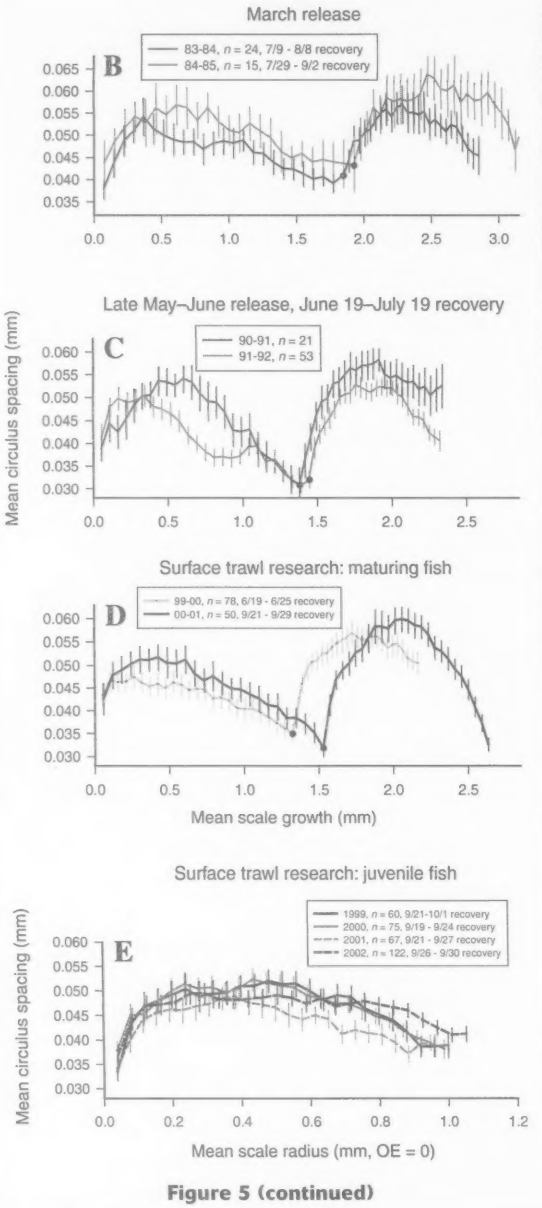
March release
B
83-84, n = 24, 7/9 - 8/8 recovery
84-85, n = 15, 7/29 - 9/2 recovery
Late May–June release, June 19–July 19 recovery
C
90-91, n = 21
91-92, n = 53
Mean circulus spacing (mm)
Surface trawl research: maturing fish
D
99-00, n = 78, 6/19 - 6/25 recovery
00-01, n = 50, 9/21 - 9/29 recovery
Mean scale growth (mm)
Surface trawl research: juvenile fish
E
1999, n = 60, 9/21-10/1 recovery
2000, n = 75, 9/19 - 9/24 recovery
2001, n = 67, 9/21 - 9/27 recovery
2002, n = 122, 9/26 - 9/30 recovery
Mean circulus spacing (mm)
Mean scale radius (mm, OE = 0)

Figure 5 (continued)

higher between the May and June research cruises (2–3 mm FL/d) than between cruises later in the summer (0.5–1.5 mm FL/d)(Fig. 7C, see also Fig. 6). The concurrent decreases in spacing of circuli at the scale margin and in apparent growth rate of coho salmon in the ocean is consistent with the hypothesis that seasonal changes in scale circulus spacing reflect seasonal changes in fish growth rate.

Additional evidence for decreasing growth rate of maturing coho salmon over the course of the summer comes from FLs of CWT fish in the hook-and-line fisheries (sport and troll fisheries). Generally, apparent growth rates in FL of maturing coho salmon originating from northern coastal Oregon streams and from both the Oregon and Washington sides of the Columbia river basin were highest from late May to mid-June and

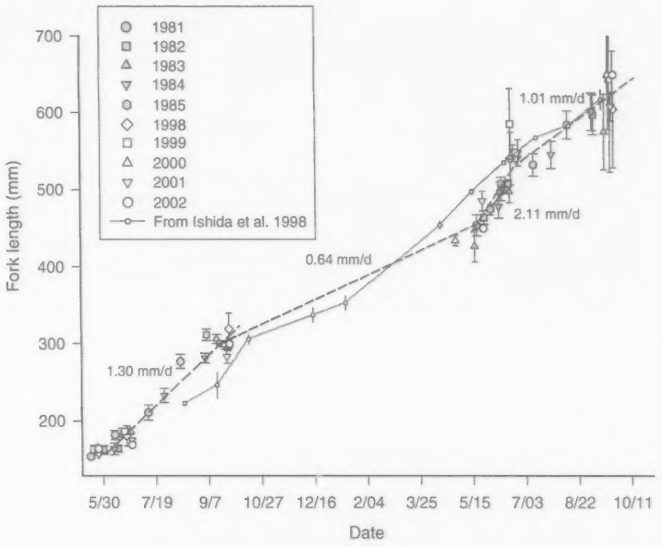

Figure 6

Average lengths (±2 SE) of juvenile and maturing coho salmon (*O. kisutch*) caught during research cruises off Oregon and Washington in different months and years (gray and white symbols. The dashed lines are linear regressions and indicate apparent growth rates in FL between the different catch periods. The late April 2000 sample of maturing coho salmon was from a single trawl off the mouth of the Columbia River (Robert L Emmett, NMFS/NWFSC/HMSC, 2030 S Marine Science Drive, Newport, OR 97365, personal commun.). The small open circles are average lengths (±2 SE) of coho salmon from Ishida et al. (1998) (their Appendix Table 6) plotted against the 15th day of the months in which they were sampled.

decreased greatly by mid-August (Fig. 8, A and B). For three periods, 20 May–29 June, 29 June–8 August, and 8 August–27 September, median apparent growth rates were 1.43 mm/d (n=19), 0.64 mm/d (n=24), and 0.24 mm/d (n=27), respectively.

Growth rates of fish from coastal Washington rivers also decreased over the summer, but the decrease was not as great as for the Oregon and Columbia River fish, and the apparent growth rates of the Washington fish were higher at comparable times during the summer (Fig. 9, A and B). The apparent growth rates of Gray Harbor basin fish were over 2 mm/d from late June to mid-July and remained comparatively high (about 1.0 mm/d) into late October (Fig. 9B). Washington fish generally were not caught in the fisheries until mid- or late June, about a month after the first catches of the Oregon and Columbia River fish. For three periods 19 June–29 July, 29 July–7 September, and 7 September–27 October, median apparent growth rates of the coastal Washington fish were 1.23 mm/d (n=13), 0.92 mm/d (n=16), and 1.06 mm/d (n=9), respectively.

The growth data for CWT fish from the sport and troll fisheries, especially those for the coastal Oregon and Columbia River stocks, were consistent with the growth data from the mixed stock catches of coho salmon in research nets off Oregon and Washington in that both data sets indicated a substantial decrease in growth rate (FL) of maturing coho salmon between the May–June period and the August–September period. The decreases over the summer in circulus spacing at the scale margin (Fig. 7B) and in apparent growth rates of maturing CWT coho salmon of known origin (Fig. 8B) is further evidence that scale circulus spacing and fish growth rate are correlated seasonally.

Discussion

Our data indicate that the seasonal cycle of changing ocean circulus spacing on scales of juvenile and adult coho salmon mirrors a similar seasonal cycle in the growth rate of these fish. We lack direct data for coho salmon collected between late September of the first calendar year of ocean residence and mid-May of the second calendar year, but growth rate during part of the fall and winter may be as low as 0.5mm/d

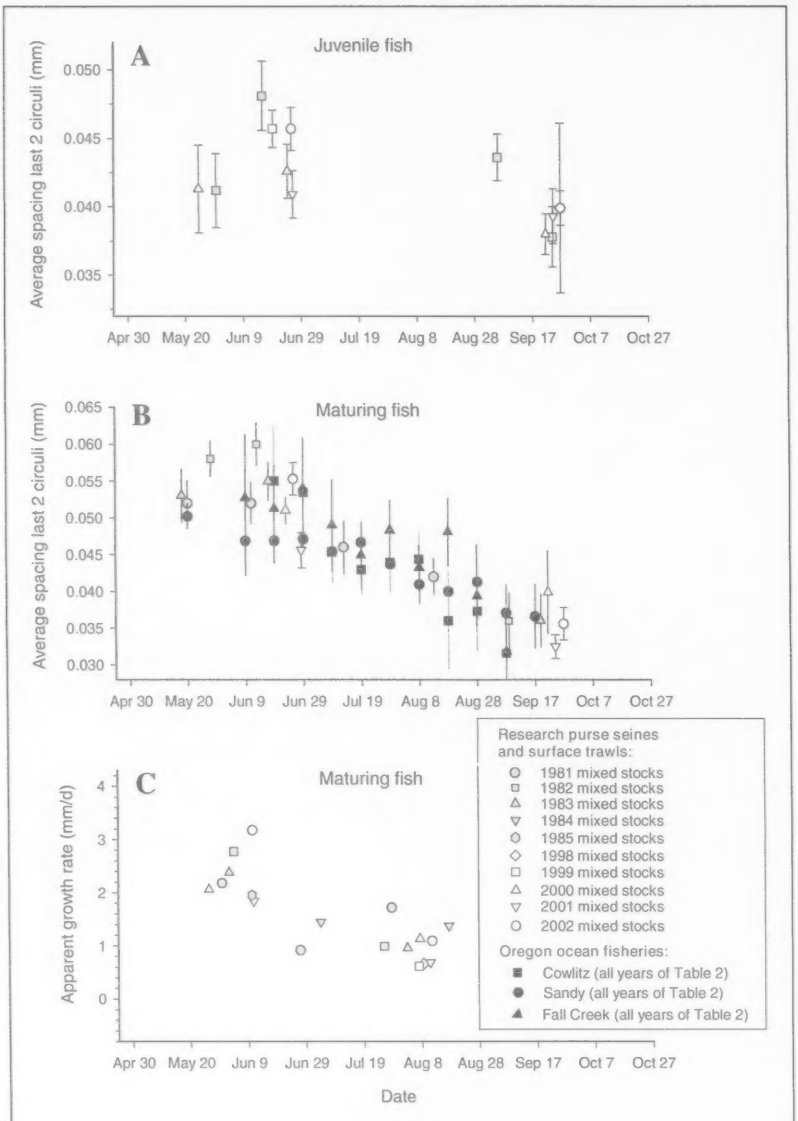

Figure 7

Average spacing of the last two intercircular spaces at the scale margin versus average catch date for (**A**) juvenile coho salmon (*O. kisutch*) caught during research cruises and (**B**) maturing coho salmon caught during research cruises (gray and white symbols) and in the ocean fisheries (black symbols, averaged by 10-day periods, all years combined). Also shown for comparison with the temporal changes in circulus spacing are (**C**) the apparent growth rates of maturing coho salmon between research cruises (based on changes in mean FL; see Fig. 6) plotted against the mid-point of each growth period.

based on data in Ishida et al. (1998). Therefore, the roughly twofold range in spacing of circuli in the ocean growth zone of scales from maturing fish that we found probably represents about a fourfold range in fish growth rate in the ocean (from about 0.5 mm/d in the winter to 2.1mm/d in the spring and early summer). Thus, changes in the spacing of scale circuli are relatively small when compared to the corresponding changes in fish growth

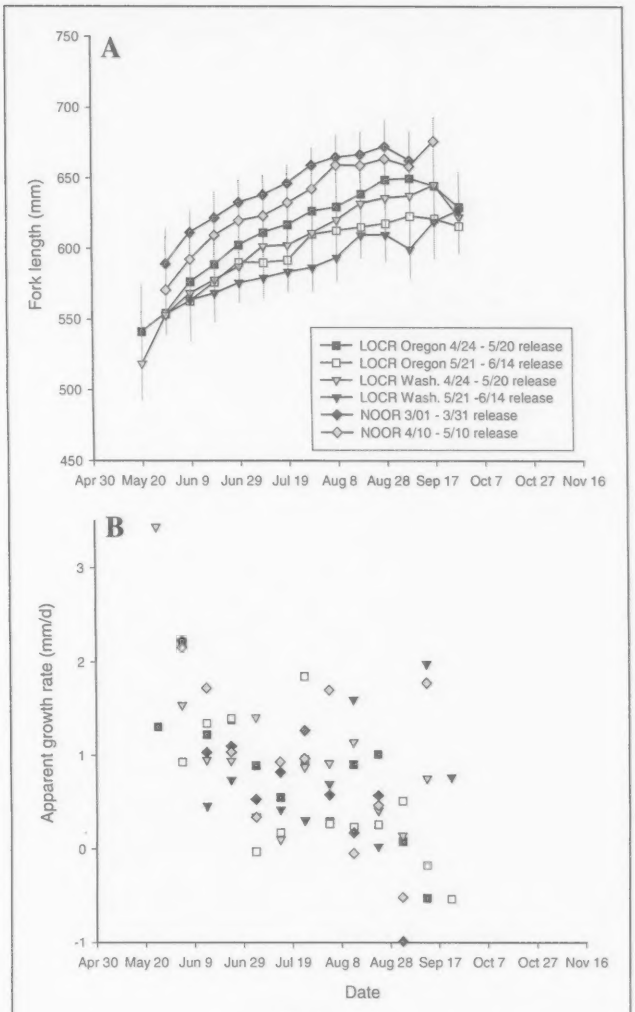
A
Fork length (mm)
750
700
650
600
550
500
450
LOCR Oregon 4/24 - 5/20 release
LOCR Oregon 5/21 - 6/14 release
LOCR Wash. 4/24 - 5/20 release
LOCR Wash. 5/21 -6/14 release
NOOR 3/01 - 3/31 release
NOOR 4/10 - 5/10 release
Apr 30 May 20 Jun 9 Jun 29 Jul 19 Aug 8 Aug 28 Sep 17 Oct 7 Oct 27 Nov 16
B
Apparent growth rate (mm/d)
3
2
1
0
-1
Apr 30 May 20 Jun 9 Jun 29 Jul 19 Aug 8 Aug 28 Sep 17 Oct 7 Oct 27 Nov 16
Date

Figure 8

(**A**) Grand-mean FLs (±2 SE) by 10-day intervals over the years 1975–2002 of CWT lower Columbia River (LOCR) Oregon and Washington stocks and northern coastal Oregon stocks (NOOR) of maturing coho salmon (*O. kisutch*). Only intervals with five or more years of data are shown. (**B**) The corresponding average apparent growth rates between each 10-day interval. Note the apparent decrease in growth rate between early and late summer.

rate. However, the large seasonal changes in growth rate of coho salmon in the ocean are readily detectable from the changes in circulus spacing on the scale.

In June 2001, 2002, and 2003 average spacing of the last two circulus pairs at the scale margin was positively correlated ($P<0.01$) with plasma IGF-I (insulin-like growth factor-I) concentrations from juvenile fish caught in the ocean in research nets (n=119, 163, and 206 and r=0.52, 0.52, and 0.59 in 2001, 2002, and 2003, respectively) (Beckman[2] and Fisher, unpubl. data). Because plasma IGF-I levels have been shown to be positively

[2] Beckman, B. 2004. Unpubl. data. Integrative Fish Biology Program, Northwest Fisheries Science Center, National Marine Fisheries Service, 2725 Montlake Boulevard East, Seattle, Washington 98112.

correlated with instantaneous growth rates (in length) of juvenile coho salmon (Beckman et al., 2004), the finding that plasma IGF-I is also correlated with the spacing of circuli at the scale margin of juvenile coho salmon is further evidence that circulus spacing and growth rate are positively related for coho salmon.

Our data suggest that growth rate in FL of maturing coho salmon is usually highest between early or mid-April and late June. This is a period of increasing photoperiod and often rising sea-surface temperature (SST) at 50°N in the northeastern Pacific Ocean, but is well before the maximum SST in late August (Fig. 10). Both increased day length and temperature stimulate growth in salmonids (Brett, 1979; Björnsson, 1997). The decreases in apparent growth rate in length of maturing coho salmon after the summer solstice could be associated with a number of factors. One possibility is that there is a shift during the summer away from skeletal growth to growth in weight (with a resultant increase in condition) or to gonadal development. Data in Ishida et al. (1998) for coho salmon caught in research nets in the North Pacific tend to support this proposition (their Appendix Table 6). Their data indicate that the rate of growth in FL of maturing coho salmon decreased from 1.45 mm/d between April and May to 0.49 mm/d between July and August. (See also Fig. 6, present study). Over the same time period the condition index (weight (g)×(10^7/FL[mm]^3)) of the fish they sampled increased from 113.3 to 143.8, an increase of 27%. Thus, skeletal growth slowed over the summer, but the condition of the fish increased.

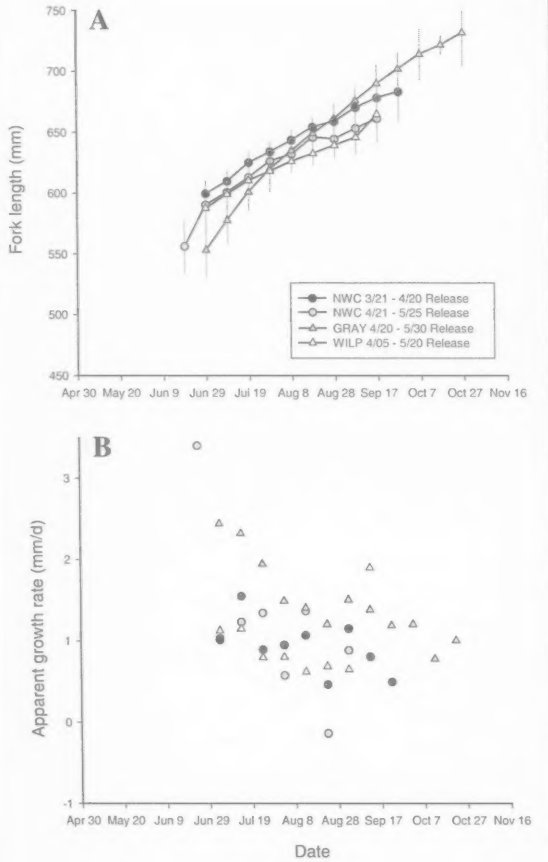

Figure 9

(**A**) Grand-mean FLs by 10-day intervals over the years 1975–2002 of CWT coastal Washington stocks of maturing coho salmon (*O. kisutch*) from the Willapa Bay basin (WILP), Grays Harbor basin (GRAY), and coast north of Grays Harbor (NWC). (**B**) The corresponding average apparent growth rates between each 10-day interval.

In contrast to growth rates of Columbia River coho salmon, which decreased greatly between early and late summer, and were quite low (≤0.5 mm/d) by August and September, the growth rates of fish from the Grays Harbor basin, although also declining during the summer, remained high well into September and early October (~0.7–1.4 mm/d), allowing the Grays Harbor fish to attain a significantly larger final average FL. Several factors may result in the differing growth patterns of maturing fish from these two groups. Many of the fish from the Columbia River are early spawners, and peak spawning occurs from late October to early November, whereas the Grays Harbor fish are mainly late spawners, and peak spawning occurs from mid-November to late-December (Weitkamp et al., 1995). Because of their later spawning the Grays Harbor fish may shift from somatic to gonadal growth later in the summer or fall than do the earlier spawners from the Columbia River. Maturing coho salmon from the Grays Harbor drainage also have a much more northerly distribution than do maturing fish from the Columbia River (Weitkamp and Neely, 2002) and, therefore, the two groups encounter very different ocean conditions (e.g., temperature, salinity, prey fields, prey distributions, and potential competitors for food) while feeding in coastal waters. The different environmental conditions experienced by the Columbia River and Grays Harbor fish may also contribute to their differing temporal growth patterns.

Because of the poor conditions for growth of fish associated with the 1983 El Niño, adult coho salmon in 1983 were exceptionally small off Oregon and were in poor condition (Pearcy et al., 1985; Johnson, 1988). Our scale analysis indicates that the small size of fish in 1983 was largely due to a failure of growth of maturing fish after formation of the winter annulus. Although the average scale radius between OE and the winter annulus was slightly smaller for the 1982–83 year class than for other year classes, the average scale radius between the winter annulus and the scale margin, representing the growth of maturing fish in spring and early summer, was

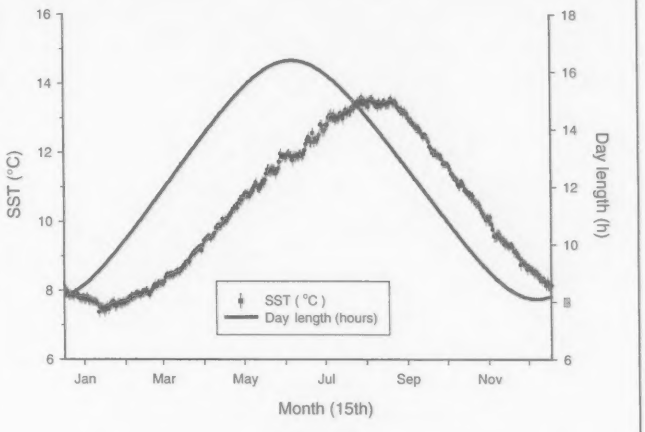

Figure 10

Yearly cycle of day length (sunrise to sunset; black line) at 50°N and of sea surface temperature (SST) (°C; ±2 SE) at Amphitrite Point, Vancouver Island, B.C. SST data from Fisheries and Oceans, Canada, Pacific Region, Science Branch, British Columbia lightstations salinity and temperature data, URL: http://www-sci.pac.dfo-mpo.gc.ca/osap/data/lighthouse/amphitr.day. SST is the daily average for the period 22 August 1934–31 July 1999.

exceptionally low for this year class (Fig. 5A). Circulus spacing revealed two notable trends. First, in 1983 the maximum spacing of circuli following the winter annulus was only very slightly lower than in other years, which indicates that spring growth in FL of maturing fish in 1983 was not unusually low. Perhaps maturing coho salmon continued to grow in length in spring 1983, when photoperiod was increasing rapidly, despite low food availability. Björnsson (1997) found that changes in photoperiod may possibly control the level of pituitary growth hormone (GH), which strongly stimulates skeletal growth in salmonids and that increased levels of GH can induce growth in length even during starvation. Second, the spacing of circuli at the scale margin for fish caught in July 1983 was unusually low, similar to the spacing at the scale margin from fish caught in August of most years. This finding indicates very slow growth rates for maturing fish by July 1983. Length data[1] for maturing CWT coho salmon from the Oregon side of the Columbia River basin caught in the ocean sport and troll fisheries indicated that between June and September 1983 the average length of fish changed very little, which would indicate that somatic growth ceased during the summer.

Our results confirm the utility of circulus spacing as an indicator of growth rate in FL of coho salmon in the ocean. Correlations between average circulus spacing and estimated average growth rates of groups of fish were significant and positive (Table 4), even when growth was measured over long intervals of time (four to five months for juveniles, and over a year for maturing coho salmon), and even when the estimates of growth rate were subject to error In addition, our data indicate large seasonal changes in growth rate in FL of coho salmon in the coastal ocean off Oregon and Washington, a result also suggested by data in Ishida et al. (1998) for coho salmon in the North Pacific (see Fig. 6), and these seasonal changes in growth rate appear to be tracked by seasonal changes in spacing of scale circuli.

Acknowledgments

We thank all personnel from the Estuarine and Ocean Ecology Division of the National Marine Fisheries Service and from Oregon State University who participated either in the research cruises or in processing samples from those cruises. We also thank Lisa Borgerson of the Oregon Department of Fish and Wildlife for supplying scales from coho salmon caught in the ocean fisheries, and the captains and crews of the FV *Sea Eagle*, FV *Ocean Harvester*, FV *Frosti* and the RV *Ricker* for their expert assistance during the cruises. Ric Brodeur and Edmundo Casillas provided helpful comments on an earlier version of this paper. This study was funded by the Bonneville Power Administration through a grant to the National Marine Fisheries Service and from NMFS to Oregon State University.

Literature cited

Bailey, K. M., and E. D. Houde.
1989. Predation on eggs and larvae of marine fishes and the problem of recruitment. Adv. Mar. Biol. 25:1–83.

Bax, N. J.
1983. Early marine mortality of marked juvenile chum salmon (*Oncorhynchus keta*) released in Hood Canal, Puget Sound, Washington, in 1980. Can. J. Fish. Aquat. Sci. 40:426–435.

Beamish, R. J., and D. R. Bouillon.
1993. Pacific salmon production trends in relation to climate. Can. J. Fish. Aquat. Sci. 50:1002–1016.

Beckman, B. R., W. Fairgrieve, and K. A. Cooper,
C. V. W. Mahnken, and R. J. Beamish.
2004. Evaluation of endocrine indices of growth in individual postsmolt coho salmon. Trans. Am. Fish. Soc. 133:1057–1067.

Bhatia, D.
1932. Factors involved in the production of annual zones on the scales of the rainbow trout (*Salmo irideus*). II. J. Exp. Biol. 9:6–11.

Bigelow, P. E., and R. G. White.
1996. Evaluation of growth interruption as a means of manipulating scale patterns for mass-marking hatchery trout. N. Am. J. Fish. Manag. 16:142–153.

Bilton, H. T.
1975. Factors influencing the formation of scale characters. Int. North Pac. Fish Comm. Bull. 32:102–108.

Bilton, H. T., and G. L. Robins.
1971. Effects of feeding level on circulus formation on scales of young sockeye salmon (*Oncorhynchus nerka*). J. Fish. Res. Board Can. 28:861–868.

Björnsson, B. T.
1997. The biology of salmon growth hormone: from daylight to dominance. Fish Physiol. Biochem. 17:9–24.

Blackbourn, D. J.
1990. Comparison of release size and environmental data with the marine survival rates of some wild and enhanced stocks of pink and chum salmon in British Columbia and Washington state. *In* Proceedings 14th northeast Pacific pink and chum salmon workshop (P. A. Knudsen, ed.), p. 82–87. Washington Dept. Fish., Olympia, WA.

Brett, J. R.
1979. Environmental factors and growth. *In* Fish physiology, vol. 8, Bioenergetics and growth (W. S. Hoar, D. J. Randall, and J. R. Brett, eds.), p. 599–675. Academic Press, New York, NY.

Clutter, R. I., and L. E. Whitesel.
1956. Collection and interpretation of sockeye salmon scales. Int. Pac. Salmon Fish. Comm. Bull. 9, 159 p.

Dawley, E. M., R. D. Ledgerwood, and A. Jensen.
1985a. Beach and purse seine sampling of juvenile salmonids in the Columbia River estuary and ocean plume, 1977–1983. Volume I: Procedures, sampling effort, and catch data. NOAA Tech. Memo. NMFS F/NWC-74. i-x, 397 p.
1985b. Beach and purse seine sampling of juvenile salmonids in the Columbia River estuary and ocean plume, 1977–1983. Volume II: Data on marked recoveries. NOAA Tech. Memo. NMFS F/NWC-75. i–vii, 260 p.

Doyle, R. W., A. J. Talbot, and R. R. Nicholas.
1987. Statistical interrelation of length, growth, and scale circulus spacing: appraisal of a growth rate estimator for fish. Can. J. Fish. Aquat. Sci. 44:1520–1528.

Emmett, R. L., and R. D. Brodeur.
2000. Recent changes in the pelagic nekton community off Oregon and Washington in relation to some physical oceanographic conditions. North Pacific Anadr. Fish Comm. Bull. 2:11–20.

Fisher, J. P., and W. G. Pearcy.
1988. Growth of juvenile coho salmon (*Oncorhynchus kisutch*) in the ocean off Oregon and Washington, USA, in years of differing coastal upwelling. Can. J. Fish. Aquat. Sci. 45:1036–1044.
1990. Spacing of scale circuli versus growth rate in young coho salmon. Fish. Bull. 88:637–643.

Friedland, K. D., and R. E. Haas.
1996. Marine post-smolt growth and age at maturity of Atlantic salmon. J. Fish Biol. 48:1–15.

Friedland, K. D., L. P. Hansen, D. A. Dunkley, and
J. C. MacLean.
2000. Linkage between ocean climate, post-smolt growth, and survival of Atlantic salmon (*Salmo salar* L.) in the North Sea area. ICES Journal of Marine Science. 57:419–429.

Friedland, K. D., and D. G. Reddin.
2000. Growth patterns of Labrador Sea Atlantic salmon postsmolts and the temporal scale of recruitment synchrony for North American salmon stocks. Can. J. Fish. Aquat. Sci. 57:1181–1189.

Friedland, K. D., D. G. Reddin, and J. F. Kocik.
1993. Marine survival of North American and European Atlantic salmon: effects of growth and environment. ICES J. Mar. Sci. 50:481–492.

Fukuwaka, M., and M. Kaeriyama.
1997. Scale analyses to estimate somatic growth in sockeye salmon, *Oncorhynchus nerka*. Can. J. Fish. Aquat. Sci. 54:631–636.

Glenn, C. L., and J. A. Mathias.
1985. Circuli development on body scales of young pond-reared walleye (*Stizostedion bitreum*). Can. J. Zool. 63:912–915.

Hare, S. R., N. J. Mantua, and R. C. Francis.
1999. Inverse production regimes: Alaska and West Coast Pacific salmon. Fisheries 24:6–15.

Healey, M. C.
1982. Timing and relative intensity of size-selective mortality of juvenile chum salmon (*Oncorhynchus keta*) during early sea life. Can. J. Fish. Aquat. Sci. 39:952–957.

Hobday, A. J., and G. W. Boehlert.
2001. The role of coastal ocean variation in spatial and temporal patterns in survival and size of coho salmon (*Oncorhynchus kisutch*). Can. J. Fish. Aquat. Sci. 58:2021–2036.

Holtby, L. B., B. C. Andersen, and R. K. Kadawaki.
1990. Importance of smolt size and early ocean growth to interannual variability in marine survival of coho salmon (*Oncorhynchus kisutch*). Can. J. Fish. Aquat. Sci. 47:2181–2194.

Ishida, Y., S. Ito, Y. Ueno, and J. Sakai.
1998. Seasonal growth patterns of Pacific salmon (*Oncorhynchus* spp.) in offshore waters of the North Pacific Ocean. N. Pac. Anadr. Fish Comm. Bull. 1:66–80.

Jaenicke, H. W., M. J. Jaenicke, and G. T. Oliver.
1994. Predicting northern southeast Alaska pink salmon returns by early marine scale growth, p. 97–110. North-

east Pacific pink and chum salmon workshop, Alaska Sea Grant Prog., Alaska Univ., Fairbanks, AK.

Johnson, S. L.
1988. The effects of the 1983 El Niño on Oregon's coho (*Oncorhynchus kisutch*) and chinook (*O. tshawytscha*) salmon. Fish. Res. 6:105–123.

Litvak, M. K., and W. C. Leggett.
1992. Age and size-selective predation on larval fishes: the bigger-is-better hypothesis revisited. Mar. Ecol. Prog. Ser. 81:13–24.

Mathews, S. B., and Y. Ishida.
1989. Survival, ocean growth and ocean distribution of differentially timed releases of hatchery coho salmon (*Oncorhynchus kisutch*). Can. J. Fish. Aquat. Sci. 46:1216–1226.

Matricia, T. A. J. Talbot and R. W. Doyle.
1989. Instantaneous growth rate of tilapia genotypes in undisturbed aquaculture systems. I. "Red" and "grey" morphs in Indonesia. Aquaculture 77:295–306.

Mantua, N. J., S. R. Hare, Zhang, Y., J. M. Wallace and F. C. Francis.
1997. A Pacific interdecadal climate oscillation with impacts on salmon production. Bull. Am. Meteorol. Soc. 78:1069–1080.

Miller, T. J., L. B. Crowder, J. A. Rice, and E. A. Marschall.
1988. Larval size and recruitment mechanisms in fishes: toward a conceptual framework. Can. J. Fish. Aquat. Sci. 45:1657–1670.

Parker, R. R.
1971. Size selective predation among juvenile salmonid fishes in a British Columbia inlet. J. Fish. Res. Board Can. 28:1503–1510.

Pearcy, W., J. Fisher, R. Brodeur, and S. Johnson.
1985. Effects of the 1983 El Niño on coastal nekton off Oregon and Washington. *In* El Niño North, Niño effects in the eastern subarctic Pacific Ocean, p. 188–204. Washington Sea Grant Program, Univ. Washington, Seattle, WA.

Pearcy, W. G., and J. P. Fisher.
1988. Migrations of coho salmon, *Oncorhynchus kisutch*, during their first summer in the ocean. Fish. Bull. 86:173–195.
1990. Distribution and abundance of juvenile salmonids off Oregon and Washington, 1981–1985. NOAA Tech. Rep. NMFS 93, 83 p.

Pyper, B. J., R. M. Peterman, M. F. Lapointe, and C.J . Walters.
1999. Patterns of covariation in length and age at maturity of British Columbia and Alaska sockeye salmon (*Oncorhynchus nerka*) stocks. Can. J. Aquat. Sci. 56: 1046–1057.

Ricker, W. E.
1973. Linear regressions in fishery research. J. Fish. Res. Board Can. 30:409–434.
1992. Back-calculation of fish lengths based on proportionality between scale and length increments. Can. J. Fish. Aquat. Sci. 49:1018–1026.

Scarnecchia, D. L.
1979. Variation of scale characteristics of coho salmon with sampling location on the body. Prog. Fish-Cult. 41:132–135.

Sogard, S. M.
1997. Size-selective mortality in the juvenile stage of teleost fishes: a review. Bull. Mar. Sci. 60:1129–1157.

Sokal, R. R., and F. J. Rohlf.
1995. Biometry. The principles and practice of statistics in biological research, 3rd ed., 887 p. W.H. Freeman and Company, New York, NY.

Talbot, A. J., and R. W. Doyle.
1992. Statistical interrelation of length, growth, and scale circulus spacing: use of ossification to detect nongrowing fish. Can. J. Fish. Aquat. Sci. 49:701–707.

Teel, D. J., D. M. Van Doornik, D. R. Kuligowski, and W. S. Grant.
2003. Genetic analysis of juvenile coho salmon (*Oncorhynchus kisutch*) off Oregon and Washington reveals few Columbia River wild fish. Fish. Bull. 101:640–652.

Weitkamp, L., and K. Neely.
2002. Coho salmon (*Oncorhynchus kisutch*) ocean migration patterns: insight from marine coded-wire tag recoveries. Can. J. Fish. Aquat. Sci. 59:1100–1115.

Weitkamp, L. A., T. C. Wainwright, G. J. Bryant, G. B. Milner, D. J. Teel, R. G. Kope, and R. S. Waples.
1995. Status review of coho salmon from Washington, Oregon, and California. NOAA Tech. Memo. NMFS-NWFSC-24, 258 p.

Willette, T. M.
1996. Impacts of the Exxon Valdez oil spill on the migration, growth, and survival of juvenile pink salmon in Prince William Sound. Am. Fish. Soc. Symp. 18:533–550.
2001. Foraging behaviour of juvenile pink salmon (*Oncorhynchus gorbuscha*) and size-dependent predations risk. Fish. Oceanogr. 10(Suppl. 1):110–131.

Escapement of the Cape rock lobster (*Jasus lalandii*) through the mesh and entrance of commercial traps

Johan C. Groeneveld

Marine and Coastal Management
5th floor Foretrust Building
Martin Hamerschlacht Street, Foreshore
Cape Town, South Africa
E-mail address: Jgroenev@deat.gov.za

Jimmy P. Khanyile

National Research Foundation
P.O. Box 2600
Pretoria 0001, South Africa

David S. Schoeman

Department of Zoology
University of Port Elizabeth
Port Elizabeth 6031, South Africa

Abstract—Metal-framed traps covered with polyethylene mesh used in the fishery for the South African Cape rock lobster (*Jasus lalandii*) incidentally capture large numbers of undersize (<75 mm CL) specimens. Air-exposure, handling, and release procedures affect captured rock lobsters and reduce the productivity of the stock, which is heavily fished. Optimally, traps should retain legal-size rock lobsters and allow sublegal animals to escape before traps are hauled. Escapement, based on lobster morphometric measurements, through meshes of 62 mm, 75 mm, and 100 mm was investigated theoretically under controlled conditions in an aquarium, and during field trials. SELECT models were used to model escapement, wherever appropriate. Size-selectivity curves based on the logistic model fitted the aquarium and field data better than asymmetrical Richards curves. The lobster length at 50% retention (L_{50}) on the escapement curve for 100-mm mesh in the aquarium (75.5 mm CL) approximated the minimum legal size (75 mm CL); however estimates of L_{50} increased to 77.4 mm in field trials where trap-entrances were sealed, and to 82.2 mm where trap-entrances were open. Therfore, rock lobsters that cannot escape through the mesh of sealed field traps do so through the trap entrance of open traps. By contrast, the wider selection range and lower L_{25} of field, compared to aquarium, trials (SR=8.2 mm vs. 2.6 mm; L_{25}=73.4 mm vs. 74.1 mm), indicate that small lobsters that should be able to escape from 100-mm mesh traps do not always do so. Escapement from 62-mm mesh traps with open entrance funnels increased by 40–60% over sealed traps. The findings of this study with a known size distribution, are related to those of a recent indirect (comparative) study for the same species, and implications for trap surveys, commercial catch rates, and ghost fishing are discussed.

Manuscript submitted 20 March 2003 to the Scientific Editor.

Manuscript approved for publication 1 July 2003 by the Scientific Editor.

Fish Bull. 103:52–62 (2005).

The traps used in lobster and crab fisheries are a versatile fishing gear that can be modified to target specific species and size ranges through choice of design and bait (Miller, 1990). Selection by traps of only the desired size classes reduces sorting time and may increase the catch rates of legal-size animals (Fogarty and Borden, 1980; Everson et al., 1992; Rosa-Pacheco and Ramirez-Rodriguez, 1996). Capture, sorting and release procedures have furthermore been implicated in accidental and stress-induced mortalities (Brown and Caputi, 1983; 1985; Hunt et al., 1986), as well as in sublethal injuries, such as limb loss (legs or antennae), which may retard somatic growth (Davis, 1981; Brown and Caputi, 1985). Air exposure, even over short periods, can induce behavioral changes such as reduced responsiveness to threatening stimuli (Vermeer, 1987) and lead to higher predation risk among released animals (Brown and Caputi, 1983). Furthermore, displacement from home reefs disrupts feeding behavior and can affect growth increments (Brown and Caputi, 1985). Managers of many crustacean trap fisheries have responded to these problems by introducing escape vents of various sizes and shapes (Krouse, 1989; Miller, 1990; Everson et al., 1992; Arana and Ziller, 1994; Rosa-Pacheco and Ramirez-Rodriguez, 1996; Treble et al., 1998; Schoeman et al., 2002a), because they successfully allow undersize specimens to escape (Arana and Ziller, 1994; Treble et al. 1998).

In fisheries management, size selectivity curves are important for estimates of incidental mortality, recruitment in yield-per-recruit analysis, and age- and length-based population models (Millar and Fryer, 1999). Notably, size selectivity can be used to evaluate the minimum legal size (MLS) and the effects of changing escape vent or mesh size regulations on the future productivity of the resource (Treble et al., 1998).

Most selectivity studies on which mesh- or escape vent size are based are comparative (indirect), implying that the size distribution of the population is unknown and that variants of the same gear type are fished simultaneously (Millar and Fryer, 1999). Results from indirect studies can, however, be influenced by trap soak times, trap saturation effects (Miller, 1990), seasonal size and sex-specific patterns in catchability (Pollock and Beyers, 1979), and by differences in morphometric ratios of subpopulations (Fogarty and Borden,

1980; Maynard et al., 1987). These disadvantages are offset by the convenience with which indirect studies measure selectivity under operational conditions. Far fewer direct studies, in which the size distribution of the fished population is known (Millar and Fryer, 1999), have been published, and those that have been published have included several laboratory studies where the escape of crustaceans from traps was monitored (Krouse and Thomas, 1975; Krouse, 1978; Everson et al., 1992). Direct studies do not recreate true commercial conditions, but rather provide a contact-selectivity curve (or retention curve) that quantifies the difference in length distribution between the catch and the population of fish coming in contact with the gear (Millar and Fryer, 1999). This information is useful as a benchmark against which operational, seasonal, and spatial selectivity patterns can be measured.

Commercial fishing for the South African Cape rock lobster (*Jasus lalandii*) originated in the late nineteenth century and reached its pinnacle in the 1950s, when nearly 11,000 tons were landed annually (Pollock, 1986). However, since then catches have declined markedly, especially during the 1990s, when annual catch restrictions based on the assumption of decreased population strength, reduced the yield to 2000–3000 tons per year (Pollock et al., 2000). In response to these operational changes, several recent modifications have been made to the regulations governing gear used in the fishery (Schoeman et al., 2002b). The changes most pertinent to this study took place in 1984, when mesh size was increased from 62 to 100 mm (stretched) to reduce the relative catch of undersize *J. lalandii* (Schoeman et al., 2002b), and during the early 1990s, when the minimum size limit was reduced from its historic level of 89 mm carapace length (CL) to 75 mm CL (Cockcroft and Payne, 1999; Pollock et al., 2000). Despite these two measures, the proportion of the commercial catch <75 mm CL that has to be released remains around 35–40% (MCM[1]). At present, the biomass of the *J. lalandii* resource that is larger than the minimum legal size is estimated at about 6% of its pristine value, whereas the spawning biomass (of mature female rock lobsters) is estimated to be 21% (Johnston, 1998). Consequently, it is clear that the resource is heavily depleted and that there is little scope for wasted production through unnecessary damage to undersize lobsters (Schoeman et al., 2002a).

Most studies on trap selectivity of *J. lalandii* (Newman and Pollock, 1969; Crous, 1976; Pollock and Beyers, 1979) predate the changes to mesh and minimum legal size described above and did not provide selectivity curves. In the only recent study, Schoeman et al. (2002a) used the SELECT (Share Each LEngth class's Catch Total) method (Millar, 1992, Milllar and Walsh, 1992) to investigate the selectivity properties of various modifications to commercial and research traps in comparison with the standard 100-mm stretched mesh trap design. This study was indirect, in that it simulated commercial fishing and compared catch rates in other traps to those made with a small-mesh (62 mm, stretched) trap, which acted as a control.

Several processes are involved in the selectivity of traps: namely the attraction of rock lobsters by bait; their ability to enter traps through trap openings of various sizes, shapes, and localities within the trap; their behavior in and around traps; their escapement through the trap opening and their escapement through mesh openings or escape vents (Miller, 1990). The present study focuses on escapement of captured *J. lalandii* through the mesh of stretched mesh traps and through trap entrances. The aims are to investigate the relationships between CL and other morphometric measures for male rock lobsters in order to use these relationships to estimate theoretical escapement curves for any given mesh size; to compare these curves to observed escapement rates through selected meshes in the aquarium; and to extend these comparisons to field conditions. The overall aim is to determine the optimum mesh characteristics that maximize efficiency in targeting legal-size male *J. lalandii*.

Material and methods

Mesh size of lobster traps

Mesh size is defined as the measurement from inside of knot to inside of knot when the net is stretched in the direction of the long diagonal of the meshes, i.e., lengthwise of the net. Netting is made of polyethylene. Commercial rock lobster traps (Fig. 1) are covered with 100-mm stretched mesh (or 50-mm bars, also measured from the insides of knots), which are stretched in such a manner over the metal frame that the openings are square.

Morphometric variables measured

Following manual trials that involved fitting lobster carapaces of different sizes through an adjustable square hole, three carapace dimensions were identified as likely to play a role in regulating escapement. These were the following: 1) carapace width (CW), measured laterally, across the widest point of the carapace; 2) carapace depth (CD), measured dorsoventrally, extending from the highest point of the dorsal carapace surface to the lowest point on the ventral surface of the thoracic plate; and 3) carapace base (CB), measured ventrally, between the distal edges of the second segment of the last walking legs, with the legs folded flush against the carapace.

Each of these dimensions was measured (±1 mm) for each of 169 male rock lobsters caught in research traps deployed off the Cape Peninsula between 1999 and 2002. Corresponding data regarding carapace length

[1] MCM (Marine and Coastal Management). 2002. Unpubl. data. MCM, Martin Hamershclacht St., Cape Town, South Africa.

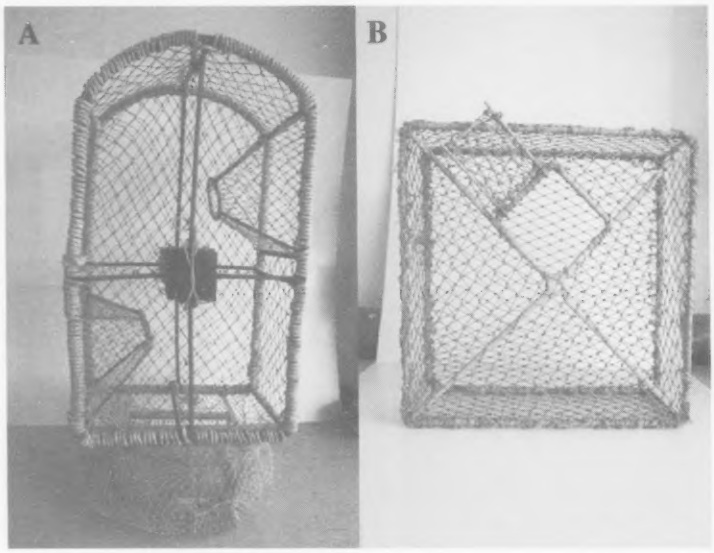

Figure 1

(**A**) Standard metal-framed traps (0.8 m × 0.5 m × 1.35 m high) covered with stretched polyethylene mesh used in the commercial fishery for *J. lalandii* and during field experiments (note the 100-mm mesh size covering on the commercial traps, and the 62-mm mesh size on the codend and entrance funnel). (**B**) Metal-framed escapement cages covered with 62-mm (shown), 75-mm, and 100-mm mesh used in the aquarium experiments (frames were 0.6 m × 0.6 m, with a depth of 0.25 m).

(CL), measured mid-dorsally from the posterior edge of the carapace to the anterior tip of the rostral spine, were also collected. This was done because CL is the dimension most frequently mentioned in legislation pertaining to this species (Schoeman et al., 2002b) and has therefore been the focus of most size-based studies (Newman and Pollock, 1969; Pollock and Beyers, 1979; Schoeman et al., 2002a). Relationships between the CL and each of CW, CD, and CB were explored by using simple least-squares regression analyses.

Theoretical calculations of escapement

In order to investigate morphological characteristics that physically limit escapement through meshes of various dimensions as a function of CL, digital photographs were taken of the posterior cross section of 46 male carapaces (tail removed) covering a range of sizes between 40 mm CL and 106 mm CL. Using standard graphics software, we superimposed a square on each image to represent a square of polyethylene mesh, similar to that used in a South African rock lobster trap.

This simulated mesh was orientated so that its base was parallel with the carapace base of the lobster under consideration. It was then proportioned so that each of its sides was equal in length to the corresponding CB. Once this procedure had been completed, the simulated mesh square was rotated and resized so that we could determine the dimensions of the smallest square through which each lobster could pass. This measure was designated the "critical mesh size" for that image.

Critical mesh size was related to CL by using simple linear regression analysis. In this way, the theoretically appropriate mesh aperture required to target all lobster larger than a given size could be predicted from the minimum CL of the target group (for convenience, this CL will be designated the "critical CL").

Aquarium trials

Having addressed the matter of whether or not lobsters theoretically should be able to escape a mesh of given dimensions, the next question to be posed is whether or not they can do so under ideal (laboratory) conditions? For these purposes, three stretched mesh sizes were considered: 1) 62 mm, which coincides with the mesh size used in the commercial fishery prior to 1984 and also with the mesh currently used on traps deployed in the Fishery Independent Monitoring Survey (FIMS) (Schoeman et al., 2002a); 2) 100 mm, which corresponds with the mesh currently used on commercial traps for *J. lalandii*; and 3) 75 mm, which was used to provide

information on selectivity for meshes of intermediate aperture dimensions.

Each of these experimental meshes was used to construct an escapement cage by stretching the mesh over a mild-steel frame in order to present square escape apertures of varying dimensions, as determined by the size of the mesh used (Fig. 1). These cages were deployed in an aquarium tank measuring 1.8 m×1.8 m and having a depth of 1.5 m. Fresh sea water was continuously supplied to this tank by a through-flow system that regulating water temperature between 12° and 16°C, well within the natural temperature range of *J. lalandii* (Heydorn, 1969).

For each mesh size, male rock lobsters of various carapace lengths (373 lobsters measuring 34–91 mm CL for 62-mm mesh; 351 lobsters measuring 34–75 mm CL for 75-mm mesh; and 142 lobsters measuring 70–91 mm CL for 100-mm mesh) were collected live from the sea and transported to the experimental aquarium tank. Care was taken to ensure that approximately equal numbers of lobsters were available for each 2-mm size-class within the respective size ranges, although fewer lobsters tended to be available in size classes towards the ends of the frequency distributions.

Once at the aquarium, lobsters were placed inside the experimental cages in groups of up to 20 and left for 30 minutes. Individuals that did not escape during this period were gently pushed towards the mesh openings, encouraging escapement, where this was possible. Subsequently, the CL frequency distributions were determined both for those lobsters that escaped the mesh as well as those that were retained. Several replicate escapement experiments were conducted for each mesh size, but because the experimental cages were too small to hold large numbers of lobsters, replicate selection curves could not be computed. Instead, all data were pooled for each mesh size for further analyses.

Field trials

The final question to be posed is whether or not lobsters do escape from traps when afforded the opportunity to do so under field conditions? To address this problem, field trials were undertaken off the Western Cape Peninsula during monthly sampling sessions conducted by the research vessel *Sardinops* in July 2000 and from December 2001 to March 2002—a total of five distinct sampling surveys.

Four categories of standard rock lobster traps (Fig. 1) were employed: 1) 62-mm stretched mesh, with entrance funnels open; 2) 62-mm stretched mesh, with entrance funnels blocked by a fine-mesh insert; 3) 100-mm stretched mesh, with entrance funnels open; and 4) 100-mm stretched mesh, with entrance funnels blocked.

Duplicate bottom long-lines consisting of 10 traps each were prepared, of which six were normal commercial traps, and the remaining four were experimental traps, and these 10 traps were spread in haphazard order along the line, excluding the end traps. Into each trap was placed a sample of approximately 40 male rock lobsters, each of which had been measured (CL) and marked by cutting a notch in its uropod. In this way, it was possible to distinguish between lobsters that had been placed in the trap and those that had entered the trap of their own accord.

Experimental traps were deployed without bait, in order to limit their ability to attract lobsters and also to remove one of the prime incentives that captive lobsters might have to remain in a trap, even when it could escape. These trap lines were soaked overnight and on their retrieval, each remaining lobster was re-measured (CL) and inspected to identify specimens that had entered the traps voluntarily. Eight replicates were completed for each of the four categories of traps.

Construction of selectivity curves

The contact-selection curves (*sensu* Millar and Fryer, 1999) for the meshes used in the laboratory and field trials were modeled by using the SELECT method (Millar and Walsh, 1992) as applied to covered codend experiments (Millar and Fryer, 1999). We felt that this approach was warranted because we collected data with respect to lobsters in both a "codend" (those retained in the traps) and a "cover" (those that escaped, but for which data were available by inference).

The logistic and Richards formulations of the general selectivity curve were fitted by using Excel (Microsoft, Redmond, WA) routines (Tokai[2]). These two selectivity functions were chosen because of their relative simplicity, their broad use over a range of different fisheries, and the availability of estimation routines for their parameters (Millar and Fryer, 1999).

The Richards curve has the equation

$$r(l)=\left(\frac{\exp(a+bl)}{1+\exp(a+bl)}\right)^{\frac{1}{\delta}},$$

where $r(l)$ is the probability that an individual of length l attempting to pass through a mesh of given size will be retained by it (Millar and Fryer, 1999); and a, b, and δ are constants. The logistic curve is the special case of this formulation, where $\delta=1$.

According to these models, the lobster length at 50% retention (L_{50}) and the selection range ($SR=L_{75}-L_{25}$) are defined as follows:

$$L_{50}=\frac{\ln\left(\frac{0.5^{\delta}}{1-0.5^{\delta}}\right)-a}{b},$$

simplifying to $L_{50}=-\frac{a}{b}$ when $\delta=1$, and

[2] Tokai, T. 2002. Personal commun. Department of Marine Science and Technology, Tokyo University of Fisheries, Konan Minatoku, Tokyo 108, Japan.

$$SR = \frac{\ln\left(\frac{0.75^{\delta}}{1-0.75^{\delta}}\right) - \ln\left(\frac{0.25^{\delta}}{1-0.25^{\delta}}\right)}{b},$$

simplifying to $SR = \frac{2\ln(3)}{b}$, when $\delta = 1$.

All calculations were made on the basis of 2-mm-CL size classes covering the entire size range for each frequency distribution. The 2-mm-CL size classes were used to ensure consistency across models, and also to balance data resolution against the number of size classes expected to have either zero catch or zero escapement (Millar and Fryer, 1999). Wherever necessary, hypothesis tests were conducted in accordance with the recommendations of Millar and Walsh (1992) and Millar and Fryer (1999).

Results

Morphometric relationships

Least-squares regression analysis indicated highly significant linear relationships between CL and each of the other morphometric variables measured (Fig. 2). In each case, at least 97% of the variability in the predictor variable was explained by CL, indicating a high degree of correlation among predictors. Nevertheless, for any given CL, CB was consistently the largest variable measured, whereas CD was the smallest. Furthermore, CB increased more rapidly in response to increasing CL than either CW or CD (ANCOVA: F=115.165; df=2, 167; P<0.001). We therefore concluded that CB would likely be the morphometric variable that limits escapement through stretched square meshes.

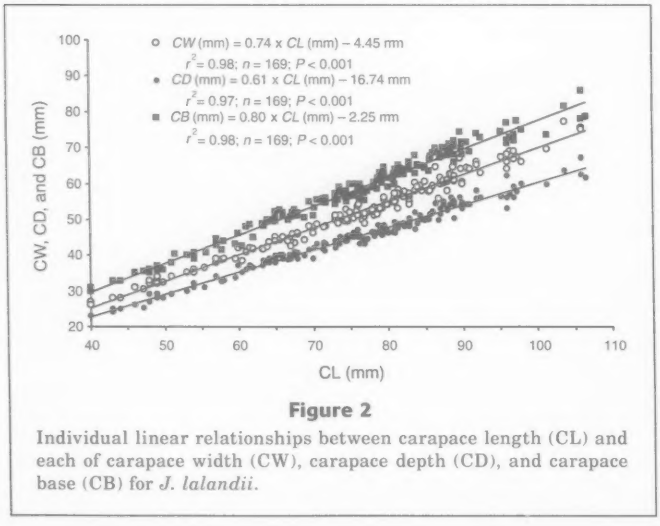

Figure 2

Individual linear relationships between carapace length (CL) and each of carapace width (CW), carapace depth (CD), and carapace base (CB) for *J. lalandii*.

Theoretical calculation of escapement

The mesh size that appeared (on the basis of visual inspection) to limit escapement was expressed as a function of CL with a simple, linear, least-squares regression model (Fig. 3). This relationship was highly significant and explained 99% of the variability in critical mesh size.

Using inverse prediction methods (Zar, 1999), we calculated the critical CL (mean ±95% confidence interval) from the regression model illustrated in Figure 3 for any mesh size. For 62-mm mesh, the critical CL is estimated at 43.8 (±4.12) mm; for the 75-mm mesh the estimate is 52.3 (±4.15) mm; whereas for the 100-mm mesh it is 68.7 (±4.12) mm. Given the implicit assumption that lobsters smaller than the critical CL can escape, but that larger lobsters are retained, the mean critical CL can be used as an estimate of L_{50}.

Aquarium trials

No lobsters larger than 48 mm CL escaped the 62-mm mesh traps in the aquarium and none smaller than 44 mm CL were retained. This finding resulted in an extremely steep selection curve with a narrow *SR* (Fig. 4; Table 1). For the 75-mm mesh, no lobsters larger than 61 mm CL escaped and no lobsters smaller than 54 mm CL were retained. This finding resulted in a slightly more gentle selection curve, but with a reasonably tight *SR* (Fig. 4, Table 1). Similarly, for the 100-mm mesh, no lobsters larger than 79 mm CL escaped and no lobsters smaller than 74 mm CL were retained. This finding resulted in a selection curve that closely resembled that for the 75-mm mesh, except that the curve shifted a few size categories to the right (Fig. 4; Table 1).

For all meshes, the symmetrical logistic model was selected in preference to the asymmetrical Richards model (Table 1), and in all cases the selected model fitted the data reasonably well (Fig. 4). It should, however, be noted that all hypothesis tests were conducted by using the deviance residuals and their degrees of freedom for all size classes sampled. This was necessary because the very tight selection curves (especially for the 62-mm mesh) resulted in relatively small numbers of size classes in which retention probability was neither zero nor one.

The above results indicate that L_{50}-estimates for each mesh size are substantially larger than the corresponding estimates of critical CL from the theoretical escapement model. In fact, assuming that the asymptotic standard errors provided in Table 1 could be converted to 95% confidence intervals by a multiplication factor of two, only the confidence intervals for these statistics from the 62 mm mesh would overlap. By contrast, confidence intervals for the critical CL are well below those for the L_{50} for both the 75 mm mesh and the 100-mm mesh. This impression is confirmed by inspecting the probabilities of

Table 1

Statistics from SELECT analysis for the aquarium escapement trials. Values in parentheses are asymptotic standard errors *sensu* Millar (1993). These standard errors are provided only for the best model fits for each of the various categories of data. Note that all hypothesis tests were conducted by using deviance residuals for the full model and their degrees of freedom (see text for explanation).

	62-mm mesh		75-mm mesh		100-mm mesh	
	Logistic	Richards	Logistic	Richards	Logistic	Richards
a	−76.479 (23.159)	−351.538	−58.217 (10.079)	−400.075	−64.101 (11.655)	−41.224
b (/mm)	1.649 (0.500)	7.463	0.991 (0.173)	6.589	0.849 (0.155)	0.615
δ		6.567		13.173		0.010
L_{50} (mm)	46.389 (0.309)	46.493	58.717 (0.302)	59.333	75.459 (0.376)	75.144
SR (mm)	1.333 (0.404)	0.989	2.216 (0.386)	2.200	2.587 (0.471)	2.567
Selection factor	0.75		0.78		0.76	
H_0: data have binomial distribution (i.e., data are not overdispersed)						
Deviance	0.802	0.209	1.984	1.092	8.675	6.435
df	27	26	19	18	12	11
P-value	1	1	0.999	0.728	0.730	0.843
H_0: δ =1						
Deviance	0.593		0.892		2.240	
df	1		1		1	
P-value	0.441		0.345		0.134	

retention, $r(l)$, by each mesh size of a lobster at its corresponding mean critical CL. For the 62-mm mesh this probability is 0.014 (0.926 at the upper 95% confidence limit for the critical CL); for the 75-mm mesh it is 0.002 (0.096 at the upper 95% confidence limit for the critical CL); and for the 100-mm mesh it is 0.003 (0.099 at the upper 95% confidence limit for the critical CL).

Field trials

Escapement from traps with 62-mm mesh was highly variable both for the traps with entrance funnels left open, as well as for those with entrance funnels that were sealed, but was surprisingly high for the latter (Fig. 5). Furthermore, it is clear that the relationship between proportion of lobsters retained and CL was not logistic, as it was for the larger mesh sizes (Figs. 5 and 6). Instead, simple, least squares regression analysis indicated linear relationships between these variables both for traps with open entrance funnels as well as for those with entrance funnels closed (Fig. 5). There was no difference between the slopes (t=1.138; df=10; P=0.282; common slope=0.795/mm), although their intercepts did differ significantly (t=14.079; df = 11; P<<0.001).

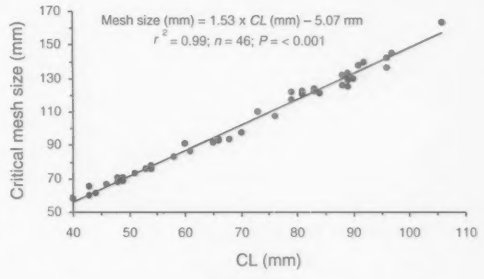

Figure 3

The relationship between carapace length of *J. lalandii* and mesh size below which escape should theoretically not be possible.

No lobsters smaller than 62 mm CL were retained in the 100-mm mesh traps with open entrances, and no upper size limit was reached beyond which escapement was completely eliminated. By contrast, when the entrance funnels to the traps were sealed, no lobsters smaller than 64 mm CL were retained and no lobsters

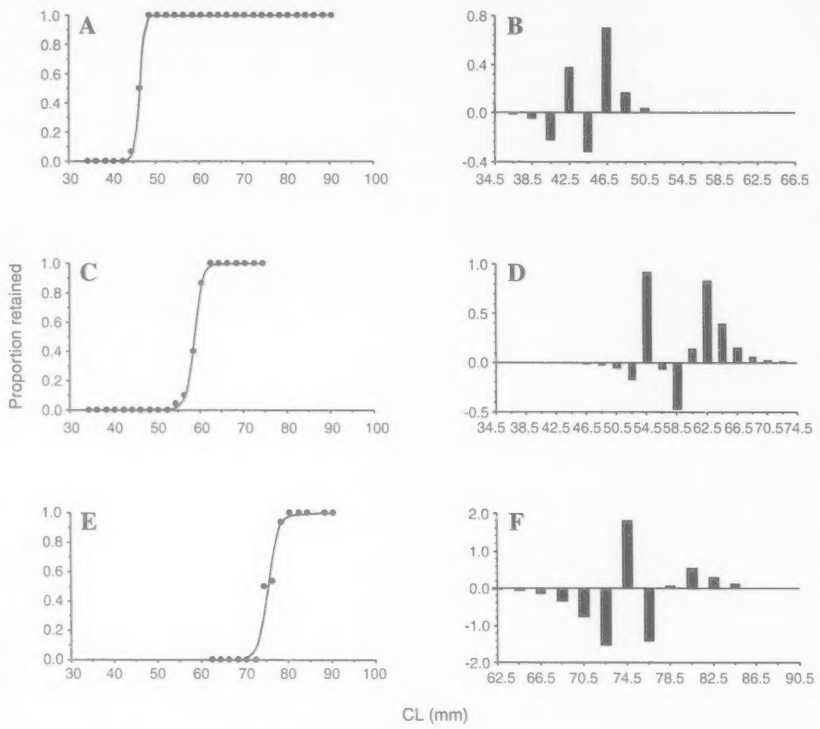

Figure 4

Fitted selectivity curves from the selected models (identified in Table 1) and their deviance residuals for a range of stretched square meshes under aquarium conditions. **A** and **B** are for 62-mm mesh, **C** and **D** are for 75-mm mesh and **E** and **F** are for 100-mm mesh.

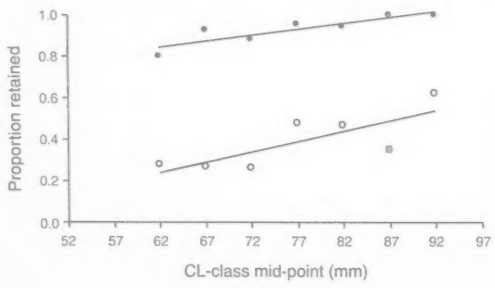

Figure 5

Relationship between proportion of rock lobsters retained by 62-mm mesh trap and carapace length (aggregated into 5-mm size classes). Filled circles represent data from traps with entrance funnels sealed (*Proportion retained*=0.58/mm×*CL* (mm)+48.35; r^2=0.79; n=7; P=0.008), whereas open circles represent data from traps with entrance funnels open (*Proportion retained*=1.01/mm×*CL* (mm)−38.94; r^2=0.62; n=7; P=0.036).

larger than 84 mm CL escaped. This resulted in contact selectivity curves for which estimates of both L_{50} and *SR* decreased when captive lobsters were denied the opportunity to escape through the entrance funnels (Fig. 6; Table 2). This finding indicates that considerable numbers of lobsters of all sizes can escape commercial traps by the entrance funnels.

Irrespective of whether the entrance funnels of the traps was sealed, the symmetrical logistic model was selected in preference to the asymmetrical Richards model (Table 2), and the selected model fitted the data reasonably well (Fig. 6; Table 2), although not as well as the models fitted to the aquarium data (Fig. 4; Table 1).

In comparison with the selectivity curves from the aquarium trials with 100-mm mesh, the corresponding curves from field trials indicated that greater numbers of larger lobsters are retained in practice than under laboratory conditions (Figs. 4 and 6). This finding indicates that some lobsters are retained in commercial traps, even though they can escape, which goes some way to explaining the more "scattered" fit of the logistic model compared to the field data.

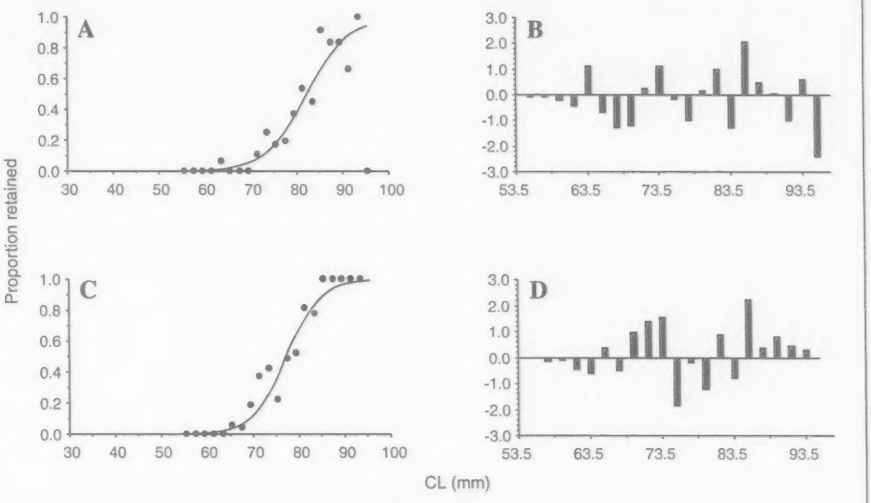

Figure 6

Fitted selectivity curves from the selected models (identified in Table 2) and their deviance residuals for escapement of *J. lalandii* from commercial rock lobster traps covered with 100-mm stretched square meshes under field conditions. **A** and **B** are for traps with open entrance funnels; **C** and **D** are for traps with sealed entrance funnels.

Discussion

This study focuses on escapement of Cape rock lobster (*J. lalandii*) through mesh openings, and on escapement through the trap entrance of commercial traps. Three questions were initially posed, namely: through what mesh size, in theory, can a lobster of given CL escape; are lobsters physically able to escape through this theoretical mesh size, or are there other factors such as orientation and mobility of lobster appendages that prevent escapement; and what proportion of sublegal and legal size lobsters escape through the mesh and trap entrance of commercial traps? In brief, the results showed a weak leak between theoretical values and the ability of the lobsters to escape.

Carapace base (CB) was isolated as the dimension most likely to limit escapement through stretched square meshes. This dimension superceded carapace width and depth, which have been more widely assumed to be the limiting factors to escapement of lobsters (Treble et al., 1998), mainly because our measurement included the width of the last pair of walking legs, folded flush against the carapace. Experimenting with lobster carapaces and an adjustable square hole showed that the joints of these appendages protrude ventrolaterally from the carapace, and the orientation and limited mobility of these appendages would prevent the lobster from escaping. Nevertheless, our theoretical escapement model included all three measurements in the underlying computer simulations to determine the appropriate mesh aperture required to target all lobsters larger than a given size.

The theoretical escapement model produced surprisingly small values of "critical CL" for all three mesh sizes in comparison with the corresponding selectivity curves from the aquarium experiment. This result implies that many rock lobsters that should theoretically not have been able to escape, did so in the aquarium trials. We therefore concluded that the theoretical model was weak and that the mechanics of escapement appear to be more complex than can be shown by simple measurements of the carapace dimensions and may rely also on the orientation of lobsters during escapement (Stasko, 1975).

Selectivity curves developed from aquarium data indicated that an 85-mm-CL lobster should not have been able to escape a 100-mm mesh trap. However, field data indicated that escapement from 100-mm mesh traps with sealed trap openings exceeded 10%. Thus, rock lobsters that should not have been able to escape, according to aquarium experiments, did escape under field conditions. This result was expected, because the mesh of traps used in the commercial fishery (and field experiments) is often unevenly stretched across the metal trap-frame, and therefore some openings lose their square dimensions. This unevenness in the stretch of the mesh was clearly illustrated by a random sample of 40 knot-to-knot aperture measurements from four 100-mm mesh commercial traps, which had diagonal dimensions significantly larger than the 70.71 mm predicted

by Pythagoras's theorem (t=4.470; df =39; P<<0.001). In addition, repairs to torn meshes often leave openings that are somewhat larger than 100 mm and that are not square (Groeneveld, personal. observ.). The wider *SR* of the selectivity curve for field data compared to the tight *SR* of the aquarium curves supports this "unevenly stretched mesh" hypothesis.

Paradoxically, a 70-mm-CL lobster, which has a 1% chance of being retained by a 100 mm mesh in the laboratory has an 11% probability of being retained by a trap with the same mesh in the field (even when its entrances are sealed). Thus, some rock lobsters that should, and could have escaped through the 100 mm mesh of the field traps did not. Schoeman et al. (2002a) suggested that small rock lobsters that can escape do not always do so because they use the trap as a refuge against predators. Alternatively, overnight soak times (as used in the field trials) may be too short for all the small rock lobsters to escape. The probability of escape is much reduced during hauling because captive specimens are then pressed into a tight mass within the fine-mesh (62-mm) codend of the trap.

Table 2

Statistics from SELECT analysis for the field escapement trials. Values in parentheses are asymptotic standard errors *sensu* Millar (1993). These standard errors are provided only for the best model fits for each of the various categories of data. Note that all hypothesis tests were conducted by using deviance residuals for the full model and their degrees of freedom (see text for explanation).

	100-mm mesh		100-mm mesh	
	Trap-entrance open		Trap-entrance sealed	
	Logistic	Richards	Logistic	Richards
a	−17.856 (2.460)	−14.299	−20.801 (2.437)	−51.967
b (/mm)	0.217 (0.031)	0.181	0.2686 (0.031)	0.626
δ		0.641		4.238
L_{50} (mm)	82.274 (0.379)	82.222	77.444 (0.379)	78.458
SR (mm)	10.124 (0.498)	10.809	8.181 (0.498)	7.997
Selection factor	0.82		0.77	
H_0: data have binomial distribution (i.e., data are not overdispersed)				
Deviance	21.593	21.257	18.698	15.807
df	19	18	17	16
P-value	0.305	0.267	0.346	0.467
H_0: $\delta = 1$				
Deviance	0.336		2.891	
df	1		1	
P-value	0.562		0.090	

No escapement from sealed 62-mm mesh traps was expected during field trials, based on the aquarium L_{50} of 46.4 (±0.3) mm and the size range of lobsters used in the field (60 mm–95 mm CL). Nevertheless, small losses (0–18%, depending on lobster size; see Fig. 5) did occur. Only two explanations are possible, namely: 1) that lobsters still managed to escaped through the mesh of the sealed 62-mm traps, despite precautions taken to ensure that the meshes of these traps were undamaged and that trap openings were properly sealed; and 2) that some individuals sustained injuries during exposure and handling, and subsequently were cannibalized by the healthy rock lobsters in the traps. This second conclusion is supported by the presence of shell fragments observed in traps after their retrieval. Because these regressions had the same positive slopes, it seems likely that smaller rock lobsters would be more susceptible to injury and cannibalism than larger animals, and their susceptibility holds irrespective of whether the trap entrance is sealed or not.

Escapement from 62-mm mesh traps with open entrance funnels increased by 40–60% compared to escapement from traps with sealed traps (Fig. 5). This finding has significant implications for the FIMS, which relies on catches made by 62-mm mesh traps and is conducted annually as a measure of the relative abundance of the *J. lalandii* resource. During a survey, it is assumed that all the Cape rock lobsters that are captured are retained and that trap-selection is uniform across all the size classes of these lobsters (Johnston, 1998). It appears that neither of these two assumptions can be met: significant escapement does occur through the trap entrance and there is a greater retention of larger specimens than smaller specimens .

When the trap entrance was left open in the 100-mm mesh field trials, L_{50} increased to 82.3 mm (from 77.4 mm in sealed traps), thus indicating that captive Cape rock lobsters can and do use the trap entrance of commercial traps to escape. The open traps also have a wider *SR* of 10.1 mm (compared to 8.2 mm in sealed traps), and therefore animals with a CL of >87 mm (L_{75}=87.3 mm), which are very unlikely to be able to get through the mesh apertures, will still be able to use the trap entrance to exit. The presence of this escape vent implies that there is little danger of ghost-fishing when using this trap type and that Cape rock lobsters of all sizes should be able to vacate the trap once the bait has been consumed. From a commercial viewpoint, however, the problem of leaving traps in the water for too long is that legal-size specimens, which cannot fit through the mesh, will escape through the entrance, thus decreasing catch rates considerably.

The aquarium result (L_{50}=75.1 mm) is considered the most accurate direct measurement of the selectivity of 100-mm square mesh for *J. lalandii*, because care was taken to ensure that the mesh was stretched

evenly with square openings across the metal trap-frame and because we made sure that all lobsters that could escape, did, resulting in a tight *SR* of 2.6 mm. This L_{50} is remarkably close to the present MLS of 75 mm CL for the commercial fishery, especially considering that 100-mm mesh was first used when the MLS was 89 mm CL, and that the commercial mesh size remained at 100 mm despite the 14 mm CL reduction in MLS during the early 1990s (Schoeman et al., 2002b). The L_{50} obtained from the field trials with sealed trap openings (77.4 mm) was also close to the present MLS.

In a recent indirect study (i.e., where the size composition of a population was unknown) Schoeman et al. (2002a) found L_{50} to be 79.2 mm (*SR*=11.1 mm) under commercial operational conditions. The increase in L_{50} (above the 75.1 mm and 77.4 mm found in the direct aquarium and field studies, respectively) is the result of the trap entrances of commercial traps remaining open, so that rock lobsters that are too large to fit through the mesh can still escape through the entrance. In the present direct study, this factor increased the L_{50} from 77.5 mm (sealed entrance) to 82.2 mm (open entrance) for 100-mm mesh. Thus, one conclusion of the indirect study, namely that the South African fishery for *J. lalandii* is unusual in that standard commercial traps are covered with mesh having an aperture considerably wider (L_{50}=79.2 mm CL) than that required to retain Cape rock lobsters of the current MLS (Schoeman et al., 2002a), must now be seen in a different light. The selectivity of the 100-mm stretched mesh itself now appears not to be wider than that which is currently required (based on the direct results). Rather, the indirectly determined L_{50} appears to have been inflated by the numbers of larger lobsters that were able to escape through the trap entrance.

Direct studies of the escapement of crustaceans from pots (Krouse and Thomas, 1975; Krouse, 1978; Everson et al., 1992) have often been criticized because these studies themselves may affect the behavior of the animals and do not include the dynamics of the processes of entry and escapement (Xu and Millar, 1993; Treble et al., 1998). We recognize these weaknesses, but felt that direct studies remain useful because they can be used to set a theoretical benchmark against which the results of indirect studies can be tested, especially if the trap selectivity of the latter depends on area and season. Various insights were gained from the present study, particularly because it closely followed an indirect study of trap selectivity for *J. lalandii* (Schoeman et al., 2002a). In conclusion, this study of escapement of *J. lalandii* through square meshes showed 1) that 100-mm mesh size is, theoretically, near optimal for the fishery; 2) that many Cape rock lobsters that are able to escape through the mesh do not do so; 3) that the rock lobsters that are shown theoretically to be unable to escape through the mesh of commercial traps, often can do so; and 4) that specimens too large to escape through the mesh can escape through the trap entrance.

Acknowledgments

This study would not have been possible without the funding and infrastructure provided by Marine and Coastal Management (Department of Environmental Affairs and Tourism, South Africa). In particular, we would like to thank our colleagues, Steven McCue, Neil van den Heever, and Danie van Zyl for technical support. We are also grateful to the skipper and crew of the research vessel *Sardinops*, which was used to conduct the field trials. J.P.K. received financial assistance from the Fridtjof Nansen and NORAD, and would like to thank his supervisors, Anders Ferno and Geir Blom, at the University of Bergen in Norway, for their assistance with an earlier draft of this manuscript. D.S.S. thanks the University of Port Elizabeth for support in terms of finance and infrastructure. Finally, the constructive comments of three anonymous referees are acknowledged; these aided substantially in clarifying certain parts of the original manuscript.

Literature cited

Arana, P. E., and S. V. Ziller.
1994. Modelling the selectivity of traps in the capture of spiny lobster (*Jasus frontalis*), in the Juan Fernandez archipelago (Chile). Investigación pesq., Santiago 38:1–21.

Brown, R. S., and N. Caputi.
1983. Factors affecting the recapture of undersize western rock lobster *Panulirus cygnus* George returned by fishermen to the sea. Fish. Res. 2:103–128.
1985. Factors affecting the growth of undersize western rock lobster, *Panulirus cygnus* George, returned by fishermen to the sea. Fish. Bull. 83:567–574.

Cockcroft, A. C., and A. I. L. Payne.
1999. A cautious fisheries management policy in South Africa: the fisheries for rock lobster. Mar. Policy 23(6):587–600.

Crous, H. B.
1976. A comparison of the efficiency of escape gaps and deck grid sorters for the selection of legal-sized rock lobsters *Jasus lalandii*. Fish. Bull. S. Afr. 8:5–12.

Davis, G. E.
1981. Effects of injuries on spiny lobster, *Panulirus argus*, and implications for fishery management. Fish. Bull. 78:979–984.

Everson, A. R., R. A. Skillman, and J. J. Polovina.
1992. Evaluation of rectangular and circular escape vents in the northwestern Hawaiian Islands lobster fishery. N. Am. J. Fish. Manag. 12:161–171.

Fogarty, M. J., and V. D. Borden.
1980. Effects of trap-venting on gear selectivity in the inshore Rhode Island American lobster, *Homarus americanus*, fishery. Fish. Bull. 77:925–933.

Heydorn, A. E. F.
1969. The rock lobster of the South African west coast *Jasus lalandii* (H. Milne-Edwards): 2. Population studies, behaviour, reproduction, moulting, growth and migration. Invest. Rep. Div. Sea Fish. S. Afr. 71, 52 p.

Hunt, J. H., W. G. Lyons, and F. S. Kennedy.
1986. Effects of exposure and confinement on spiny

lobsters, *Panulirus argus*, used as attractants in the Florida trap fishery. Fish. Bull. 84:69–76.

Johnston, S. J.
1998. The development of an operational management procedure for the South African west coast rock lobster fishery. Ph.D. diss., 370 p. Univ. Cape Town, Cape Town, South Africa.

Krouse, J. S.
1978. Effectiveness of escape vent shape in traps for catching legal-sized lobster, *Homarus americanus*, and harvestable-sized crabs, *Cancer borealis* and *Cancer irroratus*. Fish. Bull. 76:425–432.
1989. Performance and selectivity of trap fisheries for crustaceans. *In* Marine invertebrate fisheries: their assessment and management (J. F. Caddy, ed.), p. 307–325. Wiley, New York, NY.

Krouse, J. S., and J. C. Thomas.
1975. Effects of trap-selectivity and some lobster population parameters on size composition of the American lobster, *Homarus americanus* catch along the Maine coast. Fish. Bull. 73:862–871.

Maynard, D. R., N. Branch, Y. Chiasson, and G. Y. Conan.
1987. Comparison of three lobster (*Homarus americanus*) trap escape mechanisms and application of a theoretical retention curve for these devices in the southern Gulf of St. Lawrence lobster fishery. Canadian Atlantic Fisheries Scientific Advisory Committee, Research Document, 87/87, 34 p.

Millar, R. B.
1992. Estimating the size-selectivity of fishing gear by conditioning on the total catch. J. Am. Stat. Assoc. 87: 962–968.
1993. Analysis of trawl selectivity studies (addendum): implementation in SAS. Fish. Res. 17:373–377.

Millar, R. B., and R. J. Fryer.
1999. Estimating the size-selection curves of towed gears, traps, nets and hooks. Revs. Fish Biol. Fish. 9:89–116.

Millar, R. B., and S. J. Walsh.
1992. Analysis of trawl selectivity studies with an application to trouser trawls. Fish. Res. 13:205–220.

Miller, R. J.
1990. Effectiveness of crab and lobster traps. Can. J. Fish. Aquat. Sci. 47:1228–1251.

Newman, G. G., and D. E. Pollock.
1969. The efficiency of rock lobster fishing gear. S. Afr. Shipp. News Fish. Ind. Rev. 24(6):79–81.

Pollock, D. E.
1986. Review of the fishery for and biology of the Cape rock lobster *Jasus lalandii* with notes on larval recruitment. Can. J. Fish. Aquat. Sci. 43(11):2107–2117.

Pollock, D. E., and C. J. de B. Beyers.
1979. Trap selectivity and seasonal catchability of rock lobster *Jasus lalandii* at Robben Island sanctuary, near Cape Town. Fish. Bull. S. Afr. 12:75–77.

Pollock, D. E., A. C. Cockcroft, J. C. Groeneveld, and D. S. Schoeman.
2000. The commercial fisheries for *Jasus* and *Palinurus* species in the south-east Atlantic and south-west Indian oceans. *In* Spiny lobsters: fisheries and culture (B. F. Phillips and J. Kittaka, eds.), p. 105–120. Blackwell Science, UK.

Rosa-Pacheco, R. D. L., and M. Ramirez-Rodriguez.
1996. Escape vents in traps for the fishery of the California spiny lobster, *Panulirus interruptus*, in Baja California Sur, Mexico. Cienc. Mar., Baja Calif., Mex. 22:235–243.

Schoeman, D. S., A. C. Cockcroft, D. L. Van Zyl, and P. C. Goosen.
2002a. Trap selectivity and the effects of altering gear design in the South African rock lobster *Jasus lalandii* commercial fishery. S. Afr. J. Mar. Sci. 24:37–48.
2002b. Changes to regulations and the gear used in the South African commercial fishery for *Jasus lalandii*. S. Afr. J. Mar. Sci. 24:365–370.

Stasko, A. B.
1975. Modified lobster traps for catching crabs and keeping lobsters out. J. Fish. Res. Board Can. 32(12): 2515–2520.

Treble, R. J., R. B. Millar, and T. I. Walker.
1998. Size-selectivity of lobster pots with escape-gaps: application of the SELECT method to the southern rock lobster (*Jasus edwardsii*) fishery in Victoria, Australia. Fish. Res. 34:289–305.

Vermeer, G. K.
1987. Effects of air exposure on dessication rate, hemolymph chemistry, and escape behaviour of the spiny lobster, *Panulirus argus*. Fish. Bull. 85:45–51.

Xu, X., and R. B. Millar.
1993. Estimation of trap selectivity for male snow crab (*Chionoecetes opilio*) using the SELECT modeling approach with unequal sampling effort. Can. J. Fish. Aquat. Sci. 50:2485–2490.

Zar, J. H.
1999. Biostatistical analysis, 663 p. Prentice-Hall, Inc., Englewood Cliffs, NJ.

Quantification of drag and lift imposed by pop-up satellite archival tags and estimation of the metabolic cost to cownose rays (*Rhinoptera bonasus*)*

Donna S. Grusha
Mark R. Patterson
Virginia Institute of Marine Science
College of William and Mary
P.O. Box 1346
Gloucester Point, Virginia 23062-1346
E-mail address (for D. S. Grusha): dsg@vims.edu

Abstract—The recent development of the pop-up satellite archival tag (PSAT) has allowed the collection of information on a tagged animal, such as geolocation, pressure (depth), and ambient water temperature. The success of early studies, where PSATs were used on pelagic fishes, has spurred increasing interest in the use of these tags on a large variety of species and age groups. However, some species and age groups may not be suitable candidates for carrying a PSAT because of the relatively large size of the tag and the consequent energy cost to the study animal. We examined potential energetic costs to carrying a tag for the cownose ray (*Rhinoptera bonasus*). Two forces act on an animal tagged with a PSAT: lift from the PSATs buoyancy and drag as the tag is moved through the water column. In a freshwater flume, a spring scale measured the total force exerted by a PSAT at flume velocities from 0.00 to 0.60 m/s. By measuring the angle of deflection of the PSAT at each velocity, we separated total force into its constituent forces—lift and drag. The power required to carry a PSAT horizontally through the water was then calculated from the drag force and velocity. Using published metabolic rates, we calculated the power for a ray of a given size to swim at a specified velocity (i.e., its swimming power). For each velocity, the power required to carry a PSAT was compared to the swimming power expressed as a percentage, %TAX (Tag Altered eXertion). A %TAX greater than 5% was felt to be energetically significant. Our analysis indicated that a ray larger than 14.8 kg can carry a PSAT without exceeding this criterion. This method of estimating swimming power can be applied to other species and would allow a researcher to decide the suitability of a given study animal for tagging with a PSAT.

Manuscript submitted 21 May 2003 to the Scientific Editor's Office.
Manuscript approved for publication 13 July 2004 by the Scientific Editor.
Fish. Bull. 103:63–70 (2005).

The pop-up satellite archival tag (PSAT) was developed in the late 1990s primarily for the tracking of large pelagic fish (Arnold and Dewar, 2001; Gunn and Block, 2001). This electronic tag is attached to a large fish, collects data on the environment of the fish for a preprogrammed period, and then detaches from the fish by corrosion of a release pin. A float on the tag carries the tag to the surface of the water where the PSAT begins transmitting the archived environmental data. The pop-up location is determined by the Argos satellites that in turn transmit the data to a relay station. The earliest uses of these tags have been on large pelagic fishes such as Atlantic bluefin tuna (*Thunnus thynnus*) (Block et al., 1998; Lutcavage et al., 1999) and blue marlin (*Makaira nigricans*) (Graves et al., 2002). In the early tuna studies, PSATs were used to investigate geographic range and possible stock structure. Graves et al. (2002) used the tags to assess postrelease survival of blue marlin from the recreational fishery. Over their short history, the PSATs have been improved to collect even more data than the original models and currently record light levels, temperature, and pressure readings. The light levels are used to estimate geolocation and the pressure readings are converted to depth measurements. Combined with the temperature readings, the depth measurements can provide detailed information about the study animal's swimming behavior. Experiences with the first-generation tags led to the development of various fail-safe features (Arnold and Dewar, 2001). Both premature detachment (made evident by the tag floating at the surface) or lack of vertical movement (i.e., constant depth, which indicates probable death of the animal) initiate early transmission of archived data. Should the tag be carried to an extreme depth where water pressure might physically crush the tag, release mechanisms, both software-based and mechanical, have been developed to free the tag from the animal.

PSATs were developed to supplement the tracking data that could be acquired through acoustic tagging and archival tagging. Acoustic tagging is most useful for studying fine-scale movement and habitat use and for collecting physiological data (Arnold and Dewar, 2001; Gunn and Block, 2001). However, its use is limited by the need for labor-intensive, real-time tracking from a research vessel or the availability of fixed listening stations. Dagorn et al. (2001) described clear interactions between some of the yellowfin tuna (*Thunnus albacares*) being tracked and the research vessel—a violation of the assumption that the tracking operation does not alter the behavior of the fish. Archival tags also collect both environmental and physiological data but

* Contribution 2629 from the Virginia Institute of Marine Science, College of William and Mary, Gloucester Point, VA 23062.

over much longer time scales (sometimes years) and across ocean-basin geographic scales (Arnold and Dewar, 2001; Gunn and Block, 2001). These tags can provide information on both seasonal behavior and migration routes. Although data collection is fishery-independent, data retrieval is dependent on the recapture of the fish by fishermen and on the recognition and return of the archival tag. PSATs are a merger of archival and satellite telemetry technology. Because PSATs are attached externally, only environmental data can be collected. The tags can be programmed to gather data for a predetermined duration and then to disengage and transmit data at a determined time. The major advantage of this tag is that both data acquisition and retrieval are fishery-independent and the researcher knows when to expect to receive data. However, data retrieval is limited by data compression required to compensate for low data transfer rates to the Argos satellites, finite battery life, and relatively high transmission errors (Arnold and Dewar, 2001; Gunn and Block, 2001). PSATs provide accurate endpoint locations based on Doppler shifts of successive transmissions during a single satellite pass. However, geolocation throughout the tagging duration is based on light levels that estimate dawn and dusk. By determining time of local noon and day length, longitude and latitude can be calculated. According to Hill and Braun (2001), even with optimal geolocation analysis, the expected variability in longitude is a constant 0.32° but the expected variability in latitude will never be less than 0.7°. The relationship between day length and latitude is strongest at high latitudes and at the time of the solstices but weakens near the equator and becomes nearly indeterminate at the equinoxes (Sibert et al., 2003).

An implicit assumption in using these tags is that while the fish tows the tag, the tag does not affect the study animal's behavior or survival. This is a reasonable assumption for large pelagic fishes and is supported by theoretical estimates of the energetic cost of towing a PSAT (Kerstetter, 2002); however, the actual energy cost to a given fish has not previously been quantified. The success of early studies on pelagic fishes has spurred increasing interest in using these tags on a large variety of species and age groups. As studies are undertaken with PSATs, a logical extension is to pose the question: "At what point does the energy cost of carrying a PSAT negatively affect a study animal?" Blaylock (1990) addressed a similar question regarding the impact of sonic transmitters on the swimming behavior of cownose rays (*Rhinoptera bonasus*). In his study, he videotaped cownose rays for ten-minute intervals before and after attachment of a mock transmitter. Energy expenditure was estimated by counting wingbeats per second before and after attachment of the transmitter. He concluded that in the short term a transmitter-to-ray mass ratio of less than 0.03 had no statistically significant effect on ray swimming behavior.

In this study, the impact of a PSAT on a study animal is evaluated in terms of the forces that the PSAT exerts on the animal, specifically lift (i.e., buoyancy) and drag. Lift and drag are both vector quantities; lift acts in the vertical direction and drag, as measured in this study, acts in the horizontal direction. These vector components are additive to give the total force acting on the attachment site of a PSAT. At a recent tagging workshop associated with the Pelagic Fisheries Research Program,[1] the problem of premature release of some PSATs from the research animal was cited as a common difficulty. Premature release may be attributed to a number of potential failures of either the tag itself or the attachment device. Possible sources for this problem cited at this workshop include detachment of the anchor from the study animal, failure of the tether between the PSAT and the anchor, failure of the release pin on the PSAT, and failure of the release software itself. The magnitude of the total force acting on the attachment site chronically may provide some insight into whether anchor failure is a possible source for this problem.

Drag as an isolated force is the product of four defining factors:

$$F_D = \tfrac{1}{2}\,\rho\, S\, U^2\, C_D, \tag{1}$$

where F_D = force due to drag (in newtons, N);
ρ = density (kg/m^3) of the fluid through which the object is moving;
S = projected surface area (m^2) of the object;
U = relative velocity (m/s) between the object and the fluid; and
C_D = drag coefficient (dimensionless) which is largely dependent upon the shape of the object.

Furthermore, the power required to pull the tag through the water can also be related to drag mathematically:

$$P = F_D\, U = \tfrac{1}{2}\,\rho\, S\, U^3\, C_D, \tag{2}$$

where P = power (in watts, W).

Of particular note in these relationships, drag is proportional to velocity squared and power is related to velocity cubed provided that all other factors are constant. For example, as velocity is doubled, drag increases by a factor of four, whereas power increases by a factor of eight. The characteristic of the tag that most affects drag in this relationship is its projected surface area which, in turn, is defined by its size and shape. The projected surface area of the PSAT changes as the tag is pulled through the water at different velocities and in turn changes the drag coefficient at each velocity. On the other hand, lift is determined by the buoyancy of the tag. The dry weight of the tag is not a factor in either of these relationships under steady flow con-

[1] Pelagic Fisheries Research Program. 2002. PFRP PI Meeting, December 4–6, 2002. University of Hawaii at Manoa, 1000 Pope Rd., MSB 312, Honolulu, HI 96822. http://www.soest.hawaii.edu/PFRP/meetings.html. [Accessed 16 June 2004.]

ditions. The weight of the tag is only important during accelerations and decelerations. During acceleration, the mass of the tag positively affects the magnitude of two separate forces that add to the hydrodynamic drag, and likewise during deceleration, these extra forces develop on the attachment point that could cause tag loss.

The motivation for this study is to determine the feasibility of tagging cownose rays (*R. bonasus*) with PSATs to study their fall migration. By quantifying the forces that act upon an animal when a PSAT is attached, and using published metabolic rates, we can estimate the energetic cost for the ray to carry a PSAT. Moreover, this type of analysis can be used to determine the minimum size of ray suitable for tagging. Considering the wide variety of user-determined modifications that can be implemented in applying these tags, this experiment is intentionally designed to isolate the PSAT from other variables. In this way, these results can be applied to a broad range of applications so that each user can decide the manner in which a specific modification of the tag is likely to affect the forces of lift and drag.

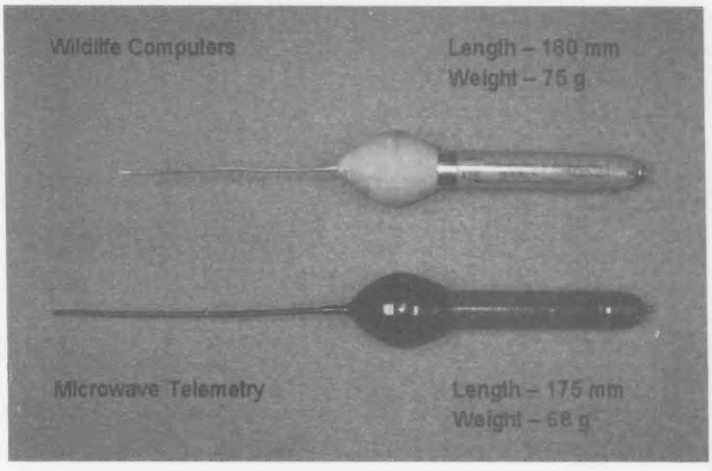

Figure 1
The shape and dimensions of two brands of pop-up satellite archival tag.

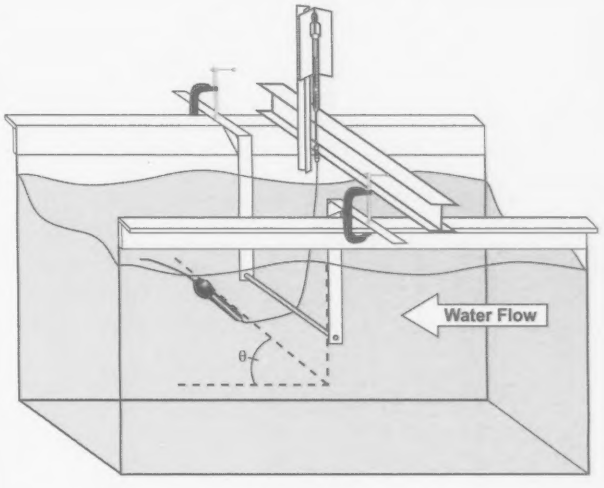

Figure 2
Diagram of experimental design, showing how θ, the angle of deflection of the tag, was measured.

Methods

Drag was measured on two brands of PSAT. One tag was manufactured by Wildlife Computers, Inc. (Model PAT, 16150 NE 85th St #226, Redmond, WA 98052) and the other was a mock tag made by Microwave Telemetry, Inc. (Model PTT-100, 10280 Old Columbia Road, Suite 260, Columbia, MD 21046) weighted to simulate a functional tag. The two tags are very similar in size and shape (Fig. 1). The Wildlife Computer PAT has a body length of 180 mm (not including the antenna) and a dry weight of 75 g and the Microwave Telemetry PTT is 175 mm long and weighs 68 g. Measurements were obtained in a 22,700-liter freshwater recirculating flume 24 meters in length located at the Virginia Institute of Marine Science. A 30-g spring scale was used to measure force and was suspended above the flume. A 1.25-cm low-friction Delrin rod was suspended approximately 55 cm below the water surface by a metal bracket and placed directly below the spring scale. A 90-cm length of 0.46-mm diameter (20-lb test) monofilament line connected the tag to the spring scale by loops tied at either end. One loop was threaded through the release pin in order to lasso the tag. The other loop was then attached to the clip on the spring scale and the tag was passed under the Delrin rod so that it floated to the other side (Fig. 2). The depth of the Delrin rod and the length of the monofilament were selected so that the tag was completely immersed in the water throughout the experiment and so that it floated within

Table 1

Spring scale measurements, angle of deflection, summary of forces exerted and power required for two brands of PSAT over flume velocities from 0.00 m/s to 0.60 m/s. The spring scale measurements include the range over a 5-minute period. The angle of deflection was measured from the horizontal. Total force, lift, and drag (in newtons, N) were calculated from Equations 3, 4, and 5, respectively. Power (in watts, W) was calculated as the product of flume velocity and drag.

PSAT	Flume velocity (m/s)	Spring scale measurement (g)	θ (°)	Total force (N)	Lift (N)	Drag (N)	Power (W)
Wildlife Computers	0.00	6.50 ±0.25	90.0	0.064	0.064	0.000	0.000
	0.15	7.50 ±0.25	76.5	0.074	0.072	0.017	0.003
	0.30	10.50 ±0.25	42.0	0.103	0.069	0.076	0.023
	0.45	15.0 ±0.5	40.0	0.147	0.094	0.113	0.051
	0.60	19.0 ±1.0	31.5	0.186	0.097	0.159	0.095
Microwave Telemetry	0.00	11.75 ±0.25	90.0	0.115	0.115	0.000	0.000
	0.15	12.25 ±0.25	75.5	0.120	0.116	0.030	0.004
	0.30	13.50 ±0.25	61.5	0.132	0.116	0.063	0.019
	0.45	16.0 ±0.5	42.5	0.157	0.106	0.116	0.052
	0.60	21.5 ±1.0	41.5	0.211	0.140	0.159	0.095

the central portion of the flume. Prior to the experiment, the monofilament line was attached to the spring scale and the spring scale was then set at zero so that the weight of the monofilament line was excluded from the subsequent measurements. The flume temperature was measured at 20°C. Measurements were taken on each tag at flume velocities of 0.0, 0.15, 0.30, 0.45, and 0.60 m/s, the maximum velocity of the flume. At each flume velocity, the flume flow was allowed to equilibrate for 10 minutes. Then spring scale measurements were observed over a period of five minutes and the mid-point measurement and its range were recorded. The raw measurement was then converted to total force, F_T (N):

$$F_T = (\text{raw measurement(g)})(1\text{kg}/1000\text{g})(9.8\text{m/s}^2). \quad (3)$$

In addition, a digital photo was taken of each tag at each velocity from the side of the flume in order to measure the angle of deflection (θ) as measured upward from horizontal. Accordingly, the total force (F_T) could then be separated into its component forces, lift (F_L) and drag (F_D):

$$F_L = \sin\theta F_T, \quad (4)$$

$$F_D = \cos\theta F_T. \quad (5)$$

Results

The spring scale measurement for the Wildlife Computers PAT increased from 6.50 g at 0.00 m/s to 19.0 g at 0.60 m/s and the Microwave Telemetry PTT increased from 11.75 g to 21.5 g over the same flume velocity increase (Table 1). Because of increasing turbulence in the flume at the two higher flume velocities, the range of the spring scale measurements also increased. The total force exerted by the Wildlife Computers PAT increased from 0.064 N to 0.186 N as the flume velocity was increased (Table 1). Similarly, the drag and calculated power required to pull the tag through the water column at the highest velocity was 0.159 N and 0.095 W, respectively. The lift of this PSAT also increased, but not continuously, from 0.064 N to 0.097 N. The forces exerted by the Microwave Telemetry PTT were very similar but had higher lift values. The total force increased from 0.115 N to 0.211 N, the drag increased to 0.159 N and the power required to pull this PSAT was 0.095 W at the highest velocity. The lift increased from 0.115 N to 0.140 N but again not in a continuous manner. Force-velocity curves for both PSATs were very similar (Fig. 3). Lift was relatively constant for each tag, although at different magnitudes. Total force and drag both increased over the range of flume velocities and roughly paralleled each other between 0.30 m/s and 0.60 m/s.

Discussion

Considered alone, the power required to pull a given PSAT at a particular velocity has little relevance, but when considered in the context of an animal's usual energy expenditure to swim at that velocity, it can be expressed as %TAX (Tag Altered eXertion), defined as the increase in energy required by the animal to pull the PSAT at the specified velocity, normalized by the routine or active metabolic rate (see below). In his biotelemetry studies, Blaylock (1992) measured mean routine swimming speeds between 0.20 m/s and 0.29 m/s in cownose rays. Maximum swimming speeds for cownose rays have

not been measured; however, with visual observation, Smith (1980) reported witnessing several undisturbed schools of cownose rays swimming near the surface at ~4–5 knots (2.06–2.57 m/s). Using data reported in first sightings during spring migration of cownose rays along the South Atlantic Bight, Smith estimated migration speeds as high as 12.5 nautical miles per day. Assuming the rays migrated continuously, that rate would require a swimming speed of 0.27 m/s; if they were actively migrating 50% of the time, they would have to swim at 0.54 m/s.

Published metabolic rates can be used to estimate the energy required for an animal to swim at various speeds. When information is not available on a study species, a suitable proxy species can be used. In the example of the cownose ray, no data are currently available regarding metabolic rates; however, DuPreez et al. (1988) published metabolic rates for the bull ray (*Myliobatis* [=*Myliobatus*] *aquila*) over a range of temperatures. *Myliobatis aquila* is a good proxy species for *R. bonasus* because the two species are morphologically similar, similar in size, and both inhabit temperate to subtropical coastal waters. Because the flume measurements were obtained at 20°C and this is also a typical mid-range temperature for either species, the equations for metabolic rates at this temperature will be used (Eq. 6, a–c). Metabolic rates are expressed as a set of three equations that yield the standard metabolic rate (SMR), the routine metabolic rate (RMR), and the active metabolic rate (AMR).

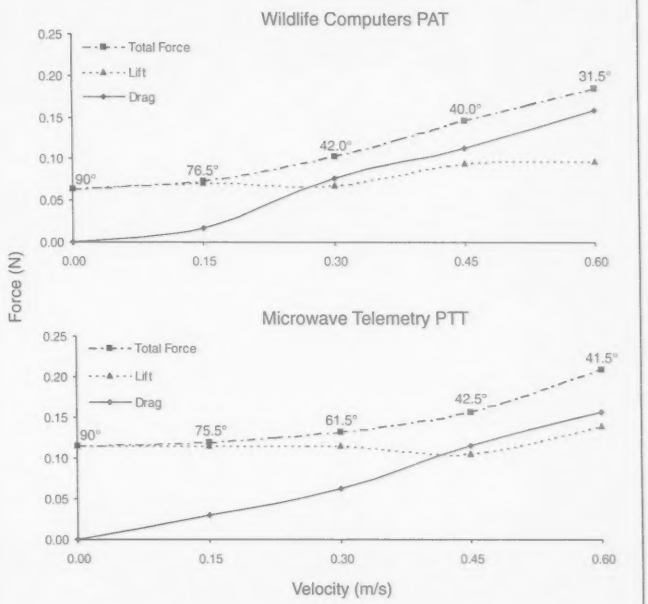

Figure 3

Comparison of force-velocity curves of two brands of PSAT. Total force (in newtons, N) and its component forces, lift and drag, are plotted against flume velocity (m/s). The angle of deflection of the PSAT as measured upward from horizontal is indicated above each set of points

$$SMR \quad \log_{10} R = 2.86 - 0.32 \times \log_{10}(M \times 1000), \tag{6a}$$

$$RMR \quad \log_{10} R = 2.79 - 0.27 \times \log_{10}(M \times 1000), \tag{6b}$$

$$AMR \quad \log_{10} R = 2.74 - 0.22 \times \log_{10}(M \times 1000), \tag{6c}$$

where M = mass (kg) of the ray (DuPreez et al.'s 1988 equations have been modified so as to express M in MKS units); and
R = metabolic rate (mg O_2/(kg × h)).

Using the size of an average female cownose ray of 15.5 kg (Smith, 1980) and solving for R, the SMR, RMR and AMR are estimated as 33.0, 45.6, and 65.8 mg O_2/(kg × h) respectively. These rates can then be used to estimate swimming power at routine and active swimming speeds:

$$SP_{?MR} = (?MR - SMR) \times (1W/kg)/\left(256mgO_2/(kg \times h)\right) \times M, \tag{7}$$

where $SP_{?MR}$ = swimming power (W) for RMR or AMR.

Making the appropriate substitutions into Equation 7 yields SP_{RMR} = 0.76 W and SP_{AMR} = 1.99 W. Drag can then be expressed as %TAX:

$$\%TAX = (P / SP_{?MR}) \times 100. \tag{8}$$

For swimming speeds of 0.15 m/s and 0.30 m/s, SP_{RMR} is used, and for swimming speeds of 0.45 m/s and 0.60 m/s, SP_{AMR} is used (Table 2).

Although lift has not been considered in the above analysis, it is an important component of the total force affecting a study animal. As a chronically applied force acting against the anchor site where the PSAT attaches, this total force may contribute to premature release of the PSAT from the study animal. Moreover, for animals where diving behavior is important for survival (e.g., diving for prey or diving to escape predators) lift becomes an additional tax on the animal's energy resouces. Using total force as an approximation of the force to be overcome by the animal when diving, we can estimate the total power required to dive as *Total force as %TAX* (Table 2).

We propose that an increase in energy requirement, *%TAX*, of <5% will not negatively impact a study ani-

Table 2

Metabolic cost to a 15.5 kg cownose ray carrying a PSAT at various velocities expressed as *%TAX*. Drag and total force are the forces created by the PSAT to be overcome by the swimming ray. Power and total power are the rates of energy expenditure required to overcome these forces. *Drag as %TAX* and *Total force as %TAX* are the increases in energy expenditures, normalized by the routine or active metabolic rate (speed dependent—see text), required to carry the PSAT at a given velocity. Drag, power, and *Drag as %TAX* apply to a ray swimming in the horizontal plane. Total force, total power, and *Total force as %TAX* account for the buoyancy of the PSAT and apply when the ray is diving.

PSAT	Flume velocity (m/s)	Drag (N)	Power (W)	Drag as %TAX	Total force (N)	Total power (W)	Total force as %TAX
Wildlife Computers	0.00	0.000	0.000	0.00	0.064	0.000	0.00
	0.15	0.017	0.003	0.34	0.074	0.011	1.44
	0.30	0.076	0.023	3.01	0.103	0.031	4.05
	0.45	0.113	0.051	2.55	0.147	0.066	3.33
	0.60	0.159	0.095	4.80	0.186	0.112	5.63
Microwave Telemetry	0.00	0.000	0.000	0.00	0.115	0.000	0.00
	0.15	0.030	0.004	0.59	0.120	0.018	2.36
	0.30	0.063	0.019	2.46	0.132	0.040	5.20
	0.45	0.116	0.052	2.62	0.157	0.071	3.55
	0.60	0.159	0.095	4.77	0.211	0.126	6.37

mal that has adequate food resources in nature; higher loads are felt to be energetically significant. In this example using a 15.5-kg cownose ray, the *Drag as %TAX* is within acceptable parameters; however, at 0.60 m/s the *Total force as %TAX* begins to exceed these guidelines. At this point, a researcher would have to consider whether diving behavior at this speed would be a significant factor in the animal's survival.

Another application of this information would be to determine the minimum reasonable size for a study animal of a particular species. Blaylock (1990) attempted to address this issue for cownose rays by considering the transmitter-to-ray mass ratio using dry weights. The advantage of using metabolic rates is that it identifies subtler but significant increases in energy requirement to carry a PSAT. In his study, Blaylock examined two age groups, a 0+ age group that had an average weight of 1.8 kg and a 1+ age group that ranged in size between 4.3 kg and 7.8 kg. He concluded that the 0+ age group was negatively impacted by the sonic tag but that the 1+ age group was not effected. A PSAT is physically smaller than the sonic tags used in his experiment; in addition, it is attached to the animal at the nose-end of the tag so that it is carried with the long axis of the tag parallel to the long axis of the animal (Blaylock's sonic tags were attached so that the long axis of the tag was carried perpendicular to the long axis of the animal). Both these factors—smaller physical size and nose-end orientation in space—decrease the projected surface area of the tag. As an example, consider the metabolic cost of carrying a Wildlife Computers PAT to each of these sizes (1.8, 4.3, and 7.8 kg) of cownose ray (Table 3). For the 1.8-kg ray, only the exertion of carrying the PSAT at 0.15 m/s horizontally was associated with a *%TAX* of <5%; higher swimming speeds or downward diving markedly increased the *%TAX*. It is obvious why short-term effects of carrying a sonic tag were evident. For the 4.3-kg ray, all swimming speeds greater than 0.15 m/s, whether horizontal or diving, required increased energy expenditures of >5%. For the 7.8-kg ray, *%TAX* was acceptable at 0.15 m/s, marginal to slightly elevated for mid-range speeds, and was clearly excessive at high speed. According to this analysis, rays of these size classes would not be good candidates for carrying a PSAT. As determined in this study, the smallest cownose ray that ought to be considered for PSAT tracking would be 14.8 kg. *Drag as %TAX* is ≤5% for all speeds and only slightly >5% for *Total force as %TAX* at 0.60 m/s. Because prolonged high speed diving behavior is not likely a factor in this ray's ability to survive, the minor elevation of *%TAX* for diving at 0.60 m/s can be disregarded.

When applying this type of analysis to other species that predominantly swim at speeds greater than 0.60 m/s, several caveats make unwise the extrapolation of these data to higher velocities. Referring back to the equations describing drag and power, Equation 1 and Equation 2, respectively, drag is proportional to velocity squared and power is proportional to velocity cubed provided that all other factors are constant. However, in examining Figure 3, as velocity increases from 0.00 m/s to 0.60 m/s, all other factors are not constant. Specifically, the angle of deflection, θ, decreases from 90° at 0.00 m/s to as low as 31.5° at 0.60 m/s. First, the projected surface area, S, over which water flows decreases as velocity increases. Second, the orientation (effective shape) of the object also effectively changes as velocity increases. Hence the drag co-efficient, C_D

Table 3

Metabolic costs to various sizes of cownose ray to carry a Wildlife Computers PSAT expressed as *%TAX*. *Drag as %TAX* is the increase in energy expenditure, normalized by the routine or active metabolic rate (speed dependent—see text), required by the ray to carry the PSAT while swimming in the horizontal plane. *Total force as %TAX* accounts for the buoyancy of the PSAT and applies when the ray is diving.

	Drag as %TAX				Total force as %TAX			
Weight of ray (kg)	Swimming velocity (m/s)				Swimming velocity (m/s)			
	0.15	0.30	0.45	0.60	0.15	0.30	0.45	0.60
1.8	2.39	21.32	18.53	34.84	10.25	28.69	24.19	40.86
4.3	1.05	9.32	8.06	15.16	4.48	12.58	10.53	17.78
7.8	0.62	5.50	4.70	8.84	2.65	7.41	6.41	10.37
14.8	0.35	3.15	2.66	5.00	1.51	4.24	3.48	5.87

also changes. At some velocity greater than 0.60 m/s, θ will approach 0°, and at that point S and C_D would remain constant for higher velocities. After that velocity is reached, then for higher velocities, drag would increase proportionately to the square of velocity and power would increase proportionately to the cube of velocity. In other words, between 0.00 m/s and 0.60 m/s, the changes in S and C_D mask the parabolic relationship of drag with velocity. Because the velocity at which S and C_D become constant is not known, extrapolations far beyond the maximum velocity for which drag was measured would be risky.

The effect of the changing values of S and C_D is evident in this data set. For example in Table 1, as velocity doubles from 0.30 m/s to 0.60 m/s, drag increases by only 2.09 and 2.52 for the Wildlife Computers PAT and the Microwave Telemetry PTT-100, respectively, rather than by a factor of four. Similarly, power increases by 4.13 and 5.00 for the two PSATs and not by a factor of eight. For both these tags, θ decreases with increasing velocity resulting in a smaller value for S and a different value for C_D.

By examining the forces exerted by a PSAT at various velocities, insights regarding the impact of these forces on a study animal can be gained. The combined forces of lift and drag act chronically on the anchor site of the PSAT. Although this study does not specifically address attachment methods, the forces of lift and drag exerted by a PSAT are not negligible and cannot be ignored when evaluating an attachment technique. A PSAT also imposes an energetic cost to the study animal. If that energy cost compromises the animal's behavior or survival, the information gained from the tag is not representative of an untagged animal. By estimating the energetic cost to an intended study animal, a researcher can make a more informed decision regarding the suitability of the animal for this type of tagging. Although direct extrapolation to higher swimming speeds is not possible with our data, the principles outlined in this study can be applied to faster swimming species such as tunas and billfishes that are frequently tagged.

Acknowledgments

We would like to thank T. Nelson, S. Wilson, W. Reisner and R. Gammisch for their assistance in running and setting up the flume, T. Mathes for his enthusiastic support, and R. Brill, D. Kersetter, and J. Hoenig for helpful discussions. Financial support was provided by NOAA Office of Sea Grant.

Literature cited

Arnold, G., and H. Dewar
2001. Electronic tags in marine fisheries research: a 30-year perspective. *In* Electronic tagging and tracking in marine fisheries (J. R. Sibert and J. L. Nielsen, eds.), p. 7–64. Kluwer Academic Publishers, Dordrecht, The Netherlands.

Blaylock, R. A.
1990. Effects of external biotelemetry transmitters on behavior of the cownose ray *Rhinoptera bonasus* (Mitchill 1815). J. Exp. Mar. Biol. Ecol. 141:213–220.
1992. Distribution, abundance, and behavior of the cownose ray, *Rhinoptera bonasus* (Mitchill 1815), in lower Chesapeake Bay. Ph.D. diss., 129 p. College of William and Mary, Williamsburg, VA.

Block, B. A., H. Dewar, C. Farwell, and E. D. Prince.
1998. A new satellite technology for tracking the movement of Atlantic bluefin tuna. Proc. Natl. Acad. Sci. 95:9384–9389.

Dagorn, L., E. Josse, and P. Bach.
2001. Association of yellowfin tuna (*Thunnus albacares*) with tracking vessels during ultrasonic telemetry experiments. Fish. Bull. 99:40–48.

DuPreez, H. H., A. McLachlan, and J. F. K. Marais.
1988. Oxygen consumption of two nearshore marine elasmobranchs, *Rhinobatos annulatus* (Muller & Henle, 1841) and *Myliobatus aquila* (Linnaeus, 1758). Comp. Biochem. Physiol. 89A:283–294.

Graves, J. E., B. E. Luckhurst, and E. D. Prince.
2002. An evaluation of pop-up satellite tags for estimating post-release survival of blue marlin. Fish. Bull. 100:134–142.

Gunn, J., and B. Block.
2001. Advances in acoustic, archival, and satellite tagging of tunas. *In* Tuna: physiology, ecology, and evolution (B. A. Block and E. D. Stevens, eds.), p. 167–224. Academic Press, San Diego, CA.

Hill, R. D., and M. J. Braun.
2001. Geolocation by light level—the next step: latitude. *In* Electronic tagging and tracking in marine fisheries (J. R. Sibert and J. L. Nielsen, eds.), p. 315–330. Kluwer Academic Publishers, Dordrecht, The Netherlands.

Kerstetter, D. W.
2002. Use of pop-up satellite tag technology to estimate survival of blue marlin (*Makaira nigricans*) released from pelagic longline gear. M.S. thesis, 109 p. College of William and Mary, Williamsburg, VA.

Lutcavage, M. E., R. W. Brill, G. B. Skomal, B. Chase, and P. Howey.
1999. Results of pop-up satellite tagging of spawning size class fish in the Gulf of Maine: Do North Atlantic bluefin tuna spawn in the mid-Atlantic? Can. J. Fish. Aquat. Sci. 56:173–177.

Sibert, J. R., M. K. Musyl, and R. W. Brill.
2003. Horizontal movements of bigeye tuna (*Thunnus obesus*) near Hawaii determined by Kalman filter analysis of archival tagging data. Fish. Oceanogr. 12: 141–151.

Smith, J. W.
1980. The life history of the cownose ray, *Rhinoptera bonasus* (Mitchill 1815), in lower Chesapeake Bay, with notes on the management of the species. M.A. thesis, 151 p. College of William and Mary, Williamsburg, VA.

Effects of El Niño events on energy demand and egg production of rockfish (Scorpaenidae: *Sebastes*): a bioenergetics approach

Chris J. Harvey

Northwest Fisheries Science Center
National Marine Fisheries Service
2725 Montlake Blvd. E
Seattle, Washington 98112
E-mail address: Chris.Harvey@noaa.gov

Abstract—Fish bioenergetics models estimate relationships between energy budgets and environmental and physiological variables. This study presents a generic rockfish (*Sebastes*) bioenergetics model and estimates energy consumption by northern California blue rockfish (*S. mystinus*) under average (baseline) and El Niño conditions. Compared to males, female *S. mystinus* required more energy because they were larger and had greater reproductive costs. When El Niño conditions (warmer temperatures; lower growth, condition, and fecundity) were experienced every 3–7 years, energy consumption decreased on an individual and a per-recruit basis in relation to baseline conditions, but the decrease was minor (<4% at the individual scale, <7% at the per-recruit scale) compared to decreases in female egg production (12–19% at the individual scale, 15–23% at the per-recruit scale). When mortality in per-recruit models was increased by adding fishing, energy consumption in El Niño models grew more similar to that seen in the baseline model. However, egg production decreased significantly—an effect exacerbated by the frequency of El Niño events. Sensitivity analyses showed that energy consumption estimates were most sensitive to respiration parameters, energy density, and female fecundity, and that estimated consumption increased as parameter uncertainty increased. This model provides a means of understanding rockfish trophic ecology in the context of community structure and environmental change by synthesizing metabolic, demographic, and environmental information. Future research should focus on acquiring such information so that models like the bioenergetics model can be used to estimate the effect of climate change, community shifts, and different harvesting strategies on rockfish energy demands.

Manuscript submitted 20 October 2003 to the Scientific Editor's Office.

Manuscript approved for publication 2 August 2004 by the Scientific Editor.

Fish. Bull. 103:71–83 (2005).

Over 90 species of rockfish (*Sebastes* spp.) are found in kelp beds, rocky reefs, pelagic habitats, and continental shelf and slope zones of the temperate and subarctic North Pacific; these species feed on a range of organisms, from zooplankton to fish (Love et al., 2002). Although they are a key component of groundfish fisheries on the U.S. Pacific Coast, many rockfish have declined considerably in recent decades, owing to overfishing and climate-induced downturns in production (Parker et al., 2000). Conservation efforts, ranging from coast-wide fishery closures to establishment of marine reserves, have been enacted in order to rehabilitate rockfish stocks. The efficacy of such actions depends in part on the dynamics of the communities in which rockfish exist. Key among these dynamics are trophic interactions, as influenced by abiotic factors and rockfish population structure.

Although rockfish are widely distributed and important to the ecology, fisheries, and conservation efforts of the Pacific Coast, little is known about their trophic dynamics. For example, of the 65 rockfish species that live along the North American West Coast, quantitative diet data are available for only 15 species (Murie, 1995). Better information on the food habits and energetics of both juvenile and adult rockfish would facilitate a greater understanding of the role they play in their communities, and how their role is affected by external forces. This is particularly true given observations that environmental variation can have strong effects on rockfish growth and condition (Lenarz et al., 1995; Woodbury, 1999).

Fish bioenergetics models relate the energy consumption, growth, and energy allocation patterns of fishes to environmental and physiological variables such as temperature, food quality, body size, and reproductive status (Kitchell et al., 1977). These models, founded in thermodynamic laws of mass and energy balance, can successfully predict patterns of energy demands by fish (Madenjian et al., 2000). At the scale of the individual fish, bioenergetics models can estimate effects of a fish on its community (in terms of the amount of prey it consumes) and effects of the environment on the fish, such as how changes in temperature or food availability influence energy consumption and growth (Rice et al., 1983). When coupled to population models, bioenergetics models can predict prey-predator supply-demand relationships (Negus, 1995) and determine how different fishery management policies will affect prey resources in the community from which the targeted fish is extracted (Kitchell et al., 1997; Essington et al., 2002; Schindler et al., 2002). Thus, these models may facilitate a more community- or ecosystem-level approach to rockfish management.

In this study, I develop a generic *Sebastes* bioenergetics model. My first objective is to detail the parameters and the sensitivity analysis of the model, thereby offering a synthesis of what is known about *Sebastes* energetic physiology and identifying parameters for which greater information is desirable. The second goal is to present a simple application of the model: an estimation of the effects of

El Niño related environmental changes on the energy demands of blue rockfish (*S. mystinus*) under unfished and fished conditions. Two relevant characteristics of El Niño events in U.S. West Coast waters are elevated temperatures and reductions in growth rates and reproductive condition of *Sebastes* (Lenarz et al., 1995; VenTresca et al., 1995; Woodbury, 1999). The bioenergetics approach can incorporate these changes and can therefore help to characterize the role of rockfish as consumers in a dynamic environment.

Methods

Model structure

I followed the basic structure of bioenergetics models established for other fishes (e.g., Kitchell et al., 1977; Hewett and Johnson, 1992), in which energy intake (consumption) equals all energy outputs (respiration, wastes, growth, and reproduction). The basic model equation is

$$C = (R + A + S) + (F + U) + (\Delta B + G), \quad (1)$$

where C = consumption, R = respiration, A = active metabolism, S = specific dynamic action (digestive costs), F = egestion, U = excretion, ΔB = somatic growth, and G = gonad production. The respiration and active metabolism portions of Equation 1 take the form

$$R = RA \times W^{RB} \times f(T) \times ACT, \quad (2)$$

where RA and RB are constants that describe the allometric respiration function, W is wet biomass, $f(T)$ is a temperature dependence function, and ACT is an activity multiplier (Kitchell et al., 1977). The function $f(T)$ (Kitchell et al., 1977) is a hump-shaped function that requires estimates of optimal (RTO) and maximum (RTM) temperatures for respiration, and a Q_{10} (RQ).

The terms S, U, and F all scale to total consumption (Kitchell et al., 1977). One can thus think of them as a general energy loss term

$$Loss = (S + U) \times (C - F) + F. \quad (3)$$

Model parameters

Although parameters are derived from studies of many rockfish species, I developed the present model to describe energetic dynamics of *S. mystinus*, for which a considerable literature exists regarding diet and responses to climate variability (e.g., Hallacher and Roberts, 1985; Bodkin et al., 1987; Hobson and Chess, 1988; Lenarz et al., 1995; VenTresca et al., 1995).

Respiration parameter estimates came from studies of other *Sebastes* species or related scorpaenid fishes (Table 1). For RTM, I used published estimates for *S. thompsoni* and *S. schlegeli* (Ouchi, 1977; Tsuchida and Setoguma, 1997), and assumed that RTO would be 5°C cooler. The resulting RTO was similar to upper temperatures at which juvenile *S. diploproa* experienced zero growth while feeding (Boehlert, 1981). RQ was based on low-temperature Q_{10} values in several scorpaenid respiration studies (Boehlert et al. 1991; Yang et al., 1992; Kita et al., 1996; Vetter and Lynn, 1997). RA, the oxygen consumption rate for a 1-g fish at RTO, was derived from data for nongestating *S. schlegeli* (Boehlert et al., 1991). RB, which describes the allometric scaling of respiration, was also derived from data for nongestating *S. schlegeli* spanning a range of roughly 0.7 to 1.9 kg body mass (Boehlert et al., 1991). Respiration terms were converted to energy units by an oxycalorific correction (13.56 J/mg O_2), and then to biomass by assuming that rockfish energy density (ED) = 6,120 J/g wet mass (Perez, 1994).

The ACT multiplier was assumed to equal 1. This assumption is best justified in cases where routine respiration rates were used to determine parameters for the model. Boehlert et al. (1991) stated that *S. schlegeli* in their analysis were generally inactive, which implies that rates derived from their data represent resting

Table 1

Parameter values for the generic *Sebastes* bioenergetics model.

Parameter	Description	Value
RA	Intercept of the allometric respiration function	0.0143
RB	Slope for allometric respiration function	−0.2485
RQ	Slope for temperature dependence of respiration (Q_{10})	2
ACT	Multiplier for active metabolism	1
RTO	Optimum temperature for respiration	23°C
RTM	Maximum temperature for respiration	28°C
SDA	Specific dynamic action coefficient	0.163
FA	Egestion coefficient	0.104
UA	Excretion coefficient	0.068
ED	Energy density (somatic tissue) of wet mass	6,120 J/g
GED	Energy density (female gonadal tissue) of wet mass	8,627 J/g
GA	Coefficient of the female length-fecundity relationship	1.559
GB	Exponent of the female length-fecundity relationship	3.179
GSI_{max}	Maximum male gonadosomatic index	0.008

metabolism. I chose to keep *ACT* at 1, however, because I could find no data describing a reasonable activity multiplier. Thus, *Sebastes* model outputs may underestimate energy consumption under conditions in which individuals are especially active.

I obtained growth (ΔB in Eq. 1) terms using von Bertalanffy length-at-age curves and data for length-to-mass conversions for *S. mystinus* as summarized by Love et al. (2002). Because female *S. mystinus* are larger at age than males, growth was modeled with sex-specific von Bertalanffy curves with the difference equation method of Gulland (1983). Digestion and waste terms *S*, *F*, and *U* were derived from previous teleost models (Hewett and Johnson, 1992).

I estimated gonad production (*G*) with gonadosomatic indexes (GSI) and size-fecundity relationships (females only), assuming that female and male *S. mystinus* mature gradually over the range of lengths observed by Wyllie-Echeverria (1987), and reproduce once annually. For males, I assumed that gonads have the same *ED* as somatic tissue; for females, I assumed that gonadal energy density (*GED*) = 8,627 J/g, which was the average of gonadal energy density at the onset of embryogenesis for *S. flavidus* and *S. jordani* (MacFarlane and Norton, 1999). Estimated maximum female GSI was based on a fecundity-length relationship:

$$fecundity = GA \times TL^{GB}, \quad (4)$$

where *GA* and *GB* were taken from a generic rockfish length-fecundity relationship (Love et al., 2002) and *TL* is total length in cm. Fecundity was converted to biomass units by assuming that each egg weighed 0.0003 g, which I derived from Love et al. (1990) by dividing the mean maximum female gonad weight by the estimated fecundity of modal mature females for several species. For mature males, I assumed a constant maximum GSI based on data for other species (Love et al., 1990). Post-spawning GSI was assumed to be 10% of the maximum for each sex, as with other rockfish (Love et al., 1990). The *G* terms were the difference between the maximum and minimum GSIs for each sex, expressed as mass (and, in females, adjusted by multiplying by *GED*/*ED*).

Rockfish are viviparous, and developing larvae may receive energy from both yolk and maternal sources (Love et al., 2002). During gestation in a laboratory, female *S. schlegeli* consumed 35% to 117% more oxygen than nongestating fish of similar size (Boehlert et al., 1991). To account for the possibility that blue rockfish may also be matrotrophically viviparous, I increased female respiration by 50% during the gestation period (assumed to be 45 days per year based on gestation times of other species [Boehlert et al., 1991]).

Model application: effects of El Niño on blue rockfish energy consumption

To examine the effects of El Niño on *S. mystinus* energy consumption, I created two model conditions: a baseline model and an El Niño model that estimated *S. mystinus* energy demands, in megajoules (MJ), required for necessary growth, reproduction, and related metabolic costs. I used MJ rather than prey biomass as the currency because quantitative, seasonal diet data for *S. mystinus* in northern California were available for average years (Hobson and Chess 1988) but not for El Niño years. During the 1982–83 El Niño, Lea et al. (1999) found that central Californian *S. mystinus* consumed large numbers of the pelagic crab *Pleuroncodes planipes*, which is typically found south of Point Conception during average years. During the same time period, *S. mystinus* ate few tunicates or scyphozoans (Lea et al., 1999), which were the predominate prey of *S. mystinus* in average years (Hobson and Chess, 1988). These findings suggest a major shift in *S. mystinus* prey composition during El Niño events.

Table 2

Changes in the *S. mystinus* bioenergetics model that were implemented in El Niño scenarios in relation to the baseline model.

Variable	Change
Temperature	Increased 1.5°C in El Niño years[1]
Growth (length increment)	Decreased 17.5% in El Niño years[1]
Female condition factor	Decreased 10% in El Niño years; decreased 5% the year following an El Niño[2]
Male condition factor	Decreased 7.5% in El Niño years; decreased 5% the year following an El Niño[2]
Fecundity	Decreased 67% in El Niño years[2]

[1] Source: Lenarz et al., 1995.
[2] Source: VenTresca et al., 1995.

The baseline model simulates energy consumption of northern California *S. mystinus* from age 0 to age 30, based on quarterly growth estimates from sex-specific von Bertalanffy curves (Love et al., 2002) and seasonal temperature data from Hobson and Chess (1988). Mature females released larvae in the fourth quarter of each year, and mature males released gametes in the third quarter (Wyllie-Echeverria, 1987). Energy consumption for both sexes from ages 0 to 30 was expressed at two scales: for the 30-year life span of an individual; and on a per-recruit basis (under the assumption that there was no fishing mortality and that the natural mortality rate [*M*] was 0.2, applied in quarterly time steps).

The El Niño model was similar to the baseline model, except an El Niño occurred every three to seven years. During these years there were changes in temperature, growth, condition, and fecundity (Table 2). Temperature increases in El Niño years were similar to temperature anomalies in northern California waters during major El Niño events from 1957 to 1993 (Lenarz et al., 1995). Changes in growth (in terms of length increment), con-

dition (the ratio of actual to expected weight, based on length-weight relationships), and fecundity were based on empirical measures of *S. mystinus* during El Niño years (Lenarz et al., 1995; VenTresca et al., 1995). As in the baseline model, I expressed energy consumption by both sexes at individual and per-recruit scales.

Finally, I ran simulations at the per-recruit scale in which the total mortality rate (Z) was increased by adding a fishing-induced mortality rate (F) in increments of 0.05 to M; fishing mortality was imposed on fish greater than 20 cm, the size at which *S. mystinus* enters fisheries in California waters (Laidig et al., 2003). The range of Z examined was 0.2 (natural mortality only) to 1.0 (a heavily overfished condition). These simulations were run under baseline conditions and El Niño conditions to determine if there was any interaction between El Niño effects and Z.

Sensitivity analysis

To measure sensitivity of the *Sebastes* bioenergetics model to different parameters, I used a Monte Carlo error analysis method (Bartell et al., 1986). In this method, parameters are drawn randomly from normal distributions with means equal to parameter estimates (Table 1) and with a coefficient of variation (CV) of either 2%, 10%, or 20%. Cases where randomly drawn *RTO* was greater than *RTM* were discarded. Female and male models were run 1000 times for each of the three CVs. Individual simulations ran to age 30 at 0.25-year increments; seasonal temperatures were those used in the baseline model. Parameter influence on 30-year cumulative consumption estimates was judged according to the parameters' relative partial sums of squares (RPSS), which quantify the influence of a parameter after all other parameters have been accounted for. RPSS for all parameters were calculated with SYSTAT (version 10.2, SYSTAT Software Inc., Richmond, CA). Additionally, means and standard deviations of consumption estimates from RPSS analyses were calculated to capture the range of energy consumption possible over the lifetime of female and male *S. mystinus*.

Results

Northern California *S. mystinus* baseline energy demands

Baseline energetic demands of northern California *S. mystinus* were a function of size, sex, and the scale of calculation (i.e., individual versus per recruit). As size increased, more energy was allocated to respiration, elimination of wastes, and reproduction, and steadily less energy was allocated to growth (Fig. 1). At the individual scale, females consumed more than males at all ages. The sexes diverged markedly as fish matured (beginning at age 3 for females, age 4 for males), and continued to diverge as fish approached asymptotic sizes (Fig. 2A). The disparity was related to sex-based differences in growth rate, maximum size, GSI, and the increased respiration of gestating females. Cumulative consumption through age 30 was 285.0 MJ for individual females, and 174.6 MJ for individual males. Assuming a prey energy density of 1500 J/g (given *S. mystinus* diets [Hobson and Chess, 1988] and prey-density measurements of the same or related prey species [Paine and Vadas, 1969; Thayer et al., 1973; Foy and Norcross, 1999]), this energy density equates to a long-term average energy consumption rate of 2.7% body mass per day for females and 2.8% body mass per day for males.

Females also had greater requirements than males at the per-recruit scale, although mortality gradually lessened the contribution of older age classes (Fig. 2B), nullifying some of the disparity between the sexes at the individual scale. Cumulative female and male per-recruit energy consumption was 20.7 MJ and 14.8 MJ, respectively. Per-recruit energy consumption, the product of age-specific consumption rate and relative fish abundance, peaked at ages 4–6, indicating that those age groups have the greatest potential to affect their prey species.

Effects of El Niño on *S. mystinus* energetics

El Niño events changed *S. mystinus* energy consumption compared to that in the baseline model, but the direction and magnitude of change were dependent on sex, age, scale of calculation (individual vs. per recruit), and the number and frequency of El Niño events experienced by a given cohort. To demonstrate this change, I modeled growth of two cohorts that experienced El Niño regimes of moderate or high intensity. The first cohort ("cohort A") experienced five El Niño events by age 30, whereas the second cohort ("cohort B") experienced eight El Niño events (Figs. 3 and 4).

At the scale of individual fish, cohorts A and B experienced lower energy consumption in El Niño events, particularly among females. During El Niño years, which first occurred at age 3 for cohort A and at age 1 for cohort B, consumption by females was always lower than the baseline value (Fig. 3A). In immature females, the disparity was 7–10% lower than the baseline value and was 12–13% lower for mature females. These reductions in consumption were a function of lower growth rates, poor condition factor, and reduced fecundity during El Niño years. In contrast, consumption by males during El Niño years was 4–9% lower than the baseline value among immature individuals, but was roughly equal to the baseline value for mature individuals (Fig. 3B), in part because males did not experience drastic changes in reproductive condition during El Niño years. Both sexes experienced years when energy consumption was greater than the baseline value, particularly two years after an El Niño event when the somatic condition factor returned to normal and greater-than-average growth for that age occurred. By age 30, sizes of fish in both El Niño models were close to the asymptotic maxima and were therefore similar to baseline sizes (Table 3). Cumulative 30-year energy consumption values were

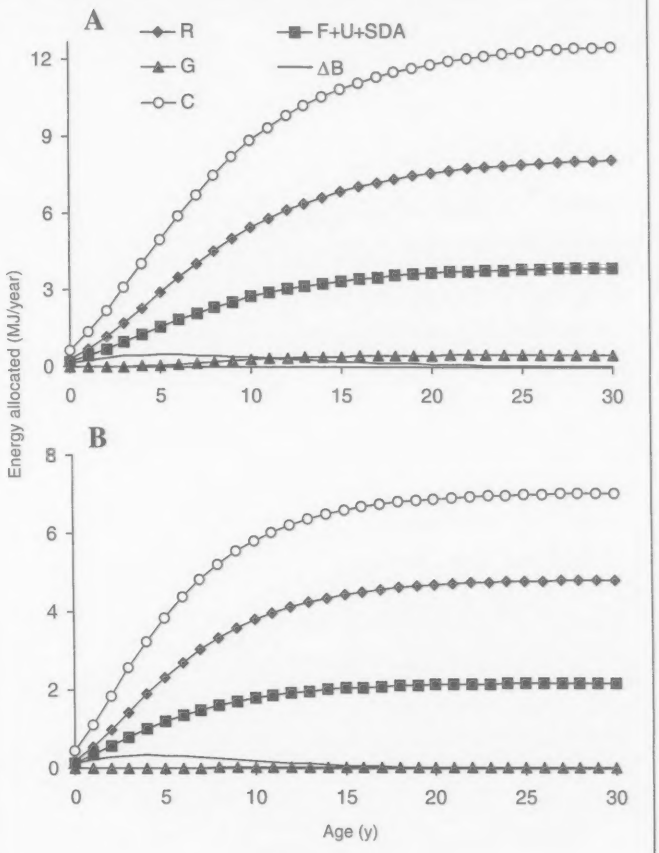

Figure 1

Estimated allocation of energy consumption by northern California *S. mystinus* from ages 0 to 30 under baseline model conditions. Consumption (C) is allocated as respiration (R), waste, and digestive costs (F+U+SDA), growth (ΔB), and reproduction (G). (**A**) Females. (**B**) Males.

also similar in all models and in both sexes, despite the declines experienced by females.

Repeated exposure to El Niño also affected reproduction by *S. mystinus*. Both sexes experienced delays in maturation as a result of slowed growth rates during El Niño events, and the delay was related to the number of El Niño years experienced at young ages. In the baseline model, 50% maturity was reached at age 6 for both sexes. In cohort A, 50% maturity was reached at age 6 by females, but at age 7 by males. Under the more arduous conditions of cohort B, both sexes reached 50% maturity at age 7. The effect of delayed maturation in terms of energy consumption should be greatest in females because of their greater investments in reproduction, although this was not especially noticeable at the scale of cumulative consumption per individual (Table 3). A further effect of El Niño events occurred in female egg production. The dramatic reduction in fecundity during El Niño years over the course of an individual female's life caused cumulative egg production in cohort A to be only 87.9% of the baseline level, and cohort B female egg production was only 81.3% of the baseline level (Fig. 3C).

More pronounced El Niño effects occurred at the per-recruit scale. El Niño conditions reduced per-recruit energy consumption in both sexes in contrast to baseline conditions (Fig. 4, A and B). Incorporating mortality lowered the contribution of older age groups, where individual consumption was highest (Fig. 3, A and B), thereby magnifying the El Niño effects on young fish. The negative effects on young age classes were exacerbated in females by slowed maturation and reduced

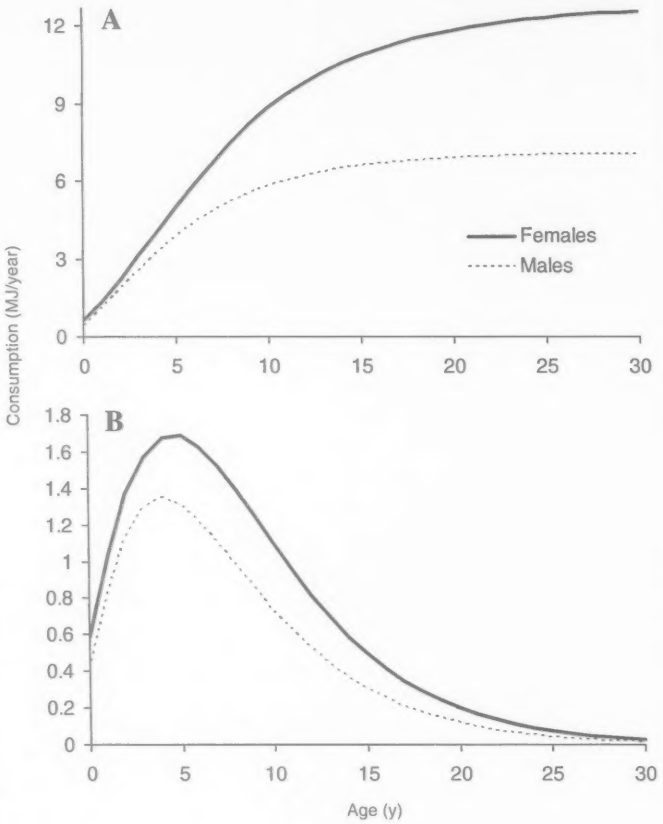

Figure 2

Estimated energy consumption by *S. mystinus* under baseline model conditions. (**A**) Females and males at the per-individual scale. (**B**) Females and males at the per-recruit scale, assuming a mortality rate (Z) of 0.2 (i.e., no fishing mortality).

Table 3

Final weights and cumulative energy consumptions for female and male *S. mystinus* from bioenergetics models run under baseline and El Niño conditions. All values are taken from the end of the 30th year. Cohort-A and cohort-B individuals experienced five and eight El Niño events, respectively (see Figs. 3 and 4).

	Final weight (g)		Total consumption (MJ)	
Model	Females	Males	Females	Males
Baseline	1,134.3	617.2	285.0	174.6
Cohort A	1,129.4	616.5	278.1	173.3
Cohort B	1,126.8	616.1	273.6	172.1

fecundity (due to slower growth), resulting in lower per-recruit consumption to meet reproductive costs. Thirty-year cumulative per-recruit energy consumption was 20.0 MJ for cohort-A females (3.2% lower than the baseline value), and 19.4 MJ for cohort-B females (6.3% less than the baseline value). Cumulative per-recruit consumption by cohort-A males was 14.5 MJ (1.9% lower than baseline), whereas cohort-B males consumed 14.2 MJ (4.4% less than the baseline level). The reduction of cumulative egg production was also more drastic at the per-recruit scale: cohort-A females produced 15% fewer eggs than the baseline level, whereas cohort-B females produced 23% fewer eggs at the per-recruit scale (Fig. 4C). These reductions in egg production were related to smaller size, lower fecundity in El Niño years, delayed maturation, and accumulative mortality, all of which allowed fewer females to reach maturity.

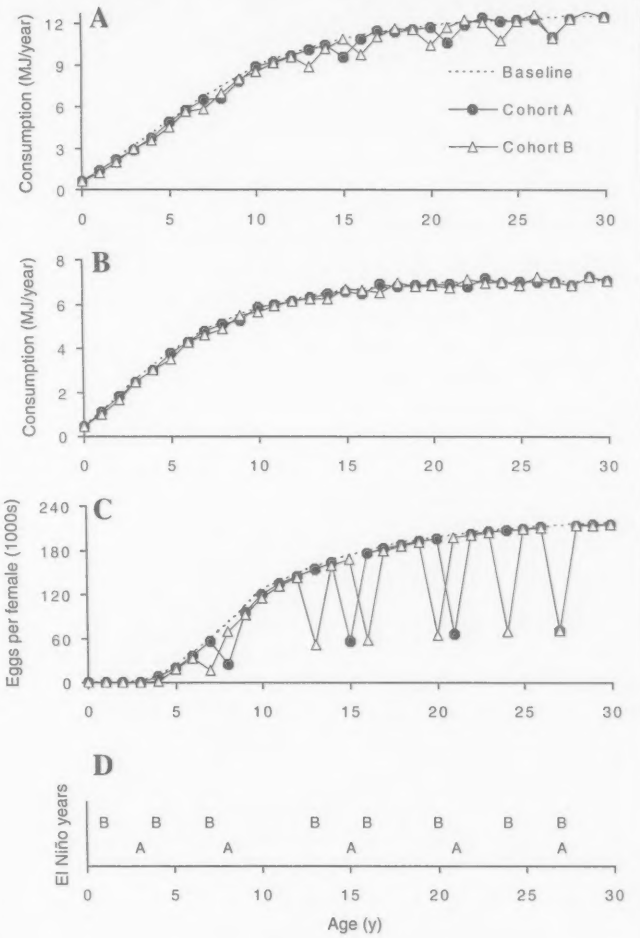

Figure 3

Estimated energy consumption and egg production by *S. mystinus* at the per-individual scale, under baseline conditions and for two cohorts (A and B) in which El Niño events occurred every three to seven years. (**A**) Female energy consumption. (**B**) Male energy consumption. (**C**) Egg production. (**D**) Timing of El Niño events for cohorts A and B.

Effects of El Niño on fished cohorts

Adding fishing mortality to the total mortality rate applied in the per-recruit simulations caused changes in the total energy consumption and egg production of *S. mystinus* experiencing repeated El Niño events, in constrast to the baseline state. Under both El Niño regimes, per-recruit consumption by both sexes increased slowly as Z increased until it was nearly identical to the baseline level for cohort A (Fig. 5A) or exceeded the baseline for cohort B (Fig. 5B). The reason for this is that the slower growth experienced during El Niño years meant that fish reached 200 mm (the size of recruitment into the fishery) later and therefore were not as rapidly subjected to fishing mortality as baseline fish. This extra period of feeding prior to reaching 200 mm was sufficient to equal or exceed the per-recruit energy consumption level in the baseline model.

In contrast, increased Z caused strong declines in egg production, and that effect was exacerbated by the frequency of El Niño years, as demonstrated by the steeper decline in cohort B (Fig. 5B). Delayed maturation caused by El Niño meant that many females were removed by fishing before they were able to reproduce;

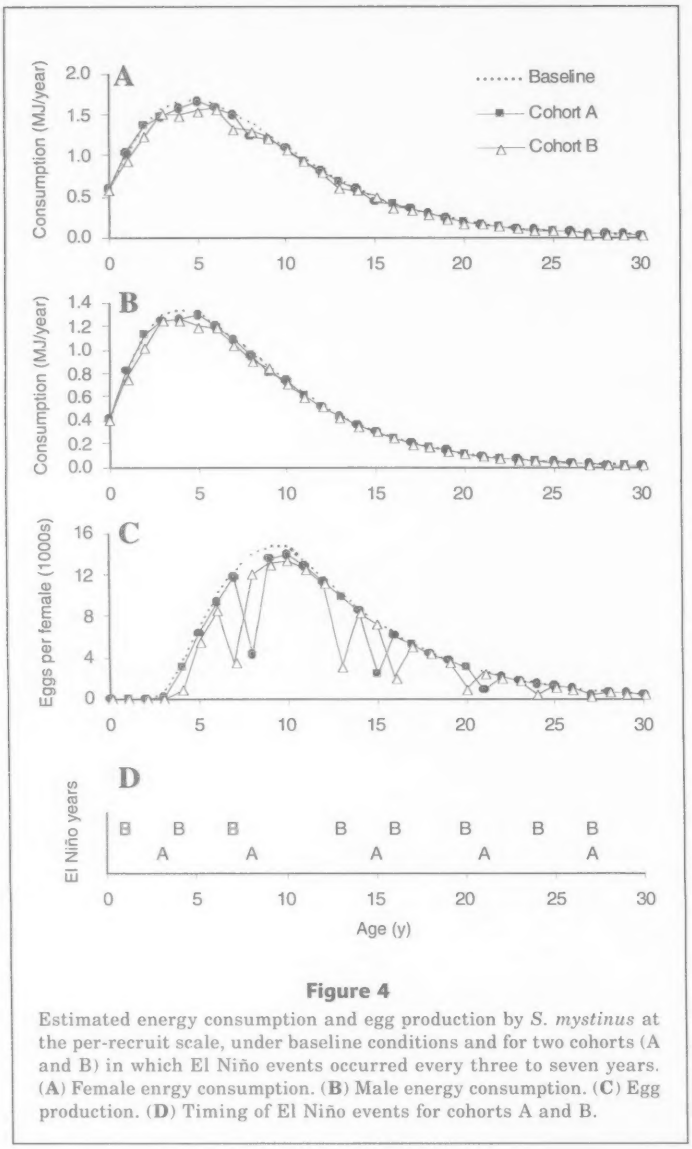

Figure 4

Estimated energy consumption and egg production by *S. mystinus* at the per-recruit scale, under baseline conditions and for two cohorts (A and B) in which El Niño events occurred every three to seven years. (**A**) Female enrgy consumption. (**B**) Male energy consumption. (**C**) Egg production. (**D**) Timing of El Niño events for cohorts A and B.

furthermore, those that escaped fishing had lower fecundities because of their smaller size and reduced egg production because of the number of El Niño years experienced.

Sensitivity analysis

Based on the RPSS analysis, sensitivity of rockfish bioenergetics models to parameter variation was a function of sex, size, and the CV of the parameter set. When CV = 2%, the model was most sensitive to respiration parameters in Equation 2 (particularly *RB*, *RQ*, and *RTO*) and to *ED*, although the rank order varied slightly by sex (Fig. 6, A and B). The sum of the $RPSS_{CV=2\%}$ for all parameters was >0.99 for both the male and female models. This result implies that energy consumption responded linearly to parameter variation because summed RPSS values scale from 0 to 1, with 1 implying a linear response to parameter perturbation (Bartell et al., 1986). When CV increased to 10%, the rank order of parameter sensitivity changed slightly, although respiration parameters and *ED* remained most important

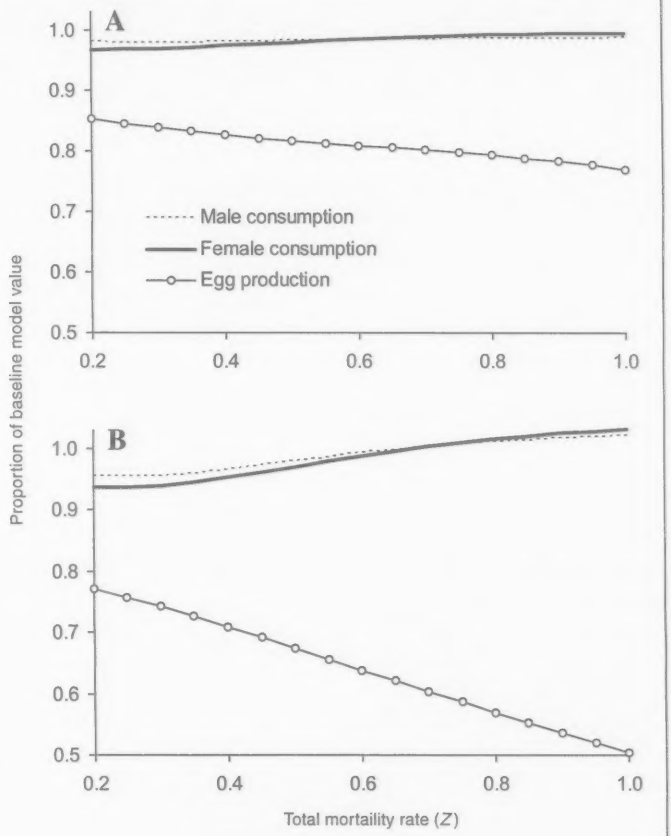

Figure 5

Effects of mortality (*Z*, increased due to fishing) on *S. mystinus* responses to El Niño events, in relation to a baseline model with identical *Z*. (**A**) Cohort A, which experienced 5 El Niño years (see Figs. 3 and 4). (**B**) Cohort B, which experienced 8 El Niño years.

(Fig. 6, C and D). $RPSS_{CV=10\%}$ values declined to 0.84 and 0.94 for females and males, respectively, indicating a greater degree of nonlinearity in response to parameter variation. Finally, when CV increased to 20%, there were major changes in parameter rank order and RPSS, especially for females (Fig. 6E). All female parameters essentially had equal weight, and $RPSS_{CV=20\%}$ dropped dramatically to 0.14, indicating a nonlinear response to parameter variation. Males experienced slight changes in parameter rank order at CV = 20% (Fig. 6F) and increasingly nonlinear behavior related to parameter variation ($RPSS_{CV=20\%}$ = 0.81). Because the major difference in the models for the two sexes is the reproductive terms (i.e., Eq. 4 for females vs. the simple GSI calculation for males), the *GA* or *GB* terms (or both) appear to be the cause of poor female model performance at high parameter uncertainty. Also, because *GA* and *GB* should only affect female energy budgets as the females mature, model sensitivity to those parameters is likely size dependent.

Energy consumption estimates generated in RPSS analyses were consistently greater than estimates generated by the baseline deterministic model, which used the parameter values from Table 1. Mean consumption estimates and standard deviations increased as the parameter CV increased (Table 4). This effect was more pronounced in females than in males, especially when parameter CV=20%. At that level of parameter uncertainty, male and especially female consumption estimates had very large standard deviations.

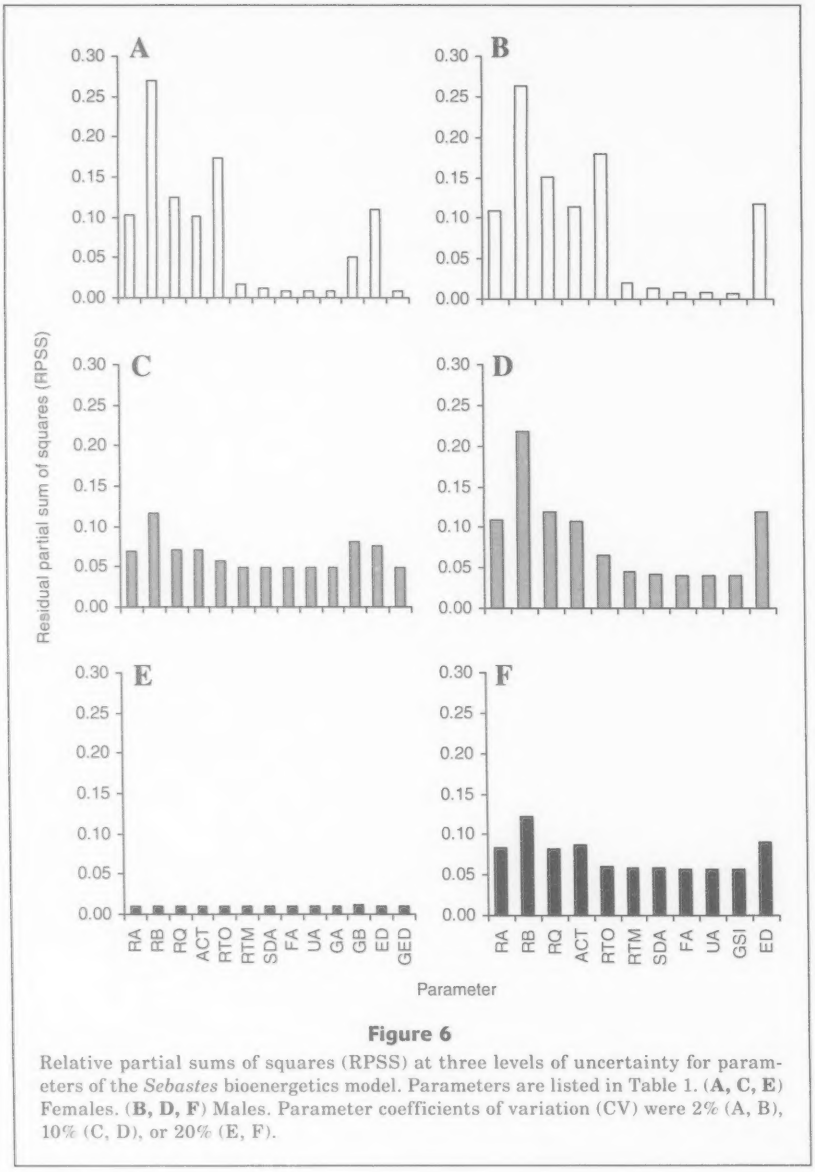

Figure 6

Relative partial sums of squares (RPSS) at three levels of uncertainty for parameters of the *Sebastes* bioenergetics model. Parameters are listed in Table 1. (**A, C, E**) Females. (**B, D, F**) Males. Parameter coefficients of variation (CV) were 2% (A, B), 10% (C, D), or 20% (E, F).

Discussion

According to the generic rockfish bioenergetics model, repeated exposure to El Niño conditions lowered the growth, maturation rate, and reproductive level of *S. mystinus*. This happened at both the individual and per-recruit scales; the latter may be most relevant when placing a cohort of fish into a community context because younger age groups have the greatest potential energy demand when mortality is accounted for. In El Niño years, increased temperatures caused respiration rates of both sexes to increase in contrast to respiration rate in the baseline model, whereas lower growth rates and poor fecundity reduced energy demands. In the long term, these rates equated to a net decrease in energy consumption, which was more pronounced in females than in males because of the higher growth rate and reproductive investment for females. Ironically, adding mortality through fishing pressure lessened the effect of El Niño on *S. mystinus* consumption in contrast to baseline conditions, but that was because rockfish in the El Niño models took longer to reach sizes vulnerable to

Table 4

Energy consumption estimates for *S. mystinus* by a deterministic baseline model (parameters given in Table 1) and simulations run for relative partial sums of squares (RPSS) analysis. Estimates from the RPSS analysis were determined at three levels of parameter uncertainty, with parameter coefficients of variation (CV) equal to 2, 10, or 20%.

	Estimated energy consumption (MJ; mean ±SD)	
Model	Females	Males
Baseline	285.0	174.6
CV = 2%	286.0 ±16.1	175.3 ±10.1
CV = 10%	314.3 ±102.8	183.9 ±57.6
CV = 20%	515.1 ±1131.4	209.0 ±131.7

fishing. However, the El Niño models may have overestimated per-recruit consumption because I did not add in direct El Niño related mortality; natural mortality may actually increase during El Niño years, as suggested by anecdotal mass mortality events affecting *S. mystinus* during the 1982–83 El Niño (Bodkin et al., 1987).

More dramatic than the effect of El Niño on energy consumption was the effect on egg production. Individual and per-recruit lifetime fecundity dropped (by roughly 12–19% and 15–23%, respectively) in the El Niño models—an effect that was even more drastic as fishing pressure increased. These declines were disproportionate in comparison to changes in long-term energy consumption, which declined by <4% at the individual scale and <7% at the per-recruit scale under even an arduous El Niño regime; and compared to changes in the size of age-30 individuals, which were essentially equal in the baseline and El Niño models. In other words, under a long-term climate regime with El Niño events, total energy demand of females is similar to a baseline regime, and lifetime gross conversion efficiency (growth/consumption) increases, but the conversion efficiency of consumption into reproduction is constrained considerably. That constraint is due largely to delayed maturity, poorer overall fecundity (particularly in El Niño years), and, at the per-recruit scale, the culling effect of natural and fishing mortality.

Of course, the implications from the models for *S. mystinus* must be viewed as hypotheses based on a generic *Sebastes* model. Although the ability of the bioenergetics approach to synthesize demographic, physiological, and environmental data makes it a powerful tool for characterizing dynamic linkages between fish, prey communities, and climate, use of this approach for studies of *Sebastes* will require additional empirical data. A rich body of information exists for some parameters, such as growth rate, fecundity, and depth distribution (Love et al., 1990; Love et al., 2002). However, many relevant data are lacking, notably diet data. Because of seasonal changes in temperature and reproductive state, rockfish energetics are also seasonal. Seasonal diet changes have been observed in several (largely inshore) species (Love and Ebeling, 1978; Hallacher and Roberts, 1985; Hobson and Chess, 1988; Murie, 1995). Diets may also change with fish size (Love and Ebeling, 1978; Murie, 1995). Data that capture the trophic ontogeny of different species would allow a better depiction of how energy consumptive patterns of a population change with demographics, particularly given the disproportionate demands of younger age classes (Fig. 4). When possible, diet data should be based on weight or volume so that estimates of energy requirements can be readily converted into masses of prey consumed.

Properly incorporating environmental variability will require information not just on temperature variability, but on how rockfish growth, reproduction, and diet vary under different climate regimes. As discussed previously, El Niño and Pacific Decadal Oscillation events have been shown to affect growth, fecundity, and recruitment success of some well-studied species of rockfish. Little information is available on how these factors are affected by La Niña events, however. Furthermore, climate variability may lead to markedly different prey communities (Brodeur and Pearcy, 1992; Lea et al., 1999), resulting in diet shifts about which we currently have little information for most rockfish. Because *S. mystinus* maintained relatively high energy demand during El Niño years, despite slower growth rates and lower fecundity, the prey quality and quantity during such events is clearly important.

Ultimately, these models can be expanded to the population level to place rockfish in the context of their communities. This approach can elucidate how factors such as fishing, environmental variability, and recruitment variability influence the role of rockfish as predators on specific prey taxa, as has been done in bioenergetics models for other predators (Kitchell et al., 1997; Essington et al., 2002; Schindler et al., 2002). Because energy budgets are influenced by fish size and reproductive state, expanding to the population level will require size- or age-structured population models, such as those used in many rockfish stock assessments (e.g., Pacific Fishery Management Council, 2000). Most *Sebastes* stock assessments to date are for species that live in shelf or slope habitats, whereas the species whose food habits and basic energetic information are best known are inshore species. Therefore, a key part of producing useful bioenergetics analysis at the population level will be to prioritize populations or species assemblages for which bioenergetics models might be most useful, and to identify which type of information (population structure or basic biology and ecology) is lacking.

Finally, the generic model parameters in this study required information from several species. Interspecies parameter borrowing has been criticized (Ney, 1993), and the results from such models deserve careful appraisal. The sensitivity analysis demonstrates the importance of this issue: with increasing parameter uncertainty,

the model not only became less reliable (i.e., RPSS decreased, especially for females), but also projected higher energy consumption rates. However, the sensitivity analysis points specifically to the parameters (respiration, energy density, female fecundity) that are most influential and deserve attention in laboratory studies. Additional work is required to better characterize *ACT*, the activity multiplier, particularly for *Sebastes* species that are more pelagically oriented. In many bioenergetics models, consumption is a parameter, such that growth, not consumption, can be the model output. Although studies of energy consumption by juvenile black rockfish (*S. melanops*) have been undertaken (Boehlert and Yoklavich, 1983), more effort is needed in this area.

Conclusion

Although there are limitations to realizing the potential of bioenergetics models in the study of rockfish ecology, those limitations do not overshadow the value of using available information to produce general heuristic models to examine important questions. Such questions include how climate variability affects rockfish consumption patterns, reproduction, and predation rates on different prey taxa; how size-selective fishing may influence rockfish consumption patterns; and how rockfish energy demands compare with available prey resources in regions where population rebuilding efforts are proposed or under way. When ultimately coupled with population models, the bioenergetics approach offers a means to clarify the role that rockfish play in their communities.

Acknowledgments

Suggestions from Phil Levin, Nick Tolimieri, Daniel Schindler, Rich Zabel, Jim Kitchell, Steve Bartell, Kevin Piner, Tina Wyllie-Echeverria, and two anonymous reviewers greatly improved this manuscript.

Literature cited

Bartell, S. M., J. E. Breck, R. H. Gardner, and A. L. Brenkert.
1986. Individual parameter perturbation and error analysis of fish bioenergetics models. Can. J. Fish. Aquat. Sci. 43:160–168.

Boehlert, G. W.
1981. The role of temperature and photoperiod in the ontogenetic migration of prejuvenile *Sebastes diploproa* (Pisces: scorpaenidae). Calif. Fish. Game 67:164–175.

Boehlert, G. W., and M. M. Yoklavich.
1983. Effects of temperature, ration, and fish size on growth of juvenile black rockfish, *Sebastes melanops*. Environ. Biol. Fishes 8:17–28.

Boehlert, G. W., M. Kusakari, and J. Yamada.
1991. Oxygen consumption of gestating female *Sebastes schlegeli*: estimating the reproductive costs of livebearing. Environ. Biol. Fishes 30:81–89.

Bodkin, J. L., G. R. VanBlaricom, and R .J. Jameson.
1987. Mortalities of kelp-forest fishes associated with large oceanic waves off central California, 1982–1983. Environ. Biol. Fishes 18:73–76.

Brodeur, R. D., and W. G. Pearcy.
1992. Effects of environmental variability on trophic interactions and food web structure in a pelagic upwelling system. Mar. Ecol. Prog. Ser. 84:101–119.

Essington, T. E., D. E. Schindler, R.J. Olson, J.F. Kitchell, C. Boggs, and R. Hilborn.
2002. Alternative fisheries and the predation rate of yellowfin tuna in the eastern Pacific Ocean. Ecol. Appl. 12:724–734.

Foy, R. J., and B. L. Norcross.
1999. Spatial and temporal variability in the diet of juvenile Pacific herring (*Clupea pallasi*) in Prince William Sound, Alaska. Can. J. Zool. 77:697–706.

Gulland, J. A.
1983. Fish stock assessment, 223 p. John Wiley and Sons, New York, NY.

Hallacher, L. E., and D. A. Roberts.
1985. Differential utilization of space and food by the inshore rockfishes (Scorpaenidae: *Sebastes*) of Carmel Bay, California. Environ. Biol. Fishes 12:91–110.

Hewett, S. W., and B. L. Johnson.
1992. Fish bioenergetics model 2, 79 p. Univ. Wisconsin Sea Grant Inst., Madison, WI.

Hobson, E. S., and J. R. Chess.
1988. Trophic relations of the blue rockfish, *Sebastes mystinus*, in a coastal upwelling system off northern California. Fish. Bull. 86:715–743.

Kita, J., S. Tsuchida, and T. Setoguma.
1996. Temperature preference and tolerance, and oxygen consumption of the marbled rockfish, *Sebasticus marmoratus*. Mar. Biol. 125:467–471.

Kitchell, J. F., D. E. Schindler, R. Ogutu-Ohwayo, and P. N. Reinthal.
1997. The Nile perch in Lake Victoria: interactions between predation and fisheries. Ecol. Appl. 7:653–664.

Kitchell, J. F., D.J. Stewart, and D. Weininger.
1977. Applications of a bioenergetics model to yellow perch (*Perca flavescens*) and walleye (*Stizostedion vitreum vitreum*). J. Fish. Res. Board Can. 34:1922–1935.

Laidig, T. E., Pearson, D. E., and L. L. Sinclair.
2003. Age and growth of blue rockfish (*S. mystinus*) from central and northern California. Fish. Bull. 101:800–808.

Lea, R. N., R. D. McAllister, and D. A. VenTresca.
1999. Biological aspects of nearshore rockfishes of the genus *Sebastes* from central California with notes on ecologically related sport fishes. Calif. Dep. Fish Game Fish Bull. 177, 109 p.

Lenarz, W. H., D. A. VenTresca, W. M. Graham, F. B. Schwing, and F. Chavez.
1995. Explorations of El Niño events and associated biological population dynamics off central California. Calif. Coop. Oceanic Fish. Invest. Rep. 36:106–119.

Love, M. S., and A. W. Ebeling.
1978. Food and habitat of three switch-feeding fishes in the kelp forests off Santa Barbara, California. Fish. Bull. 76:257–271.

Love, M. S., P. Morris, M. McCrae, and R. Collins.
1990. Life history aspects of 19 rockfish species (Scorpaenidae: *Sebastes*) from the Southern California Bight. NOAA Tech. Rep. NMFS 87, 38 p.

Love, M. S., M. Yoklavich, and L. Thorsteinson.
2002. The rockfishes of the northeast Pacific, 405 p. Univ. California Press, Berkeley, CA.

MacFarlane, R. B., and E. C. Norton.
1999. Nutritional dynamics during embryonic development in the viviparous genus *Sebastes* and their application to the assessment of reproductive success. Fish. Bull. 97:273–281.

Madenjian, C. P., D. V. O'Connor, and D. A. Nortrup.
2000. A new approach toward evaluation of fish bioenergetics models. Can. J. Fish. Aquat. Sci. 57:1025–1032.

Murie, D. J.
1995. Comparative feeding ecology of two sympatric rockfish congeners, *Sebastes caurinus* (copper rockfish) and *S. maliger* (quillback rockfish). Mar. Biol. 124:341–353.

Negus, M. T.
1995. Bioenergetics modeling as a salmonine management tool applied to Minnesota waters of Lake Superior. N. Am. J. Fish. Manag. 15:60–78.

Ney, J. J.
1993. Bioenergetic modeling today: growing pains on the cutting edge. Trans. Am. Fish. Soc. 122:736–748.

Ouchi, K.
1977. Temperature tolerance of young rockfish, *Sebastes thompsoni* (Jordan et Hubbs). Bull. Jap. Sea Reg. Fish. Res. Lab. 28:1–8.

Pacific Fishery Management Council.
2000. Status of the Pacific coast groundfish fishery through 2000 and recommended biological catches for 2001: stock assessment and fishery evaluation. Pacific Fishery Management Council, Portland, OR.

Paine, R. T., and R. L. Vadas.
1969. Calorific values of benthic marine algae and their postulated relation to invertebrate food preference. Mar. Biol. 4:79–86.

Parker, S. J., S. A. Berkeley, J. T. Golden, D. R. Gunderson, J. Heifetz, M. A. Hixon, R. Larson, B. M. Leaman, M. S. Love, J. A. Musick, V. M. O'Connell, S. Ralston, H. J. Weeks, and M. M. Yoklavich.
2000. Management of Pacific rockfish. Fisheries 25: 22–29.

Perez, M. A.
1994. Calorimetry measurements of energy value of some Alaskan fishes and squids. NOAA Tech. Memo. NMFS-AFSC-32, 32 p.

Rice, J. A., J. E. Breck, S. M. Bartell, and J. F. Kitchell.
1983. Evaluating the constraints of temperature, activity, and consumption on growth of largemouth bass. Environ. Biol. Fishes 9:263–275.

Schindler, D. E., T. E. Essington, J. F. Kitchell, C. Boggs, and R. Hilborn.
2002. Sharks and tunas: fisheries impacts on predators with contrasting life histories. Ecol. Appl. 12:735–748.

Thayer, G. W., W. E. Schaaf, J. W. Angelovic, and M. W. LaCroix.
1973. Caloric measurements of some estuarine organisms. Fish. Bull. 71:289–296.

Tsuchida, S., and T. Setoguma.
1997. Temperature responses of young Schlegel's black rockfish *Sebastes schlegeli*. Nippon Suisan Gakk. 63:317–325.

VenTresca, D. A., R. H. Parrish, J. L. Houk, M. L. Gingras, S. D. Short, and N. L. Crane.
1995. El Niño effects on the somatic and reproductive condition of blue rockfish, *Sebastes mystinus*. Cal. Coop. Oceanic Fish. Invest. Rep. 36:167–174.

Vetter, R. D., and E. A. Lynn.
1997. Bathymetric demography, enzyme activity patterns, and bioenergetics of deep-living scorpaenid fishes (genera *Sebastes* and *Sebastolobus*): paradigms revisited. Mar. Ecol. Prog. Ser. 155:173–188.

Woodbury, D.
1999. Reduction of growth in otoliths of widow and yellowtail rockfish (*Sebastes entomelas* and *S. flavidus*) during the 1983 El Niño. Fish. Bull. 97:680–689.

Wyllie-Echeverria, T.
1987. Thirty-four species of California rockfishes: maturity and seasonality of reproduction. Fish. Bull. 85: 229–250.

Yang, T.-H., N. C. Lai, J. B. Graham, and G. N. Somero.
1992. Respiratory, blood, and heart enzymatic adaptations of *Sebastolobus alascanus* (Scorpaenidae; Teleostei) to the oxygen minimum zone: a comparative study. Biol. Bull. 183:490–499.

Application of pop-up satellite archival tag technology to estimate postrelease survival of white marlin (*Tetrapturus albidus*) caught on circle and straight-shank ("J") hooks in the western North Atlantic recreational fishery*

Andrij Z. Horodysky
John E. Graves
Virginia Institute of Marine Science
College of William and Mary
Route 1208 Greate Rd.
Gloucester Point, Virginia 23062
E-mail address (for J. E. Graves, contact author): graves@vims.edu

Abstract—Short-duration (5- or 10-day) deployments of pop-up satellite archival tags were used to estimate survival of white marlin (*Tetrapturus albidus*) released from the western North Atlantic recreational fishery. Forty-one tags, each recording temperature, pressure, and light level readings approximately every two minutes for 5-day tags (n=5) or four minutes for 10-day tags (n=36), were attached to white marlin caught with dead baits rigged on straight-shank ("J") hooks (n=21) or circle hooks (n=20) in offshore waters of the U.S. Mid-Atlantic region, the Dominican Republic, Mexico, and Venezuela. Forty tags (97.8%) transmitted data to the satellites of the Argos system, and 33 tags (82.5%) transmitted data consistent with survival of tagged animals over the deployment duration. Approximately 61% (range: 19–95%) of all archived data were successfully recovered from each tag. Survival was significantly (P<0.01) higher for white marlin caught on circle hooks (100%) than for those caught on straight-shank ("J") hooks (65%). Time-to-death ranged from 10 minutes to 64 hours following release for the seven documented mortalities, and five animals died within the first six hours after release. These results indicate that a simple change in hook type can significantly increase the survival of white marlin released from recreational fishing gear.

Manuscript submitted 20 January 2004 to the Scientific Editor's Office.
Manuscript approved for publication 2 August 2004 by the Scientific Editor.
Fish. Bull. 103:84–96 (2005).

Atlantic white marlin (*Tetrapturus albidus* Poey, 1860) are targeted by a directed recreational fishery and occur as incidental bycatch in commercial fisheries throughout the warm pelagic waters of the Atlantic Ocean. Total reported recreational and commercial landings of white marlin peaked at 4911 metric tons (t) in the mid-1960s, declined steadily during the next 15 years, and have since fluctuated without trend between 1000 and 2000 t despite substantial increases in fishing effort (ICCAT, 2003). Recent population assessments conducted by the Standing Committee for Research and Statistics (SCRS) of the International Commission for the Conservation of Atlantic Tunas (ICCAT) indicate that the Atlantic-wide white marlin stock is currently at historically low levels and has been severely overexploited for over three decades (ICCAT, 2003). In the 2002 white marlin assessment, the 2001 biomass was estimated to be less than 12% of that required for maximum sustainable yield (MSY) under the continuity case (ICCAT, 2003). Current harvest is estimated to be more than eight times the replacement yield (ICCAT, 2003).

In response to the overfished status of white marlin, ICCAT has adopted binding international recommendations to decrease overall Atlantic landings of this species by 67% from 1996 or 1999 levels (whichever is greater) through the release of all live white marlin from commercial pelagic longline and purse-seine gears (ICCAT, 2001). However, even these dramatic reductions may be ineffective in rebuilding the white marlin stock. Goodyear (2000) estimated that a 60% decrease from 1999 fishing mortality levels would be required to halt the reduction of Atlantic blue marlin (*Makaira nigricans*). Because white marlin experience higher levels of fishing-induced mortality, it is expected that the reduction in mortality required to stabilize this stock will be even greater.

Management measures within the United States, established by the Atlantic Billfish Fishery Management Plan (FMP) (NMFS, 1988) and subsequent Amendment 1 (NMFS, 1999), have also been implemented to reduce white marlin fishing mortality. U.S. commercial fishermen have been prohibited from landing or possessing all Atlantic istiophorids since 1988. Dead discards of white marlin from the U.S. commercial pelagic longline fishery peaked at 107 t in 1989, and have decreased to 40–60 t over the last several years (White Marlin Status Review Team[1]). Management

* Contribution 2610 from the Virginia Institute of Marine Science, College of William and Mary, Gloucester Point, VA 23062.

[1] White Marlin Status Review Team. 2002. Atlantic white marlin status review document, 49 p. Report to the National Marine Fisheries Service. Southeast Regional Office, September 3, 2002. www.nmfs.gov/prot_res/readingrm/Candidate_Plus/white_marlin/whm_status_review.pdf

measures for U.S. recreational anglers include a minimum size of 66 inches lower jaw fork length (NMFS, 1999) and mandatory reporting of landed billfishes (NMFS, 2003). White marlin landings by U.S. recreational anglers ranged between 40 and 110 t from 1960 to the mid-1980s (Goodyear and Prince, 2003) and have decreased to about 2 t in recent years. At present, over 99% of the 4000–8000 white marlin estimated to be caught annually by U.S. recreational fishermen are released (Goodyear and Prince, 2003).

The benefit of current management measures that rely on the release of white marlin cannot be evaluated because levels of postrelease survival are not known for this species. Recapture rates of billfishes tagged with conventional tags are very low (0.4–1.83%; Prince et al., 2003; Ortiz et al., 2003), which may result from high postrelease mortality, tag shedding, or a failure to report recaptures (Bayley and Prince, 1994; Jones and Prince, 1998). Little acoustic tracking has been conducted on white marlin (Skomal and Chase, 2002; n=2 tracks), but similar work on other istiophorid species indicates relatively high postrelease survival for periods ranging from a few hours to a few days for fish released from recreational fisheries (e.g., sailfish: Jolley and Irby, 1979; blue marlin: Holland et al., 1990; Block et al., 1992; black marlin: Pepperell and Davis, 1999). However, data from acoustic tracking studies bear limitations and biases that preclude their use in estimating billfish postrelease survival (Pepperell and Davis, 1999; Graves et al., 2002). In the absence of better data, all recreationally released billfishes have been assumed to survive (Peel, 1995), and estimates of white marlin postrelease mortality are currently not incorporated into ICCAT landing statistics or assessments (White Marlin Status Review Team, 2002).

Developments in pop-up satellite archival tag (PSAT) technology have greatly improved scientific understanding of the behavior, movements and postrelease survival of highly migratory marine fishes, including bluefin tuna (Block et al., 2001), swordfish (Sedberry and Loefer, 2001), white sharks (Boustany et al., 2002), blue marlin (Graves et al., 2002; Kerstetter et al., 2003), black marlin (Gunn et al., 2003), and striped marlin (Domeier et. al, 2003). To estimate the postrelease survival of billfishes, researchers have used PSAT deployment durations ranging from five days to seven months (Graves et al., 2002; Domeier et al., 2003; Kerstetter et al., 2003). Goodyear (2002) cautioned that longer duration deployments increase the potential for tag shedding, tag malfunction, and data corruption, and may bias postrelease survival estimates by including additional sources of mortality other than the capture event. Graves et al. (2002) considered five days to be an appropriate window to detect mortality in blue marlin released from recreational gear in offshore waters of Bermuda, citing recaptures of blue marlin tagged with conventional tags within five days of the initial tagging event as evidence that some istiophorids may recover sufficiently to resume feeding shortly after capture.

Survival estimates for other istiophorid species released from recreational fishing gear may not be applicable to white marlin. One reason may involve body size: recreationally caught blue marlin and striped marlin are generally larger than white marlin. Inter- and intra-specific differences in body size may affect feeding behavior, fight time, handling time, as well as postrelease recovery (Kieffer, 2000). Another reason may involve the different angling techniques used to catch certain istiophorid species. Blue marlin often hook themselves in the mouth and head while aggressively pursuing high speed trolled lures (Graves et al., 2002). In contrast, as white and striped marlin approach a specific baitfish in the trolling spread, many anglers free-spool (i.e., "drop-back") rigged natural baits to feeding marlin to imitate stunned baitfish (Mather et al., 1975). This process increases the probability that straight-shank ("J") hooks rigged with natural baits will damage vital internal areas such as the gills, esophagus, and stomach (Prince et al., 2002a). Recently, several studies have documented a reduction in hook-induced trauma associated with the use of circle hooks in fisheries targeting estuarine and pelagic fishes (Lucy and Studholme, 2002). However, there is little research specifically comparing levels of postrelease survival of pelagic fishes caught on circle and straight-shank ("J") hooks. Prince et al. (2002a) and Skomal et al. (2002) examined hooking locations and injuries in sailfish and bluefin tuna caught on both hook types but lacked postrelease survival data from study animals. Domeier et al. (2003) did not detect a significant difference between striped marlin caught on circle and straight-shank ("J") hooks, although the authors did observe significantly decreased rates of deep-hooking and tissue trauma with circle hooks compared to straight-shank ("J") hooks.

We used data recovered from PSATs to estimate the survival of 41 white marlin caught on circle and straight-shank ("J") hooks in the recreational fishery and released in the western North Atlantic Ocean during 2002–2003. In addition, differences in hooking locations and hook-induced trauma for white marlin caught on circle and straight-shank ("J") hooks were assessed.

Methods

Tags

The Microwave Telemetry, Inc. (Columbia, MD) PTT-100 HR model PSAT tag was used in our study. This tag is slightly buoyant, measures 35 cm by 4 cm, and weighs <70 grams. The body of the tag contains a lithium composite battery, a microprocessor, a pressure sensor, a temperature gauge, and a transmitter, all housed within a black resin-filled carbon fiber tube. Flotation is provided by a spherical resin bulb embedded with buoyant glass beads. This tag model is programmed to record and archive a continuous series of temperature,

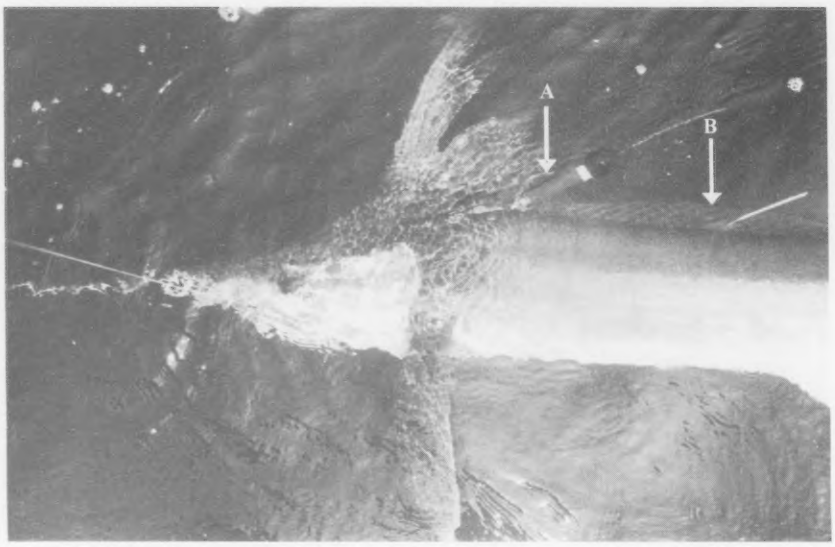

Figure 1

White marlin (*Tetrapturus albidus*) tagged with a Microwave Telemetry PTT-100 HR pop-up satellite tag (**A**) and conventional streamer tag (**B**).

light, and pressure (depth) measurements, and can withstand pressure equivalent to a depth of 3000 m. Tags programmed to disengage after five days (n=5) recorded measurements approximately every two minutes, whereas tags programmed to disengage after ten days (n=35) recorded measurements about every four minutes. Additionally, both 5-day and 10-day tag models transmitted archived and real-time surface temperature, pressure, and light level readings to orbiting satellites of the Argos system for 7–10 days following release from the study animals.

PSATs were attached to white marlin by an assembly composed of 16 cm of 400-pound test Momoi® brand (Momoi Fishing Co., Ako City, Japan) monofilament fishing line attached to a large hydroscopic, surgical-grade nylon intramuscular tag anchor according to the method of Graves et al. (2002). Anchors were implanted with 10-cm stainless steel applicators attached to 0.3-m, 1-m, or 2-m tagging poles (the length of the tagging pole varied depending on the distance from a boat's gunwhales to the water) and were inserted approximately 9 cm deep into an area about 10 cm posterior to the origin of the dorsal fin and 5 cm ventral to the base of the dorsal fin (Fig. 1). In this region, the nylon anchor has an opportunity to pass through and potentially interlock with pterygiophores supporting the dorsal fin well above the coelomic cavity (Prince et al., 2002b; Graves et al., 2002). When possible, a conventional tag was also implanted posterior to the PSAT.

Deployment

White marlin were tagged in the offshore waters of the U.S. Mid-Atlantic Bight, the Dominican Republic, Mexico, and Venezuela (Table 1). These locations were chosen for vessel availability and seasonal concentrations of white marlin. All tagging operations were conducted on private or charter recreational fishing vessels targeting billfishes and tunas. White marlin were caught on 20–40 lb class sportfishing tackle and fought in a manner consistent with typical recreational fishing practice (G. Harvey, personal commun.[2]). The first 41 white marlin caught and successfully positioned boatside were tagged. Fish were not brought to the boat until they were sufficiently quiet to facilitate optimal tag placement. When possible, crew members positioned white marlin for tagging by holding them by the bill and dorsal fin in the water alongside the boat, a technique often used when controlling a billfish to remove hooks. On boats with high gunwhales that prohibited holding the captured fish by the bill, the marlin were "leadered" to the boat's side and moved into position for tagging when calm. Six hooked white marlin escaped prior to tagging because frayed leaders broke or hooks slipped during this process. Hooks were removed when feasible;

[2] Harvey, G. 2002. Personal commun. Guy Harvey Enterprises. 4350 Oakes Rd. Suite 518. Davie, FL 33314.

Table 1

Summary of white marlin (*Tetrapturus albidus*) tagging locations during 2002–2003.

Location	Dates of tagging	Tag deployment duration (in days)	Number of tags deployed
Mid-Atlantic Coast	2002: 18–22 Aug, 5–21 Sep	10	11
	2003: 22 Aug	10	1
Punta Cana, Dominican Republic	2002: 15–19 May	5	5
Isla Mujeres, Mexico	2003: 10–12 June	10	3
La Guaira, Venezuela	2002: 23–25 Nov	10	6
	2003: 12–13 Sep 1 Oct	10	15

otherwise, they were left in the fish and the leader was cut as close to the animal as possible prior to release. Both practices are common in the recreational billfish fishery. After capture and positioning alongside tagging vessels, six white marlin were observed to have lost color, and were lethargic and unable to maintain vertical position in the water. These fish were resuscitated alongside the moving boat for 1–5 minutes prior to release—also a common practice in the recreational fishery.

Gear type, fight time, handling time, fight behavior, hooking location, overall fish condition, estimated weight, and GPS coordinates of the release location were recorded for each tagged white marlin. Fight time was defined as the interval from the time the fish was hooked to the time it was "leadered" alongside the boat prior to tagging. Handling time included tagging and resuscitation, if applicable. In accordance with Prince et al. (2002a), straight-shank ("J") hooks were defined as those with a point parallel to the main hook shaft, whereas circle hooks were defined as having a point perpendicular to the main hook shaft. All circle and straight-shank ("J") hooks were rigged with dead ballyhoo (*Hemiramphus brasiliensis*) bait. Size 7/0 Mustad straight-shank ("J") hooks (models 9175 and 7731) were rigged with the hook exiting the ventral surface of the ballyhoo. Two models of circle hooks were employed in this study: Mustad Demon Fine Wire (model C39952BL, size 7/0; 5° offset, n=9) and Eagle Claw Circle Sea (L2004EL, sizes 7/0–9/0; non-offset, n=11). All circle hooks were rigged so that they pointed upwards from the head of the ballyhoo (see Prince et al., 2002a). The rigging designations and fishing techniques unique to each hook type were maintained in our study to reflect the usual application of circle and straight-shank ("J") hooks in the white marlin recreational fishery. Other than these differences, all handling, tagging, and recording methods were the same for both treatments.

Hooking locations were pooled into two categories: jaw, externally visible (including all lip-hooked, foul-hooked, and bill-entangled white marlin) and deep, not externally visible (including all white marlin hooked in the palate, gills, esophagus, and everted stomachs). Bleeding was recorded as present or absent, and the general location of bleeding was recorded when it was possible to identify the source.

Data analysis

Survival of released white marlin was determined from two distinct lines of evidence provided by the satellite tags: net movement, and water temperature and depth profiles. Time series of water temperature and depth measurements taken about every 2 minutes (5-day tags) or 4 minutes (10-day tags) were used to discriminate surviving from moribund animals. Net movement was determined as a minimum straight line distance traveled between the coordinates of the initial tagging event and the coordinates of the first reliable satellite contact with the detached tag (inferred to be the location of tag pop-up) derived from Argos location codes 1, 2, or 3 for the first or second day of transmission. In cases where tags did not report more precise location codes, an average of all location code 0 readings for the first day of transmission was used as a proxy for the location of the tag pop-up. To determine the directions (and magnitudes) of observed surface currents in areas where fish were tagged, GPS coordinates (Argos location codes of 1, 2, or 3, or a daily mean of location code 0, for tags lacking these) were plotted for the 7–10 days that the tags were floating at the surface and transmitting data to satellites. Maps, tracks, and distances were generated by using MATLAB (version 6.5, release 13.1, Mathworks Inc, Natick, MA).

Cochran-Mantel-Haenszel (CMH) tests were used to address the effect of circle and straight-shank ("J") hooks on survival, hooking location, and the degree of hook-induced trauma. A Yates correction for small sample size was applied when expected cell values were less than 5 (Agresti, 1990). The effects of fight time and total handling time on survival were assessed with Wilcoxon-Mann-Whitney exact tests, with the null hypothesis that there was no difference between surviving and moribund white marlin. All statistical analyses were conducted by using SAS (version 8, SAS Institute, Cary, NC). The lone nonreporting tag observed in our study was excluded from all subsequent analyses.

We conducted bootstrapping simulations to examine the effect of sample size on the 95% confidence intervals of the release mortality estimates using software developed by Goodyear (2002). Distributions of estimates were based on 10,000 simulations with an underlying release mortality equivalent to that observed for straight-shank ("J") hooks for experiments containing 10–200 tags and no sources of error (e.g., no premature release of tags, no tagging-induced mortality, and no natural mortality).

Results

Forty-one white marlin were tagged in four geographic locations during 2002–2003 (Table 1). Information for each fish is summarized in Table 2. Fight times were fairly typical for this fishery (mean: 15.8 min, range: 3–83 min), although two animals required more than 30 minutes before they were sufficiently calm at boatside for tag placement. Overall, forty tags (97.6%) transmitted data to the satellites of the Argos system and of these, thirty-seven tags remained attached to study animals for the full five- or ten-day duration. One five-day tag was released prematurely from a surviving white marlin after 2.5 days, presumably because it had not been attached securely. This individual showed behavior similar to other surviving white marlin while the tag was attached and was presumed to have survived for the purposes of our study. Additionally, two 10-day tags attached to moribund white marlin disengaged from the carcasses prior to the expected date after an extended amount of time at a constant depth and temperature on the seafloor. Approximately 61% of data (range: 19–95%) were successfully transmitted from reporting tags.

Overall, 33 of 40 tags (82.5%) returned data that indicated the survival of tagged animals throughout the duration of tag deployment. Surviving white marlin exhibited daily variations in water temperature and depth data while carrying PSATs (Fig. 2A). The net movement of surviving animals could not be explained by the speed or direction of current patterns alone over the course of the tag deployment (Table 2, Fig 3A). In contrast, moribund white marlin (Fig. 2B) sank to the seafloor (237–1307 m) and to constant water temperatures (3.7–12.5°C), where they remained until the tags disengaged and floated to the surface not far from the initial tagging location (Fig 3B). Five of the seven moribund white marlin died within the first six hours of release; four of these five animals died within the first hour (Table 2).

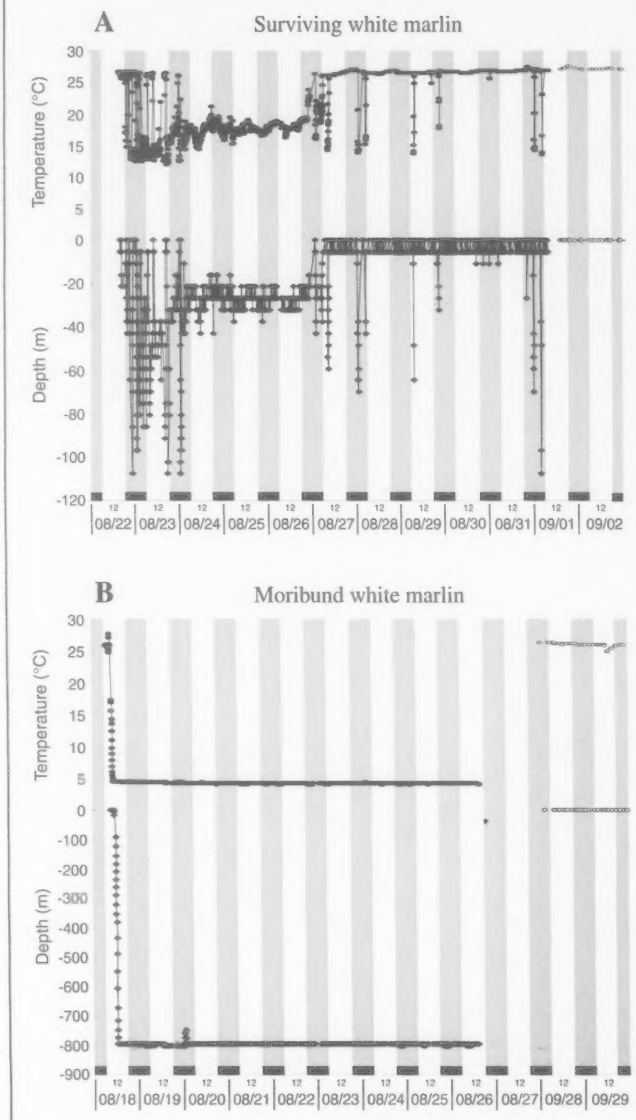

Figure 2

Depth and temperature tracks for a surviving (**A**) (MA12) and moribund (**B**) (MA01) white marlin (*Tetrapturus albidus*). Filled symbols correspond to measurements taken while tags were attached to animals, hollow symbols refer to measurements taken after pop-up while tags were transmitting data to Argos satellites. Gray bars denote periods of local night.

The two white marlin that experienced the longest fight times (46 and 83 min) died more than 24 hours following their release. White marlin VZ03-11 had a

Table 2

Summary information for tagged white marlin (*Tetrapturus albidus*) released from recreational fishing gear in the western North Atlantic Ocean. Total fight time is defined as the interval between the time that the fish was hooked and the time that it was brought to the side of the boat prior to tagging. Handling time included tagging and resuscitation, where applicable. "D/N" refers to deep, not externally visible hooking locations, "foul" refers to a white marlin hooked in the dorsal musculature. Tail-wrapped fish are denoted with the symbol "*T*", resuscitated marlin are denoted with the symbol "*R*".

Tag number	Estimated weight (kg)	Fight time (minutes)	Handling time (minutes)	Hook type	Location of hook in or on fish	Bleeding (Yes/No)	Fate (living or dead)	Movement (nmi/km direction)
DR02-01	23	19	1	"J"	D/N	N	L	23/43 NW
DR02-02	20	29	1	"J"	D/N	N	L	39/72 NW
DR02-03	20	29	1	"J"	D/N	Y	L	33/61 NE
DR02-04	25	83	1	"J"	D/N	Y	D	—
DR02-05	20	6	1	"J"	D/N	N	L	60/111 SE
MA01	18	7	1	"J"	D/N	Y	D	—
MA02	20	24	1	"J"	jaw	N	L	63/117 S
MA03	18	9	1	"J"	D/N	Y	L	51/94 S
MA05	20	17	1	"J"	D/N	Y	L	24/44 S
MA06	18	7	1	"J"	D/N	Y	D	—
MA07	20	7	1	"J"	jaw	Y	D	—
MA08[T, R]	25	17	2	"J"	jaw	N	D	—
MA09	23	9	1	"J"	jaw	N	L	103/191 NE
MA10	23	13	1	"J"	jaw	Y	L	102/189 SE
MA11[T]	27	16	1	"J"	jaw	N	L	260/482 SE
MA12[R]	23	11	1	"J"	jaw	N	L	59/109 SE
VZ02-01	27	8	1	circle	jaw	N	L	118/219 NW
VZ02-02	23	12	1	circle	jaw	N	L	80/148 NE
VZ02-03[T, R]	20	4	2	circle	jaw	N	L	69/128 NW
VZ02-04	18	9	1	circle	jaw	N	L	63/117 NE
VZ02-05	20	7	1	circle	jaw	N	L	67/124 N
VZ02-06	23	9	1	circle	jaw	N	L	98/181 NW
MX03-01[T]	27	15	1	circle	jaw	N	L	172/319 NW
MX03-02	18	14	1	circle	jaw	N	L	422/782 NW
MX03-03[T, R]	23	21	5	circle	jaw	N	L	211/391 NW
VZ03-01	20	3	1	circle	jaw	N	L	85/157 NE
VZ03-02	30	6	1	circle	jaw	N	L	127/235 NE
VZ03-03	23	12	1	circle	jaw	N	L	16/30 N
VZ03-04	27	10	1	circle	jaw	Y	L	114/211 NE
VZ03-05	34	23	1	circle	jaw	N	L	40/74 W
VZ03-06	23	9	1	circle	jaw	N	L	49/91 NE
VZ03-07	23	15	1	circle	jaw	N	L	23/43 NE
VZ03-08	23	7	1	circle	jaw	N	L	39/72 NE
VZ03-09[T]	23	10	1	circle	jaw	N	L	127/235 NE
VZ03-10[T, R]	23	28	2	"J"	jaw	N	L	81/150 NE
VZ03-11[T, R]	23	46	3	"J"	foul	N	D	—
VZ03-12	18	23	1	"J"	jaw	N	L	19/35 NW
VZ03-13	16	17	1	"J"	D/N	Y	D	—
VZ03-14	20	14	1	circle	jaw	N	L	131/243 NW
VZ03-15	20	8	1	circle	jaw	N	L	128/237 NE

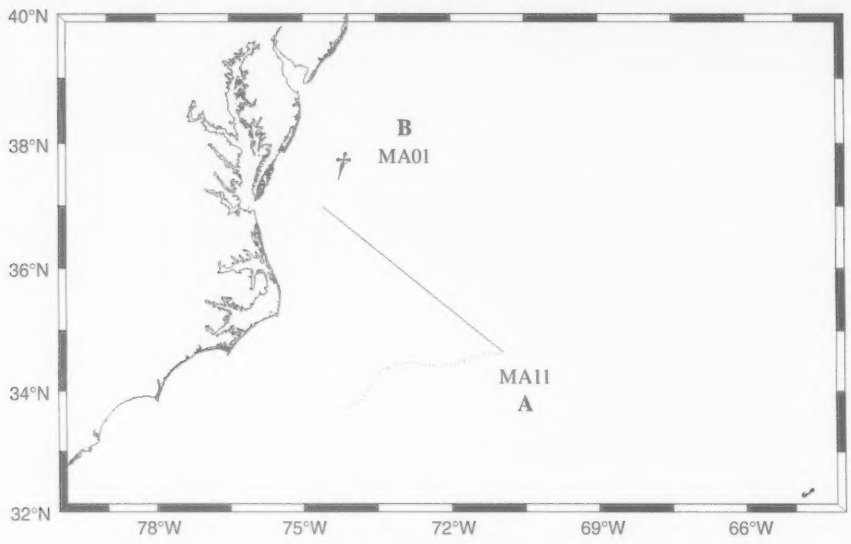

Figure 3

Minimum straight line distances traveled by a surviving white marlin (*Tetrapturus albidus*) (solid line) (**A**) and the drifting track of a transmitting tag (dotted line) in offshore waters of the U.S. Mid-Atlantic Bight. The cross (**B**) denotes a moribund white marlin that sank to the seafloor shortly after it was released, illustrating that dead fish did not travel far from the initial tagging coordinates.

fight time of 46 minutes and died 27 hours after tagging, and DR02-04 had a fight time of 83 minutes and died 64 hours after tagging (Fig. 4). There was no significant difference in fight time (Z=0.4996, P=0.62) between surviving and moribund white marlin, largely due to the large range of fight times for moribund animals. Handling times ranged from 1 to 5 minutes per fish.

Hook type had a highly significant effect on the postrelease survival of white marlin (Fig. 5). Fish caught on circle hooks experienced significantly higher survival (20 of 20; 100%) than those caught on straight-shank ("J") hooks (13 of 20; 65%) (Yates's corrected CMH χ^2=7.386, P<0.007). There were also highly significant differences in hooking locations and hook-induced trauma between hook types (Fig. 5). Odds ratios revealed that white marlin caught on straight-shank ("J") hooks were 41 times more likely to be hooked deeply (Yates's corrected CMH χ^2=11.48, P<0.001) and over 15 times more likely to sustain hook-induced tissue trauma resulting in bleeding (CMH χ^2=8.3, P<0.005) than fish caught on circle hooks. Of the white marlin caught on straight-shank ("J") hooks, half were hooked in deep locations, and 70% of these fish were bleeding. Four of the seven observed mortalities were those of deep-hooked and bleeding fish. Overall, 56% of bleeding, 40% of deep-hooked, and 57% of deep-hooked and bleeding white marlin perished following release. In contrast, all white marlin caught on circle hooks were hooked in the jaw, and bleeding was evident only in a single animal in which the hook point exited the edge of the eye socket but did not damage the eye. Additionally, 20% (8 of 40) of the white marlin in our study became entangled in the line during the fight and were "leadered" to the boat tail-first, a condition known as "tailwrapped" (Holts and Bedford, 1990). This phenomenon was equally distributed with respect to hook type. Five tailwrapped white marlin required resuscitation, and two tailwrapped white marlin hooked in the jaw with straight-shank ("J") hooks died.

With the model developed by Goodyear (2002), the results of 10,000 simulated experiments at an underlying true mortality rate of 35% indicated that approximate 95% confidence intervals for mortality estimates for an experiment deploying 20 tags on white marlin caught on straight-shank ("J") hooks range from 15% to 59% in the absence of confounding factors. A dramatic increase in sample size would be required to improve the precision of mortality estimates (Fig 6). Doubling the sample size (n=40) would decrease the 95% confidence intervals to about ±15% of the true value and quadrupling the number of tags (n=80 PSATs) would reduce confidence intervals to about ±10% of the true value. More than 200 PSATs would have to be deployed to lower the confidence intervals to ±5% of the true value.

The net displacement of released white marlin was variable among individuals and across locations and was used as an independent line of evidence to assess survival. Surviving white marlin demonstrated movement patterns that cannot be explained by surface currents alone. Distances and directions of displacement are summarized in Table 2. White marlin tagged with

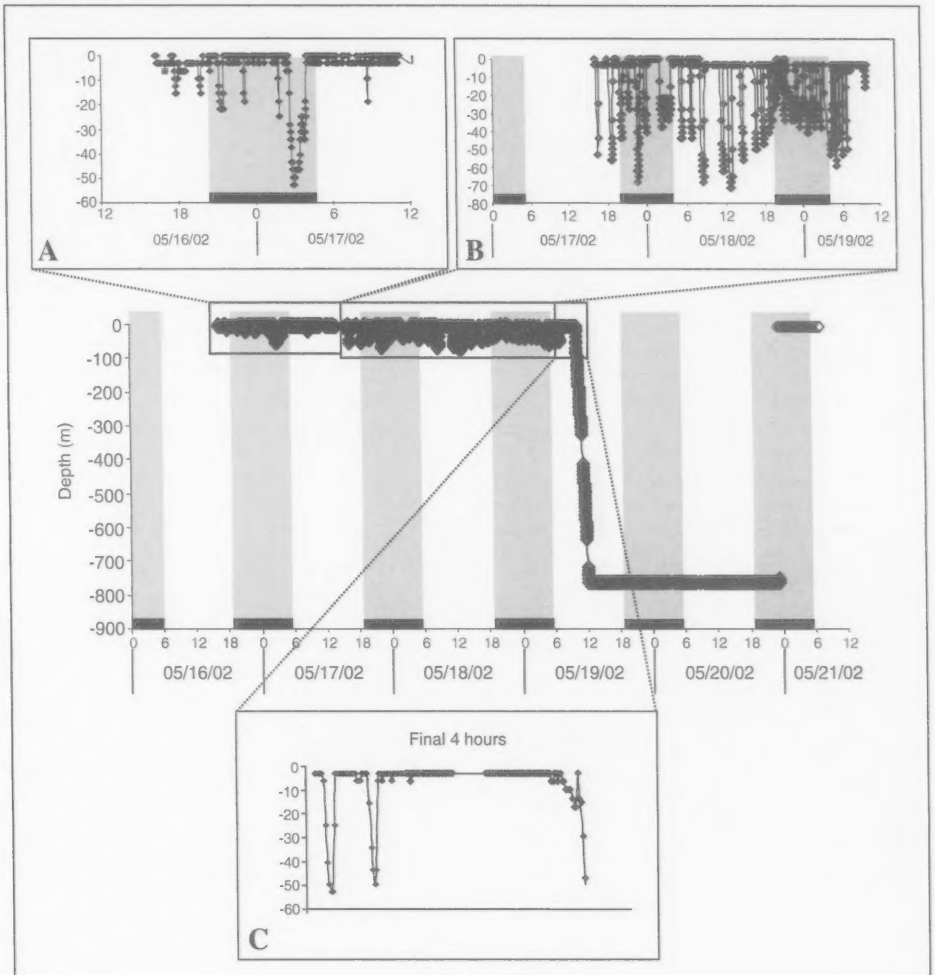

Figure 4

Track of DR02-04 showing mortality 64 hours after release: (**A**) the first 20 hours following release, (**B**) the next 40 hours showing behavior similar to other surviving tagged marlin, and (**C**) the four hours prior to mortality.

10-day PSATs moved an average of 101 (±84) nautical miles (nmi) or 188 km (±155) and those tagged with 5-day PSATs moved an average of 38.8 nmi (±15.6) or 72 km (±29).

Discussion

The results of this study clearly indicate that hook type significantly affects the survival of white marlin released from recreational fishing gear. White marlin caught on circle hooks were much more likely to survive release from recreational fisheries than those caught on straight-shank ("J") hooks. These results concur with previous research across a broad range of fishes caught by diverse recreational fishing techniques (Muoneke and Childress, 1994; Diggles and Ernst, 1997; Lukacovic and Uphoff, 2002; Malchoff et al., 2002; Skomal et al., 2002; Zimmerman and Bochenek, 2002). However, the results of our study differ with those of Domeier et al. (2003), who noted differences in deep-hooking and bleeding between striped marlin caught on circle hooks and those caught on "J" hooks but did not detect a significant difference in mortality between hook types. Differences between the two studies may result from a disparity in body size between the two species, specific bait types (white marlin were caught on dead baits in the present study, Domeier et al. [2003] used live baits),

or sampling error (or a combination of these factors). It should be noted that Domeier et al. (2003) and the crew of the present study both used non-offset and 5° offset circle hooks.

The survival rate observed for white marlin caught on straight-shank ("J") hooks in our study (65%) is slightly lower than that reported for other istiophorid species (blue marlin 89%, Graves et al., 2002; striped marlin 71%, Domeier et al., 2003) caught on this type of hook. Differences in the recreational fishing practices for these species may account for the variation in levels of istiophorid postrelease survival. In recreational fisheries that target striped marlin and white marlin, longer drop-back durations with natural baits rigged on "J" hooks increase the probability of deep-hooking and internal damage, which influence mortality. The postrelease mortality rates of white marlin and striped marlin from drop-back fisheries are similar and are notably higher than that of blue marlin caught on high-speed trolled baits.

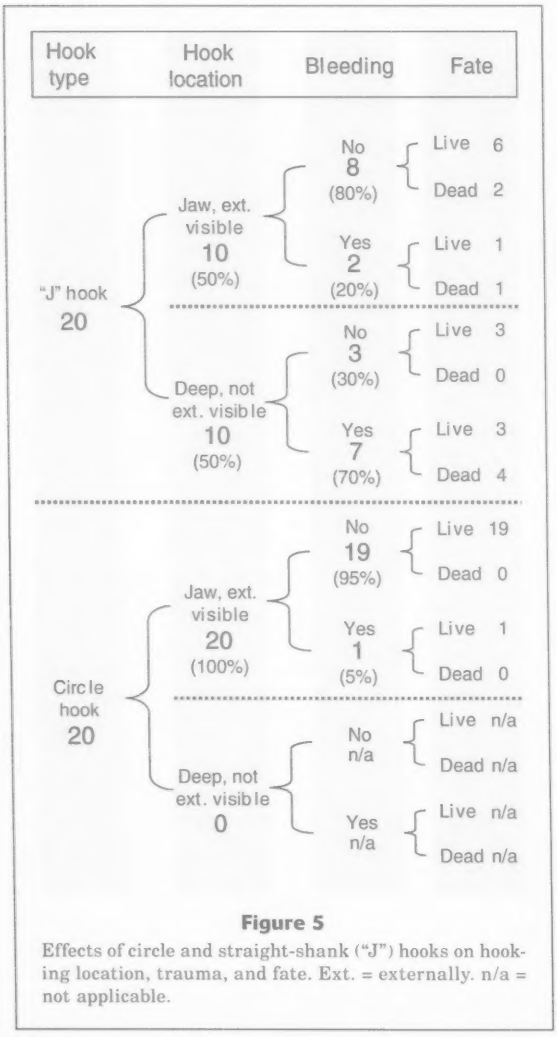

Figure 5

Effects of circle and straight-shank ("J") hooks on hooking location, trauma, and fate. Ext. = externally. n/a = not applicable.

The results of our study also agree with previous research documenting increased deep-hooking and tissue trauma associated with the use of straight-shank ("J") hooks. In contrast to circle hooks, "J" hooks are over 20 times more likely to cause bleeding in sailfish (Prince et al., 2002a), five times more likely to cause bleeding in striped marlin (Domeier et al., 2003), and 15 times more likely to cause bleeding in white marlin (present study). Slightly more than half of the bleeding white marlin and less than half of the deep-hooked fish caught on "J" hooks died in our study. Observations of rusted hooks encapsulated in the viscera of otherwise healthy istiophorids (Prince et al., 2002a) have indicated that wounds resulting from deep-hooking are not necessarily lethal. Furthermore, the results of the present study also indicate that jaw hooking locations are not exclusively nonlethal. Straight-shank ("J") hooks can cause lacerations to vital organs such as the eye, brain, pharynx, esophagus, and stomach before detaching from the initial hooking location and rehooking in regions that are typically considered less lethal, such as the jaw and bill (Prince et al., 2002a). These internal injuries are difficult to record without additional handling and internal examination and confound relationships between hooking location and mortality in the absence of other predictors. Regardless, the significantly higher survival rate for white marlin caught on circle hooks, coupled with reduced rates of deep-hooking and tissue trauma, indicate that this terminal gear may decrease postrelease mortality rates in drop-back fisheries that currently use "J" hooks.

None of the white marlin caught on circle hooks in this study were hooked deeply. Despite documenting significantly lower deep-hooking rates with circle hooks, previous studies have nonetheless observed that both non-offset and offset circle hooks may occasionally hook fish deeply (Prince et al., 2002a; Skomal et al. 2002). This is especially true of severely offset (e.g., 15°) circle hooks, which are highly associated with increased levels of deep hooking and which may mitigate any conservation benefits associated with the use of this terminal gear (Prince et al., 2002a).

Resuscitation of exhausted istiophorids is a common practice in the recreational fishery. Five white marlin that were tailwrapped and unable to ram-ventilate during the fight were resuscitated in our study. For example, white marlin MX03-03 was tailwrapped for the final seven minutes of the 21-minute fight and appeared to be severely exhausted at boatside. This fish was unable to regulate its position in the water when the PSAT was implanted, and required the longest resuscitation of any white marlin in this study (~5 min.). After release, a diver confirmed that this marlin regained color and actively swam away upon reaching cooler water at a depth of about 20 m (G. Harvey[2]). Depth and temperature data showed that this fish survived for the entire 10-day tag deployment duration. Failure

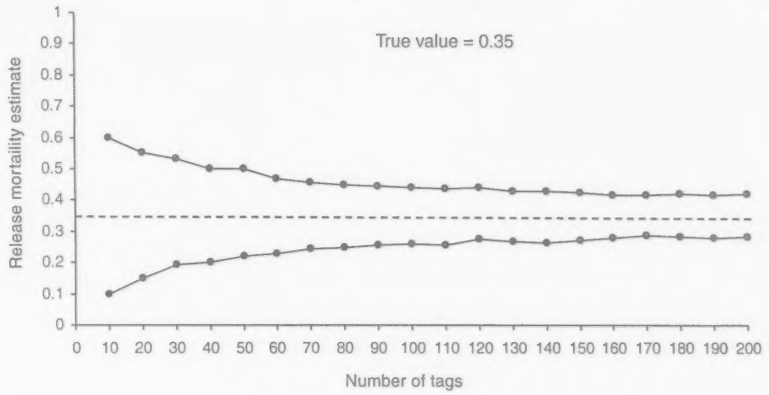

Figure 6

Effect of sample sizes ranging from 10 to 200 PSATs on the 95% confidence intervals for estimates of release mortality. Estimates were derived from 10,000 simulations of hypothetical experiments with increasing numbers of tags (by using software developed by Goodyear [2002]). The dashed line represents the underlying true value of 0.35.

to revive any of the exhausted or tailwrapped white marlin in this study would have biased the mortality estimate upwards if any of these animals perished as a result of exhaustion.

It is unlikely that trauma induced by boatside handling or tagging contributed to the difference between the mortality of white marlin caught on circle hooks and those caught on "J" hooks. Holts and Bedford (1990) and Domeier et al. (2003) suggested that striped marlin in their studies may have died as a result of striking the tagging vessel rather than from hook-induced injury. We observed only one white marlin (DR02-01) strike the side of a tagging vessel; this fish survived and exhibited behavior similar to other healthy white marlin for the full five-day tag deployment duration.

The implications for stomach eversion on billfish survival are unclear because of fairly few observations in studies assessing survival. Stomach eversion appears to be a natural behavioral mechanism by which undesired food items and remnants may be expelled, and stomachs quickly retracted (Holts and Bedford, 1990). In addition, the generally weakened condition of some marlin with everted stomachs indicates that this condition may occur in response to stress (Holts and Bedford, 1990; Pepperell and Davis, 1999). A striped marlin with an everted stomach tracked by Holts and Bedford (1990) survived, whereas a black marlin with an everted stomach tracked by Pepperell and Davis (1999) and a white marlin in this condition tagged by Kerstetter et al. (2004) were both attacked by sharks and died. In the present study, two white marlin (DR02-03 and MA01) everted their stomachs during the fight. White marlin DR02-03 showed behavior consistent with survival until the tag was prematurely released after 2.5 days. In contrast, white marlin MA01 was hooked in its everted stomach and bled profusely during the fight. Depth data recovered from the PSAT attached to this animal indicated that it died less than 10 minutes after release. The survival of some istiophorids with everted stomachs supports the release of fish in this condition; however, without further observations of animals in this condition, the relevance of stomach eversion in predicting mortality of released billfishes remains uncertain.

The majority of mortalities observed in our study occurred within the first six hours of release; however two mortalities (DR02-04 and VZ03-13) occurred more than 24 hours after tagging. Insights into the behavior of VZ03-13 prior to mortality are compromised by large sections of missing data; however, it should be noted that the final four hours prior to death were associated with surface waters. Likewise, white marlin DR02-04 (Fig. 3A) spent the majority of the first day almost entirely within nearsurface waters following release. Similar prolonged surface associations have been documented in blue marlin (Block et al., 1992) and striped marlin (Brill et al., 1993)—a behavioral pattern that has been attributed to that of a badly injured fish (Brill et al., 1993). White marlin DR02-04 resumed diving behavior similar to that observed in healthy tagged fish (Fig. 3B) after 20 hours, indicating possible recovery from catch-and-release procedures. This white marlin again returned to the surface for four hours prior to its death 64 hours after release.

The two white marlin that had the longest fight times in our study, DR02-04 and VZ03-11 (83 and 46 min, respectively), may have experienced delayed postrelease mortality associated with physiological stress, such as intracellular acidosis following exhaustive exercise (Wood et al., 1983) or haemodilution (Bourke et al.,

1987). These mortalities appear to have occurred too soon to have been caused by infection (Bourke et al., 1987) and too late to have been caused by lactic acidosis. Postexertion recovery in istiophorid billfishes is poorly studied, but Skomal and Chase (2002) reported significant perturbations in blood chemistry, including elevation in blood cortisol levels in bluefin tuna (*Thunnus thynnus*), yellowfin tuna (*Thunnus albacares*), and white marlin exposed to prolonged angling bouts (mean=46 min). Acoustic tracks of these animals revealed recovery periods characterized by limited diving behavior for two hours or less after release. The death of white marlin DR02-04 after apparent recovery (Fig. 3C) may be the result of natural mortality, another capture event, or delayed mortality associated with release from recreational fishing gear. Mortality associated with the trauma induced by retained fishing hooks need not be immediate. Blue sharks with fishing hooks embedded in the esophagus or perforating the gastric wall have been found to experience systemic debilitating disease that may affect survival over longer time intervals (Borucinska et al., 2001, 2002).

We also cannot discount predation as a possible cause of mortality for any of the white marlin that died in our study. Acoustic tagging studies have described predation on tagged and released sailfish (Jolley and Irby, 1979), blue marlin (Block et al., 1992) and black marlin (Pepperell and Davis, 1999) by sharks. Recently, Kerstetter et al. (2004) observed results consistent with scavenging and predation on PSAT-tagged white marlin and opah (*Lampris guttatus*) by sharks. Both Block et al. (1992) and Kerstetter et al. (2004) documented attacks on tagged marlin that exhibited prolonged surface associations—the same pattern shown by DR02-04 immediately following its release and prior to mortality.

One tag (MA04) in our study failed to transmit data and was eliminated from all analyses. In previous PSAT studies demonstrating billfish survival, mortalities of tagged istiophorids were not directly observed (Graves et al., 2002; Kerstetter et al., 2003), and the authors conservatively regarded nonreporting tags to be evidence of mortality. The early tag models used in these studies may have failed to transmit data because moribund animals were located at depths that exceeded the tolerance limit (650 m) of the tags or because of other factors, including tag malfunction, mechanical damage (Graves et al., 2002; Kerstetter et al., 2003) or tag ingestion (Kerstetter et al., 2004), or a combination of these factors. Other authors, using newer models of PSATs rated to withstand pressure equivalent to a depth of 3000 m, have clearly documented several mortalities and have chosen to eliminate nonreporting tags from their analyses (Domeier et al, 2003, present study). Treating nonreporting tags as mortalities will bias mortality estimates upwards if tags fail to report for reasons other than catch-and-release–induced mortality (Goodyear, 2002).

Relatively small sample sizes and fairly limited spatial coverage in the present study precluded the use of these data to infer Atlantic-wide estimates of postrelease mortality rates for white marlin. Given the need to account for geographical differences in body sizes of white marlin, fishing gears, drop-back durations, angler skill level, habitat variables, predator densities, and locations, the sample size needed to generate an accurate estimate of postrelease mortality for the entire Atlantic recreational sportfishery could easily require more than a thousand tags (Goodyear, 2002). Results of simulated experiments suggest that if the true underlying J-hook mortality rate is 35%, more than 200 PSATs would have to be deployed on white marlin caught on this terminal tackle to reduce the 95% confidence intervals to ±5% of the true value. The cost of such an experiment (~$1 million for tags alone) is presently prohibitive, particularly considering that these estimates are derived under the assumption of ideal conditions (no premature releases, no tag-induced mortality, and no natural mortality) (Goodyear, 2002). The presence of any confounding factors would increase the necessary sample size and the total cost of such an experiment (Goodyear, 2002).

Despite a relatively small sample size, the present study clearly demonstrates the importance of hook type for the postrelease survival of white marlin. Our results indicate that a highly significant proportion of released white marlin caught on straight-shank ("J") hooks perish and that these hooks are significantly more likely to hook fish deeply and cause internal damage. In contrast, the survival rate of all white marlin caught on circle hooks indicates that a simple change in terminal tackle can significantly reduce postrelease fishing mortality in the recreational fishery.

Acknowledgments

The authors would like to thank Captains Mike Adkins (*South Jersey Champion*), O. B. O'Bryan (*Sea-D*), Jimmy Grant (*Vintage*), Gene Hawn (*Ocean Fifty Seven*), Ryan Higgins (*Caliente*), Ken Neill (*Healthy Grin*), Steve Richardson (*Backlash*), Rod Ryan (*White Witch*), and Rom Whittaker (*Release*), as well as their crews, for their skill in finding white marlin and for their patience with us as we deployed PSATs. We thank Phil Goodyear for kindly providing the bootstrapping software for simulations, Eric Prince (NMFS) for suggestions regarding bait rigging techniques, Paul Howey and Lissa Werbos (Microwave Telemetry, Inc) for technical assistance with the tags, Lorraine Brasseur (VIMS) for assistance with MATLAB programming, Robert Diaz (VIMS) for advice with statistical methods, and David Kerstetter (VIMS) for helpful comments on this manuscript. We gratefully acknowledge the logistical support of Guy Harvey, Dick Weber, and John Wendkos. This project was funded by the National Marine Fisheries Service and Marine Ventures, Inc.

Literature cited

Agresti, A.
1990. Categorical data analysis, 558 p. John Wiley and Sons, Inc., New York, NY.

Bayley, R. E., and E. D. Prince.
1994. A review of the tag release and recapture files for Istiophoridae from the Southeast Fisheries Science Center's Cooperative Gamefish Tagging Program. Int. Comm Cons. Atl. Tunas (ICCAT) Coll. Vol. Sci. Pap. Vol. 41:527–548.

Block, B. A., D. T. Booth, and F. G. Carey.
1992. Depth and temperature of the blue marlin, *Makaira nigricans*, observed by acoustic telemetry. Mar. Biol. 114:175–183.

Block, B. A., H. Dewar, S. B. Blackwell, T. D. Williams, E. D. Prince, C. J. Farwell, A. Boustany, S. L. H. Teo, A. Seitz, A. Walli, and D. Fudge.
2001. Migratory movements, depth preferences, and thermal biology of Atlantic bluefin tuna. Science 293 (5533):1310–1314.

Brill, R. W., D. B. Holts, R. K. C. Chang, S. Sullivan, H. Dewar, and F. G. Carey.
1993. Vertical and horizontal movements of striped marlin (*Tetrapturus audax*) near the Hawaiian Islands, determined by ultrasonic telemetry, with simultaneous measurement of oceanic currents. Mar. Biol. 117: 567–574.

Borucinska, J., N. Kohler, L. Natanson, and G. Skomal.
2002. Pathology associated with retained fishing hooks in blue sharks (*Prionace glauca*) with implications for their conservation. J. Fish Disease 25(9):515–521.

Borucinska, J., J. Martin, and G. Skomal.
2001. Peritonitis and pericarditis associated with gastric perforation by a retained fishing hook in a blue shark (*Prionace glauca*) (Linnaeus, 1758). J. Aquat. Animal Health 13:347–254.

Bourke, R. E., J. Brock, and R. M. Nakamura.
1987. A study of delayed capture mortality syndrome in skipjack tuna, *Katsuwonus pelamis* (L). J. Fish Disease 10:275–287.

Boustany, A. M., S. F. Davis, P. Pyle, S. D. Anderson, B. J. LeBoef, and B. A. Block.
2002. Satellite tagging: expanded niche for white sharks. Nature 412(6867):35–36.

Diggles, B. K., and I. Ernst.
1997. Hooking mortality of two species of shallow-water reef fish caught by recreational angling methods. Mar. Freshw. Res. 48(6):479–483.

Domeier, M. L, H. Dewar, and N. Nasby-Lucas.
2003. Mortality rate of striped marlin (*Tetrapturus audax*) caught with recreational tackle. Mar. Freshw. Res. 54(4):435–445.

Goodyear, C. P.
2000. Biomass projections for Atlantic blue marlin: potential benefits of fishing mortality reductions. ICCAT (Int. Comm. Conserv. Atl. Tunas) Coll. Vol. Sci. Pap. 52:1502–1506.
2002. Factors affecting robust estimates of the catch-and-release mortality using pop-off tag technology. *In* Catch and release in marine recreational fisheries (J. A. Lucy and A. Studholme, eds.), p. 172–179. Am. Fish. Soc. Symp. 30, Bethesda, MD.

Goodyear, C. P., and E. Prince.
2003. U.S. recreational harvest of white marlin. ICCAT (Int. Comm. Conserv. Atl. Tunas) Coll. Vol. Sci. Pap. 55:624–632.

Graves, J. E., B. E. Luckhurst, and E. D. Prince.
2002. An evaluation of pop-up satellite tags for estimating postrelease survival of blue marlin (*Makaira nigricans*) from a recreational fishery. Fish. Bull. 100:134–142.

Gunn, J. S., T. A. Patterson, and J. G. Pepperell.
2003. Short-term movement and behavior of black marlin *Makaira indica* in the Coral Sea as determined through a pop-up satellite archival tagging experiment. Mar. Freshw. Res. 54:509–513.

Holts, D., and D. Bedford.
1990. Activity patterns of striped marlin in the southern California Bight. *In* Planning the future of billfishes (R. H. Stroud, ed.), p. 81–93. National Coalition for Marine Conservation Inc., Savannah, GA.

Holland, K., R. Brill, and R. K. C. Chang.
1990. Horizontal and vertical movements of Pacific blue marlin captured and released using sportfishing gear. Fish. Bull. 88:397–402.

ICCAT (International Commission for the Conservation of Atlantic Tunas).
2001. Report of the fourth ICCAT billfish workshop. Int. Comm. Cons. Atl. Tunas (ICCAT) Coll. Vol. Sci. Pap. 53:1–22.
2003. Report of the 2002 white marlin stock assessment meeting. Int. Comm. Cons. Atl. Tunas (ICCAT) Coll. Vol. Sci. Pap. 55(2): 350–452.

Jolley, J. W., and E. W. Irby.
1979. Survival of tagged and released Atlantic sailfish (*Istiophorus platypterus*: Istiophoridae) determined with acoustic telemetry. Bull. Mar. Sci. 29:155–169.

Jones, C. D., and E. D. Prince.
1998. The cooperative tagging center mark-recapture database for Istiophoridae (1954–1995) with an analysis of the west Atlantic ICCAT billfish tagging program. Int. Comm. Cons. Atl. Tunas (ICCAT) Coll. Vol. Sci. Pap. Vol. 47:311–322.

Kerstetter, D. W., B. E. Luckhurst, E. D. Prince, and J. E. Graves.
2003. Use of pop-up satellite archival tags to demonstrate survival of blue marlin (*Makaira nigricans*) released from pelagic longline gear. Fish. Bull. 101:939–948.

Kerstetter, D. W., J. J. Polovina, and J. E. Graves.
2004. Evidence of shark predation and scavenging on fishes equipped with pop-up satellite archival tags. Fish. Bull. 102:750–756.

Kieffer, J. D.
2000. Limits to exhaustive exercise in fish. Comp. Biochem. Physiol. A. 126:161–179.

Lucy, J. A. and A. L. Studholme, editors.
2002. Catch and release in marine recreational fisheries. Am. Fish. Soc. Symp. 30, Bethesda, MD, 250 p.

Lukacovic, R., and J. H. Uphoff.
2002. Hook location, fish size, and season as factors influencing catch-and-release mortality of striped bass caught with bait in Chesapeake Bay. Extended abstract. *In* Catch and release in marine recreational fisheries (J. A. Lucy and A. Studholme, eds.) p. 97–100. Am. Fish. Soc. Symp. 30, Bethesda, MD.

Malchoff, M. H., J. Gearhart, J. Lucy, and P.J. Sullivan.
2002. The influence of hook type, hook wound location, and other variables associated with post catch-and-release mortality in the US summer flounder recreational fishery. Extended abstract. *In* Catch and release in marine recreational fisheries (J. A. Lucy ann A. Studholme, eds.), p. 101–105. Am. Fish. Soc. Symp. 30, Bethesda, MD.

Mather, F. J. III, H. L. Clark, and J. M. Mason Jr.
1975. Synopsis of the biology of the white marlin *Tetrapturus albidus* Poey (1861). *In* Proceedings of the International Billfish Symposium Kailua-Kona, Hawaii, 9–12

August 1972. Part 3: Species Synopses (R. S. Shomura and F. Williams, eds.), p. 55–94. NOAA Tech. Rep. NMFS SSRF-675.

Muoneke M. I., and W. M. Childress.
1994. Hooking mortality: a review for recreational fisheries. Rev. Fish. Sci. 2(2):123–156.

NMFS. (National Marine Fisheries Service.)
1988. The Atlantic billfish fishery management plan. NOAA-NMFS-F/SF-Highly Migratory Species Division, Silver Spring, MD.
1999. Amendment 1 to the Atlantic billfish fishery management plan. NOAA-NMFS-F/SF-Highly Migratory Species Division, NMFS, Silver Spring, MD.
2003. Final rule: Atlantic highly migratory species: monitoring of recreational landings. 50 F.R. 711–715.

Ortiz, M., E. D. Prince, J. E. Serafy, D. B. Holts, K. B. Davy, J. G. Pepperell, M. B. Lowry, and J. C. Holdsworth.
2003. Global overview of the major constituent-based billfish tagging programs and their results since 1954. Mar. Freshw. Res. 54(4):489–507.

Peel. E.
1995. No place to hide: highly migratory fish in the Atlantic Ocean, 125 p. Center for Marine Conservation, Washington, D.C.

Pepperell, J. G., and T. L. O. Davis.
1999. Post-release behavior of black marlin (*Makaira indica*) caught and released using sportfishing gear off the Great Barrier Reef (Australia). Mar. Biol. 135:369–380.

Prince, E. D., M. Ortiz, and A. Venizelos.
2002a. A comparison of circle hook and "J" hook performance in recreational catch-and-release fisheries for billfish. *In* Catch and release in marine recreational fisheries (J. A. Lucy and A. Studholme, eds.), p. 66–79. Am. Fish. Soc. Symp. 30, Bethesda, MD.

Prince, E. D., M. Ortiz, A. Venizelos, and D. S. Rosenthal.
2002b. In-water conventional tagging techniques developed by the cooperative tagging center for large, highly migratory species. *In* Catch and release in marine recreational fisheries (J. A. Lucy and A. Studholme, eds.), p. 155–171. Am. Fish. Soc. Symp. 30, Bethesda, MD.

Prince, E. D., C. Rivero, J. E. Serafy, C. Porch, G. P. Scott, and K. B. Davy.
2003. An update of the tag release and recapture files for Atlantic white marlin. Int. Comm. Cons. Atl. Tunas (ICCAT) Coll. Vol. Sci. Pap. Vol. 55(2):578–593.

Sedberry, G. R., and J. K. Loeffer.
2001. Satellite telemetry tracking of swordfish, *Xiphias gladius*, off the eastern United States. Mar. Biol. 139:355–360.

Skomal, G. B., and B. C. Chase.
2002. The physiological effects of angling on post-release survivorship in tunas, sharks, and marlin. Extended abstract. *In* Catch and release in marine recreational fisheries (J. A. Lucy and A. Studholme, eds.), p. 135–138. Am. Fish. Soc. Symp. 30, Bethesda, MD.

Skomal, G. B., B. C. Chase, and E. D. Prince.
2002. A comparison of circle and straight hook performance in recreational fisheries for juvenile Atlantic bluefin tuna. *In* Catch and release in marine recreational fisheries (J. A. Lucy and A. Studholme, eds.), p. 57–65. Am. Fish. Soc. Symp. 30, Bethesda, MD.

Zimmerman, S. R., and E. A. Bochenek.
2002. Evaluation of the effectiveness of circle hooks in New Jersey's recreational summer flounder fishery. Extended abstract. *In* Catch and release in marine recreational fisheries (J. A. Lucy and A. Studholme, eds.), p. 106–109. Am. Fish. Soc. Symp. 30, Bethesda, MD.

Wood, C. M., J. D. Turner, and M. S. Graham.
1983. Why do fish die after severe exercise? J. Fish. Biol. 22:189–201.

Age validation of quillback rockfish (*Sebastes maliger*) using bomb radiocarbon

Lisa A. Kerr

Allen H. Andrews

Moss Landing Marine Laboratories
California State University
8272 Moss Landing Road
Moss Landing, California 95039
Present address (for L. A. Kerr): Chesapeake Biological Laboratory
University of Maryland Center
for Environmental Science
P.O. Box 38,
Solomons, Maryland 20688

E-mail address (for L.A. Kerr, contact author): kerr@cbl.umces.edu

Kristen Munk

Alaska Department of Fish and Game
Division of Commercial Fisheries
1255 W. 8th Street
Juneau, Alaska 99801

Gregor M. Cailliet

Moss Landing Marine Laboratories
California State University
8272 Moss Landing Road
Moss Landing, California 95039

Kenneth H. Coale

Moss Landing Marine Laboratories
California State University
8272 Moss Landing Road
Moss Landing, California 95039

Thomas A. Brown

Center for Accelerator Mass Spectometry
Lawrence Livermore National Laboratory
7000 East Avenue
Livermore, California 94551

Brian R. Frantz

Center for Accelerator Mass Spectrometry
Lawrence Livermore National Laboratory
7000 East Avenue
Livermore, California 94551

Abstract—Rockfishes (*Sebastes* spp.) support one of the most economically important fisheries of the Pacific Northwest and it is essential for sustainable management that age estimation procedures be validated for these species. Atmospheric testing of thermonuclear devices during the 1950s and 1960s created a global radiocarbon (^{14}C) signal in the ocean environment that scientists have identified as a useful tracer and chronological marker in natural systems. In this study, we first demonstrated that fewer samples are necessary for age validation using the bomb-generated ^{14}C signal by emphasizing the utility of the time-specific marker created by the initial rise of bomb-^{14}C. Second, the bomb-generated ^{14}C signal retained in fish otoliths was used to validate the age and age estimation method of the quillback rockfish (*Sebastes maliger*) in the waters of southeast Alaska. Radiocarbon values from the first year's growth of quillback rockfish otoliths were plotted against estimated birth year to produce a ^{14}C time series spanning 1950 to 1985. The initial rise in bomb-^{14}C from prebomb levels ($\sim -90‰$) occurred in 1959 [±1 year] and ^{14}C levels rose relatively rapidly to peak $\Delta^{14}C$ values in 1967 (+105.4‰) and subsequently declined through the end of the time series in 1985 (+15.4‰). The agreement between the year of initial rise of ^{14}C levels from the quillback rockfish time series and the chronology determined for the waters of southeast Alaska from yelloweye rockfish (*S. ruberrimus*) otoliths validated the aging method for the quillback rockfish. The concordance of the entire quillback rockfish ^{14}C time series with the yelloweye rockfish time series demonstrated the effectiveness of this age validation technique, confirmed the longevity of the quillback rockfish up to a minimum of 43 years, and strongly confirms higher age estimates of up to 90 years.

Manuscript submitted 11 April 2003 to the Scientific Editor's Office.

Manuscript approved for publication 24 August 2004 by the Scientific Editor.

Fish. Bull. 103:97–107 (2005).

Rockfishes (*Sebastes* spp.) comprise one of the most commercially important fisheries in the northeast Pacific Ocean. Some rockfish species possess life history characteristics, such as long life, slow growth, late age at maturity, low natural mortality, and variable juvenile recruitment success, all of which make them particularly vulnerable to overfishing (Adams, 1980; Archibald et al., 1981; Leaman and Beamish, 1984; Cailliet et al., 2001.). Rockfish population biomass and size composition have declined to very low levels today in part because of continued high exploitation rates (Love et al., 2002). Prevention of further population declines is a management imperative. Sustainable management of marine fisheries requires accurate life history information, of which validated age and growth characteristics can be one of the most important aspects.

Underestimated age can lead to inflated estimates of total allowable catch for a fishery that is unsustainable at that level of exploitation (Beamish and McFarlane, 1983; Campana, 2001). For example, underestimated longevity and improper management allowed overfishing that accelerated the decline of the Pacific ocean perch (*Sebastes alutus*) of the northeastern Pacific Ocean (Beamish, 1979; Archibald et al., 1983). Reliable estimates of age are also essential for understanding life history traits,

such as age at maturity, rate of growth, longevity, and reproduction frequency (Beamish and McFarlane, 1983). For production (large-scale) aging purposes, age validation is especially important because it provides a standardized basis for ongoing aging efforts to identify strong and weak cohorts (Campana, 2001).

The most common method of age estimation of bony fishes is counting growth zones in their calcified inner ear bones, or otoliths (Chilton and Beamish, 1982; Beamish and McFarlane, 1987). A pair of translucent and opaque growth zones is often assumed to represent one year of growth (Williams and Bedford, 1974). By counting growth zones an estimate of fish age is possible; however, growth patterns are not easily discernible for all species. Age interpretations in long-lived species can be particularly difficult and subjective because of the compression of growth zones within the otolith (Munk, 2001). Therefore, it is necessary to validate the periodicity of growth zones in otoliths with an independent and objective method. Despite the importance of accurate age estimates for understanding and managing fish populations, validated age and growth characteristics are often not available (Beamish and McFarlane, 1983; Campana, 2001). Traditional age validation techniques, such as captive rearing, mark-recapture, and tag-recapture, can be difficult or impractical for long-lived and deep-dwelling fishes.

An alternative technique to traditional age validation methods uses radiocarbon (^{14}C) produced by the atmospheric testing of thermonuclear devices in the 1950s and 1960s as a time-specific marker (Kalish, 1993). This established method of validating otolith-derived age estimates of fishes involves relating the discrete temporal variation of ^{14}C recorded in otoliths to an established ^{14}C chronology. Otoliths are closed systems, accreting calcium carbonate throughout the life of the fish and this calcium carbonate is conserved through time. The measurement of bomb-produced ^{14}C in otoliths of fishes is considered one of the best objective means to validate otolith-based age estimates in long-lived fishes (Campana, 2001).

This technique is most reliable for fishes that inhabit the surface mixed layer of the ocean, at least during a portion of their life history. Uncertainty regarding mixing rate at depth and limited data on the ^{14}C signal in deeper waters make it difficult to use this technique for organisms that live below the mixed layer throughout their lives (Kalish, 1995, 2001). Studies indicate that the main source of carbon (70–90%) for otoliths is from dissolved inorganic carbon (DIC) in seawater and that the remainder (10–30%) is dietary (Kalish, 1991; Farrell and Campana, 1996; Schwarcz et al., 1998). An understanding of the life history of the fish (in particular diet, movement, and habitat) and the regional oceanography of the area are integral for interpreting otolith ^{14}C data. One caveat of this technique is that it must use otoliths with birth dates, including the period of initial increase in ^{14}C (mid-1950s to mid-1960s; Kalish, 1995). Consequently, this technique is well suited for age validation of long-lived species or species for which there is an archived otolith collection with birth years that span this period. The application of bomb ^{14}C for age validation of long-lived species is advantageous, in that it provides a minimum longevity and verifies the periodicity of growth zones in otoliths with only a small amount of material and with a high degree of precision (Kalish, 1993; Campana, 2001). However, the high cost of ^{14}C analysis (~$400–$500 per sample) has been a limiting factor in the widespread application of this technique.

The quillback rockfish (*Sebastes maliger*) is a commercially important rockfish that represents a portion (~8%) of the demersal shelf rockfish assemblage landings in the Gulf of Alaska (O'Connell et al.[1]). Species within the demersal shelf group are considered long-lived, late maturing, and sedentary as adults, making them highly susceptible to fishing pressure (O'Connell et al.[1]). Estimated exploitation rates are low; once exploited beyond a sustainable level, recovery is slow (Leaman and Beamish, 1984; Francis, 1985; O'Connell et al.[1]). Longevity estimates for the quillback rockfish are wide ranging, from 15 to 90 years (38 years, Barker, 1979; 55 years, Richards and Cass, 1986; 15 years, Reilly et al.[2]; 76 years, Yamanaka and Kronland, 1997; >32 years, Casillas et al., 1998; 90 years, Munk, 2001), and no age validation has been performed for this species to date.

Quillback rockfish are found associated with rocky substrate in relatively shallow continental shelf waters (9 to 146 m)—their abundance decreasing with increasing depth below 73 m (Kramer and O'Connell, 1995). As juveniles, quillback rockfish inhabit nearshore benthic habitat. Tagging studies confirmed that they do not demonstrate migratory behavior and are residents in their shallow-water habitat (Matthews, 1990). Because 1) most longevity estimates indicate that some present-day adult quillback rockfish were born in the prebomb era, 2) quillback rockfish in the juvenile stage are found in the ocean mixed layer, and 3) a suitable ^{14}C time series exists for the waters off southeast Alaska (previously determined from yelloweye rockfish [*S. ruberrimus*] otoliths [Kerr et al., 2004]), the quillback rockfish is an ideal candidate for ^{14}C age validation.

The objectives of our study were 1) to develop a method for determining the minimum number of samples required for bomb ^{14}C age validation to minimize cost, 2) to validate both age and age estimation methods of the quillback rockfish by measuring ^{14}C in aged otoliths and to compare the timing of the initial rise in ^{14}C with

[1] O'Connell, V. M., D. W. Carlile, and C. Brylinsky. 2002. Demersal shelf rockfish assessment for 2002. Stock assessment and fishery evaluation report for the groundfish resources of the Gulf of Alaska, 36 p. North Pacific Fishery Management Council (NPFMC), P.O. Box 103136, Anchorage AK 99510.

[2] Reilly, P. N., D. Wilson-Vandenberg, R. N. Lea, C. Wilson, and M. Sullivan. 1994. Recreational angler's guide to the common nearshore fishes of Northern and Central California. California Department of Fish and Game, Marine Resources Leaflet, 57 p. Calif. Dep. Fish and Game, 20 Lower Ragsdale Drive, Suite 100, Monterey, CA 93940.

the chronology determined for the waters of southeast Alaska (i.e., yelloweye rockfish), and 3) to analyze ^{14}C in aged quillback rockfish otoliths, spanning the pre- to postbomb era, in order to examine the complete ^{14}C time series and demonstrate the effectiveness of using the timing of the initial rise in ^{14}C as an age validation method.

Materials and methods

Sample size assessment

Because of the considerable cost of accelerator mass spectrometry (AMS) analyses, the minimum number of ^{14}C samples required to validate the aging method of the quillback rockfish was mathematically determined from a previously determined yelloweye rockfish otolith ^{14}C time series for the waters of southeast Alaska (Kerr et al., 2004). To assess minimum sample size, estimated years of initial rise in ^{14}C levels (and associated errors) were determined for different numbers of data points (n=3, 5, 7, 9, and 11) subsampled from the bomb-rise region of the yelloweye rockfish data set. The estimated years of initial rise from each subsample set were then compared to the initial year of rise and error determined from all bomb-rise yelloweye rockfish ^{14}C samples (n=23). Because the error associated with the yelloweye rockfish bomb-rise data set is limited by the uncertainty associated with age estimates for yelloweye rockfish, a maximum error of ±2 years for fish with birth years during the bomb rise (1956 to 1971; Kerr et al., 2004) was our precision criterion for defining the minimum number of quillback rockfish otolith samples.

Twenty-three yelloweye rockfish otolith ^{14}C values with birth years from 1956 to 1971 were divided into data sets of 3, 5, 7, 9, and 11 data points. A stratified sampling approach was applied by creating bomb ^{14}C linear regressions from repeated selection of 3, 5, 7, 9, and 11 data points at uniform intervals from 1956 to 1971. Random selection of data points was not practical because it is established that the careful choice of sample year during the rapid rise in ^{14}C is required for this technique (Baker and Wilson, 2001). The year of initial rise in ^{14}C, and associated error, was determined from the bomb ^{14}C regressions. The year of initial ^{14}C rise was calculated with the following formula:

$$x = (y - b)/m,$$

where x = year of initial rise in ^{14}C values;
y = average prebomb ^{14}C value;
m = slope of the line; and
b = y-intercept.

The error associated with the year of initial rise in ^{14}C values (σ_x) was calculated by using the delta method (treating b as a scaler; Wang et al., 1975):

$$\sigma_x = \sigma_y / \sigma_m,$$

where σ_y = error associated with average prebomb ^{14}C value
σ_m = error associated with the slope of the line.

Radiocarbon analysis

Sagittal otoliths of quillback rockfish were collected from a random subsampling of catches from commercial longline fishing vessels in the coastal waters off southeast Alaska by the Alaska Department of Fish and Game (ADFG), Juneau, AK in 2000 (Fig. 1). A single otolith from a pair taken from each fish was aged by using the break-and-burn method developed by researchers at the Mark, Tag, and Age Laboratory, ADFG in Juneau, AK, and the corresponding intact otolith was analyzed for ^{14}C. Whole and broken-and-burned otoliths were stored dry in paper envelopes. Year of capture, estimated final age, assigned year class, readability code, and reader identification information were archived and provided by ADFG for each sample.

Fifteen quillback rockfish otoliths, with estimated birth years ranging from the prebomb 1950s to the postbomb mid-1980s were selected for ^{14}C analysis. The core of each otolith, which constitutes the first year of growth, was analyzed for ^{14}C. From life history information, it is known that the core was formed while the fish inhabited the ocean mixed layer during its early growth stage (Yoklavich et al., 1996). To determine the average length and width, and minimum depth of the core, whole and broken-and-burnt otoliths from adult quillback rockfish were examined under a Leica® dissecting microscope with an attached Spot RT® video camera and were measured using Image Pro Plus® image analysis software (version 4.1 for Windows, Media Cybernetics, Silver Spring, MD). Cores were extracted with a milling machine with a 1.6-mm (1/16″) diameter end mill. To minimize the extraction of material deposited after the first year of growth, length, width, and depth parameters of the otolith core were used to guide coring. Because the first year of growth in quillback rockfish otoliths is clearly visible from the distal surface of the otolith we were able to visually correct for individual variability in otolith core size. The core (first year of growth in the otolith) was reduced to powder, collected, and weighed to the nearest 0.1 mg.

For ^{14}C analysis, otolith calcium carbonate ($CaCO_3$) was converted to pure carbon in the form of graphite (Vogel et al., 1984, 1987) and measured for ^{14}C content by using AMS at the Center for Accelerator Mass Spectrometry, Lawrence Livermore National Laboratory. The ^{14}C values were reported as $\Delta^{14}C$ (Stuvier and Polach, 1977).

The ^{14}C values measured in quillback rockfish otolith cores were plotted with respect to corresponding birth years assessed from break-and-burn age estimates, taking into consideration the potential variation of the age estimate (coefficient of variation=2.6%, rounded to the nearest whole number; Chang, 1982). The ^{14}C time series for the waters of southeast Alaska established from the otoliths of the age-validated yelloweye rockfish

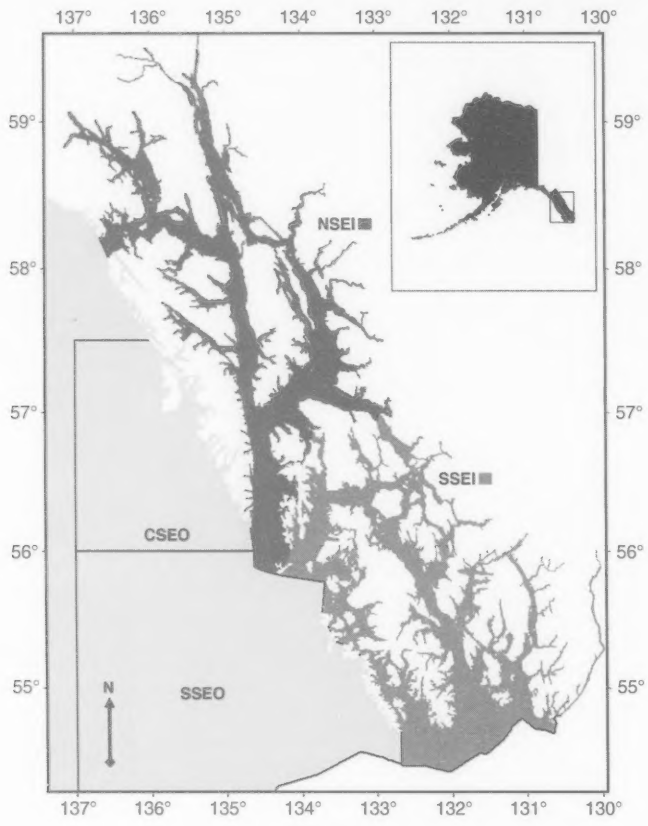

Figure 1

Map of southeast Alaska with regions where quillback rockfish (*Sebastes maliger*) used for otolith radiocarbon analyses were captured. Quillback rockfish were collected from random subsampling of catches from commercial longline fishing vessels in the coastal waters off southeast Alaska (CSEO: Central Southeast Offshore (outside), SSEI: Southern Southeast Inshore, SSEO: Southern Southeast Offshore, and NSEI Northern Southeast Inshore (inside)) by the Alaska Department of Fish and Game, Juneau, AK, in 2000. Note that the specific geographic location for individual fish during the first year of life is unknown; however, life history information indicates that quillback rockfish are not migratory and exhibit residential behavior in shallow-water habitat. Hence, the general location of the fish collected and used in this study may be useful in a broad context.

(n=43) was used for temporal calibration of the quillback rockfish record (Andrews et al., 2002; Kerr et al., 2004). The level of concordance between the years of initial rise in ^{14}C in the two time series was the basis for validating the otolith-based age estimates of the quillback rockfish. The degree of agreement between the ^{14}C time series, spanning the pre- to postbomb era, for the quillback and yelloweye rockfishes was examined to demonstrate the effectiveness of determining the year of initial rise in ^{14}C as an age validation method, and whether the entire time series for the quillback provided any further information relevant to age validation. To do this, the yelloweye rockfish ^{14}C time series was divided into three intervals (prebomb, bomb rise, and postbomb) and fitted with confidence intervals. The prebomb era ^{14}C values (1950–57) were fitted with an average (±2 SD); the bomb rise (1959–71) and postbomb era values (1966–85) were fitted with a linear regression and corresponding 95% prediction intervals. A qualitative comparison of the quillback rockfish ^{14}C record was made with other existing marine records: two Hawaiian Islands coral records—Oahu (Toggweiler et al., 1991)

Table 1

Range of the year of calculated initial rise in radiocarbon and the associated range of error calculated for bomb radiocarbon regressions. Each regression comprised varying numbers of yelloweye rockfish radiocarbon data points (n=3, 5, 7, 9, and 11) and was compared to the year of initial ^{14}C rise and error was determined from all bomb-rise yelloweye rockfish ^{14}C samples (n=23, last row) to determine the minimum number of quillback rockfish otolith samples sufficient to achieve the desired degree of precision (±2 years).

Number of data points in regression	Number of regressions	Range of the year of calculated initial rise in ^{14}C	Error range (± years)
3	8	1954.1–1960.3	0.8–6.8
5	5	1956.0–1959.4	1.3–2.9
7	4	1956.5–1957.9	1.0–2.5
9	3	1957.1–1957.3	0.9–1.8
11	2	1957.0–1957.8	1.2–1.5
23	1	1957.3	n/a

and Kona (Druffel et al., 2001)—and two otolith-based northern hemisphere ^{14}C records—for northwest Atlantic haddock (Campana, 1997) and the Barents Sea Arcto-Norwegian cod (Kalish et al., 2001).

Results

Sample size assessment

The estimated years of initial rise in ^{14}C calculated for the bomb-^{14}C regressions, composed of 3, 5, 7, 9, and 11 yelloweye rockfish data points spanning 1956 to 1971, converged towards the calculated year for all 23 data points as the number of samples comprising the regressions increased (Table 1). In parallel, the errors associated with the estimated years of initial rise in ^{14}C decreased as the number of ^{14}C samples increased (Table 1). The degree of precision within the quillback rockfish record was limited by the uncertainty associated with age estimates for yelloweye rockfish (a maximum error of ±2 years based on growth zone counts for fish with birth years from 1956 to 1971; Kerr et al., 2004). Examination of the error (years) associated with the year of initial rise in ^{14}C for the number of data points comprising each regression in relation to our ±2 year criterion indicated that a sample size of nine data points resulted in error values that ranged below 2 years (Table 1). Therefore, it was concluded that nine ^{14}C samples spanning 1956–71 would be sufficient to provide a suitable degree of precision in the quillback rockfish record. In addition, a limited number of samples, in this case 4, were required to establish an average prebomb level for the intercept year.

Radiocarbon analysis

The ^{14}C measured in 15 previously aged quillback rockfish otoliths with presumed birth years from 1950 to 1985 varied considerably over time (Table 2). Otoliths from quillback rockfish with birth years 1950–57 contained prebomb ^{14}C levels. Although there was more variation in these prebomb values than expected from ^{14}C uncertainties, the level was relatively consistent over time, averaging −90.7 (±11.5)‰ (mean ±SD). A sharp rise in otolith ^{14}C values was evident in 1959 (±1 year);

Table 2

Summary of fish and otolith data from quillback rockfish collected off the coast of southeast Alaska. Resolved age is the final age estimate given by Alaska Department of Fish and Game. Birth year is the collection year (2000) minus the resolved age. Age error is the uncertainty associated with the age estimate (CV=2.6%; year rounded to the nearest whole number). Radiocarbon values in the otolith cores of yelloweye rockfish are expressed as $\Delta^{14}C$ with the AMS analytical uncertainty.

Resolved age (years)	Birth year (± age error)	$\Delta^{14}C$ (‰)
50	1950 ±1	−76.9 ±3.3
46	1954 ±1	−104.8 ±3.2
45	1955 ±1	−89.0 ±4.0
43	1957 ±1	−92.2 ±3.8
41	1959 ±1	−66.9 ±3.3
40	1960 ±1	−54.7 ±4.2
39	1961 ±1	−57.8 ±3.7
37	1963 ± 1	−49.1 ±3.3
35	1965 ±1	28.2 ±3.7
33	1967 ±1	105.4 ±4.2
31	1969 ±1	19.4 ±4.0
30	1970 ±1	47.5 ±3.6
25	1975 ±1	43.9 ±4.0
20	1980 ±1	76.3 ±5.5
15	1985 ±0	15.4 ±3.7

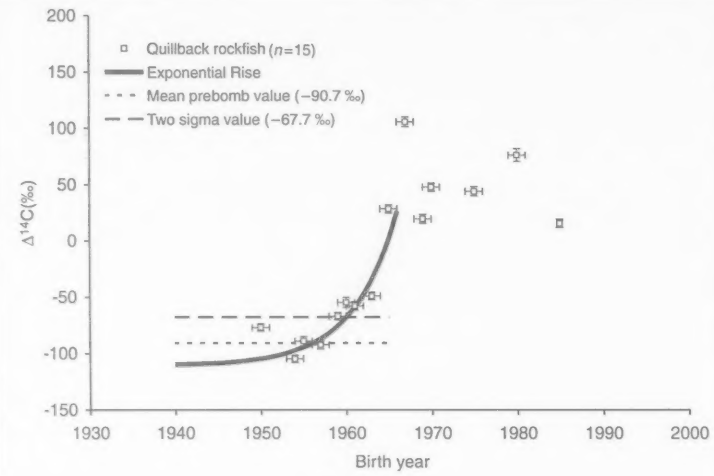

Figure 2

Radiocarbon ($\Delta^{14}C$) values for quillback rockfish (*Sebastes maliger*) otolith cores (n=15) in relation to estimated birth year. Horizontal error bars represent the age estimate uncertainty from growth zone counts (CV=2.6%, year rounded to the nearest whole number) and vertical error bars represent the 1–σ AMS (accelerator mass spectometry) analytical uncertainty. The solid line represents the exponential curve fitted to the data that was used to determine the year of initial rise in ^{14}C levels from prebomb levels (the fitted function had the form $Y=A+B\ \exp(CX)$ with $Y=^{14}C$, X=birth year, and A, B, and C as fitted parameters). The dashed line represents the +2 SD level (−67.7‰) associated with the average prebomb ^{14}C value (−90.7 ±11.5‰; dotted line); the intersection of the +2 SD line and the curve was used to define the year-of-initial-rise in ^{14}C values.

this sample was the first to have a ^{14}C value (−66.9 [±3.3]‰) that was above prebomb radiocarbon levels with a +2 SD criteria (upper limit of −67.7‰). This first indication of a rise in ^{14}C related to the rise of the bomb was in agreement with the exponential fit of the quillback rockfish ^{14}C times series (Fig. 2). The ^{14}C record for quillback rockfish otoliths peaked in 1967 with a maximum ^{14}C concentration of +105.4 (±4)‰. This peak was followed by a generally declining, but inconsistent, trend in ^{14}C values to 1985 (last birth year sampled).

The ^{14}C values measured in quillback rockfish otoliths plotted against estimated birth years produced a characteristic increasing and decreasing curve representative of bomb-generated ^{14}C changes over time (Fig. 3). The quillback rockfish ^{14}C record was synchronous with a ^{14}C time series for southeast Alaskan waters determined from yelloweye rockfish otoliths (Kerr et al., 2004); the average prebomb ^{14}C values for the quillback rockfish were in close agreement with the average yelloweye rockfish prebomb levels (−102.2 [±9.3]‰ [mean ±SD]). The year of initial rise in the quillback and yelloweye rockfish records (1959 [±1 year] *cf.* 1958 [±2 years]) and peak in ^{14}C values (1967 *cf.* 1966) for these two species coincided within one year, a period encompassed within the uncertainty associated with break-and-burn age estimates. Furthermore, the postbomb decline in quillback rockfish ^{14}C values was similar to that of the yelloweye rockfish. In addition, thirteen of the fifteen quillback rockfish ^{14}C values fell within the confidence intervals of the yelloweye rockfish ^{14}C curve (Fig. 3).

The comparison of the quillback rockfish ^{14}C record with that for Hawaiian Islands corals (Toggweiler et al., 1991; Druffel et al., 2001) and two otolith-based northern hemisphere ^{14}C chronologies (northwest Atlantic haddock [Campana, 1997] and Barents Sea Arcto-Norwegian cod [Kalish et al., 2001]) revealed similarities in the year of initial rise and rate of rise of ^{14}C values, and differences in the pre- and postbomb eras that can be explained by regional oceanographic effects (Fig. 4).

Discussion

Sample size assessment

Although the ^{14}C technique has great potential for validating the age of many long-lived fishes, one of the main disadvantages has been the high cost of AMS ^{14}C analyses. By providing a means of defining the

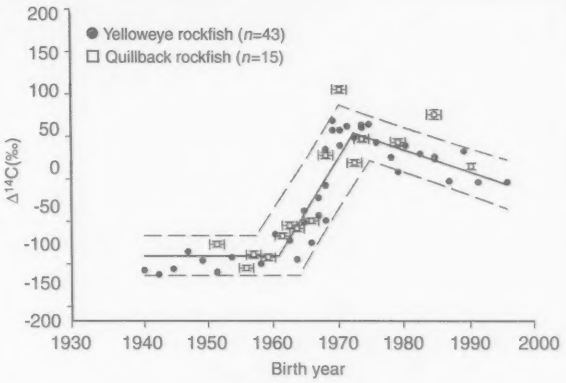

Figure 3

Radiocarbon ($\Delta^{14}C$) values from quillback rockfish (*Sebastes maliger*) otoliths and the yelloweye rockfish (*S. ruberrimus*) ^{14}C time series for the waters of southeast Alaska. The yelloweye rockfish ^{14}C data were divided into three intervals (prebomb, bomb rise, and postbomb) and fitted with confidence intervals. The prebomb era ^{14}C values (1950–57) were fitted with an average (±2 SD), and the bomb rise (1959–71) and postbomb era values (1966–85) were fitted with a linear regression and corresponding 95% prediction intervals.

minimum number of samples required to achieve the desired degree of precision, the present study takes a step toward reducing the number of prescribed samples, (i.e., 20–30 otoliths; Campana, 2001), effectively making age validation more affordable.

To determine the number of samples necessary for an age validation study, an assessment of the degree of precision is required. The degree of precision may be defined by the level of variation in the chronology or the uncertainty associated with age estimates. It can also be dependent on the estimated longevity of the fish and the resolution of age that is sufficient for the purposes of the study. For example, a resolution of ±5 years may be sufficient for a species estimated to live 100 years, but would not be satisfactory for a species estimated to live 20 years. The higher degree of precision, the greater the cost will be for a study. However, a maximum precision can be attained at a minimum cost by taking into consideration the precision of the ^{14}C time series, the error associated with age estimates, and the age resolution necessary to accomplish the goals of the study.

In our study, the ±2-year variation of the yelloweye rockfish ^{14}C time series limited the precision to which the age of the quillback rockfish could be determined through comparison. Stratified sampling of nine quillback rockfish ^{14}C values between 1956 and 1971 revealed an average year of initial rise in ^{14}C of 1959 (±1 year) that was in close agreement with the year of initial rise determined for the yelloweye rockfish time series. Thus, given the unique circumstances for this species, we have quantitatively reduced the number of samples required for age validation to 9 (given that some sampling or additional information is used to establish prebomb levels). It can also be envisioned that ^{14}C analysis of a single fish otolith could establish a minimum longevity for a species if the ^{14}C levels measured in the otolith core of an adult fish with a known capture year were consistent with established prebomb ^{14}C levels for the regional waters in which that fish spent its first year. This exercise illustrates the necessity of defining precision on a species-by-species basis prior to beginning a ^{14}C study. Despite the high cost of AMS analyses, the overall project cost may be lower and of shorter duration than traditional age validation studies because of the relatively short time required to prepare and process the minimum number of otoliths. Currently, the ^{14}C technique is considered one of the most effective methods for age validation of long-lived fishes (Campana, 2001) and as costs are minimized, future application of the bomb ^{14}C age-validation technique of marine fishes should increase.

Radiocarbon analysis

To interpret radiocarbon values recorded in marine organisms it is essential to put them in the context of the regional oceanography. The Alaska coastal current, driven by wind stress and enriched with freshwater runoff, is the driving force behind the coastal dynamics off southeast Alaska (Royer, 1982). The coastal environment off southeast Alaska is characterized by significant

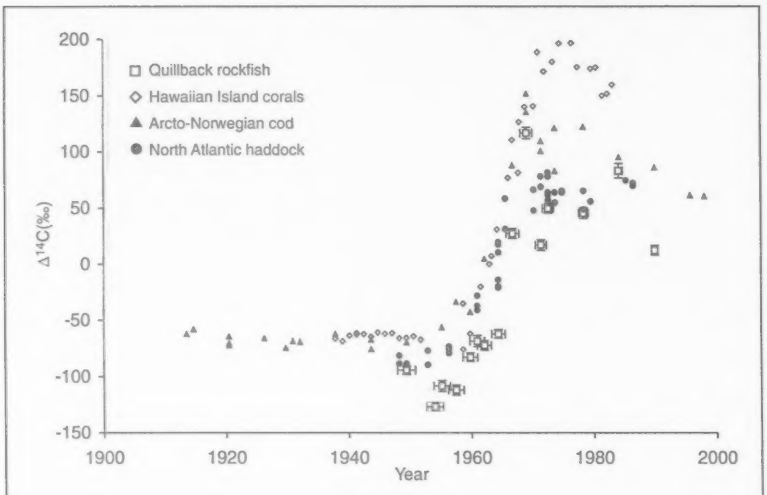

Figure 4

Radiocarbon data ($\Delta^{14}C$) from otolith cores of quillback rockfish (*Sebastes maliger*), Hawaiian hermatypic corals (Toggweiler et al., 1991; Druffel et al., 2001), and two age-validated fishes, the northwest Atlantic haddock (*Melanogrammus aeglefinus*; Campana, 1997) and the Arcto-Norwegian cod (*Gadus morhua*; Kalish et al., 2001). Note the strong agreement in the timing of the year of initial rise in ^{14}C values.

downwelling, high wind stress, eddies, and storm activity, resulting in a high degree of mixing. The rapid rise and early peak recorded in quillback rockfish otoliths, followed by a postbomb decline, indicated rapid ocean-atmosphere gas exchange in the shelf waters off southeast Alaska. Shallow continental shelf waters, such as the environment inhabited by juvenile quillback rockfish, have a thin mixed layer and relatively long surface residence time, resulting in a relatively fast response and build up of bomb-^{14}C from the atmospheric signal. In addition, low prebomb ^{14}C values in the quillback rockfish record may indicate the influence of upwelled ^{14}C-depleted waters on southeast Alaskan coastal surface waters. This is expected because surface waters sampled off the Alaskan Peninsula (GEOSECS; Ostlund and Stuvier, 1980) in 1973 had low ^{14}C values (+62‰) in relation to the subtropical Pacific (Oahu coral, +174.5‰ in 1973, Toggweiler et al., 1991), indicating the influence of upwelled ^{14}C-depleted waters.

A comparison of the ^{14}C time series determined from quillback rockfish otoliths to the established ^{14}C time series exhibited synchronicity with the global rise in radiocarbon. The quillback rockfish record and high latitude northern hemisphere records from Arcto-Norwegian cod and haddock exhibited nearly identical years of initial rise and rates of ^{14}C increase. Note that there are differences among these records in the prebomb and peak ^{14}C levels attained and the behavior of bomb-^{14}C after the peak, but it is irrelevant to the utility of the technique as an age validation tool. The quillback rockfish record was also temporally similar to a Hawaiian Island corals record (Oahu, Toggweiler et al., 1991; Hawaii, Druffel et al., 2001), both increasing rapidly from the late 1950s. However, as expected, the corals had higher prebomb levels (−50‰ *cf.* −90‰), a later peak (1971 *cf.* 1967) at a higher value (174‰ *cf.* 105‰), and the indication of a more rapid decline in the postbomb years. These differences are indicative of the different oceanographic influences on the subtropical waters (e.g., lesser relative influence of upwelled, ^{14}C-depleted, deep water).

Possible sources of error in the quillback rockfish ^{14}C record are the specific location of each fish during its first year of growth, possible inaccuracies in the method of extracting the core, age estimate uncertainty, and variable oceanographic conditions during the year of otolith formation. The unknown geographic location of individual fish during the first year of life is a potential source of ^{14}C variation. Although juvenile quillback rockfish occupy relatively limited regions, factors such as local bathymetry, coastal upwelling, and freshwater input are likely to impact the ^{14}C content of the local waters. Two of the quillback otolith samples (birth years 1967 and 1980) had considerably higher (~50‰) ^{14}C values when compared to the highest yelloweye rockfish value for that same year. These elevated ^{14}C values may indicate that the individuals resided in different water masses. The variability of otolith ^{14}C values from regional effects is evident in the observed ±11.5‰ (1 SD) associated with prebomb values, a higher variability than expected from the analytical uncertain-

ties of the AMS ^{14}C measurements (~±3–4‰). Elevated ^{14}C levels have also been recorded in otoliths of the black drum (*Pogonias cromis*), known to reside in estuaries during the juvenile stage (Campana and Jones, 1998); these elevated values are attributed to the rapid exchange of atmospheric ^{14}C in the well-mixed estuarine environment and the influence of river input. Quillback rockfish are known to inhabit more nearshore waters than those inhabited by yelloweye rockfish (Love et al., 2002), which could explain the elevated ^{14}C levels.

The core-extraction method was designed to limit the inclusion of more recently formed material (older than age 1); however, the inclusion of some of this material may have inadvertently occurred, perhaps introducing error to the quillback rockfish ^{14}C record. This kind of error could alter the ^{14}C value from the actual core year value depending on the time of otolith formation in relation to the bomb ^{14}C signal. A small addition of material with ^{14}C content different from the core material, however, may not produce a significant change in the timing of the initial rise and the shape of the rise. We feel that in most cases this would lead to an underaging of the fish and provide us with a minimum age estimate.

Perhaps the most significant potential source of error is the uncertainty associated with age estimation methods (coefficient of variation=2.6%). Growth zone counting error could have contributed to variation in the quillback rockfish record; however, the otoliths used in our study were chosen specifically to provide clearly definable growth zones and the highest rank in age-estimate confidence. The samples chosen were best-case examples of precise age determinations.

Short-term regional-scale changes in oceanographic conditions, such as upwelling events, may have affected ^{14}C levels at the time of otolith formation. The variation in postbomb measurements exemplifies this factor.

Considering the discussions above and the similar biology, ecology, and distribution of the two rockfish species, we believe that the use of the yelloweye rockfish ^{14}C time-series (Kerr et al., 2004) as a means of temporal calibration for the quillback rockfish record is well supported. The year of initial rise in ^{14}C for quillback rockfish otoliths (1959 [±1 year]) is in agreement with the yelloweye rockfish record (1958 [±2 years]); this finding validates the age estimates of the quillback rockfish and the accuracy of the break-and-burn age estimation method. In addition, the concordance of the quillback time series (1950 to 1985) provides further support for the age validation. Note that the ^{14}C levels, timing of the peak, and the subsequent decline were similar between species. In addition, all but two of the quillback rockfish ^{14}C values (sample years 1967 and 1980) fell within the confidence intervals for the yelloweye rockfish ^{14}C curve, further supporting the concordance of the two rockfish records. If there had been consistent underaging or overaging of quillback rockfish otoliths, this discrepancy would have resulted in a chronology that was not in phase with the yelloweye rockfish time series (Campana et al., 2002).

This application of the bomb-^{14}C technique has confirmed the longevity of quillback rockfish to a minimum of 43 (±1) years. This minimum age estimate is based on the last individual fish sample (estimated birth year of 1957 from growth zone counting) to have prebomb levels, immediately preceding the significant rise in ^{14}C levels observed in 1959 (±1) year. These findings effectively refute previous longevity estimates less than 43 years (Barker, 1979; Reilly et al.[2]). In addition, it is reasonable to assume that the annual growth pattern continues throughout life; hence, these findings strongly support longevity estimates exceeding 43 years and ranging up to 90 years (Richards and Cass, 1986; Yamanaka and Kronland, 1997; Casillas et al., 1998; Munk, 2001).

Conclusions

It is our intention to not only validate the age and age estimation method for the quillback rockfish, but to determine the most effective number of samples for age validation with bomb radiocarbon. From our results, it appears that the concordance of the full ^{14}C time series is not entirely necessary for validating the age of fish, and perhaps of any other organism. Because the evolution and magnitude of the bomb-^{14}C rise from the prebomb to postbomb era is subject to variations due to the specific oceanography of the region, the ^{14}C time series are in fact regional and are not universally applicable to all validation studies. The agreement of the entire ^{14}C time series does not provide additional information relevant to age validation. Hence, we propose that the year-of-initial-rise method be considered an effective ^{14}C age validation approach. This method both reduces the number of samples required for age validation and effectively precludes the perceived need to establish a pre- to postbomb ^{14}C reference time series for every region of the world's oceans. Because the year of initial rise in ^{14}C levels in surface waters is well defined (1958 [±2 years]), it should be treated as a time-specific marker for organisms that inhabit the mixed layer of the oceans for some or all of their life cycle.

Acknowledgments

We thank the Alaska Department of Fish and Game for providing aged otolith samples. This article was supported in part by the National Sea Grant College Program of the U.S. Department of Commerce's National Oceanic and Atmospheric Administration under NOAA Grant no. NA06RG0142, project number R/F-190, through the California Sea Grant College Program, and in part by the California State Resources Agency. This work was performed, in part, under the auspices of the U.S. Department of Energy by University of California, Lawrence Livermore National Laboratory under contract no. W-7405-Eng-48. This research was also funded in part by the Pacific States Marine Fisheries Commission, Earl H. and Ethel M. Myers Oceanographic

and Marine Biological Trust, Packard Foundation, and Project AWARE.

Literature cited

Adams, P. B.
1980. Life history patterns in marine fishes and their consequences for fisheries management. Fish. Bull. 78:1–12.

Andrews, A. H., G. M. Cailliet, K. H. Coale, K. M. Munk, M. M. Mahoney, and V. M. O'Connell.
2002. Radiometric age validation of the yelloweye rockfish (*Sebastes ruberrimus*) from southeastern Alaska. Mar. Freshw. Res. 53:139–146.

Archibald, C. P., D. Fournier, and B. M. Leaman.
1983. Reconstruction of stock history and development of rehabilitation strategies for Pacific ocean perch in Queen Charlotte Sound, Canada. N. Am. J. Fish. Manag. 3:283–294.

Archibald, C. P., W. Shaw, and B. M. Leaman.
1981. Growth and mortality estimates of rockfish (Scorpaenidae) from B.C. coastal waters. 1977–1979. Can. Tec. Rep. Fish Aquat. Sci. 1048, 57 p.

Baker, M. S., and C. A. Wilson.
2000. Use of bomb radiocarbon to validate otolith section ages of red snapper *Lutjanus campechanus* from the northern Gulf of Mexico. Limnol. Oceanogr. 46(7):1819–1824.

Barker, M. W.
1979. Population and fishery dynamics of recreationally exploited marine bottomfishes of northern Puget Sound. Ph.D. diss., 135 p. Univ. Wash., Seattle, WA.

Beamish, R. J.
1979. New information on the longevity of Pacific ocean perch (*Sebastes alutus*). J. Fish. Res. Board Can. 36:1395–1400.

Beamish, R. J., and G. A. McFarlane.
1983. The forgotten requirement for age validation in fisheries biology. Trans. Am. Fish. Soc. 112:735–743.
1987. Current trends in age determination methodology. *In* The age and growth of fish (R. C. Summerfelt and G. E. Hall, eds.), p. 15–42. The Iowa State Univ. Press, Ames, IA.

Cailliet, G. M., A. H. Andrews, E. J. Burton, D. L. Watters, D. E. Kline, and L. A. Ferry-Graham.
2001. Age determination and validation studies of marine fishes: do deep-dwellers live longer? Exp. Geron. 36:739–764.

Campana, S. E.
1997. Use of radiocarbon from nuclear fallout as a dated marker in the otoliths of haddock *Melanogrammus aeglefinus*. Mar. Ecol. Prog. Ser. 150:49–56.
2001. Accuracy, precision and quality control in age determination, including a review of the use and abuse of age validation methods. J. Fish Biol. 59:197–242.

Campana, S. E., and C. M. Jones.
1998. Radiocarbon from nuclear testing applied to age validation of black drum, *Pogonias cromis*. Fish. Bull. 96:185–192.

Campana, S. E., L. J. Natanson, and S. Myklevol.
2002. Bomb dating and age determination of large pelagic sharks. Can. J. Fish. Aquat. Sci. 59:450–455.

Casillas, E., L. Crockett, Y. DeReynier, J. Glock, M. Helvey, B. Meyer, C. Schmitt, M. Yoklavich, A. Bailey, B. Chao, B. Johnson, and T. Pepperell.
1998. Essential fish habitat West Coast groundfish appendix, 778 p. NMFS, Montlake, Seattle, WA.

Chang, W. Y. B.
1982. A statistical method for evaluating reproducibility of age determination. Can. J. Fish. Aquat. Sci. 39:1208–1210.

Chilton, D. E., and R. J. Beamish.
1982. Age determination methods for fishes studied by the groundfish program at the Pacific biological station. Can. Spec. Publ. Fish. Aquat. Sci. 60. 102 p.

Druffel, E. R. M., S. Griffin, T. P. Guilderson, M. Kashgarian, J. Southon, and D. P. Schrag.
2001. Changes in subtropical North Pacific radiocarbon and correlation with climate variability. Radiocarbon 43(1):15–25

Farrell, J., and S. E. Campana.
1996. Regulation of calcium and strontium deposition on the otoliths of juvenile tilapia, *Oreochromis niloticus*. Comp. Biochem. Physiol. 115A:103–109.

Francis, R. C.
1985. Fisheries research and its application to west coast groundfish management. *In* Proceedings of the conference on fisheries management: issues and options (T. Frady ed.), p. 285–304. Alaska Sea Grant Report. 85-2, Univ. Alaska, Fairbanks, AK.

Kalish, J. M.
1991. ^{13}C and ^{18}O isotopic disequilibria in fish otoliths: metabolic and kinetic effects. Mar. Ecol. Prog. Ser. 75:191–203.
1993. Pre- and post-bomb radiocarbon in fish otoliths. Earth Planet. Sci. Lett. 114:549–554.
1995. Radiocarbon and fish biology. *In* Recent developments in fish otolith research (D. H. Secor, J. M. Dean, and S. E. Campana, eds.), p. 637–653. Univ. South Carolina Press, Columbia, SC.
2001. Use of the bomb radiocarbon chronometer to validate fish age. Final Report FRDC Project 93/109, 384 p. Fisheries Research and Development Corporation, Canberra, Australia.

Kalish, J. M., R. Nydal, K. H. Nedreaas, G. S. Burr, and G. L. Eine.
2001. A time history of pre- and post-bomb radiocarbon in the Barents Sea derived from Arcto-Norwegian cod otoliths. Radiocarbon 43(2B):843–855.

Kerr, L. A., A. H. Andrews, B. R. Frantz, K. H. Coale, T. A. Brown, and G. M. Cailliet.
2004. Radiocarbon in otoliths of yelloweye rockfish (*Sebastes ruberrimus*): a reference time series for the waters of southeast Alaska. Can. J. Fish. Aquat. Sci. 61:443–451.

Kramer, D. E., and V. M. O'Connell.
1995. Guide to northeast Pacific rockfishes: genera *Sebastes* and *Sebastolobus*. Alaska Sea Grant Advisory Bulletin 25, 78 p. Univ. Alaska, Fairbanks, AK.

Leaman, B. M., and R. J. Beamish.
1984. Ecological and management implications of longevity in some northeast Pacific groundfishes. Int. North Pac. Fish. Comm. Bull. 42:85–97.

Love, M. S., M. Yoklavich, and L. Thorsteinson.
2002. The rockfishes of the Northeast Pacific, 404 p. Univ. California Press, Berkeley, CA.

Matthews, K. R.
1990. An experimental study of the habitat prefer-

ences and movement patterns of copper, quillback, and brown rockfishes (*Sebastes* spp.). Environ. Biol. Fishes 29:161–178.

Munk, K. M.
2001. Maximum ages of groundfishes in waters off Alaska and British Columbia and considerations of age determination. Alaska Fish. Res. Bull. 8(1):12–21.

Ostlund, H. G., and M. Stuiver.
1980. GEOSECS Pacific Radiocarbon. Radiocarbon 22(1):25–53.

Richards, L. J., and A. J. Cass.
1986. The British Columbia inshore rockfish fishery: Stock assessment and fleet dynamics of an unrestricted fishery, p. 299–308. *In* Proceedings of the international rockfish symposium, Lowell Wakefield fisheries symposium, Anchorage, Alaska, October 20–22, 1986. Alaska Sea Grant Report 87–2:

Royer, T. C.
1982. Coastal fresh water discharge in the northeast Pacific. J. Geophys. Res. 87(C3):2017–2021

Schwarcz, H. P., Y. Gao, S. Campana, D. Browne, M. Knyf, and U. Brand.
1998. Stable carbon isotope variations in otoliths of Atlantic cod (*Gadus morhua*). Can. J. Fish. Aquat. Sci. 55:1798–1806.

Stuvier, M., and H. A. Polach.
1977. Discussion: reporting of ^{14}C data. Radiocarbon 19(3):355–363.

Toggweiler, J. R., K. Dixon, and W. S. Broecker.
1991. The Peru upwelling and the ventilation of the South Pacific thermocline. J. Geophys. Res. 96:20467–20497.

Vogel, J. S., D. E. Nelson, and J. R. Southon.
1987. ^{14}C background levels in an accelerator mass spectrometry system. Radiocarbon 29(3):323–333.

Vogel, J. S., J. R. Southon, D. E. Nelson, and T. A. Brown.
1984. Performance of catalytically condensed carbon for use in accelerator mass spectrometry. Nucl. Instr. Methods B5:289–293.

Wang, C. H., D .L. Willis, and W. D. Loveland.
1975. Radiotracer methodology in the biological, environmental, and physical sciences, 480 p. Prentice Hall, Englewood Cliffs, NJ.

Williams, T., and B. C. Bedford.
1974. The use of otoliths for age determination. *In* The ageing of fish. Proceedings of an international symposium (T. B. Bagenal, ed.), p. 114–123. Unwin Brothers Limited, Surrey, England.

Yamanaka, K. L., and A. R. Kronlund.
1997. Inshore rockfish stock assessment for the west coast of Canada in 1996 and recommended yields for 1997. Can. Tech. Rep. Fish. Aquat. Sci. 2175, 80 p.

Yoklavich, M. M., V. J. Loeb, M. Nishimoto, and B. Daly.
1996. Nearshore assemblages of larval rockfishes and their physical environment off central California during an extended El Nino event, 1991–1993. Fish. Bull. 94:766–782.

Cross-shelf and seasonal variation in larval fish assemblages on the southeast United States continental shelf off the coast of Georgia

Katrin E. Marancik

Department of Biology
East Carolina University
East Fifth Street
Greenville, North Carolina 27858
Present address: Center for Coastal Fisheries and Habitat Research
NOAA Beaufort Laboratory
101 Pivers Island Road
Beaufort, North Carolina 28516
E-mail address: Katey.Marancik@noaa.gov

Lisa M. Clough

Department of Biology
East Carolina University
East Fifth Street
Greenville, North Carolina 27858

Jonathan A. Hare

Center for Coastal Fisheries and Habitat Research
NOAA Beaufort Laboratory
101 Pivers Island Road
Beaufort, North Carolina 28516

Abstract—Seasonal and cross-shelf patterns were investigated in larval fish assemblages on the continental shelf off the coast of Georgia. The influence of environmental factors on larval distributions also was examined, and larval transport processes on the shelf were considered. Ichthyoplankton and environmental data were collected approximately every other month from spring 2000 to winter 2002. Ten stations were repeatedly sampled along a 110-km cross-shelf transect, including four stations in the vicinity of Gray's Reef National Marine Sanctuary. Correspondence analysis (CA) on untransformed community data identified two seasonal (warm weather [spring, summer, and fall] and winter) and three cross-shelf larval assemblages (inner-, mid-, and outer-shelf). Five environmental factors (temperature, salinity, density, depth of the water column, and stratification) were related to larval cross-shelf distribution. Specifically, increased water column stratification was associated with the outer-shelf assemblage in spring, summer, and fall. The inner shelf assemblage was associated with generally lower temperatures and lower salinities in the spring and summer and higher salinities in the winter. The three cross-shelf regions indicated by the three assemblages coincided with the location of three primary water masses on the shelf. However, taxa occurring together within an assemblage were transported to different parts of the shelf; thus, transport across the continental shelf off the coast of Georgia cannot be explained solely by two-dimensional physical factors.

Manuscript submitted 20 December 2003 to the Scientific Editor's Office.

Manuscript approved for publication June 25 2004 by the Scientific Editor.

Fish. Bull. 103:108–129 (2005).

The study of larval fish assemblages provides information on community structure, spawning, and larval transport. Larval fish assemblages are groups of larvae with similar temporal and spatial distributions (Cowen et al., 1993). Larval distribution patterns are initially determined by spawning time and location; larvae of species with similar spawning patterns are initially in the same larval assemblage (Rakocinski et al., 1996). Physical forcing and larval behavior then modify the structure of larval assemblages and ultimately determine the outcome of larval transport (Cowen et al., 1993; Smith et al., 1999; Hare et al., 2001).

Marine protected areas (MPAs) are portions of the marine environment designated to "provide lasting protection for part or all of the natural and cultural resources therein" (Federal Register, 2000). A number of specific conservation objectives are encompassed by this definition, such as protecting small areas with historical significance or aesthetic quality, or protecting much larger areas to enhance fisheries through increases in spawning stock biomass and the supply of recruits to surrounding areas (Crowder et al., 2000). However, whether an MPA provides recruits to other areas is difficult to quantify and involves determining the fate of larvae and juveniles spawned in a protected area (Stephenson, 1999; Warner et al., 2000).

MPAs are under consideration as a fisheries management tool on the southeast United States continental shelf (Plan Development Team, 1990), and larval assemblage studies would provide useful information regarding spawning and larval transport. Although substantial larval fish research has been conducted on the southeast U.S. continental shelf, no studies have examined the dynamics

of larval fish assemblages in this area. For example, during the RV *Dolphin* cruises, the Marine Resources Monitoring, Assessment, and Prediction (MARMAP) cruises, and the Southeast Area Monitoring and Assessment Program (SEAMAP) cruises, ichthyoplankton surveys were conducted on the southeast United States continental shelf. From these surveys, spawning time was defined for a large group of species (Fahay, 1975), and the temporal and spatial distribution of larvae were described for a few select species (Kendall and Walford, 1979; Collins and Stender, 1987; 1989; Smith et al., 1994) and for multiple taxa, but mostly at the family level (Powles and Stender, 1976). Similarly, other programs (e.g., the South Atlantic Bight Recruitment Experiment) examined spawning and larval transport of "estuarine-dependent" species such as Atlantic menhaden (e.g., Judy and Lewis, 1983; Hoss et al., 1997; Hare et al., 1999; Checkley et al., 1999), but results for the entire suite of species sampled were not reported. For studies where the broader community of larval fish on the southeast U.S. shelf was addressed, the structure and dynamics of larval assemblages were not defined (Powell and Robbins, 1994, 1998; Govoni and Spach, 1999; Powell et al., 2000).

The purpose of this study was to examine larval fish assemblages on the continental shelf off the coast of Georgia, USA. This region of the continental shelf was targeted because of 1) the nature of the broad shallow shelf, 2) the location of Gray's Reef National Marine Sanctuary 20 km from shore, and 3) the location of several proposed deepwater MPAs (70–200 m water depth) in the region. Temporal and spatial patterns in larval distributions were described to explain spawning and larval transport processes on the continental shelf off the coast of Georgia, and the implications for MPAs in the region were addressed.

Materials and methods

Study site

The southeast United States continental shelf extends from West Palm Beach, Florida, to Cape Hatteras, North Carolina. Moving north from West Palm Beach (15 km), the shelf widens to Georgia (200 km) and then narrows to Cape Hatteras (35 km). Physical forcing by the Gulf Stream, which is part of the North Atlantic Western Boundary Current system, varies along the shelf. As the Gulf Stream flows northward along the shelf edge, it meanders, and cyclonic frontal eddies form in meander troughs (Lee et al., 1991). Meanders and frontal eddies grow in dimension from just north of the Straits of Florida (27°N latitude) to St. Augustine, Florida (30°N latitude), and then decrease from St. Augustine to just south of Charleston, South Carolina (32°N latitude). Meanders and frontal eddies grow in dimension again downstream of the Charleston Bump (32–33°N latitude), and then decrease again from Cape Fear, North Carolina (33°N latitude), to Cape Hatteras, North Carolina (36°N latitude).

Table 1

Year, month, and season of ichthyoplankton sampling and number of stations sampled in the Georgia Bight region of the southeast United States continental shelf.

Year	Month	Season	Number of stations
2000	April	spring	4
2000	August	summer	8
2000	October	fall	7
2001	January	winter	8
2001	March	winter	8
2001	May	spring	7
2001	June	summer	7
2001	August	summer	10
2001	October	fall	8
2002	February	winter	10

In addition to along-shelf variation in geophysical structure and Gulf Stream forcing, the southeast United States continental shelf can be divided into three cross-shelf zones based on physical circulation dynamics (Boicourt et al., 1998). Circulation on the inner-shelf (0–20 m water depth) is influenced by tidal currents, river inflow, and wind (Atkinson and Menzel, 1985; Pietrafesa et al., 1985a). Wind-driven flow predominates on the mid-shelf (20–40 m water depth) and there is only minor Gulf Stream and tidal influence (Atkinson and Menzel, 1985). Flow on the outer-shelf (40–75 m water depth) is dominated by the passage of Gulf Stream frontal eddies and upwelling at the shelf break (Pietrafesa et al., 1985b).

Inner and mid-shelf physical processes are relatively more important off the coast of Georgia compared to other segments of the southeast United States continental shelf (Boicourt et al., 1998). The continental shelf off the coast of Georgia is the area of diminishing meanders and eddies from St. Augustine, Florida, to Charleston, South Carolina. Tidal range and freshwater inflow is greatest in the Georgia portion of the southeast shelf (Atkinson and Menzel, 1985). Further, because the shelf is widest off the coast of Georgia (approximately 200 km), the Gulf Stream is less influential on mid- and inner-shelf dynamics compared to the rest of the southeast United States continental shelf (Lee et al., 1991).

Collection of larval fish and CTD data

Ichthyoplankton sampling was conducted approximately every other month from April 2000 through February 2002 (Table 1). A maximum of ten stations, approximately 18.5 km apart, were sampled during each cruise. Stations were missed on some cruises owing to weather and equipment failure. The transect was 110 km long and spanned 10 to 50 m water depth (Fig. 1). Four sta-

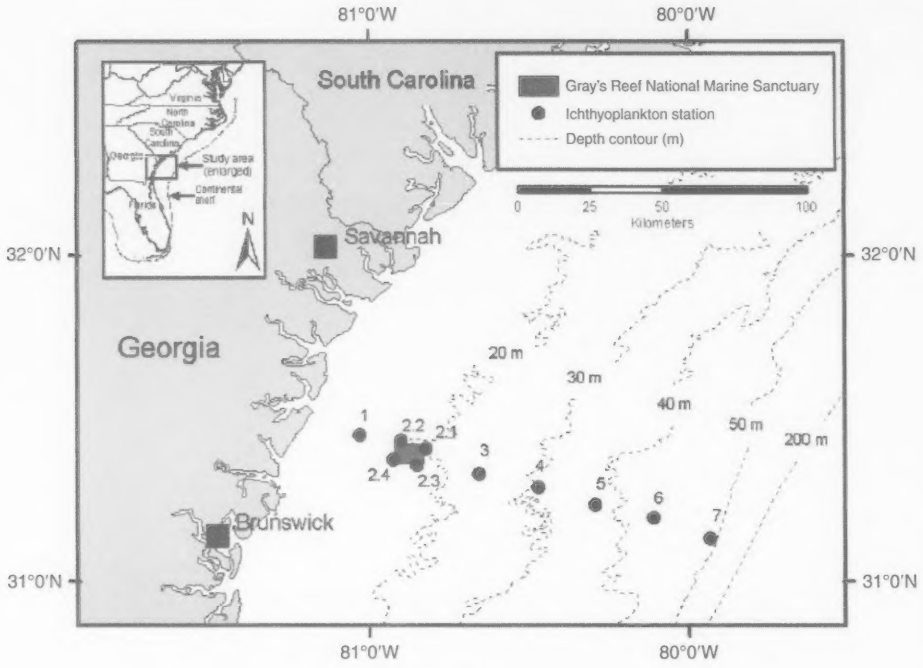

Figure 1

Map of the study area and the cross-shelf transect used for sampling larval abundance and environmental data bimonthly from April 2000 to February 2002 (see Table 1). Four stations (stations 2.1–2.4) were located around Gray's Reef National Marine Sanctuary.

tions were placed immediately adjacent to the four sides of Gray's Reef National Marine Sanctuary. At each station, temperature, salinity, density, and water depth were measured from the water's surface to one meter above the bottom with a Seabird conductivity-temperature-depth (CTD probe (SBE19, Seabird Electronics, Inc., Bellevue, WA). Ichthyoplankton was collected at each station with a five-minute single oblique net tow to within one meter of the bottom. For all but one cruise (August 2000), a 61-cm paired bongo frame fitted with 333-μm or 505-μm mesh nets was used. During the remaining cruise, a 1-m ichthyoplankton sled with 333-μm mesh net was used because of the smaller size of the research vessel. A flow meter (General Oceanica) was used to measure the volume of water filtered.

A gear comparison study, conducted during October 2000, showed that ichthyoplankton samples collected with the two gear types (61-cm bongo versus 1-m^2 ichthyoplankton sled) were similar. An analysis of variance (ANOVA) on the mean larval concentration revealed no significant differences between the two gear types (one-way ANOVA: F=0.489; df=1; P>0.5). Also, an analysis of similarities (ANOSIM, Clarke and Warwick, 2001) determined that the community structure varied more within than between gear types (ANOSIM: R=−0.11; S=77.57). Similarly, preliminary analysis of the effect of gear selectivity due to mesh size indicated that the larval communities collected by 333-μm mesh and by 505-μm mesh nets were similar. Thus, data from all cruises were combined in the subsequent analyses (see Marancik, 2003, for more details).

Preparation of ichthyoplankton data

All ichthyoplankton samples were sorted and larval fish were identified to the lowest possible taxonomic level by using previously published descriptions (e.g., Fahay, 1983; Johnson and Keener, 1984; Richards, 2001) and descriptions developed as part of this study. Identification to species was not easy given the diversity of species along the southeast United States continental shelf (see Kendall and Matarese, 1994), yet every effort was made to identify larvae to species-level (46.3% to species, 27.4% to genus, 6.7% unidentified). Larval concentrations were calculated as number of larvae/100 m^3.

Two data sets were used for statistical analyses, differing in the inclusion of rare taxa. Rare taxa pose a problem in community analyses. Some rare taxa occur because of transport anomalies (Cowen et al., 1993), and their inclusion in data analyses can confound the definition of larval assemblages. However, rare taxa can also be indicative of consistent, but low larval abun-

Table 2

Taxa collected during two years of sampling (April 2000–February 2002) constituting one or ten percent of any one sample from the continental shelf off the coast of Georgia and included in the analyses. The taxonomic codes used in the figures of this article are also shown. Taxa included in the one percent and ten percent data sets are marked by an "X." Also indicated are the seasonal assemblage (warm weather [WA] and winter [WI]) and larval assemblage (I=inner-shelf, M=mid-shelf, O=outer-shelf) in which larvae were collected (based on correspondence analyses).

Family	Species	Taxonomic code	Included in 1% data set	Included in 10% data set	Season	Assemblage
Muraenidae	*Gymnothorax* sp.		X		WA/WI	I/O
Ophichthidae	*Ophichthus* sp.		X		WA/WI	M/O
	Myrophis punctatus	Mpun	X	X	WI	M
Clupeidae	*Brevoortia tyrannus*	Btyr	X	X	WI	M
	Etrumeus teres		X		WI	O
	Opisthonema oglinum	Oogl	X	X	WA	I/O
Engraulidae	*Anchoa hepsetus*	Ahep	X	X	WA	I/M
	Engraulis eurystole		X		WA	O
Gonostomatidae	*Cyclothone* spp.		X		WA	O
Phosichthyidae	*Vinciguerria nimbaria*		X		WA	O
Paralepidae	*Lestidium atlanticum*		X		WI	O
Myctophidae	*Diaphus* spp.		X		WA/WI	M/O
	Lepidophanes spp.		X		WA	O
	Ceratoscopelus maderensis		X		WA/WI	M/O
	Ceratoscopelus warmingii		X		WI	M
	Electrona risso		X		WI	O
	Hygophum hygemii		X		WI	O
	Hygophum reinhardtii		X		WA	O
	Lampadena urophaos		X		WA	M
	Myctophum affini		X		WA	O
	Myctophum selenops		X		WA	O
Bregmacerotidae	*Bregmaceros atlanticus*		X		WA	O
	Bregmaceros cantori		X		WA/WI	I/O
	Bregmaceros houdei		X		WA/WI	M
Gadidae	*Urophycis* sp.		X		WI	M
Ophidiidae	*Ophidion antipholus/holbrooki*		X		WA/WI	I/M
	Ophidion josephi		X		WA/WI	I/O
	Ophidion marginatum	Omar	X	X	WA	M
	Ophidion selenops		X		WA	M
	Otophidium omostigmum	Oomo	X	X	WA/WI	M
Holocentridae	Holocentridae		X		WA	O
Syngnathidae	*Hippocampus* sp.		X		WA	I
	Syngnathus fuscus/louisianae		X		WA	I
	Syngnathus louisianae		X		WA	I
Scorpaenidae	Scorpaenidae		X		WA/WI	M/O

continued

dance (Leis, 1989); excluding these taxa could remove data useful in defining larval assemblages. Thus, two taxa inclusion data sets were selected. The first data set comprised taxa that made up greater than one percent abundance at any one station, and the second data set included those taxa that made up at least 10 percent abundance at any one station (Table 2).

The data sets were further truncated by eliminating, with a few exceptions, all taxa not identified to genus or species level. Priacanthidae, Scaridae, Scorpaenidae, and Epinephalinae were included because, despite potential inclusion of multiple species, these larvae represent some of the only reef taxa collected, and larval assemblage data including these taxa would be useful

Table 2 (continued)

Family	Species	Taxonomic code	Included in 1% dataset	Included in 10% dataset	Season	Assemblage
Serranidae	Epinephalinae		X		WA/WI	M/O
	Serraninae		X		WA/WI	M/O
	Diplectrum spp.		X		WA/WI	I/M/O
	Hemanthias vivanus		X		WA	O
	Serraniculus pumilio		X		WA	M
Priacanthidae	Priacanthidae		X		WA	M/O
Pomatomidae	*Pomatomus saltatrix*		X		WA	O
Carangidae	*Elagatus bipinnulata*		X		WA	M/O
Coryphaenidae	*Coryphaena hippurus*		X		WA	I/O
Lutjanidae	*Lutjanus* sp.		X		WA	O
	Rhomboplites aurorubens		X		WA	O
Sparidae	*Lagodon rhomboides*	Lrho	X	X	WI	I
Sciaenidae	*Bairdiella chrysura*		X		WA	I
	Cynoscion nothus		X		WA	I/M
	Cynoscion regalis		X		WA	I
	Larimus fasciatus		X		WA	I/M
	Leiostomus xanthurus	Lxan	X	X	WI	I/M
	Menticirrhus americanus	Mame	X	X	WA	I
	Micropogonias undulatus	Mund	X	X	WA/WI	I/M
	Pogonias cromis		X		WA	I
	Sciaenops ocellatus		X		WA	I
Pomacentridae	*Abudefduf* sp.		X		WA	O
	Chromis spp.		X		WA	O
Mugilidae	*Mugil curema*		X		WI	M
Labridae	*Halichoeres* sp.		X		WA/WI	M
	Xyrichthys spp.	Xyr	X	X	WA	M/O
Scaridae	Scaridae		X		WA/WI	I/M/O
Dactyloscopidae	Dactyloscopidae type 1 (*D. moorei*)		X		WA	I
	Dactyloscopidae type 2		X		WA	M
	Dactyloscopidae type 3		X		WA/WI	O
Callionymidae	*Diplogrammus pauciradiatus*	Dpau	X	X	WA/WI	M
Scombridae	*Euthynnus alletteratus*		X		WA	O
	Scomberomorus cavalla		X		WA	O
	Scomberomorus maculatus		X		WA	I
	Auxis rochei	Aroc	X	X	WA	O
	Scomber japonicus		X		WA/WI	M/O
Stromateidae	*Ariomma* sp.		X		WA/WI	M/O
Bothidae	*Bothus ocellatus/robinsi*	Boce	X	X	WA/WI	M/O
Paralichthyidae	*Cyclopsetta* sp.		X		WA/WI	M/O
	Engyophrys spp.		X		WA	O
	Syacium spp.		X		WA	M/O
	Paralichthys albiguta/lethostigma		X		WI	O
	Citharichthys arctifrons		X		WI	I
	Citharichthys cornutus		X		WA	O
	Citharichthys gymnorhinus		X		WA/WI	I/M/O
	Citharichthys spilopterus	Cspi	X	X	WI	M
	Etropus crossotus	Ecro	X	X	WA	M
	Hippoglossina oblongatta		X		WA	M
	Paralichthys lethostigma		X		WI	M
Soleidae	*Trinectes maculatus*		X		WA	I
Balistidae	*Monocanthus hispidus*		X		WA	O

Table 3

Mean values for each station (station 2 is the average of stations 2.1–2.4) of the sixteen environmental variables used in canonical correspondence analysis to determine which environmental variables were most significantly linked to the larvae of the Georgia Bight. Temperature, salinity, and density gradients are horizontal gradients based on the difference between adjacent stations. Stratification of the water column was calculated by using Simpson's stratification parameter and is a measure of vertical change in density.

		Station						
Environmental variables	Code	1	2	3	4	5	6	7
Depth (m)	DEP	12.44	18.51	23.15	33.05	37.03	41.48	45.94
Average temperature (°C)	AVGTEM	19.51	20.76	21.67	22.33	21.97	22.73	23.10
Temperature gradient (°C)	TEMGRAD	−0.29	−0.67	−1.10	−0.82	−0.52	−1.33	−0.59
Average salinity	AVGSAL	34.78	35.70	36.11	36.32	36.35	36.30	36.24
Salinity gradient	SALGRAD	−0.88	−1.13	−0.56	−0.25	0.03	0.12	0.19
Average density (kg/m^3)	AVGDEN	24.56	24.97	25.04	25.05	25.18	24.92	24.79
Density gradient (kg/m^3)	DENGRAD	−0.64	−0.74	−0.18	0.01	0.16	0.44	0.31
Stratification	STRAT	3.10	1.47	3.37	6.19	13.41	42.41	98.44

for managing reef fish on the southeast United States continental shelf (see Powell and Robbins, 1994; 1998). Serraninae were also included because the majority of these larvae are likely one type: *Serranus subligarius*. In contrast, larvae identified to some genera were excluded because there are multiple species common in the area within each genus, and each species likely has different larval distributions: *Etropus* spp. (3 species), *Prionotus* spp. (14 species), *Sphoeroides* spp. (11 species), *Symphurus* spp., (22 species), and *Syngnathus* spp. (10 species). In summary, 86 taxa were included in the one percent data set, and 16 taxa were included in the ten percent data set (Table 2).

Preparation of environmental data

Season, water mass, and eight environmental variables (mostly derived from temperature and salinity data) were chosen in an attempt to explain variation in the ichthyoplankton data (Table 3). For subsequent use in multivariate analyses, all environmental variables were standardized to a mean of zero and a standard deviation of one.

CTD data were processed with the manufacturer's software (Seasave vers. 5.3, Seabird Electronics, Inc., Bellevue, WA) and averaged into 0.5-m bins. Two parameters were derived to describe each hydrographic variable (salinity, temperature, density): an average value through the entire water column and a horizontal gradient value (calculated as the difference in value between the two adjacent stations). Vertical stratification was estimated by using Simpson's stratification parameter (Simpson and James, 1986):

$$\Phi = 1/h \int_{-h}^{0} (\bar{\rho} - \rho) g z dz,$$

where h = water column depth;
$\bar{\rho}$ = average water column density;
ρ = water density;
g = acceleration due to gravity; and
z = depth.

The stratification parameter, Φ (jowles/m^3), is a measure of the resistance of water to mixing; higher numbers signify higher resistance to mixing.

Temperature and salinity data were further used to define water masses on the continental shelf off the coast of Georgia. Pietrafesa et al. (1994) defined four water masses on the southeast U.S. continental shelf: Georgia Bight Water, Carolina Capes Water, Virginia Coastal Water, and Gulf Stream Water. However, temperature data collected on the continental shelf off the coast of Georgia exhibited greater seasonal variability (10–29°C) than reported by Pietrafesa et al. (1994; 14–29°C). As a result, water mass definitions for our study, although based largely on the definitions of Pietrafesa et al. (1994), reflect the greater range of temperature and reflect the natural breaks in temperature, salinity, and stratification data. Specifically, two water masses (inner-shelf water and mid-shelf water) and two mixes (inner-shelf–mid-shelf mixed water and mid-shelf–Gulf Stream mixed water) were defined (Fig. 2). Inner-shelf water was characterized by salinities <35 ppt and seasonally variable temperatures. This water mass was found during winter and spring and was distributed inside the 20-m isobath (Fig. 3). Mid-shelf water, with salinities >36 (Fig. 2), was typically well mixed vertically (Simpson's stratification parameter value <10). Mid-shelf water was found year round over large sections of the shelf, particularly in the fall (Fig. 3). A mixture between inner-shelf and mid-shelf water was defined with salinities between 35 and 36 (Fig. 2). A mixture was also defined

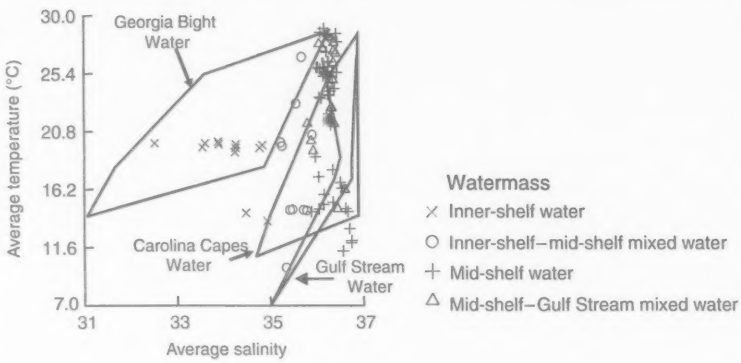

Figure 2

The average temperature and salinity for each station; symbols used represent the water mass designation for each station. The black polygons represent the temperature and salinity boundaries (data for all seasons bounded by one polygon) of three water masses defined by Pietrafesa et al. (1994; Georges Bight water; Carolina Capes water, and Gulf Stream water). Four water masses were defined in our study (inner-shelf water, inner-shelf–mid-shelf water, mid-shelf water, and mid-shelf–Gulf Stream mixed water).

as mid-shelf water and Gulf Stream water (Fig. 2). Gulf Stream water was not encountered, but its temperature and salinity properties are well documented (Churchill et al., 1993; Pietrafesa et al., 1994). Mid-shelf–Gulf Stream mixed water was highly stratified (Simpson's stratification parameter value >10), with warm highly saline water intruding on the surface during fall, winter, and spring and cool highly saline water intruding at depth during summer. Mid-shelf–Gulf Stream mixed water was encountered on most cruises and was found farthest offshore (Fig. 3).

Cruises were assigned to one of four seasons (Table 1) based on wind and temperature regimes. Although Blanton et al. (1985) identified five seasons for the southeast United States based on wind regimes (Spring [March–May], summer [June–July], transition [August], autumn [September–October], and winter [November–February]), the temperature data collected in our study supported classifying both August cruises as summer and the March cruise as winter.

Data analyses

Multivariate analyses were used to define larval assemblages and to explore the factors that influence distribution of larval assemblages on the continental shelf off the coast of Georgia. Multivariate analyses arrange sites and species along environmental gradients creating a low dimensional map (an ordination). Analyses can be conducted for samples where the distance between points in the ordination represents the similarity of species abundance between samples. Analyses also can be conducted for species where the distance between points in the ordination represents the similarity in the sample distribution between species. Ordinations, then, can be analyzed in two ways: with regard to proximity and dimensionality. Points that occur in close proximity can be considered similar based on similar composition. Points that occur on the same dimension define gradients in the data.

The effects of data transformation (untransformed, square root transformed, and fourth root transformed) and species inclusions (1% and 10% data sets) on the ordination of community and environmental data by two multivariate ordination techniques, multidimensional scaling and correspondence analysis (CA), were compared to determine which method was more effective at analyzing the larval fish data collected on the continental shelf off the coast of Georgia (Marancik, 2003). Overall, the two analytical methods produced similar ordinations and were robust to the inclusion of rare species and to the type of data transformation.

Correspondence analysis on untransformed larval fish concentration data was used to define larval assemblages in relation to season and the entire two-year data set. One of the strengths of CA is that it allows one to plot analyses of species and station data simultaneously on one ordination, thereby, allowing immediate comparisons between those stations that occur in close proximity in ordination space and those taxa that influence that proximity. Eigenvalues are a measure of the importance of each CA dimension (ter Braak and Smilauer, 2002). Thus, the dimensions needed to describe patterns in the data can be determined by an abrupt drop in the magnitude of eigenvalues from one dimension to the next.

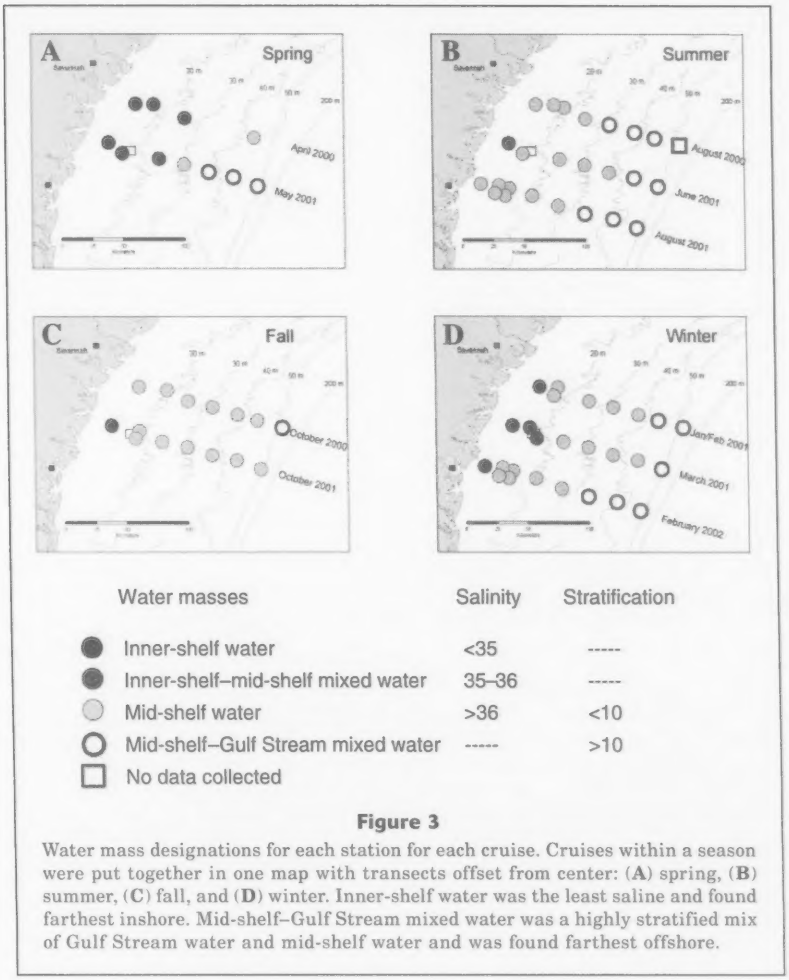

Figure 3

Water mass designations for each station for each cruise. Cruises within a season were put together in one map with transects offset from center: (**A**) spring, (**B**) summer, (**C**) fall, and (**D**) winter. Inner-shelf water was the least saline and found farthest inshore. Mid-shelf–Gulf Stream mixed water was a highly stratified mix of Gulf Stream water and mid-shelf water and was found farthest offshore.

Canonical correspondence analysis (CCA), which incorporates environmental variables by aligning species and station data along environmental gradients, was used to explore the relationship between larval assemblages and the environment. The species-environment correlation is a measure of the strength of the relation between the species data and the environmental data for each CCA dimension (ter Braak and Smilauer, 2002). The product of the species-environment correlation and the eigenvalue can be used to describe the variance in the data. CA and CCA were performed by using the statistical package CANOCO (Ter Braak, 1988).

Multivariate analyses were used to determine which fish species spawn on the continental shelf off the coast of Georgia, to examine what environmental factors influence larval distribution, and to explore the physical factors affecting the transport of larvae spawned on the shelf. Specifically, six objectives were addressed: 1) cross-shelf patterns in the larval fish community; 2) larval assemblages associated with cross-shelf patterns in the larval fish community; 3) the relation among cross-shelf patterns in the larval fish community, larval assemblages, and environmental variables; 4) the relation between water mass and larval assemblages; 5) seasonal patterns in the larval fish community and larval assemblages; and 6) the relation between seasonal larval assemblages and environmental variables.

In addition to addressing the six specific objectives, the implications for larval transport were considered. By comparing the distributions of specific taxa to the patterns discerned by addressing the objectives above, some insights were gained into larval transport processes. The distribution of taxa representative of each larval assemblage was examined for patterns through space and time. Mechanisms driving larval transport were then explored by linking these patterns to water mass and other environmental variables.

Results

Two dimensions were sufficient to explain the majority of the variance in the larval concentration data (Table 4). The winter data eigenvalues indicated the relevance of a third dimension; yet, inspection of three dimensions did not define any patterns not indicated by the first two dimensions. Thus, two dimensions were analyzed for each season in both the CA and CCA analyses.

Cross-shelf patterns in the larval fish community

A cross-shelf pattern in the larval community was observed. In spring, summer, and fall, the inshore stations (stations 1–3) were in close proximity, forming an inner-shelf station group in the ordination resulting from the CA (Fig. 4). Along the same dimension (axis) as the inner-shelf group was a mid-shelf station group of stations 3–6 (stations 2.1–2.4 were also included in this group in spring, summer, and winter). An outer-shelf group composed of offshore stations (stations 5–7) was distributed along a nearly perpendicular dimension, and the mid-shelf group was at the intersection of the two dimensions (Fig. 4). Analysis of the one-percent species data set revealed an identical pattern for each season (not shown).

The winter station ordination resulted in a less distinct cross-shelf pattern (Fig. 4D). In January 2001, stations 1, 2, 3, and 6 were in the inner-shelf group; whereas, stations 4 and 7 from the same cruise were in the mid-shelf group, and station 5 was in the outer-shelf group. Some of this blurring of the cross-shelf pattern in the ordination may be explained by a lower total catch, giving the taxa found across the shelf (*Brevoortia tyrannus* and *Leiostomus xanthurus*) more influence over the data. In addition, most of the variance was explained by the first dimension (Table 4), meaning that the separation of the outer-shelf group (stations 5 and 6) from the mid- and inner-shelf groups is based on a weak relationship among the stations.

Larval assemblages associated with cross-shelf patterns in the larval fish community

Three larval assemblages were defined that corresponded to the three station groups (Fig. 5). The inner-shelf assemblage was composed of species that spawn in coastal and estuarine habitats. Larvae in this assemblage were distributed within the 20-m isobath and confined largely to stations classified as inner-shelf (Fig. 6). The inner-shelf assemblage was primarily represented by *Menticirrhus americanus* during spring, summer, and fall, and by *Micropogonius undulatus* and *Lagodon rhomboides* during winter (Table 5). Taxa included in the mid-shelf assemblage were generally found between the 20- and 40-m isobaths. Some mid-shelf taxa, however, were found across the shelf (stations 1–7) and a large percentage of the larvae occurring in each region were mid-shelf taxa (Fig. 6). The outer-shelf assemblage comprised offshore or deepwater spawned taxa and was

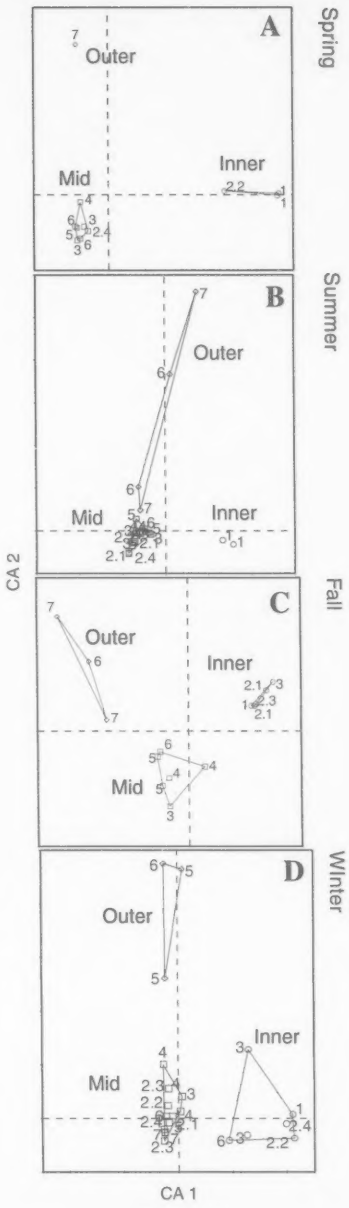

Figure 4

Correspondence analysis ordinations (portraying the first and second dimension scores) of the larval fish community data showing station groups in each season (**A**) spring, (**B**) summer, (**C**) fall, and (**D**) winter. Three cross-shelf station groups were identified within each season. Solid lines enclose the boundary of each station group with three or more stations. Station groups comprising one or two stations are not enclosed by a solid line. Each station group is labeled and portrayed with a different symbol. The dashed lines intersect at the origin of the plot. Analyses were conducted with larval concentration data only. Data from each cruise within a season are shown together.

Table 4

Eigenvalues and species-environment correlations (r^2) for each axis analyzed (correspondence analysis [CA] and canonical correspondence analysis [CAA]) by season and the entire year. A sharp drop in the eigenvalue marks the axes that explain most of the data. Species and environment correlations represent the strength of the relation between the species data and the environmental data for each axis within each season. Values of zero denote no relation; values of one denote a perfect relation. The product of the species-environment correlation and the eigenvalue explains the variance in the data for CCA. Eigenvalues alone explain the variance in the data for CA.

	CA axis				CCA axis			
Season	1	2	3	4	1	2	3	4
Spring								
Eigenvalue	0.932	0.674	0.348	0.107	0.89	0.631	0.329	0.068
r^2					0.98	0.969	0.969	0.796
Summer								
Eigenvalue	0.792	0.621	0.537	0.292	0.703	0.564	0.409	0.159
r^2					0.959	0.959	0.889	0.799
Fall								
Eigenvalue	0.738	0.544	0.273	0.106	0.707	0.443	0.228	0.053
r^2					0.983	0.909	0.935	0.946
Winter								
Eigenvalue	0.526	0.287	0.197	0.165	0.42	0.104	0.059	0.041
r^2					0.894	0.665	0.645	0.496
Year								
Eigenvalue	0.937	0.788	0.607	0.54	0.773	0.61	0.319	0.276
r^2					0.923	0.899	0.8	0.735

Table 5

Three cross-shelf larval assemblages (inner-shelf, mid-shelf, and outer-shelf) were persistent in the Georgia Bight with seasonal changes in membership. Shown are the assemblages from the ten-percent data set. *"Bothus ocellatus/robinsi"* means *B. ocellatus* and *B. robinsi* or one of either of them.

Season	Inner	Mid	Outer
Spring	*Menticirrhus americanus*	*Diplogrammus pauciradiatus*	*Auxis rochei*
		Otophidium omostigmum	*Opisthonema oglinum*
		Bothus ocellatus/robinsi	
		Xyrichthys spp.	
		Micropogonias undulatus	
		Etropus crossotus	
		Anchoa hepsetus	
Summer	*M. americanus*	*D. pauciradiatus*	*A. rochei*
	O. oglinum	*O. omostigmum*	*B. ocellatus/robinsi*
		Ophidion marginatum	
		Xyrichthys spp.	
		E. crossotus	
		M. undulatus	
		A. hepsetus	
Fall	*M. americanus*	*D. pauciradiatus*	*Xyrichthys* spp.
	A. hepsetus	*M. undulatus*	*B. ocellatus/robinsi*
	O. marginatum	*E. crossotus*	
	Leiostomus xanthurus	*O. omostigmum*	
Winter	*M. undulatus*	*B. tyrannus*	*B. ocellatus/robinsi*
	L. rhomboides	*M. punctatus*	
		C. spilopterus	
		D. pauciradiatus	
		O. omostigmum	
		L. xanthurus	

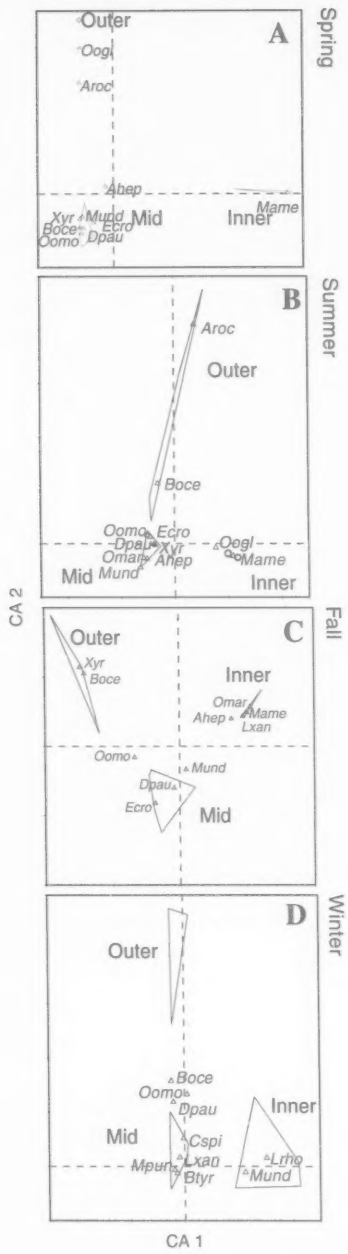

Figure 5

Correspondence analysis (CA) ordinations (portraying the first and second dimension scores) of the larval fish community data showing species in each season: (**A**) spring, (**B**) summer, (**C**) fall, and (**D**) winter. A larval fish assemblage was associated with each cross-shelf station group. Each station group is outlined and labeled as in Figure 4. The dashed lines intersect at the origin of the plot. Analyses were conducted by using larval concentration data only. Refer to table 2 for definitions of larval taxa codes. Three larval fish assemblages were defined based on species association with station groups (see table 5).

found primarily at outer-shelf stations (Fig. 6). *Auxis rochei* and *Bothus ocellatus/robinsi* [where the slash (/) means "*B. ocellatus* and *B. robinsi*" or one of these species] represented the outer-shelf assemblage (Table 5).

The region of the shelf with the highest species richness depended on the inclusion of rare taxa and season. With the exception of fall, species richness was highest in the mid-shelf group when only abundant taxa were included in analyses (Table 5, Fig. 7A). When rare taxa were included (the 1% data set), species richness was highest in the mid-shelf group during spring and summer and highest in the outer-shelf group during fall and winter (Fig. 7B).

Relationship among cross-shelf patterns in the larval fish community, larval assemblages, and environmental variables

Five environmental variables were correlated to the cross-shelf pattern in station groups and larval assemblages. Water density, salinity, temperature, depth, and stratification of the water column had a significant relation to the structure of larval assemblages and the grouping of stations in the CCA ($P<0.05$ for each variable, Monte Carlo permutation test; Table 6). The species-environment correlation for the first two axes of the ordination was greater that 0.79, indicating a strong association between the environment and larval assemblages (Table 6). Although the portrayal of station groups and larval assemblages in ordination space was not identical when environmental data were included (compare Figs. 4 and 5 to 8), the cross-shelf pattern in station groups and larval assemblages was maintained (Fig. 8).

The first CCA dimension, in all seasons, was most highly influenced by the depth, temperature, salinity, and density of the water (Fig. 8). In spring, summer, and winter, the mid- and outer-shelf stations were aligned along CCA 1 and separated from the inner-shelf stations along this gradient (Fig. 8). Similarly, in fall, the three station groups were arranged separately along this gradient with the mid-shelf groups intermediate to the inner- and outer-shelf stations. Thus, the separation between inner-shelf and mid- and outer-shelf stations is related to a gradient in depth, temperature, salinity, and density.

The second dimension separated outer-shelf stations from inner- and mid-shelf station groups. In spring and summer, the second dimension (CCA 2) was clearly influenced by stratification (Fig. 8). The outer-shelf stations experienced a higher degree of stratification, separating them from the inner- and mid-shelf stations. During fall and winter, stratification still impacted the second dimension, but less dramatically. In summary, outer-shelf stations were distinguished from mid- and inner-shelf stations by increased stratification of the water.

Relation between larval assemblages and water mass distributions

When hydrographic variables were combined to define water mass, a possible explanation for the cross-shelf

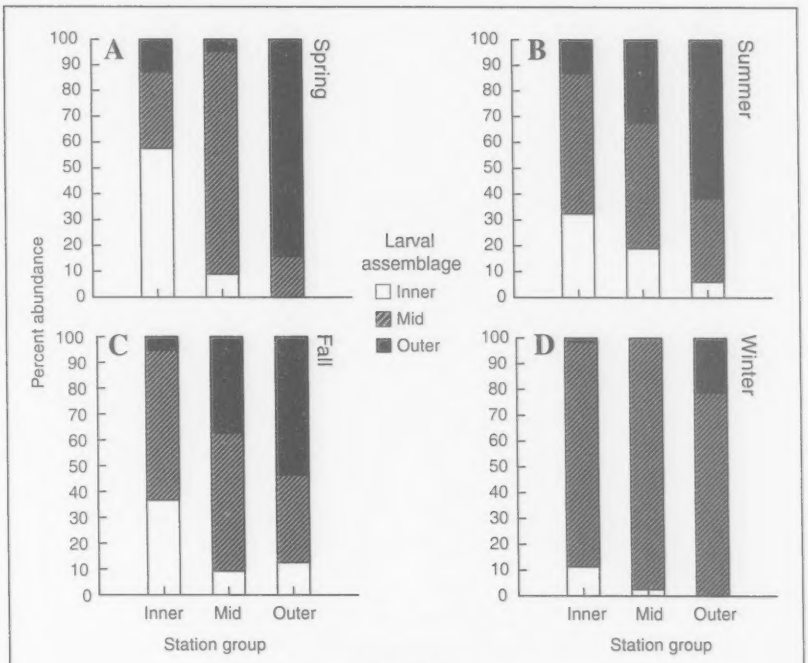

Figure 6

Percent abundance of taxa in larval assemblages associated with each station group (inner-, mid-, and outer-shelf) in (**A**) spring, (**B**) summer, (**C**) fall, and (**D**) winter.

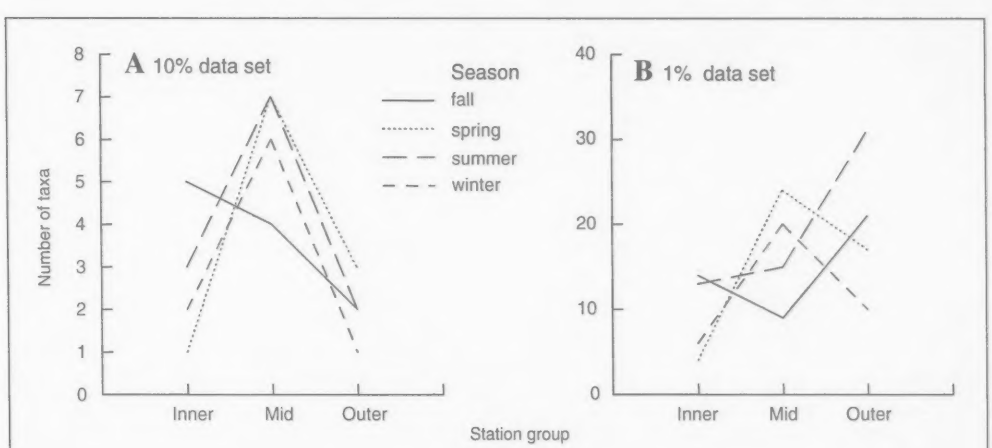

Figure 7

The number of taxa collected in each station group during each season for the (**A**) ten-percent and (**B**) one-percent data sets.

pattern in the larval community was revealed. Physical data delineated four water masses (Fig. 3). Larval fish assemblages differentiated only three of these water masses. Stations associated with inner-shelf water (the inshoremost water mass) and mid-shelf–Gulf Stream mixed water (the offshoremost water mass) formed distinct groups in the ordination of larval community data (Fig. 9). Stations associated with mid-shelf water also

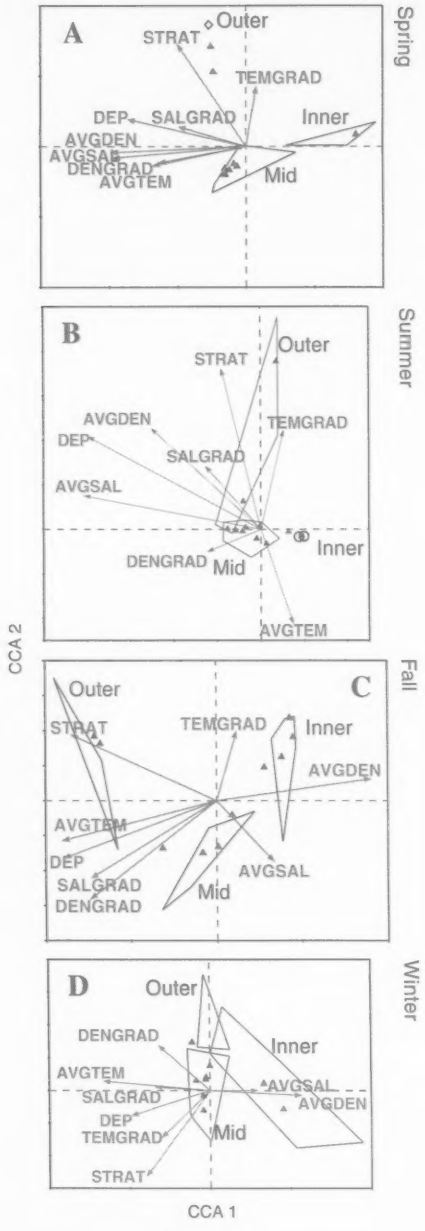

Figure 8

Canonical correspondence analysis (CCA) ordinations (portraying the first and second dimension scores) of the larval fish community data showing the correlations between environmental variables, species, and station groups: (**A**) spring, (**B**) summer, (**C**) fall, and (**D**) winter. The solid triangles mark the location of taxa (as in Fig. 5), and the polygons surround the three cross-shelf station groups (as in Fig. 4). The arrows depict the gradient of each environmental variable. The dashed lines intersect at the origin of the plot. Analyses were conducted with both larval and environmental data. Refer to Table 3 for definitions of environmental variable codes.

Table 6

The *P* values from a Monte Carlo permutation test on the environmental variables for each season. Significant values ($P<0.05$) are shown in bold font. See Table 3 for definitions of variable codes.

	Season			
Variable code	Spring	Summer	Fall	Winter
AVGDEN	**0.002**	**0.01**	0.34	0.494
AVGSAL	**0.002**	**0.022**	**0.016**	**0.004**
AVGTEM	0.152	0.1	**0.04**	**0.016**
DENGRAD	0.836	0.076	0.466	0.958
SALGRAD	0.456	0.086	0.78	0.634
TEMGRAD	0.074	0.076	0.38	0.574
DEP	0.468	**0.002**	**0.002**	0.68
STRAT	**0.036**	**0.014**	**0.012**	0.504

formed distinct groups. The fourth water mass, inner-shelf–mid-shelf mixed water overlapped with either inner-shelf or mid-shelf water depending on season. In summary, the cross-shelf distribution and assemblages of water masses coincided with the three cross-shelf regions described: inner-shelf, mid-shelf, and outer-shelf characterized by inner-shelf water, mid-shelf water, and mid-shelf–Gulf Stream mixed water, respectively.

Seasonal patterns in the cross-shelf distributions of the larval fish community

The ten percent data set revealed two distinct seasonal station groups (Fig. 10). The winter stations occurred in close proximity and were separate from stations sampled during the rest of the seasons (Fig. 10A). However, inner-shelf stations sampled during fall overlapped with the winter stations because of the presence of winter and fall spawning species (*L. xanthurus* and *M. undulatus*). There was also overlap of the winter and the warm weather outer-shelf stations (Fig. 10, A and B).

Similarly, the ten percent data set revealed two seasonal assemblages in the larval community data (Fig. 10, C and D). The warm weather assemblage comprised taxa associated with the warm weather station group and were collected during spring, summer, and fall. The winter assemblage was associated with the winter station group and comprised taxa collected during winter. Taxa from the warm weather inner- and mid-shelf assemblages were different from those representing the winter inner- and mid-shelf assemblages (Table 5). The outer-shelf assemblage, however, was less seasonally distinct, represented by *Bothus ocellatus/robinsi* in summer, fall, and winter and by *Auxis rochei* in spring, summer, and fall (Table 5).

Relation between seasonal larval assemblages and environmental variables

The seasonal pattern in the larval concentration data described above was maintained when constrained by environmental variables in the CCA. The community data clearly showed a seasonal influence on the first dimension in ordination space; winter taxa were separate from taxa collected during the rest of the seasons. This seasonal pattern was also reflected in the environmental data (Fig. 11). Salinity, density, temperature, depth, and stratification of the water column were again the most significant environmental variables for explaining variance in the species data ($P<0.05$, Monte Carlo permutation test, Table 6). The warm weather stations and taxa coincided with higher water temperature, lower density, and a lower density gradient. In addition, the cross-shelf pattern evident in the second and third dimensions of the full larval concentration data (Fig. 10, A and B) appeared to correlate with depth of the water column, the degree of stratification in the water column, and salinity (Fig. 11).

Implications for larval transport

The structure of larval assemblages was linked to water mass distributions and the cross-shelf zonation of physical circulation processes. Three cross-shelf zones of physical dynamics have been defined previously (Atkinson and Menzel, 1985; Pietrafesa et al., 1985a, 1985b; Lee et al., 1991; Boicourt et al., 1998). Three analogous cross-shelf zones were delineated in the larval community data. The cross-shelf larval assemblages were linked to three water masses with cross-shelf structure, and to the physical-chemical characteristics of the region (temperature, salinity, density, and stratification of the water column). The three cross-shelf zones identified previously in terms of physical dynamics coincided with the station groups and larval assemblages identified in our study. Thus, larval distribution and physical properties of the ocean are linked and indicate a strong influence of physical properties and processes on the distribution of larval fish on the southeast United States continental shelf.

Retention on the inner-shelf was a clear larval transport pattern identified in the analyses. *Menticirrhus americanus* represents the inner-shelf group (Table 5) and were always found inshore of the 20-m isobath in inner-shelf water, in inner-shelf–mid-shelf mixed water, or in mid-shelf water, (Fig. 12). Spawning likely occurs on the inner-shelf (Cowan and Shaw, 1988), and larvae are retained in the inner-shelf region.

The analyses also demonstrated that transport from offshore onto the shelf is limited on the continental shelf off the coast of Georgia. *Ceratoscopelus maderensis* and *Auxis rochei* were found only at offshore stations (Fig. 13), representing the outer-shelf group (Table 5) and the mid-shelf–Gulf Stream mixed water mass. The presence of *C. maderensis* identified transport of a mesopelagic fish to waters inshore of the shelf break; how-

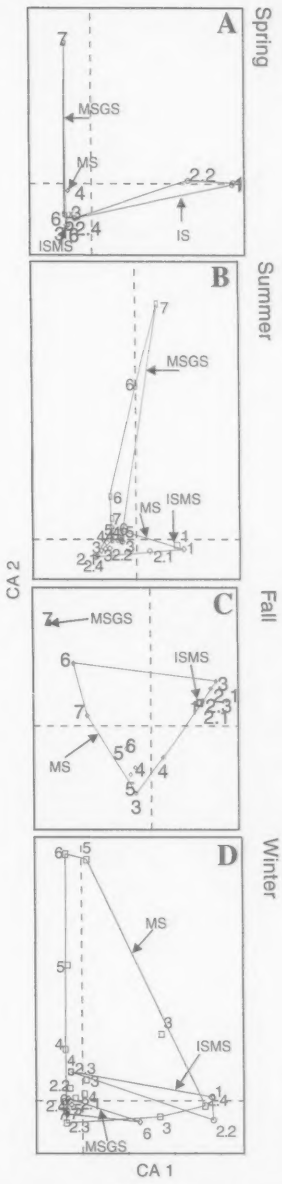

Figure 9

Correspondence analysis (CA) ordinations (portraying the first and second dimension scores) of the larval fish community data showing the full ten-percent data set: (**A**) spring, (**B**) summer, (**C**) fall, and (**D**) winter. The points represent stations classified by water mass. Solid lines enclose the boundary of each station group with three or more stations. Station groups comprising one or two stations are not enclosed by a solid line. Each station group is labeled and portrayed with a different symbol. Stations with inner-shelf water are labeled with IS (inner-shelf), inner-shelf–mid-shelf mixed water with ISMS, mid-shelf water with MS, and mid-shelf–Gulf Stream mixed water with MSGS. The dashed lines intersect at the origin of the plot. Analyses were conducted using larval data only.

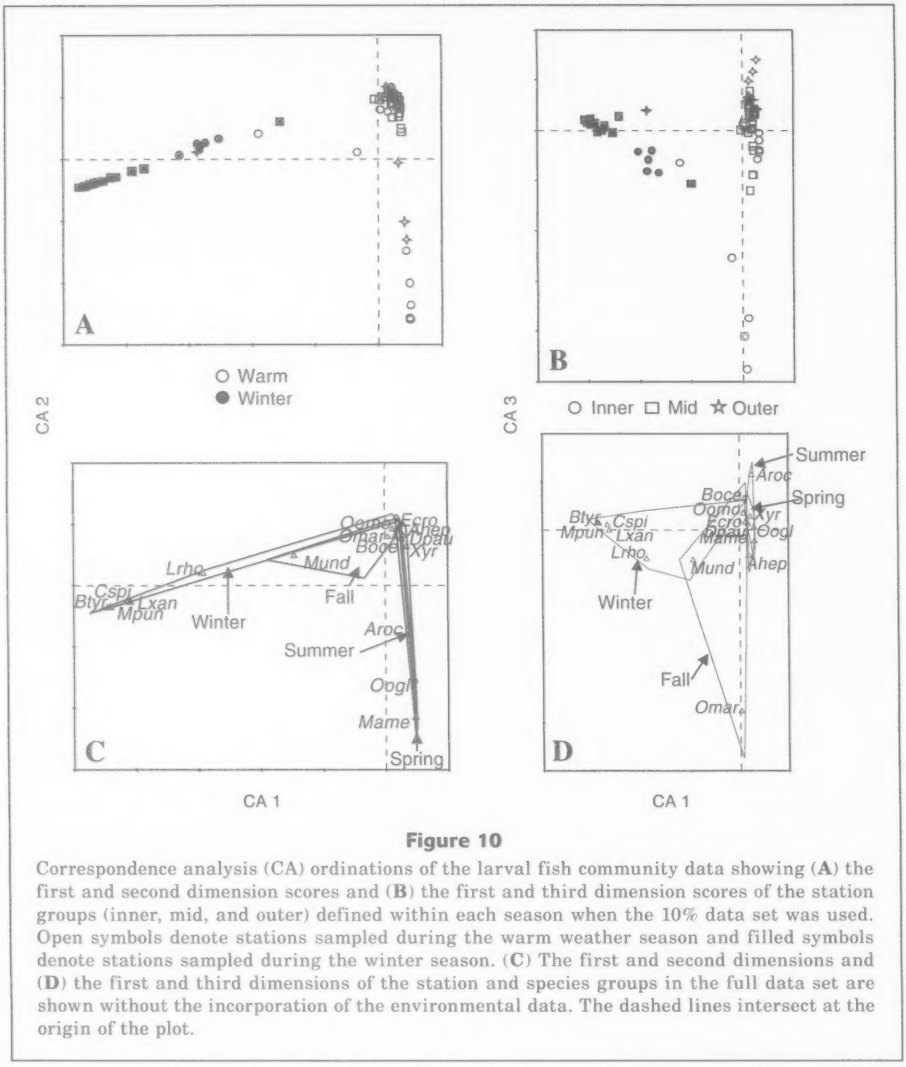

Figure 10

Correspondence analysis (CA) ordinations of the larval fish community data showing (**A**) the first and second dimension scores and (**B**) the first and third dimension scores of the station groups (inner, mid, and outer) defined within each season when the 10% data set was used. Open symbols denote stations sampled during the warm weather season and filled symbols denote stations sampled during the winter season. (**C**) The first and second dimensions and (**D**) the first and third dimensions of the station and species groups in the full data set are shown without the incorporation of the environmental data. The dashed lines intersect at the origin of the plot.

ever, the rarity of this species on the continental shelf off the coast of Georgia provides evidence for relatively limited onshore transport from off the shelf. Powell and Robins (1994, 1998) and Govoni and Spach (1999) also collected tropical and deepwater taxa inshore of the shelf break. The presence of these taxa was likely due to frequent but variable exchange of larvae across the Gulf Stream front (Govoni and Spach, 1999). Less is known about spawning of *A. rochei* but the species' larval distribution represents restriction to offshore waters (always collected offshore of the 40-m isobath).

During winter, when *B. tyrannus* was found across the shelf (Fig. 14), *Bothus ocellatus/robinsi* was collected only on the outer part of the shelf (Fig. 14). Both *B. tyrannus* and *B. ocellatus/robinsi* likely spawn on the outer shelf. However, unlike *B. tyrannus, Bothus ocellatus/robinsi* was never collected inshore of station 3 (the boundary between the inner- and mid-shelf zones), indicating that the two taxa may experience different transport pathways or different seasonal spawning patterns (see "Discussion" section).

Discussion

Three cross-shelf regions were defined on the continental shelf off the coast of Georgia based on the distribution and abundance of larval fish: inner-shelf, mid-shelf, and outer-shelf. Each region was dominated by a distinct group of species (i.e., larval assemblage). The inner-shelf

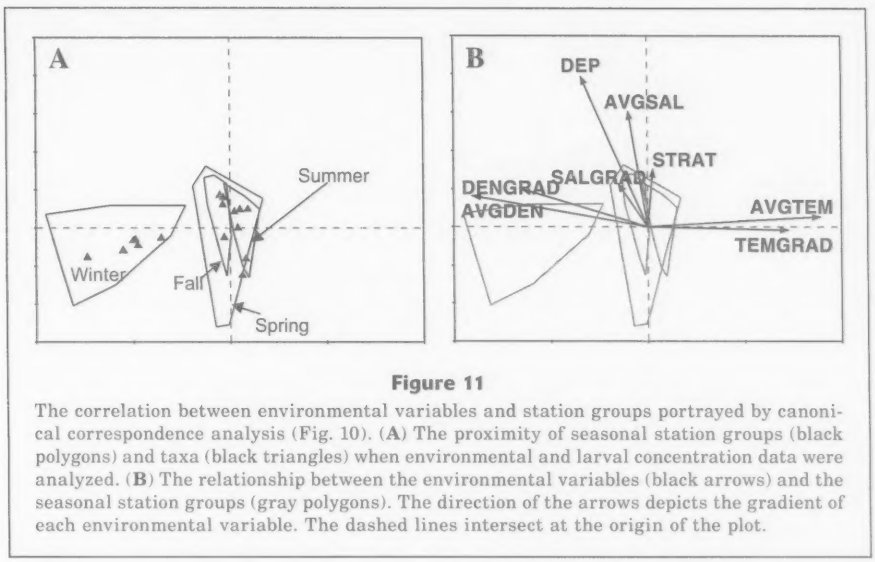

Figure 11

The correlation between environmental variables and station groups portrayed by canonical correspondence analysis (Fig. 10). (**A**) The proximity of seasonal station groups (black polygons) and taxa (black triangles) when environmental and larval concentration data were analyzed. (**B**) The relationship between the environmental variables (black arrows) and the seasonal station groups (gray polygons). The direction of the arrows depicts the gradient of each environmental variable. The dashed lines intersect at the origin of the plot.

region was defined inshore of the 20-m isobath (Figs. 4, 5, 12). The inner-shelf larval assemblage was the least diverse taxonomically (Table 2, Fig. 7B), and most taxa in the assemblage were nearshore or estuarine spawning species (e.g., *Cynoscion regalis*, *Menticirrhus americanus*, Table 2). Gradients in salinity and density were associated with the separation of the inner-shelf region but the direction of the gradient varied among seasons; in the spring and summer the inner-shelf region was characterized by lower salinity and density, whereas in the fall and winter, the inner-shelf region was characterized by higher salinities and densities (Fig. 8). The restricted inshore distribution of the assemblage indicated mechanisms of larval retention in the inner-shelf zone.

The mid-shelf region was defined between the 20- and 40-m isobaths (Figs. 4, 5, 12). The mid-shelf larval assemblage was distributed over the widest area (Figs. 4, 5, 12) and species in the assemblage were found in all three regions defined (Fig. 6). The mid-shelf region and larval assemblage were related to the average environmental parameters encountered on the shelf (Fig. 8), which varied seasonally. The broad distribution of the assemblage indicated either broad spawning distributions of member species or mechanism of larval transport to both the inner- and outer-shelf regions.

The outer-shelf region was defined as the area offshore from the 40-m isobath (Figs. 4, 5, 12). The outer-shelf region was related to increased stratification of the water column, which was likely a result of Gulf Stream waters mixing onshore. These periodic intrusions would help explain the higher species richness of rare taxa found on the outer-shelf during fall and winter (Fig. 7B). Taxa in the outer-shelf assemblage were either spawned on the outer-shelf (e.g., *Hemanthias vivanus*), spawned offshore of the shelf break and transported onto the shelf (e.g., *Ceratoscopelus maderensis*), or spawned south of the study area and transported onto the shelf (e.g., *Abudefduf* sp.). Most outer-shelf taxa, however, were restricted to outer-shelf stations indicating limited onshore exchange between the outer- and mid-shelf regions.

Larval assemblages on the continental shelf off the coast of Georgia are derived from a combination of spawning distributions and larval transport; *Brevoortia tyrannus* and *Bothus ocellatus/robinsi* provide an example. *Brevoortia tyrannus* spawn in water temperatures between 16° and 23°C during winter (Checkley et al. 1999); these temperatures were experienced in the mid- and outer-shelf regions during winter. *Bothus ocellatus/robinsi* adults also occur on the mid- and outer-shelf of the continental shelf off the coast of Georgia (Gutherz, 1967). Thus, during winter the spawning distribution of these two species are likely similar. The larval distributions, however, are different: *B. tyrannus* larvae were collected in all three regions of the shelf during winter, whereas *B. ocellatus/robinsi* were collected on the mid- and outer-shelf (Fig. 14). The vertical distributions of the two species also are different. *B. tyrannus* larvae occur higher in the water column than do *B. ocellatus/robsini* (Hare and Govoni[1]). The observed differences in horizontal distribution could result from the differences in vertical distributions. Alternatively, the distributional differences could result from physiological differences that allow *B. tyrannus* larvae to survive cooler inshore waters or could result from seasonal cross-shelf spawning patterns that result

[1] Hare, J. A., and J. J. Govoni. 2004. In review. Vertical distribution and the outcome of larval fish transport along the southeast US continental shelf during winter.

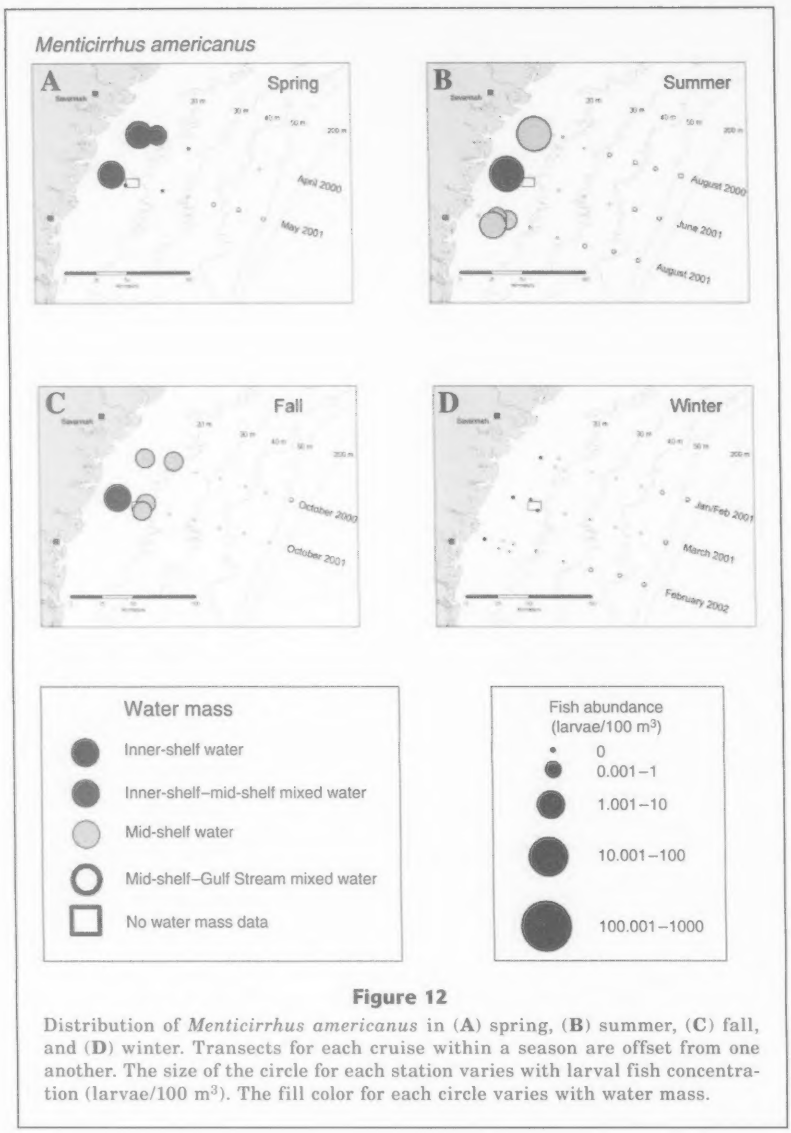

Figure 12

Distribution of *Menticirrhus americanus* in (**A**) spring, (**B**) summer, (**C**) fall, and (**D**) winter. Transects for each cruise within a season are offset from one another. The size of the circle for each station varies with larval fish concentration (larvae/100 m^3). The fill color for each circle varies with water mass.

in *B. tyrannus* spawning inshore during the fall. This example demonstrates that there are multiple mechanisms or pathways that affect the transport of larval fish, and that each species may be subject to different transport regimes. Therefore, to understand larval transport, many factors, including physical forcing mechanisms, the horizontal and vertical distributions of larvae, seasonal patterns, and the physiology of a species, need to be considered.

Temporal larval assemblages were defined in addition to the spatial assemblages. Larvae clearly separated into two seasonal spawning groups: winter and warm seasons (Fig. 10). The winter assemblage was associated with cool, denser water, whereas the warm water assemblage was associated with warmer, less dense water (Fig. 11). The cross-shelf structure in larval assemblages was still evident in the two seasonal assemblages, but there was overlap in the winter and warm-weather outer-shelf assemblages (Fig. 10). This overlap occurred in waters with the least seasonal variability in temperature and salinity and likely results from year-round spawning by species in the outer-shelf assemblage or year-round supply of larvae to the outer-shelf region by the Gulf Stream.

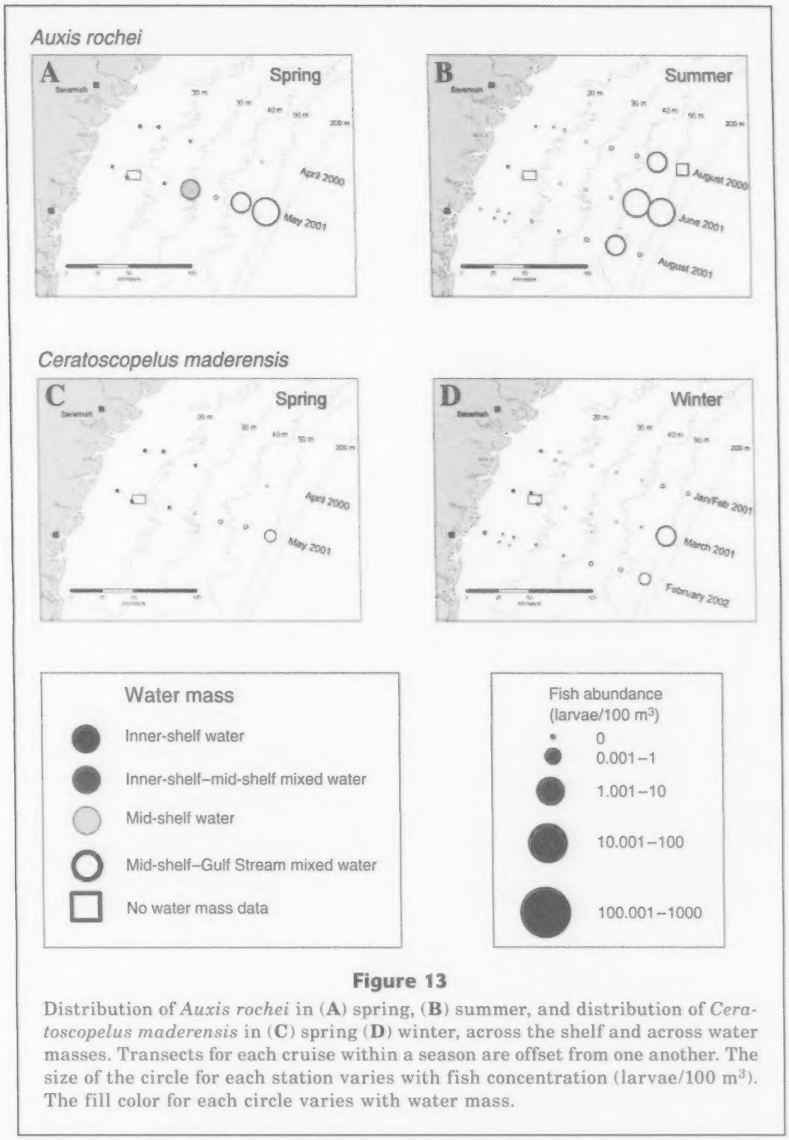

Figure 13

Distribution of *Auxis rochei* in (**A**) spring, (**B**) summer, and distribution of *Ceratoscopelus maderensis* in (**C**) spring (**D**) winter, across the shelf and across water masses. Transects for each cruise within a season are offset from one another. The size of the circle for each station varies with fish concentration (larvae/100 m^3). The fill color for each circle varies with water mass.

Winter-spawning species that use estuaries are frequently grouped together as "estuarine-dependent" taxa (*sensu* Warlen and Burke, 1990). However, Hare and Govoni[1] found that vertical distributions of these winter taxa are different. In addition, our study demonstrated that the horizontal distributions of these species are distinct: *Lagadon rhomboides* and *Micropogonias undulatus* were members of the inner-shelf assemblage and *Leiostomus xanthurus*, *Myrophis punctatus*, and *Brevoortia tyrannus* were members of the mid-shelf assemblage. These findings imply that often grouped "estuarine-dependent" species have different spawning locations or experience different larval transport processes (or both) and may not reflect a single group.

The definition of three regions based on larval fish distributions is consistent with the division of the shelf into three cross-shelf zones based on physical dynamics. The inner-shelf (0–20 m) is dominated by freshwater discharge, tides, and winds; the mid-shelf (20–40 m) is influenced by wind and tides; and the outer-shelf (40–75 m) is affected by the Gulf Stream and wind (Atkinson and Menzel, 1985; Pietrafesa et al., 1985a, 1985b; Lee et al., 1991; Boicourt et al., 1998). Thus, the physical dynamics of the shelf appear to be closely linked to spa-

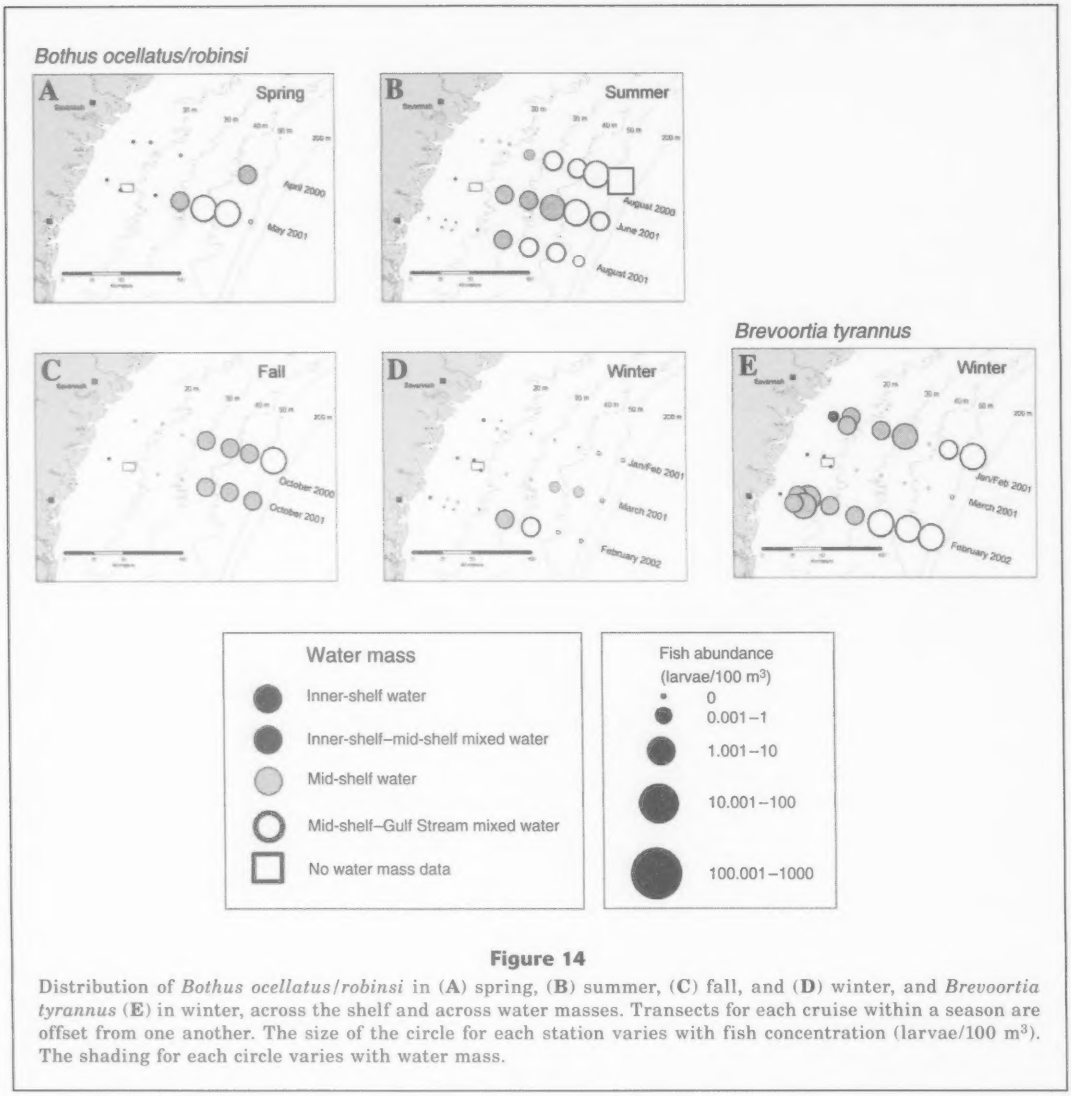

Figure 14

Distribution of *Bothus ocellatus/robinsi* in (**A**) spring, (**B**) summer, (**C**) fall, and (**D**) winter, and *Brevoortia tyrannus* (**E**) in winter, across the shelf and across water masses. Transects for each cruise within a season are offset from one another. The size of the circle for each station varies with fish concentration (larvae/100 m^3). The shading for each circle varies with water mass.

tial patterns in the distribution of larval fish. Further physiochemical characteristics of the environment (e.g., temperature, salinity, water masses) are highly associated with the structure of larval assemblages (Tables 4, 6, Fig. 9), again indicating a strong link between physical dynamics and larval distribution. However, patterns in spawning and behaviorally modified vertical distributions also have an influence on larval distributions and thus a simple two-dimensional passive model will not adequately explain the distribution of larval fish on the continental shelf off the coast of Georgia.

The three regions defined in our study have important implications for the consideration of MPAs on the southeast United States shelf. The described cross-shelf zones (inner-, mid-, or outer-shelf) provide information needed to protect spawning habitat of specific species (e.g., *Rhomboplites aurorubens* spawns on the outer-shelf; Table 2). Conversely, the species included in an area under consideration for protection can also be derived (e.g., Gray's Reef National Marine Sanctuary potentially protects species spawning at the interface between the inner- and mid-shelf, Table 2). Further, spawning location information can be derived for several species protected under the South Atlantic Fisheries Management Council's coastal migratory pelagics management plan (e.g., *Rachycentron canadum*, *Scomberomorus cavalla*, *Scomberomorus maculatus*, or *Coryphaena hippurus*, Table 2), but individuals of

these species range so widely (Sutter et al., 1991), only very large MPAs would afford protection from fishing (Parrish 1999, Beck and Odaya 2001). Unfortunately, many species in the snapper-grouper complex, a more sedentary group of species of particular importance in the southeast United States, were not collected. Either these taxa do not spawn on the continental shelf off the coast of Georgia and their larvae are rarely transported into the area, or snapper-grouper spawning on the continental shelf off the coast of Georgia is at a very low level and larvae are quite rare.

Another aspect of MPAs designed for fisheries management is production of individuals in the MPA and their supply to surrounding areas; larval transport is a major mechanism of supply. On the continental shelf off the coast of Georgia, larval assemblages suggest that the supply of larvae from the south (by the Gulf Stream) and even between cross-shelf zones is limited. Members of the outer-shelf assemblage rarely occurred on the mid- and inner-shelf, and members of the inner-shelf assemblage rarely occurred on the mid- and outer-shelf. Thus, larvae spawned on the inner-shelf and to a lesser degree on the mid-shelf likely remain on the continental shelf off the coast of Georgia and appear to be subject to local retention. MPAs in the region, therefore, could provide a local benefit by supplying recruits to nonprotected areas on the continental shelf off the coast of Georgia.

Acknowledgments

We would like to thank all who helped with sample collections, sorting, and analyses: G. Bohne, R. Bohne, C. Bonn, J. Burke, M. Burton, B. Degan, M. Duncan, J. Govoni, M. Greene, E. Jugovich, S. Lem, J. Loefer, R. Mays, R. McNatt, A. Powell, R. Rogers, S. Shoffler, S. Varnam, H. Walsh, and T. Zimanski. We appreciate the hard work and dedication of the officers and crew of the NOAA Ship *Ferrel*, NOAA Ship *Jane Yarn*, NOAA Ship *Oregon II*, and RV *Cape Fear*. Frank Hernandez provided invaluable help with the CTD processing and stratification calculations. We would also like to thank J. Johnson, S. Norton, A. Powell, F. Hernandez, E. Williams, P. Marraro, W. Richards, and an anonymous reviewer for their comments on previous drafts. Most of all, we thank Gray's Reef National Marine Sanctuary and the National Marine Sanctuary Office for funding the project.

Literature cited

Atkinson, L. P., and D. W. Menzel.
1995. Introduction: Oceanography of the southeast United States continental shelf. *In* Oceanography of the southeastern U.S. continental shelf (L. P. Atkinson, D. W. Menzel, and K. A. Bush, eds.), p 1–9. Am Geophysical Union, Washington, D. C.

Beck, M. W., and M. Odaya.
2001. Ecoregional planning in marine environments: identifying priority sites for conservation in the northern Gulf of Mexico. Aquat. Conserv.: 11:235–242

Blanton, J. O., F. B. Schwing, A. H. Weber, L. J. Pietrafesa, and D. W. Hayes.
1985. Wind stress climatology in the south Atlantic Bight. *In* Oceanography of the Southeastern U.S. continental shelf (L. P. Atkinson, D. W. Menzel, and K. A. Bush, eds.). p. 10–22. American Geophysical Union, Washington, D.C.

Boicourt, W. C., W. J. Wiseman Jr., A. Valle-Levinson, and L. P. Atkinson.
1998. Chapter 6. Continental shelf of the southeastern United States and the Gulf of Mexico: in the shadow of the western boundary current. *In* The sea, vol. 11 (A. R. Robinson and K. H. Brink, eds.), p. 135–182. John Wiley and Sons, Inc., New York, NY.

Checkley, Jr., D. M., P. B. Ortner, F. E. Werner, L. R. Settle, and S. R. Cumming.
1999. Spawning habitat of the Atlantic menhaden in Onslow Bay, North Carolina. Fish. Oceanogr. 8:22–36.

Churchill, J. H., E. R. Levine, D. N. Connors, and P. C. Cornillon.
1993. Mixing of shelf, slope and Gulf Stream water over the continental slope of the Middle Atlantic Bight. Deep-Sea Res. 40:1063–1085.

Clarke, K. R., and R. M. Warwick.
2001. Change in marine communities: an approach to statistical analysis and interpretation. PRIMER-E, 2nd ed., 144 p. Plymouth Marine Laboratory, Plymouth, Cornwall, UK.

Collins, M. R., and B. W. Stender.
1987. Larval king mackerel (*Scomberomorus cavalla*), Spanish mackerel (*S. maculates*), and bluefish (*Pomatomus saltatrix*) off the southeast coast of the United States, 1973–1980. Bull. Mar. Sci. 41:822–834.
1987. Larval striped mullet (*Mugil cephalus*) and white mullet (*Mugil curema*) off the southeastern United States. Bull. Mar. Sci. 45:580–589.

Cowan, J. H., and R. F. Shaw.
1988. The distribution, abundance, and transport of larval sciaenids collected during winter and early spring from the continental shelf waters off west Louisiana. Fish. Bull. 86:129–142.

Cowen, R. K. , J. A. Hare, and M. P. Fahay.
1993. Beyond hydrography: can physical processes explain larval fish assemblages within the Middle Atlantic Bight? Bull. Mar. Sci. 53:567–587.

Crowder, L. B., S. J. Lyman, W. F. Figueira, and J. Priddy.
2000. Source-sink population dynamics and the problem of siting marine reserves. Bull. Mar. Sci. 66:799–820.

Fahay, M. P.
1975. An annotated list of larval and juvenile fishes captured with surface-towed meter net in the South Atlantic Bight during four RV *Dolphin* cruises between May 1967 and February 1968. NOAA/NMFS Technical Report SSRF 685, 39 p
1983. Guide to the early stages of marine fishes occurring in the western North Atlantic Ocean, Cape Hatteras to the southern Scotian Shelf. Northwest Atl. Fish. Sci. 4:1–423.

Federal Register.
2000. Presidential documents. Executive Order 13158 of

May 26, 2000. Volume 65, number 105, May 31 2000. U.S. Government Printing Office, Washington, D.C.

Govoni, J. J., and H. L. Spach.
1999. Exchange and flux of larval fishes across the western Gulf Stream front south of Cape Hatteras, USA, in winter. Fish. Oceanogr. 8(suppl. 2):77–92.

Gutherz, E. J.
1967. Field guide to the flatfishes of the family Bothidae in the Western North Atlantic, 47 p. United States Department of the Interior, Washington, D.C.

Hare, J. A., J. A. Quinlan, F. E. Werner, B. O. Blanton, J. J. Govoni, R. B. Forward, L. R. Settle, and D. E. Hoss.
1999. Larval transport during winter in the SABRE study area: results of a coupled vertical larval behavior-three-dimensional circulation model. Fish. Oceanogr. 8:57–76.

Hare, J. A., M. P. Fahay, and R. K. Cowen.
2001. Springtime ichthyoplankton of the Slope Sea: larval assemblages, relation to hydrography and implications for larval transport. Fish. Oceanogr. 10:164–192.

Hoss, D. E., H. L. Spach, L. R. Settle, J. A. Hare, and E. H. Laban.
1997. The growth and behaviour of two species of clupeid larvae and how it affects their oceanic transport. *In* Ichthyoplankton ecology (A. J. Geffen, J. M. Fives, J. E. Thorpe, eds.), 22 p. Fisheries Society of the British Isles, Galway, Ireland.

Johnson, G. D., and P., Keener.
1984. Aid to the identification of American grouper larvae. Bull. Mar. Sci. 34:106–134.

Judy, M. H., and R. M. Lewis.
1983. Distribution of eggs and larvae of Atlantic menhaden, *Brevoortia tyrannus* along the Atlantic coast of the United States. U. S. National Marine Fisheries Service, Special Scientific Report—Fisheries 774, 23 p.

Kendall, A. W., Jr., and A. C. Materese.
1994. Status of early life history descriptions of marine teleosts. Fish. Bull. 92:725–36.

Kendall, A. W., Jr, and L. A. Walford.
1979. Sources and distribution of bluefish, Pomatomus saltatrix, larvae and juveniles off the east coast of the United States. Fish. Bull. 77:213–27.

Lee, T. N., J. A. Yoder, and L. P. Atkinson.
1991. Gulf Stream frontal eddy influence on productivity of the southeast U.S. continental shelf. J. Geophy. Res. 96:22191–2205.

Leis, J. M.
1989. Larval biology of butterflyfishes (Pisces, Chaetodontidae): what do we really know? Environ. Biol. Fishes 25:87–00.

Marancik, K. E.
2003. Larval fish assemblages of the Georgia Bight. M.S. thesis, 149 p. East Carolina Univ., Greenville, NC.

Parrish, R.
1999. Marine reserves for fisheries management: why not. CalCOFI Rep. 40:77–6

Pietrafesa, L. J., J. O. Blanton J. D. Wang, V. Kourafalou, T. L. Lee, and K. A. Bush.
1985a. The tidal regime in the South Atlantic Bight. *In* Oceanography of the southeastern U.S. continental shelf (L. P. Atkinson, D. W. Menzel, K. A. Bush, eds.), p. 63–6. American Geophysical Union, Washington, D.C.

Pietrafesa, L. J., G. S. Janowitx, and P. A. Wittman.
1985b. Physical oceanographic processes in the Carolina Capes. *In* Oceanography of the southeastern U.S. continental shelf (L. P. Atkinson, D. W. Menzel, K. A. Bush, eds.), p. 23–32. American Geophysical Union, Washington, D.C.

Pietrafesa, L. J., J. M. Morrison, M. P. McCann, J. Churchill, E. Bohm, and R. W. Houghton.
1994. Water mass linkages between the Middle and South Atlantic Bights. Deep-Sea Res. II 41:365–89.

Plan Development Team.
1990. The potential of marine fishery reserves for reef fish management in the U.S. southern Atlantic. NOAA Tech. Memo. NMFS-SEFC-261, 40 p.

Powell, A. B., D. G. Lindquist, and J. A. Hare.
2000. Larval and pelagic juvenile fishes collected with three types of gear in Gulf Stream and shelf waters in Onslow Bay, North Carolina, and comments on ichthyoplankton distribution and hydrography. Fish. Bull. 98:427–38.

Powell, A. B., and R. E. Robbins
1994. Abundance and distribution of ichthyoplankton along an inshore-offshore transect in Onslow Bay, North Carolina. NOAA Tech. Report NMFS 120, 28 p.
1998. Ichthyoplankton adjacent to live-bottom habitats in Onslow Bay, North Carolina. NOAA Tech. Report NMFS 133, 32 p.

Powles, H., and B. W. Stender.
1976. Observations on composition, seasonality and distribution of ichthyoplankton from MARMAP cruises in the South Atlantic Bight in 1973. South Carolina Marine Resources Center, Technical Report Series Number 11, Charleston, SC.

Rakocinski, C. F., J. Lyczkowski-Shultz, and S. L. Richardson.
1996. Ichthyoplankton assemblage structure in Mississippi Sound as revealed by canonical correspondence analysis. Estuar. Coast. Shelf Sci. 43:237–57.

Richards, W. J. (ed.).
2001. Preliminary guide to the identification of the early life history stages of fishes of the Western Central Atlantic. (http://www4.cookman.edu/noaa). [Accessed 12 May 2004.]

Simpson, J. H., and I. D. James.
1986. Coastal and estuarine fronts. *In* Baroclinic processes on continental shelves (C. N. K. Mooers, ed.), p. 63–93. American Geophysical Union, Washington, D.C.

Smith, W., P. Berrien, and T. Potthoff.
1994. Spawning patterns of bluefish, Pomatomus saltatrix in the northeast continental shelf ecosystem. Bull. Mar. Sci. 54:8–6.

Smith, K. A., M. T. Gibbs, J. H. Middleton, and I. M. Suthers.
1999. Short term variability in larval fish assemblages of the Sydney shelf: tracers of hydrographic variability. Mar. Ecol. Prog. Ser. 178:1–5.

Stephenson, R. L.
1999. Stock complexity in fisheries management: A perspective of emerging issues related to population sub-units. Fish. Res. 43:247–249

Sutter, F. C., III, R. I. Williams, and M. F. Godcharles.
1991. Movement patterns and stock affinities of king mackerel in the southeast United States. Fish. Bull. 89:315–324

ter Braak, C. F. J.
1988. CANOCO—a FORTRAN program for canonical community ordination by correspondence analysis, principal components analysis and redundancy analysis. Technical Report: LWA-88-02. Groep Landbouw-wiskunde, Wageningen, The Netherlands.

ter Braak, C. F. J., and P. Smilauer.
2002. CANOCO Reference manual and CanoDraw for Windows User's guide: software for canonical community ordination (vers. 4.5), 500 p. Microcomputer Power Ithaca, New York, NY.

Warlen, S. M., and J. S. Burke.
1990. Immigration of larvae of fall/winter spawning marine fishes into a North Carolina estuary. Estuaries 13:453–61.

Warner, R. R., S. E. Swearer, and J. E. Caselle.
2000. Larval accumulation and retention: Implications for the design of marine reserves and essential fish habitat. Bull. Mar. Sci. 66:821–830.

Year-class formation in Pacific herring (*Clupea pallasi*) estimated from spawning-date distributions of juveniles in San Francisco Bay, California

Michael R. O'Farrell

Ralph J. Larson

Department of Biology
San Francisco State University
1600 Holloway Avenue
San Francisco, CA 94132
Present address (for M. R. O'Farrell, contact author): Department of Wildlife,
Fish and Conservation Biology
University of California, Davis
One Shields Avenue
Davis, California 95616

E-mail address (for M. R. O'Farrell): mrofarrell@ucdavis.edu

Abstract—Inter and intra-annual variation in year-class strength was analyzed for San Francisco Bay Pacific herring (*Clupea pallasi*) by using otoliths of juveniles. Juvenile herring were collected from March through June in 1999 and 2000 and otoliths from subsamples of these collections were aged by daily otolith increment analysis. The composition of the year classes in 1999 and 2000 were determined by back-calculating the birth date distribution for surviving juvenile herring. In 2000, 729% more juveniles were captured than in 1999, even though an estimated 12% fewer eggs were spawned in 2000. Spawning-date distributions show that survival for the 2000 year class was exceptionally good for a short (approximately 1 month) period of spawning, resulting in a large abundance of juvenile recruits. Analysis of age at size shows that growth rate increased significantly as the spawning season progressed both in 1999 and 2000. However, only in 2000 were the bulk of surviving juveniles a product of the fast growth period. In the two years examined, year-class strength was not predicted by the estimated number of eggs spawned, but rather appeared to depend on survival of eggs or larvae (or both) through the juvenile stage. Fast growth through the larval stage may have little effect on year-class strength if mortality during the egg stage is high and few larvae are available.

Manuscript submitted 27 February 2003 to the Scientific Editor's Office.

Manuscript approved for publication 2 August 2004 by the Scientific Editor.

Fish. Bull. 103:130–141 (2005).

Both biological and physical sources of mortality have been suggested as important in determining year-class strength in fish populations. Food limitation at first feeding (Hjort, 1914; Cushing, 1975; Lasker, 1975; Cushing, 1996), larval retention (Iles and Sinclair, 1982; Sinclair and Iles, 1985), a juvenile critical period (Bollens et al., 1992; Thorisson, 1994), as well as predation and environmental conditions may ultimately affect recruitment. Egg development time and larval growth rate have the capacity to adjust the relative impacts of these mortality sources on individual propagules by modifying stage duration (Houde, 1989; Yoklavich and Bailey, 1990).

Juvenile fishes can be used to assess both inter- and intra-annual variation in egg and larval survival. Interannual variation in year-class strength is often inferred from measures of juvenile abundance (e.g., Baxter et al., 1999). In addition, when the total number of eggs spawned is known, juvenile abundance can be used to assess overall variation in egg and larval survival. Intra-annual variation in egg and larval survival can be estimated from the birth-date distribution of surviving juveniles, as determined from otolith daily increment analysis. Particularly when data on actual spawning-date distributions are available, the birth date distribution of survivors can be used to identify periods of spawning that contributed differentially to juvenile recruitment (Methot, 1983; Rice et al., 1987; Yoklavich and Bailey, 1990; Moksness and Fossum, 1992; Fox, 1997; Takahashi et al., 1999).

Recruitment of juvenile Pacific herring (*Clupea pallasi*) varies interannually by over an order of magnitude in San Francisco Bay (Baxter et al., 1999) and is the culmination of several processes. Schools of adult herring enter San Francisco Bay in discrete batches during the fall and winter. These schools shoal and deposit eggs and milt during spawning events that often correspond to the quarter moon phase. Spawning events can vary in duration from approximately one day to one week, and simultaneous events may occur at different spawning sites throughout the bay. Herring lay adhesive eggs intertidally and subtidally on rocks, algae, aquatic plants, pier pilings, and other substrates (Alderdice and Velsen, 1971; Hay, 1985). Eggs can experience extremely high mortality due to predation (McGurk, 1986; Bishop and Green, 2001), suboptimal temperature and salinity conditions (Alderice and Velsen, 1971; Griffin et al., 1998), as well as reduced hatching and developmental abnormalities associated with certain substrate se-

lection (Vines et al., 2000). Larvae hatch from eggs after an incubation period, and the San Francisco Bay estuary can serve as a larval nursery area until after metamorphosis into the juvenile stage (Hay, 1985).

Our objectives were 1) to identify periods in the spawning season that lead to successful (or unsuccessful) juvenile recruitment and 2) to evaluate larval and juvenile growth variation for two herring year classes. We used otoliths of juvenile herring from the 1999 and 2000 year classes to back-calculate spawning-date distributions and determine spawning times that lead to successful recruitment. Distributions of spawning were obtained from management surveys. Growth was then evaluated to determine its role in year-class formation.

Methods

Surveys

All information on adult herring spawning events and juvenile herring specimens were obtained from ongoing monitoring and management surveys conducted by the California Department of Fish and Game (CDFG).

Data on timing, location, and magnitude of herring spawning events for the 1998–99 and 1999–2000 spawning seasons were obtained from the herring spawn survey conducted by the California Department of Fish and Game (CDFG). The survey is conducted from November through March throughout central San Francisco Bay, the area of most herring spawning (Watters et al., 2004). The central bay region is searched for herring spawning on a daily basis from a small boat, and the entire spawning region is covered at least once per week. Eggs are located visually at low tide and by rake in shallow subtidal areas. When a spawning area is located, the number of eggs per square meter is measured from a subsample of the spawning area and is expanded to an estimate of total eggs spawned (for spawning survey method details, see Spratt, 1981; Watters et al., 2004). At the end of the 1998–99 and 1999–2000 spawning seasons, information on date, location, spawning area, average eggs/m^2, total eggs, and the spawning biomass estimate was provided for the purpose of this study (Watters[1]).

Juvenile (age-0) herring were sampled monthly from 30 stations in San Francisco Bay aboard the RV *Longfin* as part of CDFG's Bay/Delta Division's Bay study (Fig. 1). Each station was visited once a month and juvenile herring were retained from catches during the months of April–June 1999 and March–June 2000. Stations were sampled by mid-water trawl with a 3.7-m^2 mouth and 1.3-cm mesh codend, towed against the current, for 12 minutes. Volume of water filtered was calculated by using a flowmeter and was used to calculate

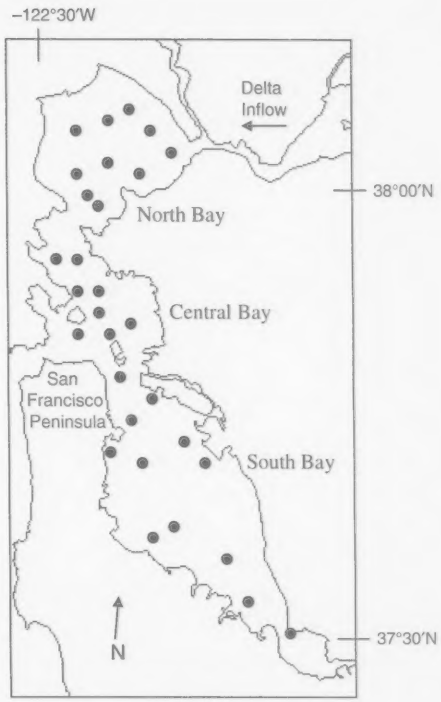

Figure 1
Midwater trawl sampling stations in San Francisco Bay.

catch per unit of effort (CPUE) for each station. Juvenile herring were measured onboard, sorted from the catch, kept on ice, and transported to the laboratory, where they were frozen. Relative recruitment in each year was calculated by summing the CPUE at each station for the months of March–June in 1999 and 2000.

Otolith preparation and analysis

Frozen juvenile herring, separated by date and station, were thawed in batches and all fish were re-measured for standard length to the nearest mm. If the catch was small at a particular station (less than approximately 10 individuals), all specimens from that station were reserved for otolith analysis. If the catch was large, a subsample of the measured catch was reserved for otolith analysis. Subsampling consisted of randomly selecting at least two specimens from each 1-mm length bin in the catch.

Both sagittal otoliths were extracted from each fish, cleaned with fresh water, and transferred to a microscope slide where they were allowed to dry. When completely dry, both otoliths were mounted on the slide, convex side up, with clear nail polish.

Otoliths were read with a compound microscope. Because otoliths were too thick to allow sufficient light transmission for increment reading, all otoliths were

[1] Watters, D. 2000. Personal commun. Calif. Dep. Fish and Game, 411 Burgess Dr., Menlo Park, CA 94025.

ground with 2000 grit sandpaper. Otoliths were alternately ground and examined under the microscope at 100× to ensure that the section was thin enough to allow sufficient light transmission, yet not over-ground so that the edges of the otolith were lost.

Daily increment deposition in herring begins at yolksac absorption, corresponding with the first heavy ring near the nucleus (Geffen, 1982; McGurk, 1984a; McGurk, 1987; Moksness and Wespestad, 1989). This heavy ring was located in all herring examined and increment counts were initiated there. Increment counts were made at 1000× (with an oil immersion objective) and 400× (without oil immersion) magnification along the axis of maximum resolution. All increments were counted from the first heavy ring until the last ring on the edge of the otolith.

Several days after the first reading, the same reader performed a reading on the second otolith. If the two increment counts differed by more than a value of 7, a third reading was conducted at a later date on the highest quality otolith. If the three increment counts differed from each other by more than a value of 7, otolith data from that fish were not used in further analyses. Where two readings differed by 7 or fewer increments, the final increment number for each fish was determined by averaging the two increment counts.

Daily otolith increment deposition has been demonstrated in Pacific herring larvae reared in captivity (McGurk, 1984a; Moksness and Wespestad, 1989) and in the field (McGurk, 1987). In our study, otolith increments were assumed to be deposited daily and the validity of this assumption is treated in the "Results" and "Discussion" sections. Precision of otolith increment counts was determined by computing the average percent error for each otolith examined (Beamish and Fournier, 1981).

Spawning-date distributions

Spawning-date distributions were constructed from specimens retained for otolith analysis in 1999 and 2000. Distributions were calculated 1) by adding a constant of 14 days to the otolith increment count and 2) by subtracting that value (otolith increments+14) from the Julian date of capture. Because Pacific herring begin daily increment deposition at yolksac absorption, the constant of 14 days was added to the increment value to account for egg incubation and the yolksac larval period. Taylor (1971) reported a 9-day egg incubation period for a British Columbia Pacific herring stock between 13.4°C and 13.8°C. For San Francisco Bay spawned herring, Griffin et al. (1998) found developmental rate to be influenced by salinity; the greatest hatching rate occurred 10 days after fertilization at a salinity of 14 ppt. Yolksac absorption occurs in Pacific herring 4–7 days after hatching (McGurk, 1987; Griffin et al., 2004, and references therein). The final value of 14 days for egg incubation and yolksac absorption used in our study was determined 1) from laboratory-derived values reported for British Columbia (Taylor, 1971; McGurk, 1987) and San Francisco Bay (Griffin et al., 1998) herring populations and 2) by visually matching back-calculated spawning-date distributions with the observed spawning-date distribution from the CDFG spawn-deposition survey.

The back-calculated spawning-date distributions determined from specimens used for otolith analysis were extrapolated to include as many herring as possible caught in the juvenile surveys of 1999 and 2000. Length-frequency distributions were converted to spawning-date distributions by using age-length keys. Separate age-length keys were constructed for each survey in both 1999 and 2000. In some cases, the monthly survey was split into two legs separated by several days. When the monthly survey was split into legs, separate age-length keys were constructed for each leg.

It was not possible to fit all herring caught between the months of March and June into age-length keys because some samples were inadvertently discarded after measurement in the field. If the range of lengths in the discarded samples extended beyond the sizes of samples aged, a complete age-length key could not be constructed. To avoid ascribing a possibly inaccurate age to a fish outside the size range of the age-length key, those fish were not included in the spawning-date distribution. Table 1 displays the number of herring caught in each leg, the number of otoliths used to construct the age-length key for that survey leg, and the total number and proportion of juveniles caught that are represented in the spawning-date distribution. The number of juveniles caught was greater than the number of juveniles in the spawning-date distribution for all but one survey leg. This discrepancy was due to discarded fish (in the field) with lengths not within the range of the age-length key constructed from the subsampled individuals.

Mortality estimate corrections are often superimposed upon spawning-date or hatching-date distributions to account for different size juveniles captured (Methot, 1983). Presumably a larger juvenile is older, and thus has been exposed to mortality factors for a longer period of time than has a smaller juvenile. The lack of a correction for juvenile mortality can lead to an underrepresentation of larger juveniles in the distribution. Because of the noncontinuous mid-water trawl sampling schedule, mortality rates could not be estimated from the data used in our study. As a result, mortality corrections were calculated by using an instantaneous mortality rate value of 0.016/d, corresponding to the greater of two mortality rates calculated from juvenile Pacific herring in Prince William Sound, Alaska (Stokesbury et al., 2002).

Spawning-date distributions were corrected for mortality by calculating abundance at age 100 days (N_{100}). For fishes aged at less than 100 days:

$$N_{100} = N_a e^{-0.016(100-a)}, \quad (1)$$

where a is the age of the fish in days.

Table 1

Summary of the catch, number of *Clupea pallasi* otoliths examined from the catch, number and percent available for use in the spawning-date distributions, and catch per unit of effort (CPUE) for the midwater trawl survey in 1999 and 2000. ΣCPUE represents summed CPUE for all stations in each survey leg. Juveniles were not used in analysis if they were inadvertently discarded in the field and if a complete age-length key could not be constructed.

Survey dates	Area surveyed	Juveniles caught	Otoliths examined	Used in analysis	Percent used	ΣCPUE
1999						
Mar 99	entire bay	0	0	0	0	0
21 Apr 99	central and north	41	0	0	0%	1653
26–28 Apr 99	south and north	66	53	60	91%	2360
18–19 May 99	north	19	4	2	11%	771
24–27 May 99	north, central, and south	280	251	273	98%	12,856
9–10 Jun 99	north and central	91	25	45	49%	3457
15 Jun 99	south	61	0	0	0%	2551
Total		558	333	380	68%	23,648
2000						
8–9 Mar 00	north and central	11	0	0	0%	637
13–14 Mar 00	south	7	7	6	86%	294
4–5 Apr 00	north	25	25	25	100%	1053
10–11 Apr 00	central and south	302	115	284	94%	14,712
10 May 00	north	898	77	740	82%	38,270
22–24 May 00	central and south	2244	77	2237	100%	102,516
6–7 Jun 00	central and south	569	74	569	100%	25,352
13 Jun 00	north	13	0	0	0%	539
Total		4069	375	3861	95%	183,373

For fishes aged greater than 100 days:

$$N_{100} = \frac{N_a}{e^{-0.016(a-100)}}. \quad (2)$$

Combining the results of Equations 1 and 2 produced the mortality-corrected spawning-date distributions.

Growth

To evaluate correlates of both inter- and intra-annual variation in survival to the juvenile stage, we wanted to compare growth rates of herring up to the juvenile stage. However, because it was apparent that growth rates may have differed for specimens spawned at different times of the year, either a linear or nonlinear growth curve fitted to size-at-age data would be erroneous (O'Farrell, 2001). Larger (older) and smaller (younger) individuals would have experienced different growth histories; therefore a plot of size versus age for any sample of fish would not reflect the growth history of any one cohort. Furthermore, consecutive samples rarely contained individuals from any given cohort because older juveniles appeared to leave San Francisco Bay. Finally, we did not have data on size at age of larvae; therefore growth curves would be incomplete.

Instead, we used age at size to compare growth within and between years. To do this, we computed the number of otolith increments (days after yolksac absorption) present in fish between 40 mm and 50 mm standard length. This size group was chosen to analyze growth because it was well represented in both in the 1998–99 and 1999–2000 spawning seasons. The mean and stan-

Table 2

Summary statistics and distribution of juvenile *Clupea harengus* lengths within the 40–50 mm size bin for sampling events where size-at-age data were used. Other sampling events were not included in growth analyses because they did not contain juvenile herring between the sizes of 40 mm and 50 mm.

Survey leg	*n*	Mean (mm)	SD (mm)
26–27 Apr 99	15	43.80	2.54
24–27 May 99	162	45.02	2.63
9 Jun 99	10	42.20	2.82
5 Apr 00	16	46.25	3.00
10–11 Apr 00	23	46.43	2.94
10 May 00	9	43.67	3.04
22–24 May 00	36	44.81	3.19
6–7 Jun 00	36	46.56	2.82

dard deviation of the length distribution within the 40–50 mm bin for each sampling event is provided in Table 2. Thus, the amount of time (measured by otolith increments) needed for fish to grow to the 40 mm–50 mm size group was used to compare growth. Differences in age at length were evaluated and compared with observed variation in juvenile abundance.

Results

Egg and juvenile abundance

Both the magnitude and timing of estimated egg deposition differed little between the 1998–99 and 1999–2000 spawning seasons (Fig. 2). Total egg deposition was estimated to be 9.66×10^{11} eggs for 1998–1999 and 8.59×10^{11} eggs for 1999–2000 (Watters[2]). Peak egg deposition in both spawning years occurred in January (Fig. 2).

Abundance of juvenile herring resulting from these two spawning seasons differed greatly. The cumulative estimated relative recruitment ($\Sigma CPUE$) of juvenile herring was 7.75 times greater in 2000 than 1999 (Table 1).

General patterns of juvenile herring distribution were similar in 1999 and 2000. Juvenile herring recruited to the sampling gear in March and April and were widely distributed throughout the bay (Fig. 3). Peak abundances occurred in May for both 1999 and 2000, and juveniles were caught throughout the study area. By June, abundances decreased and herring became more concentrated in the central Bay region, presumably aggregating in this area prior to exiting San Francisco Bay for the coastal ocean (Fig. 3).

[2] Watters, D. 2000. Unpubl. data. Calif. Dep of Fish and Game, 411 Burgess Dr., Menlo Park, CA 94025.

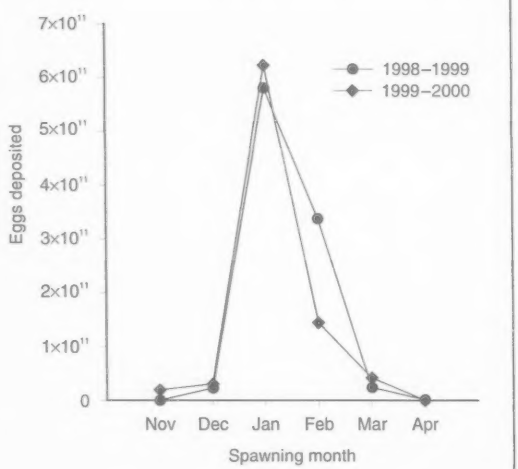

Figure 2

Total egg deposition by Pacific herring (*Clupea pallasi*), summed by spawning month for the 1998–99 and 1999–2000 spawning seasons. Data provided by the California Department of Fish and Game, Menlo Park.

Spawning-date distributions

The temporal distribution of successful spawning-dates differed between the 1999 and 2000 year classes (Fig. 4, A and B). In 1999, the earliest spawning-date that resulted in juvenile recruitment was 30 November 1998. The greatest numbers of juvenile recruits were a product of the middle of the spawning season, from approximately early January 1999 though early February 1999, and the highest recruitment occurred from spawnings between 10 January and 14 January 1999 (Fig. 4A). An additional spike of recruitment was observed from spawning events at the end of the season (early March). The period of highest recruitment came at the same time as the highest spawning intensity. Spawning events early in the spawning season (November–December) appeared to produce few juveniles (Fig. 4A).

In 2000, juveniles recruited from much earlier spawning events. Back-calculated spawning dates indicated that spawning may have occurred as early as 13 October 1999 (Fig. 4B). Both the March 2000 and April 2000 juvenile surveys contained herring with back-calculated spawning dates that ranged from mid to late October, indicating that a spawning event occurred extremely early in the spawning season and was undetected by the spawn-deposition survey (which commences in November). Although early spawnings appeared to produce some recruitment success, a near lack of success was noted for many of the mid-season spawnings that occurred from mid-November through mid-January 2000 (Fig. 4B). This period of poor survival was then followed by the period of highest recruitment; spawning dates ranged from mid-January to early March and peak recruitment resulted from February spawning (Fig. 4B).

Juvenile mortality corrections superimposed upon the spawning-date distributions had little effect on the general results. An instantaneous juvenile mortality rate of 0.016/d produced minor adjustments on the percent recruitment resulting from particular spawning periods in both years (Fig. 4, A and B). This mortality correction did not alter the general spawning periods that resulted in juvenile recruitment. Increasing the instantaneous juvenile mortality rate to 0.05/d (O'Farrell, unpubl. data) also had negligible effects on the general results of the spawning-date distributions.

Data for both 1999 and 2000 are not totally complete. The spawning-date distribution for 1999 was based on a total of 380 herring, whereas 558 herring were caught between the months of March and June. Similarly, the 2000 spawning-date distribution was based on a total of 3861 herring, whereas 4069 herring were caught during the same months (Table 1). Fish were omitted from

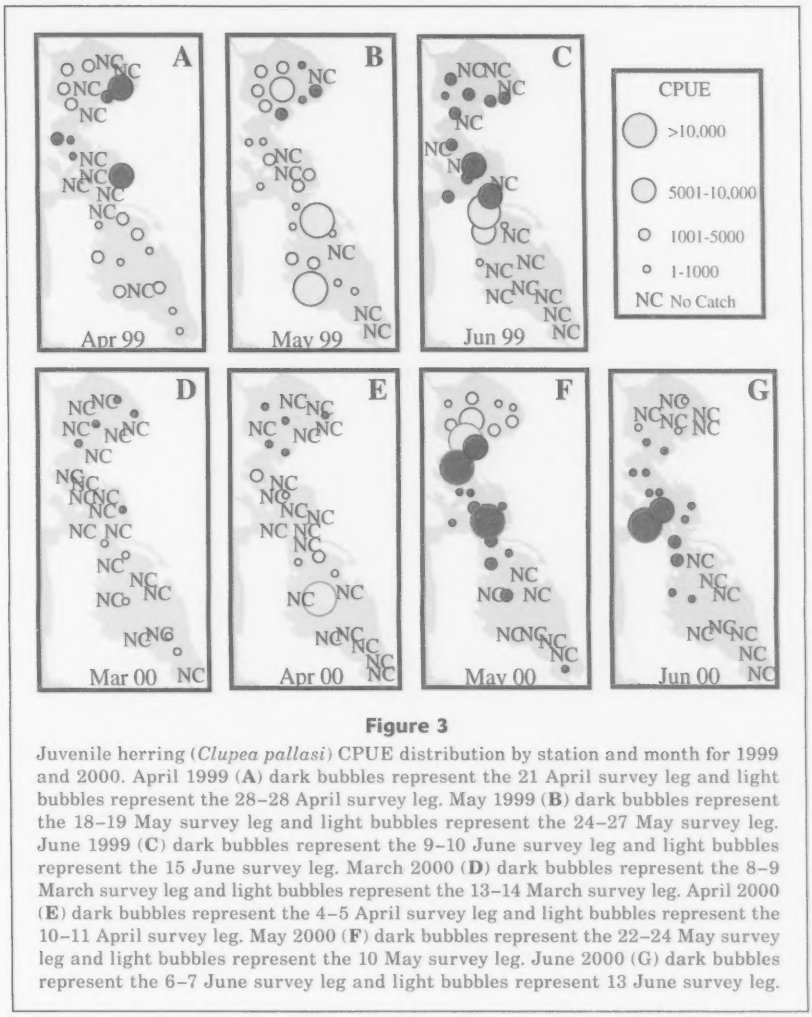

Figure 3

Juvenile herring (*Clupea pallasi*) CPUE distribution by station and month for 1999 and 2000. April 1999 (**A**) dark bubbles represent the 21 April survey leg and light bubbles represent the 28–28 April survey leg. May 1999 (**B**) dark bubbles represent the 18–19 May survey leg and light bubbles represent the 24–27 May survey leg. June 1999 (**C**) dark bubbles represent the 9–10 June survey leg and light bubbles represent the 15 June survey leg. March 2000 (**D**) dark bubbles represent the 8–9 March survey leg and light bubbles represent the 13–14 March survey leg. April 2000 (**E**) dark bubbles represent the 4–5 April survey leg and light bubbles represent the 10–11 April survey leg. May 2000 (**F**) dark bubbles represent the 22–24 May survey leg and light bubbles represent the 10 May survey leg. June 2000 (G) dark bubbles represent the 6–7 June survey leg and light bubbles represent 13 June survey leg.

the spawning-date distribution because some samples were discarded and otoliths were unavailable. Because of evidence for intrayear growth-rate variation, other age-at-length data were not used to infer spawning dates for these fish. The standard length data for the fish not included in this analysis were used for all other analyses in our study.

Precision of multiple otolith readings was calculated for all otoliths examined. Average percent error (Beamish and Fournier, 1981) was 3.60% in 1999 and 1.64% in 2000, indicating that aging precision was less than 4 days for 100-day old herring in both years.

Growth

Different patterns of age at length (40–50 mm) were observed in 1999 and 2000. In 1999, specimens between 40 mm and 50 mm were captured in three survey legs. A significant decrease in the number of otolith increments for juveniles 40 mm–50 mm standard length was detected in 1999 (Fig. 5A; Kruskal-Wallis test; H=27.93, P<0.0001). Nonparametric multiple comparisons indicated that there was a nonsignificant difference in otolith increment counts for herring caught in the April 1999 and the May 1999 surveys, but herring from these surveys had significantly higher median otolith increment counts than those from the June 1999 survey. In this later survey, juvenile herring were caught that were a product of spawning events occurring late in the spawning season. Figure 5C displays the median and range of spawning dates of the specimens aged for Figure 5A. Juvenile herring that were a product of spawning between 27 February 1999 and 7 March 1999 reached a 40–50 mm size range significantly faster than

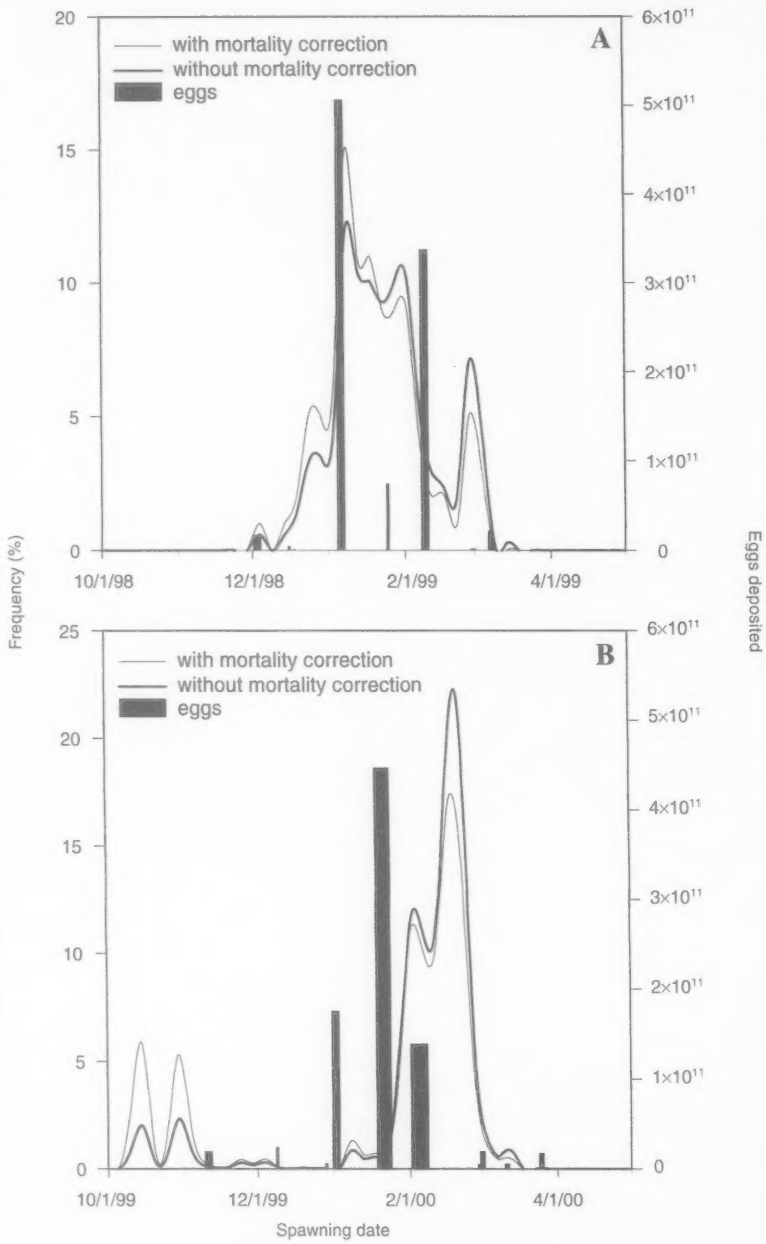

Figure 4

Spawning-date distributions for juvenile herring (*Clupea pallasi*) caught in (**A**) 1999 and (**B**) 2000. Vertical bars represent dates and magnitude of observed spawning (eggs deposited), heavy lines represent the spawning-date distribution of juveniles without the mortality correction, and light lines represent the spawning-date distribution corrected for juvenile mortality at an instantaneous rate of 0.016/d. Distributions are smoothed with a cubic spline interpolation. Data on observed spawning were provided by D. Watters, CDFG (see Footnote 2 in the text).

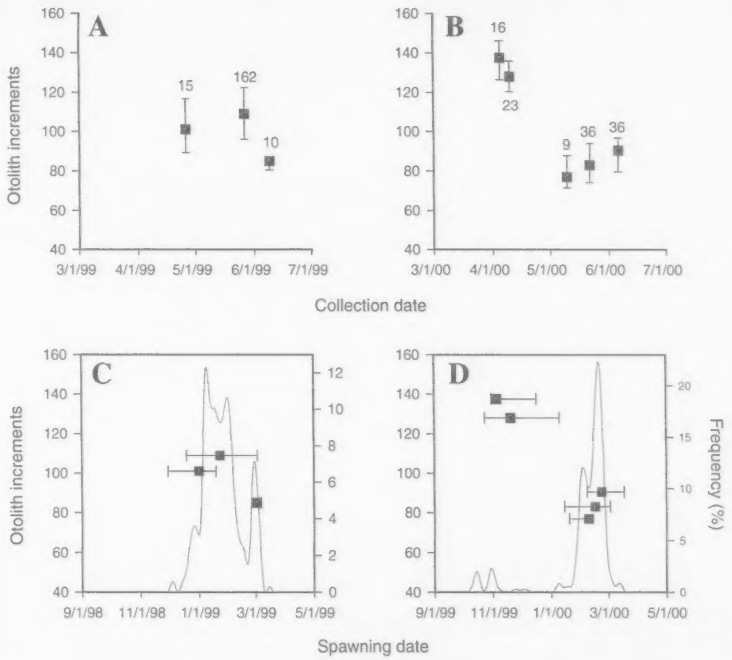

Figure 5

The upper panels display otolith increments present in 40 mm–50 mm juvenile herring (*Clupea pallasi*) arranged by capture date for (**A**) 1999 and (**B**) 2000. Boxes represent median number of otolith increments, bars indicate ±1 SD, and the number above each point is the sample size. The lower panel displays growth histories for juvenile herring originating from various periods within the spawning season for (**C**) 1999 and (**D**) 2000. Boxes represent median spawning-dates and bars represent range of spawning dates at that growth rate. The spawning-date distribution (uncorrected for juvenile mortality) is superimposed upon C and D to ascertain how changes in growth are reflected in survival to the juvenile stage.

specimens recruiting from earlier spawning periods. The period of greatest recruitment occurred during the slower growth period in 1999 (Fig. 5C).

In 2000, 40 mm–50 mm juvenile herring were caught in five survey legs conducted during three months (April, May, and June). The data are displayed by survey leg; pooling the data by month, however, does not change the result. Median increment counts differed significantly for the 2000 surveys (Fig. 5B; H=76.39, P<0.0001). Otolith increment counts for 40 mm–50 mm specimens did not differ for the 5 April 2000 and 10–11 April 2000 surveys. However, the age at length for these surveys was significantly greater than for the three later survey legs (10 May 2000, 22–24 May 2000, and 6 June 2000), which did not significantly differ from each other. Herring caught in the three later surveys grew significantly faster than herring caught in the two earlier surveys. The significant decrease in age at length indicates that juvenile herring that were a product of spawning between 15 January 2000 and 18 March 2000 grew faster than specimens recruiting from earlier spawning events. The majority of juvenile recruits in 2000 were a product of the fast growth period (Fig. 5D).

Accuracy of growth-rate estimates determined from growth increments on otoliths

The above analyses depended upon the assumption that increments were deposited daily in the otoliths examined. Two lines of evidence point to the validity of this assumption. First, back-calculated spawning-dates generally agreed with the known spawning season of San Francisco Bay herring, and several peaks in back-calculated spawning dates match known spawning events quite closely (Fig. 4, A and B).

Second, juvenile growth rates appear to be high enough for daily growth (McGurk, 1984b). Clear length-frequency modes were visible for three sampling events

in 2000. Assuming linear growth between these time periods, the advancement of these length-frequency modes resulted in growth rates of 0.75 mm/d (Fig. 6, arrow in A), 0.83 mm/d (arrow in B), and 0.64 mm/d (arrow in C). McGurk (1984b) demonstrated daily increment deposition in herring if the larval growth rate exceeded 0.36 mm/d. Our data did not allow us to estimate growth rates of larvae; however, the estimated juvenile growth rates presented above are much greater than necessary for daily increment deposition.

Discussion

Catches of juvenile herring were much greater in 2000 than in 1999. Between the months of March and June 2000, cumulative CPUE was more that seven times greater than during the same period in 1999, yet an estimated 12% more eggs were deposited during the 1988–99 spawning season. Because observed differences in recruitment between 1999 and 2000 far exceeded differences in the total eggs spawned, differential survivorship during the egg or larval stages (or both) must be responsible for disparate year-class strengths.

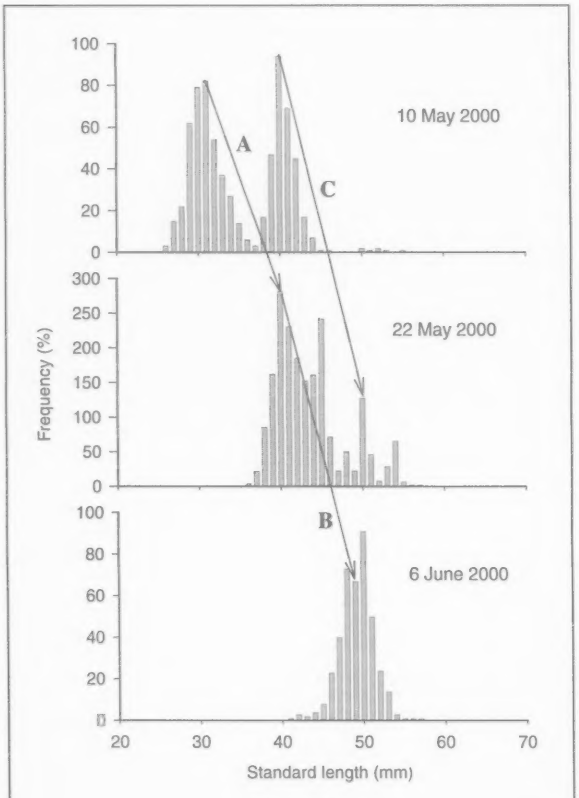

Figure 6

Length frequencies for juvenile herring (*Clupea pallasi*) captured on 10 May 2000, 22 May 2000, and 6 June 2000. Arrows represent the estimated propagation of length modes through time. Linear growth rates, calculated from each trajectory, are as follows: A=0.75 mm/d; trajectory B=0.83 mm/d); and C=0.64 mm/d.

The spawning-date distributions presented for 1999 and 2000 did not contain all herring caught by the mid-water trawl survey between the months of March and June. Because they could not be accurately assigned ages with an age-length key (Table 1), 178 herring were omitted from the distribution in 1999. Most specimens omitted from this distribution were caught in the early April 1999 and late June 1999 survey legs. As a result, the spawning-date distribution likely underestimated the recruitment from very early and very late season spawnings. In 2000, 208 specimens, from a variety of survey legs, were omitted from the spawning-date distribution (Table 1). Because a large number of herring were caught in 2000, it is unlikely that these omissions would significantly change the shape of the spawning-date distribution. The loss of data in this case does not change the overall result of large year-class-strength variation.

The noncontinuous sampling schedule for juveniles may have resulted in either an underestimation or overestimation of CPUE and thus year-class strength. In several months, the mid-water trawl survey was conducted over two legs separated by several days (Table 1, Fig. 3). This noncontinuous sampling could have produced error in our estimates because aggregations of juveniles, through movement between areas, could conceivably have escaped detection by trawls (resulting in CPUE underestimation) or have been sampled twice in the same month (resulting in CPUE overestimation). However, O'Farrell (2001) showed that dispersal of herring from a successful spawning event could occur through much of San Francisco Bay. Therefore, we do not believe that aggregations of juveniles were completely missed by the mid-water trawl survey. The degree to which aggregations of juveniles were sampled more than once in a sampling month is not known.

Variation in age estimates undoubtedly produced back-calculated spawning-dates that did not match exactly with true spawning dates. Yet, for some spawning events, very good matches between back-calculated and reported spawning events indicate that the age estimations were accurate for many of the cohorts examined (O'Farrell, 2001). Other cohorts that did not match as well with reported spawnings may be the result of 1) a spawning event undetected by the spawn-deposition study, 2) a small, "spot" spawning that did not qualify as a true spawning event for the spawn-deposition study, or 3) very slow or fast growth through a portion of the larval life history that interrupted daily increment deposition (McGurk, 1984b, 1987).

Increased survival did not occur throughout the entire 2000 spawning season. Instead, periods of good survival and poor survival were present, yet the

periods of good survival in 2000 led to a much stronger year class than that of 1999. Detecting a "match" of favorable conditions that led to recruitment success was not possible in our study because of the myriad factors that can determine recruitment success. Rather than attempting to explain the observed survival differences with specific mechanisms, we suggest what may possibly contribute to the observed patterns.

Larval survival

The degree to which larval survival depends upon biotic or abiotic factors is difficult to estimate. Fox (2001) presented data showing that year-class strength in the Blackwater stock of Atlantic herring (*Clupea harengus* L.) was determined by survival after the egg stage. However, it is not clear whether variation in survival was due to density-dependent or environmental factors. A recent study has shown that salinity can affect larval survival after hatching in San Francisco Bay herring (Griffin et al., 2004). Here, the salinity during embryonic development was a factor in yolksac larval survival in different salinity treatments. Regardless of the form of mortality operating on larvae, small changes in larval growth rate can lead to large changes in levels of recruitment (Houde, 1987). Faster larval growth results in shorter larval stage duration and thus decreased exposure to the characteristically high mortality of the larval stage. Age at size for herring in this study decreased significantly as the spawning season progressed both in 1999 and 2000. From this finding, we infer that positive changes in growth rate occurred during the spring and summer. Seasonal positive shifts in growth have also been observed in Pacific herring populations in Prince William Sound, Alaska, between the months of June and October (Stokesbury et al., 1999).

In 1999, the greatest number of recruits came from mid to late-season spawning events. The late February to early March spike in recruitment (Fig. 4A) may be partially explained by within-year growth variation. This group of survivors appeared to be derived from a relatively small number of eggs. Recruits from that spawning period grew significantly faster than recruits from earlier spawning events. The largest spawning events of the 1998–99 spawning season produced recruits that grew slower than the recruits spawned in early March and thus may have experienced lower relative survival.

Within-year growth rate variation also partially explains the 2000 year class. The 2000 year class was dominated by late season recruitment, primarily from spawning in February 2000. Herring from spawning events occurring between late October 1999 and mid-January 2000 had a significantly higher median age at length than herring produced from subsequent spawning times. This slow growth may in part explain the near lack of recruitment from the two highest magnitude spawns occurring from 1 to 3 Jan 2000 and from 19 to 24 Jan 2000. However, age at length decreased (and thus growth rate increased) for spawning events occurring from late January 2000 to early March 2000. The timing of the growth rate switch (from slow to fast) coincided closely with the spawning period producing the greatest amount of recruitment. The general trend of high levels of recruitment from late season spawning events indicates that increased growth rate played a role in the good survival during this period. However, recruitment from very early spawning events and the small number of recruits resulting from late March 2000 spawning was not explained solely by this within-year growth variation.

Egg mortality

Variation in mortality during the egg stage may also affect recruitment in San Francisco Bay herring. Fertilization, embryonic development, and hatching success of Pacific herring are strongly tied to environmental conditions (Alderdice and Velsen, 1971, Griffin et al., 1998). The optimal range for fertilization and development of the San Francisco Bay population is between 12 ppt and 24 ppt, and both percent fertilization and percent hatching is maximized at 16 ppt (Griffin et al., 1998). The herring spawning season in San Francisco Bay is a time of rapidly changing salinities. High salinities generally persist through the fall months. In winter, rapid decreases in salinity due to freshwater from the San Joaquin–Sacramento Delta, storm drain runoff and local creek purges (Oda[3]) are common, yet the magnitude varies between years (Conomos et al., 1985). In the two years examined, salinity during the winter spawning season varied both above and below the optimum range determined by Griffin et al. (1998). These salinity fluctuations could have a large effect on the supply of larvae into the San Francisco Bay system.

Mortality during the egg stage can be exceedingly high in Pacific herring due to predation and other biotic interactions (Alderdice and Velsen, 1971; McGurk, 1986; Rooper et al., 1999, Bishop and Green, 2001). As a result, egg incubation time may have a significant effect upon eventual recruitment. The length of times of egg incubation and the yolksac larval stage were combined in our study and the combined period was given a constant value of 14 days. In actuality, egg incubation time (Taylor, 1971; McGurk, 1987) and embryonic development (Alderdice and Velsen, 1971; Griffin et al., 1998) are strongly linked to environmental factors and likely have a significant effect upon recruitment before growth rates can determine survival. Analysis of egg incubation and yolksac larval duration for separate cohorts was not performed in our study. It may, however, play a large role in larval abundance.

Conclusion

The 1999 and 2000 spawning-date distributions indicate that year classes can be shaped by periods of good and

[3] Oda, K. 2000. Personal commun. Calif. Dep. Fish and Game, 411 Burgess Dr., Menlo Park, CA 94025.

poor survival lasting shorter than the duration of the spawning season, yet longer than the duration of an individual spawning event. The distributions indicated that variation in survivorship was not only a function of individual spawn success. Rather, periods of good and poor survivorship in 1999 and 2000 were of longer duration than one spawning event. The period of exceptionally good survival that led to the majority of the strong 2000 year class was approximately one month in duration and incorporated several spawning events. Yet this window of good survival was much shorter than the entire 2000 spawning season. Variation in survivorship between individual spawnings may be less important in shaping the year class than survivorship variation on a longer time scale.

Visual examination of the spawning-date distribution superimposed upon juvenile age at length indicate that faster growth had a positive effect on recruitment in 2000, and a negligible effect in 1999. For larval growth to affect recruitment, larvae must be available from hatching eggs. Year-class strength variation in Pacific herring could depend upon both egg and larval survival.

The timing of peak herring spawning in San Francisco Bay may be a tradeoff between maximizing larval growth rates and spawning when hydrographic conditions are optimal for embryonic development. In the two years examined, growth rate increased with the progression of the spawning season. It follows that the herring population could maximize recruitment by spawning later so that larvae grow faster. However, because delta outflow is generally high in February and March on account of winter storms, late season spawning may expose eggs to low salinities and thus decreased hatching rates. Peak spawning may occur in January as a trade off between growth-rate and egg-hatching success.

Acknowledgments

This research would not have been possible without the extensive cooperation of the California Department of Fish and Game Belmont and Stockton offices. In particular, we would like to thank Diana Watters, Ken Oda, Sara Peterson, Kathy Hieb, Kevin Fleming, Tom Greiner, Suzanne Deleon, and the entire crew of the RV *Longfin*. Stephen Bollens, Steven Obrebski, Ken Oda, and three anonymous reviewers provided very helpful comments on various drafts of this manuscript.

Literature cited

Alderdice, D. F., and F. P. J. Velsen.
1971. Some effects of salinity and temperature on early development of Pacific herring (*Clupea harengus pallasi*). J. Fish. Res. Board Can. 28:1545–1562.

Baxter, R., K. Hieb, S. DeLeon, K. Fleming, and J. Orsi.
1999. Report on the 1980–1995 fish, shrimp and crab sampling in the San Francisco estuary. Technical Report 63, California Department of Fish and Game, Stockton, CA.

Beamish, R. J., and D. A. Fournier.
1981. A method for comparing the precision of a set of age determinations. Can. J. Fish. Aquat. Sci. 38:982–983.

Bishop, M. A., and P. G. Green.
2001. Predation on Pacific herring (*Clupea pallasi*) spawn by birds in Prince William Sound, Alaska. Fish. Oceanogr. 10(suppl. 1):149–158.

Bollens, S. M., B. W. Frost, H. R. Schwaninger, C. S. Davis, K. J. Way, and M. C. Landsteiner.
1992. Seasonal plankton cycles in a temperate fjord and comments on the match-mismatch hypothesis. J. Plankton Res. 14:1279–1305.

Conomos, T. J., R. E. Smith, and J. W. Gartner.
1985. Environmental setting of San Francisco Bay. Hydrobiologia 129:1–12.

Cushing, D. H.
1975. Marine ecology and fisheries. Cambridge Univ. Press, Cambridge, UK.
1996. Toward a science of recruitment in fish populations. Excell. Ecol. 7, 175 p.

Fogarty, M. J., M. P. Sissenwine, and E. B. Cohen.
1991. Recruitment variability and the dynamics of exploited marine populations. Trends Ecol. Evol. 6: 241–246

Fox, C. J.
2001. Recent trends in stock-recruitment of Blackwater herring (*Clupea harengus* L.) in relation to larval production. ICES J. Mar. Sci. 58:750–762.

Fox, D. A.
1997. Otolith increment analysis and the application toward understanding recruitment variation in Pacific hake (*Merluccius productus*) within Dabob Bay, WA. M.S. thesis, 73 p. Univ. Washington, Seattle, WA.

Geffen, A. J.
1982. Otolith ring deposition in relation to growth rate in herring (*Clupea harengus*) and Turbot (*Scophthalmus maximus*) larvae. Mar. Biol. 71:317–326.

Griffin, F. J., M. R. Brenner, H. M. Brown, E. H. Smith, C. A. Vines, and G. N. Cherr.
2004. Survival of Pacific herring larvae is a function of external salinity. *In* Early life history of fishes in the San Francisco Estuary and watershed (F. Feyrer, L. R. Brown, R. L. Brown, and J. J. Orsi, eds.), p. 37–46. Am. Fish. Soc. Symp. 39, Bethesda, MD.

Griffin, F. J., M. C. Pillai, C. A. Vines, J. Kaaria, T. Hibbard-Robbins, R. Yanagimachi, and G. N. Cherr.
1998. Effects of salinity on sperm motility, fertilization, and development in the Pacific herring, *Clupea pallasi*. Biol. Bull. 194:25–35.

Hay, D. E.
1985. Reproductive biology of Pacific herring (*Clupea harengus pallasi*). Can. J. Fish. Aquat. Sci. 42(supp. 1.):111–126.

Hjort, J.
1914. Fluctuations in the great fisheries of northern Europe viewed in light of biological research. Rapp. P.V. Reun. Cons. Int. Explor. Mer 20:1–228.

Houde, E. D.
1987. Fish early life dynamics and recruitment variability. Am. Fish. Soc. Symp. 2:17–29.
1989. Subtleties and episodes in the early life of fishes. J. Fish Biol. 35(suppl. A):29–38.

Iles, T. D. and M. Sinclair.
1982. Atlantic herring: stock discreteness and abundance. Science 215(5):627–633.
Lasker, R.
1975. Field criteria for survival of anchovy larvae: the relation between inshore chlorophyll maximum layers and successful first feeding. Fish. Bull. 73:453–462.
McGurk, M. D.
1984a. Ring deposition in the otoliths of larval Pacific herring, *Clupea harengus pallasi*. Fish. Bull. 82: 113–120.
1984b. Effects of delayed feeding and temperature on the age of irreversible starvation and on the rates of growth and mortality of Pacific herring larvae. Mar. Biol. 84:13–26.
1986. Natural mortality rates of marine pelagic fish eggs and larvae: role of spatial patchiness. Mar. Ecol. Prog. Ser. 34:227–242.
1987. Age and growth of Pacific herring based on length-frequency analysis and otolith ring number. Env. Biol. Fish. 20(1):33–47.
Methot, R. D., Jr.
1983. Seasonal variation in survival of larval northern anchovy, *Engraulis mordax*, estimated from the age distribution of juveniles. Fish. Bull. 81:741–750.
Moksness, E., and P. Fossum.
1992. Daily growth rate and hatching-date distribution of Norwegian spring-spawning herring (*Clupea harengus* L.). ICES J. Mar. Sci. 49:217–221.
Moksness, E., and V. Wespestad.
1989. Ageing and back-calculating growth rates of Pacific herring, *Clupea pallasii*, larvae by reading daily otolith increments. Fish. Bull. 87(3):509–513.
O'Farrell, M. R.
2001. Year class formation of Pacific herring in San Francisco Bay. M.A. thesis, 73 p. San Francisco State Univ., San Francisco, CA.
Rice, J. A., L. B. Crowder, and M.E. Holey.
1987. Exploration of mechanisms regulating larval survival in Lake Michigan bloater: a recruitment analysis based on characteristics of individual larvae. Trans. Am. Fish. Soc. 116:703–718.
Rooper, C. N., L. J. Haldorson, and T. J. Quinn II.
1999. Habitat factors controlling Pacific herring (*Clupea pallasi*) egg loss in Prince William Sound, Alaska. Can. J. Fish. Aquat. Sci. 56:1133–1142.
Sinclair, M., and T. D. Iles.
1985. Atlantic herring (*Clupea harengus*) distribution in the Gulf of Maine-Scotian Shelf area in relation to oceanographic features. Can. J. Fish. Aquat. Sci. 42:880–887.
Spratt, J. D.
1981. Status of the Pacific herring, *Clupea harengus pallasi*, resource in California 1972 to 1980. Cal. Dep. Fish and Game, Fish. Bull. 171, 107 p.
Stokesbury, K. D. E., R. L. Foy, and B. L. Norcross.
1999. Spatial and temporal variability in juvenile Pacific herring, *Clupea pallasi*, growth in Prince William Sound, Alaska. Environ. Biol. Fish. 56:409–418.
Stokesbury K. D. E., J. Kirsch E. V. Patrick, and B. L. Norcross.
2002. Natural mortality estimates of juvenile Pacific herring (*Clupea pallasi*) in Prince William Sound, Alaska. Can. J. Fish. Aquat. Sci. 59:416–423.
Takahashi, I., K. Azuma, H. Hiroyuki, and F. Shinji.
1999. Different mortality in larval stage of Ayu *Plecoglossus altivelis* by birth dates in the Shimanto estuary and adjacent coastal waters. Fish. Sci. 65(2):206–210.
Taylor, F. H. C.
1971. Variation in hatching success in Pacific herring (*Clupea pallasi*) eggs with water depth, temperature, salinity, and egg mass thickness. Rapp. P.-V. Reun. Cons. Perm. Int. Explor. Mer 160:128–136.
Thorisson, K.
1994. Is metamorphosis a critical interval in the early-life of marine fishes? Environ. Biol. Fish. 40:23–36.
Vines, C. A., T. Robbins, F. J. Griffin, and G. N. Cherr.
2000. The effects of diffusible creosote-derived compounds on development in Pacific herring (*Clupea pallasi*). Aquat. Toxicol. (NY) 51:225–239.
Watters, D. L., H. M. Brown, F. J. Griffin, E. J. Larson, and G. N. Cherr.
2004. Pacific herring *Clupea pallasii* spawning grounds in San Francisco Bay: 1973 to 2000. *In* Early life history of fishes in the San Francisco Estuary and watershed (F. Feyrer, L. R. Brown, R. L. Brown, and J. J. Orsi, eds.), p. 3–14. Am. Fish. Soc. Symp. 39, Bethesda, MD.
Yoklavich, M. M., and K. M. Bailey.
1990. Hatching period, growth and survival of young walleye pollock *Theragra chalcogramma* as determined from otolith analysis. Mar. Ecol. Prog. Ser. 64:13–23.

Diet of oceanic loggerhead sea turtles (*Caretta caretta*) in the central North Pacific

Denise M. Parker

Joint Institute for Marine and Atmospheric Research
8604 La Jolla Shores Drive
La Jolla, California 92037
Present address: Northwest Fisheries Science Center
National Marine Fisheries Service, NOAA
Newport, Oregon 97365-5275
E-mail address: Denise.Parker@noaa.gov

William J. Cooke

AECOS, Inc.
970 N. Kalaheo Avenue, Suite C311
Kailua, Hawaii 96734

George H. Balazs

Pacific Islands Fisheries Science Center, Honolulu Laboratory
National Marine Fisheries Service
2570 Dole Street
Honolulu, Hawaii 96822-2396

Abstract—Diet analysis of 52 loggerhead sea turtles (*Caretta caretta*) collected as bycatch from 1990 to 1992 in the high-seas driftnet fishery operating between lat. 29.5°N and 43°N and between long. 150°E and 154°W demonstrated that these turtles fed predominately at the surface; few deeper water prey items were present in their stomachs. The turtles ranged in size from 13.5 to 74.0 cm curved carapace length. Whole turtles (n=10) and excised stomachs (n=42) were frozen and transported to a laboratory for analysis of major faunal components. Neustonic species accounted for four of the five most common prey taxa. The most common prey items were *Janthina* spp. (Gastropoda); *Carinaria cithara* Benson 1835 (Heteropoda); a chondrophore, *Velella velella* (Hydrodia); *Lepas* spp. (Cirripedia), *Planes* spp. (Decapoda: Grapsidae), and pyrosomas (*Pyrosoma* spp.).

Manuscript submitted 15 July 2003 to the Scientific Editor's Office.

Manuscript approved for publication 8 July 2004 by the Scientific Editor.

Fish. Bull. 103:142–152 (2005).

Loggerhead sea turtles are circumglobal, inhabiting temperate, subtropical, and tropical waters of the Atlantic, Pacific, and Indian Oceans. In the Pacific, loggerhead sea turtles have been found in nearshore waters of China, Taiwan, Japan, Australia, and New Zealand and are seen in offshore waters of Washington, California, and northwestern Mexico (Dodd, 1988; Pitman, 1990). Nesting in the North Pacific Ocean occurs in Japan; there is no known nesting in the eastern North Pacific (Márquez and Villanueva, 1982; Frazier, 1985; Bartlett, 1989). Trans-Pacific migrations of juveniles have been documented from mitochondrial DNA analyses of individuals found feeding off Baja California. Bowen et al. (1995) identified these Baja sea turtles as originating from Japanese rookeries, although a a small percentage come from Australia. Recent research indicates that all loggerhead sea turtles found in the oceanic realm of the central North Pacific Ocean are of Japanese stock (Dutton et al., 1998). Tagging studies in Japan and the Eastern Pacific also demonstrate transpacific migrations of loggerhead sea turtles between the east and west Pacific (Balazs, 1989; Resendiz et al., 1998; Uchida and Teruya[1]).

Recent oceanic satellite tracking studies of loggerhead sea turtles indicate that they are active in their oceanic movements. These turtles follow subtropical fronts as they travel toward Japan from east to west across the Pacific Ocean, often swimming against weak geostrophic currents (Polovina et al., 2000; Polovina et al., 2004). One hypothesis discussed in Polovina et al. (2000; 2004) suggests that this species obtains prey items from the subtropical fronts along which they travel. A sharp gradient in surface chlorophyll is observed along the main frontal area where these turtles are commonly encountered. This frontal area, the transition zone chlorophyll front

[1] Uchida, S., and H. Teruya. 1991. A) Transpacific migration of a tagged loggerhead, *Caretta caretta*. B) Tag-return result of loggerhead released from Okinawa Islands, Japan. *In* International symposium on sea turtles '88 in Japan (I. Uchida, ed.), p. 169–182. Himeji City Aquarium, Tegarayama 440 Nishinobusue, Himeji-shi, Hyoyo 670, Japan.

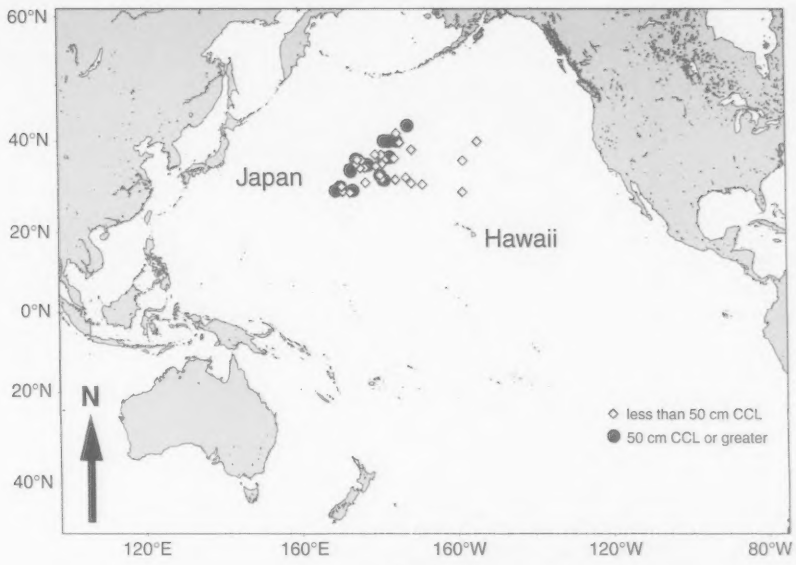

Figure 1

Distribution of loggerhead sea turtles (*Caretta caretta*) incidentally captured in the international high seas driftnet fishery in the central North Pacific Ocean. Turtles smaller than 50 cm curved carapace length (CCL) are shown as open diamonds and those larger than 50 cm CCL are shown as black circles.

(TZCF), is an area of concentrated phytoplankton that also collects and attracts a variety of neustonic and oceanic organisms—many of which may be potential prey times, as well as predators, of oceanic-stage loggerhead sea turtles in the Pacific. Polovina et al. (2000, 2004) have suggested that the turtles are foraging along the TZCF.

The duration of the juvenile oceanic stage for loggerhead sea turtles in the Pacific is currently unknown. In the Atlantic, juvenile turtles inhabit the oceanic zone for approximately 10 years (Bjorndal et al., 2000). Based on growth analyses (Zug et al., 1995; Chaloupka, 1998), it is probable that this sea turtle from the Pacific can have a similar extended oceanic stage, which in some cases may last until sexual maturity (30+ years).

Understanding the diets of sea turtles is important for their conservation. Foraging studies have been done with oceanic-stage turtles in the Atlantic (Van Nierop and den Hartog, 1984). However, there is a paucity of information regarding the foraging ecology of oceanic-stage loggerhead sea turtles in the Pacific. Such information can help identify important food resources and foraging areas necessary for guiding decisions regarding the management of endangered sea turtle populations (Bjorndal, 1999). The objective of the present study is to determine the diet composition of loggerhead sea turtles from the central North Pacific Ocean and to discuss the possibility of interactions between these turtles and commercial fisheries that may occur as a result of the foraging behavior of these sea turtles.

Method

National Marine Fisheries Service (NMFS) observers between 1990 and 1992 obtained 52 dead loggerhead sea turtles. These specimens were taken as bycatch in the international high-seas driftnet fishery, which targeted squid and albacore (Wetherall et al., 1993). NMFS observers recorded capture position and sea surface temperature aboard commercial driftnet vessels. Samples were collected between latitude 29.5°N and 43°N and longitude 150°E and 154°W (Fig. 1). A total of 10 whole specimens and 42 excised stomachs were frozen and transported to a Honolulu laboratory for analysis. Stomachs were removed from whole specimens and all stomachs were examined from anterior to posterior. Gross observations of stomach contents were made and the contents were sorted to the lowest identifiable taxonomic level by using a dissecting microscope. Major fauna were identified, quantified by volume, and the percent contribution (to stomach contents) of each major organism was calculated (Forbes, 1999). Presence of jellyfish or other jellies were identified by presence of tentacles, nematocysts, and whole or partial individuals. *Planes* spp. were identified from descriptions of Spivak and Bas (1999). Frequency of occurrence of major components was calculated by dividing the number of stomachs in which the prey item occurred by the total number of turtle stomachs examined. Percent sample volume was calculated for all prey items by summing the total volume of each prey item and dividing it by the total volume of all

prey collected. Summing the total volume of each prey item and dividing it by the total stomach volume for those samples, where the prey item was present, yielded the mean percent volume. Regression analysis was done to determine if any correlation existed between sea surface temperature, sample volume, and size of turtle.

Results

Loggerhead sea turtles collected in our study were found widely distributed over the central North Pacific Ocean and there was no apparent difference in distribution between size classes (Fig. 1). The turtle specimens ranged from 13.5 cm to 74.0 cm curved carapace length (CCL, Fig. 2); the mean was 44.8 [±14.5] cm CCL. Figure 2 shows the distribution of turtles in each 10-cm size class. Sea surface temperatures in the area of capture ranged from 16° to 20°C. There was no correlation between size of turtle and sea surface temperature in the area of capture (F=0.58, r^2=0.01, Fig. 3).

All 52 stomachs examined contained prey items; the level of fill varied from 6 mL to 1262 mL. Items found in the anterior portion of the stomach were the most identifiable and contents varied between turtles. Unidentifiable remains were located mainly in the posterior end of the stomach or the intestines if a whole gastrointestinal tract was analyzed. Only one of the samples analyzed included an entire gastrointestinal tract.

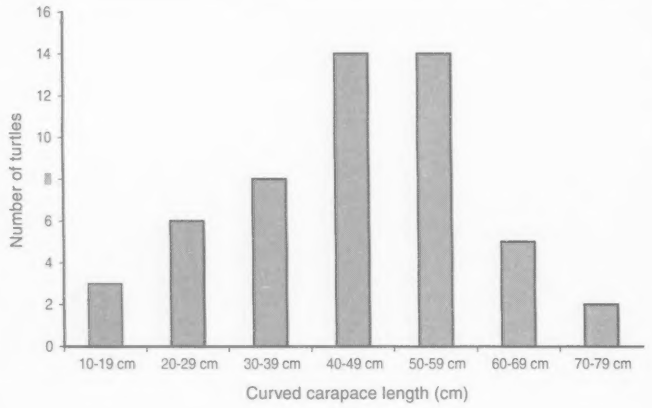

Figure 2

Size distribution for the 52 loggerhead sea turtles (*Caretta caretta*) obtained as samples in the high-seas driftnet fishery. Sizes were grouped into 10-cm size classes.

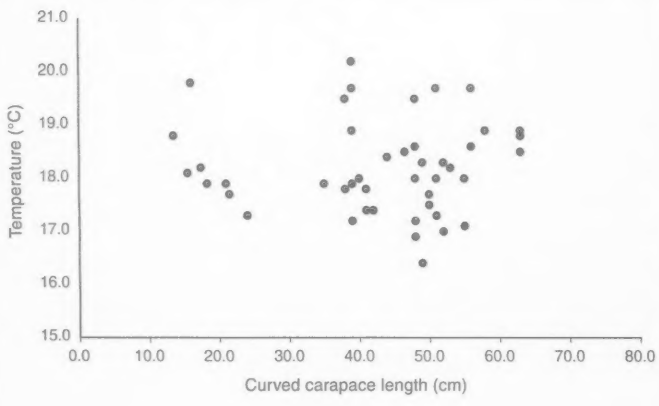

Figure 3

Relationship between curved carapace length (CCL, cm) of loggerhead sea turtles (*Caretta caretta*) and sea surface temperature (SST, n=52).

A taxonomic listing of diet items identified for the loggerhead sea turtles of the central North Pacific is shown in Table 1 along with frequency of occurrence and mean percent sample volume of each prey item. The six most common (frequent) prey items were identified. These included *Janthina* spp., which occurred in 75% of samples, and *Planes* spp., which occurred in 56% of samples. *Lepas* spp. occurred in 52% of the samples, and *Carinaria cithara* was found in 50% of samples. *Velella velella*, was found in 25% of the samples, and pyrosomas were found in 21% of samples (Table 1). Other common food items found in stomachs were fish eggs (25% of stomachs), salps, amphipods (46% of stomachs), small fish, and plastic items (35% of stomachs, Table 1). Some plastic items included small plastic beads, thin plastic sheets, polypropylene line, and even a small plastic fish, which had been an individual soy sauce container. Although *Velella*, pyrosomas, and salps were represented as prey items in our samples, other types of jellies may not have been well represented because their soft bodies may dissolve more quickly in stomach acids. It is also possible that unidentified jellies may comprise the unidentified remains, which occurred in 71% of stomachs and comprised 13.8% of total sample volume; however, a portion of the unidentified remains were likely masticated portions of identified prey items. Table 2 shows the mean percent prey item volumes for the six most common prey items. The six most common prey items can be ranked from largest to smallest mean volumes in

Table 1

Percent occurrence and percentage of total sample volume (volume of prey for all stomachs combined) for prey items (listed to lowest taxonomic order) found in loggerhead sea turtles (*Caretta caretta*, n=52 turtles).

Prey group	Occurrence (%)	Percent volume (%)
Carinaria cithara Benson 1835	50.0	43.8
Janthina spp. (includes *J. janthina* and *J. prolongata* = *J. globosa*)	75.0	14.4
Lepas spp. (includes *L.anserifera* Linnaeus 1767 and *L.anatifera anatifera* Linnaeus 1758)	51.9	6.7
Velella velella Linneaus 1758 (by-the-wind-sailor)	25.0	10.6
Planes spp. Dana 1852	55.8	1.2
Pyrosoma spp.	21.0	3.4
Fish eggs (*Hirundicthys speculiger* and unidentified spp.)	25.0	1.9
Cephalopoda (squid and octopus fragments and paralarvae)	21.2	0.5
Debris (plastic, styrofoam, paper, rubber, polypropylene, etc.)	34.6	0.3
Debris (wood, bird feathers)	11.5	<0.1
Salpidae	13.5	0.5
Family Sternoptychidae (hatchetfish)	7.7	0.1
Electrona sp.—Myctophidae	1.9	0.1
Gammaridea and Hyperiidea amphipods	46.2	<0.1
Thecosomate pteropods	13.5	<0.1
Cavolinia globulosa (Gray 1850)	11.5	<0.1
POLYCHAETA (polychaete worms)—Alciopidae	5.8	<0.1
ISOPODA	3.8	<0.1
MYSIDACEA—mysid	3.8	<0.1
Creseis sp.	1.9	<0.1
PHAEOPHYTA (brown algae)—*Cystoseira* sp.	1.9	<0.1
EUPHAUSIACEA—euphausiid	1.9	<0.1
Unidentified tunicate spp.	13.5	1.0
Unidentified jellies	13.5	0.5
Unidentified crustaceans	5.8	0.5
Unidentified remains	71.2	13.8

the following order: 1) *Carinaria cithara*, 2) *Pyrosoma* spp., 3) *Janthina* spp., 4) *Velella velella*, 5) *Lepas* spp., and 6) *Planes* spp.

Mean sample volume was 370.2 [±319.4] mL. Size of loggerhead sea turtles did not influence the volume of prey items for turtle sizes 35–70+ cm (F=0.11, r^2=0.05). However, the smaller turtles did have smaller volumes of prey items present in their stomachs, because all turtles 13–34 cm had less than 80 mL total stomach volume (Fig. 4). The size of the turtle did not appear to be a factor in the type of prey ingested. The one exception may be *Velella velella*. Turtles smaller than 30 cm CCL in our sample did not ingest this prey item, albeit sample size for less than 30-cm turtles was relatively small compared to the number of 40- and 50-cm size class turtles (Fig. 2); therefore, this apparent trend may not be the case for the general population.

Of the six most common prey items, *Carinaria cithara* had the highest percent sample volume, 43.8% of total sample volume. In general, percent volumes of *C. cithara* were high; 20 of the 27 turtle stomachs had percent volumes greater than 30% with this prey item and a number of stomachs had percent volumes greater than 90%. *Janthina* spp. had the next highest

Table 2

Mean percent volume and percent volume ranges for the six most frequently observed prey items found in driftnet captured loggerhead sea turtles (*Caretta caretta*).

Prey item	Mean percent volume	Standard deviation (±%)	Range
Janthina spp.	30.7%	34.8%	1–97%
Carinaria cithara	52.8%	33.1%	1–98%
Lepas spp.	19.1%	24.7%	1–99%
Velella velella	22.7%	29.4%	1–84%
Planes spp.	5.6%	10.1%	1–38%
Pyrosoma spp.	44.7%	33.7%	1–88%

percent sample volume at 14.4%. The percent volume of *Janthina* was generally high; 15 of 37 turtle stomachs had greater than 30% volume of this species. Only 4 of the 13 stomachs with *Velella velella* had greater than 30% sample volume; yet *Velella* made up almost 11% of total sample volume, and one of the stomach samples was almost entirely filled (84% volume) with *Velella* prey. In the samples that contained pyrosomas, this prey item often comprised a high percent of the total gut content—up to 88% stomach volume—and 7 out of 11 stomachs had greater than 30% stomach volume of pyrosomas. *Planes* spp. comprised more than 30% of stomach volume in only 2 of the 29 stomachs containing this species. *Lepas* spp. often occurred in very high percent volumes (up to 99% of total gut content in one sample), although only 6 of 21 stomachs had percent volumes greater than 30% for *Lepas*.

Discussion

Prey items

Loggerhead sea turtles in North Pacific oceanic habitats are opportunistic feeders that ingest items floating at or near the surface. Availability of prey in the oceanic realm is generally characterized as patchy. This means that the majority of the ocean contains little to no forage, but in some areas high densities of prey can be found. This unpredictability of prey availability likely contributes to the opportunistic feeding behavior of the loggerhead sea turtle. The TZCF, an area of convergence created within the subtropical frontal zone by cooler denser water masses converging and sinking below warmer lighter water masses (Roden, 1991), may serve to help concentrate different prey items. Prey items such as *Velella* can often concentrate in large numbers in such areas (Evans, 1986). All size classes of this sea turtle collected in our study were found between 16° and 21°C (Fig. 3), which typically are the temperatures that define the subtropical frontal zone and TZCF (Roden, 1991). Eighty-three percent of prey items that were recorded were found floating on the surface or were found on floating objects and would also likely be concentrated at convergent fronts such as the TZCF, driven there by the currents and winds (Polovina, et al., 2000; Polovina et al., 2004). It is suggested that this concentration of prey, along the convergent fronts, may be aggregating the loggerhead sea turtles traveling along this area, which are likely foraging on the increased densities of prey (Polovina et al., 2003a). Turtles in our study smaller than 30-cm CCL had very low volumes of prey in their stomachs. It is unknown whether the paucity of prey items in these turtle stomachs was related to the individual's size, e.g. they were physically not able to capture or ingest certain types of prey items, or perhaps to a lack of experience in foraging due to youth, given that turtles in this size range were determined to be between 1 and 4 years of age by Zug et al. (1995), or to other mitigating factors.

Another indication that loggerhead sea turtles are opportunistic feeders is the presence of oceanic, mesopelagic fish as prey items. The total number of fish (lanternfish and hatchetfish) in the samples was low (only 0.1 % of total stomach volume). These species of fish tend to stay below the photic zone usually at depths greater than 300 m during the day and migrate up near the surface at night. Lanternfish make diel vertical migrations where they reach maximum densities at 100 m at night. During nightly movements some species can also come directly to the surface (Hulley, 1990). Some species of hatchetfish also make diel vertical migrations, which would bring them to within 100 m of the surface at night (Weitzman, 1986; Froese and Pauly, 2003). Because of the low numbers, it is likely that loggerhead sea turtles ingest only dead or debilitated fish rather than actively hunt and chase such species. The presence of these species also indicates that the turtles may be feeding at night when they would be more likely to encounter the fish during their diel movement. Another prey item exhibiting diel vertical migration is the pyrosomas. Pyrosomas, which are a part of Pacific leatherback sea turtle diets (Davenport and Balazs, 1991), were also present in loggerhead sea turtle stomach samples. Pyrosomas are colonial tunicates comprising individual zooids embedded in the walls of a gelatinous tube. These colonies can become quite large (some greater that 4 meters in length) and tend to drift with ocean currents and accumulate along frontal zones which make them accessible to the sea turtle that forages opportunistically. At least one species (*P. atlanticum*) has been recorded to stay below 300 m during the

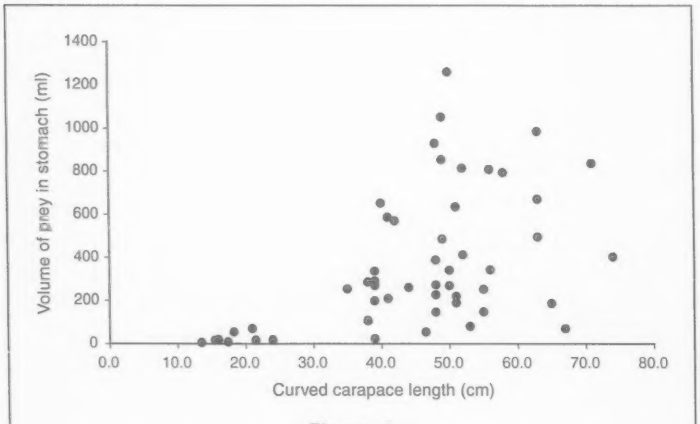

Figure 4

Relationship between curved carapace length (CCL, cm) of loggerheads (*Caretta caretta*) and stomach volume (mL, n=52)

day and move up near the surface at night (Andersen and Sardou, 1994); this activity again may indicate active night foraging by the loggerhead sea turtle.

Loggerhead sea turtles may feed by swallowing floating prey whole and also by biting whole prey (or portions off a whole prey) found on large floating objects. A commonly ingested prey item, *Velella velella*, known as "by-the-wind-sailor" (Eldredge and Devaney, 1977), typically was found intact. *Janthina* spp., predatory gastropods whose main prey item is *Velella velella*, were also frequently found whole in stomachs. Small *Janthina* spp. have been observed directly on *Velella*, and it has been hypothesized that *Janthina* use *Velella* to settle on and use the *Velella* as floatation until they become too large for the host (Bayer, 1963). This behavior may be a reason why whole *Janthina* and *Velella* were often found together in stomach samples. *Janthina* spp. had been previously noted as a prey item of loggerhead sea turtles in the Azores and South Africa (Dodd, 1988) but was first identified as a prey item in the Pacific Ocean in a preliminary unpublished report by Cooke in 1992[2]—data that are included in the present study. The high frequency of occurrence of *Velella velella* and whole *Janthina* spp. support the hypothesis that loggerhead sea turtles will feed on the surface, swallowing their prey whole. Distribution of *Velella velella* is patchy; densities range from <1/1000 m^3 to 1000/1000 m^3 and densities of *Janthina* spp. are considerably less than those of *Velella*. When optimum combinations of prevailing winds and currents converge, densities of *Velella velella* have been observed to be in concentrations upward of 10,000/1000 m^2, forming patches so large and dense they have been likened to oil tanker sludge by mariners (Evans, 1986; Parker, personal observ.). It is possible that the one turtle that had a stomach volume of 84% *Velella* found one of these patches on which to feed. *Velella velella* was the one common prey item that was not found in stomachs of turtles less than 30-cm CCL. Because *Velella* were commonly swallowed whole, it is possible that an average size *Velella*, which range from 5 to 10 cm (Evans, 1986), might have been too large for a 13–29 cm CCL turtle to swallow whole.

The epibiotic oceanic crabs and the gooseneck barnacles (*Lepas* spp.) usually occur on floating objects; *Planes* sometimes even rides on *Velella* (Chace, 1951). *Planes* spp. also have been observed and collected from the tail area of loggerhead sea turtle themselves (Davenport, 1994; NMFS observers[3]). Although approximately 80% of stomach samples with *Planes* spp. contained whole crabs, which were identified as *P. cyaneus*, there were also numerous masticated crabs and pieces of crabs. These pieces could have been *P. marinus* because whole specimens are necessary to identify *Planes* spp. (Spivak and Bas, 1999); therefore the lowest taxonomic identification for this study was limited to *Planes* spp. Densities of *Planes* spp. and *Lepas* spp. are not well documented but are likely limited by the amount of substrate on which they can settle or on the amount of floating objects available. Natural drifting objects such as tree logs or pumice from volcanic eruptions have been documented since the nineteenth century (Kew, 1893, cited in Jokiel, 1990). The "floating islands," as they have been called, continue to be important for transporting organisms, from corals to reef fish across the oceans (Jokiel, 1990). Man-made objects also supply substrate and habitat on which different organisms can settle. Buoys and logs that wash ashore often have *Lepas* spp. attached to them, some with *Lepas* spp. covering 100% of the area that was underwater (Parker, personal observ.). Although the frequency of occurrence of *Planes* spp. in stomach samples was high, the percent sample volume of *Planes* was relatively low (1.2% total volume) and the mean volume of *Planes* found was also low (5.6%, Table 2), indicating that this prey was either taken opportunistically or accidentally. It is not known whether the *Planes* were ingested along with other prey items or were actually grazed from larger floating objects. In contrast, *Lepas* spp. often occurred in very high percent volumes, indicating that the turtles were actively grazing these prey. The constant presence of *Lepas* spp. in samples strongly supports the hypothesis that loggerhead sea turtles feed not only by swallowing prey whole, but also by biting prey off larger floating objects. Small chunks of Styrofoam were still attached to the bases of some *Lepas* specimens indicating that the turtle had bitten off some of the floating object itself while grazing on prey found on the floating debris.

Among other floating items that often occurred in the turtles' stomachs, one common element was fish eggs. Some of these fish eggs were identified as *Hirundicthys speculiger* or flying fish eggs. Amphipods were another common item but comprised a very small fraction of total gut content (<1%), indicating that they were not a targeted prey item. Amphipods were possibly ingested incidentally as epiphytes on other items or as part of the gut contents of other prey items. The proportion of man-made drift debris in our sample was low in contrast to prior studies (Balazs, 1985; Allen, 1992; Bjorndal et al., 1994; Kamezaki, 1994; Tomas et al., 2002). Plastics and other man-made debris were commonly found, occurring in about 35% of stomachs, but they comprised a very small fraction of the total gut content (<1%).

Loggerhead sea turtles also actively forage at deeper depths if high densities of prey items are present. An initial study of pelagic dive behavior of this species (Polovina et al., 2003) indicates that they regularly dive down to depths of 100 m and may also forage at those depths, which may account for the high frequency of occurrence and high total percent volume of

[2] Cooke, W. J. 1992. A taxonomic analysis of stomach contents from loggerhead turtles (*Caretta caretta*). AECOS report no. 697, 12 p. Prepared for NOAA, NMFS, Honolulu Laboratory, 2570 Dole Street, Honolulu, Hawaii 96822. [Available from AECOS, Inc., 45-939 Kamehameha Hwy., Rm. 104, Kaneohe, Hawaii 96744.]

[3] NMFS (National Marine Fisheries Service) observers. 1997–2000. Personal commun. Pacific Islands Fisheries Science Center. 2570 Dole Street, Honolulu, HI 96822-2396.

the heteropod *Carinaria cithara*. Okutani (1961) first recorded sea turtles consuming *Carinaria* (including *Carinaria cithara*, Benson 1835), in the western North Pacific. Heteropods are found in the upper photic zone (within 100 m of the surface) but are not typically a neustonic or floating species. Recorded heteropod densities in the Pacific are variable (<1/1000 m^3 to 150/1000 m^3, Seapy, 1974, cited in Lalli and Gilmer, 1989). Although these densities seem very low, it is clear that in this area of the central North Pacific heteropods are numerous enough within diving depths of loggerhead sea turtles to make this an attractive prey item for the turtles.

Conclusion—Interactions with fisheries

The bycatch of nontargeted species in different fisheries has been an issue for many years (Wetherall et al., 1993; Wetherall, 1996; Gardner and Nichols, 2001; Suganuma[4]). Bycatch of sea turtles has also been an issue for the conservation management of most sea turtle species. Sea turtle mortalities have occurred in nearly all fisheries (gillnet, driftnet, trawl, and longline). During their transpacific migrations loggerhead sea turtles move through areas of multinational longline fishing (Lewison et al., 2004). Mortalities of sea turtles after longline fishery interactions have been estimated between 28% and 50% by both U.S. and Japanese researchers (Nishemura and Nakahigashi, 1990; Kleiber,[5] McCracken[6]) and loggerhead sea turtles comprise a large percentage of the sea turtle interactions in longline fisheries, as high as 59% of sea turtles captured in the Hawaii-based longline fleet. The longline fishery as well as various other fisheries in the Pacific (Gardner and Nichols, 2001) have been implicated as part of the reason for recent declines in the loggerhead sea turtle populations both in Japan (Kamezaki and Matsui, 1997; Sato et al., 1997; Suganuma[4]) and also in Australia, and southern nesting areas (Limpus and Couper, 1994; Limpus and Reimer[7]). Research on feeding behavior may help with the mitigation of fisheries interactions.

Learning more about the life history of loggerhead sea turtles and understanding more about the movements, foraging behavior, and prey of these turtles are important for making well-informed management decisions because foraging behavior may change as seasons change and as these turtles move through different habitats (Bjorndal, 1997). Although our study indicates that these turtles forage mainly on floating or near-surface prey in the open ocean, studies in different areas show different feeding habits. The oceanic, near-surface feeding behavior of loggerhead sea turtles is likely one reason for the numerous longline fishery interactions in the central North Pacific. The recorded dive data for these turtles indicate that they spend a large percentage of their time near the surface—as much as 78% of their time is spent within 10 m of the surface (Polovina et al., 2003b). Juvenile loggerhead sea turtles are rarely found in the waters adjacent to Japan (Uchida, 1973); the juvenile turtles are thought to use the Kuroshiro Current to move out into the Pacific and the southern edge of the Subartic Gyre during their eastward movement toward foraging grounds in the Eastern Pacific (Bowen et al., 1995). In the Atlantic, however, small neonate loggerhead sea turtles have been found associated with drifts of floating material, especially *Sargassum* rafts (Witherington, 2002), and although large, regular drifts of floating material are rare in the Pacific, small loggerhead sea turtles may also be associated with floatsam (Pitman, 1990).

Studies have indicated that foraging changes throughout the lifecycle of loggerhead sea turtles (van Nierop and den Hartog, 1984; Plotkin et al., 1993; Godley et al., 1997; Tomas et al., 2001). In the Pacific, oceanic immature turtles (present study) forage on different prey from that foraged by subadults in the pelagic and neritic areas off Baja California (Nichols et al., 2000; Peckham and Nichols, 2003; Seminoff et al., 2004), and adults in benthic neritic habitats, in turn, forage on different prey near Japan and China (Hitase et al., 2002). Japanese loggerhead sea turtles foraging in the Eastern Pacific target *Pleuroncodes planipes*, the pelagic red crab, which occurs year round off Baja California. These turtles interact with the artisanal fisheries in the area which are both pelagic and benthic fisheries (Gomez-Gutierrez and Sanchez-Ortiz, 1997; Bartlett, 1998; Gomez-Gutierrez et al., 2000; Peckham and Nichols, 2003). Loggerhead sea turtles have also been found on the Gulf of California side of Baja California, likely foraging on the large abundance of invertebrate fauna found there (Brusca, 1980), and these turtles face fishing pressure from the artisanal gillnet fishery in this area (Seminoff et al., 2004).

[4] Suganuma, H. 2002. Population trends and mortality of Japanese loggerhead turtles, *Caretta caretta*, in Japan. *In* Proc. Western Pacific Sea Turtle Coop. Res. and Mgmt. Workshop (I. Kinan, ed.), p. 74–77. Western Pacific Regional Fishery Management Council, 1164 Bishop Street, Suite 1400, Honolulu, HI 96813.

[5] Kleiber, P. 1998. Estimating annual takes and kills of sea turtles by the Hawaiian longline fishery, 1991–1997, from observer program and logbook data. Administrative report H-98-08, 21 p. Southwest Fisheries Science Center, Nat. Mar. Fish. Serv., NOAA, 2570 Dole St., Honolulu, HI 96822.

[6] McCracken, M. L. 2000. Estimation of sea turtle take and mortality in the Hawaiian longline fisheries. Administrative report H-00-06, 29 p. Southwest Fisheries Science Center, Nat. Mar. Fish. Serv., NOAA, 2570 Dole St., Honolulu, HI 96822.

[7] Limpus, C. J., and D. Reimer. 1994. The loggerhead turtle, *Caretta caretta*, in Queensland: a population in decline. *In* Proceedings of the Australian marine turtle conservation workshop (R. James, compiler), p. 39–59. Queensland Dep. Environ and Heritage and Aust. Nat. Conserv. Agency, GPO Box 787, Canberra ACT 2601, Australia.

Converting CCL to straight carapace length (SCL; using the conversion equation: $CCL=1.388+(1.053)\ SCL$, in Bjorndal et al., 2000), size classes found in our study ranged from 11.5 cm to 68.9 cm SCL with a mean of 41.2 [±12.4] cm SCL. The East Pacific recruits were slightly larger with means of 46.9–61.9 cm SCL (Seminoff et al., 2004). Most of these turtles were immature to subadult turtles, and only a few were adult-size turtles. According to Zug et al. (1995), the loggerhead sea turtles recruiting to the nearshore and neritic habitats of Baja California are likely 10 years of age or older, indicating that these turtles might spend as many as 10 years before arriving at their East Pacific foraging habitat. After returning to the West Pacific, satellite telemetry has found that adult loggerhead sea turtles also reside in both neritic and pelagic habitats (Baba et al., 1992, 1993; Kamezaki et al., 1997; Sakamoto et al., 1997) putting them at risk of interaction with nearshore gillnet fisheries as well as pelagic longline fisheries. Hitase et al. (2002) found a size difference between adults in neritic and oceanic habitats—the postnesting females that chose oceanic habitats were smaller (mainly <80.0 cm) than those that used neritic habitats for postnesting foraging—and also suggested that some adult turtles may not recruit to neritic areas near Japan and China. This may be evidence that some loggerhead sea turtles remain in the oceanic habitat their whole life cycle, returning nearshore only to mate or nest. In the Atlantic, juveniles as well as adults of this species can be found in neritic foraging habitats of the Gulf of Mexico, and these turtles can have interactions with coastal trawl and other coastal fisheries in the area (Plotkin et al., 1993). Juvenile turtles have also been observed and captured in areas along the eastern coast of the United States where they have been found feeding on benthic invertebrates (Burke et al., 1990; Epperly et al., 1990). Very small, neonate loggerhead sea turtles have been found associating with and foraging in *Sargassum* drifts while they are transported by the Gulf Stream into the mid-Atlantic (Witherington, 2002); therefore, the harvest of *Sargassum* or trawling through this area would affect these juveniles. There is some evidence that juvenile Atlantic loggerhead sea turtles may move between coastal and pelagic forage habitats, which would expose them to both coastal and pelagic fisheries (Witzell, 2002). In the Mediterranean, both juvenile and adult loggerhead sea turtles also have variety of foraging behaviors. In the eastern Mediterranean, postpelagic juveniles and adults forage mainly in neritic habitats on benthic prey items where they would interact with coastal trawl and other artesianal fisheries (Godley et al., 1997). In the western Mediterranean, juvenile turtles of this species forage in both pelagic as well as neritic habitats, where they are at risk of fishery interactions in many different fisheries including longline, trawling, and coastal fisheries (Tomas et al., 2001). Postpelagic juveniles in the Mediterranean may be recruits from the Atlantic Ocean or may come from the endemic Mediterranean population. Adult loggerhead sea turtles have been noted to also move between the eastern and western basins of the Mediterranean in response to seasonal temperature changes (Bentivegna, 2002). During this migration between two benthic feeding areas, some of the turtles would spend extensive amounts of time in the pelagic habitat likely foraging on pelagic prey items. This intra-Mediterranean movement puts these turtles at risk of interactions with a multinational fishery contingent of pelagic as well as coastal fisheries (Bentivegna, 2002).

One possible way to mitigate increased fisheries interactions in the Pacific and other areas might be to identify specific loggerhead foraging areas for protection, such as the area around Baja California, Mexico. In the central North Pacific, our study (Fig. 1), as well as recent satellite tracking studies of juvenile and adult loggerhead sea turtles (Hitase et al., 2002; Parker et al., 2003; Polovina et al., 2004), has indicated that the area west of and around the Emperor seamounts, between 160° and 180°E might also be an important foraging habitat. Most of the turtles in our study were collected from this area (Fig. 1) and one juvenile spent 10 months west of the Emperor Seamounts, between 160° and 170°E, before its satellite transmitter stopped transmitting data (Parker et al., 2003). In this area, the southern edge of the Kuroshiro Extension Current forms numerous eddies that are semipermanent features throughout the year. Reduction of fishing effort or other fishery mitigation techniques in this area may greatly decrease the number of fisheries interactions that Pacific loggerhead sea turtles experience. International cooperation is needed in order to manage these foraging habitats. More studies also need to be done on the ecology of these turtles so that fishery interactions at all life stages can be addressed and so that a total picture of the life history of this species can be obtained.

Acknowledgments

We would like to acknowledge the hard work of all the NMFS fishery observers for obtaining the samples, Russ Miya and Bryan Winton for their help in the initial sorting, and Mike Seki and Kevin Landgraf for their help in identifying prey items. We would also like to acknowledge the review and comments of Alan Bolten, Jeffrey Seminoff, George Antonelis, Jerry Wetherall, Colin Limpus, Judith Kendig, Francine Fiust, Shawn Murakawa, and two anonymous reviewers.

Literature cited

Allen, W.
1992. Loggerhead dies after ingesting marine debris. Mar. Turtle Newsl. 58:10.

Andersen, V., and J. Sardou.
1994. *Pyrosoma atlanticum* (Tunicata, Thaliacea): diel migration and vertical distribution as a function of colony size. J. Plankton Res. 16(4):337–349.

Baba, N., M. Kiyota, H. Suganuma, and H. Tachikawa.
1992. Research on migratory routes of loggerhead turtles and green turtles by the Argos system. Report on commissioned project for data analysis by scientific observers aboard fishing vessels in 1991. Fish. Agency Jpn., Tokyo, p. 89–99. [In Japanese.]
1993. Research on migratory routes of loggerhead turtles and green turtles by the Argos system. Report on commissioned project for data analysis by scientific observers aboard fishing vessels in 1992. Fish. Agency of Jpn, Tokyo, p. 86–99. [In Japanese.]

Balazs, G.
1989. New initiatives to study sea turtles in the eastern Pacific. Mar. Turtle Newsl. 47:19–21.
1985. Impact of ocean debris on marine turtles: entanglement and ingestion. *In* R.S. Shomura and H.O. Yoshida (eds.), Proceedings of the workshop on the fate and impact of marine debris, 26–29 November 1984, Honolulu, Hawaii, p. 387–429. NOAA Tech. Memo. NMFS, NOAA-TM-SWFC-54.

Bartlett, G.
1989. Juvenile *Caretta* off Pacific coast of Baja California. Not. Caguamas 2:2–10.

Bayer, F. M.
1963. Observations on pelagic mollusks associated with siphonophores *Velella* and *Physalia*. B. Mar. Sci. 13(3):454–466.

Bentivegna, F.
2002. Intra-Mediterranean migrations of loggerhead sea turtles (*Caretta caretta*) monitored by satellite telemetry. Mar. Biol. 141: 795–800.

Bjorndal, K. A.
1997. Foraging ecology and nutrition of sea turtles. *In* The biology of sea turtles (P. Lutz and J. Musick, eds.), p. 199–32. CRC Press, Boca Raton, FL.
1999. Priorities for research in foraging habitats. *In* Research and management techniques for the conservation of sea turtles (K. L. Eckert, K. A. Bjorndal, F. A. Abreu-Grobois, and M. Donnely, eds.), p. 12–18. IUCN (International Union for the Conservation of Nature and Natural Resources)/SSC (Species Survival Commision), Mar. Turtle Spec. Group Publ. No. 4, Washington, DC.

Bjorndal, K. A., A. B. Bolten, and C. J. Lagueux.
1994. Ingestion of marine debris by juvenile sea turtles in coastal Florida habitats. Mar. Pollut. Bull. 28: 154–158.

Bjorndal, K. A., A. B. Bolten, and H. R. Martins.
2000. Somatic growth model of juvenile loggerhead sea turtles *Caretta caretta*: duration of pelagic stage. Mar. Ecol. Prog. Ser. 202: 265–272.

Bowen, B. W., F. A. Abreu-Grobois, G. H. Balazs, N. Kamezaki, C. J. Limpus and R. J. Ferl.
1995. Trans-Pacific migrations of the loggerhead turtle (*Caretta caretta*) demonstrated with mitochondrial DNA markers. Proc. Natl. Acad. Sci. 92: 3731–3734.

Brusca, R. C.
1980. Intertidal invertebrates of the Gulf of California, 513 p. Univ. Arizona Press, Tucson, AZ.

Burke, V. J., S. J. Morreale, and E. A. Standora.
1990. Comparisons of diet and growth of Kemp's Ridley and loggerhead turtles from the Northeastern U.S. *In* Proceedings of the tenth annual workshop on sea turtle biology and conservation (T. H. Richardson, J. I. Richardson, and M. Donnelly (comps.), p. 135. NOAA Tech. Memo NMFS-SEFC-278.

Chace, F. A.
1951. The oceanic crabs of the genera *Planes* and *Pachygrapus*. Proc. U.S. Natl. Mus. 101:65–103.

Chaloupka, M.
1998. Polyphasic growth in pelagic loggerhead sea turtles. Copeia 1998(2):516–518.

Davenport, J.
1994. A cleaning association between the oceanic crab (*Planes minutus*) and the loggerhead sea turtle (*Caretta caretta*). J. Mar. Biol. Assoc. UK 74(3):735–737.

Davenport, J., and G. H. Balazs.
1991. Fiery Bodies: Are pyrosomas an important component of the diet of leatherback turtles. Brit. Herpt. Soc. 37:33–38.

Dodd, C. K., Jr.
1988. Synopsis of the biological data on the loggerhead sea turtle *Caretta caretta* (Linnaeus 1758). U.S. Fish Wildl. Serv. Biol. Rep. 88(14), 110 p.

Dutton, P. H., G. H. Balazs, and A. E. Dizon.
1998. Genetic stock identification of sea turtles caught in the Hawaii-based pelagic longline fishery. *In* Proceedings of the seventeenth annual sea turtle symposium (S. P. Epperly and J. Braun, compilers), p. 43. NOAA Tech. Memo. NMFS-SEFSC-415.

Eldredge, L. G., and D. M. Devaney.
1977. Other hydrozoans. *In* Reef and shore fauna of Hawaii, Sec.1: Protozoa through Ctenophora. B. P. Bishop Mus. Spec. Publ. 64(1):105–107.

Epperly, S. P., J. Braun, and A. Veishlow.
1990. Distribution and species composition of sea turtles in North Carolina. *In* Proceedings of the tenth annual workshop on sea turtle biology and conservation (T. H. Richardson, J. I. Richardson, and M. Donnelly (comps.), p. 95–96. NOAA Tech. Memo NMFS-SEFC-278.

Evans, F.
1986. *Velella velella* (L.), the 'by-the-wind-sailor,' in the North Pacific Ocean in 1985. Mar. Obs. 56(7): 196–200.

Forbes, G. A.
1999. Diet sampling and diet component analysis. *In* Research and management techniques for the conservation of sea turtles (K. L. Eckert, K. A. Bjorndal, F. A. Abreu-Grobois, and M. Donnelly, eds.), p. 144–148. IUCN/SSC Mar. Turtle Spec. Group Publ. no. 4., Washington, D.C.

Frazier, J.
1985. Misidentification of sea turtles in the East Pacific: *Caretta caretta* and *Lepidochelys olivacea*. J. Herpetol. 1:1–11.

Froese, R., and D. Pauly, eds.
2003. FishBase. World Wide Web electronic publication. www.fishbase.org. [Accessed 6 March 2004.]

Gardner, S. C., and W. J. Nichols.
2001. Assessment of sea turtle mortality rates in the Bahia Magdalena region, Baja, California Sur, México. Chel. Cons. Biol. 4:197–199.

Godley, B. J., S. M. Smith, P. F. Clark, and J. D. Taylor.
1997. Molluscan and crustacean items in the diet of the loggerhead turtle, *Caretta caretta* (Linnaeus, 1758) [Testudines: Chelonidae] in the eastern Mediterranean. J. Molluscan Stud. 63:474–476.

Gomez-Gutierrez, J., E. Dominguez-Hernandez, C. J. Robinson, and V. Arenas.
2000. Hydroacoustical evidence of autumn inshore residence of the pelagic red crab *Pleuroncodes planipes* at Punta Eugenia, Baja California, Mexico. Mar. Ecol. Prog. Ser. 208:283–291.

Gomez-Gutierrez, J., and C. A. Sanchez-Ortiz.
1997. Larval drift and population structure of the pelagic phase of *Pleuroncodes planipes* (Stimpson) (Crustacea: Galatheidae) off the southwest coast of Baja California, Mexico. B. Mar. Sci. 61(2):305–325.

Hitase, H., N. Takai, Y. Matsuzawa, W. Sakamoto, K. Omuta, K. Goto, N. Arai, and T. Fujiwara.
2002. Size-related differences in feeding habitat use of adult female loggerhead turtles *Caretta caretta* around Japan determined by stable isotope analyses and satellite telemetry. Mar. Ecol. Prog. Ser. 233: 273–281.

Hulley, P. A.
1990. Myctophidae. *In* Fishes of the Southern Ocean (O. Gon and P. C. Heemstra, eds.), p. 146–178. J. L. B. Smith Institute of Ichthyology, Grahamstown, South Africa. [ref. 5182 from website FishBase: www.fishbase.org.]

Jokiel, P. L.
1990. Long-distance dispersal by rafting: reemergence of an old hypothesis. Endeavour, New Series. 14(2):66–73.

Kamezaki, N.
1994. Review of quantitative data on plastic debris found in the intestine (*sic*) of the sea turtle. Umigame Newsl. 22: 9–14. [In Japanese.]

Kamezaki, N., and M. Matsui.
1997. A review of biological studies on sea turtles in Japan. Jpn. J. Herpetol. 17(1):16–32.

Kamezaki, N., I. Miyawaki, H. Suganuma, K. Omuta, Y. Nakajima, K. Goto, K. Sato, Y. Matsuzawa, M. Samejima, M. Ishii, and T. Iwamoto.
1997. Post-nesting migration of Japanese loggerhead turtle, *Caretta caretta*. Wildl. Conserv. Jpn. 3:29–39. [In Japanese with English abstract.]

Lalli, C. M., and R. W. Gilmer.
1989. Pelagic snails: the holoplanktonic gastropod mollusks, 259 p. Stanford Univ. Press, Stanford, CA.

Lewison, R. L., S. A. Freeman, and L. D. Crowder.
2004. Quantifying the effects of fisheries on threatened species: the impact of pelagic longlines on loggerhead and leatherback sea turtles. Ecol. Lett. 7(3):221–231.

Limpus, C. J., and P. Couper.
1994. Loggerheads: a species in decline. Wildl. Aust. 30:11–13.

Márquez, M. R., and A. O. Villanueva.
1982. Situación actual y recomendaciones para el manejo de las tortugas marinas de la costa occidental de México, en especial la tortuga golfina *Lepidochelys olivacea*. Cienc. Pesquera INP 2:83–91.

Nichols, W. J., A. Resendiz, and C. Mayoral-Russeau.
2000. Biology and conservation of loggerhead turtles in Baja California, Mexico. *In* Proceedings of the nineteenth annual symposium on sea turtle biology and conservation (H. J. Kalb and T. Wibbels, comps), p. 169–171. NOAA Tech. Memo. NMFS-SEFSC-443.

Nishemura W., and S. Nakahigashi.
1990. Incidental capture of sea turtles by Japanese research and training vessels: results of a questionnaire. Mar. Turtle Newsl. 51:1–4.

Okutani, T.
1961. Notes on the genus *Carinaria* (Heteropoda) from Japanese and adjacent waters. Publs. Seto Mar. Biol. Lab. 9:333–353.

Parker, D. M., J. Polovina, G. H. Balazs, and E. Howell.
2003. The lost years: long-term movement of a maturing loggerhead turtle in the northern Pacific Ocean. *In* Proceedings of the twenty-second annual symposium on sea turtle biology and conservation (J. A. Seminoff, comp.), p. 294–296. NOAA Tech. Memo. NMFS-SEFSC-503.

Peckham, H., and W. J. Nichols.
2003. Why did the turtle cross the ocean? Pelagic red crabs and loggerhead turtles along the Baja California coast. *In* Proceedings of the twenty-second annual symposium on sea turtle biology and conservation (J. A. Seminoff, comp.), p. 47. NOAA Tech. Memo. NMFS-SEFSC-503.

Pitman, R. L.
1990. Pelagic distribution and biology of sea turtles in the Eastern Tropical Pacific. *In* Proceedings of the tenth annual workshop on sea turtle biology and conservation (T. H. Richardson, J. I. Richardson, and M. Donnelly, comps.), p. 143–148. 1. NOAA Tech. Memo. NMFS-SEFC-278.

Plotkin, P. T., M. K. Wicksten, and A. E. Amos.
1993. Feeding ecology of the loggerhead sea turtle *Caretta caretta* in the Northwestern Gulf of Mexico. Mar. Biol. 115:1–15.

Polovina, J. J., G. H. Balazs, E. A. Howell, D. M. Parker, M. P. Seki, and P. H. Dutton.
2004. Forage and migration habitat of loggerhead (*Caretta caretta*) and olive ridley (*Lepiodchelys olivacea*) sea turtles in the central North Pacific Ocean. Fish. Oceanogr. 13:36–51.

Polovina, J. J., E.A. Howell, D. M. Parker, and G. H. Balazs.
2003. Dive depth distribution of loggerhead (*Caretta caretta*) and olive ridley (*Lepiodchelys olivacea*) turtles in the central North Pacific Ocean: Might deep longline sets catch fewer turtles. Fish. Bull. 101: 189–193.

Polovina, J. J., D. R. Kobayashi, D. M. Parker, M. P. Seki and G. H. Balazs.
2000. Turtles on the edge: movement of loggerhead turtles (*Caretta caretta*) along oceanic fronts spanning longline fishing grounds in the Central North Pacific, 1997–1998. Fish. Oceanogr. 9:71–82.

Resendiz, A., B. Resendiz, W. J. Nichols, J. A. Seminoff, and N. Kamezaki.
1998. First confirmed east-west transpacific movement of a loggerhead sea turtle, *Caretta caretta*, released in Baja California, Mexico. Pac. Sci. 52(2):151–153.

Roden, G. I.
1991. Subartic-subtropical transition zone of the North Pacific: large-scale aspects and mesoscale structure. *In* Biology, oceanography, and fisheries of the North Pacific Transition Zone and Subartic Frontal Zone (J. A. Wetherall, ed.), p. 1–38. NOAA Tech Rep. NMFS, SWFSC 105.

Sakamoto, W., T. Bando, N. Arai, and N. Baba.
1997. Migration paths of adult female and male loggerhead turtles, *Caretta caretta*, determined through satellite telemetry. Fisheries Sci. 63:547–552.

Sato, K., T. Bando, Y. Matsuzawa, H. Tanaka, W. Sakamoto, S. Minamikawa, and K. Goto.
1997. Decline of the loggerhead turtle, *Caretta caretta*, nesting on Senri beach in Minabe, Wakayama, Japan. Chel. Conserv. Biol. 2:600–603.

Seminoff, J. A., A. Resendiz, B. Resendiz, and W. J. Nichols.
2004. Occurrence of loggerhead sea turtles (*Caretta caretta*) in the Gulf of California, Mexico: evidence of life-history variation in the Pacific Ocean. Herpetol. Rev. 35(1):24–27.

Spivak, E. D., and C. C. Bas.
1999. First finding of the pelagic crab *Planes marinus* (Decapod: Grapsidae) in the Southwestern Atlantic. J. Crustacean Biol. 19(1):72–26.

Tomas, J., F. J. Aznar, and J. A. Raga.
2001. Feeding ecology of the loggerhead turtle *Caretta caretta* in the western Mediterranean. J. Zool. Lond. 255:525–532.

Tomas, J., R. Guitart, R. Mateo, and J. A. Raga.
2002. Marine debris ingestion in loggerhead sea turtles, *Caretta caretta*, from the western Mediterranean. Mar. Poll. Bull. 44:221–216.

Uchida, I.
1973. Pacific loggerhead turtle—pursuing its mysterious oceanic life. Anima 1(3):5–17. [In Japanese.]

Weitzman, S. H.
1986. Sternoptychidae. *In* Smith's sea fishes (M. M. Smith and P. C. Heemstra, eds.), p. 253–259. Springer-Verlag, Berlin.

Wetherall, J. A.
1996. Assessing impacts of Hawaiian longline fishing on Japanese loggerheads and Malaysian leatherbacks: some exploratory studies using TURTSIM. *In* Status of marine turtles in the Pacific Ocean relevant to incidental take in the Hawaii-based pelagic longline fishery (A. Bolten, J. A. Wetherall, G. H. Balazs, and S. G. Pooley, comps.), p. 57–75. NOAA Tech. Memo. NMFS-SWFSC-230.

Wetherall, J. A., G. H. Balazs, R. A. Tokunaga, and M. Y. Y. Yong.
1993. Bycatch of marine turtles in North Pacific high-seas driftnet fishery and impacts on stock. *In* INPFC symposium on biology, distribution, and stock assessment of species caught in the high seas driftnet fishery in the North Pacific Ocean, 53(III) (J. Ito et al., eds.), p. 519–538. Int. N. Pac. Fish. Comm., Vancouver, Canada.

Witherington, B. E.
2002. Ecology of neonate loggerhead turtles inhabiting lines of downwelling near a Gulf Stream front. Mar. Biol. 140:843–853.

Witzell, W. N.
2002. Immature Atlantic loggerhead turtles (*Caretta caretta*): suggested changes to the life history model. Herpetol. Rev. 33:266–269.

Van Nierop, M. M., and J. C. den Hartog.
1984. A study of the gut contents of five juvenile loggerhead turtles, *Caretta caretta* (Linnaeus) (Reptilia Cheloniidae), from the south-Eastern part of the North Atlantic Ocean, with emphasis on coelenterate identification. Zool. Meded. Leiden 59:35–54.

Zug, G. R., G. H. Balazs, and J. A. Wetherall.
1995. Growth in juvenile loggerhead sea turtles (*Caretta caretta*) in the North Pacific pelagic habitat. Copeia 2:484–487.

Indirect validation of the age-reading method for Pacific cod (*Gadus macrocephalus*) using otoliths from marked and recaptured fish

Nancy E. Roberson
Daniel K. Kimura
National Marine Fisheries Service, NOAA
Alaska Fisheries Science Center
7600 Sand Point Way, NE
Seattle, Washington 98115
E-mail address (for N. E. Roberson): Nancy.Roberson@noaa.gov

Donald R. Gunderson
University of Washington
School of Aquatic and Fishery Sciences
1122 N.E. Boat Street
Seattle, Washington 98105

Allen M. Shimada
National Marine Fisheries Service, NOAA
Office of Research
1315 East-West Hwy
Silver Spring, Maryland 20910-3282

Abstract—Two examples of indirect validation are described for age-reading methods of Pacific cod (*Gadus macrocephalus*). Aging criteria that exclude faint translucent zones (checks) in counts of annuli and criteria that include faint zones were both tested. Otoliths from marked and recaptured fish were used to back-calculate the length of each fish at the time of its release by using measurements of the area of annuli. Estimated fish size at time of release and actual observed fish size were similar, supporting the assumption that translucent zones are laid down on an annual basis. A second method for validating reading criteria used otolith age and von Bertalanffy parameters, estimated from the tagging data, to predict how much each fish grew in length after tagging. We found that otolith aging criteria applied to otoliths from tagged and recovered Pacific cod predicted quite accurately the growth increments that we observed in these specimens. These results provide further evidence that the current aging criteria are not underestimating the age of the fish and support our current interpretation of checks (i.e., as subannual marks). We expect these indirect validations to advance age determination for Pacific cod, which in turn would enhance development of stock assessment methods based on age structure for this species in the eastern Bering Sea.

Manuscript submitted 7 November 2002 to the Scientific Editor's Office.
Manuscript approved for publication 20 September 2004 by the Scientific Editor.
Fish. Bull. 103:153–160 (2005).

Pacific cod (*Gadus macrocephalus* Tilesius, 1810) is an important species in eastern Bering Sea commercial fisheries and is second only to walleye pollock (*Theragra chalcogramma*) in landings (Thompson and Dorn[1]). It is also considered to be one of the most difficult of all commercially important Alaska groundfish species to age. Scientists from both Canada and the United States have experienced similar difficulties in finding an appropriate aging structure, which can be consistently interpreted to track large year classes of cod through time. Historically, scales and otoliths have been the two most common structures used for determining the ages of fish species. Unfortunately, age-readers employing these structures have experienced limited success in the case of Pacific cod (Kimura and Lyons, 1990).

The Pacific Biological Station in Canada stopped aging Pacific cod in 1978, after age estimates derived from scale readings began yielding year classes that were inconsistent with length-frequency time series from field surveys (Westrheim and Shaw, 1982). The Alaska Fisheries Science Center's (AFSC) Resource Ecology and Fisheries Management (REFM) Division is responsible for stock assessment of Pacific cod in the Gulf of Alaska and eastern Bering Sea. The REFM Division's Age and Growth Program used scales for determining the age of Pacific cod from 1976 to the early 1980s. Thereafter, the program used the break-and-burn method with otoliths to age Pacific

[1] Thompson, G. G., and M. W. Dorn. 1999. Pacific cod. *In* Stock assessment and fishery evaluation report for the groundfish resources for the Bering Sea/Aleutian Islands regions (plan team for groundfish fisheries of the Bering Sea/Aleutian Islands), p. 151–205. North Pacific Fishery Management Council, 605 W. 4th Avenue Suite 306, Anchorage, AK 99501.

cod (Thompson and Methot[2]). In the otoliths of young Pacific cod (under 6 years), there is a tendency for subannual marks (also known as "checks") to be very dark and evenly spaced, making them difficult to distinguish from annuli. This confusion makes it difficult to age the species to an exact age.

From 1990 through 1992, the AFSC noticed that the average length at a specific age was smaller than it had been in previous years. The decrease was noticed in ages 1–6 but was especially dramatic in 1-, 2-, and 3-year-olds. It is generally theorized that the shift was the result of one of two scenarios: either the fish population experienced an actual decrease in length-at-age or the age readers were over-aging fish by counting marks other than annuli. Unable to pinpoint the reason for the shift and given the inherent difficulty of aging cod, production (large-scale) aging of Pacific cod was indefinitely suspended at the AFSC.

Pacific cod stock assessments in Alaska have since depended largely on length-frequency data alone to model population age structure because of the difficulties in obtaining age estimates (Thompson and Dorn[1]). However, the use of length-frequency data as proxies for age data can be problematic. If external factors such as ocean conditions affect somatic growth to such a degree that length-at-age within the population is highly variable, such as appears to be the case for Pacific cod, then the population becomes difficult to model. Otoliths, on the other hand, are permanent records of growth that are more independent of external factors.

Consequently, the Age and Growth Program initiated a new study in 1998 to re-examine the otolith aging structure for Pacific cod. This study used otoliths from tagged Alaska Pacific cod to validate aging criteria for otoliths.

Methods

Otoliths and length data were collected during a tagging study conducted by the AFSC. Between 1982 and 1990, 12,396 Pacific cod were tagged and released in the eastern Bering Sea during summer bottom-trawl surveys (See Shimada and Kimura, 1994). Fish were measured to the nearest 0.5 cm fork length, tagged with uniquely marked spaghetti tags, and set free. Over a period of 13 years, commercial fishing vessels recaptured 375 (3%) of the tagged fish and returned otoliths from 112 fish (106 of which were usable) (Table 1). More details on the tagging methods can be found in Shimada and Kimura (1994).

[2] Thompson, G. G., and R. D. Methot. 1993. Pacific cod. *In* Stock assessment and fishery evaluation report for the groundfish resources for the Bering Sea/Aleutian Islands regions as projected for 1994 (plan team for groundfish fisheries of the Bering Sea/Aleutian Islands), p. 2–28. North Pacific Fishery Management Council, 605 W. 4th Avenue Suite 306, Anchorage, AK 99501.

Otolith preparation

One sagittal otolith from each recaptured fish was selected for our study. We did not discriminate between left and right otoliths based on the results of Sakurai and Hukuda (1984) who were unable to detect any consistent differences between the weight and length of right and left Pacific cod otoliths.

Each otolith was cleaned and preserved in 95% ethanol. After having been preserved for approximately one month, a line was penciled across the otolith center from the dorsal apex to the ventral apex to ensure that the otoliths would later be sectioned at the core.

The otolith was then placed in a polyester mold and set in black resin (Technovit 3040, Energy Beam Sciences, Agawam, MA), forming a block of resin. A slow-speed saw was used to cut the blocks in half. This produced two smaller blocks, each with an exposed view of the otolith in the transverse plane and cut through the center. One of the two blocks was selected and glued (otolith side down) to a glass slide. The glass slide was mounted to a Hillquist thin section machine (Hillquist Inc., Fall City, WA) and the section was ground down to a thickness of 0.25 mm. A coverslip was permanently glued on the top of the section with marine-grade epoxy.

Sections were placed on a piece of black velvet (which added contrast) on the stage of a 50× dissecting microscope, and reflected light was used for illumination. The sections were viewed on a computer monitor by using a Cohu 6500 monochrome video camera, Integral Flashpoint 128 frame grabber and Optimas 6.5 imaging software (Media Cybernetics, Silver Spring, MD).

Age-reading criteria

Traditional qualitative aging criteria were used to distinguish annuli from checks. The criterion for identification as an annulus was a continuous translucent band that could be seen along the entire structure or as a ridge or groove on the structure (Secor et al., 1995). Checks (i.e., subannual marks) are translucent zones that appear very similar to annuli. They were determined primarily by the incompleteness of the zone around the entire section, by zone darkness, and by spacing between zones. When translucent zones could be classified as either annuli or additional subannular marks, they were classified as checks. Annuli, checks, and edges (the space between the last annulus and the edge of the otolith) were traced by using the Optimas 6.5 software package and measurements of their areas and major axis lengths were collected (Fig. 1). All otoliths were read blind; that is, information about fish length and date of capture (Table 1) was withheld from the reader to prevent bias.

When all the otoliths had been aged and measured, the age reader returned to each otolith section to estimate the area and length of the otolith when the fish was tagged. This was accomplished by following a two-step process. The first step was to approximate the location of the otolith cross-section that corresponded to

Table 1

Mark and recapture data for spaghetti-tagged Pacific cod (*Gadus macrocephalus*). L_1 = fork length at tagging (mm), L_2 = fork length at recapture (mm), d_1 = time at liberty (months), a_1 = age estimated from L_1 and d_1, a_2 = age at recapture estimated by using the fish's otolith and age-reading criteria, and NR = not reported.

L_1	L_2	d_1	a_1	a_2	a_1–a_2	L_1	L_2	d_1	a_1	a_2	a_1–a_2
430	480	9	4	3	1	625	550	3	6.5	5	1.5
680	875	21	8	7	1	740	850	26	8	8	0
690	830	30	8	8	0	650	670	4	6	7	–1
590	500	4	6	7	–1	525	550	5	5	4	1
530	690	30	7	7	0	645	720	9	7	6	1
430	500	10	4	4	0	835	890	14	7	8	–1
600	620	8	6	7	–1	560	600	5	5	4	1
390	490	11	3.5	3	0.5	645	830	38	9	8	1
630	660	5	6.5	4	2.5	405	412	4	3.5	2	1.5
670	750	9	7	8	–1	460	550	8	4	3	1
630	850	49	9.5	10	–0.5	735	760	1	6	7	–1
590	650	7	6	6	0	620	650	1	5	6	–1
450	570	25	5	6	–1	545	550	4	4	6	–2
630	660	7	6.5	6	0.5	555	560	2	4	5	–1
440	525	14	4.5	5	–0.5	680	730	19	7.5	6	1.5
705	890	35	9	8	1	640	680	4	6.5	4	2.5
556	680	25	6	8	–2	730	730	6	7	7	0
480	540	7	5.5	3	2.5	540	655	12	5	5	0
620	660	2	5	9	–4	600	720	14	6	6	0
630	730	17	7	8	–1	540	700	17	5	6	–1
600	730	44	8.5	7	1.5	530	920	50	8	9	–1
630	623	1	5.5	6	–0.5	610	691	16	6	8	–2
702	760	11	7	8	–1	690	800	10	7	5	2
330	530	22	4	3	1	555	630	7	5	6	–1
540	706	20	6	5	1	790	NR	21	8	7	1
390	578	22	4.5	4	0.5	560	630	8	5	5	0
670	710	4	6	9	–3	520	550	2	4	4	0
820	825	2	6	8	–2	535	NR	18	5.5	6	–0.5
690	710	8	7	8	–1	460	530	7	4	3	1
725	850	17	7.5	6	1.5	590	930	93	12.5	15	–2.5
530	590	9	5	5	0	690	742	5	6.5	6	0.5
660	690	3	6	7	–1	720	770	8	7	9	–2
580	770	57	9.5	10	–0.5	870	924	7	7	8	–1
450	695	25	5	5	0	520	523	7	5	3	2
815	860	10	7	8	–1	470	530	6	4.5	3	1.5
540	670	22	6	7	–1	630	740	13	6.5	7	–0.5
740	670	7	7	6	1	510	630	13	5	6	–1
670	705	2	6	8	–2	650	720	13	7	6	1
650	640	0	6	7	–1	570	675	20	6	8	–2
710	860	19	8	7	1	690	660	20	7.5	8	–0.5
670	810	20	8	7	1	660	760	23	8	8	0
780	770	1	6	8	–2	690	750	7	7	7	0
810	850	7	7	8	–1	560	630	8	5	5	0
485	640	21	5.5	6	–0.5	530	700	7	5	7	–2
305	850	39	4.5	8	–3.5	600	620	10	5.5	4	1.5
695	710	9	7	6	1	595	970	50	8.5	9	–0.5
610	810	30	8	6	2	520	910	32	6.5	7	–0.5
660	820	30	9	7	2	540	800	30	6	7	–1
610	725	26	7	7	0	820	830	2	6	6	0
580	720	30	7.5	7	0.5	585	782	34	7.5	6	1.5
530	830	33	7	6	1	680	790	9	7	6	1
600	760	17	7	6	1	676	1080	70	11.5	11	0.5
515	730	26	6	5	1	585	590	0	4.5	5	–0.5

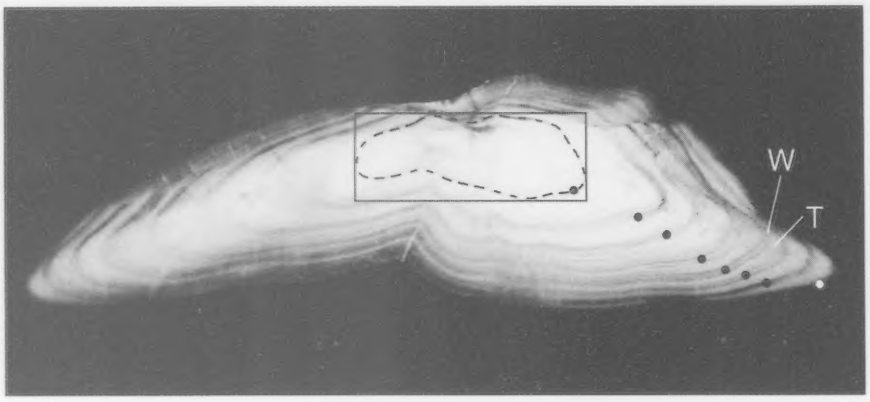

Figure 1

Transverse cross-section of a Pacific cod (*Gadus macrocephalus*) otolith with an unusually clear annulus pattern. The otolith was taken from a 830-mm, 8-year-old fish that was recaptured 30 months after tagging. Annuli (black dots), checks, and edges (the space between the last annulus and edge [white dot]) were traced and measurements of their areas (from the center of the otolith to the outer margin of the translucent zone [dotted line]) and major axis lengths (from the smallest rectangular box that will hold the translucent zone) were collected. *T* is the estimated otolith size (length and area) at the time of tagging and was used to back-calculate fish length at tagging. *W* corresponds to the annulus preceding *T*.

the time of tagging. The second step was calculating the area and length of that region, producing an estimated otolith size at the time of tagging

First, to approximate the location of the otolith that corresponded to the time of tagging required the reader to know how long (years) the fish had been at liberty, after tagging. Using this knowledge and starting from the last annulus before the edge, the reader counted towards the center of the otolith, the number of years (as represented by annuli) that the fish had been at liberty. (In cases where the fish had been at liberty for less than one year before being caught again, the reader began at the edge rather than at the last annulus before the edge). Assuming that all annuli are laid down by late winter, the reader would end up on the annulus that preceded the summer of tagging. This annulus represents the size of the otolith just prior to tagging and for sake of further explanation, its area and length will be identified as *W* (Fig. 1). To complete the procedure, the reader needed only to measure the summer increment which followed *W*, divide it in half and add it to *W*. These calculations were assumed to reflect the size of the fish's otolith at time of tagging and were used as O_i values (the size of the otolith at tagging) to back-calculate fish size at initial capture.

Estimating fish length by using tagged fish and back-calculations

Annuli on tagged fish otoliths can be used to estimate the length of each fish at an earlier age. Smedstad and Holm (1996) compared six different back-calculation formulae on tagged Atlantic cod (*Gadus morhua*) and found that the age-independent, nonlinear, body proportional (nbp) hypothesis worked the best. Pacific cod is a gadid closely related to the Atlantic cod; therefore we also used the nonlinear, body proportional formula

$$L_i = (O_i / O_c)^v L_c,$$

where L_i = the predicted fish length at tagging or desired age;

O_i = the size (either radius or area) of otolith at tagging;

O_c = the size of otolith at time of recapture;

v = the slope from the regression of Ln(L) on Ln(O); and

L_c = the fish length at recapture.

This analysis was performed by using two different measures of otolith size, the cross-sectional area and major axis (i.e., length) of otolith increments (Fig. 1).

Estimating growth increments in fish length from tagged fish

We can use tagged fish otolith ages to estimate how much each fish grew in length after tagging, in a manner similar to Fabens' equation (Ricker, 1975), using the von

Table 2

Results of regressing Ln *fish length* on Ln *otolith area* and Ln *fish length* on Ln *otolith major axis* by using tagged fish data. Fish length was measured in mm, otolith area in mm^2, and otolith major axis in mm, n=96.

	Coefficients	Standard error	t stat	P-value
Regression of Ln *Fish length* on Ln *Otolith area*				
Intercept	4.637299	0.117551	39.44929	2.75E-60
Slope (v)	0.65732	0.040471	16.24168	4.96E-29
Regression of Ln *Fish length* on Ln *Otolith major axis*				
Intercept	4.27009	0.229693	18.5904	3.01E-33
Slope (v)	1.012865	0.102305	9.900426	2.99E-16

Bertalanffy equation (Ricker, 1975). However, because we could estimate the age of fish at time of recapture, we were able to manipulate the von Bertalanffy equation to obtain the following equation:

$$L_2 - L_1 \approx L_{inf}\left[\left(e^{-K(a_2-d-t_0)}\right)-\left(e^{-K(a_2-t_0)}\right)\right],$$

where L_1 = length at tagging;
L_2 = length at recapture;
L_{inf} = maximum size;
K = growth rate;
a_2 = estimated age at recovery determined from our otolith ages;
d = time at liberty; and
t_0 = age at length 0 mm.

Given von Bertalanffy parameters and age at recovery, a (fish) length increment for time after tagging can be predicted. Using published L_{inf} and K estimates from tagging data, L_{inf} = 1043 mm, K = 0.222 (Kimura et al., 1993), we estimated L_2–L_1. One weakness in these estimates is that the growth parameters estimated by Kimura et al. (1993) were based on only positive growth increments (there were some instances where recaptured fish were smaller than they were at tagging, demonstrating negative growth increments).

A value for t_0 was estimated iteratively in the von Bertalanffy equation by using the subroutine Solver (Frontline Systems Inc., Incline Village, NE) from the Excel software package with the following parameter values: K = 0.222, t = 1 year old, L_{inf} = 1043 mm (Kimura et al., 1993), l_t = length at age one = 180 mm (from the 1977 year class [Foucher et al., 1984]). Because these von Bertalanffy parameters are not based on age determination, they provide an indirect method for validating aging criteria. In addition, ages determined by readers were scaled smaller (by 0.75) and larger (by 1.25) in order to simulate the results of younger and older aging criteria. Plots of observed and predicted growth increments should agree if the aging criteria for a_2 reflect the true age of fish.

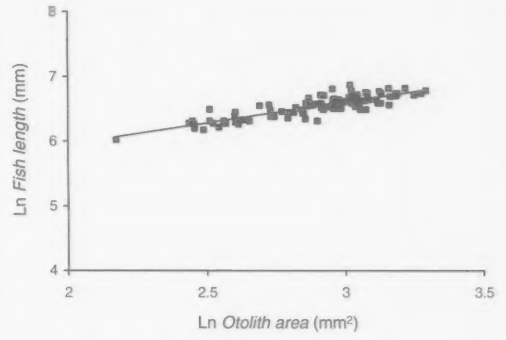

Figure 2

Relationship between Ln *fish length* and Ln *otolith area* based on tagged and recaptured Pacific cod (r^2=0.735, Y=4.6+0.66X, n=96).

Results

Predicting fish length from tagged fish and back-calculations

The parameter v used in all back-calculations in our study was estimated by using otolith area and again by using the major axis of the otolith (Fig. 1). Based on the slopes from the regression of Ln *fish length* on Ln *otolith size* (Table 2, [Fig. 2]), the coefficients should be v=1.01 for otolith length and v=0.66 for otolith areas.

Back-calculations were performed by using the otolith area and were repeated by using the major axis. Scatter plots of estimated and observed fish lengths were used to visually inspect how well back-calculation determines fish length (Fig. 3). Assuming that the residuals of the back-calculated length at tagging have independent chi-square distributions, an F-test indicates that back-calculations derived from otolith areas are significantly more accurate than back-calculations derived from the major axis (P<0.05). However, because we used the two

different methods on the same otoliths, the residuals were correlated and thus this result can be considered only approximate.

Predicting growth increments of fish length from tagged fish

Using the von Bertalanffy curve fitted with the data from the tagged fish sample, we estimated the value of t_0 to be 0.147.

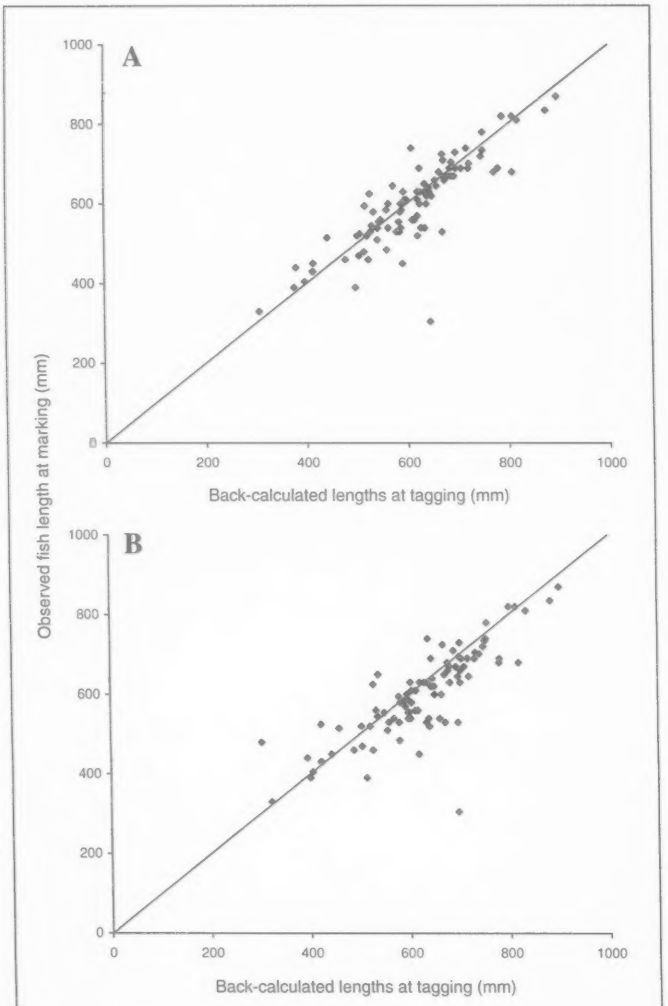

Figure 3

Fish length at tagging was back-calculated from estimated otolith size at tagging and time at liberty. Two separate back-calculations were performed, each with a different measure of the otolith size at tagging: one using (**A**) the area; the other using (**B**) the major axis.

The amount that each tagged fish grew after tagging was calculated three times by using fish age at recovery and the von Bertalanffy equation (Fig. 4). The calculated sums of squared deviations for the three sets of predicted values are as follows: 433,955 when fish age is scaled by 0.75, 419,477 when fish age is scaled by 1.0, and 761,545 when fish age is scaled by 1.25. The lowest sum of squared deviations accompanied ages that were scaled by 0.86. Assuming that the residuals of the estimated growth increments have independent chi-square distributions, an F-test indicates that residuals were significantly larger ($P<0.05$) when ages were scaled 25% older and there was no significant difference ($P<0.05$) between reader-determined ages and ages scaled 25% younger. The three sets of residuals came from the same otoliths and would be correlated; therefore, this result can be considered only approximate.

Another test of our reading criteria was performed through a more direct comparison: simply "aging" the tagged fish from estimated age at tagging (based on length), plus the time after tagging (Table 1). Out of 106 samples, 75% of these fish were within one year of the age that we had determined from otolith readings, and 94% were within two years. The average percent error (Beamish and Fournier, 1981) was 8.70, and the average deviation from tagged-based age was −0.075. Results of a Z-test indicated that the average deviation was not significantly different from zero ($P=0.724$) and indicated no bias in the age estimates.

Discussion

Beamish and McFarlane (1983) noted that "validating a method of age determination is as important in fishery biology as standardizing solutions or calibrating instruments are in other sciences." Age determination must reflect the actual age of each fish in order to be a useful tool for use in stock assessments. Although much effort has been devoted in the past to finding an appropriate aging structure for Pacific cod, particularly with dorsal fin rays (Beamish, 1981; Lai et al., 1987; Kimura and Lyons, 1990), scales and otoliths (Lai et al., 1987; Kimura and Lyons, 1990), a directly validated method of age determination has yet to be found (Westrheim, 1996). The otolith seems to be the most promising structure for production (large-scale) age reading of Pacific cod (Kimura and Lyons, 1990); however it is not without weaknesses (i.e., the faint patterns of some translucent zones can lead to low precision between readers and are a constant concern in regard to

under- or overestimated ages). The key difficulty of the cod otolith patterns is differentiating the translucent zones that are annual from the translucent zones that are checks, particularly in young fish. It is necessary to have validated criteria in order to confidently eliminate checks without under-aging the fish. In our study, we have given two examples of indirect validation for Pacific cod age determination by using otoliths from marked and recaptured fish.

In the first example, we used back-calculations to test our reading criteria, which exclude counting lighter translucent zones. Early in the study, we found a strong relationship between otolith size and fish length, which supported using back-calculations as a vehicle to test accuracy. Overall, using strong translucent zones to back-calculate fish length at tagging gave fairly accurate results. This finding supports the assumption that translucent zones are laid down on an annual basis.

An ancillary finding was that otolith area measurements provided more accurate estimates of fish length than otolith lengths. Although back-calculations are typically performed by using radial or diametral measurement, the more accurate estimates of fish length from otolith area measurements are not surprising in that otolith area is a more comprehensive measure of otolith three-dimensional growth.

A second indirect validation of reading criteria was possible by estimating how much each tagged fish grew (millimeters) between tagging and recapture by its estimated age at recovery and von Bertalanffy growth parameters (derived only from tagging data). When compared to the observed growth increments, we found that the results support our proposed aging criteria (which exclude lighter translucent zones) because these criteria give the best fit to growth increments based on the mark-recapture growth increments. Aging the fish older (by counting light translucent zones) or younger (counting less annuli by banding translucent zones together) increases the residual fit to the mark-recapture growth increments. Large growth increments of fish length were difficult to estimate (Fig. 4). A possible explanation is that the longer a fish remains at liberty, the more likely that the growth becomes asymptotic, making the relationship between the growth increment and time at liberty less exact.

The final test for reading criteria was performed through a more direct comparison: simply "aging" the tagged fish by its length-at-release plus its time at liberty after tagging and comparing that age to the otolith-based age at recovery. Dwyer et al. (2003) also used this method in their study of yellowtail flounder (*Limanda ferruginea*). Average deviation from tag-based age was −0.075; 75% of these fish were found to be within one year of our age according to otolith readings, and 94% were within two years. These results provide further evidence that the current criteria do not result in the underestimation of the age of the fish and support the practice of not counting checks.

We found that growth information residing in otoliths from tagged and recovered Pacific cod provided significant information applicable to indirectly validating otolith aging criteria. Therefore, it seems that otoliths from other species that were tagged and recovered might be useful for indirect age validation as well. The

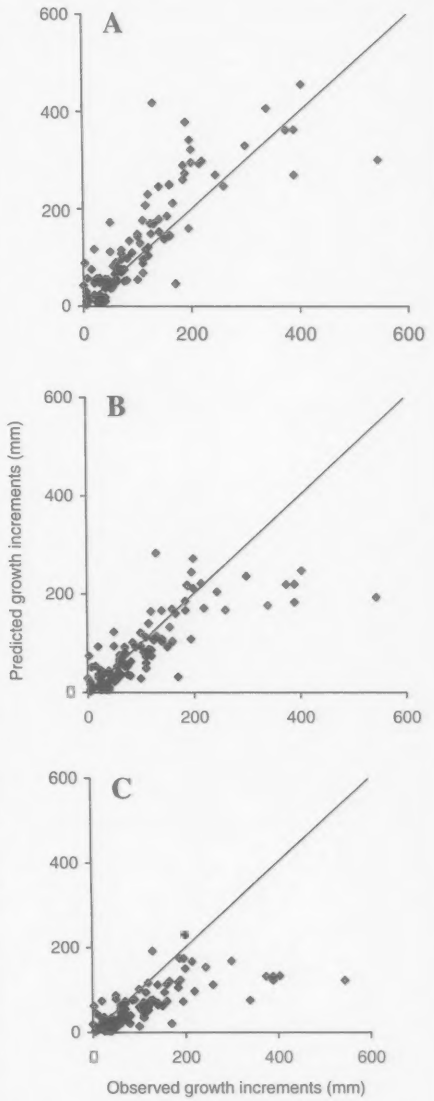

Figure 4

Three plots comparing predicted and observed fish-length growth increments by using recaptured fish from tagging experiments (n=97). Estimated ages at recovery (**B**) were scaled 25% smaller (**A**) and 25% larger (**C**). The lines indicate theoretical 1:1 line of perfect agreement.

information provided in our study indicates that our aging criteria for Pacific cod are roughly correct and that errors are probably within plus or minus 1 or 2 years. However, the problem of the shift in length at age alluded to in the introduction is more difficult to elucidate. Analysis made during this study seems to indicate that both environmental growth factors and changes in otolith aging criteria could have played a role in this apparent shift.

Acknowledgments

This work was performed in partial fulfillment of the requirements for an M.S. degree at the School of Aquatic and Fishery Sciences at the University of Washington and was supported by the National Marine Fisheries Service. We would like to express our appreciation to those individuals who assisted in the tagging and recapture process and to the two anonymous reviewers for their helpful comments on the manuscript.

Literature cited

Beamish, R. J.
1981. Use of sections of fin-rays to age walleye pollock, Pacific cod, albacore, and the importance of this method. Trans. Am. Fish. Soc. 110:287–299.

Beamish, R. J., and D. A. Fournier.
1981. A method for comparing the precision of a set of age determinations. Can. J. Fish. Aquat. Sci. 38:982–983.

Beamish, R. J., and G. A. McFarlane.
1983. The forgotten requirement for age validation in fisheries biology. Trans. Am. Fish. Soc. 112:735

Dwyer, K. S., S. J. Walsh, and S. E. Campana.
2003. Age determination, validation and growth of Grand Bank yellowtail flounder (*Limanda ferruginea*). ICES J. Mar. Sci. 60:1123–1138.

Foucher, R. P., R. G. Bakkala, and D. Fournier.
1984. Comparison of age frequency derived by length-frequency analysis and scale reading for Pacific cod in the North Pacific Ocean. Int. North Pac. Fish. Comm. Bull. 42:232–242.

Kimura, D. K., and J. J. Lyons.
1990. Choosing a structure for the production aging of Pacific cod (*Gadus macrocephalus*). Int. N. Pac. Fish. Comm. Bull. 50:9–23.

Kimura, D. K., A. M. Shimada, and S. A. Lowe.
1990. Estimating von Bertalanffy growth parameter of sablefish (*Anoplopoma fimbria*) and Pacific cod (*Gadus macrocephalus*) using tag-recapture data. Fish. Bull. 91:271–280.

Lai, H. L., D. R. Gunderson, and L. L. Loh.
1987. Age determination of Pacific cod, *Gadus macrocephalus*, using five aging methods. Fish. Bull. 85:713–723.

Ricker, W. E.
1975. Computation and interpretation of biological statistics of fish populations. Bull. Fish. Res. Board Can. 191, p. 382.

Sakurai, Y., and S. Hukuda.
1984. The age and growth of the spawning Pacific cod in Mutsu Bay. Sci. Rep. Aquat. Cen., Aomori Pref. 3:9–14.

Secor, D. H., J. M. Dean, and S. E. Campana (eds.).
1995. Recent developments in fish otolith research. Belle W. Baruch Institute for Marine Biology and Coastal Research., Univ. South Carolina Press, Columbia, SC.

Shimada, A. M., and D. K. Kimura.
1994. Seasonal movements of Pacific cod, *Gadus macrocephalus*, in the eastern Bering Sea and adjacent waters based on tag-recapture data. Fish. Bull. 92:800–816.

Smedstad, O. M., and J. C. Holm.
1996. Validation of back-calculation formulae for cod otoliths. J. Fish Biol. 49:973–985.

Westrheim, S. J.
1996. On the Pacific cod (*Gadus macrocephalus*) in British Columbia waters, and a comparison with Pacific cod elsewhere, and Atlantic cod (*G. morhua*). Can. Tech. Rep. Fish. Aquat. Sci. 2092, 390 p.

Westrheim, S. J., and W. Shaw.
1982. Progress report on validating age determination methods for Pacific cod (*Gadus macrocephalus*). Can. Manuscr. Rep. Fish. Aquat. Sci. 1670, 41 p.

Age and growth estimates of the thorny skate (*Amblyraja radiata*) in the western Gulf of Maine

James A. Sulikowski
Jeff Kneebone
Scott Elzey
Zoology Department, Spaulding Hall
46 College Road
University of New Hampshire
Durham, New Hampshire 03824
E-mail address (for J. A. Sulikowski, senior author): jsulikow@hotmail.com

Joe Jurek
Yankee Fisherman's Cooperative
P.O. Box 2240
Seabrook, New Hampshire 03874

Patrick D. Danley
Department of Biology
University of Maryland
College Park, Maryland 20724

W. Huntting Howell
Zoology Department, Spaulding Hall
46 College Road
University of New Hampshire
Durham, New Hampshire 03824

Paul C.W. Tsang
Department of Animal and Nutritional Sciences
Kendall Hall
129 Main St.
University of New Hampshire
Durham, New Hampshire 03824.

Abstract—The northwest Atlantic population of thorny skates (*Amblyraja radiata*) inhabits an area that ranges from Greenland and Hudson Bay, Canada, to South Carolina. Despite such a wide range, very little is known about most aspects of the biology of this species. Recent stock assessment studies in the northeast United States indicate that the biomass of the thorny skate is below the threshold levels mandated by the Sustainable Fisheries Act. In order to gain insight into the life history of this skate, we estimated age and growth for thorny skates, using vertebral band counts from 224 individuals ranging in size from 29 to 105 cm total length (TL). Age bias plots and the coefficient of variation indicated that our aging method represents a nonbiased and precise approach for the age assessment of *A. radiata*. Marginal increments were significantly different between months (Kruskal-Wallis $P<0.001$); a distinct trend of increasing monthly increment growth began in August. Age-at-length data were used to determine the von Bertalanffy growth parameters for this population: L_∞ = 127 cm (TL) and $k=0.11$ for males; L_∞ = 120 cm (TL) and $k=0.13$ for females. The oldest age estimates obtained for the thorny skate were 16 years for both males and females, which corresponded to total lengths of 103 cm and 105 cm, respectively.

Manuscript submitted 21 August 2003 to the Scientific Editor's Office.

Manuscript approved for publication 8 July 2004 by the Scientific Editor.

Fish. Bull. 103:161–168 (2005).

The northeast skate complex consists of seven species endemic to the waters off the New England coast of the United States (New England Fisheries Management Council (NEFMC[1,2]). In the past, these skates were generally discarded because of their low commercial value (NEFMC[1,2]). More recently, the rapidly expanding markets for human consumption of skate wing and for use as lobster bait have made three of these species (winter skate [*Leucoraja ocellata*], little skate [*L. erinacea*], and thorny skate [*Amblyraja radiata*]) commercially more viable (Sosebee, 2000; NEFMC[1,2]). Despite an increasing commercial importance, harvests for skate in the U.S. portion of the western north Atlantic remain unregulated and have the potential to over-exploit the stocks. Moreover, life history information is almost nonexistent for most of these elasmobranch fishes (Frisk, 2000 NEFMC[1,2]).

The available information from the few skates that have been studied categorizes them as equilibrium strategists (K selected) because they reach sexual maturity at a late age, have a low fecundity, and are relatively long-lived (Holden 1977; Winemiller and Rose, 1992; Zeiner and Wolfe, 1993; Francis et al., 2001; Frisk et el., 2001, Sulikowski et al., 2003). These characteristics, coupled with the practice of selective removal of large individuals, make these animals more likely to be over-exploited by commercial fisheries (Brander 1981; Hoenig and Gruber, 1990; Casey and Myers 1998; Dulvey et al., 2000; Frisk et al., 2001).

The thorny skate (*Amblyraja radiata*) is a cosmopolitan species found on both sides of the Atlantic ocean from Greenland and Iceland to the English Channel in the eastern Atlantic (Compagno et al., 1989) and from Greenland and Hudson Bay, Canada, to South Carolina, United States, in the western Atlantic (Robins and Ray, 1986; Collette and Klein, 2002). Along with this broad geographic range, marked differences in size exist for specimens captured in different regions of the Atlantic. For

[1] NEFMC (New England Fishery Management Council. 2001. 2000 stock assessment and fishery evaluation (SAFE) report for the northeast skate complex. NEFMC, 50 Water Street, Mill 2 Newburyport, MA 01950.

[2] NEFMC (New England Fishery Management Council). 2003. Skate fisheries management plan. NEFMC, 50 Water Street, Mill 2 Newburyport, MA. 01950.

example, the thorny skate reaches total lengths of over 100 cm in the Gulf of Maine (Collette and Klein, 2002), whereas specimens captured off the Labrador coast do not reach total lengths >72 cm (Templeman, 1987). Although no directed fisheries for this species exists in the Gulf of Maine, this skate meets the minimum 1¼ pound-cut pectoral-fin size sought after by wing processors (Sosebee, 2000; NEFMC[1,2]). Unfortunately, because landings are not reported by species, the proportion of thorny skates to the total wing market is unknown. Recent assessment studies in the northeast United States (NEFSC[3]) indicate that the biomass of thorny skates is declining, and is below threshold levels mandated by the Sustainable Fisheries Act (SFA; NMFS[4]). Thus, owing to the recent commercial interest in this species and the concomitant decline in population size, obtaining life history information for this species has become more important. In order to provide insight into the biology of this species and to determine the stock status (Simpfendorfer, 1993; Frisk et al., 2001), our objectives were to estimate age and growth rates of *A. radiata* based on banding patterns in vertebral centra from specimens collected in the western Gulf of Maine.

Materials and methods

Sampling

Thorny skates were captured by otter trawl in an approximate 900 square mile area centered at 42°50′N and 70°15′W in the Gulf of Maine between June 2001 and May 2002. These locations varied from 30 to 40 km off the coast of New Hampshire. Approximate depths at this location ranged between 100 and 120 m. This area was chosen for two reasons: 1) these waters support the vast majority of commercial fishing in New Hampshire and can be easily accessed during normal fishing operations; and 2) because of rolling closures within the Gulf of Maine, an experimental fishing permit was granted to us by the National Marine Fisheries Service (NMFS) to collect thorny skates in this location during the months of April, May, and June, when these waters are closed to commercial fishing. Although our sampling was conducted in a small portion of the species' range, the sizes of thorny rays collected corresponded to those collected during the NEFSC bottom trawl surveys conducted throughout the Gulf of Maine and Georges Bank (NEFMC[1]; NEFSC[3]). From this information, it is unlikely that differences in other biological parameters exist.

Skates were maintained alive on board the vessel until arrival at the University of New Hampshire's Coastal Marine Laboratory (CML). There, individual fish were euthanized (0.3g/L bath of MS222). Total length (TL in cm) was measured as a straight line distance from the tip of the rostrum to the end of the tail, and disc width (DW in cm) as a straight line distance between the tips of the widest portion of pectoral fins. Total wet weight (kg) was also recorded.

Preparation of vertebral samples

Vertebral samples, taken from above the abdominal cavity, were removed from 320 thorny skates (154 females and 166 males), labeled, and stored frozen. After having been thawed, three centra from each specimen were removed from the vertebral column, stripped of excess tissue and air dried. Large centra were cut sagittally with a Dremel™ tool fitted with a mini saw attachment while held with a vice-like device. Smaller centra were sanded with a Dremel™ tool to replicate a sagittal cut. Processed vertebrae were mounted horizontally on glass microscope slides and ground with successively finer-grit (no. 180, no. 400, no. 600) wet-dry sandpaper. Each vertebra was then remounted and the other side ground to produce a thin (300-micrometer) hourglass section.

Band counts

Vertebral sections were digitally photographed with a Canon Powershot S40 attached to a Leica S8PO dissecting microscope and reflected light. Magnification depended on the size of the section and varied from 4× to 12× (Fig. 1). A growth ring (band count) was defined as one opaque and translucent band pair that traversed the intermedialia and that clearly extended into the corpus calcareum (Casey et al., 1985; Brown and Gruber, 1988; Sulikowski et al., 2003). The birth mark (age zero) was defined as the first distinct mark distal to the focus that coincided with a change in the angle of the corpus calcareum (Casey et al., 1985; Wintner and Cliff, 1996; Sulikowski et al, 2003).

Precision and bias

Nonconsecutive band counts were made independently by two readers for each specimen used in the study without prior knowledge of the skate's length or of previous counts. A Tukey test was used to test for differences between ages. Age determination bias between readers was assessed through the use of an age-bias plot. This type of graph displays band counts of one reader against a second reader in reference to an equivalence line. Specifically, reader 2 is represented as mean age and 95% confidence intervals corresponding to each of the age classes estimated by reader 1 (Campana et al., 1995). Divergence from the equivalence line, where reader 1 = reader 2, would indicate a systematic difference between readers. Precision estimates of each reader were calculated by using the coefficient of variation (CV) as described by Chang (1982) and Campana et al. (1995).

[3] NEFSC (Northeast Fisheries Science Center). 1999. 30th Northeast regional stock assessment workshop. NEFSC, 166 Water Street, Woods Hole, MA 02543-1026.

[4] NMFS (National Marine Fisheries Service). 2002. Annual report to Congress on the status of U.S. fisheries 2001, 142 p. NMFS, NOAA, Silver Spring, MD 20910.

Marginal increment analyses

The annual periodicity of band pair formation was investigated using marginal increment analyses (MIA). Because the annuli in older adult specimens were compressed, marginal increments were calculated from randomly selected juvenile specimens (Simpfendorfer, 1993; Sulikowski et al., 2003). For MIA, the distance of the final opaque band and the penultimate opaque band, from the centrum edge, was measured with a compound microscope and optical micrometer. The marginal increment was calculated as the ratio of the distance between the final and penultimate bands (Branstetter and Musick, 1984; Cailliet, 1990; Simpfendorfer, 1993; Simpfendorfer et al., 2000; Sulikowski et al., 2003). Average increments were plotted by month of capture to identify trends in band formation, and a Kruskal-Wallis one-way analysis of variance on ranks was used to test for differences in marginal increment by month (Simpfendorfer et al., 2000; Sulikowski et al., 2003).

Growth estimates

A von Bertalanffy growth function (VBGF) was fitted to the data with the following equation (von Bertalanffy, 1938):

$$L_t = L_\infty(1 - e^{-k(t - t_0)}),$$

where l_t = total length at time t (age in years);
L = theoretical asymptotic length;
k = Brody growth constant; and
t_0 = theoretical age at zero length.

The VBGF was calculated by using FISHPARM, a computer program for parameter estimation of nonlinear models with Marquardt's (1963) algorithm for least-square estimation of nonlinear parameters (Prager et al., 1987).

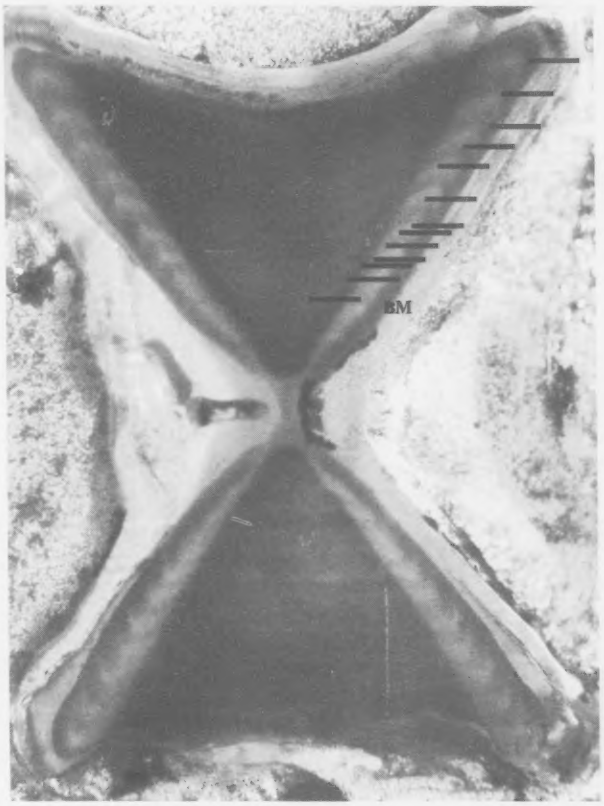

Figure 1

Longitudinal cross-section of a vertebral centrum from a 97-cm-TL female *Amblyraja radiata* estimated to be 12 years. BM = birth mark; Black dots represent age in years.

Results

Morphological measurements

Out of the 320 specimens collected, a total of 224 were used for our study (Table 1). Males (n=103) ranged between 29 and 103 cm TL, 18–75 mm DW, and 0.125–10.5 kg body weight (data not shown), whereas females (n=121) ranged between 31 and 105 cm TL, 18–74 cm DW, and 0.170–11.4 kg body weight (data not shown). Total length, disk width, and body weight were strongly correlated in males, females, and when data from the sexes were combined (all coefficient of determination [r^2] values were greater than 0.87).

Vertebral analyses

Comparison of counts between two readers indicated no appreciable bias in the counting process (Fig. 2) and the coefficient of variation for all sampled vertebrae was 2.8% This level of precision is considered acceptable (Campana, 2001) and counts generated by both readers were combined (averaged) for the analyses (Skomal and Natanson, 2003).

The relationship between TL and centrum diameter was linear (r^2=0.93; P<0.05) and there were no significant differences in this relationship (ANCOVA, P<0.05) between males and females. Because no significant difference existed between TL and centrum diameter between the sexes, these data were combined (Fig. 3).

A total of 120 skates (10 per month) were used for marginal increment analyses. Marginal increments were significantly different between months (Kruskal-Wallis P<0.001); there was a distinct trend of increasing

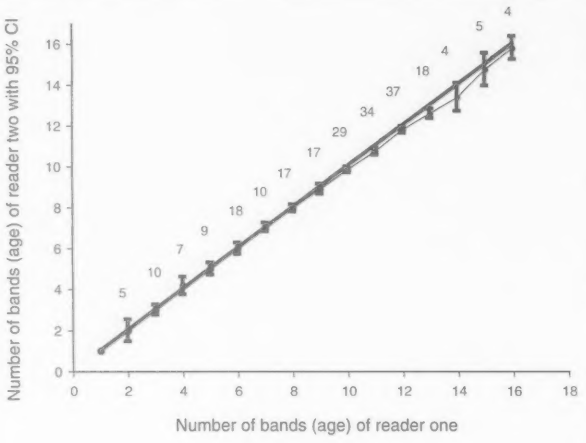

Figure 2

Age bias graph for pair-wise comparison of 224 thorny skate (*Amblyraja radiata*) vertebral counts by two independent readers. Each error bar represents the 95% confidence interval for the mean age assigned by reader 2 to all fish assigned a given age by reader 1. The diagonal line represents the one-to-one equivalence line. Sample sizes are given above each corresponding age.

Table 1

Average total length (TL) and disc width (DW) at age for male and female thorny skates (*A. radiata*). Sizes are presented as mean ±1 SEM; sample sizes are given in parentheses.

Age (years)	Male TL (cm)	Female TL (cm)	Sexes combined	Male DW (cm)	Female DW (cm)	Sexes combined
2	33 (5) ±1		33 (5) ±1	23±1		2±1
3	37 (3) ±1	37 (7) ±1	37 (10) ±1	26 ±1	27 ±0	27 ±1
4	43 (5) ±1	42 (2) ±2	42 (7) ±1	29 ±0	29 ±1	29 ±1
5	48 (2) ±2	49 (7) ±2	48 (9) ±1	33 ±0	35 ±0	34 ±1
6	64 (1) ±1	54 (17) ±1	54 (18) ±1	44 ±0	39 ±2	39 ±2
7	69 (5) ±1	62 (5) ± 3	64 (10) ±1	50 ±1	44 ±2	47 ±1
8	71 (6) ±1	73 (11) ±2	72 (17) ±2	52 ±1	53 ±2	53 ±1
9	78 (9) ±1	78 (8) ±2	78 (17) ±1	57 ±2	57 ± 1	57 ±1
10	86 (14) ±1	82 (15) ±1	84 (29) ±1	63 ±2	60 ±1	61 ±1
11	88 (17) ±1	89 (17) ±1	89 (34) ±1	65 ±1	65 ±1	65 ±1
12	93 (18) ±1	92 (19) ±0	92 (37) ±1	68 ±1	66 ±1	67 ±1
13	99 (10) ±1	95 (8) ±1	97 (18) ±1	73 ±1	68 ±1	70 ±1
14	97 (3) ±3	98 (1) ±0	96 (4) ±2	70 ±2	70 ±0	70 ±1
15	102 (2) ±1	101 (3) ±0	101 (5) ±1	70 ±1	74 ±2	74 ±1
16	101 (3) ±2	105 (1) ±0	102 (4) ±2	75 ±1	70 ±1	75 ±1

monthly increment growth that peaked in July, followed by a large decline in August (Fig. 4). Based on this information, the increment analyses support the likelihood that a single opaque band may be formed annually on vertebral centra during August or September. The marginal analysis was only conclusive for juvenile-size animals (skates ≤80 cm TL). As thorny skates matured, their growth slowed dramatically and the band counts in older specimens became compressed, making it difficult to discern monthly changes in margin width.

Age and growth estimates

The von Bertalanffy growth curves (VBGC) fitted to total length-at-age data (Fig. 5) provided a reasonable fit with a low standard error for males, females, and both sexes combined (Table 2). Furthermore, the VBGC parameters for males, females, and the sexes combined were similar, and because no differences in age-at-size existed between males and females ($P>0.05$ ANOVA), those data were combined (Fig. 5).

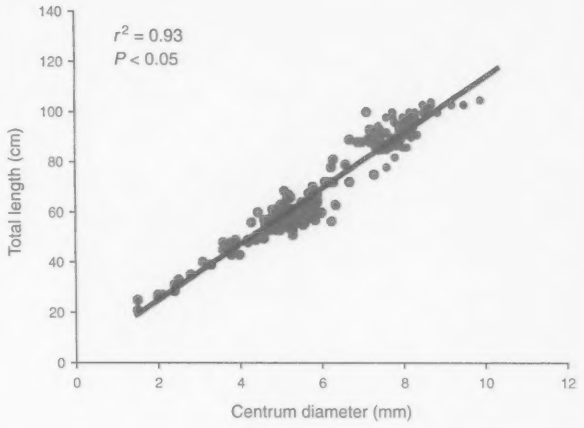

Figure 3

The relationship of total length (cm) to centrum diameter (mm) for combined sexes of thorny skate (*Amblyraja radiata*).

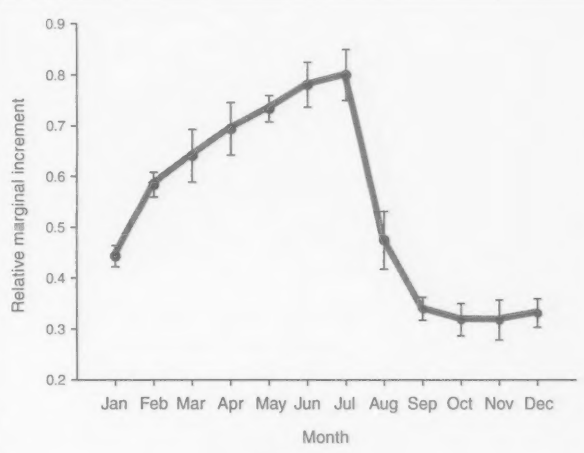

Figure 4

Mean monthly marginal increments of opaque bands for *Amblyraja radiata* from the Gulf of Maine. Marginal increments were calculated each month from 10 specimens whose centra contained less than 10 annuli. Error bars represent 1 ±SEM.

Discussion

Precision estimates, the relationship between TL and centrum diameter, and marginal increment analysis support the use of vertebral centra for age analyses of thorny skates captured in the Gulf of Maine (Conrath et al., 2002; Sulikowski et al., 2003). Furthermore, the 2.8% coefficient of variation indicates that our aging method represents a precise approach for the age assessment of *A. radiata* (Campana, 2001). Minimal width of the marginal increment for thorny skates captured in August and September (Fig. 4) supports the hypothesis of annual band formation in this species. Moreover, these results compare favorably to cycles in marginal increments (Sulikowski et al., 2003) and to annual vertebral band patterns in other skate species (Holden and Vince, 1973; Waring, 1984; Natanson, 1993; Zeiner and Wolfe, 1993; Walmsley-Hart et al., 1999; Francis et al., 2001). However, because the band counts of the largest and oldest animals in the population were compressed (too small for us to discern marginal increments from their widths), the marginal increment analysis included only juvenile skates that were ≤80 cm total length and the annular nature of the growth bands was verified for only those length groups. Nevertheless, we assumed that as the skates grew larger and older, the annual nature of growth ring deposition continued throughout their lifetime (Conrath et al, 2002).

During 42 sampling trips from June 2001 through May 2002 (approximately three trips per month), individuals <30 cm TL were rarely captured. The lack of specimens in this size class and smaller size classes was most likely due to the mesh size of the commercial trawl nets. Trawl nets used by commercial fishermen in the Gulf of Maine are restricted to a 6½-inch diamond mesh-size opening, which facilitates the release of most fish below 30 cm TL.

Our estimates of L_∞ exceed the largest specimens in our field collections for both females and males. Growth parameters estimated from the Gompertz and logistics equations also produced over-estimations of L_∞ for the thorny skates in our study. Because the von Bertalanffy growth curve (VBGC) is most widely used and accepted in elasmobranch age and growth studies, we chose to use this function to fit our data. Over estimation of L_∞ with the VBGC has been documented in most skate species studied to date (Table 3). Campana (2001) suggested that the smallest and largest specimens are the most influential in the estimation of growth. Moreover, both Walmsley-Hart et al. (1999) and Sulikowski et

al. (2003) suggested that rareness of large individuals was most likely responsible for their over estimation of L_∞. Similarly, in a study of the blue shark (*Prionace glauca*) in the northwest Atlantic, Skomal and Natanson (2003) suggested that earlier studies on the same species contained artificially inflated L_∞ estimates and lower growth rates because of the lack of maximum-size fish. The rareness of large specimens in our study may have been due to these larger individuals being able to avoid the fishing gear or may indicate that mortality, natural or fishing induced, prevents them from attaining these lengths. Exploratory manipulation of our data indicated that inclusion of maximum observed sizes (i.e., thorny skates over 103 cm TL) produced divergent results with regard to von Bertalanffy parameters. For example, the addition of maximum-size fish, using 20 years as the maximum age (Templeman, 1984) and 105 cm as the maximum total length (from the present study), reduced the combined sex L_∞ from 124 cm TL to 116 cm TL. However, the same effect was not documented when adding hatching size (age zero) fish (note: because no documented size for thorny skates exists within the Gulf of Maine, the authors used known hatching sizes for a similar congener species, the winter skate [*Leucoraja ocellata*]). Be that as it may, the reasonable fit of the thorny skate data (Table 2) to the VBGC (Fig. 5) for *A. radiata*, along with a comparison with other batoid studies (Table 3), indicates that this is an appropriate model for this skate species.

Growth rates were similar for both sexes of thorny skate (k=0.13 for females and k=0.11 for males) and commensurate with other skate species of a similar size. The oldest age obtained for male and female thorny skates was 16 years (Table 1). These data are in agreement with the assumption that larger batoids, such as *A. radiata, R. pullopunctata* (Walmsley-Hart et al., 1999), and *L. ocellata* (Sulikowski et al., 2003) are longer lived and slower growing than smaller species. For instance, *R. erinacea,* which reaches a total length of 52 cm, has been aged to 8 years and found to have a corresponding k value of 0.352 (Johnson, 1979; Waring, 1984).

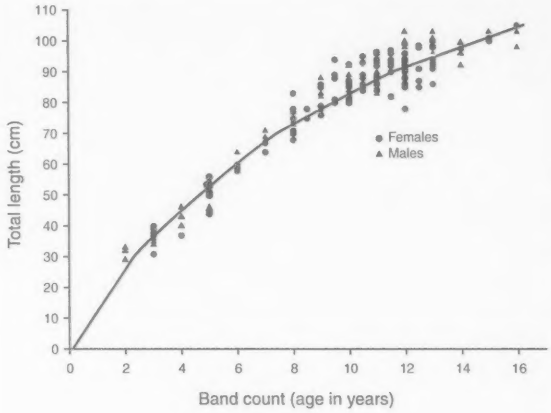

Figure 5

Von Bertalanffy growth curve generated from combined vertebral data for female and male thorny skates (*Amblyraja radiata*) from the western Gulf of Maine. Individual VBGC parameters are given in Table 2.

Table 2

Calculated von Bertalanffy parameters for male, female, and combined sexes of *A. radiata*.

Parameter	Male	Female	Combined sexes
L_∞ (cm TL)	127.00	120.00	124.00
K (/year)	0.11	0.13	0.12
t_0 (year)	−0.37	−0.4	−0.35
r^2	0.96	0.92	0.94
SE	0.01	0.01	0.001
n	103.00	121.00	224.00

The reduction in biomass of the thorny skate below threshold levels mandated by the SFA necessitates the development of management measures to rebuild these stocks in accordance with the Magnuson-Stevens Fishery Conservation and Management Act. However, the development and implementation of a successful fisheries management plan for the species require in-depth analyses of appropriate biological information. Moreover, accurate stock assessment data for skates is difficult to collect in the northeast U.S. because individual species are rarely differentiated in landings information (NEFMC[1,2]). As a result, fluctuations in stock size will continue to be difficult to detect and successful implementation of fisheries management plans will remain problematic. This article is the first in a series aimed at providing life history data for the management of thorny skates indigenous to the Gulf of Maine. The basic age and growth parameters for the thorny skate provided in the present study support the hypothesis that *A. radiata*, like other elasmobranchs, require conservative management because of their slow growth rate and susceptibility to over-exploitation (Brander, 1981; Kusher et al., 1992; Zeiner and Wolf, 1993; Frisk et al., 2001; Sulikowski et al., 2003).

Acknowledgments

Collection of skates was conducted on the FV *Mystique Lady*. We thank Noel Carlson for maintenance of the fish at the U.N.H. Coastal Marine Laboratory and Matt Ayer for his help in digitizing the vertebrae samples. This

Table 3

Comparison of von Bertalanffy derived L_∞ to the observed total lengths (L) for a number of skate species. L_∞ (mm) = disk width.

Scientific name	Sex	L_∞ (mm)	L observed (mm)	Max. age (yr)	Source
Raja microocellata	♀ ♂	1370 (TL)	875[1]	9	Ryland and Ajayi, 1984
Raja montagui	♀ ♂	978 (TL)	710[1]	7	Ryland and Ajayi, 1984
Raja clavata	♀	1047 (TL)	1392	7	Ryland and Ajayi, 1984
Raja erinacea	♀ ♂	527 (TL)	520	8	Waring, 1984
Raja rhina	♂	967 (TL)	1322	13	Zeiner and Wolf, 1993
Raja rhina	♀	1067 (TL)	1047	12	Zeiner and Wolf, 1993
Raja wallacei	♂	405 (DW)	512	15	Walmsley-Hart et al., 1999
Raja wallacei	♀	435 (DW)	571	15	Walmsley-Hart et al., 1999
Raja pullopunctata	♂	771 (DW)	696	18	Walmsley-Hart et al., 1999
Raja pullopunctata	♀	1327 (DW)	747	14	Walmsley-Hart et al., 1999
Raja pullopunctata	♀	1327 (DW)	747	14	Walmsley-Hart et al., 1999
Dipturus nasutus	♀ ♂	700 (TL)	913	9	Francis et al., 2001
Dipturus innominatus	♀ ♂	1330 (TL)	1505	24	Francis et al., 2001
Leucoraja ocellata	♀ ♂	1314 (TL)	936[1]	19	Sulikowski et al., 2003
Amblyraja radiata	♀ ♂	1240 (TL)	1020[1]	16	Present study

[1] Average of male and female observed TL.

project was supported by a Northeast Consortium grant (no. NA16FL1324) to PCWT, JAS, and PDD.

Literature cited

Brander, K.
1981. Disappearance of common skate *Raia batis* from Irish Sea. Nature 290 (5801):48–49.

Branstetter, S., and J. A. Musick.
1984. Age and growth estimates for the sand tiger in the northwestern Atlantic ocean. Trans. Am. Fish. Soc. 123:242–254.

Brown, C. B., and S. H. Gruber.
1988. Age assessment of the lemon shark, *Negaprion brevirostris*, using tetracycline validated vertebral centra. Copeia 3:747–753.

Casey, J. G., H. L. Pratt, and C. E. Stillwell.
1985. Age and growth of the sandbar shark (*Carcharhinus plumbeus*) from the western North Atlantic. Can. J. Fish. Aquat. Sci. 42(5):963–975.

Casey, J. M., and R. A. Myers.
1998. Near extinction of a large widely distributed fish. Science 28:690–692.

Cailliet, G. M.
1990. Elasmobranch age determination and verification: an updated review. *In* Elasmobranchs as living resources: advances in the biology, ecology, systematics and the status of the fisheries (L. Pratt Jr, S. H. Gruber, and T. Tanuichi (eds.), p. 157–165. NOAA Tech. Report NMFS 90.

Campana, S. E.
2001. Accuracy, precision and quality control in age determination including a review of the use and abuse of age validation methods. J. Fish. Biol. 59:197–242.

Campana, S. E., M. C. Annand, and J. I. Mcmillan.
1995. Graphical and statistical methods for determining the consistency of age determinations. Trans. Am. Fish. Soc. 124:131–138.

Chang, W. Y. B.
1982. A statistical method for evaluating the reproducibility of age determination. Can. J. Fish. Aquat. Sci. 39:1208–1210.

Collette, B., and G. Klein-MacPhee, eds.
2002. Bigelow and Schroeder's fishes of the Gulf of Maine, 3rd ed., p. 62–66. Smithsonian Institution Press, Washington, D. C.

Compagno, L. J. V., D. A. Ebert, and M. J. Smale.
1989. Guide to the sharks and rays of southern Africa, 158 p. New Holland (Publ.) Ltd., London.

Conrath, C. L., J. Gelsleichter, and J. A. Musick.
2002. Age and growth of the smooth dogfish, *Mustelus canis*, in the northwest Atlantic. Fish. Bull. 100:674–682.

Dulvey, N. K., J. D. MetCalfe, J. Glanville, M. G. Pawson, and J. D. Reynolds.
2000. Fishery stability, local extinctions, and shifts in community structure in skates. Cons. Biol. 14 (1): 283–293.

Francis, M., C. O. Maolagain, and D. Stevens.
2001. Age, growth, and sexual maturity of two New Zealand endemic skates, *Dipturus nasutus* and *D. innominatus*. N. Z. J. Mar. Freshw. Res. 35:831–842.

Frisk, M. G.
2000. Estimation and analysis of biological parameters in elasmobranch fishes and the population dynamics of the little skate *Raja erinacea*, thorny skate *R. radiata* and Barndoor skate *R. laevis*. M.S. thesis, 112 p. Center for Environmental Science, Univ. Maryland, Cambridge, MD.

Frisk, M. G., T. J. Miller, and M. J. Fogarty.
2001. Estimation and analysis of biological parameters in elasmobranch fishes: a comparative life history study. Can. J. Fish. Aquat. Sci. 58(5):969–981.

Hoenig, J., and S. H. Gruber.
1990. Life history patterns in the elasmobranchs: implications for fisheries management. *In* Elasmobranchs as living resources: advances in the biology, ecology, systematics and the status of the fisheries (H. L. Pratt Jr, S. H. Gruber, and T. Tanuichi, eds.), p. 1–16. NOAA Tech. Report, NMFS 90.

Holden, M. J.
1977. Elasmobranchs. *In* Fish population dynamics (J. A. Gulland, ed.), p. 187–214. J. Wiley and Sons, London, England.

Holden, M. J., and M. R. Vince.
1973. Age validation studies on the centra of *Raja clavata* using tetracycline. J. Cons. Int. Explor. Mer 35:13–17.

Johnson, G. F.
1979. The biology of the little skate, *Raja erinacea*, in Block Island Sound, Rhode Island. Unpubl. M.A. thesis, 119 p. Univ. Rhode Island. Kingston, RI.

Kusher, D. I., S. E. Smith, and G. M. Cailliet
1992. Validated age and growth of the leopard shark, *Triakis semifasciata*, with comments on reproduction. Environ. Biol. Fish. 35:187–203.

Magnuson Fishery Conservation and Management Act.
1994. 16 U.S.C.1801-1882 (1994), amended by Sustainable Fisheries Act, Pub. L. No. 104-297, 110 Stat. 3559 (1996).

Marquardt, D. W.
1963. An algorithm for the least squares estimation of nonlinear parameters. J. Soc. Ind. Appl. Math. 2: 431–441.

Natanson, L. J.
1993. Effect of temperature on band deposition in the little skate, *Raja erinacea*. Copeia 1993:199–206.

Prager, M. H., S. B. Saila, and C. W. Recksiek.
1987. Fishparm: a microcomputer program for parameter estimation of nonlinear models in fishery science. Old Dominion University, Norfolk Virginia, Tech. Rep. (87–10):1–37.

Robins, C. R., and G. C. Ray.
1986. A field guide to Atlantic coast fishes of North America, 354 p. Houghton Mifflin Co., Boston, MA.

Ryland, J. S., and T. O Ajayi.
1984. Growth and population dynamics of three *Raja* species (Batoidei) in Carmarthen Bay, British Isles. J. Cons. Int. Explor. Mer 41:111–120.

Simpfendorfer, C.A.
1993. Age and growth of the Australian sharpnose shark, *Rhizoprionodon taylori*, from north Queensland, Australia. Environ. Biol. Fish. 36:(3):233–241.
2000. Age and growth of the whiskery shark, *Furgaleus macki*, from south-western Australia. Environ. Biol. Fish. 58:335–343.

Skomal, G. B, and L. J. Natanson.
2003. Age and growth of the blue shark (*Prionace glauca*) in the North Atlantic Ocean. Fish. Bull. 101:627–639.

Sosebee, K.
2000. Skates. Status of fishery resources off the northeastern United States. NOAA Tech. Mem. NMFS-NE. 115:114–115.

Sulikowski, J. A., M. D. Morin, S. H. Suk, and W. H. Howell.
2003. Age and growth of the winter skate, *Leucoraja ocellata*, in the Gulf of Maine. Fish. Bull. 101:405–413.

Templeman, W.
1984. Migrations of thorny skate, *Raja radiata*, tagged in the Newfoundland area. J. Northw. Atl. Fish. Sci. 5(1):55–63.
1987. Differences in sexual maturity and related characteristics between populations of thorny skate *Raja-radiata* in the northwest atlantic. J. Northw. Atl. Fish. Sci. 44 (1):155–168.

Von Bertalanffy, L.
1938. A quantitative theory of organic growth (inquiries of growth laws II). Human Biology 10:181–183.

Walmsley-Hart, S. A., W. H. H. Sauer, and C. D. Buxton.
1999. The biology of the skates *Raja wallacei* and *R. pullopunctata* (Batoidea:Rajidae) on the Agulhas Bank, South Africa. S. Afr. J. Mar. Sci. 21:165–179.

Waring, G. T.
1984. Age, growth and mortality of the little skate off the northeast coast of the United States. Trans. Am. Fish. Soc. 113:314–321.

Winemiller, K. O., and K. A. Rose.
1992. Patterns of life history diversification in North American fishes: implication for population regulation. Can. J. Fish. Aquat. Sci. 49:2196–2218.

Wintner, S. P., and G. Cliff.
1996. Age and growth determination of the blacktip shark, *Carcharhinus limbatus*, from the east coast of South Africa. Fish. Bull. 94 (1):135–144.

Zeiner, S. J., and P. G. Wolf.
1993. Growth characteristics and estimates of age at maturity of two species of skates (*Raja binoculata* and *Raja rhina*) from Monterey Bay, California. *In* Conservation biology of elasmobranches (S. Branstetter, ed.), p. 87–90. NOAA Tech. Report NMFS 115.

Age validation, growth modeling, and mortality estimates for striped trumpeter (*Latris lineata*) from southeastern Australia: making the most of patchy data

Sean R. Tracey
Jeremy M. Lyle
Marine Research Laboratories
Tasmanian Aquaculture and Fisheries Institute
Private Bag 49
Hobart 7001, Tasmania, Australia
E-mail address (for S R. Tracey): stracey@utas.edu.au

Abstract—Age estimates for striped trumpeter (*Latris lineata*) from Tasmanian waters were produced by counting annuli on the transverse section of sagittal otoliths and were validated by comparison of growth with known-age individuals and modal progression of a strong recruitment pulse. Estimated ages ranged from one to 43 years; fast growth rates were observed for the first five years. Minimal sexual dimorphism was shown to exist between length, weight, and growth characteristics of striped trumpeter. Seasonal growth variability was strong in individuals up to at least age four, and growth rates peaked approximately one month after the observed peak in sea surface temperature. A modified two-phase von Bertalanffy growth function was fitted to the length-at-age data, and the transition between growth phases was linked to apparent changes in physiological and life history traits, including offshore movement as fish approach maturity. The two-phase curve was found to represent the mean length at age in the data better than the standard von Bertalanffy growth function. Total mortality was estimated by using catch curve analysis based on the standard and two-phase von Bertalanffy growth functions, and estimates of natural mortality were calculated by using two empirical models, one based on longevity and the other based on the parameters L_∞ and k from both growth functions. The interactions between an inshore gillnet fishery targeting predominately juveniles and an offshore hook fishery targeting predominately adults highlight the need to use a precautionary approach when developing harvest strategies.

Manuscript submitted 20 December 2003 to the Scientific Editor's Office.
Manuscript approved for publication 7 September 2004 by the Scientific Editor.
Fish. Bull. 103:169–182 (2005).

Striped trumpeter (*Latris lineata*) are widely distributed around the temperate latitudes of southern Australia, New Zealand (Last et al., 1983), the Gough and Tristan Da Cunha Island groups in the southern Atlantic Ocean (Andrew et al., 1995), and the Amsterdam and St. Paul Island groups in the southern Indian Ocean (Duhamel, 1989). They are opportunistic carnivores associated with epibenthic communities over rocky reefs at moderate depths from 5 to 300 m along the continental shelf. The species can grow to a relatively large size, 1200 mm in total length and 25 kg in weight (Gomon et al., 1994). Spawning apparently occurs offshore, and females are highly fecund multiple-spawners (Furlani and Ruwald, 1999). Although there have been a number of ichthyoplankton surveys in Tasmanian waters, only a few striped trumpeter larvae have been collected, caught during the late austral winter through early spring months at nearshore (30–50 m) and shelf edge sites (~200 m) (Furlani and Ruwald, 1999). Larval rearing trials have shown that the presettlement phase is complex and extended; individuals can remain in this neritic-pelagic phase for up to 9 months after hatching before metamorphosis into the juvenile stage takes place (Morehead[1]). As juveniles striped trumpeter settle on shallow rocky reefs.

In Tasmania striped trumpeter are taken commercially over inshore reefs (5 to 50 m), generally as a bycatch of gillnetting, and are targeted with hook methods (handline, dropline, longline, and trotline) on deeper reefs (80 to 300 m). Small, subadult individuals dominate inshore catches, whereas larger individuals are taken from offshore reefs. In recent years the combined annual commercial catch has been typically less than 100 metric tons (Lyle[2]). Striped trumpeter also attract significant interest from recreational fishermen, who use both hooks and gill nets. Furthermore, the aquaculture potential for this species is currently being assessed in Tasmania (Furlani and Ruwald, 1999; Cobcroft et al., 2001). Despite wide interest in this species, there is a general paucity of information on age, growth, and stock structure of wild populations.

Assessing the growth of a species is a fundamental part of fisheries population dynamics. Ever since Beverton and Holt (1957) introduced the von Bertalanffy growth model to fisheries research it has become ubiquitous in descriptions of the increase in size

[1] Morehead. D. 2003. Personal commun. Tasmanian Aquaculture and Fisheries Institute, Univ. Tasmania. GPO Private Bag 49, Hobart, Tasmania, Australia 7001.

[2] Lyle. J. M. 2003. Tasmanian scalefish fishery—2002. Fishery assessment report of the Marine Research Laboratories, Tasmanian Aquaculture and Fisheries Institute, Tasmania. [Available from TAFI GPO Private Bag 49, Hobart, Tasmania, Australia 7001.]

of a species as a function of age. The parameters common to the von Bertalanffy growth function (VBGF) are used in stock assessment models such as empirical derivatives of natural mortality (Pauly, 1980) and assessments of yield per recruit and spawning stock biomass (Beverton and Holt, 1957). Despite the von Bertalanffy growth parameters being well established as cornerstones of many stock assessment models, several authors have highlighted limitations of the original derivation of the growth function to adequately represent growth of a population (Knight, 1968; Sainsbury, 1979; Roff, 1980; Schnute, 1981; Bayliff, et al, 1991; Hearn and Polacheck, 2003). This limitation becomes especially evident with limited or patchy data. The limitations of the von Bertalanffy growth function have created three scenarios: 1) use the VBGF and retain the use of the parameters to derive per-recruit estimates at the possible expense of physiological integrity; 2) derive or employ a model that is not based on the von Bertalanffy parameters (such as a linear or logistic model) or another polynomial function (for instance, the Gompertz equation [Schnute, 1981]) and in doing so the expediency of the von Bertalanffy parameters in stock assessments is compromised; 3), use or develop an extension of the von Bertalanffy equation with the caveat that, by introducing additional parameters, the problem of reduced parsimony by over parameterisation would need to be considered.

While investigating the life history characteristics of striped trumpeter, we became aware that the original description of the VBGF would not adequately represent growth of this species, in part because of the patchy data available for analysis.

This study aims to describe the age and growth of striped trumpeter from Tasmania. Seasonal growth oscillations are considered for the first four years by using actual length-at-age data from a strong cohort. We then employ and evaluate an extension of the VBGF that offers a better fit to the sample population of aged individuals and allows the flexibility of assigning representative growth and mortality parameters to different life phases of the population. Growth parameters derived from both the standard von Bertalanffy and extended von Bertalanffy models are used in our catch curve analyses, and the empirical models of Pauly (1980) and Hoenig (1983) are used to allow comparison of mortality estimates.

Materials and methods

Striped trumpeter were collected opportunistically from various sites off the east and southeast coasts of Tasmania from a variety of fisheries dependent and independent sources spanning the period 1990–2002 (Table 1). Inshore catches were predominately taken with gill nets ranging in mesh sizes from 64 to 150 mm. Offshore catches were taken by hook-and-line methods. Samples ranged from intact specimens, for which the full range of biological information was collected, to processed frames from which length and, depending on condition of the body, sex and gonad weight were recorded. All specimens were measured for fork length (±1 mm) and, where possible, total weight was recorded (±1 gram). Otoliths were collected when possible. This *ad hoc* sampling approach created a temporally irregular data set.

Table 1

Composition of Tasmanian sampling data from 1990 through 2002 showing data from inshore gill net and offshore hook fisheries. Numbers in parentheses represent the number of individuals aged from each particular sampling regime.

Year	Gill net	Hook	Total
1990	—	45	45
1991	—	332	332
1992	—	126	126
1994	3	8	11
1995	228	12	240
1996	529	55	585
1997	193	2	195
1998	7	171	178
1999	205	902	1107
2000	—	91	91
2001	—	60	60
2002	—	97	99
Total	1165	1901	3069
	(268)	(508)	(776)

Kolmogorov-Smirnov tests (α=0.05) were used to determine whether significant differences existed between male and female length-frequency distributions or between length-frequency distributions by depth strata.

Analysis of residual sums of squares (Chen, 1992) was used to determine whether a significant difference existed between the sex-specific length-weight relationships that were fitted by minimizing the sum of square residuals and that are described by the power function

$$W = aL^b, \quad (1)$$

where W = whole weight (g);
L = fork length (mm); and
a and b = constants.

Sex ratios were compared for significant deviation from 1:1 by chi-square tests.

Aging technique

Sagittal otoliths were removed from 873 individuals and a subsample of 295 otoliths were individually weighed to the nearest milligram. One randomly selected otolith from each fish was embedded in clear polyester casting resin. A transverse section was taken through

the primordial region (width approximately 300 μm) and mounted on a microscope slide. A stereo dissector microscope at 25× magnification was used to aid the interpretation of increments in the mounted sections. Increment measurements were made by using Leica IM© image digitization and analysis software (Leica Microsystems, Wetzlar, Germany). All counts and increment measurements were made without knowledge of fish size, sex, or date at capture to avoid reader bias.

Position of the first annual increment was determined by testing the close correspondence of otolith microstructure and body size between known-age individuals reared from eggs in aquaria and wild-caught specimens. To ensure that growth in cultured individuals also reflected growth in wild specimens, a hypothesis of comparable growth was tested by fitting traditional VBGFs to the length-at-age data of 288 cultured individuals (maximum known age: 4 years) and 268 wild specimens (maximum otolith-derived age: 4 years). A likelihood ratio test (Kimura, 1980) was then used to test for significance. The VBGF model was in the form

$$L_t = L_\infty(1 - e^{-(t - t_0)}) + \varepsilon. \quad (2)$$

where L_t = length at age t;
L_∞ = average asymptotic length;
k = a constant describing how rapidly L_∞ is achieved;
t_0 = the theoretical age where length equals zero; and
ε = independent normally distributed (O, σ^2) error term.

Modal progression of length frequencies from a strong cohort of juvenile fish was sampled over a three-year period (1995–97). This cohort provided an opportunity to validate annual periodicity in increment deposition. By applying an aging protocol based on position of the first increment and assuming that each opaque+translucent zonal pair represented one year of growth, this recruitment pulse could be tracked over seven years in age-frequency progression.

A random subsample of 335 otoliths was read a second time by the primary reader, and a second subsample of 46 otoliths by a second reader, both experienced in otolith interpretation. Precision was assessed by determining percentage agreement between repeated readings, age bias plots (Campana et al., 1994), and calculating the average percent error (APE) (Beamish and Fournier, 1981).

Growth modeling

The length-frequency progression of a strong and discrete cohort of fish indicated that striped trumpeter may be subject to seasonal growth variability. This variability was described by integrating a sinusoidal function (Pitcher and MacDonald, 1973; Haddon, 2001) into a standard VBGF and by applying this function to the actual weekly length-at-age data of individuals sampled from the strong 1993 cohort over the period 1995 through 1997, where the model was described as

$$L_t = L_\infty\left(1 - e^{-\left[C\sin\left(\frac{2\pi(t-S)}{52}\right) + k(t-t_0)\right]}\right) + \varepsilon, \quad (3)$$

where C = the magnitude of the oscillations above and below the nonseasonal growth curve of the sinusoidal cycle;
S = the starting point in weeks of the sinusoidal cycles; and
52 = the cycle period in weeks.

The timing of seasonal growth was compared with weekly average sea surface temperature (SST) on the southeast coast of Tasmania over the sampling period, calculated by using optimum interpolation (Reynolds et al., 2002) of raw remotely sensed data from the area (NOAA-CIRES[3]). A sine function was fitted to the weekly average SST by using least squares regression to compare the timing and phase of growth and temperature and test for a significant correlation.

All individuals aged were assigned a "decimal" age, where the decimal portion represented the proportion of the year between a nominal average date of spawning (1st October) and the date of capture. We assumed a nominal peak spawning date of 1 October based on an assessment of monthly averaged gonadosomatic index (Tracey, unpubl. data), which is consistent with that observed for wild-caught broodstock held under ambient conditions (Morehead[1]).

Growth of the sampled population was initially described by using the standard von Bertalanffy growth function (Eq. 2). However, a preliminary visual assessment of the fit suggested it did not produce an adequate representation of the entire data set. In an attempt to find a model that better represented the data, the fit of the standard von Bertalanffy growth function ($VBGF_S$) was compared with an extension of the traditional von Bertalanffy growth model fitted by minimization of the sum of negative log-likelihood; normal distribution of the error term. The model chosen was similar to that used by Hearn and Polacheck (2003) and involved fitting a VBGF function either side of an age at transference, described as

$$L_t = \begin{cases} \left(L_{\infty 1}(1 - e^{-k_1(t - t_{01})}\right) + \varepsilon & \text{for } t < t^\delta \\ \left(L^\delta + (L_{\infty 2} - L^\delta)(1 - e^{-k_2(t - t_{02})}\right) + \varepsilon & \text{for } t \geq t^\delta \end{cases}, \quad (4)$$

[3] Data sourced from the NOAA-CIRES Climate Diagnostics Center, Boulder, CO 80305. http://www.cdc.noaa.gov/. [Accessed 15 Sep. 2002]

where $L_{\infty 1}$, k_1, t_{01} = VBGF parameters applied to the first growth phase;
$L_{\infty 2}$, k_2, t_{02} = VBGF parameters applied to the second growth phase;
L^{δ} = length of transference from one growth phase to the next; and
t^{δ} = age of transference from one growth phase to the next; calculated as,

$$t^{\delta} = t_{01} - \frac{1}{k_1}\ln\left(1 - \frac{L_t}{L_{\infty 1}}\right). \quad (5)$$

Having fitted Equation 4, we smoothed the discontinuity from the first growth stanza to the second, assuming normal distribution around the age at transference by integrating a normal probability cumulative distribution function (PDF) where the mean is equal to the age of transference (4.4 years) and where the standard deviation is arbitrarily set at 1.0. This model is referred to as the two-phase von Bertalanffy growth function ($VBGF_{TP}$) and is now represented as

$$L_t = \begin{cases} \left(1 - \int_{t=-t_0}^{+t^{\delta}} \frac{1}{\sigma\sqrt{2\pi}} e^{\left(\frac{-(t-t_{01})^2}{2\sigma^2}\right)}\right)\left(L_{\infty 1}(1-e^{-k_1(t-t_{01})}) + \varepsilon\right) + \\ \left(\int_{t=t^{\delta}}^{+t_{max}} \frac{1}{\sigma\sqrt{2\pi}} e^{\left(\frac{-(t-t^{\delta})^2}{2\sigma^2}\right)}\right)\left(L^{\delta} + (L_{\infty 2} - L^{\delta})(1-e^{-k_2(t-t_{02})}) + \varepsilon\right) \end{cases}, \quad (6)$$

where t_{max} = maximum age present in the sample; and
σ^2 = standard deviation of cumulative density function with mean t^{δ}.

The model that best represented the data was judged on a combination of parsimony as determined by the Akaike information criterion (AIC) (Akaike, 1974), quality of fit by minimization of the negative log-likelihood value derived from each model, visual inspection of the residuals, and as an index of fit, the percent deviation of L_{∞} for each model from the maximum observed length (L_{max}).

The hypothesis of sexual dimorphism in growth was tested by using likelihood ratio tests (Kimura, 1980) for both the $VBGF_S$ and $VBGF_{TP}$ models fitted to the length-at-age data of all individuals whose sex had been determined.

Mortality estimation

Mortality estimates were calculated by using the parameters of both the $VBGF_S$ and $VBGF_{TP}$ functions. An estimate of instantaneous rate of total mortality (Z) for the offshore hook fishery was calculated for 1998 by applying a length converted catch curve analysis (LCCCA *sensu* Pauly, 1983) to the length-frequency data.

Estimates of instantaneous rate of natural mortality (M) were calculated by using two empirical equations. The first equation, derived by Pauly (1980), is described as

$$\log_{10} M = -0.0066 - 0.279 \log_{10} L_{\infty\gamma} + 0.6543 \log_{10} k_{\gamma} + 0.4634 \log_{10} T, \quad (7)$$

where $L_{\infty\gamma}$ and k_{γ} = parameters derived from the $VBGF_S$ or from the second growth phase of the $VBGF_{TP}$; and
T = average annual sea surface temperature (°C) at the area of capture.

The mean annual sea surface temperature on the east coast of Tasmania in 1998 was estimated as 14°C (NOAA-CIRES[3]). The second equation used was the regression equation of Hoenig (1983):

$$\ln Z = 1.46 - 1.01 \ln t_{max}; \quad M \sim Z \text{ assuming } F \sim 0, \quad (8)$$

where t_{max} = the maximum age for the species in years.

Estimates of fishing mortality (F) were calculated by subtracting natural mortality from total mortality.

Results

Males ranged in length from 203 mm to 815 mm (n=504) and females ranged from 269 mm to 950 mm (n=565). Length-frequency distributions did not differ significantly between sexes (Kolmogorov-Smirnov; Z=0.91 P=0.38).

Pooling the length-frequency data of all individuals produced a bimodal frequency distribution. However, when grouped by depth (Fig. 1), the data revealed a significant depth-based stratification between the shallow (<50 m stratum) and the deeper strata (Kolmogorov-Smirnov; Z=13.8 P<0.001), occurring at around 450 mm in length.

Analysis of residual sums of squares indicated no significant difference between the sex-specific length-weight relationships (F=0.02 df=2 P=0.10); consequently a power regression was applied to the length-weight data of all individuals combined (Table 2).

The sex ratio of males to females (1.0:1.3) from the inshore net fishery showed a low level of significant difference from 1:1 (χ^2=3.88 P=0.049 n=232), whereas, the ratio of males to females (1.0:1.1) caught from the offshore hook fishery did not show significant difference from 1:1 (χ^2=0.933 P=0.334 n=840).

Age estimates

Age was successfully estimated for 776 (89%) individuals. Transverse otolith sections showed typical distinct alternate light and dark zone formations within the

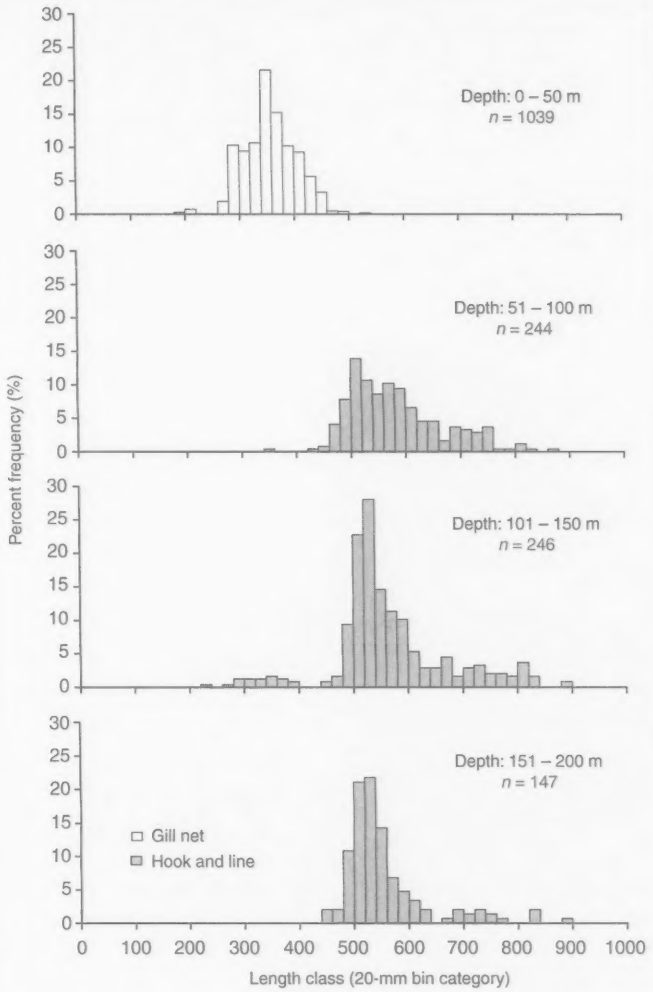

Figure 1

Length-frequency distribution by 50-m depth strata for striped trumpeter (*Latris lineata*) samples collected from 1990 through 2002.

Table 2

Predictive equations used to compare weight and length, otolith weight and age, and reader variability across age classes, for striped trumpeter (*Latris lineata*).

Dependent variable	Independent variable	n	Equation	r^2
Weight (W)	Fork length (L)	491	$W = 2 \times 10^{-5} \times L^{3.00}$	0.99
Otolith weight (OW)	Age (t)	295	$OW = 7.32 + (1.70 \times t)$	0.89
Primary reader, count 2 (P_2)	Primary reader, count 1 (P_1)	339	$P_2 = 0.05 + (0.99 \times P_1)$	0.99
Secondary reader, count 1 (S_1)	Primary reader, count 1 (P_1)	46	$S_1 = 0.27 + (0.97 \times P_1)$	0.97

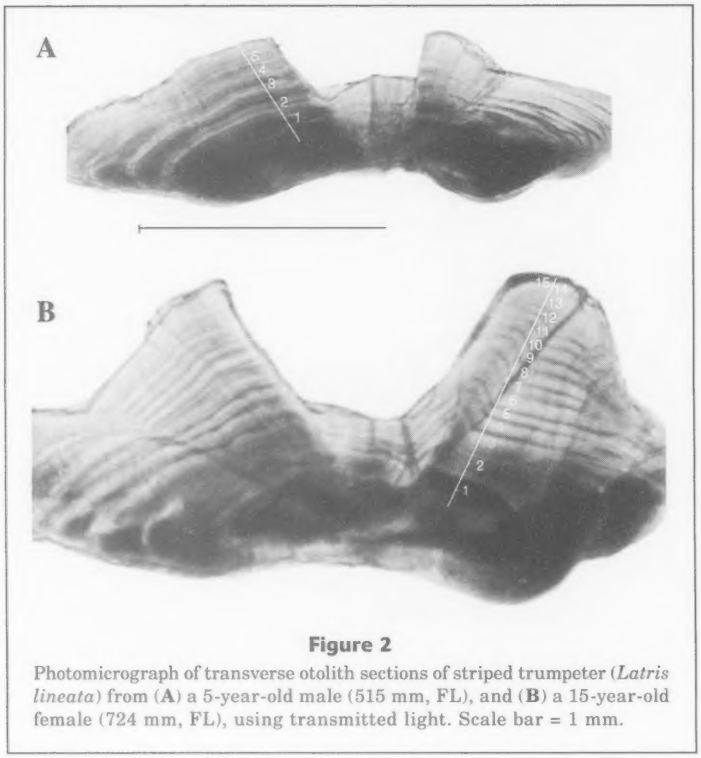

Figure 2

Photomicrograph of transverse otolith sections of striped trumpeter (*Latris lineata*) from (**A**) a 5-year-old male (515 mm, FL), and (**B**) a 15-year-old female (724 mm, FL), using transmitted light. Scale bar = 1 mm.

otolith matrix. Viewed under transmitted light the zones showed as dark (opaque) and light (translucent) (Fig. 2). A robust linear relationship existed between otolith mass and individual age (Table 2).

The core area of each section consisted of an opaque region. Immediately adjacent to this was a faint thin translucent zone followed by the first broad opaque annual increment. In some cases the transition from core to the first expected increment could not be discerned because of a continuation of the opaque region (the expected thin translucent zone was too faint to see). In such cases, increment measurements were required to ensure that the annulus was not overlooked. Mean increment radius (±SD) from the primordia to the first annulus was 491 ±63 μm (n=122); and the deposition of the second annulus occurred at a mean radius of 733 ±55 μm (n=122). The next four opaque and translucent zone pairs were relatively broad compared with subsequent zones that consistently narrowed as they approached the growing edge (Fig. 2).

To validate the first increment we compared somatic and otolith growth of wild individuals with that of individuals cultured under ambient conditions. Larval-rearing trials of striped trumpeter juveniles have produced mean lengths of 190 mm at 14 months and 261 mm at 24 months. The smallest individuals recorded from the wild in our study were 190–220 mm and were captured in January 1995. From the rearing trials it seemed reasonable to assume that the wild-caught individuals of this size were between 1 and 2 years of age. If a birth date of 1 October is assumed, these individuals would have been about 16 months old and therefore were spawned in 1993. Viewing the sectioned otoliths of these small wild-caught individuals revealed only one increment within the margin, analogous to the increment composition of cultured individuals at a similar length.

To test for comparable growth between wild and cultured individuals as a means to facilitate confident validation of the first increment deposition, von Bertalanffy growth curves were fitted to length-at-age data of both wild (based on otoliths) and cultured individuals (of known age) to age four. A likelihood ratio test indicated that wild-caught individuals increased in length slightly faster than those cultured to the same age (χ^2=5.3 df=6 P=0.51); however, this trend was not significant (F=4.4 df=23 P=0.04).

Tracking length-frequency distributions (Fig. 3) from 1995 through 1997, from inshore gillnet samples, revealed progression of a strong cohort. Based on its size structure, the spawning year for this cohort was assumed to be 1993. A second cohort was evident in the last quarter of 1996, assumed to have been spawned in 1994. The progression of the cohort spawned in 1993 was clearly evident in the age structure of the samples over the period 1995–2001, proving useful in the valida-

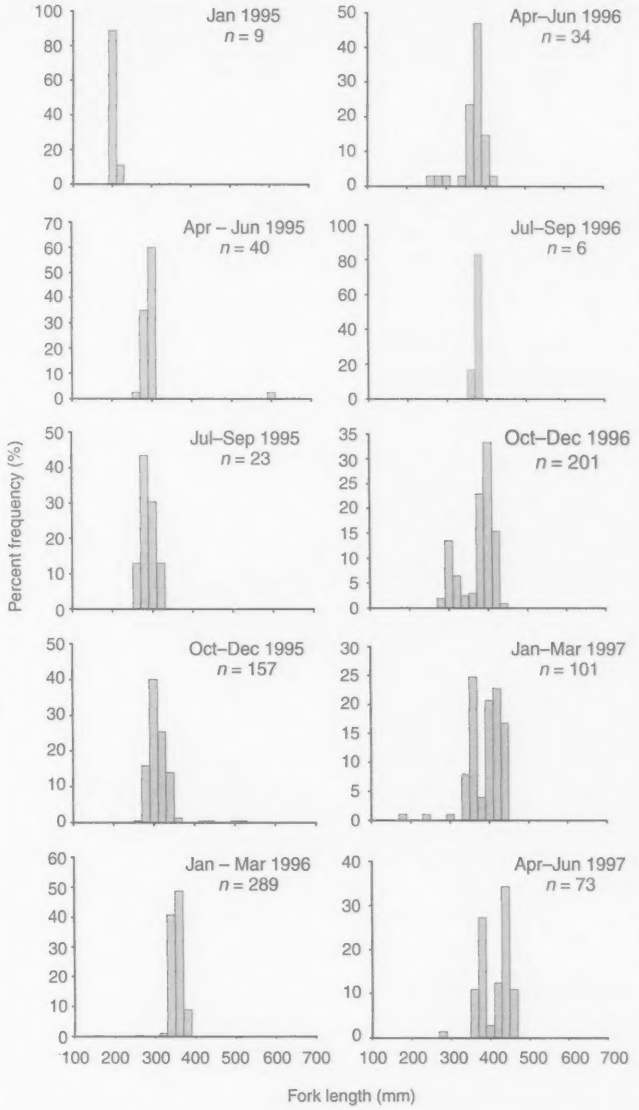

Figure 3

Quarterly length-frequency distribution (by 20-mm size class) of striped trumpeter (*Latris lineata*) sampled from January 1995 to June 1997.

tion of annual periodicity (Fig. 4). However, inferences about population age structure cannot be drawn from the age-frequency histograms because some sample sizes were low and there was discriminatory sampling (by gear type) over the period. For instance up to 1996–97 most of the aged samples were from inshore gillnet catches, whereas subsequent samples were derived primarily from hook catches.

Precision of repeated age estimation was high. Second readings by the primary reader were 79% in agreement with first readings, yielding an APE of 0.93%. Eighteen percent of second readings gave rise to a one-year difference and 3% of second readings differed by 2 years, and no significant tendency to overestimate or underestimate age was evident. An age bias plot did not differ significantly from 1:1 for the primary reader (Table 2).

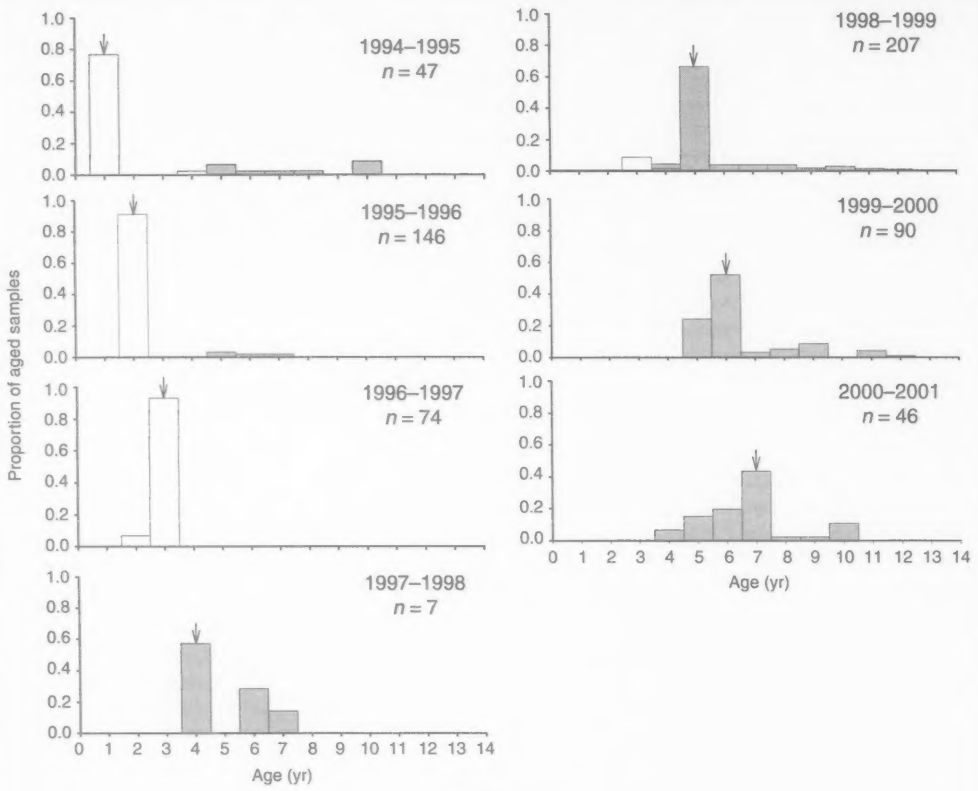

Figure 4

Age-frequency distribution (based on biological year, October–September) for striped trumpeter (*Latris lineata*) from 1994 through 2001. Gillnet-caught fish are represented by unshaded columns, hook-caught fish are represented by shaded columns. Arrows represent the progression of the cohort spawned in 1993.

Precision of the second reader's age estimates when compared with those of the primary reader were also satisfactory, yielding an APE of 1.59%, and no significant bias was revealed at any age class (Table 2).

The maximum observed ages for males and females were 29 and 43 years, respectively. From the available data, it is unclear whether apparent differences in longevity between the sexes are representative because very few individuals over the age of 25 were sampled. However, there was no significant difference in the age-frequency composition of the pooled samples based on sex (Kolmogorov-Smirnov; Z=1.05 P=0.22).

Growth modeling

The strong 1993 cohort allowed us to closely monitor the actual length at age of striped trumpeter. Average size increased from 190 mm (1.3 years) in January 1995 to 300 mm (2.1 years) by November 1996 (Fig. 3) and 420 mm (4.0 years) by November 1997. The seasonal VBGF model indicated that the majority of observed growth in this cohort occurred between January and May (late austral summer through autumn) and that there was little growth apparent between June and December (Fig. 5). The sine wave representing seasonal fluctuations indicated that the peak growth rate occurred in May. Comparing this sine function with that derived for SST (Fig. 6), we identified a first-order serial correlation—the strongest correlation identified when a 34-day lag period was incorporated in the growth phase.

The parameters of the $VBGF_S$ and $VBGF_{TP}$ fitted to the aged individuals are presented in Table 3. The $VBGF_{TP}$ gave the more parsimonious fit to the pooled length-at-age data according to the deterministic AIC value and underestimated L_∞ in relation to L_{max} to a lesser extent than the $VBGF_S$ (Table 3), reflecting a better fit to the data in the older age classes. In conjunction with a visual assessment of residuals, it was apparent that the $VBGF_S$ underestimated length at age above 20 years (Fig. 7). The better fit by the $VBGF_{TP}$

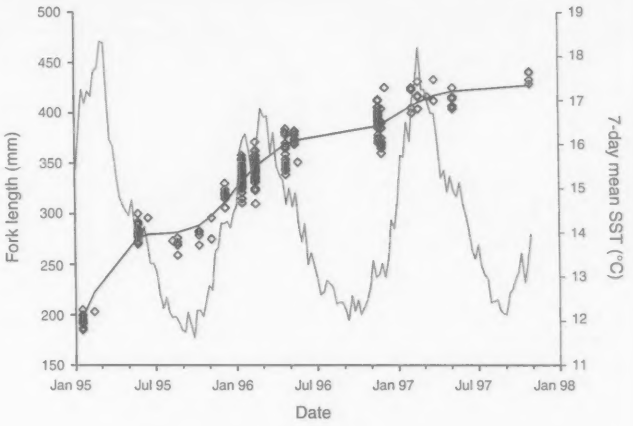

Figure 5

Length-at-age data (◇) of the 1993 striped trumpeter (*Latris lineata*) cohort fitted with a modified von Bertalanffy growth function to represent seasonal growth (black line), plotted against a 7-day average SST at the time of sampling (gray line).

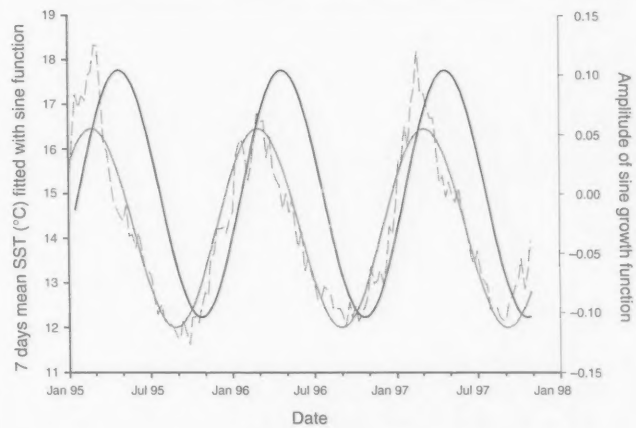

Figure 6

Seven-day mean SST (broken gray line) fitted with a sine wave (gray line) plotted against the sine function (black line) extracted from the seasonal von Bertalanffy growth function fitted in Figure 5.

supports the hypothesis that a more complex growth model was required for striped trumpeter.

The $VBGF_{TP}$ was sensitive to the value *age at transference*. A profile of negative log likelihood for a range of age-at-transference values (Fig. 8) assisted in determining the correct absolute minima. The negative log-likelihood profile revealed a low minima range across age at transference from 3.5 to 4.6 years, which, however, converged to a lowest value at age 4.4 years. Fitting the PDF to the growth curve substantially smoothed the point of transition, producing a curve that represented the data well. Setting an arbitrary standard deviation of 1.0 around the age at transference provided a normally distributed two-tailed range at transference (90 percent confidence adjusted for bias) from 1.3 to 7.8 years.

A likelihood ratio test (LRT) identified a slight significant difference between male and female $VBGF_S$ growth curves (χ^2=13.20 df=3 P=0.04), but there was no significant difference when the $VBGF_{TP}$ was tested (χ^2=10.83 df=6 P=0.09).

Mortality estimation

Ages 9–23 and 7–25 were included in the LCCCA regressions of the $VBGF_S$ and the $VBGF_{TP}$, respectively, to estimate Z (Fig. 9). Individuals below these ranges were assumed, by their respective model, not to have fully recruited to the offshore fishery, and individuals over the age of 25 were excluded due to poor sample size. These age ranges effectively excluded the strong 1993 recruitment pulse from the regression, thereby avoiding the complication of including a known strong year class in the analysis.

Application of the $VBGF_{TP}$ model resulted in lower estimates of Z and M (based on the Pauly equation), compared with those calculated by using the $VBGF_S$ parameters (Table 4). The estimate of Z based on the Hoenig (1983) equation was assumed to be close to M because F is low for this species. The Hoenig M was very similar to the Pauly estimate when $VBGF_{TP}$ parameters were used. In this case M was just below 0.1, indicating an annual natural mortality rate of about 9%. The $VBGF_{TP}$ estimates indicate that F was slightly higher than M in the offshore fishery. By contrast, the standard $VBFG_S$ parameters produced a substantially higher estimate of M (0.15) based on the Pauly equation than predicted by the Hoenig approximation, indicating an annual natural mortality rate of about 14%. Derived estimates of F with the $VBGF_{TP}$ were slightly higher than M, whereas F in relation to M was variable for the $VBGF_S$, depending on the equation used to derive M.

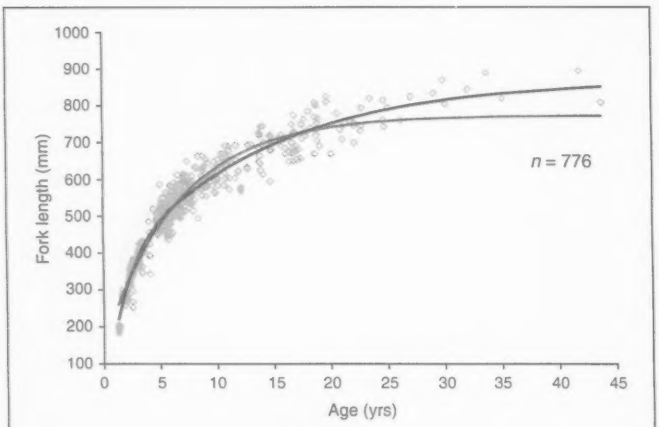

Figure 7

Pooled length-at-age data for striped trumpeter (*Latris lineata*). The black line represents the optimal two-phase von Bertalanffy growth function ($VBGF_{TP}$), with a mean age at transference of 4.4 years and a standard deviation equal to 1; the gray line represents the optimal standard von Bertalanffy growth function ($VBGF_S$).

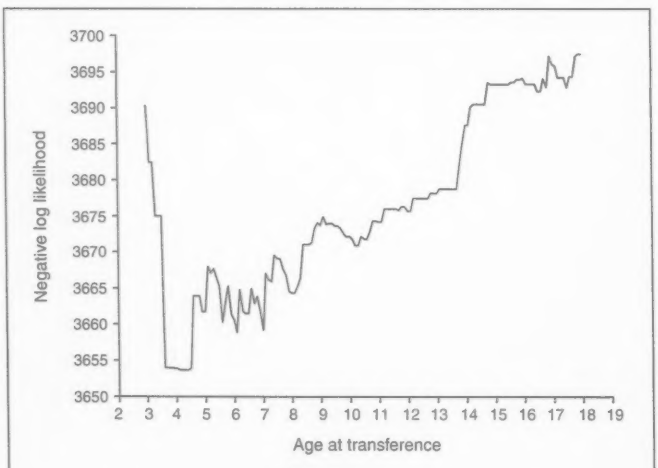

Figure 8

Negative log-likelihood profile plot of increasing age-at-transference values for striped trumpeter (*Latris lineata*).

Discussion

The present study represents the first report of age and growth of striped trumpeter. Despite having available a patchy data set, we were able to validate age and overcome the limitations of the von Bertalanffy equation to represent these data by the use of a robust growth model. Striped trumpeter are long lived, have a maximum age in excess of 40 years, and growth is particularly rapid up to age five, after which it slows dramatically.

The species has a complex early life history involving a long planktonic larval phase of around nine months (Morehead[1]), an inshore juvenile phase, and then movement offshore into deepwater.

Gear selectivity (gill nets in the shallow and hook catches in the deeper waters) may have influenced the fish-size structure of our samples, especially when grouped by depth, although it is highly unlikely that the size differences could be completely attributed to gear type alone. For instance, small individuals (<400 mm) were occasionally taken by hooks in the deeper strata and individuals over 500 mm were taken by gill nets in less than 50 m. The commercial hook fishery

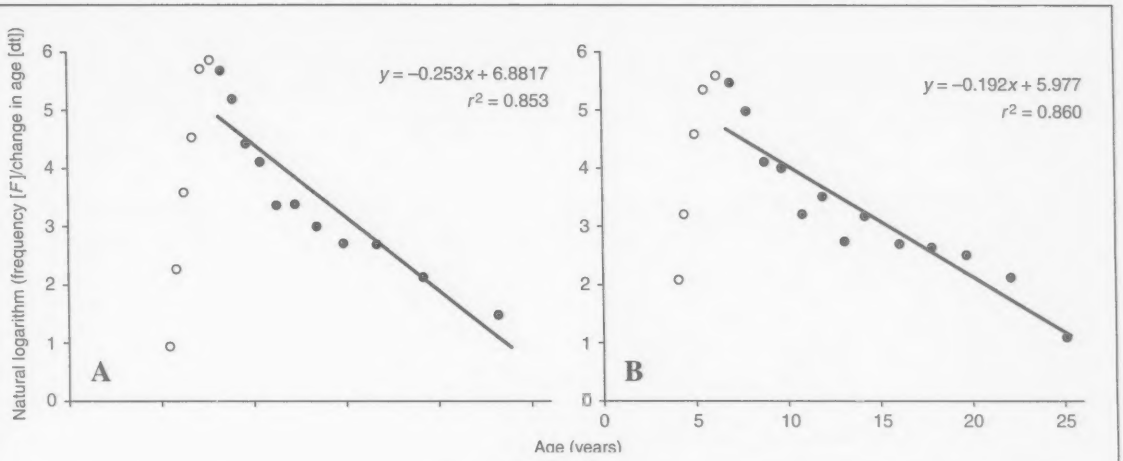

Figure 9

Length-converted catch curve analysis for striped trumpeter (*Latris lineata*) length and age data from 1998. (**A**) Age composition was based on the standard von Bertalanffy growth function ($VBGF_S$), (**B**) age composition was based on the second stanza of the two-phase von Bertalanffy growth function ($VBGF_{TP}$). Solid points were included in the respective linear regressions.

for striped trumpeter is largely restricted to depths of greater than 50 m, and despite considerable hook-fishing effort at shallower depths targeting other demersal reef species, notably the wrasses *Notolabrus fucicola* and *N. tetricus*, minimal catches of striped trumpeter are taken and those that are caught tend to be small in size (Lyle[2]). Rather, size structuring by depth is believed to reflect the movement of striped trumpeter offshore into deeper water as they grow and mature.

Seasonal growth was dramatic in young striped trumpeter (Fig. 5). This phenomenon is common in temperate species (Haddon, 2001; Jordan, 2001; McGarvey and Fowler, 2002), and has been linked to fluctuations in environmental factors, such as water temperature and oceanographic conditions, as well as biotic factors, such as seasonality in primary productivity (Harris et al., 1991; Jordan, 2001). Our study supports a correlation between water temperature and seasonal growth (Fig. 6); maximum growth was observed to take place consistently over a three-year period, approximately one month after the peak sea-surface temperatures.

Knowledge of growth and growth variability is essential to the understanding of a stock's population dynamics. To achieve an accurate assessment of these characteristics, several issues need to be addressed. Foremost, is a rigorous approach to the validation and precision testing of age estimates (Campana, 2001). In this study, a combination of age validation protocols outlined by Fowler and Doherty (1992) and Campana (2001) were subscribed to: 1) otoliths must display an internal structure of increments, (Fig. 3); 2) otoliths must grow throughout the lives of fish at a perceptible rate, which was confirmed by the otolith weight-at-age regression (Table 2); 3) the age of first increment formation must be determined; and 4) increment periodicity across the entire age range of interest must be veri-

Table 3

Parameter estimates derived from the two growth functions (standard von Bertalanffy growth function, [$VBGF_S$] and the two-phase von Bertalanffy growth function [$VBGF_{TP}$]) applied to the length-at-age data of striped trumpeter (*Latris lineata*) in Tasmania. Growth parameters are defined in the text, NOP = number of parameters in the model, AIC = Akaike information criterion, and L_{max} = the maximum length of all individuals included in the growth models.

		$VBGF_S$	$VBGF_{TP}$
Growth parameters	$L_{\infty 1}$	773.27	532.77
	k_1	0.15	0.43
	t_{01}	−1.46	0.03
	L^{δ}	—	450.11
	$L_{\infty 2}$	—	871.59
	k_2	—	0.08
	t_{02}	—	3.49
	t^{δ}	—	4.4
	σ^2 of t^{δ}	—	1.0
Diagnostics	NOP	3.0	9.0
	−log likelihood	3759.98	3700.13
	AIC	5335.12	5211.30
	% deviation of $L_{\infty 2}$ from L_{max}	−13.7	−2.7

Table 4

Estimates of instantaneous rates of total (Z), natural (M), and fishing (F) mortality for striped trumpeter (*Latris lineata*) determined with age-based catch curve analysis and the empirical equations of Hoenig (1983) and Pauly (1980). $VBGF_{TP}$ = estimates derived from the parameters of the two-phase von Bertalanffy growth function, $VBGF_S$ = estimates derived from the parameters of the standard von Bertalanffy growth function and LCCCA = length converted catch curve analysis.

	Z		M		F	
Method	$VBGF_S$	$VBGF_{TP}$	$VBGF_S$	$VBGF_{TP}$	$VBGF_S$	$VBGF_{TP}$
LCCCA	0.253	0.192	—	—	—	—
Hoenig	—	—	0.096	0.096	0.157	0.096
Pauly	—	—	0.151	0.092	0.102	0.100

fied. We used cultured individuals to determine which opaque or translucent zone represented the first growth increment, although the accuracy of age validation with cultured individuals has been questioned by Campana (2001). In our study, the close correspondence between the growth of cultured and wild fish over a period of several years gives us confidence in using this approach to validate first increment position. The slightly slower growth rate observed in cultured striped trumpeter can be attributed to jaw malformation—a phenomenon that has been shown to affect feeding ability (Cobcroft et al., 2001).

Modal progression of the 1993 cohort through time provided indirect validation for annual periodicity in increment formation up until age seven. Validation across all age classes was not possible in our study, although validation after the age of five years was significant. That is, validation was achieved past the average age at which fish moved offshore into deeper water, and past the age at which there was a significant reduction in growth rate.

The second consideration to address when studying animal growth is model selection. Akaike's information criterion is a standard method for model selection that provides an implementation of Occam's razor, in which parsimony or simplicity is balanced against goodness-of-fit (Forster, 2000). However, model selection should not rely on statistical fit alone; it should also provide a biologically sensible interpretation across the entire range of ages in the sampled population (Haddon, 2001). In the case of striped trumpeter, the standard von Bertalanffy function provided a poor representation of growth in older individuals, resulting in an unrealistically low L_∞. This problem was largely overcome by the application of a two-phase growth function. Similar to that used on large pelagics, such as *Thunnus maccoyii* (Bayliff et al., 1991; Hearn and Polacheck, 2003). In their application of the model, Hearn and Polacheck (2003) considered biological traits when discussing the justification for age at transference, namely the reduction in growth rate, and inshore to offshore migration. In the present study we have considered analogous traits to seed the age of transference for striped trumpeter. In this species there is a marked transition in size structure between shallow and deeper reefs that occurs at around 450 mm or between 4 and 5 years (Fig. 8). In addition, a visual assessment of the length-at-age data highlighted a marked decrease in growth rate at a similar age.

Solving for the age at transference produced a point estimate that results in a sharp discontinuity in the growth curve; an observation that Hearn and Polacheck (2003) highlighted as biologically unrealistic. The range of low negative log likelihood values described by the age at transference profile is due to the patchiness of data around these ages, creating uncertainty in the model. We have assumed in this case that the converged value of 4.4 years is accurate and that the variability around this point is normally distributed with a standard deviation equal to one. By including the normal probability distribution function we have effectively created a smooth transition between growth phases. This function implies that age at transference has some level of inherent variability, which is likely to be more biologically plausible than knife-edge transition.

A further extension of the two-phase model was tested by applying the seasonal growth version of the VBGF (described in Eq. 3) to the first phase and a standard VBGF to the second phase, but was disregarded because of the effect of over parameterization on parsimony. However, this approach did highlight the flexibility of the two-phase model to allow for a more dynamic representation of population growth characteristics.

This study supports the assertion by Hearn and Polacheck (2003) that discontinuity in growth rate may be a more common phenomenon in fish than implied by growth models reported in the literature. Such a two-phase growth model, where age at transference coincides with the transition phase from one fishery to another, has proven useful. It allows separate growth parameters to be tracked to each fishery, and as such, provides a precursor to developing a more biologically robust production model with dynamic parameters at age and for fishing method.

The predictive regression developed by Pauly (1980) that estimates natural mortality is based on the direct

relationship between longevity (t_{max}) and the magnitude of the physiological growth parameters k and L_∞. As such, it would be reasonable to assume that if a good fit exists between length at age that the growth parameters, when employed in such an empirical model, would yield a natural mortality estimate approximately equal to that determined by a regression model that is based on t_{max} (Hoenig, 1983). The two-phase growth function also provided a more conservative estimate of M than the standard von Bertalanffy model. Overestimates of M can lead to unrealistically high estimates of productivity and a potential yield that may in turn lead to overexploitation of a stock.

Protracted longevity, slow growth in later life, large body size, recruitment variability, and relatively low natural mortality once individuals reach adulthood are all characteristics typical of a K-selected species (where equilibrium is the biological strategy). Such species are often regarded as being susceptible to growth over-fishing and stock depletion (Booth and Buxton, 1997). For instance, increased fishing effort on the inshore fishery, as has been observed with the recruitment of strong cohorts, will affect subsequent recruitment to the offshore fishery and spawning stock. The current analysis indicates that fishing mortality is slightly higher than natural mortality and, in the absence of further strong recruitment, a decline in the stock size is likely if fishing pressure is not reduced.

Acknowledgments

The authors gratefully acknowledge Ray Murphy and Alan Jordan who collected many of the earlier samples and undertook preliminary examination of the otoliths. The assistance of the captain and crew of FRV *Challenger* in collecting samples is also thankfully acknowledged. Philippe Ziegler, Dirk Welsford, and Malcolm Haddon provided constructive criticism and ideas in terms of the analyses and reviewed the manuscript; Sarah Irvine and an anonymous reviewer provided constructive feedback on final versions of this manuscript.

Literature cited

Akaike, H.
1974. A new look at the statistical model identification. Institute of Electrical and Electronic Engineers Transactions on Automatic Control, AC-19, p. 716–723. IEEE Control Systems Society, New York, NY.

Andrew, T. G., T. Hecht, P. C. Heemstra, and J. R. E. Lutjeharms.
1995. Fishes of the Tristan Da Cunha group and Gough Island, South Atlantic Ocean. JLB Smith Institute of Ichthyology. Ichthyol. Bull. 63:1–41.

Bayliff, W. H., I. Ishizuka, and R. B. Deriso.
1991. Growth, movement, and attrition of northern bluefin tuna, *Thunnus thynnus*, in the Pacific Ocean, as determined by tagging. Inter-Am. Trop. Tuna Comm. Bull. 20(1):1–94.

Beamish, R. J., and D. A. Fournier.
1981. A method for comparing the precision of a set of age determinations. Can. J. Fish. Aquat. Sci. 38: 982–983.

Beverton, R. J. H , and S. J. Holt.
1957. On the dynamics of exploited fish populations. U.K. Ministry of Agriculture and Fisheries, Fisheries Investigations (series 2), 19:1–533.

Booth, A. J. and C. D. Buxton.
1997. Management of the panga *Pterogymnus laniarius* (Pisces: Sparidae), on the Agulhas Bank, South Africa using per-recruit models. Fish. Res. 32:1–11.

Campana, S. E.
2001. Accuracy, precision and quality control in age determination, including a review of the use and abuse of age validation methods. J. Fish. Biol. 59:197–242.

Campana, S. E., M. C. Annand, and J. I. Mcmillan.
1994. Graphical and statistical methods for determining the consistency of age determinations. Trans. Am. Fish. Soc. 124(1):131–138.

Chen, Y, D. A, Jackson, and H. H. Harvey.
1992. A comparison of von Bertalanffy and polynomial functions in modelling fish growth data. Can. J. Fish. Aquat. Sci. 49:1228–1235.

Cobcroft, J. M., P. M. Pankhurst, J. Sadler, and P. R. Hart.
2001. Jaw development and malformation in cultured striped trumpeter *Latris lineata*. Aquaculture 199(3–4): 267–282.

Duhamel, G.
1989. Ichtyofaune des iles Saint-Paul et Amsterdam (Océan Indien sud). Mésogée. 49:21–47.

Forster, M. R.
2000. Key concepts on model selection: performance and generalizability. J. Math. Psych. 44:205–231.

Fowler, A. J., and P. J. Doherty.
1992. Validation of annual growth increments in the otoliths of two species of damsel fish from the southern Great Barrier Reef. Aust. J. Mar. Freshw. Res. 43: 1057–1068.

Furlani, D. M., and F. P. Ruwald
1999. Egg and larval development of laboratory-reared striped trumpeter *Latris lineata* (Forster *in* Bloch and Schneider 1801) (Percoidei: Latridiidae) from Tasmanian waters. N.Z. J. Mar. Freshw. Res. 33:16–83.

Gomon, M. F., J. C. M. Glover, and R. H. Kuiter.
1994. The fishes of Australia's south coast, 992 p. The Flora and Fauna of South Australia Handbooks Committee. State Printers, Adelaide, South Australia, Australia.

Haddon, M.
2001. Modelling and quantitative methods in fisheries. Chapman and Hall, Boca Raton, FL.

Harris, G. P., F. B. Griffiths, L. A. Clementson, V. Lyne, and H. Van der Doe.
1991. Seasonal and interannual variability in physical processes, nutrient cycling and the structure of the food chain in Tasmanian shelf waters. J. Plankton Res. 13 (Suppl.):109–131.

Hearn, W. S., and T. Polacheck.
2003. Estimating long-term growth-rate changes of southern bluefin tuna (*Thunnus maccoyii*) from two periods of tag-return data. Fish. Bull.101:58–74.

Hoenig, J. M.
1983. Empirical use of longevity data to estimate mortality rates. Fish. Bull. 82:898–902.

Jordan, A. R.
2001. Age, growth and spatial and interannual trends in age composition of jackass morwong, *Nemadactylus*

macropterus, in Tasmania. Aust. J. Mar. Freshw. Res. 52:651–660.

Kimura, D. K.
1980. Likelihood methods for the von Bertalanffy growth curve. Fish. Bull. 77:765–776.

Knight, W.
1968. Asymptotic growth: an example of nonsense disguised as mathematics. J. Fish. Res. Board Can. 25:1303–1307.

Last, P. R., E. O. G. Scott, and F. H. Talbot.
1983. Fishes of Tasmania, 563 p. Tasmanian Fish-eries Development Authority, Hobart, Tasmania, Australia.

McGarvey, R., and A. J. Fowler
2002. Seasonal growth of King George whiting (*Sillaginodes punctata*) estimated from length-at-age samples of the legal-size harvest. Fish. Bull. 100:545–558.

Pauly, D.
1980. On the interrelationships between natural mortality, growth parameters, and mean environmental temperature in 175 fish stocks. J. Cons. Int. Explor. Mer 39(2):175–192.
1983. Length-converted catch curves: a powerful tool for fisheries research in the tropics (part 1). Fishbyte 1(2):9–13.

Pitcher, T. J., and P. D. M. MacDonald.
1973. Two models for seasonal growth in fishes. J. Appl. Ecol. 10:559–606.

Reynolds, R. W., N. A. Rayner, T. M. Smith, D. C. Stokes, and W. Wang.
2002. An improved in situ and satellite SST analysis for climate. J. Climate 15:1609–1625.

Roff, D. A.
1980. A motion for the retirement of the von Bertalanffy function. Can. J. Fish. Aquat. Sci. 37:127–129.

Sainsbury, K. J.
1979. Effect of individual variability on the von Bertalanffy growth equation. Can. J. Fish. Aquat. Sci. 37: 241–247.

Schnute, J.
1981. A versatile growth model with statistically stable parameters. Can. J. Fish. Aquat. Sci. 38:1128–1140.

Larval development of estuary perch (*Macquaria colonorum*) and Australian bass (*M. novemaculeata*) (Perciformes: Percichthyidae), and comments on their life history

Thomas Trnski
Amanda C. Hay
Ichthyology, Australian Museum
6 College Street
Sydney, New South Wales 2010, Australia
E-mail address (for T. Trnski, senior author): tomt@austmus.gov.au

D. Stewart Fielder
New South Wales Fisheries
Port Stephens Fisheries Centre
Private Bag 1
Nelson Bay, New South Wales 2315, Australia

Abstract—Morphological development of the larvae and small juveniles of estuary perch (*Macquaria colonorum*) (17 specimens, 4.8–13.5 mm body length) and Australian bass (*M. novemaculeata*) (38 specimens, 3.3–14.1 mm) (Family Percichthyidae) is described from channel-net and beach-seine collections of both species, and from reared larvae of *M. novemaculeata*. The larvae of both are characterized by having 24–25 myomeres, a large triangular gut (54–67% of BL) in postflexion larvae, small spines on the preopercle and interopercle, a smooth supraocular ridge, a small to moderate gap between the anus and the origin of the anal fin, and distinctive pigment patterns. The two species can be distinguished most easily by the different distribution of their melanophores. The adults spawn in estuaries and larvae are presumed to remain in estuaries before migrating to adult freshwater habitat. However, larvae of both species were collected as they entered a central New South Wales estuary from the ocean on flood tides; such transport may have consequences for the dispersal of larvae among estuaries. Larval morphology and published genetic evidence supports a reconsideration of the generic arrangement of the four species currently placed in the genus *Macquaria*.

Manuscript submitted 20 November 2003 to the Scientific Editor's Office.

Manuscript approved for publication 15 June 2004 by the Scientific Editor.

Fish. Bull. 103:183–194 (2005).

The Percichthyidae is a family of freshwater fishes restricted to Australia (8 genera, 17 species) and South America (2 genera, 7 species) (Johnson, 1984; Nelson, 1994; Allen et al., 2002; Paxton et al., in press). There is continuing debate regarding the monophyly of the family; several genera are variously allocated to separate families: *Gadopsis* is allocated to Gadopsidae (Allen et al., 2002; see Johnson, 1984 for a history of the systematic placement of the genus) and *Edelia*, *Nannatherina*, and *Nannoperca* are allocated to Nannopercidae (Allen et al., 2002). Other Australian genera of Percichthyidae include *Bostockia*, *Guyu*, *Maccullochella*, and *Macquaria* (Pusey and Kennard, 2001; Allen et al., 2002; Paxton et al., in press). The genera *Percalates* and *Plectroplites* were synonymized with *Macquaria*, based on morphological and biochemical characters (MacDonald, 1978), and although this arrangement was accepted by Paxton and Hanley (1989), Paxton et al. (in press), Eschmeyer (1998), Johnson (1984), and Nelson (1994) recognized both *Percalates* and *Plectroplites* as valid genera.

There are four described species in the genus *Macquaria*, all confined to southeastern Australia. *Macquaria ambigua* occurs naturally in freshwaters of the Murray-Darling river system and has been translocated outside of its natural range (Kailola et al., 1993; Allen et al., 2002). There is genetic evidence for an additional undescribed freshwater species closely related to *M. ambigua* from central Australian drainages (Musyl and Keenan, 1992). *Macquaria australasica* is also confined to freshwater of the Murray-Darling river system, and an isolated population exists from the Shoalhaven and Hawkesbury Rivers, New South Wales (Allen et al., 2002) that may be a separate species (Dufty, 1986). The other two species (*M. colonorum* and *M. novemaculeata*) are catadromous and occur in coastal southeastern Australian drainages between southern Queensland and eastern South Australia (Paxton et al., in press). They are sympatric from northern New South Wales (NSW) to eastern Victoria. Adults of *M. novemaculeata* occur in freshwater, whereas *M. colonorum* prefers brackish water of estuaries (Williams, 1970). Both species migrate to estuarine areas to breed in winter (Allen et al., 2002). Both species are protected from commercial fishing but are highly prized by recreational fishermen (Harris and Rowland, 1996; Allen et al., 2002) and *M. novemaculeata* is an important aquaculture species.

Of the 17 Australian percichthyids, larvae of only *Maccullochella macquariensis*, *M. peelii peelii*, and *Macquaria ambigua* have been described (Dakin and Kesteven, 1938; Lake, 1967; Brown and Neira, 1998). Larval and early juvenile development of the estuary perch (*Macquaria colonorum*) and the Australian bass (*Macquaria novemaculeata*) is described from specimens collected from the central and southern coast of NSW, and from reared larvae of the latter species obtained from brood stock from central NSW. This is the first description of the morphological development of the early life history of these two species.

Materials and methods

Morphological definitions, measurements, and abbreviations follow Neira et al. (1998) and Leis and Carson-Ewart (2000). Larvae and juveniles were examined and measured under a dissecting microscope at magnifications from 6 to 50×. Precision of the measurements varied with magnification but ranged from 0.02 to 0.16 mm. Where morphometric values are given as a percentage, they are as a proportion of body length (BL) unless otherwise indicated. All pigment described is external unless otherwise specified. The juveniles collected are in transition from larvae to juveniles because they retain some of their larval characters and squamation is incomplete; these are called "transitional juveniles" (Vigliola and Harmelin-Vivien, 2001). Illustrations were prepared with a Zeiss SR with an adjustable drawing tube.

Field-caught larvae were collected in a fixed 2-m^2 channel net with about 1-mm mesh in Swansea Channel, Lake Macquarie, central NSW. The net filtered surface waters to 1 m depth during night flood tides (Trnski, 2002). Small juveniles were collected in a 30-m beach seine dragged over sand, mud, and *Zostera* seagrass in the Clyde River, southern NSW. Reared larvae of *M. novemaculeata* were obtained from rearing tanks at the Port Stephens Fisheries Centre, an aquaculture research facility of NSW Fisheries. Brood stock came from the Williams River, central NSW. All specimens were initially fixed in 10% formalin and subsequently transferred to 70% ethanol.

Field-caught larvae were restricted to a narrow size range: 4.8–7.1 mm body length (BL) for *M. colonorum* (n=12), and 4.6–7.6 mm BL for *M. novemaculeata* (n=15). Juveniles of both species ranged from 10.3 to 13.5 (n=5) and from 10.1 to 14.1 mm BL (n=5), respectively. Reared larvae of *N. novemaculeata* were available to confirm the identification of the larvae and to extend the developmental series for this species to 3.3–10.2 mm BL (n=18).

All material examined is registered in the fish collection at the Australian Museum. Registration numbers of *M. colonorum* larvae are AMS I.20052-010, I.41690-005 to -008, I.41691-002, I.41692-001, I.41693-001; *M. novemaculeata* are AMS I.20052-012, I.27051-013, I.41561-001 to -008, I.41590-001, I.41641-001, I.41661-001 and -002, I.41662-001, I.41668-001, I.41690-001 to -0004, I.41691-001, I.41694-001.

Identification

Field-caught larvae and juveniles were identified as percichthyids by using the characters in Brown and Neira (1998), particularly the combination of a relatively large gut, the small to moderate gap between the anus and origin of the anal fin prior to complete formation of the anal-fin, continuous dorsal fin, fin-ray, and vertebral counts, and head spination including small preopercular spines, a small interopercular spine, and a smooth supraocular ridge. The larvae and juveniles described here were confirmed as being *Macquaria colonorum* and *M. novemaculeata* because of their coastal distribution and meristics; all other species in the family are restricted to freshwater. The overlap in meristics between *M. colonorum* and *M. novemaculeata* made separation of the species difficult. The availability of reared *M. novemaculeata* from positively identified adults determined the species allocations.

Results

Development of *Macquaria colonorum*

Adult meristic data Dorsal (D) IX–X,8–11; Anal (A) III,7–9; Pectoral (P_1) 12–16; Pelvic (P_2) I,5; Vertebrae 25 17 specimens: 4.8–7.1 and 10.3–13.5 mm BL

General morphology (Tables 1 and 2, Fig. 1) Larvae and transitional juveniles are moderately deep bodied (body depth, BD 30–35%). The body and head are laterally compressed. There are 24–25 myomeres (12–14 preanal and 11–13 postanal). The large, triangular gut is fully coiled in the smallest larva examined. The preanal length ranges from 60% to 67%. The conspicuous gas bladder located over the midgut is small to moderate in size but difficult to distinguish in transitional juveniles. The round to slightly elongate head is large (head length, HL 32–41%). The snout is slightly concave to straight. The snout is approximately the same length as the eye diameter but becomes shorter from 7 mm. The eye is round and moderate in size (27–32% of HL) in larvae but becomes moderate to large in transitional juveniles (32–36% of HL). The large mouth reaches to the middle of the pupil. Small canine teeth are present in both jaws in all larvae examined. The nasal pit closes shortly after settlement, by 12.5 mm.

Head spination is weak. Three short spines are present on the posterior preopercular border in the smallest larva examined; a fourth spine is present in some postflexion larvae from 6.3 mm and in all transitional juveniles. The spine at the angle of the preopercle is longest but remains shorter than the pupil diameter. A minute interopercular spine is present from 6.0 mm and persists in all transitional juveniles. A low, smooth

Table 1

Morphometric data for *Macquaria colonorum* larvae from channel-net samples and juveniles from beach-seine samples. Measurements are in mm. VAFL = vent to anal-fin length.

Body length	Preanal length	Predorsal length	Body depth	Head length	Snout length	Eye diameter	VAFL
Flexion							
4.80	3.40	2.48	1.49	1.96	0.58	0.58	0.04
5.10	3.40	3.00	1.60	1.88	0.60	0.56	0
5.40	3.40	2.80	1.60	1.72	0.50	0.50	0
5.48	3.32	2.91	1.74	1.80	0.56	0.56	0
Postflexion							
5.73	3.49	2.80	1.99	2.08	0.56	0.60	0
5.98	3.68	3.24	1.99	2.04	0.60	0.60	0
6.00	3.72	2.60	1.92	2.00	0.50	0.60	0
6.31	3.98	2.57	2.16	2.20	0.60	0.68	0
6.60	4.00	3.00	2.20	2.40	0.64	0.64	0
6.81	4.15	3.07	2.16	2.32	0.66	0.66	0
7.00	4.32	3.32	2.08	2.24	0.60	0.72	0
7.10	4.36	2.91	2.32	2.28	0.60	0.72	0
Settled							
10.29	6.81	4.81	3.15	3.74	0.91	1.25	0
10.62	6.81	4.98	3.24	3.90	0.95	1.25	0
11.29	7.47	5.56	3.74	4.48	1.00	1.58	0
12.45	7.97	5.64	4.15	4.57	1.00	1.66	0
13.45	8.70	6.64	4.48	5.23	1.41	1.83	0

Table 2

Meristic data for *Macquaria colonorum* larvae and juveniles. ( ) indicates only fin bases present, [ ] incipient rays or spines, {} ray transforming to a spine, d = damaged.

Body length	Dorsal	Anal	Pectoral	Pelvic	Caudal	Myomeres
Flexion						
4.80	(V), 9	(I), 8[1]			9+7[1]	14+11=25
5.10	d, (10)	(I), 9			[1]8+7[1]	13+11=24
5.40	d, (9)	(II), 9	[2]		9+8	13+12=25
5.48	(III), 9	(II), 8	3		9+8	12+12=25
Postflexion						
5.73	(IV), 11	(II), 8	5		9+8	13+12=25
5.98	(V), 10	(II), 8	2		9+8	13+12=25
6.00	(IV), 10	(II), 8	3		9+8	13+12=25
6.31	(IV)I, 11	[II], 9	9	buds	9+8	13+12=25
6.60	IV, 11	II, 9	5	buds	9+8	13+12=25
6.81	VII, 11	II, 10	9	buds	9+8	13+12=25
7.00	VII, 11	II, 10	5 (d)	buds	9+8	12+13=25
7.10	VIII, 10	II{I}, 9	11[1]	buds	9+8	14+11=25
Settled						
10.29	VIII {I}, 10	II{I}, 8	15	I,5	7+9+8+6	13+12=25
10.62	VIII {I}, 10	II{I}, 8	13	I,5	7+9+8+4	12+13=25
11.29	IX, 10	III,8	15	I,5	7+9+8+8	12+13=25
12.45	IX, 10	III, 8	14	I,5	12+9+8+7	12+13=25
13.45	IX, 10	III, 9	14	I,5	9+9+8+8	12+13=25

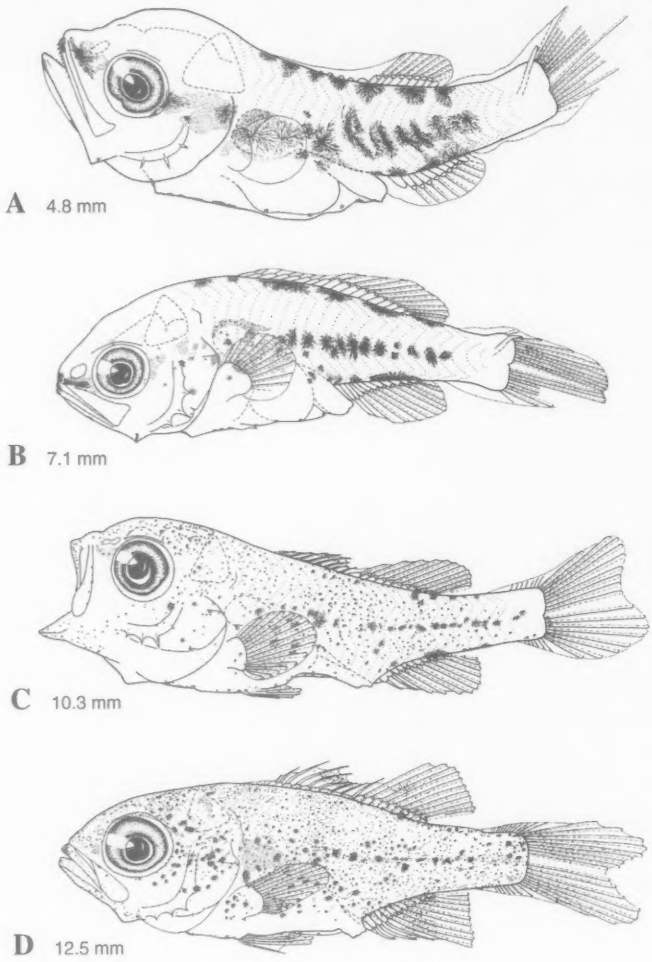

Figure 1

Larvae of *Macquaria colonorum*. (**A** and **B**) postflexion larvae from Swansea Channel, central New South Wales (NSW) (**C** and **D**) recently settled juveniles from the Clyde River, southern NSW.

supraocular and supracleithral ridge form by the time notochord flexion is complete. A weak posttemporal ridge is present from 7 mm, and a small spine develops in transitional juveniles from 11.3 mm. A small spine develops on the supracleithrum from 10.6 mm. An opercular spine is present in transitional juveniles.

Dorsal-fin soft rays are ossified by the completion of notochord flexion, the posteriormost rays being the last to ossify. The pterygiophores of the spinous rays of the dorsal fin develop from posterior to anterior and begin to form during notochord flexion. Spines begin to ossify in postflexion larvae by 6.3 mm, and the full complement of dorsal-fin elements is present by 7.1 mm. All soft rays of the anal fin are ossified by the completion of notochord flexion, by which time 1–2 pterygiophores of the spinous rays are present. The first two anal-fin spines are ossified by 6.6 mm. The last spinous soft ray of the dorsal and the third spinous ray of the anal fin transforms from a soft ray after settlement and they are fully transformed by 11.3 mm. Incipient rays begin to form in the pectoral fin during notochord flexion, and the rays ossify from dorsal to ventral in postflexion larvae. A few pectoral-fin rays remain unossified at 7.1 mm and are fully ossified prior to settlement.

Pelvic-fin buds appear in postflexion larvae from 6.3 mm, but no elements have formed in the largest specimen; they are all ossified in the transitional juveniles. All primary caudal-fin rays are ossified by the end of notochord flexion. Procurrent caudal rays are present in the transitional juveniles. Notochord flexion commences before 4.8 mm, and is complete by 5.7 mm. Scales have not begun to develop in the largest transitional juvenile examined (13.5 mm).

Pigment (Fig. 1, A–D) Larvae are moderately to heavily pigmented; melanophores are concentrated on the dorsal and ventral midlines, and midlateral surface of the trunk and tail. Small expanded melanophores are present at the tips of the upper and lower jaws, and there are one or two melanophores ventral to the nasal pit. Additional internal melanophores are present along the roof of the mouth, and posterior to the eye below the mid- and hindbrain. External melanophores may be present on the operculum in line with the eye. One or two melanophores are present on the ventral midline of the lower jaw, and there is one at the angle of the lower jaw.

Four to seven large, expanded melanophores are present along the dorsal midline of the trunk and tail, from the nape to just posterior to the dorsal-fin base. There are one or two melanophores on the nape and four or five along the dorsal-fin base. A series of large, expanded melanophores is present along the lateral midline of the trunk and tail, commencing at the gas bladder and extending to the posterior end of the dorsal and anal fins. In postflexion larvae, this series extends onto the anterior third of the caudal peduncle. Internal melanophores are present over the gas bladder, the mid- and hindgut, and may be present along the notochord. The external and internal pigment series thus give the impression of a line of heavy pigment from the tip of the snout, across the head and trunk, to the tail.

Small melanophores are present along the ventral midline of the gut; one melanophore on the isthmus immediately anterior to the cleithral symphysis, usually three (range: 2–4) melanophores between the cleithral symphysis and pelvic-fin base, and usually three (range: 1–4) melanophores between the pelvic-fin base and the anus. Expanded melanophores are present along the ventral midline of the tail, from above the anus to the posterior end of the anal-fin base. Between one and three melanophores occur along the anal-fin base. A small melanophore is occasionally present in early postflexion larvae at the base of ventral primary caudal-fin rays 1–2.

In transitional juveniles, the expanded melanophores are relatively smaller, and are most prominent midlaterally along the trunk and tail. The expanded melanophores along the dorsal and ventral midlines become small to absent during the juvenile stage. Additional expanded melanophores develop laterally on the head and body, and the dorsal and anal fins become pigmented. Small melanophores cover the head and body—coverage lightest ventrally on the head and gut. Three broad vertical bands become apparent dorsally on the nape, below the center of the spinous dorsal fin and below the center of the soft dorsal fin by 13.5 mm.

Development of *Macquaria novemaculeata* larvae

Adult meristic data D VIII–X,8–11; A III,7–9; P_1 12–16; P_2 I,5; Vertebrae 25; 38 specimens: 3.3–14.1 mm BL

Eggs and hatching Eggs are approximately 900 μm in diameter and have multiple oil globules. Larvae are 3.3 mm SL at time of hatching.

General morphology (Tables 3 and 4, Fig. 2) Yolksac and early preflexion larvae are elongate (BD 15–18%), but in late preflexion and flexion larvae, body depth becomes moderate (BD 26–34%). Body depth of field-caught postflexion larvae ranges from 29% to 35%, and in transitional juveniles from 33% to 34%. Reared postflexion larvae and transitional juveniles are deeper than wild larvae, ranging from 32% to 44%, which is an artifact of the extremely full guts in the reared larvae. Body depth decreases abruptly posterior to the anus, although this becomes less marked with development. The head and body are laterally compressed. There are 25 myomeres (10–13 preanal+12–15 postanal). In general, there are 10–12 preanal myomeres in preflexion and flexion larvae, and 12–13 preanal myomeres in postflexion larvae and transitional juveniles. The gut is initially straight in yolksac larvae but is coiled by 3.9 mm. The gut is oval to triangular in shape; preanal length reaches 44–56% of BL in yolksac and preflexion larvae, 54–60% in flexion stage larvae, and 54–66% in postflexion larvae and transitional juveniles. The gut mass is large, particularly in reared postflexion larvae and transitional juveniles. The conspicuous gas bladder, which is located over the midgut, is moderate to large in size, except in the yolksac larvae where it is small and inconspicuous. The head is round and small in yolksac larvae (HL 15–16%), moderate in preflexion larvae (HL 22–31%), and becomes moderate to large in flexion (29–35%) and postflexion larvae and transitional juveniles (32–38%). The snout is always shorter than the eye diameter and is initially concave, but becomes convex to straight in postflexion larvae. The eye is moderate to large (27–36% of HL) but is relatively larger in yolksac larvae (42–45% of HL). The eye is initially unpigmented, but is fully pigmented by 3.6–3.8 mm, prior to the complete absorption of the yolk. The moderate mouth reaches to the middle of the pupil. Small canine teeth appear in both jaws in late preflexion larvae by 4.4 mm. The number of teeth increases with development. The nasal pit begins to close by 8.6 mm, and both nostrils are developed by 10.3 mm.

Head spination is weak. A small spine appears at the preopercular angle by the end of the preflexion stage. By the time notochord flexion is complete, there are three spines on the posterior preopercular border, and the spine at the angle is the longest. All spines are shorter than the pupil diameter. Additional spines

Table 3

Morphometric data for *Macquaria novemaculeata* larvae from channel net samples and reared in aquaria (body length preceded by "R"), and juveniles from beach-seine samples. Measurements are in mm. VAFL = vent to anal-fin length.

Body length	Preanal length	Predorsal length	Body depth	Head length	Snout length	Eye diameter	VAFL
Yolksac							
R 3.32	1.48		0.52	0.53	0.16	0.24	
R 3.60	1.60		0.58	0.53	0.16	0.22	
Preflexion							
R 3.60	2.00		0.92	0.96	0.24	0.34	
R 3.80	2.00		1.00	1.04	0.30	0.38	
R 3.90	1.76		0.64	0.84	0.18	0.30	
R 4.20	2.00		0.64	0.93	0.20	0.33	
R 4.40	2.00		0.78	1.06	0.26	0.34	
4.57	2.36	2.16	1.20	1.40	0.28	0.40	0.22
Flexion							
5.00	2.72	2.40	1.52	1.48	0.32	0.48	0.12
5.14	2.90	2.32	1.48	1.76	0.44	0.48	0.10
R 5.31	2.84	2.60	1.40	1.60	0.48	0.56	0.20
5.39	2.74	2.66	1.58	1.60	0.40	0.48	0.12
R 5.39	2.90	2.66	1.36	1.56	0.40	0.56	0.20
5.47	2.80	2.74	1.60	1.72	0.44	0.48	0.12
R 5.47	3.00	2.60	1.56	1.76	0.52	0.60	0.12
5.70	3.40	2.92	1.96	2.00	0.52	0.56	0.06
5.90	3.32	2.90	1.80	1.88	0.52	0.56	0.04
Postflexion							
5.64	3.07	2.41	1.66	2.00	0.52	0.60	0.08
5.89	3.52	2.64	2.00	2.00	0.52	0.60	0.06
6.06	3.32	2.81	1.99	2.00	0.52	0.56	0.10
6.30	3.40	2.57	1.91	1.99	0.50	0.60	0.20
6.60	3.73	2.91	2.24	2.08	0.50	0.66	0
6.72	3.74	2.82	2.24	2.16	0.60	0.64	0.08
R 6.72	3.74	2.60	2.16	2.16	0.52	0.76	0.08
R 7.20	3.98	3.00	2.32	2.28	0.52	0.68	0.08
7.40	4.15	3.02	2.49	2.32	0.66	0.72	0
R 7.47	4.15	3.04	2.49	2.48	0.64	0.72	0.08
7.55	4.30	3.15	2.66	2.57	0.66	0.72	0
R 8.18	5.31	3.49	3.07	2.91	0.75	0.91	0
R 8.60	5.56	4.15	3.24	3.24	0.83	1.08	0
R 9.20	5.56	3.98	3.75	3.50	0.75	1.21	0
Settled							
10.13	6.64	4.81	3.49	3.65	0.83	1.33	0
R 10.20	6.64	4.57	3.74	3.74	0.83	1.33	0
R 10.30	6.64	4.57	3.99	3.82	1.05	1.33	0
11.62	7.55	5.56	3.82	4.23	1.00	1.49	0
11.62	7.55	5.47	3.98	4.39	1.07	1.49	0
13.28	8.30	5.98	4.56	4.98	1.41	1.66	0
14.10	8.63	6.47	4.65	5.15	1.41	1.74	0

Table 4

Meristic data of *Macquaria novemaculeata* larvae and juveniles. Body length preceded by "R" indicates larvae reared in aquarium. ( ) indicates only fin bases present, [ ] incipient rays or spines, { } ray transforming to a spine.

Body length	Dorsal	Anal	Pectoral	Pelvic	Caudal	Myomeres
Yolksac						
R 3.32						10+15=25
R 3.60						11+14=25
Preflexion						
R 3.60						12+13=25
R 3.80						11+14=25
R 3.90						11+14=25
R 4.20						10+15=25
R 4.40						10+15=25
4.57	(9)	(8)			[2+3]	10+15=25
Flexion						
5.00	(VI), (6)	(8)			7+6	10+15=25
5.14	(VI), (8)	(9)			8+7	10+15=25
R 5.31	(III), (9)	(8)			[7+6]	12+13=25
5.39	(IV), [9]	(I), [9]			8+7	11+14=25
R 5.39	(III), (9)	(9)			6+6	12+13=25
5.47	(V), [8]	[I], [7]			[1]7+7[1]	11+14=25
R 5.47	(VI), [10]	(I), [8](1)			[1]8+7[1]	12+13=25
5.70	VI, 10	(I), 8	6		9+8	13+13=26
5.90	[I]V, 10	(I), 8	6		9+8	12+13=25
Postflexion						
5.64	VI, 10	(I), 9	5		9+8	10+15=25
5.89	[VI], 10	(I), 9	5		9+8	12+13=25
6.06	VI, 10	(I), 9	6		9+8	12+13=25
6.30	VI, 11	I, 9	6	buds	9+8	11+14=25
6.60	VI, 11	I, 9	8		9+8	12+13=25
6.72	VI, 11	I, 9	8	buds	9+8	12+13=25
R 6.72	VI, 10	I, 9	12	buds	9+8	12+13=25
R 7.20	VII, 11	II, 9	10	buds	9+8	12+13=25
7.40	VII, 11	II, 9	12	buds	9+8	13+12=25
R 7.47	VII, 11	II, 9	13	buds	9+8	12+13=25
7.55	VII, 11	II, 9	12	buds	9+8	12+13=25
R 8.18	VIII, 11	II, 9	13	I, 5	9+8	13+12=25
R 8.60	VIII, 11	II, 8	13	I, 5	9+8	13+12=25
R 9.20	IX, 10	II{I}, 7	15	I, 5	9+8	13+12=25
Settled						
10.13	IX, 10	II{1}, 8	14	I,5	7+9+8+7	12+13=25
R 10.20	IX, 10	II{1}, 8	14	I, 5	9+8	13+12=25
R 10.30	IX, 10	II{1}, 8	14	I, 5	9+8	13+12=25
11.62	VIII {1},10	II {1}, 8	14	I,5	9+9+8+8	13+12=25
11.62	IX, 9	II {1}, 8	14	I,5	8+9+8+7	13+12=25
13.28	IX, 10	III, 8	14	I,5	7+9+8+9	12+13=25
14.1	IX, 10	III, 8	14	I,5	9+9+8+7	12+13=25

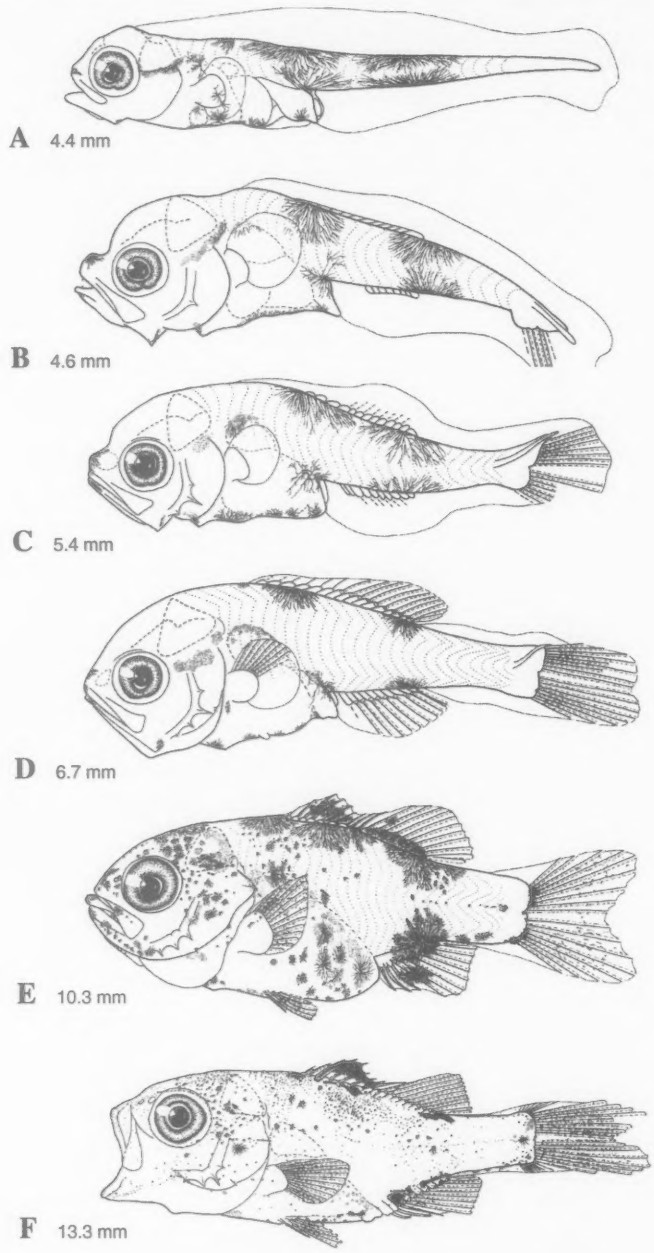

Figure 2

Larvae of *Macquaria novemaculeata*. **(A)** yolksac larva, 10 days after hatching, note remnant of yolk below pectoral-fin base; **(B)** preflexion larva; **(C)** flexion stage larva; **(D)** postflexion larva; **(E)** postflexion larva, 57 days after hatching; **(F)** recently settled juvenile. Specimens A and E were reared at Port Stevens Fisheries Centre, New South Wales (NSW); B–D from Swansea Channel, central NSW; specimen F is a recently settled juvenile from the Clyde River, southern NSW.

form as larvae develop; four or five spines are present in larvae and transitional juveniles from 7.5–8.2 mm. A minute spine (rarely two) develops on the anterior preopercular border from 9 mm; a third spine develops in transitional juveniles from 13.3 mm. A small interopercular spine develops by the time notochord flexion is complete. Low posttemporal and supraocular ridges, but no spines, develop during notochord flexion; they both become inconspicuous in postflexion larvae from 8.2 and 8.6 mm, respectively. An opercular spine is present from 8.6 mm. A small supracleithral spine is present in transitional juveniles from 10.1 mm.

The pterygiophores of all the soft rays and up to six of the pterygiophores of the first dorsal fin form during notochord flexion. Soft rays of the dorsal fin are ossified by the time notochord flexion is complete, whereas spinous rays ossify from posterior to anterior in late flexion and early postflexion larvae by 5.7–6.1 mm. The full complement of spines is present by 8.2 mm. Anal-fin pterygiophores form during notochord flexion, and all soft rays are ossified by the time notochord flexion is complete. Spinous rays of the anal fin begin to ossify in postflexion larvae by 6.3 mm, and all anal-fin elements are present by 7.2 mm. The last spinous ray of the dorsal fin and the third spinous ray of the anal fin transform from a soft ray between 7.6 and 9.2 mm. Pectoral-fin elements begin to ossify by the time notochord flexion is complete, and all rays are present in postflexion larvae by 7.5 mm. Pelvic-fin buds form in postflexion larvae by 6.7 mm, and all elements are ossified by 8.2 mm. Caudal-fin rays first appear in preflexion larvae from 4.6 mm, and all principal rays are ossified by the time notochord flexion is complete. Procurrent caudal rays are present in field-caught transitional juveniles. Notochord flexion commences between 4.6 and 5.0 mm, and is complete by 5.6–6.1 mm. There is a prominent gap between the anus and anal fin while the anal fin forms (vent to anal-fin length [VAFL] up to 5% of BL). The gap reduces in size as the anal fin develops, and it is absent by 7.6 mm. Scales have not developed in the largest specimen examined.

Pigment (Fig. 2, A–F) Larvae are moderately to heavily pigmented. An expanded melanophore is present on the tip of the snout and a small melanophore develops under the tip of the lower jaw in preflexion larvae from 3.6 mm. A second melanophore on the snout develops posterior to the first by the time notochord flexion is complete. A single melanophore is present at the angle of the lower jaw. A few small melanophores develop ventrally along the lower jaw in postflexion larvae from 7.2 mm. A series of internal melanophores underlie the mid- and hindbrain.

There are two very large expanded melanophores on the dorsal midline of the tail; the first is on the trunk centered over the hindgut, and the second is mid way along the tail. Once the dorsal fin forms they are centred under the middle of the spinous portion of the dorsal fin and under the posterior end of the soft dorsal fin, respectively. An additional smaller expanded melanophore is present from 7.2 to 7.5 mm on the dorsal midline of the nape above the pectoral-fin base.

Two very large expanded melanophores occur ventrally, opposite the two large dorsal melanophores. The anteriormost of these melanophores reduces in prominence as larvae develop and is inconspicuous to absent by metamorphosis. Internal expanded melanophores over the gas bladder may have filaments that emerge externally, particularly in preflexion and flexion larvae. Internal melanophores along the notochord may be apparent on the caudal peduncle in postflexion larvae from 7 mm. There is an expanded melanophore on the midline of the isthmus, immediately anterior to the cleithral symphysis. A series of three to six small, expanded melanophores is present along the ventral midline of the gut. In postflexion larvae there is a bilaterally paired melanophore anterior to the pelvic-fin base, and two to four melanophores along the midline of the gut between the pelvic-fin base and the anus. A small contracted melanophore ventrally on the posterior margin of the caudal-fin base develops between 5.0 and 6.1 mm, and is located between ventral rays 1–5. This melanophore expands from 6.7 to 7.6 mm and spreads across up to four ray bases.

Pigment distribution spreads rapidly over most of the head from 7.2 to 7.5 mm, and laterally on the trunk, gut and tail from 8.2 mm. The expanded melanophores on the dorsal and ventral midlines of the trunk and tail remain large as the larvae develop; the posteriormost of these increases in intensity in reared larvae. The expanded melanophores on the dorsal and ventral midlines of the body become relatively smaller after settlement. By settlement, small melanophores develop on the membranes of the pectoral, pelvic, anal, and caudal fins, and the membrane of the spinous portion of the dorsal fin becomes heavily pigmented. After settlement, small melanophores cover most of the head and body, but the heaviest cover is seen dorsally. Three broad vertical bands become apparent dorsally on the nape, below the center of the spinous dorsal fin, and below the center of the soft dorsal fin in the largest specimen examined (14.1 mm).

Discussion

Adults of *M. colonorum* and *M. novemaculeata*, which have only minor morphological differences, such as the relative length of the snout, the profile of the head dorsally, postorbital head length, and gill-raker counts, are difficult to distinguish (Williams, 1970). None of these characters are useful for distinguishing larvae. The larvae of these two species could be positively identified only by comparison with reared larvae derived from positively identified brood stock.

Melanophore distribution is the most distinguishing character between the larvae of *M. colonorum* and *M. novemaculeata*. *Macquaria colonorum* has between four and seven expanded melanophores along the dorsal midline of the trunk and tail between 4.8 and 7.1 mm.

Macquaria novemaculeata has only two melanophores, and these are much larger; a third expanded melanophore develops on the nape from 7.2 mm. In addition, *M. novemaculeata* lacks a midlateral series of melanophores along the tail until settlement, and it is never as well developed as that in *M. colonorum*. On the other hand, *M. colonorum* has a prominent midlateral series until after settlement. One other morphological character that distinguishes the larvae is a snout length which is about equal to eye diameter in *M. colonorum* larvae until 7 mm, but snout length is always smaller than the eye diameter in *M. novemaculeata*.

Within the genus *Macquaria*, larval development of only *M. ambigua* has been described (Lake, 1967; Brown and Neira, 1998). There are several differences in the life history and development of the larvae of *M. ambigua* compared with *M. colonorum* and *M. novemaculeata*. *Macquaria ambigua* is restricted to freshwater, the eggs are large (3.3–4.2 mm in diameter, compared with 0.9 mm in reared *M. novemaculeata*) and the yolk sac in *M. ambigua* is large in small larvae and is not resorbed until the flexion stage (Brown and Neira, 1998). Compared with the larvae described in the present study, larvae of *M. ambigua* have more myomeres (24–28, but typically 26–27), and these larvae are relatively large by the time they complete notochord flexion (7.3 mm). They also lack an interopercular spine and supraocular ridge, and lack dorsal and lateral pigment on the tail until the postflexion stage.

Larvae of several other generalized percoid families are morphologically similar to *Macquaria*, including Latidae (Trnski et al., 2000), Microcanthidae (Walker et al., 2000a), Kyphosidae (Walker et al., 2000b), and some Apogonidae (Leis and Rennis, 2000). The latid genus *Lates* is morphologically most similar to the *Macquaria* larvae described in the present study but is tropical and does not have an overlapping distribution with *Macquaria*. *Lates* can be distinguished by the small size at notochord flexion (3.0–3.8 mm), dorsal and pectoral fin-ray counts when complete, and heavier melanophore distribution at a given size. Microcanthid and kyphosid larvae can be distinguished from coastal percichthyid larvae by the higher number of fin elements in the dorsal and anal fins, and the presence of supracleithral spines that are absent in larval percichthyids until the juvenile stage. Some deep-bodied apogonids resemble *Macquaria* larvae but can be distinguished by having separate spinous and soft dorsal fins and a large, conspicuous gas bladder.

Larvae of *M. colonorum* and *M. novemaculeata* were collected in Swansea Channel from July to August. This collection period coincides with adults of *M. novemaculeata* spawning from June to September in central New South Wales (Harris, 1986). *Macquaria colonorum* probably spawns at a similar time (McCarraher and McKenzie, 1986), and eggs have been collected from June to November in western Victoria (Newton, 1996). Adults of both species are thought to spawn in the middle reaches of estuaries at salinities above 8–10 g/kg (Harris, 1986; McCarraher, 1986), but *M. novemaculeata* will spawn in waters up to 35 g/kg in culture (Battaglene and Selosse, 1996). The optimal conditions for incubation and hatching of *M. novemaculeata* eggs are 18 [±1]°C and salinity at 25 to 35‰ (van der Wal, 1985). Eggs are buoyant within this salinity range and hatch in 42 h at 18°C.

The presence of field-caught larvae of both species on incoming tides in Swansea Channel indicates that the larvae have spent some time in the ocean and that the eggs were potentially spawned in the ocean rather than in an estuary if they were not carried out to sea by outgoing tides. *Macquaria novemaculeata* adults move downstream into estuaries to spawn in water of suitable salinity. In low rainfall years, the spawning location is further upstream than in wet years, when spawning can occur in shallow coastal waters adjacent to estuaries (Searle[1]). Mature *M. novemaculeata* adults can be found outside of estuaries in wet years (Williams 1970). This is verified by the collection of mature adults by trawl in July 1995 in 11–17 m of water off Newcastle, NSW (AMS I.37358-001). *Macquaria colonorum* adults have also been collected on the continental shelf (McCarraher and McKenzie, 1986). In addition, larvae can tolerate waters of marine salinity in culture, and late in their larval phase wild larvae can tolerate marine salinity as shown from our field collections. The presence of larvae and adults in continental shelf waters may provide two modes of dispersal among estuaries. Thus, these two species of *Macquaria* may not be confined to freshwater and estuarine conditions as often assumed (Harris and Rowland, 1996; Allen et al., 2002).

The smallest juveniles of *M. colonorum* and *M. novemaculeata* collected in the wild are from the Clyde River estuary, southern NSW. These range in size from 10 to 14 mm SL, and were collected among *Zostera* seagrass. They are morphologically similar to the largest pelagic larvae collected in the channel net in Swansea Channel. Based on the largest larvae and smallest juveniles, settlement occurs between 7.1 and 10.3 mm SL in *M. colonorum* and between 9.2 and 10.1 mm in *M. novemaculeata*. Transition to the juvenile stage is gradual, because scales are not present and juvenile pigmentation is still forming at about 15 mm. Juveniles of both species have been collected in estuarine waters until at least 100 mm SL (AMS fish collection). Juveniles of *M. novemaculeata* would be expected to migrate to freshwater because this is the nominal adult habitat (Williams, 1970), but the size at which this migration occurs is unclear.

The two species described in the present study were the only members of the genus *Percalates*, until this genus (along with *Plectroplites*) was synonymized with *Macquaria* by MacDonald (1978). Analyzing morphological and biochemical similarities of the three genera, MacDonald (1978) listed eight morphological differences that distinguished *Percalates* from *Macquaria* and *Plectroplites*. Protein electrophoresis similarities were stron-

[1] Searle, G. 2002. Personal commun. Searle Aquaculture, 255 School Rd, Palmers Island NSW 2463.

ger between *Pe.* (currently *Macquaria*) *colonorum* and *Pe.* (*Macquaria*) *novemaculeata* (similarity coefficient 0.95), and *M. australasica* and *Pl.* (*Macquaria*) *ambigua* (0.71) than between the *Percalates* and *Macquaria* + *Plectroplites* (0.63) (MacDonald, 1978). The species of *Percalates* are euryhaline, whereas *Macquaria* and *Plectroplites* are strictly freshwater. This fact, combined with the difference in larval morphological features between *Macquaria ambigua* (Brown and Neira, 1998) and *M. colonorum* and *M. novemaculeata*, provides evidence that the genus *Macquaria* as defined by MacDonald may be polyphyletic. Recent phylogenetic analysis of the Percichthyidae with the use of molecular data indicates that *M. colonorum* and *M. novemaculeata* are more closely related to *Maccullochella* species than to *Macquaria* (*sensu stricto*) (Jerry et al., 2001). Molecular and larval evidence indicates the two catadromous species (*M. colonorum* and *M. novemaculeata*) belong in a genus separate from the freshwater species (*M. ambigua* and *M. australasica*).

Acknowledgments

Comments by Dave Johnson, Jeff Leis, and Tony Miskiewicz improved the manuscript. Sue Bullock illustrated the larvae from camera lucida sketches by TT. Glen Searle provided information on spawning habits that aided interpretation of larval distributions. Mark McGrouther provided access to specimens held in the Fish Collection at the Australian Museum (AMS). Larval collections in the field were supported by funds from Lake Macquarie City Council. Preparation of this paper was supported by a NSW Government Biodiversity Enhancement Grant to AMS, and by AMS.

Literature cited

Allen, G. R., S. H. Midgley, and M. Allen.
2002. Field guide to the freshwater fishes of Australia, 394 p. Western Australian Museum, Perth, Western Australia, Australia.

Battaglene, S. C., and P. M. Selosse.
1996. Hormone-induced ovulation and spawning of captive and wild broodfish of the catadromous Australian bass, *Macquaria novemaculeata* (Steindachner), (Percichthyidae). Aquacult. Res. 27:191–204.

Brown, P., and F. J. Neira.
1998. Percichthyidae: basses, perches, cods. *In* Larvae of temperate Australian fishes: laboratory guide for larval fish identification (F. J. Neira, A. G. Miskiewicz and T. Trnski, eds.), p. 259–265. Univ. Western Australia Press, Perth, Western Australia, Australia.

Dakin, J. W., and G. L. Kesteven.
1938. The Murray cod (*Maccullochella macquariensis* (Cuv. And Val.)). Bull. New South Wales State Fish. 1:1–18.

Dufty, S.
1986. Genetic and morphological divergence between populations of macquarie perch (*Macquaria australasica*) east and west of the Great Dividing Range. Honours thesis, 43 p. Univ. New South Wales, Sydney, New South Wales, Australia.

Eschmeyer, W. N. (ed.)
1998. Catalog of fishes, 2905 p. Special publication 1, Center for Biodiversity Research and Information, California Academy of Sciences, San Francisco, CA.

Harris, J. H.
1986. Reproduction of the Australian bass, *Macquaria novemaculeata* (Perciformes: Percichthyidae) in the Sydney Basin. Aust. J. Mar. Freshw. Res. 37:209–235.

Harris, J. H., and S. J. Rowland.
1996. Family Percichthyidae: Australian freshwater cods and basses. *In* Freshwater fishes of south-eastern Australia (R. M. McDowall, ed.), p 150–163. Reed Books, Chatswood, New South Wales., Australia.

Jerry, D. R., M. S. Elphinstone, and P. B. Baverstock.
2001. Phylogenetic relationships of Australian members of the family Percichthyidae inferred from mitochondrial 12s rRNA sequence data. Molec. Phylogenetics Evol. 18:335–347.

Johnson, G. D.
1984. Percoidei: development and relationships. *In* Ontogeny and systematics of fishes (H. G. Moser, W. J. Richards, D. M. Cohen, M. P. Fahay, A. W. Kendall Jr., and S. L. Richardson, eds.), p 464–498. Am. Soc. Ichthyol. Herpetol., Spec. Publ. 1.

Kailola, P. J., M. J. Williams, P. C. Stewart, R. E. Reichelt, A. McNee, and C. Grieve.
1993. Australian fisheries resources, 422 p. Bureau of Resource Sciences, and Fisheries Research and Development Corporation, Canberra, New South Wales, Australia.

Lake, J. S.
1967. Rearing experiments with five species of Australian Freshwater fishes. II. Morphogenesis and ontogeny. Aust. J. Mar. Freshw. Res. 18:155–173.

Leis, J. M., and B. M. Carson-Ewart.
2000. The larvae of Indo-Pacific coastal fishes: an identification guide to marine fish larvae. Fauna Malesiana Handbooks, 2850 p. Brill, Leiden, The Netherlands.

Leis, J. M., and D. S. Rennis.
2000. Apogonidae (cardinalfishes). *In* The larvae of Indo-Pacific coastal fishes: an identification guide to marine fish larvae (J. M. Leis and B. M.Carson-Ewart, eds.), p. 273–279. Fauna Malesiana Handbooks 2, Brill, Leiden, The Netherlands.

McCarraher, D. B.
1986. Observations on the distribution, spawning, growth and diet of Australian bass (*Macquaria novemaculeata*) in Victorian waters. Arthur Rylah Inst. Environ. Res. Tech. Rep. Ser. 47.

McCarraher, D. B., and J. A. McKenzie.
1986. Observations on the distribution, growth, spawning and diet of estuary perch (*Macquaria colonorum*) in Victorian waters. Arthur Rylah Inst. Environ. Res. Tech. Rep. Ser. 42.

MacDonald, C. M.
1978. Morphological and biological systematics of Australian freshwater and estuarine percichthyid fishes. Aust. J. Mar. Freshw. Res. 29:667–698.

Musyl, M. K., and C. P. Keenan.
1992. Population genetics and zoogeography of Australian freshwater golden perch, *Macquaria ambigua* (Richardson 1845) (Teleostei: Percichthyidae), and electrophoretic identification of a new species from the Lake Eyre Basin. Aust. J. Mar. Freshw. Res. 43:1585–1601.

Neira, F. J., A. G. Miskiewicz, and T. Trnski.
1998. Larvae of temperate Australian fishes: laboratory guide for larval fish identification, 474 p. Univ. Western Australia Press, Perth, Western Australia, Australia.

Nelson, J. S.
1994. Fishes of the world, 3rd ed., 600 p. John Wiley and Sons, New York, NY.

Newton, G. M.
1996. Estuarine ichthyoplankton ecology in relation to hydrology and zooplankton dynamics in a salt-wedge estuary. Mar. Freshw. Res. 47:99–111.

Paxton, J. R., and J. E. Hanley.
1989. Percichthyidae. *In* Zoological catalogue of Australia, vol. 7: Petromyzontidae to Carangidae (J. R. Paxton, D. F. Hoese, G. R. Allen, and J. E. Hanley (eds.), p. 509–515. Australian Government Publishing Service, Canberra, New South Wales, Australia.

Paxton, J. R., J. E. Hanley, D. J. Bray, and D. F. Hoese.
In press. Percichthyidae. *In* Pisces (part 2), Mugilidae to Molidae. Zoological catalogue of Australia, vol. 7 (part 2) (D. F. Hoese, D. J. Bray, D. J., G. R. Allen, C. J. Allen, N. J. Cross, and J. R. Paxton, eds.). Australian Government Publishing Service, Canberra, New South Wales, Australia.

Pusey, B. J., and M. J. Kennard.
2001. *Guyu wujalwujalensis*, a new genus and species (Pisces: Percichthyidae) from north-eastern Queensland, Australia. Ichthyol. Explor. Freshw. 12:17–28.

Trnski, T.
2002. Behaviour of settlement-stage larvae of fishes with an estuarine juvenile phase: *in situ* observations in a warm-temperate estuary. Mar. Ecol. Progr. Ser. 242:205–214.

Trnski, T., D. J. Russell, and J. M. Leis.
2000. Latidae (barramundi, sea basses). *In* The larvae of Indo-Pacific coastal fishes: an identification guide to marine fish larvae (J. M. Leis and B. M.Carson-Ewart, eds.), p. 313–316. Fauna Malesiana Handbooks 2, Brill, Leiden, The Netherlands.

Van der Wal, E.
1985. Effects of temperature and salinity on the hatch rate and survival of Australian bass (*Macquaria novemaculeata*) eggs and yolk-sac larvae. Aquaculture 47:239–244.

Vigliola, L., and M. Harmelin-Vivien.
2001. Post-settlement ontogeny in three Mediterranean reef fish species of the genus *Diplodus*. Bull. Mar. Sci. 68:271–286.

Walker Jr, H. J., A. G. Miskiewicz, and F. J. Neira.
2000a. Microcanthidae (stripey). *In* The larvae of Indo-Pacific coastal fishes: an identification guide to marine fish larvae (J. M. Leis and B. M.Carson-Ewart, eds.), p. 470–473. Fauna Malesiana Handbooks 2, Brill, Leiden, The Netherlands.

Walker Jr, H. J., F. J. Neira, A. G. Miskiewicz, and B. M. Carson-Ewart.
2000b. Kyphosidae (rudderfishes, sea chubs). *In* The larvae of Indo-Pacific coastal fishes: an identification guide to marine fish larvae (J. M. Leis and B. M.Carson-Ewart, eds.), p. 466–469. Fauna Malesiana Handbooks 2, Brill, Leiden, The Netherlands.

Williams, N. J.
1970. A comparison of the two species of the genus *Percalates* Ramsay and Ogilby (Percomorphi: Macquariidae), and their taxonomy. State Fisheries Research Bulletin 11, 60 p. Chief Secretary's Department, Sydney, New South Wales, Australia.

Early life history of the Argentine sandperch *Pseudopercis semifasciata* (Pinguipedidae) off northern Patagonia

Leonardo A. Venerus
Centro Nacional Patagónico–Consejo Nacional de Investigaciones Científicas y Técnicas
Boulevard Brown s/n, (U9120ACV)
Puerto Madryn, Chubut, Argentina
E-mail address: leo@cenpat.edu.ar

Laura Machinandiarena
Martín D. Ehrlich
Instituto Nacional de Investigación y Desarrollo Pesquero
PO Box 175, (B7602HSA)
Mar del Plata, Buenos Aires, Argentina

Ana M. Parma
Centro Nacional Patagónico–Consejo Nacional de Investigaciones Científicas y Técnicas
Boulevard Brown s/n, (U9120ACV)
Puerto Madryn, Chubut, Argentina

Abstract—The Argentine sandperch *Pseudopercis semifasciata* (Pinguipedidae) sustains an important commercial and recreational fishery in the northern Patagonian gulfs of Argentina. We describe the morphological features of larvae and posttransition juveniles of *P. semifasciata* and analyze the abundance and distribution of early life-history stages obtained from 19 research cruises conducted on the Argentine shelf between 1978 and 2001. *Pseudopercis semifasciata* larvae were distinguished from other larvae by the modal number of myomeres (between 36 and 38), their elongated body, the size of their gut, and by osteological features of the neuro- and branchiocranium. *Pseudopercis semifasciata* and *Pinguipes brasilianus* (the other sympatric species of pinguipedid fishes) posttransition juveniles were distinguished by their head shape, pigmentation pattern, and by the number of spines of the dorsal fin (five in *P. semifasciata* and seven in *P. brasilianus*). The abundance and distribution of *P. semifasciata* at early stages indicate the existence of at least three offshore reproductive grounds between 42–43°S, 43–44°S, and 44–45°S, and a delayed spawning pulse in the southern stocks.

Manuscript submitted 20 November 2003 to the Scientific Editor's Office.
Manuscript approved for publication 16 September 2004 by the Scientific Editor.
Fish. Bull. 103:195–206 (2005).

The family Pinguipedidae (Osteichthyes, Perciformes) includes six genera and about 50 marine species and one freshwater species (Froese and Pauly, 2004). On the Argentine continental shelf this family is represented by two species, *Pseudopercis semifasciata* (Cuvier, 1829) and *Pinguipes brasilianus* Cuvier, 1829.

The Argentine sandperch *P. semifasciata* is an important incidental catch in the bottom trawl and longline commercial fisheries that target hake (*Merluccius hubbsi*) in the northern Patagonian coast off Argentina (Otero et al., 1982; Elías and Burgos, 1988; González, 1998). In recent years, the reported annual landings have oscillated between 1900 and 3780 metric tons (official statistics, SAGPyA-DNPyA[1]). In northern Patagonia, *P. semifasciata* is also targeted by sport anglers and spear fishermen and represents a tourist attraction for recreational divers. It inhabits rocky and sandy bottoms, from 23°S in Brazil to 47°S in Argentina (Cousseau and Perrotta, 2000), mainly in coastal waters, although it has been found in depths of up to 100 m (Menezes and Figueiredo, 1985).

Very little is known about the ecology and behavior of *P. semifasciata*, and most of what is known is based on limited observations during underwater visual censuses on shallow reefs where adults concentrate (González, 1998). Previous studies have focused on morphological features (Herrera and Cousseau, 1996; Rosa and Rosa, 1997; Gosztonyi and Kuba[2]), age and growth (Elías and Burgos, 1988; Fulco, 1996; González, 1998), diet (Elías and Rajoy, 1992; González, 2002), and reproductive traits, including reproductive season, spawning modality, and age at first maturity (Macchi et al., 1995;

[1] SAGPyA-DNPyA. 2003. Capturas marítimas totales 1992–2002. Manuscript, 71 p. [Available from Secretaría de Agricultura, Ganadería y Pesca de la Nación, Dirección de Pesca y Acuicultura, Paseo Colón 982 P.B. Of. 59 – (C1063ACW) Buenos Aires, Argentina.] http://www.sagpya.mecon.gov.ar [Accessed July 2004.]

[2] Gosztonyi, A. E., and L. Kuba. 1996. Atlas de huesos craneales y de la cintura escapular de peces costeros patagónicos. Inf. Téc. FPN 4, 29 p. [Available from CENPAT, Blvd. Brown s/n (U9120ACV), Puerto Madryn, Chubut, Argentina.]

Fulco, 1996; González, 1998). *Pseudopercis semifasciata* is a multiple spawner with low batch fecundity and an extended reproductive season (Macchi et al., 1995; González, 1998). There is little information on the early life history of the species because only specimens >20–25 cm are found on reefs and the habitat of juveniles has not been described. In general, information about the early stages of pinguipedid fishes from the southwest Atlantic Ocean is scarce. De Cabo[3] reported pinguipedid larvae from the Argentine shelf but did not identify the specimens to species level.

In the present study, we describe development of *P. semifasciata* from larvae to the posttransition juvenile stage (*sensu* Vigliola and Harmelin-Vivien, 2001) and analyze data on distribution and abundance on the northern Patagonian shelf. This information is needed to locate main reproductive and nursery grounds for the species.

[3] De Cabo, L. 1988. Descripción de tres larvas de peces teleósteos del Mar Argentino: Mugiloididae, Ophidiidae (*Genypterus blacodes*) y Tripterygidae (*Tripterygion cunninghami*). Unpubl. manuscript, 58 p. Facultad de Ciencias Exactas y Naturales, Universidad de Buenos Aires–INIDEP. [Available from INIDEP: P.O. Box 175 (B7602HSA) Buenos Aires, Argentina.]

Materials and methods

Fish larvae and posttransition juveniles were collected during 19 research cruises conducted by INIDEP (Instituto Nacional de Investigación y Desarrollo Pesquero) between 1978 and 2001. A total of 592 ichthyoplankton samples and 277 juvenile trawl samples were analyzed (Table 1).

Larvae

Ichthyoplankton was sampled by using Bongo, Nackthai, and PairoVET nets. The Bongo net was fitted with 300-μm mesh and a flowmeter. The Nackthai sampler, a German modification of the Gulf V high-speed sampler (Nellen and Hempel, 1969), was fitted with a 400-μm mesh net and a flowmeter. Both samplers were towed obliquely from bottom to surface. The PairoVET sampler, a Bongo-type version of the CalVET, was fitted with two 200-μm mesh nets to sample fish eggs (Smith et al., 1985) and was towed vertically. Samples were fixed in a solution of 5% formalin to seawater. During most cruises, depths at which *P. semifasciata* were located were determined by a SCANMAR sensor mounted on the sampler.

Table 1

Research cruises in the Argentine Sea during 1978–2001. Only those cruises with at least one positive station containing larvae or posttransition juveniles of *Pseudopercis semifasciata* were included in the analysis. EH=RV *Dr. Eduardo L. Holmberg*; OB=RV *Capitán Oca Balda*; SM= RV *Shinkai Maru*.

Year	Cruise	Dates	No. of stations	Lat. S range	Long. W range
Ichthyoplankton surveys					
1978–79	SM-IX	26 Dec–07 Jan	28	42°27′–45°30′	61°58′–66°01′
1982	EH-05/82	19 Nov–03 Dec	65	35°55′–40°53′	54°45′–61°57′
1983	EH-01/83	14 Jan–26 Jan	43	38°30′–44°32′	58°00′–65°07′
1985	OB-02/85	25 Mar–04 Apr	30	44°41′–46°52′	65°05′–67°18′
1986	OB-01/86	20 Jan–03 Feb	40	41°34′–44°36′	61°27′–65°05′
	OB-07/86	09 Dec–22 Dec	43	43°01′–46°50′	62°40′–66°51′
1991	OB-07/91	01 Nov–11 Nov	35	35°49′–36°51′	56°03′–56°59′
1995	OB-14/95	05 Dec–18 Dec	75	41°16′–45°22′	60°00′–67°00′
1996	EH-17/96	12 Dec–21 Dec	18	42°29′–44°01′	62°03′–65°16′
1998	OB-10/98	07 Dec–20 Dec	87	42°21′–45°36′	61°00′–65°44′
1999	OB-09/99	11 Dec–17 Dec	15	43°21′–44°01′	62°59′–65°12′
2000	OB-14/00	09 Dec–21 Dec	27	43°19′–46°24′	63°37′–66°48′
2001	EH-01/01	06 Jan–29 Jan	28	43°19′–46°54′	62°12′–67°33′
	OB-02/01	12 Feb–25 Feb	40	42°54′–45°25′	62°30′–66°12′
	OB-13/01	10 Nov 13 Nov	18	42°21′–43°42′	61°55′–65°01′
Posttransition juvenile trawls					
1992	EH-02/92	02 Mar–21 Mar	45	42°04′–45°43′	62°45′–66°14′
1998	EH-04/98	01 Apr–10 Apr	41	43°18′–47°02′	63°51′–66°43′
1999	EH-04/99	20 May–31 May	56	43°10′–47°01′	63°51′–66°42′
2000	OB-05/00	01 Jun–20 Jun	112	43°45′–47°02′	61°53′–67°25′
2001	OB-02/01	12 Feb–25 Feb	23	42°54′–45°25′	62°30′–66°12′

A total of 68 preserved larvae, ranging in body length (BL) from 3.3 to 11.7 mm, were used to describe larval development. Terminology for morphometrics followed Neira et al. (1998). Additionally, head depth (HD) was defined as the maximum depth of the head. Preserved larvae were measured to the nearest 0.1 mm with an ocular micrometer fitted to a dissecting microscope, and their pigmentation pattern was recorded. Possible shrinkage was not considered in the measurements. Whenever possible, the number of vertebrae and numbers of dorsal, anal, caudal, pectoral, and pelvic fin rays were recorded. In addition, 14 larvae from 3.4 to 11.7 mm BL were cleared and stained following the methods of Potthoff (1984) and Taylor and Van Dyke (1985), and then examined for meristics and osteological features. Myomere and fin-ray counts and morphometric measurements were made on the left side of the body. Larval abundance was expressed as the number of larvae/10 m^2 of sea surface as recommended by Smith and Richardson (1977).

Posttransition juveniles

Posttransition juveniles were collected with a small bottom trawl called "Piloto," with the following features: 6 m total length, 6-m headrope and groundrope, 25-mm wing mesh size, 10-mm codend mesh size, 0.25-m^2 otter board surface and 12 kg weight, 10-m bridles and 0.80-m vertical opening. In Argentina, commercial fishing vessels use this gear for locating shrimp concentrations. Additionally, an epibenthic sampler (Rothlisberg and Pearcy, 1976) fitted with 1-mm mesh was used on one cruise (EH-02/92). We believe that individuals up to 12 cm total length were well represented in samples obtained with this gear.

A total of 27 posttransition juveniles, ranging from 22 to 83 mm body length (BL), were used to describe Argentine sandperch developmental stages. Samples were either frozen or fixed in 5% formalin to seawater solution. Measurements and degree of pigmentation were recorded after preservation.

Total length (TL), body length (=standard length), head length (HL), predorsal length (PDL), and preanal length (PAL) were measured to the nearest 1 mm. Head depth (HD), body depth (BD), and eye diameter (ED) were measured to the nearest 0.2 mm. Three juveniles between 22 and 33 mm BL were cleared and stained (Potthoff, 1984; Taylor and Van Dyke, 1985) and examined for meristics.

The density of posttransition juveniles, expressed as individuals/square nautical mile (nmi^2), was estimated from swept area. The family Pinguipedidae includes two species (morphologically very similar as juveniles) that overlap in the Argentine Sea. Unfortunately, not all individuals caught during the cruises were examined by us; therefore, to avoid biases caused by identification errors, the posttransition juveniles of both species were considered as a group. Distributional centroids and ellipses were calculated by following the method of Kendall and Picquelle (1989), that is by weighting each station by the density of juveniles caught. For this purpose each density value was standardized with respect to the maximum density observed for each survey season over all years.

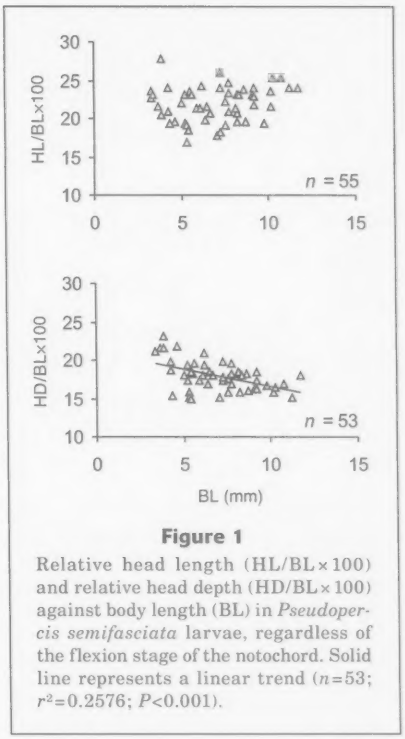

Figure 1

Relative head length (HL/BL × 100) and relative head depth (HD/BL × 100) against body length (BL) in *Pseudopercis semifasciata* larvae, regardless of the flexion stage of the notochord. Solid line represents a linear trend (n=53; r^2=0.2576; P<0.001).

Results

Description of larvae

General morphological features The larval body was elongate and relative BD was <25% in all stages of development (Table 2). The smallest larva collected (yolksac larva) was 3.3 mm BL. Its yolk sac was small and the single oil globule was located on the anterior part of the yolk mass. Notochord flexion began at 6 mm and was complete by 7–8 mm BL. As development proceeded, larvae became slightly deeper and laterally compressed. The head was small, with a rounded snout and no spines. The oblique mouth was open by the end of the yolksac larval stage. By 10 mm BL, premaxilla and dentary bones were covered with caniniform teeth. The premaxilla was an elongated bone with three processes on its dorsal margin—the first one perpendicular to the premaxilla. Relative head length remained constant, whereas relative head depth diminished during development (Fig. 1). The eyes were pigmented and their relative diameter decreased during the preflexion stage, and

Table 2

Body proportions of *Pseudopercis semifasciata* larvae, according to the flexion stage of the notochord. Mean (±SE), range and number of observations are shown in the table. BD=body depth; BL=body length; ED=eye diameter; HD=head depth; HL=head length; PAL=preanal length.

		BD/BL×100	HD/BL×100
Preflexion	3.3–7.1 mm BL; n=36:	16.4 ±3.1 (12.4–25.5) n=27	18.5 ±2.3 (14.8–23.1) n=25
Flexion	6.2–8.7 mm BL; n=8:	14.5 ±1.4 (12.2–16.1) n=5	17.1 ±1.2 (15.9–19.4) n=8
Postflexion	7.3–11.7 mm BL; n=20:	16.8 ±1.3 (14.3–19.5) n=20	17.4 ±1.4 (15.2–19.8) n=20
		PAL/BL×100	ED/BL×100
Preflexion		53.6 ±4.1 (45.0–62.5) n=29	7.8 ±1.1 (5.9–10.9) n=29
Flexion		52.0 ±2.2 (49.4–56.5) n=8	6.1 ±0.3 (5.6–6.5) n=8
Postflexion		52.5 ±2.7 (47.3–57.5) n=20	6.1 ±0.7 (4.9–7.6) n=20
		HL/BL×100	
Preflexion		21.2 ±2.4 (17.0–27.7) n=27	
Flexion		20.5 ±1.9 (18.2–24.2) n=8	
Postflexion		23.4 ±1.5 (19.3–26.0) n=20	

then remained constant (Fig. 2, A and B). The gut was initially straight but began to constrict at 4 mm BL and was loosely constricted throughout development (Fig. 3, A–C). It was moderate to long and extended to near the midpoint of the body, resulting in a relative preanal length of 0.45 to 0.62 BL.

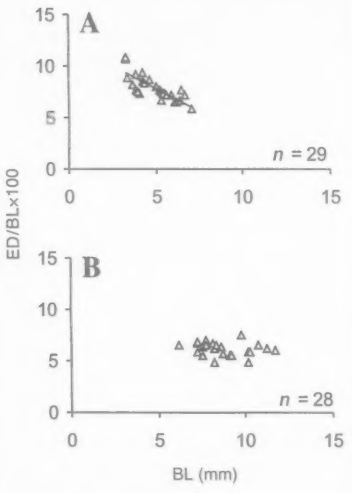

Figure 2

Relative eye diameter (ED/BL × 100) against body length (BL) in *Pseudopercis semifasciata* larvae. (**A**) Preflexion larvae. Solid line represents a linear trend (n=29; r^2=0.6228; P<0.001). (**B**) Flexion and postflexion larvae.

Body pigmentation Argentine sandperch larvae were lightly pigmented during all stages of development (Fig. 3; A–C). The pigmentation on the ventral body surface, between the isthmus and the anus, consisted of small stellate melanophores. Several small melanophores were scattered on the lateral surface of the anterior part of the gut. A double row of minute melanophores along the ventral surface ended in a single melanophore at the constriction of the gut. Pigmentation along the lateral midline of the tail consisted of four to seven stellate melanophores.

In preflexion larvae (Fig. 3A), small spots were evident along the lower jaw and the ventral part of the head. Several small stellate melanophores were present on the dorsal surface of the gut. A few melanophores were scattered at the base of the pectoral fin bud.

Preflexion and flexion larvae (Fig. 3, A and B) showed a distinct pattern of 12 to 23 small postanal melanophores serially arranged, about one per myomere, along the ventral midline. A total of 11 to 18 melanophores, about one melanophore per anal fin pterygiophore, was observed in postflexion larvae (Fig. 3C). As flexion progressed (Fig. 3, B and C), the number of melanophores on the ventral part of the head and over the gut diminished.

Fins and meristic features Modes of preanal and postanal myomeres were 14 and 23, respectively. All specimens examined had 33–40 total myomeres (mode:36–38 myomeres). Vertebral column ossification started anteriorly. A total of 38–39 vertebrae were recorded in 10–12 mm BL postflexion larvae (n=2).

In yolksac larvae, finfold and pectoral buds were the first fin development distinguished. In preflexion and flexion larvae, the finfold was present and it was gradually lost as the true fins developed. The sequence of fin-ray formation, characterized by initial development of fin elements, was caudal (7–8 mm BL), then pectoral

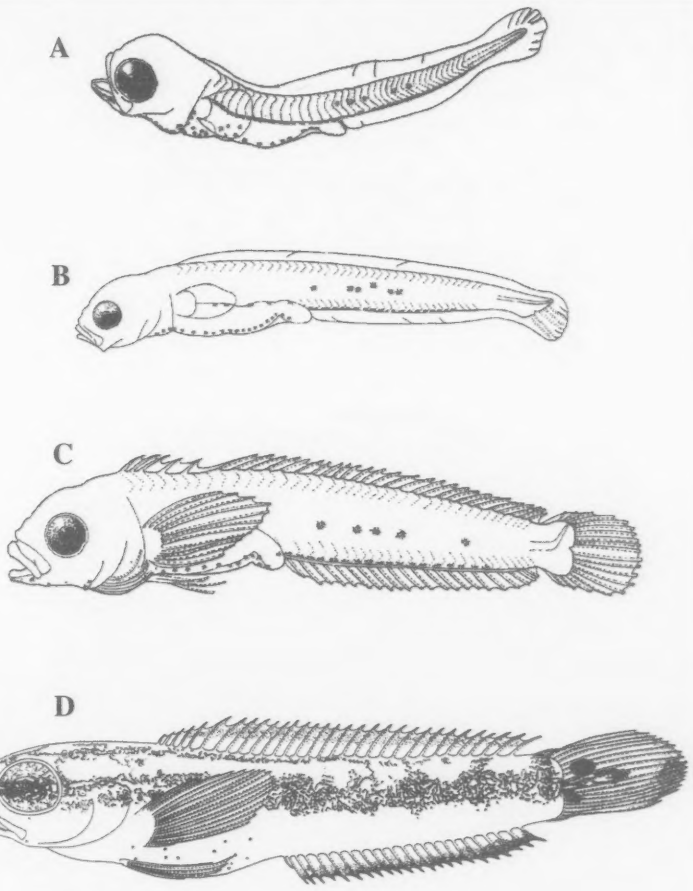

Figure 3

Larvae and posttransition juvenile of *Pseudopercis semifasciata*. (**A**) Preflexion (4.3 mm BL). (**B**) Flexion (8.7 mm BL). (**C**) Postflexion (10.7 mm BL). (**D**) transition juvenile (22 mm BL).

(9–10 mm BL), anal (9–10 mm BL), dorsal (9–10 mm BL), and pelvic (10–11 mm BL). Elements of the caudal fin began forming at flexion stage, and remaining fins at the postflexion stage. By 9–10 mm BL, dorsal (V+26–27) and anal (II+20–22) fin elements reached their full complement.

Description of posttransition juveniles

The posttransition juvenile stage was characterized by the acquisition of complete fin-ray complements and by morphological similarities with the adults (Table 3, Fig. 4). The transition from pelagic to benthic habitat in this species, i.e. settlement, probably occurred at about 20 mm BL because the smallest benthic juvenile of *Pseudopercis semifasciata* reported was 22 mm BL.

Table 3

Body proportions (mean [±SE] and range) of *Pseudopercis semifasciata* posttransition juveniles. BD=body depth; BL=body length; ED=eye diameter; HD=head depth; HL=head length; PAL=preanal length; PDL=predorsal length.

BD/BL×100	HD/BL×100
15.1 ±1.4 (12.7–19.3)	13.8 ±1.5 (11.9–19.3)
PAL/BL×100	ED/BL×100
41.7 ±2.2 (37.7 – 48.0)	8.4 ±1.1 (6.4–11.9)
HL/BL×100	PDL/BL×100
23.0 ±2.4 (17.6–31.6)	27.8 ±1.3 (25.7–30.2)

Individuals became more thick bodied as they developed. The body was elongate and relative body depth remained fairly constant throughout development. The snout was longer and rounded, and relative head length was moderate. The mouth was terminal, reaching to the middle of the eye, and had fleshy lips. Both jaws presented only caniniform teeth. Two opercular spines were also present in all specimens studied. Relative head depth decreased slightly during development, but not relative eye diameter. Gut length was moderate (PAL/BL 0.38–0.48), and the anus was situated near the midpoint of the body (Fig. 3D). Relative predorsal length (0.26–0.30) diminished during development.

The scales were ctenoid. Smaller posttransition juveniles (BL ≤33 mm) retained some of the larval pigmentation pattern. Larger juveniles showed several dark vertical bars, not completely defined at this stage of development, and three horizontal stripes along the body (Fig. 3D). Vertical bars developed progressively from the caudal peduncle to the head. Two lateral stripes formed continuous bands along each side of the body, almost entirely above the midline. The upper stripe developed from the tip of the snout and the lower one began below the eye, both extending to the anterior caudal peduncle. Another stripe developed from the dorsal region of the head between the eyes and extended along the dorsal fin, joining the upper lateral stripe at the posterior third part of the body. In large posttransition juveniles (≥47 mm BL), the membrane of the dorsal fin was pigmented more densely between the spines than between the rays; there were also dark blotches on the membrane between the rays. Anal-fin membranes were more pigmented than those of the dorsal fin. The membranes of the pectoral, pelvic, and caudal fins, and the external border of the membranes of the dorsal fin, were yellow in frozen individuals. By 22 mm BL, the conspicuous dark blotch observed in adult *P. semifasciata* on the base of the caudal fin upper lobe (Herrera and Cousseau, 1996) was already present (Fig. 3D). The pelvic fin was large and slightly shorter than the pectoral fin, whose margin was rounded.

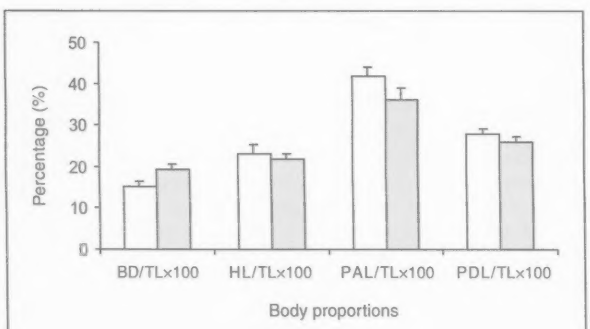

Figure 4

Comparisons between body proportions in posttransition juveniles (white bars) and adults (gray bars) of *Pseudopercis semifasciata*. Relative measures were taken with respect to total length (TL). Body depth (BD), head length (HL), preanal length (PAL), predorsal length (PDL). Proportions for adults were estimated from 99 individuals between <30 cm and 90 cm TL (González, 1998).

Abundance and distribution

Larvae Larvae of Argentine sandperch occurred between 36°42′S and 46°30′S, mainly in coastal waters, in the vicinity of the 50-m isobath (Fig. 5). The southernmost limit where larvae were collected was within San Jorge Gulf, which was surveyed in late March (fall). Larvae were present in only 3.55% of the stations in densities that varied between two and 74 larvae/10 m^2 of sea surface (Table 4). Greater densities (>20 larvae/10 m^2 of sea surface) were obtained in December 1986, 1996, and 1999, off the coast between Engaño Bay and Isla Escondida. Positive stations formed scattered clumps along the whole distributional area of the species. Minimum and maximum depths sampled were 20 and 71 m, respectively. Water temperature at 10 m depth at positive stations varied between 12.3°C (March 1985) and 18.7°C (December 1999) (mean temperature [±SE]: 15.2°C [±2.1°C]).

Posttransition juveniles Posttransition pinguipedid juveniles were found between 42°27′S and 43°37′S in February and March, and between 43°17′S and 44°58′S from April to June, primarily in the vicinity of the 50-m isobath (Fig. 6, A and B). The percentages of positive stations were 5.9% and 7.7% in summer and fall surveys, respectively. Maximum juvenile densities were 4410 individuals/nmi^2 in summer and 27,027 individuals/nmi^2 in fall (Table 5).

The grid of stations used during the summer and fall cruises overlapped (Fig. 6, A and B), covering the main area of concentration of *P. semifasciata* (Otero et al., 1982). Minimum and maximum depths were 54 and 74 m in summer surveys (mean depth [±SE]: 64.5 [±10.0] m), and 34 and 79 m in fall surveys (mean depth [±SE]: 60.4 [±13.7] m). The distributional ellipses calculated for summer and fall from the positive stations were small and widely separated. Maximum summer densities of posttransition pinguipedids were found southeast of Península Valdés, whereas greatest fall densities were detected northeast of Camarones Bay (Fig. 6, A and B).

Discussion

Literature describing the early stages of species belonging to the family Pinguipedidae (formerly Mugiloididae) is scarce. The few available studies refer to the larval development of *Parapercis* spp. (Leis and Rennis, 1983; Watson et al., 1984; Houde et al., 1986; Neira, 1998; Leis and Rennis, 2000)

and *Prolatilus jugularis* (Vélez et al., 2003). Larval abundance and distribution have been studied for a few species of *Parapercis* (Houde et al., 1986; Gaughan et al., 1990; Neira et al., 1992) and, more recently, for *Prolatilus jugularis* (Vélez et al., 2003); no information is available for posttransition pinguipedid juveniles.

Larvae of *P. semifasciata* resembled the larvae of other pinguipedids in their gut size, meristics, and general pattern of pigmentation. They differed from *Parapercis* spp. and *P. jugularis* larvae in some relevant features:

- The head had no spines and was less rotund, rather moderate instead of large (HL ranged from 0.17 to 0.30 BL; mean HL/BL=0.22 [±0.02]);
- The body was rather elongate instead of moderate (BD ranged from 0.12 to 0.26 BL; mean BD/BL=0.16 [±0.03]);
- The notochord flexion occurred between 6.2 and 8.7 mm BL, at a relatively large size range compared to that for *Parapercis* spp. (3.7–4.8 mm BL) and to *P. jugularis* (5.7–6.9 mm BL). *Pseudopercis semifasciata* is a larger and more rotund species;
- The finfold was still present in preflexion and flexion larvae.

De Cabo[3] described some osteological, meristic, and morphological characteristics of Argentine Sea pinguipedid larvae. Like De Cabo[3] we found that the first cranial bones that appeared during larval development in *P. semifasciata* were the premaxilla, the dentary and the cleithrum. These structures were already ossified in 3.4 mm BL preflexion larvae. From the adult osteological descriptions by Herrera and Cousseau (1996) and Gosztonyi and Kuba,[2] we determined that the larvae studied were *P. semifasciata*. The only other sympatric species of Pinguipedidae in the Argentine shelf is the Brazilian sandperch (*Pinguipes brasilianus*), which shares several similarities in meristic counts with *P. semifasciata* (Rosa and Rosa, 1987; Herrera and Cousseau, 1996). However, some osteological features from the neuro- and branchiocranium are of great value for identification of larval stages of *P. semifasciata*. The two species could be distinguished by the placement of the first process of the premaxilla, which is perpendicular to the premaxilla in the Argentine sandperch, and backinclined in the Brazilian sandperch, drawing an acute angle with the premaxilla (Herrera and Cousseau, 1996). The dentary in *P. semifasciata* has a quadrangulate anterior end and a margin almost straight, whereas the margin of the dentary in *P. brasilianus* is oblique (Herrera and Cousseau, 1996). In addition, the head and the teeth patch of the vomer are quadrangulate in *Pinguipes* and triangular in *Pseudopercis* (Herrera and Cousseau, 1996).

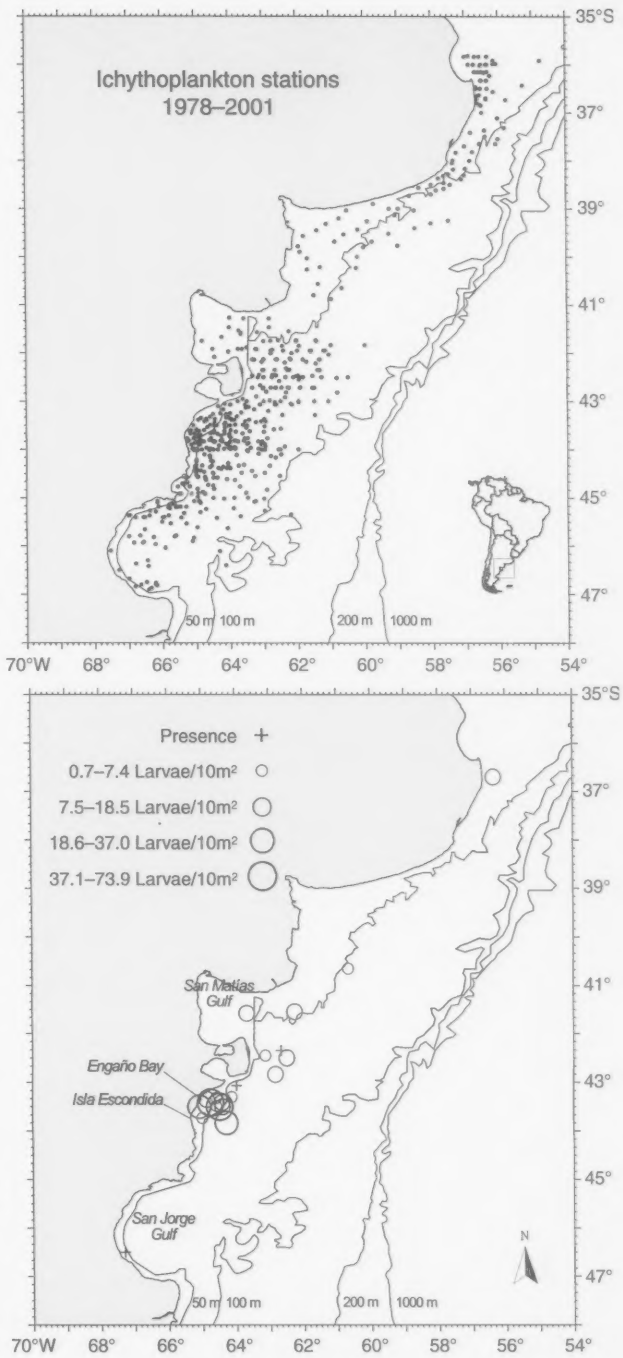

Figure 5

Distribution of ichthyoplankton stations (upper) and *Pseudopercis semifasciata* larvae (lower) in the Argentine Sea in the period 1978–2001. Dot diameter, classified into four categories, is proportional to larval abundance at each station (expressed as larvae/10 m² of sea surface).

Table 4

Positive stations for *Pseudopercis semifasciata* larvae in the Argentine Sea, during 1978–2001. Temperature values in parentheses indicate that only surface temperature was registered. W/d=missing data.

Cruise	Date	Sampler	Lat. S	Long. W	Abundance (larvae/10 m^2 of sea surface)	Water temperature (at 10 m depth)	Depth (m)
SM-IX	28 Dec 1978	Bongo	42°27′	63°08′	7.36	w/d	70
EH-05/82	22 Nov 1982	Bongo	40°39′	60°40′	5.85	(12.8)	53
EH-01/83	21 Jan 1983	Bongo	43°44′	65°00′	4.82	16.7	52
OB-02/85	30 Mar 1985	Bongo	46°30′	67°18′	Presence	12.3	56
OB-07/86	20 Dec 1986	Nackthai	43°25′	64°45′	73.91	14.2	34
OB-07/86	20 Dec 1986	Nackthai	43°50′	64°17′	19.78	14.0	47
OB-01/86	22 Jan 1986	Nackthai	41°33′	62°15′	13.76	18.7	45
OB-01/86	22 Jan 1986	Nackthai	41°35′	63°40′	8.64	17.6	51
OB-07/91	02 Nov 1991	Nackthai	36°42′	56°21′	15.33	w/d	20
OB-14/95	12 Dec 1995	Pairovet	43°04′	63°59′	Presence	13.0	65
EH-17/96	15 Dec 1996	Nackthai	43°30′	65°05′	23.92	14.3	24
OB-10/98	10 Dec 1998	Nackthai	42°21′	62°40′	Presence	w/d	66
OB-09/99	12 Dec 1999	Nackthai	43°21′	64°52′	17.22	(14.6)	20
OB-09/99	12 Dec 1999	Nackthai	43°30′	64°29′	41.00	(21.0)	49
OB-14/00	11 Dec 2000	Bongo	43°19′	64°35′	1.81	(12.8)	37
OB-14/00	11 Dec 2000	Bongo	43°30′	64°24′	8.44	13.8	52
EH-01/01	26 Jan 2001	Bongo	43°29′	64°35′	2.51	15.9	47
OB-02/01	16 Feb 2001	Bongo	43°18′	64°08′	5.20	15.8	59
OB-13/01	10 Nov 2001	Bongo	42°30′	62°30′	9.30	w/d	71
OB-13/01	11 Nov 2001	Bongo	42°50′	62°55′	9.36	w/d	71
OB-13/01	13 Nov 2001	Bongo	43°25′	64°49′	7.99	w/d	38

The modal number of myomeres (36–38; n=47) in *P. semifasciata* larvae matched the number of vertebrae reported for adults (36–37; n=50) by González (1998). The dorsal and anal fin elements reached their full complement by 9–10 mm BL, whereas the caudal-, pelvic-, and pectoral-fin elements were still incomplete in the size range analyzed in this study (3.3 to 11.7 mm BL). *Pseudopercis semifasciata* and *P. brasilianus* posttransition juveniles differ in their head shape, pigmentation pattern, and in the number of spines of the dorsal fin. The snout is larger in the Brazilian sandperch and the dorsal profile of the head is less convexly shaped than in *P. semifasciata*. These head shape differences increased with size. In *P. brasilianus*, the lateral stripes were less conspicuous than in *P. semifasciata*, and the vertical bars appeared earlier in the development (seven vertical bars were present in *ca.* 50 mm BL individuals). Furthermore, vertical bars in *P. semifasciata* were more defined at the base of the dorsal fin, whereas they extended below the midline in *P. brasilianus*. *Pseudopercis semifasciata* had five dorsal-fin spines, and *P. brasilianus* had seven spines, both in the range reported by Herrera and Cousseau (1996).

Both the epibenthic sampler and the "Piloto" trawl used to collect juveniles sample the fauna from the bottom to approximately one meter above the bottom. The fact that juveniles were caught in the lowest strata of the water column indicates that juveniles had settled to benthic habitat, even though the *P. semifasciata* posttransition juveniles still conserved some larval pigmentation, had not completely developed adult pigmentation pattern, and had already acquired morphological proportions similar to adults.

Even though the abundance and distribution data used in our study came from cruises that targeted other species, they provide satisfactory spatiotemporal coverage. This was particularly true for the ichthyoplancton surveys, which covered a great portion of the distributional area of *P. semifasciata* in the northern Patagonian shelf, mainly during the peak of the reproductive season (November–December). Among the Piloto positive stations (n=20), *P. brasilianus* was found by itself only at three stations. Also, *P. brasilianus* was far less abundant than *P. semifasciata* posttransition juveniles in the trawl samples. As a consequence, we consider that the abundance and distribution patterns of posttransition pinguipedid juveniles adequately reflect the abundance and distribution of *P. semifasciata* posttransition juveniles in the Argentine shelf.

The abundance and distribution of *P. semifasciata* larvae and posttransition juveniles indicate the presence of at least three main reproductive grounds, one

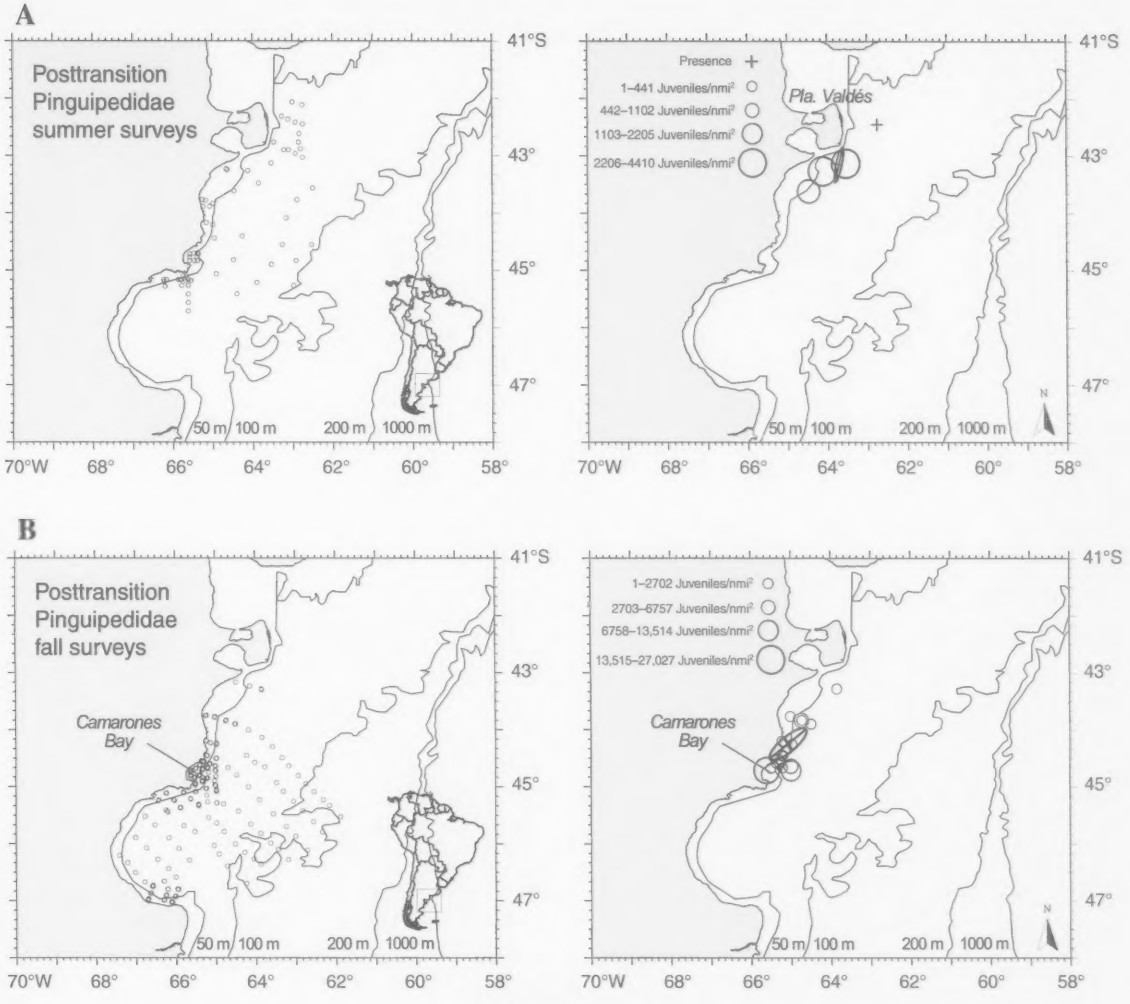

Figure 6

Distribution of "Piloto" or epibenthic sampler stations (left) and Pinguipedidae posttransition juveniles (right) in the Argentine Sea by season. (**A**) Summer surveys. (**B**) Fall surveys. Dot diameter, classified into four categories, is proportional to posttransition juvenile abundance at each station (expressed as no. of juveniles/nmi^2).

located off Peninsula Valdés (42–43°S, 63°W), another off the coast between Engaño Bay and Isla Escondida (43–44°S, 64°W to the coast), and the third off northeastern Camarones Bay (44–45°S, 65°W to the coast). These areas are linked to a frontal zone, the Northern Patagonia frontal system, which is highly productive during the spring and summer and could offer retention mechanisms for larvae (Bogazzi et al., in press). In December 1978, Argentine sandperches of both sexes were observed running near Isla Escondida (Ehrlich, personal observ.). In addition, Elías and Burgos (1988) reported great concentrations of Argentine sandperches off Península Valdés (42–44°S) between October and December, based on commercial fishery data for the period 1981–88. These reproductive grounds are consistent with the principal areas of summer concentration described by Otero et al. (1982). Furthermore, Elías and Burgos (1988) attributed the decline in yields and average size observed in January and February to the dispersal of postspawning individuals. However, initial results from an ongoing tag-recapture program in San José Gulf indicate that this species may have a high site fidelity and a limited dispersal (Venerus et al., 2003). In this case, the declines in yield and average size as the fishing season progresses could be a consequence of the fishing effort itself. Macchi et al. (1995) detected a decrease in the proportion of females in January, which also may imply an emigration from the reproductive sites.

Table 5

Positive stations for posttransition pinguipedids in the Argentine Sea, during 1992–2001. The "Species" column show the categories assigned in the survey reports. Underlined items in the "Abundance" column indicate that some or all of the specimens were preserved and at least one individual was correctly identified as *Pseudopercis semifasciata*. EBS= epibenthic sampler.

Cruise	Date	Season	Sampler	Lat. S	Long. W	Species	Abundance (individuals/nmi²)	Depth (m)
EH-02/92	18 Mar 1992	Summer	EBS	42°27′	62°45′	*Pseudopercis*	Presence	71
OB-02/01	14 Feb 2001	Summer	Piloto trawl	43°08′	63°32′	Both	4409.5	74
OB-02/01	16 Feb 2001	Summer	Piloto trawl	43°16′	64°07′	Pinguipedidae	2572.2	59
OB-02/01	17 Feb 2001	Summer	Piloto trawl	43°37′	64°28′	Pinguipedidae	1286.1	54
EH-04/98	07 Apr 1998	Fall	Piloto trawl	44°40′	65°13′	*Pseudopercis*	1492.6	74
EH-04/98	07 Apr 1998	Fall	Piloto trawl	44°43′	65°00′	*Pseudopercis*	10,204.1	79
EH-04/98	07 Apr 1998	Fall	Piloto trawl	44°38′	65°01′	*Pseudopercis*	4761.9	78
EH-04/98	07 Apr 1998	Fall	Piloto trawl	44°34′	65°20′	*Pseudopercis*	3448.3	52
EH-04/98	07 Apr 1998	Fall	Piloto trawl	44°28′	65°14′	*Pseudopercis*	1587.3	61
EH-04/99	28 May1999	Fall	Piloto trawl	44°12′	65°14′	*Pseudopercis*	1449.3	34
EH-04/99	28 May1999	Fall	Piloto trawl	43°50′	64°44′	*Pinguipes*	1315.8	64
EH-04/99	29 May1999	Fall	Piloto trawl	43°54′	64°30′	*Pinguipes*	1265.8	65
EH-04/99	29 May1999	Fall	Piloto trawl	43°17′	63°51′	*Pseudopercis*	1250.0	73
OB-05/00	11 Jun 2000	Fall	Piloto trawl	44°27′	65°13′	*Pinguipes*	2631.6	64
OB-05/00	11 Jun 2000	Fall	Piloto trawl	44°34′	65°19′	*Pseudopercis*	1250.0	58
OB-05/00	11 Jun 2000	Fall	Piloto trawl	44°41′	65°31′	*Pseudopercis*	1351.4	43
OB-05/00	11 Jun 2000	Fall	Piloto trawl	44°43′	65°37′	Both	27,027.0	38
OB-05/00	15 Jun 2000	Fall	Piloto trawl	44°15′	64°59′	*Pinguipes*	1449.3	72
OB-05/00	18 Jun 2000	Fall	Piloto trawl	43°50′	64°44′	Both	5194.8	59
OB-05/00	18 Jun 2000	Fall	Piloto trawl	43°46′	65°01′	*Pseudopercis*	1388.9	52

The low number of positive stations in spite of the intense sampling conducted within the area of distribution of *P. semifasciata* suggests a reduced spawning site. Both the area off Península Valdés and the one near Isla Escondida have rocky bottoms, which complicates trawling operations. A few experienced captains were able to target *P. semifasciata* by trawling along sandy corridors between rocky outcrops off Peninsula Valdés during the reproductive season (Elías[4]). Likewise, where running Argentine sandperches were observed near Isla Escondida, trawling is possible only in one orientation (Ehrlich, personal observ.). This could indicate that spawning grounds are associated with rocky outcrops. Spawning associated with rocky reefs and the existence of chromatic sexual dimorphism is compatible with Macchi et al.'s (1995) and González's (1998) suggestions of a complex mating system involving sexual courtship.

Spawning activity of *P. semifasciata* in northern Patagonia (42–44°S) peaks in November and December (Elías and Burgos, 1988; Macchi et al., 1995), and in October within San Matías Gulf (González, 1998). Maximum densities of larvae (>20 larvae/10 m^2 of sea surface) were found in December 1986, 1996, and 1999. The temperature at 10 m depth at positive ichthyoplankton stations varied between 12.3°C and 18.7°C. Such a wide range of temperature reflects the wide latitudinal range in the distribution of *P. semifasciata* and the extended time period (November–March) in which larvae were collected.

Posttransition pinguipedid juveniles were mainly collected at depths between 60 and 65 m, in both seasons sampled (summer and fall). A total of seven *P. semifasciata* juveniles ranging in total length from 66 to 82 mm were collected in fall (June), near the northern coast of San Matías Gulf (40°58′S–41°00′S; 64°18′W–64°24′W), at 29–54 m depth, associated with rib mussel beds (*Aulacomya ater*) (González[5]). Our distributional data indicate that settlement and nursery grounds could be located near shore. The absence of posttransition juveniles off northeast of Camarones Bay during summer and their presence in the fall could be a consequence of a delayed spawning pulse in the southern stocks. Some independent observations support this hypothesis: 1) back-calculations of hatching date based on daily growth increments from 19 post-

[4] Elías, I. 2004. Personal commun. Centro Nacional Patagónico, Puerto Madryn, Chubut, Argentina.

[5] González, R. A. C. 2004. Personal commun. Instituto de Biología Marina y Pesquera "Alte. Storni," San Antonio Oeste, Río Negro, Argentina.

transition juveniles collected in northeast Camarones Bay, between 43°50′S and 44°43′S, indicated birth dates between February and March (Venerus and Brown, 2003); 2) the collection of one *P. semifasciata* larva in San Jorge Gulf (46°30′S 67°18′W) on 30 March 1985; and 3) macroscopic observations of the ovaries from 24 mature females angled near Islas Blancas, Camarones Bay (ca. 44°46′S 65°38′W) on 26 and 27 January 2002, most of which (58.3%) were in the late developing stage (n=4) or in the gravid and running stage (n=10) (macroscopic maturation stages *sensu* González, 1998). This delayed spawning pulse in the southern stocks apparently follows the annual cycle of seawater warming on the Argentine shelf (Ciancio[6]). Similar delays have been reported for the Argentine hake (*Merluccius hubbsi*) (Pájaro and Macchi[7]; Machinandiarena et al.[8]).

Further investigations focused on the seasonal distribution of spawners are needed to confirm the existence of spawning aggregations indicated by the presence of larvae and posttransition juveniles. Mark-recapture and telemetry studies could be used to investigate the spatial dynamics of reproductive activity of this species in the Argentine Sea. Given the relative sedentary habits of adult Argentine sandperches, the use of reproductive refuges appear *a priori* to provide a suitable approach to protect this species.

Acknowledgments

We thank the crew and scientific staff on board for collecting the material. We also thank Atila Gosztonyi, Rául González, and two anonymous reviewers for providing useful comments on the manuscript. L.A.V. was supported by a fellowship from Consejo Nacional de Investigaciones Científicas y Técnicas (CONICET).

Literature cited

Bogazzi, E., A. Baldoni, A. Rivas, P. Martos, R. Reta, J. M. Orensanz, M. Lasta, and P. Dell'Arciprete.
In press. Spatial correspondence between areas of concentration of Patagonian scallop (*Zygochlamys patagonica*) and frontal systems in the Southwestern Atlantic. Fish. Oceanograph.

Cousseau, M. B., and R. G. Perrotta.
2000. Peces marinos de Argentina: Biología, distribución, pesca, 163 p. INIDEP, Mar del Plata, Buenos Aires, Argentina.

Elias, I., and G. Burgos.
1988. Edad y crecimiento del "salmón de mar," *Pseudopercis semifasciata* (Cuvier, 1829) (Osteichthyes, Pinguipedidae) en aguas norpatagónicas argentinas. Inv. Pesq. 52:533–548.

Elias, I., and C. R. Rajoy.
1992. Hábitos alimentarios del "salmón de mar" *Pseudopercis semifasciata* (Cuvier, 1829): Pinguipedidae en aguas norpatagónicas argentinas. Rev. Biol. Mar. 27:133–146.

Froese, R., and D. Pauly (eds.)
2004. Fishbase. World wide web electronic publication. www.fishbase.org. [Accessed April 2004].

Fulco, V. K.
1996. Aspectos ecológicos y pesqueros del "salmón de mar" *Pseudopercis semifasciata* (Cuvier, 1829) (Osteichthyes, Pinguipedidae) en aguas norpatagónicas. Licenciatura diss., 21 p. Facultad de Ciencias Naturales, Universidad Nacional de la Patagonia San Juan Bosco, Puerto Madryn, Chubut, Argentina.

Gaughan, D. J., F. J. Neira, L. E. Beckley, and I. C. Potter.
1990. Composition, seasonality and distribution of ichthyoplankton in the lower Swan Estuary, south-western Australia. Aust. J. Mar. Freshw. Res. 41:529–543.

González, R. A. C.
1998. Biología y explotación pesquera del salmón de mar *Pseudopercis semifasciata* (Cuvier, 1829) (Pinguipedidae) en el Golfo San Matías, Patagonia, Argentina. Ph.D. diss., 135 p. Universidad Nacional del Sur, Bahía Blanca, Buenos Aires, Argentina.
2002. Alimentación del salmón de mar *Pseudopercis semifasciata* (Cuvier, 1829) en el golfo San Matías. IBMP–Serie Publicaciones 1:14–21.

Herrera, M., and M. B. Cousseau.
1996. Comparación del esqueleto óseo de dos especies de peces de la familia Pinguipedidae. Nat. Patagon. (Cienc. Biol.) 4:95–110.

Houde, E. D., S. Almatar, J. C. Leak, and C. E. Dowd.
1986. Ichthyoplankton abundance and diversity in the Western Arabian Gulf. Kuwait Bull. Mar. Sci. 8:107–393.

Kendall Jr., A. W., and S. J. Picquelle.
1989. Egg and larval distributions of walleye pollock *Theragra chalcogramma* in the Shelikof Strait, Gulf of Alaska. Fish. Bull. 88:133–154.

Leis, J. M., and D. S. Rennis.
1983. The larvae of Indo-Pacific coral reef fishes, 269 p. New South Wales University Press, Sidney, Australia, and Univ. Hawaii Press, Honolulu, HI.
2000. Pinguipedidae—grubfishes, sandperches. *In* The larvae of Indo-Pacific coastal fishes: an identification guide to marine fish larvae (Fauna Malesiana Handbooks 2) (J. M. Leis and B. M. Carson-Ewart, eds.), p. 565–658. E. J. Brill, Leiden, The Netherlands.

Macchi, G. J., I. Elías, and G. E. Burgos.
1995. Histological observations on the reproductive cycle of the Argentinean sandperch, *Pseudopercis semifasciata* (Osteichthyes, Pinguipedidae). Sci. Mar. 59: 119–127.

Menezes, N. A., and J. L. Figuereido.
1985. Manual de peixes marinhos do sudeste do Brasil.

[6] Ciancio, J. 2004. Unpubl. data. Centro Nacional Patagónico, Puerto Madryn, Chubut, Argentina.

[7] Pájaro, M., and G. J. Macchi. 2001. Distribución espacial y estimación de la talla de primera maduración del stock patagónico de merluza (*Merluccius hubbsi*) en el período de puesta diciembre 2000–abril 2001. INIDEP Inf. Téc. Int. 100, 14 p. [Available from INIDEP: P.O. Box 175 (B7602HSA) Buenos. Aires, Argentina.]

[8] Machinandiarena, L., M. D. Ehrlich, D., Brown, M. Pájaro, and E. Leonarduzzi. 2004. Distribución y abundancia de huevos y larvas de merluza (*Merluccius hubbsi*) en el litoral norpatagónico. Período diciembre 2000 a marzo–abril 2001. Inf. Téc. Int. DNI-INIDEP 29, 16 p. [Available from INIDEP: P.O. Box 175 (B7602HSA) Beunos Aires, Argentina.]

V. Teleostei (4), 105 p. Mus. Zool. Univ. São Paulo, Brazil.

Neira, F. J.
1998. Pinguipedidae: sandperches, grubfishes *In* Larvae of temperate Australian fishes: Laboratory guide for larval fish identification (F. J. Neira, A. G. Miskiewicz, and T. Trnski, eds.), p. 362–365. Univ. Western Australia Press, Nedlands, Western Australia, Australia.

Neira, F. J., A. G. Miskiewicz, and T. Trnski. (eds.)
1998. Larvae of temperate Australian fishes. Laboratory guide for larval fish identification, 474 p. Univ. Western Australia Press, Nedlands, Western Australia.

Neira, F. J., I. C. Potter, and J. S. Bradley.
1992. Seasonal and spatial changes in the larval fish fauna within a large temperate Australian estuary. Mar. Biol. 112:1–16.

Nellen, W., and G. Hempel.
1969. Versuche zur Fängigkeit des "Hai" und des modifizierten Gulf-V-plankton-samplers "Nackthai. Meeresforsch. 20:141–154.

Otero, H., S. I. Bezzi, M. Renzi, and G. Verazay.
1982. Atlas de los recursos pesqueros demersales del Mar Argentino, 248 p. Contrib. INIDEP 423, Mar del Plata, Buenos Aires.

Potthoff, T.
1984. Clearing and staining techniques. *In* Ontogeny and systematics of fishes (G. Moser, W. J. Richards, D. M. Cohen, M. P. Fahay, A. W. Kendall, and S. L. Richardson, eds.), p. 35–37. Am. Soc. Ichthy. Herp., Spec. Publ. 1.

Rosa, I. L., and R. S. Rosa.
1997. Systematic revision of the South American species of Pinguipedidae (Teleostei, Trachinoidei). Revta. Bras. Zool. 14:845–865.

Rothlisberg, P. C., and W. G. Pearcy.
1976. An epibenthic sampler used to study the ontogeny of vertical migration of *Pandalus jordani* (Decapoda, Caridea). Fish. Bull. 74:994–998.

Smith, P. E., and S. L. Richardson.
1977. Standard techniques for pelagic fish egg and larva surveys. FAO Fish. Tech. Paper 175, 100 p.

Smith, P. E., W. C. Flerx, and R. P. Hewitt.
1985. The CalCOFI vertical egg tow (CalVET) net. *In* An egg production method for estimating spawning biomass of pelagic fish: application to the northern anchovy (*Engraulis mordax*) (R. Lasker, ed.), p. 27–33. NOAA Tech. Rep. NMFS 36.

Taylor, W. K. and G. C. Van Dyke.
1985. Revised procedures of staining and clearing small fishes and other vertebrates for bone and cartilage study. Cybium 9:107–119.

Vélez, J., W. Watson, and E. M. Sandknop.
2003. Larval development of the Pacific sandperch (*Prolatilus jugularis*) (Pisces: Pinguipedidae) from the Independencia Bight, Pisco, Peru. J. Mar. Biol. Assoc. UK 83:1137–1142.

Venerus, L. A., and D. Brown.
2003. Análisis de la microestructura de otolitos *lapilli* en juveniles de edad 0 del salmón de mar, *Pseudopercis semifasciata*. Abstracts of the V Jornadas Nacionales de Ciencias del Mar, Instituto Nacional de Investigación y Desarrollo Pesquero and Universidad Nacional de Mar del Plata, 8–12 Dec. 2003, p. 181. Mar del Plata, Buenos Aires, Argentina.

Venerus, L. A., A. M. Parma, and D. E. Galván.
2003. Dinámica espacial del salmón de mar, *Pseudopercis semifasciata*, en los arrecifes rocosos del golfo San José, Argentina. Resultados iniciales de un programa de marcación. Abstracts of the XXIII Congreso de Ciencias del Mar, Sociedad Chilena de Ciencias del Mar, 5–8 May 2003, p. 152. Sociedad Chilena de Ciencias del Mar and Universidad de Magallanes, Punta Arenas, Chile.

Vigliola, L., and M. Harmelin-Vivien.
2001. Post-settlement ontogeny in three Mediterranean reef fishes of the genus *Diplodus*. Bull. Mar. Sci. 68:271–286.

Watson, W., A. C. Matarese, and E. G. Stevens.
1984. Trachinoidea: development and relationships. *In* Ontogeny and systematics of fishes (G. Moser, W. J. Richards, D. M. Cohen, M. P. Fahay, A. W. Kendall, and S. L. Richardson, eds.), p. 554–561. Am. Soc. Ichthyol. Herpet. Spec. Publ. 1.

Geographic variation among age-0 walleye pollock (*Theragra chalcogramma*): evidence of mesoscale variation in nursery quality?*

Matthew T. Wilson
Annette L. Brown
Kathryn L. Mier

Alaska Fisheries Science Center
National Marine Fisheries Service, NOAA
7600 Sand Point Way, NE
Seattle, Washington 98115

E-mail address (for M. T. Wilson): matt.wilson@noaa.gov

Abstract—Nurseries play an important part in the production of marine fishes. Determining the relative importance of different nurseries in maintaining the parental population, however, can be difficult. In the western Gulf of Alaska, the Kodiak Island vicinity may be particularly well suited as a pollock nursery because of a prey-rich nearshore environment. Our objectives were 1) to examine age-0 pollock body condition, growth, and diet for evidence of a nearshore-shelf effect, and 2) to determine if variation in the potential prey field of zooplankton was associated with this effect. This was a pilot study that occurred in three bays and over the adjacent shelf off east Kodiak Island during 5–18 September 1993. Sampling occurred only during night at locations where echo sign indicated the presence of age-0 pollock. Echo sign was targeted to increase the chance of collecting fish given the limited vessel time. Fish condition was indicated by length-specific body weight. Growth rate indices were estimated for three different periods by using fish length-age data and daily otolith increment widths: 1) from hatching date to capture, 2) 1–5 d before capture, and 3) 6–10 d before capture. Fish diet was determined from gut content analysis. Considerable variation among areas was evident in zooplankton composition, and fish condition, growth, and diet. However, relatively high prey densities, as well as fish condition and growth rates indicated that Chiniak Bay was particularly well suited as a pollock nursery. Hatching-date distributions indicated that most of the age-0 walleye pollock from bays were spawned earlier than were those from the shelf. The benefit of being reared in nearshore areas is therefore realized more by individuals that were spawned early than by individuals spawned relatively late.

Manuscript submitted 20 November 2003 to the Scientific Editor's Office.

Manuscript approved for publication 16 September 2004 by the Scientific Editor.

Fish. Bull. 103:207–218 (2005).

The location of suitable fish nurseries has long been of interest to fishery scientists (Kendall and Duker, 1998). Such areas are a link in the chain of resources that sustain the productivity of a population and shape its evolution. Although the presence of juvenile fish in an area may indicate a nursery, relative importance among nursery areas ultimately depends on the number and reproductive fitness of reared individuals that contribute to the parental population. These qualities, however, are usually not measurable. Instead, we focus on measuring the size of juveniles, their body condition, diet, growth, and other characteristics that are accessible and relevant to fish survival. However, because these indices are not free of measurement error, it is advisable to consider more than one index (Suthers, 1998).

In the North Pacific Ocean, walleye pollock (*Theragra chalcogramma*) have adapted to the heterogeneity and productivity of coastal areas; they now support one of the world's most productive fisheries. Walleye pollock are a semidemersal gadid. Spawning typically occurs in mid-water during the spring at locations near, or over, the continental shelf (Kendall and Picquelle, 1989; Bailey et al., 1997). Fertilization is external. The eggs and larvae are pelagic, remaining in the plankton for *ca.* 4 months while they are dispersed over large areas. At 25–40 mm standard length (SL), larvae transform to juveniles (Brown et al., 2001) and become increasingly nektonic. Juveniles are referred to as "age-0" when they are between transition and 12-months old (40~130 mm SL, Brodeur and Wilson, 1996a). They are zooplanktivorous, feeding mostly on copepods and euphausiids, but other taxa sometimes dominate their diet (Brodeur and Wilson, 1996a). Age-0 juveniles commonly occur in various habitats from nearshore to the outer continental shelf (Nakatani and Maeda, 1987; Sobolevskiy et al., 1992; Carlson, 1995; Natsume and Sasaki, 1995; Brodeur and Wilson, 1996a; Wilson, 2000). Occasionally, they are found farther offshore (Tang et al., 1995), but probably in small numbers (Brodeur et al., 1999; Shida et al., 1999).

The early life stages of walleye pollock have been extensively studied in the Gulf of Alaska (GOA) (Kendall et al., 1996). In the Gulf, young pollock are most abundant in the western region (Brodeur and Wilson, 1996a). This region is naturally divided into two areas by the Shelikof Sea Valley, which cuts through the shelf at *ca.*156°N longitude (Fig. 1). To the east, the Kodiak vicinity includes the continental shelf around the Kodiak Island Archipelago. To the west, the lower Alaska Peninsula vicinity extends to Unimak Pass at the Peninsula's southwestern terminus. During the 1980s, age-0 abundance in the

* Contribution FOCI-0417 to NOAA's Fisheries-Oceanography Coordinated Investigations, 7600 Sand Point Way NE, Seattle, WA 98115.

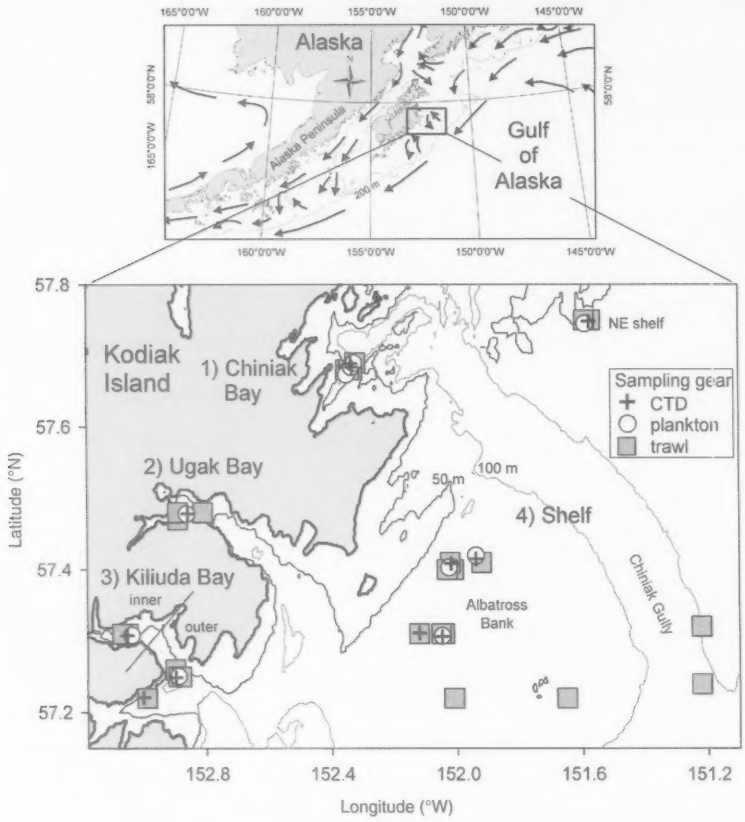

Figure 1

Location of sampling operations (CTD, plankton, and trawl) conducted during 5–18 September 1993, Kodiak Island, Alaska, to examine geographic variation among age-0 walleye pollock (*Theragra chalcogramma*). The ocean currents, shown as arrows on upper map, are adapted from Reed and Schumacher (1986).

Kodiak vicinity was related to the recruitment of pollock to the GOA fishery (Wilson, 2000). Furthermore, age-0 juveniles in this vicinity were large in comparison to those collected elsewhere (Wilson, 2000). The large size of the "Kodiak" juveniles may reflect faster growth (Bailey et al., 1996) due to a rich diet of euphausiids (Merati and Brodeur, 1996). In contrast, the diet of age-0 pollock along the Lower Peninsula was dominated by larvaceans (Merati and Brodeur, 1996). Interestingly, high densities of age-0 pollock were closer to shore in the Kodiak vicinity than along the Lower Peninsula where the shelf is relatively broad.

The apparent richness of the Kodiak Island vicinity may reflect its relative upstream position in the Alaska Coastal Current (ACC) (Fig. 1). Stabeno et al. (2004) integrated much research on the ACC to provide a comprehensive view of its importance in circulation over the GOA shelf. The ACC is wind driven and structured by seasonal influxes of fresh water. Flow is generally southwestward over the shelf but there is considerable topographic influence. For example, landmasses at the northern entrance to Shelikof Strait (Kennedy-Stevenson Entrance) allow only about 70% of the ACC water to enter the Strait. The remaining 30% of the water flows south around the northeastern end of the Kodiak Archipelago. This bifurcation of flow occurs in an area of vigorous tidal mixing and localized upwelling, both of which contribute to increased biological productivity. Off the northeastern Archipelago, Stabeno et al. (2004) have shown that the ACC follows bathymetric contours into and out of sea valleys, thus, providing some across-shelf movement of water. Advection of water was found by Coyle et al. (1990) to be important in the enhancement of zooplankton in Auke Bay, which is in the eastern GOA. Less is known about the exchange of water and zooplankton between the bays and fjords of the western GOA and the adjacent shelf. Thus, the ACC probably helps enrich the waters off northeastern

Kodiak Island, but we do not yet understand how this actually affects walleye pollock in nearshore nurseries.

In this article, we present information from a pilot study to better understand the environmental basis for the apparent richness of the Kodiak Island vicinity as a pollock nursery. Our objectives were 1) to examine age-0 pollock size, body condition, growth, and diet for evidence of geographic effect (nearshore versus shelf), and 2) to determine if their potential prey field (i.e., zooplankton) was associated with this effect.

Materials and methods

This study was conducted as an ancillary project during a research cruise off east Kodiak Island, 5–18 September 1993 (Fig. 1). In this area, the shelf is about 50 nmi wide and has an offshore bank (Albatross Bank) crossed by deep gullies (Barnabas and Chiniak gullies) extending from the slope to the coast. Bays form the upper reaches of these troughs and receive seasonal influxes of freshwater (Rogers et al.[1]). Over the shelf, net transport is southwestward (*ca.* 5 cm/s) (Stabeno et al., 1995). A boundary current, the Alaska Stream, exists farther offshore and flows rapidly to the southwest (Reed and Schumacher, 1986).

Sampling was conducted from the NOAA ship *Miller Freeman* (Fig. 1). Sampling occurred only at night to avoid complications of diel fish movement (Brodeur and Wilson, 1996b) and feeding patterns (Merati and Brodeur, 1996). A 38-kHz, Simrad-EK500 echo-sounder system was used to help guide our sampling to locations where age-0 pollock were likely present. The targeting of echo signs resulted in an irregular sample-location pattern and biased estimation of fish abundance; however, it focused our sampling at locations where age-0 pollock were likely present and thereby contributed to successful fish collections. Sampling was accomplished in four areas: Chiniak Bay, Ugak Bay, Kiliuda Bay, and over the adjacent shelf. All data analyses included these four areas as geographic strata; finer divisions (e.g., inner and outer Kiliuda Bay, and NE and Albatross Bank) were not possible given the available data and chosen analytical methods.

Age-0 pollock were obtained from the four areas with a bottom trawl and a midwater trawl (Wilson et al., 1996). The codend of each trawl was lined with a 3-mm mesh net. Towing speed averaged 4.5 k/h. Previous comparisons between these trawls indicated no significant difference with regard to estimation of age-0 pollock size or abundance (Brodeur and Wilson, 1996a; Wilson et al., 1996). Differences in the sampling effort used to collect each sample were corrected by dividing the age-0 catch by the volume filtered. Volume filtered was estimated by multiplying the distance fished (meters traveled while at depth) by the mouth opening of the trawl (m^2) (Wilson, 2000). Thus, age-0 catches are reported as number of fish per m^3.

Size composition of walleye pollock for each area was estimated by measuring the standard length (SL) of fresh age-0 pollock to the nearest millimeter. For large catches, a random subsample of about 300 individuals was used to represent the entire catch; otherwise, SL on every individual was measured. Length frequencies were expanded to the standardized catch estimates. Age-0 juveniles were clearly distinguishable from older pollock (<130 mm versus >150 mm SL) as indicated by Brodeur and Wilson (1996a). Random subsamples of age-0 pollock were also frozen at sea for subsequent determination of body condition, age, growth, and diet.

In the laboratory, length-specific weights of 776 age-0 pollock were used to examine area differences in body condition (Table 1). The fish were thawed within four months of collection. Excess water was blotted from each individual, and each specimen was measured to the nearest millimeter SL and weighed whole to the nearest 0.01 gram. Afterwards, each carcass was stored in 95% ethanol for eventual gut content analysis. Lengths and somatic weights, obtained from the subset of fish used in the gut analysis, were also analyzed to verify that geographic differences in condition were not dependent on whole versus somatic weight.

Growth rate was estimated for 128 individuals by using fish length and age data. Age, in days, was estimated as the number of daily increments visible in the microstructure of sagittal otoliths following Brown and Bailey (1992). Length-age relationships were examined for evidence of an area effect on growth rates integrated over the period from hatching to capture. We used these relationships to convert the length composition for each sample to a hatching-date distribution, and by summing across samples we then obtained area-specific hatching-date distributions.

To estimate growth rate realized near the point of capture we measured the width of recent daily otolith increments. Following Bailey (1989), we measured the width of the two outermost, nonoverlapping 5-increment bands on each of 97 sagittal otoliths. These widths were assumed to relate directly to body growth during the first (1–5 days) and second (6–10 days) 5-d periods before capture, and that the increments were deposited while individuals were near the point of capture. Thus, growth rate indices were obtained for three different periods: 1) hatching date to capture date, 2) 1–5 days before capture, and 3) 6–10 days before capture.

Gut content analysis was conducted on 300 individuals according to the method of Merati and Brodeur (1996) to determine feeding intensity and taxonomic composition of age-0 prey. No more than 15 fish per sample were examined. Each fish was measured (SL), blotted dry, and weighed immediately prior to dissection. Stomachs were excised between the esophagus and

[1] Rogers, D. E., D. J. Rabin, B. J. Rogers, K. J. Garrison, and M. E. Wangerin. 1979. Seasonal composition and food web relationships of marine organisms in the nearshore zone of Kodiak Island—including ichthyoplankton, meroplankton (shellfish), zooplankton, and fish. Annual rep. OCSEAP RU553, FRI-UW-7925, 291 p. Fish. Res. Inst., Univ. Washington, Seattle, WA.

Table 1

Number of age-0 walleye pollock (*Theragra chalcogramma*) collected near Kodiak Island, Alaska, September 1993, measured for standard length, and examined in the laboratory to estimate condition, growth, and the weight and taxonomic composition of stomach contents. Sample is the number of trawl hauls.

		At-sea collections (no. of fish)		Laboratory examinations (no. of fish)					
				Condition		Growth			
							Band width		Evaluated for gut content weight and composition
Location	Sample (n)	Caught	Measured for SL	whole[1] wt.	somatic[2] wt.	Age	1–5[3]	6–10[4]	
Chiniak Bay	7	1858	709	223	75	23	17	17	75
Ugak Bay	4	2506	773	218	91	28	12	12	91
Kiliuda Bay	7	562	279	165	66	41	33	33	66
Shelf	14	358	358	170	68	36	35	35	65
All combined	32	5284	2119	776	300	128	97	97	297

[1] Whole wet weights from thawed fish.
[2] Somatic wet weights from fish preserved in 95% ethanol after freezing at sea.
[3] Collective width of daily otolith increments 1–5; numbering begins with the most peripheral increment.
[4] Collective width of daily otolith increments 6–10.

pylorus. Gut contents were dissected from the specimens and weighed to the nearest 0.001 gram. Somatic weight represented whole wet weight minus the gut content weight. Three fish were omitted from further consideration because of apparent regurgitation. Taxonomic composition of age-0 diets was determined by counting the organisms in the gut after sorting them into broad taxonomic groups.

Zooplankton was collected by using a 1-m Tucker net (333-μm mesh) to sample where age-0 pollock had been collected. The net was fished through acoustic echo layers believed to be age-0 pollock in order to characterize their immediate prey field. Potential prey items were sorted into broad taxonomic groups and enumerated at the Polish Plankton and Identification Center, Szezcin, Poland.

Temperature and salinity profiles (near surface to 10 m off bottom) were obtained by using a Seabird SBE-911+ CTD system. Profile data were collected during deployment at a descent rate of ca. 0.5 m/s.

Statistically significant differences in age-0 condition, growth, and feeding intensity among geographic areas were detected with split-plot analysis of covariance (ANCOVA) and *post hoc* multiple comparison tests (Proc Mixed, SAS software, Littell et al., 1996). The covariates were fish length or age (days since hatching). Following Milliken and Johnson (2002), we first tested for covariate significance (H_0: all slopes=0) and homogeneity of slopes (H_0: equal slopes) to ensure appropriateness of the following reduced, common-slope model:

$$Y = \alpha + \beta x_{ij} + Area_j + Sample_i\{Area_j\} + e_{ijk},$$

where Y = dependent variable;
α = intercept parameter;
β = slope parameter;
x_{ij} = covariate for sample i and area j; and
e_{ijk} = replicate error for sample i, area j, and fish k.

A split-plot design was necessary to account for the nesting of samples (trawl catches) within area, and individuals within sample. To avoid pseudoreplication, trawl catch was the sampling unit instead of individual fish. Area was a fixed effect; sample was a random effect. For body condition, lengths and weights were $\log_e$-transformed according to the method of Patterson (1992); two points were omitted because of suspiciously low length-specific, whole-body weight. For feeding intensity, gut content weights (GCW) were fourth-root transformed ($GCW^{0.25}$) to linearize the GCW-length relationship and remove heteroscedasticity (Clarke and Warwick, 2001). Significance of *post hoc* pairwise differences was based on a Bonferroni-corrected, 0.05-level of significance. The standardized catch data were not incorporated into these tests; therefore the conclusions pertain to the samples not weighted by catch.

Nonmetric multidimensional scaling (NMS, PC-Ord, McCune and Mefford, 1999) was used to ordinate the diet and plankton samples according to taxonomic composition. Each diet sample represented the average numerical composition of the diet of all fish in the sample. This value was calculated by dividing the sum of all items within each taxonomic category by the number of fish in the sample. The ordinations, one for diet and another for plankton, were based on Bray-Curtis similarity coefficients of fourth root-transformed data. Differences among the four areas were statistically tested by using a two-way nested analysis of similarity

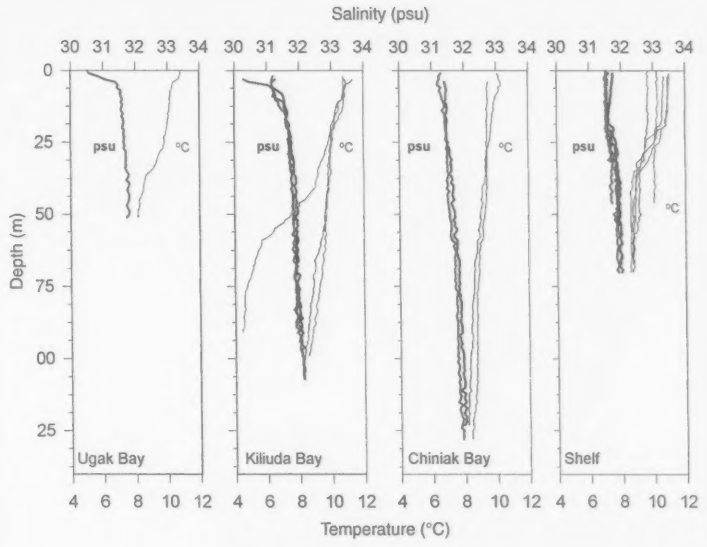

Figure 2

Water salinity and temperature profiles obtained in 10 casts at locations where age-0 walleye pollock (*Theragra chalcogramma*) were collected near Kodiak Island, Alaska, during 5–18 September 1993.

(ANOSIM, PRIMER, Clarke and Warwick, 2001) applied to the Bray-Curtis similarity matrices.

Results

Overall, salinity ranged from 30.3 to 33.0 ppt, and water temperature ranged from 4.4 to 11.3°C (Fig. 2). Shallow surface layers of relatively fresh water were evident from low near-surface salinities in Ugak Bay and in the inner part of Kiliuda Bay. This part of Kiliuda Bay was also well stratified thermally. Unfortunately, it was not possible to include inner Kiliuda Bay as a fifth area in subsequent statistical analyses because of insufficient sampling. Thermal stratification was also evident at shelf sampling locations.

A total of 5284 age-0 pollock were collected in 25 of the 32 successful trawl hauls (Table 1). These fish were absent only at the four most-offshore locations over Albatross Bank and Chiniak Gully (Fig. 3). In addition, no age-0 pollock were caught in shallow (<35-m depth) tows at locations on Albatross Bank; a dense and expansive school of capelin (*Mallotus villosus*) may have displaced them downward. Median age-0 density was 0.0006 fish/m^3; the maximum (0.095 fish/m^3) was found in Ugak Bay.

Standard lengths of 2119 age-0 pollock ranged from 25 to 121 mm SL (Table 1, Fig. 4). The fish in Chiniak Bay (91 mm SL), Ugak Bay (90 mm SL), and Kiliuda Bay (89 mm SL) all had a median SL that were larger than the median length of fish collected over the shelf (71 mm SL). A surprising number of individuals <50 mm SL were collected in Ugak Bay and inner Kiliuda Bay.

Body condition, based on the reduced, common-slope ANCOVA model, varied among the four areas (Table 2). Because of this effect, area-specific equations were used to describe the length-weight relationship (Table 3, Fig. 5A). After accounting for differences in length, we found that fish from the shelf weighed less than the individuals collected in Chiniak Bay and Ugak Bay. Individuals from Kiliuda Bay were intermediate in weight, differing only from the Ugak Bay fish (Table 4). Similar conclusions from the somatic-weight data of fish used in the diet examinations indicated that gut-content weight was not responsible for the relatively low length-specific weights of fish from Kiliuda Bay and the shelf (Tables 2 and 4).

The fish age-length relationship also varied by area. The relationship was described by using a reduced, common-slope model (Table 2). The common slope was 0.78 mm/d (Table 3, Fig. 5B). Differences in line elevation, or age-specific length, indicated that fish from the shelf grew more slowly during the hatch-to-capture period than did the fish from Chiniak or Kiliuda bays (Table 4). Applying these equations to the length data resulted in hatching-date distributions that ranged from mid March to mid July (Fig.6). The fish collected in Chiniak Bay (17 April), Kiliuda Bay (20 April), and Ugak Bay (25 April) all had earlier median hatching

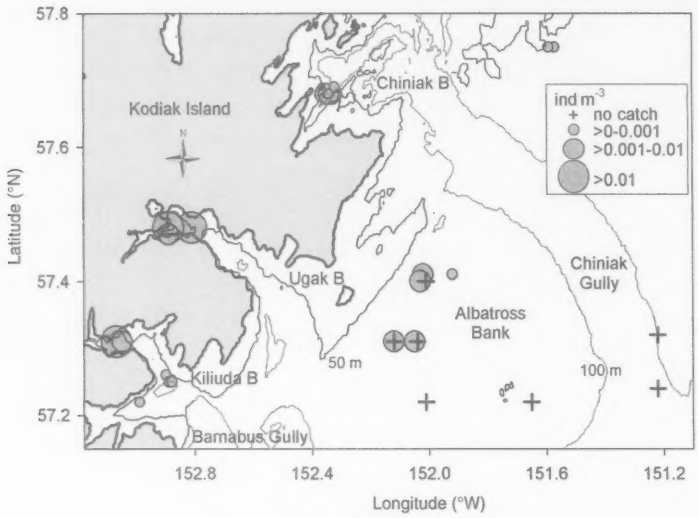

Figure 3

Geographic distribution of standardized catches (no. of individuals/m^3) of age-0 walleye pollock (*Theragra chalcogramma*) collected in trawl hauls conducted near Kodiak Island during 5–18 September 1993.

dates in comparison to fish from the shelf (8 May). Interestingly, the hatching dates of the cohort of small individuals from Ugak Bay and inner Kiliuda Bay ranged from June to July.

Mean otolith increment width varied with area. It was not necessary to include fish length as a covariate (Table 2). For the 1–5 d precatch period, the large mean increment width associated with fish from Chiniak Bay (0.036-mm band width) was different from the means of each other area (Table 4). The only other difference was between the Kiliuda Bay (0.026 mm) and shelf (0.030 mm) areas. The only difference for the 6–10 d precatch period was again between the Kiliuda Bay (0.029 mm) and shelf (0.036 mm) areas.

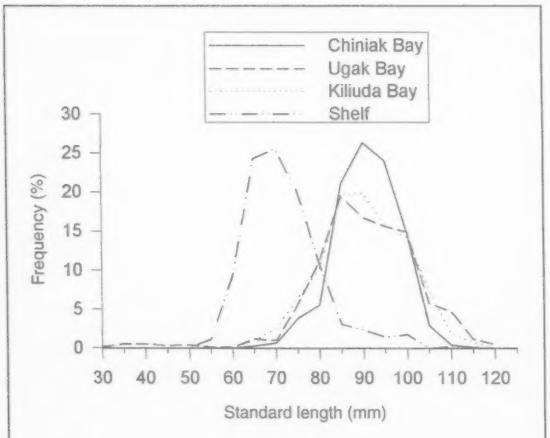

Figure 4

Size composition (mm SL) of age-0 walleye pollock (*Theragra chalcogramma*) by area from samples collected near Kodiak Island, 5–18 September 1993.

No area effect on gut content weight (GCW) was detected (Table 2). There was, however, a significant fish length effect (Fig. 5C), and this was incorporated in the final model (Table 3). After adjusting for length, area-specific mean GCW agreed in rank with area-specific fish weight (Table 4).

Differences in taxonomic composition of age-0 pollock diets resulted in a good separation of samples by area (Fig. 7A, ANOSIM, R=0.533, P=0.001). Each pair-wise comparison of areas resulted in a significant difference (P<0.05) (the one sample of small fish from Kiliuda Bay, and two samples from the shelf of fish with empty stomachs were omitted from the ANOSIM). The diet of fish from Ugak Bay and Kiliuda Bay were mostly crab larvae or copepods, depending on fish size (Table 5A). Over the shelf, fish diets comprised mostly euphausiids (74%). In contrast, fish from Chiniak Bay had a much more varied diet; no single prey category exceeded 40% of the items per stomach. Note the correspondence between the number of prey per fish (Table 5A) and mean gut-content weight (Table 4); both were lowest for fish from the shelf.

Differences in taxonomic composition also resulted in separation of the plankton samples by area (Fig. 7B, ANOSIM, R=0.886, P=0.001). Pair-wise comparisons indicated a difference between Chiniak Bay and the shelf (R=0.813, P=0.029). Ugak Bay was not included in the comparisons because only one sample was avail-

Table 2

Summary results of six ANCOVA tests of an area effect on six dependent variables obtained from laboratory analysis of age-0 pollock: body condition (whole or somatic weight), three indices of growth, and gut content weight. NDF and DDF are numerator and denominator degrees of freedom for the *F* test, respectively.

Dependent variable	H_0: all slopes = 0	*Ho*: equal slopes	Reduced model				
			Source	NDF	DDF	Type III *F*	*P* > *F*
Condition							
whole weight	*P*=0.0001	*P*=0.3340	Area	3	14.2	6.81	0.0045
			ln(SL)	1	769	105824	0.0001
somatic weight	*P*=0.0001	*P*=0.3115	Area	3	17.8	10.01	0.0004
			ln(SL)	1	294	31000	0.0001
Growth							
age-specific length	*P*=0.0001	*P*=0.4140	Area	3	4.3	14.43	0.0106
			Age	1	117	475.39	0.0001
1–5 d band width	*P*=0.2645		Area	3	93	8.05	0.0001
6–10 d band width	*P*=0.2267		Area	3	5.76	3.89	0.0768
Gut content weight	*P*=0.0001	*P*=0.7208	Area	3	16.2	0.36	0.7850
			SL	1	285	201.99	0.0001

able. Copepods dominated the catches in Chiniak Bay and over the shelf, whereas larval crabs were most prevalent in the Ugak and Kiliuda samples (Table 5B). In terms of overall abundance, mean prey densities were lowest among samples collected from the shelf and highest for the Chiniak Bay samples.

Table 3

Least-squares linear relationships used to describe the condition, growth, and feeding intensity of age-0 walleye pollock collected September 1993, Kodiak Island, Alaska. GCW = gut content weight.

Relationship	Location	Equation
Condition		
whole weight	Chiniak Bay	$\ln(g) = 3.228(\ln SL\text{mm}) - 12.646$
	Ugak Bay	$\ln(g) = 3.228(\ln SL\text{mm}) - 12.609$
	Kiliuda Bay	$\ln(g) = 3.228(\ln SL\text{mm}) - 12.659$
	Shelf	$\ln(g) = 3.228(\ln SL\text{mm}) - 12.698$
somatic weight	Chiniak Bay	$\ln(g) = 3.127(\ln SL\text{mm}) - 12.708$
	Ugak Bay	$\ln(g) = 3.127(\ln SL\text{mm}) - 12.702$
	Kiliuda By	$\ln(g) = 3.127(\ln SL\text{mm}) - 12.774$
	Shelf	$\ln(g) = 3.127(\ln SL\text{mm}) - 12.816$
Growth		
length-at-age	Chiniak Bay	$\text{age}(d) = 0.782(SL\text{mm}) - 22.294$
	Ugak Bay	$\text{age}(d) = 0.782(SL\text{mm}) - 26.928$
	Kiliuda Bay	$\text{age}(d) = 0.782(SL\text{mm}) - 21.346$
	Shelf	$\text{age}(d) = 0.782(SL\text{mm}) - 31.011$
Gut content weight		
	All combined	$\text{GCW}(g^{0.25}) = 0.007(SL\text{mm}) - 0.192$

Discussion

The presence of age-0 pollock in bays and over the inner shelf, but not over the outer shelf, indicates that the principal pollock nursery off east Kodiak Island during autumn is relatively close to shore. Earlier studies of age-0 pollock in the western GOA focused on nearshore areas (Smith et al., 1984; Wilson, 2000) and did not document the absence of age-0 pollock over the outer shelf. Our results point to prey resource as a likely explanation for the observed distribution of and differences among age-0 walleye pollock.

Seasonal declines in zooplankton density underscore the importance of nearshore areas as pollock nurseries. Rogers et al.[1] and Kendall et al.[2] observed an order-of-magnitude autumnal decline in prey[3] density off Kodiak Island during 1977–79 (Fig. 8). This decline was accompanied by a shoreward shift in the region of highest eu-

[2] Kendall, A. W., Jr., J. R. Dunn, R. J. Wolotira Jr., J. H. Bowerman Jr., D. B. Dey, A. C. Matarese, and J. E. Munk. 1980. Zooplankton, including ichthyoplankton and decapod larvae, of the Kodiak shelf. NOAA NWAFC proc. rep. 80-8, 393 p. Alaska Fishery Science Center, Seattle, WA.

[3] All invertebrate zooplankters are considered potential age-0 pollock prey except cnidarians, ctenophores, siphonophores, and larval shrimps and crabs. Shrimp and crab were omitted from Figure 8 because density estimates were not available separately for the shelf and slope regions.

phausiid density. Similar to our findings, the estimates of larval crab densities from Rogers et al.'s and Kendall et al.'s studies were always highest in bays. In autumn, the larger zooplankters are of principal importance to age-0 pollock because of size-related changes in diet (Table 5A, Merati and Brodeur, 1996).

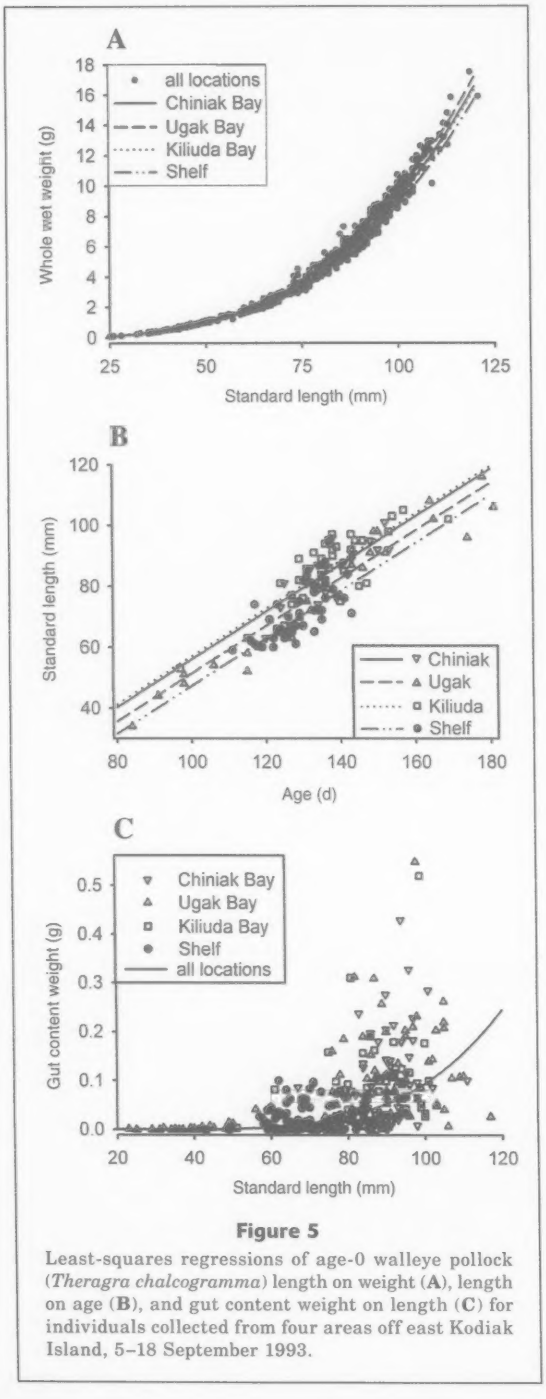

Figure 5

Least-squares regressions of age-0 walleye pollock (*Theragra chalcogramma*) length on weight (**A**), length on age (**B**), and gut content weight on length (**C**) for individuals collected from four areas off east Kodiak Island, 5–18 September 1993.

By all accounts, age-0 pollock collected from Chiniak Bay fared as well or better than individuals in each of the other areas sampled. Wilson (2000) found that the density of age-0 pollock in the Chiniak Bay vicinity predicted Gulf-wide recruitment. However, these fish represent a minuscule part of the Gulf-wide population of age-0 pollock. Even if two cohorts, from spring- and summer-spawnings, were produced, it seems unreasonable to expect that local production would dramatically affect gulf-wide recruitment. Alternatively, the abundance and condition of age-0 pollock in this vicinity might reflect larger-scale processes that relate to gulf-wide recruitment. Identifying large-scale processes based on small-scale sampling, however, is complicated by variation at high spatial and temporal frequencies. For example, the relatively high density of pea crab (*Fabia subquadrata*) megalopae in combination with influxes of freshwater (Epifanio, 1988) indicate that local dynamics are important in sustaining prey populations in Ugak and Kiliuda bays. In contrast, Chiniak Bay might be more affected by influxes of oceanic prey. Such influxes could be facilitated by cross-shelf sea valleys, which extend into all the fjords that we sampled. Indeed, Kendall et al.,[2] Lagerloef (1983), and Stabeno et al. (2004) have all shown that the local sea valleys induce cross-shelf flow in the ACC. Furthermore, Inzce et al. (1997) found that zooplankton density was elevated in the Shelikof Sea Valley above the density found at adjacent shelf areas; a similar phenomenon, however, was not observed off northeastern Kodiak Island (Kendall et al.[2]). Compared to the other bays, Chiniak Bay might be best positioned to receive enriched ACC water that flows south from where it bifurcates at the entrance to Shelikof Strait. Such enriched water may also be an important transport mechanism for immigrating larval and juvenile pollock (Wilson, 2000).

Because of the inconsistency among our various indices (i.e., weight-at-length, length-at-age, otolith increment width), it is difficult to conclude that fish over the shelf and in Ugak and Kiliuda bays were prey limited. Over the shelf, recent growth rates were not low despite relatively small individual size and low prey density. For example, the low prey densities and small fish sizes over the shelf contrasted with recent fish growth that was not low. Age-0 pollock are capable of social foraging behavior to compensate for food scarcity (Ryer and Olla, 1992), but it is unclear that the associated energetic cost (Ryer and Olla, 1997) would depress body weight before slowing otolith growth. In contrast, fish in Kiliuda Bay had relatively slow recent growth and low body weight, but age-specific length was large. The observed differences in age-specific length are somewhat discounted by the fact that such differences may have arisen any time after hatching and are not necessarily indicative of recent differences in growth. Another complication was our inability to reconstruct the spatial history of the sampled fish;

Table 4

Least-squares adjusted means of indices of body condition, growth, and gut content weight (GCW) of age-0 walleye pollock collected September 1993, Kodiak Island, Alaska. Means sharing the same superscript letter are not different (*post hoc* multiple comparison tests, $P>0.05$).

	Condition		Growth			
Location	whole wt. (ln *g*)	somatic wt. (ln *g*)	age-specific SL (mm)	1–5 d band width (mm)	6–10 d band width (mm)	GCW ($g^{0.25}$)
Chiniak Bay	1.47^{ab}	0.82^{a}	82.3^{a}	0.036^{a}	0.033^{ab}	0.40
Ugak Bay	1.50^{b}	0.83^{a}	77.6^{ab}	0.027^{bc}	0.032^{ab}	0.43
Kiliuda Bay	1.45^{ac}	0.76^{b}	83.2^{a}	0.026^{b}	0.029^{a}	0.39
Shelf	1.42^{c}	0.72^{b}	73.6^{b}	0.030^{c}	0.036^{b}	0.36

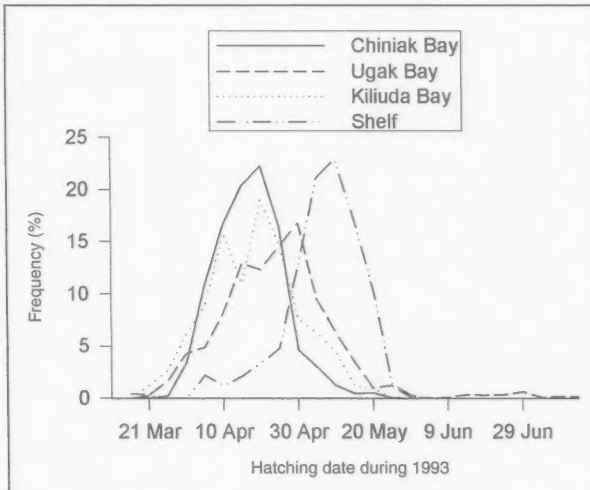

Figure 6

Hatching-date composition of age-0 walleye pollock (*Theragra chalcogramma*) by area from samples collected near Kodiak Island, 5–18 September 1993.

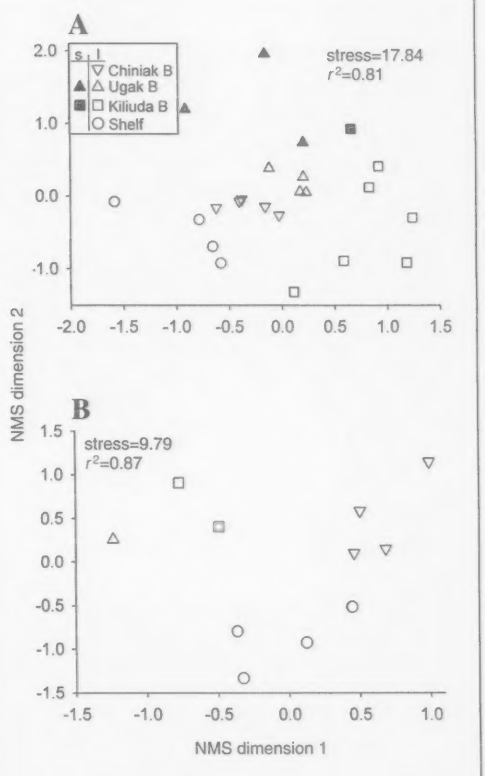

Figure 7

Nonmetric multidimensional scaling (NMS) of samples based on age-0 walleye pollock (*Theragra chalcogramma*) diet composition (**A**), or zooplankton composition (**B**). Symbols indicate four different sampling areas. For diet, the small (<66 mm SL) fish in bays are represented by filled symbols.

in other words, we did not know where they had been prior to capture.

As evidenced by geographic variation in hatching-date distributions, cohort-specific differences persisted well into the juvenile stage and had important implications for inter-cohort differences in survival. The median hatching dates of fish in bays were similar to those estimated for north Kodiak Island by Brown and Bailey (1992). In contrast, fish over the shelf had substantially later hatching dates. There is little evidence of pollock spawning within our study area; therefore it seems likely that the differences in hatching dates reflect successive immigration of sequential cohorts. However, the presence of the youngest cohort, fish hatched during

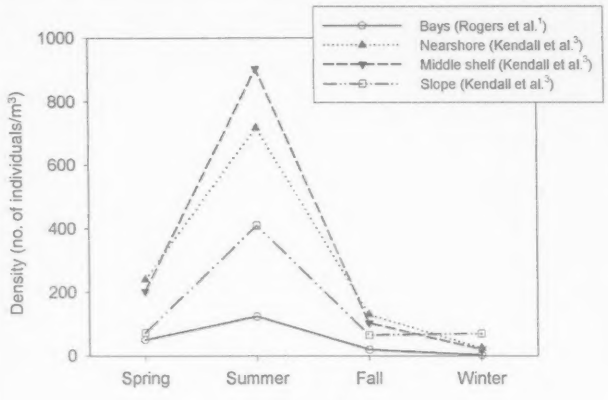

Figure 8

Seasonal variability in densities (no. of individuals/m^3) of invertebrate zooplankton near Kodiak Island based on samples collected with 60-cm bongo nets with 0.333-mm mesh (modified from Rogers et al.[1], Kendall et al.[2]).

June and July, only in the innermost parts of Kiliuda Bay and Ugak Bay, may indicate an alternative mechanism such as local spawning and geographic differences in retention. Regardless, the relationship between fish size and hatching date indicates that large individuals were spawned early; thus, early spawned individuals might experience higher overwinter survival, which often increases with fish size (Sogard, 1997).

We chose to track echo sign in our study to reduce the sampling effort expended in areas devoid of age-0 pollock. This method maximized our chance of collecting the samples needed to study differences among age-0 pollock given the limited vessel time. Unfortunately, this method also introduced a bias, thereby reducing the utility of density estimates to indicate habitat suitability (Brown et al., 2000; Stoner et al., 2001) and to extrapolate from samples to at-sea populations. Our focus, however, was on other measures that might eventually provide a

Table 5

Numerical composition of age-0 pollock diet by location and predator SL (**A**), and composition of the plankton in 1-m^2 Tucker samples (**B**) concurrently collected during 5–18 September 1993, Kodiak Island, Alaska. "t" signifies trace (<0.05).

A			Prey (number of individuals/fish)[1]								
Area	Sample (n)	no. of fish	amphipod	chaetognath	copepod	crab larvae	cumacean	euphausiid	mysid	shrimp larvae	No. of prey/ fish
Chiniak Bay	5	75	2.8	t	4.1	0.1	0.0	3.7	0.4	t	11.0
Ugak Bay											
≤66 mm	3	31	0.1	0.6	11.2	0.6	0.0	0.1	t	0.0	12.6
>66 mm	4	60	0.1	t	5.9	15.9	t	3.3	0.2	t	25.6
Kiliuda Bay											
≤66 mm	1	5	0.0	0.2	2.2	1.0	0.0	0.2	0.0	0.0	3.6
>66 mm	6	61	t	t	t	6.4	t	2.7	t	t	9.2
Shelf	6	65	0.3	0.0	0.1	0.1	t	2.8	0.4	0.1	3.8

[1] $0<t<0.05$.

B			Zooplankton (number of individuals/m^3)[1]								
Area	Sample (n)	amphipod	chaetognath	copepod	crab larvae	euphausiid	fish larva	larvacean	mysid	shrimp larvae	total no./ m^3
Chiniak Bay	4	t	9	332	1	23	t	4	2	4	375
Ugak Bay	1	t	13	12	48	2	t	3	1	t	80
Kiliuda Bay	2	t	13	40	82	28	t	17	4	3	188
Shelf	4	t	1	51	1	4	t	15	t	2	74

[1] $0<t<0.05$. In zooplankton samples, cumaceans were not enumerated.

useful supplement to abundance distribution data (Beutel et al., 1999).

This study enabled us to conclude that Chiniak Bay is particularly well suited for rearing pollock probably because of influxes of zooplankton. It remains to be seen if Chiniak Bay contributes relatively high numbers of recruits, or if other counteracting factors such as predation exist. Nevertheless, we have demonstrated that differences among juvenile pollock exist at mesogeographic scales and that these differences are useful for inferring how specific areas might relate to the population dynamics of walleye pollock.

Acknowledgments

R. Brodeur provided the initial impetus for this study. P. Munro and D. Somerton accommodated our request to share ship time. The captain and crew of the NOAA ship *Miller Freeman* helped make our at-sea operations efficient and pleasurable. M. Busby assisted with field operations. We gratefully appreciate the comments of many people: K. Bailey, J. Napp, A. Stoner, S. Syrjala, N. Bartoo, the AFSC Publications Unit, and several anonymous reviewers.

Literature cited

Bailey, K. M.
1989. Interaction between the vertical distribution of juvenile walleye pollock *Theragra chalcogramma* in the eastern Bering Sea, and cannibalism. Mar. Ecol. Prog. Ser. 53:205–213.

Bailey, K. M., A. L. Brown, M. M. Yoklavich, and K. L. Mier.
1996. Interannual variability in growth of larval and juvenile walleye pollock, *Theragra chalcogramma*, in the western Gulf of Alaska, 1983–91. Fish. Oceanogr. 5(suppl. 1):137–147.

Bailey, K. M., P. J. Stabeno, and D. A. Powers.
1997. The role of larval retention and transport features in mortality and potential gene flow of walleye pollock. J. Fish. Biol. 51(suppl. A):135–154.

Beutel, T. S., R. J. S. Beeton, and G. S. Baxter.
1999. Building better wildlife-habitat models. Ecography 22(2):219–223.

Brodeur, R. D., and M. T. Wilson.
1996a. A review of the distribution, ecology and population dynamics of age-0 walleye pollock in the Gulf of Alaska. Fish. Oceanogr. 5 (suppl. 1):148–166.

Brodeur, R. D., and M. T. Wilson.
1996b. Mesoscale acoustic patterns of juvenile walleye pollock (*Theragra chalcogramma*) in the western Gulf of Alaska. Can. J. Fish. Aquat. Sci. 53(9):1951–1963.

Brodeur, R. D., M. T. Wilson, G. E. Walters, and I. V. Melnikov.
1999. Forage fishes in the Bering Sea: distribution, species associations, and biomass trends. *In* Dynamics of the Bering Sea (T. R. Loughlin, K. Ohtani, eds.), p. 509–536. Univ. Alaska Sea Grant, Fairbanks, AK.

Brown, A. L., and K. M. Bailey.
1992. Otolith analysis of juvenile walleye pollock *Theragra chalcogramma* from the western Gulf of Alaska. Mar. Biol. 112:23–30.

Brown, A. L., M. S. Busby, and K. L. Mier.
2001. Walleye pollock *Theragra chalcogramma* during transformation from the larval to juvenle stage: otolith and osteological development. Mar. Biol. 139: 845–851.

Brown, S. K., K. R. Buja, S. H. Jury, M. E. Monaco, and A. Banner.
2000. Habitat suitability index models for eight fish and invertebrate species in Casco and Sheepscot Bays, Maine. N. Am. J. Fish. Manag. 20:408–435.

Carlson, H. R.
1995. Consistent yearly appearance of age-0 walleye pollock, *Theragra chalcogramma*, at a coastal site in southeastern Alaska, 1973–1994. Fish. Bull. 93(2): 386–390.

Clarke, K. R., and R. M. Warwick.
2001. Change in marine communities: an approach to statistical analysis and interpretation, 2nd ed., 87 p. PRIMER-E, Plymouth, Cornwall, U.K.

Coyle, K. O., A. J. Paul, and D. A. Zieman.
1990. Copepod populations during the spring bloom in an Alaskan subarctic embayment. J. Plank. Res. 12(4):759–797.

Epifanio, C. E.
1988. Transport of invertebrate larvae between estuaries and the continental shelf. *In* Larval fish and shellfish transport through inlets (M. P. Weinstein, ed.), p. 104-114. Am. Fish. Soc. Symp. 3, Bethesda, MD.

Incze, L. S., D. W. Siefert, and J. M. Napp.
1997. Mesozooplankton of Shelikof Strait, Alaska: abundance and community composition. Cont. Shelf Res. 17(3):287–305.

Kendall, A. W., Jr., and G. J. Duker.
1998. The development of recruitment fisheries oceanography in the United States. Fish. Oceanog. 7(2): 69–88.

Kendall, A. W. Jr., and S. J. Picquelle.
1989. Egg and larval distributions of walleye pollock *Theragra chalcogramma* in Shelikof Strait, Gulf of Alaska. Fish. Bull. 88:133–154.

Kendall, A. W. Jr., J. D. Schumacher, and S. Kim.
1996. Walleye pollock recruitment in Shelikof Strait: applied fisheries oceanography. Fish. Oceanogr. 5(suppl. 1):4–18.

Lagerloef, G.
1983. Topographically controlled flow around a deep trough transecting the shelf off Kodiak Island, Alaska. J. Phys. Oceanogr. 13:139–146.

Littell, R. C., G. A. Milliken, W. W. Stroup, and R. D. Wolfinger.
1996. SAS System for mixed models, 633 p. SAS Institute Inc., Cary, NC.

McCune B., and M. J. Mefford.
1999. PC-ORD. multivariate analysis of ecological data, vers. 4, 237 p. MjM Software Design, Gleneden Beach, OR.

Merati, N., and R. D. Brodeur.
1996. Feeding habits and daily ration of juvenile walleye pollock, *Theragra chalcogramma*, in the western Gulf of Alaska. *In* Ecology of juvenile walleye pollock, *Theragra chalcogramma* (R. D. Brodeur, P. A. Livingston, T. R. Loughlin, A. B. Hollowed, eds.), p. 65–79. NOAA Tech. Rep. NMFS 126.

Milliken, G. A., and D. E. Johnson.
2002. Analysis of messy data, vol. III, analysis of covariance, 605 p. Chapman and Hall/CRC, New York, NY.

Nakatani, T., and T. Maeda.
1987. Distribution and movement of larval and juvenile walleye pollock (*Theragra chalcograma*) in Funka Bay and adjacent waters. Bull. Jap. Soc. Sci. Fish. 53(9):1585–1591.

Natsume, M., and M. Sasaki.
1995. Distribution of walleye pollock, *Theragra chalcogramma*, larvae and juveniles off the northern coast of Hokkaido. Sci. Rep. Hokkaido Fish. Exp. Stn. 47: 33–40.

Patterson, K. R.
1992. An improved method for studying the condition of fish, with an example using Pacific sardine *Sardinops sagax* (Jenyns). J. Fish. Biol. 40:821–831.

Reed, R. K., and J. D. Schumacher.
1986. Physical oceanography. *In* The Gulf of Alaska physical environment and biological resources (D. W. Hood and S. T. Zimmerman, eds.), p. 57–75. OCS Study MMS86-0095. Minerals Management Service, Springfield, VA.

Ryer, C. H., and B. L. Olla.
1992. Social mechanisms facilitating exploitation of spatially variable ephemeral food patches in a pelagic marine fish. Anim. Behav. 44:69–74.
1997. Altered search speed and growth: social versus independent foraging in two pelagic juvenile fishes. Mar. Ecol. Prog. Ser. 153:273–281.

Shida, O., O. Yamamura, and H. Miyake.
1999. Distribution and migration to offshore of age-0 walleye pollock, *Theragra chalcogramma*, along the Pacific coast of southeastern Hokkaido. Sci. Rep. Hokkaido Fish. Exp. Stn. 54:1–7.

Sobolevskiy, E. I., L. V. Cheblykova, and V. I. Radchenko.
1992. Distribution of first-year pollock, *Theragra chalcogramma*, in the western Bering Sea. J. Ichthyol. 1: 119–130.

Sogard, S. M.
1997. Size-selective mortality in the juvenile stage of teleost fishes: a review. Bull. Mar. Sci. 60(3):1129–1157.

Smith, G. B., G. E. Walters, P. A. Raymore Jr., and W. A. Hirschberger.
1984. Studies of the distribution and abundance of juvenile groundfish in the northwestern Gulf of Alaska, 1980–1982. NOAA Tech. Memo. F/NWC-59, 100 p.

Stabeno, P., N. A. Bond, A. J. Hermann, N. B. Kachel, C. W. Mordy, and J. E. Overland.
2004. Meteorology and oceanography of the northern Gulf of Alaska. Cont. Shelf Res. 24:859–897.

Stabeno, P. J., R. K. Reed, and J. D. Schumacher.
1995. The Alaska Coastal Current: continuity of transport and forcing. J. Geophys. Res. 100(C2):2477–2485.

Stoner, A. W., J. P. Manderson, and J. P. Pessutti.
2001. Spatially explicit analysis of estuarine habitat for juvenile winter flounder: combining generalized additive models and geographic information systems. Mar. Ecol. Prog. Ser. 213:253–271.

Suthers, I. M.
1998. Bigger? Fatter? Or is faster growth better? Considerations on condition in larval and juvenile coral-reef fish. Aust. J. Ecol. 23:265–273.

Tang, Q., W. Wang, Y. Chen, F. Li, X. Jin, X. Zhao, J. Chen, and F. Dai.
1995. Stock assessment of walleye pollock in the north Pacific Ocean by acoustic survey. J. Fish. China 19(1):8–20.

Wilson, M. T.
2000. Effects of year and region on the abundance and size of age-0 walleye pollock, *Theragra chalcogramma*, in the western Gulf of Alaska, 1985–1988. Fish. Bull. 98:823–834.

Wilson, M. T., R. D. Brodeur, and S. Hinckley.
1996. Distribution of age-0 walleye pollock (*Theragra chalcogramma*) in the western Gulf of Alaska. *In* Ecology of juvenile walleye pollock (R. D. Brodeur, P. A. Livingston, T. R. Loughlin, A. B. Hollowed, eds.), p. 11–24. NOAA Tech. Rep. NMFS 126.

Tagging studies on the jumbo squid (*Dosidicus gigas*) in the Gulf of California, Mexico

Unai Markaida

Departamento de Ecología, Centro de Investigación Científica y de Educación Superior de Ensenada (CICESE)
Ctra. Tijuana-Ensenada km 107
Ensenada, Baja California, Mexico
Present address: Departamento de Aprovechamiento y Manejo de Recursos Acuáticos
El Colegio de la Frontera Sur
Calle 10 x 61 No 264
Colonia Centro, 24000 Campeche, Mexico

Joshua J. C. Rosenthal

Institute of Neurobiology
University of Puerto Rico
201 Blvd del Valle
San Juan, Puerto Rico 00901

William F. Gilly

Hopkins Marine Station
Stanford University
Pacific Grove, California 93950
Email address (for W. F. Gilly, contact author): lignje@stanford.edu

In Sta. Rosalia the fishery operates from May to November, which is also the period of peak landings (see Fig. 1; SEMARNAP, 1996, 1997, 1998, 1999, 2000; SAGARPA, 2001; SAGARPA[1]) (see also Markaida and Sosa-Nishizaki, 2001). These generally reciprocal landing patterns are consistent with the abundance patterns described by Klett (1982), although the exact migrations proposed by Ehrhardt et al. (1983) have never been directly observed (Morales-Bojórquez et al., 2001).

All these studies concerning jumbo squid migrations have relied on analyses of landing statistics and catch data acquired by fishing stations on commercial squid-jigging vessels. Although migratory patterns of several other ommastrephid species of commercial importance have been directly demonstrated with conventional tag-and-recapture methods (Nagasawa et al., 1993), to our knowledge jumbo squid has not been studied in this manner. Given the commercial and ecological importance of this species, such studies would be valuable.

This paper describes conventional tag-and-recapture experiments on jumbo squid in the central Gulf of California. Tag-return rates were higher than in most previous studies of other ommastrephid species, and seasonal migrations between the Sta. Rosalia and Guaymas areas were directly demonstrated. Growth rates were also directly determined for the first time.

Dosidicus gigas, the only species in the genus *Dosidicus*, is commonly known as the jumbo squid, jumbo flying squid (FAO, see Roper et al., 1984), or Humboldt squid. It is the largest ommastrephid squid and is endemic to the Eastern Pacific, ranging from northern California to southern Chile and to 140°W at the equator (Nesis, 1983; Nigmatullin, et al., 2001). During the last two decades it has become an extremely important fisheries resource in the Gulf of California (Ehrhardt et al., 1983; Morales-Bojórquez et al., 2001), around the Costa Rica Dome (Ichii et al., 2002) and off Peru (Taipe et al., 2001). It is also an active predator that undoubtedly has an important impact on local ecology in areas where it is abundant (Ehrhardt et al., 1983; Nesis, 1983; Nigmatullin et al., 2001; Markaida and Sosa-Nishizaki, 2003).

Ommastrephid squid, including the jumbo squid, are largely pelagic and may migrate long distances as part of their life cycle (Mangold, 1976). A general pattern of long-distance migration for the jumbo squid over its entire range was proposed by Nesis (1983) and smaller-scale migrations within the Gulf of California have also been proposed according to the distribution of the fishery during 1979–80 (Klett, 1982; Ehrhardt et al., 1983). During this period squid were reported to enter the Gulf from the Pacific in January, to reach their northernmost limit (29°N) by April, and to remain in the central Gulf from May through August; the highest concentrations were found along the western (Baja California) coast. From September onward these squid appear to migrate eastward to the Mexican mainland coast and then southwards, to the mouth of the Gulf and back into the Pacific (Klett, 1982; Ehrhardt et al., 1983).

Since 1994 a seasonal pattern in the jumbo squid fishery has emerged in which large squid are abundant in the central Gulf essentially all year. During November to May, the fishery is centered in the area of Guaymas.

[1] SAGARPA (Secretaría de agricultura, ganadería, desarrollo rural, pesca y alimentación). Anuario Estadístico de Pesca, http://www.sagarpa.gob.mx/conapesca/planeacion/anuario/anuario2001.zip and http://www.sagarpa.gob.mx/conapesca/planeacion/anuario 2002. [Accessed 26 July 2004.]

Manuscript submitted 21 March 2003 to the Scientific Editor's Office.

Manuscript approved for publication 8 September 2004 by the Scientific Editor.

Fish. Bull. 103:219–226 (2005).

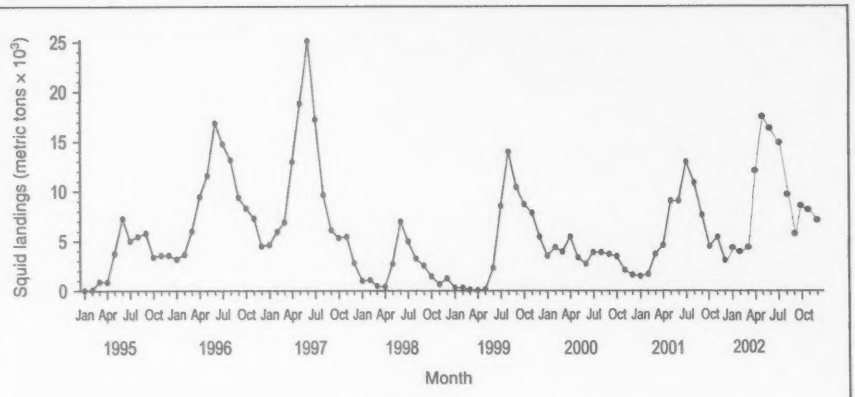

Figure 1

Monthly landings (in metric tons) of *Dosidicus gigas* in Mexico from 1995 through 2002.

Materials and methods

Fieldwork was carried out in two separate experiments along both coasts of the Guaymas basin (see Fig. 2). This area of the central part of the Gulf of California accounts for more than 95% of Mexican jumbo squid landings. A total of 996 squid were tagged between 9 and 16 October 2001, in the general vicinity of Sta. Rosalia, Baja California Sur (B.C.S.), as indicated in Figure 2. Another 997 squid were tagged off Guaymas, Sonora, between 3 and 7 April 2002. Both experiments were conducted close to the anticipated end of the respective fishing seasons for each zone, because we hoped to obtain recaptures both locally and from more distant sites after the squid had migrated away from the fishing areas.

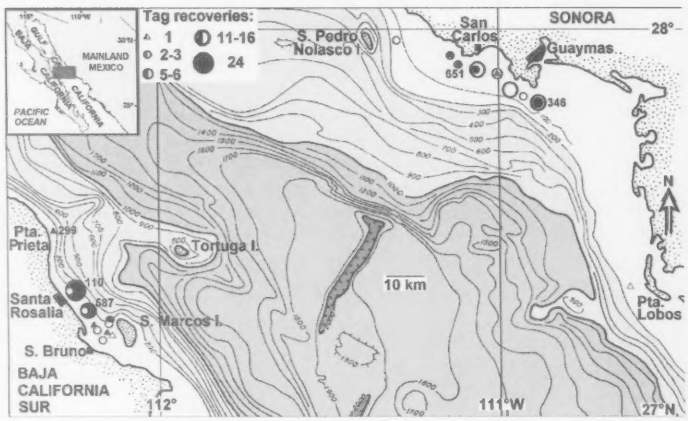

Figure 2

Map of the Guaymas basin in the central Gulf of California showing both coasts where the tagging experiments were performed. Area of detailed main map is indicated by a gray rectangle in upper leftmost inset. Numbers of tags deployed are in bold type in main map. Symbols for the numbers of tags recovered are indicated in the inset "Tag recoveries." Black symbols represent squid tagged off Sta. Rosalia; white symbols represent squid tagged off Guaymas. Depth contours are in meters. Adapted from Bischoff and Niemitz (1980).

Squid were caught by commercial fishermen using hand-lines with 30-cm jigs and were tagged on deck with spaghetti-type, plastic cinch-up tags (Floy Tag Co., Seattle, WA) through the anterior edge of the dorsal mantle. This process took about 30 seconds, and the squid was then immediately released. All squid quickly jetted away with no obvious sign of trauma or physical impairment. Animals with any visible damage, primarily form cannibalistic attacks by other squid, were not tagged. In addition, dorsal mantle length (ML) was measured to the nearest mm for all squid in the Guaymas experiment.

Tag-return information was imprinted on the tag, and posters announcing the experiment were distributed at squid-landing ports and at local processing facilities in Sta. Rosalia, San Lucas, San Bruno, Mulege, Loreto and La Paz (B.C.S.), as well as in San Carlos, Guaymas, Yavaros (Sonora) and Mazatlan (Sinaloa) (Fig. 2). A monetary reward ($50 US) was offered for each tag returned with information on recapture date and location. During the second experiment an additional reward was offered for information on squid ML and stage of sexual maturity as defined by Lipinski and Underhill (1995): immature (stages I–II), maturing (III) and mature (IV–V). Average daily growth rate (DGR) was calculated from the increase in ML between tagging and recapture divided by the number of days elapsed during this period.

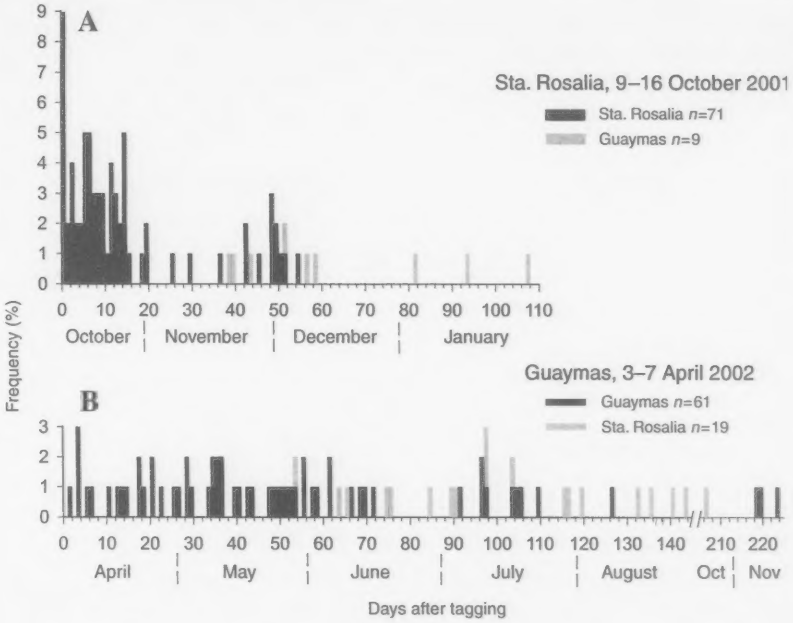

Figure 3

Time course for recapture data for squid tagged off Santa Rosalia (**A**) and off Guaymas (**B**). In both sections, black bars represent squid recaptured from the same coast where tagging was done, and gray bars represent squid recaptured from the opposite coast. Note that a gap exists between August and October in panel B.

Results

Timing of tag returns

A total of 80 tags (8.03%) were recovered for the squid tagged off Sta. Rosalia. Of these, 71 were recovered in the general vicinity of this port. More than a third of these tags (25) were discovered at commercial squid processing plants, where the mantles are manually cleaned before final processing. Squid were captured generally shortly after tagging; most of the tags (52) were recovered during the first 15 days (Fig. 3A). The shortest recapture period was only several hours. In this case, a squid tagged by the crew of one of our boats was caught about one km away by our second boat.

In addition to the Sta. Rosalia returns, another nine squid (0.9%) were recaptured off Guaymas, from 39 to 108 days after tagging (Fig. 3A). The temporal overlap in returns from the two localities (days 39–55) and the total lack of any subsequent Sta. Rosalia returns would indicate that a significant number, if not most, of the squid migrated from Sta. Rosalia to Guaymas and potentially elsewhere during this period (17 Nov–4 Dec).

In the second experiment, conducted off Guaymas, 80 tags (8%) were also recovered. Sixty-one were recovered in the Guaymas area over an extended period from 2 to 224 days after tagging (Fig. 3B). In this case, the squid were recaptured more or less constantly at a low rate over the first 60 days. Surprisingly, only one tag was recovered at a processing plant during this period. Sporadic returns then continued in Guaymas over the next three months. It should be noted that there was little squid fishing activity in the area during September because of the beginning of the commercial shrimp season. The final three tags were recovered after 219–224 days (8–13 Nov). These squid were tagged on the same night and location seven months earlier.

Of the tags deployed in Guaymas, 19 (1.9%) were recovered in the Sta. Rosalia area in summer 2002 (28 May–29 August) from 54 to 207 days after tagging (Fig. 3B). Seven of these tags were recovered at squid factories. A period of overlapping returns occurred over days 54–72, and we interpreted this overlap in returns as being consistent with a seasonal mass migration form Guaymas to Sta. Rosalia. A second period of overlapping returns of similar duration occurred in July. However, in this case, returns from Guaymas continued throughout the entire summer and into the fall. It thus appears that some squid remained in the Guaymas area during this period.

Dependence of recapture rate on squid size

Squid tagged off Guaymas ranged from 32.7 to 83 cm ML (mean [±SD] of 56.6 [±7.5] cm ML [Fig. 4]). Recapture rate is clearly size dependent. No squid smaller than 46 cm ML were recaptured, and recapture rates were low (1.3–3.4%) for squid of 46–50 cm ML. However, recapture increased in roughly direct proportion to ML, reaching 15–20% for squid >70 cm ML.

Determination of daily growth rate (DGR)

Dorsal ML was measured from forty-four squid tagged off Guaymas after recapture at 4 to 224 days. ML values ranged between 46 and 80.7 cm. Variability in DGR determination, as indicated by the standard deviation (SD) of binned data from 20-day intervals, clearly decreased as the time to recapture increased. Thus, a significant negative correlation exists between the SD of DGR and recovery time (r^2=0.88, P<0.01, n=6) (Fig. 5). Six measurements of squid caught before 40 days yielded negative growth rates. This finding indicates that large discrepancies in DGR calculations exist in measurements on squid with short recapture times, because any errors in ML measurement are generally much larger. Growth rate estimates from squid captured after 40 days yielded values of 1.0–1.5 mm/day (SD of 0.05–0.6). We regard these as the only reliable data.

Further analysis of DGR was limited to squid captured after 40 days. Figure 6 illustrates DGR versus "mean" ML (average of ML at times of tagging and recapture) for selected squid of different sexes and stages of maturity. Probably the most reliable DGR estimates come from the four squid that grew from 47–53 to 71–74 cm ML in 207–224 days, and these measurements yield a mean DGR of 1.05 [±0.05] mm/day (Fig. 5 and ▽ in Fig. 6). Solid and dashed curves in Figure 6 represent DGR independently determined for both sexes through analysis of statolith increments (Markaida et al., 2004) for squid of a comparable size range. These growth rates are about twice those determined in the present study by direct ML measurements.

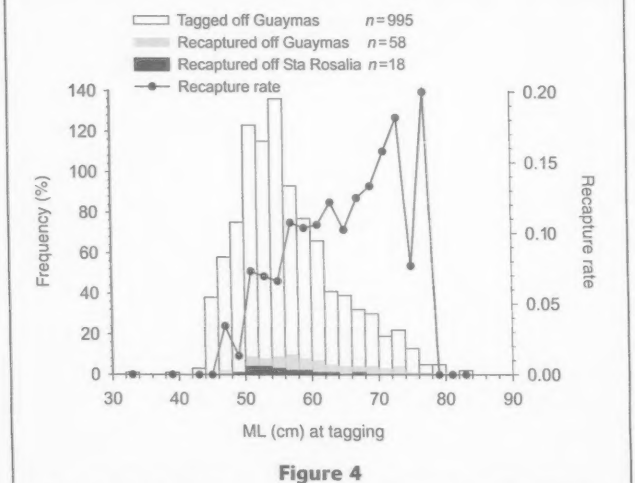

Figure 4

Mantle length (ML) distribution for all squid tagged off Guaymas (white bars) and for those recaptured off Guaymas (gray bars) and Santa Rosalia (black bars). Black circles represent recapture rate.

Discussion

Tag return rates

High recovery rates obtained in our study clearly demonstrate that *D. gigas* in the Gulf of California is suitable for tagging studies. This large species is relatively easily tagged with conventional plastic tags, and the tagging operation produced no obviously deleterious effects on the squid. These features make jumbo squid an attractive species for application of archival electronic tags or telemetry devices.

Despite extensive tagging efforts and intense commercial fisheries, recapture rates for other species of ommastrephid squid have generally been much lower. In the extreme case, no recaptures whatsoever were obtained for the northern shortfin squid (*Illex illecebrosus*) tagged in offshore waters of Newfoundland (Hurley and Dawe, 1981). In other studies recaptures ranged from 0.03–0.1% for the Argentine shortfin squid (*I. argentinus*) in the Southwest Atlantic (Brunetti et al., 2000), to 1.0–6.2% for the European flying squid (*Todarodes sagittatus*) off Norway (Wiborg et al.[2]). The neon flying squid (*Ommastrephes bartramii*) from the North Pacific also yielded low rates (0.1–0.5%; Murata and Nakamura, 1998; see also Nagasawa et al., 1993). In 62 years of tagging studies of Japanese flying squid (*Todarodes pacificus*), only a few experiments carried out in the Sea of Japan and Tsugaru Strait yielded return rates that match those of the present study (up to 16.4%; see Nagasawa et al., 1993). The highest tag recovery rate (19–32%) was found for the northern shortfin squid in Newfoundland inshore areas (Hurley and Dawe, 1981). Recapture rates of up to 12.7% have also been reported for large, neritic loliginid squid (Nagasawa et al., 1993; Sauer et al., 2000).

In the present study, recapture rate was found to be directly proportional to mantle length, ranging from <3.5% for squid <50 cm

[2] Wiborg, K. F., J. Gjøsaeter, I. M. Beck, and P. Fossum. 1982. The squid *Todarodes sagittatus* (Lamarck). Distribution and biology in Northern waters, August 1981–April 1982. Council Meet. Int. Coun. Explor. Sea (K:30):1–17. ICES, Palægade 2-4, DK-1261, Copenhagen K, Denmark. info@ices.dk.

ML to 20% for squid close to 80 cm ML (Fig. 4). Reasons for this strong size-dependence are not clear. Smaller squid may either suffer a higher natural mortality rate or migrate southward out of the Guaymas basin more readily than the larger squid. We do not believe that the tagging process itself leads to such a difference in mortality rate, but this possibility cannot be ruled out.

Several factors are relevant to evaluating differences in recapture rates for jumbo squid and other ommastrephids. First, squid of the other species are not as large as jumbo squid. We are not aware of any other published data on size-dependence of recapture rates, but this phenomenon may be relevant. Second, the localized nature of the fisheries surrounding the Guaymas basin equates with high concentrations of squid in relatively small areas that are intensively fished. Most recent tagging studies of other ommastrephids have taken place in oceanic waters in the Sea of Japan and North Pacific, where the fishing zone is extremely large and far from any localized coastal fishing areas (Nagasawa et al, 1993). The extreme disparity in return rates for nearshore versus offshore studies in Newfoundland supports this idea. Third, an ambitious advertising campaign (posters) and the substantial reward offered for tag returns undoubtedly stimulated a high degree of cooperation in the largely artisanal Mexican fishery that is highly concentrated in Sta. Rosalia and Guaymas. A strong dependence of tag-return rate on rewards and advertising has been previously noted (see Nagasawa et al., 1993).

Seasonal migration

Results from this study directly demonstrate that jumbo squid in the Guaymas basin migrate across the Gulf on a seasonal basis. Squid appear to migrate from Sta. Rosalia to Guaymas during the second half of November and early December and to make the reverse trip in late May and early June. Thus, large squid (40–80 cm ML) remain available to fisheries surrounding the Guaymas basin throughout the year. These data support the idea that these fishing areas are feeding grounds (Markaida and Sosa-Nishizaki, 2001). What fraction of squid, if any, migrate southward out of the Guaymas basin and potentially into the Pacific cannot be ascertained from our data.

Transit time across the Gulf for the migrating squid appears to be fairly brief—probably less than 16 days based on the overlap of recaptures in both fishing areas. Assuming a straight-line distance of 130 km between

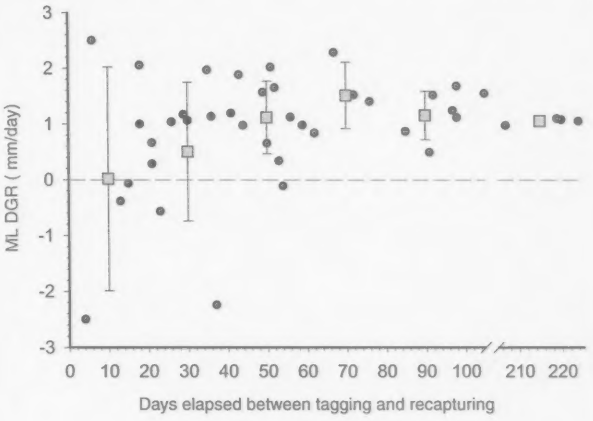

Figure 5

Daily growth rate (DGR) in mantle length (ML) determined for squid recaptured at different times after tagging. Black circles represent measurements from individual animals. Gray squares represent means ±1 SD for squid grouped in 20-day bins. Note that a gap exists between 100 and 200 days.

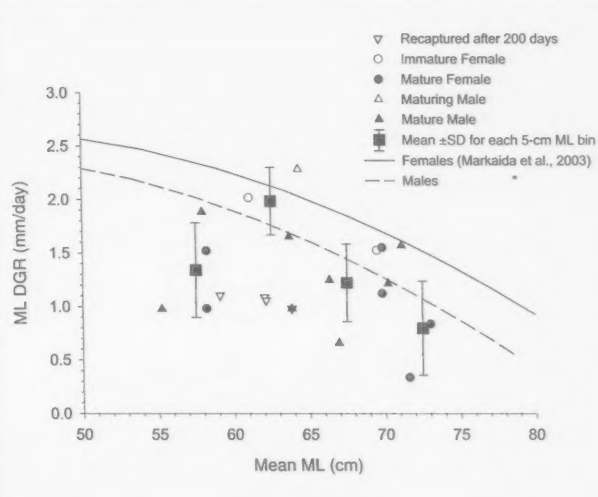

Figure 6

Relationship of daily growth rate (DGR) and mean mantle length (ML) (average of measured ML at time of tagging and time of recapture). Small symbols represent measurements from selected individual animals as follows: squid recaptured after >200 days (▽), immature female (○), mature female (●), maturing male (△), mature male (▲). Larger squares (■) indicate means ±1 SD for all data pooled into 5-cm bins. Analysis was limited to squid recaptured after 40 days and of identified sex. Curves represent DGR vs. ML relationship as determined by counting statolith increments for females (solid) and males (dashed) and are adapted from Markaida et al. (2004).

these areas, the average maintained speed during the migration would be about 8 km/day. A comparable figure can be derived from one of our first squid to be recaptured. This animal was tagged at Pt. Prieta (see Fig. 2) and recaptured 20 km away off Sta. Rosalia (Fig. 2) after three days.

This estimated velocity for a trans-Gulf migration is well within the range of rates observed in other studies of ommastrephids (O'Dor, 1988). Jumbo squid tracked with acoustic telemetry off Peru covered 3–5 miles in 8–14 hours, or about 14 km/day (Yatsu et al., 1999). Neon flying squid tracked in the same way covered up to 22 km per day (Nakamura, 1993). Migration rates obtained from tagging studies yielded even higher estimates. Maximum speed for migrating short-finned squid has been estimated at 20–30 km/day (Dawe et al., 1981; Hurley and Dawe, 1981), and high rates have also been reported for the Japanese squid (see Nagasawa et al., 1993). Large loliginid squid have been reported to migrate at rates of 3 to 17 km/day (see Sauer et al., 2000).

Daily growth rates

Variance in DGR estimates from ML measurements decreased dramatically after 30 days after tagging, and became fairly consistent by 50 days. Clearly, estimates of DGR in our study are only reliable for these later times, and a DGR of 1–1.5 mm/day in ML is evident for squid in the 50–70 cm range of ML (Fig. 6). These absolute rates would correspond to relative rates of 0.15–0.22% increase in ML per day.

There are few comparable estimates of growth rates for other ommastrephid squids based on tag-recapture studies. However, the neon flying squid grows 0.5–2.7 mm/day in the 18–48 cm ML range (Araya, 1983), and good agreement exists between growth rates obtained from tag-recapture studies and those from statolith aging studies (Yatsu et al., 1997). When converted to relative growth rate, this species would thus appear to grow substantially faster than the jumbo squid. The common Japanese squid grows 0.45 mm/day (Nagasawa et al., 1993), but for this species, mantle lengths were not given; therefore relative rates cannot be estimated.

More importantly, absolute growth rates determined by direct ML measurements in the present study disagreed with those derived from statolith aging methods (Markaida et al., 2004), and this discrepancy merits re-evaluation of previous longevity estimates. Squid of 50 cm ML are thought to be about 260 days old based on statolith ring counts, and our tag-recapture study revealed that it can take another 200 days to grow to 70 cm ML. The estimated age at this size would therefore be 460 days, about 100 days more than that estimated by statolith aging for squid of 70 cm ML (Markaida et al., 2004). Thus, the largest squid found in the Gulf of California (about 90 cm ML) might be up to 2 years old.

Reasons for the apparent underestimates in longevity with statolith aging are unclear. Difficulty in resolving discrete rings late in life of a specimen is one possibility. Another is that the assumed daily ring deposition may not occur throughout the lifetime of a jumbo squid. No successful validation studies have been reported for this species, either in the laboratory or in the wild.

Squid distributions in the Gulf in relation to commercial landings

Although large-scale migrations of jumbo squid within the Guaymas basin are apparently responsible for the seasonal pattern in the commercial landings (Fig. 1; see also Markaida and Sosa-Nishizaki, 2001), the biological and oceanographic reasons for these migrations are not well established. The reciprocal pattern in squid distribution between the eastern and western central Gulf is correlated with the wind-driven upwelling seasonality in this area (Roden and Groves, 1959) and is probably highly influenced by this oceanographic feature. A similar situation exists in the life cycle of another important pelagic resource, the Pacific sardine (*Sardinops caeruleus*) (Hammann et al., 1988).

However, other biological factors are also probably important. Summer upwelling in the western Gulf is actually less intense than off the eastern coast in winter (Hammann et al., 1988; Santamaría-del-Angel et al., 1999), yet 80% of squid landings were made at Sta. Rosalia between 1995 and 1997 (Markaida and Sosa-Nishizaki, 2001). We propose that concentrations of spawning myctophids (lanternfishes) off Baja California in the summer (Moser et al., 1974) may be largely responsible for this disparity because these fish are a major prey item for squid in the Guaymas basin (Markaida and Sosa-Nishizaki, 2003).

Data in the present study also indicate that jumbo squid may be available to commercial fishing efforts off each coast for a longer period than previously thought. Our data indicate that squid were recovered in the waters off Guaymas throughout the year; therefore it is likely that some squid do not undergo the westward spring migration (Fig. 3B). However, it is not certain that the final returns from Guaymas after 7 months were of this resident stock, because they would have had time to migrate to Sta. Rosalia and back again. It is also unclear whether a resident stock of squid exists in the Sta. Rosalia area year-round. Strong northern winds in this area lead to a cessation of commercial fishing efforts during the winter months, and the lack of tag returns during winter may simply reflect this fact.

Long-distance migrations into and out of the Gulf of California

Although data in this paper have demonstrated seasonal migrations of jumbo squid within the Guaymas basin, migration patterns into this region from the southern Gulf and open Pacific (and back out) remain unknown. The much lower level of commercial fishing effort in these latter areas will greatly constrain efforts to elu-

cidate migrations over these longer distances using conventional tag-and-recapture approaches.

Presumably, as the largest eunektonic squid, jumbo squid should be able to perform large-scale migrations covering its whole geographic range as do other ommastrephids (O'Dor, 1988). The high tag return rates achieved in the present study, in conjunction with the large size of the squid, make application of a variety of archival electronic tagging devices an attractive possibility. Such devices could reveal long-distance migrations across the large range of jumbo squid in a fishery-independent manner.

Acknowledgments

We acknowledge funding for this project by the Tagging of Pacific Pelagics (TOPP) program and the Census of Marine Life (COML). We thank Oscar Sosa-Nishizaki (CICESE, Ensenada) for administering this project in Mexico and providing laboratory space and facilities. Volunteer field workers in Sta. Rosalia included A. Novakovic, J. Schulz, S. Sethi (Stanford Univ.), and L. Roberson (California State University, Northridge). We are also indebted to personnel of Centro Regional de Investigación Pesquera, especially Manuel O. Nevárez, Paco Méndez, and Araceli Ramos, for their support during tagging and tag recovering at Guaymas, and to Sandra Patricia Garaizar and Vicente Monreal for recovering tags in Sta. Rosalia. We extend our sincere gratitude to all fishermen and squid factory personnel for their cooperation.

Literature cited

Araya, H.
1983. Fishery, biology and stock assessment of *Ommastrephes bartrami* in the North Pacific Ocean. Mem. Nat. Mus. Victoria 44:269–283.

Bischoff, J. L., and J. W. Niemitz.
1980. Bathymetric maps of the Gulf of California: bathymetry of the Central Gulf Province, Map I-244. Miscellaneous Investigation Series, U. S. Geological Survey, Denver, CO. Sheet 3 of 4 sheets.

Brunetti, N. E., M. L. Ivanovic, G. R. Rossi, B. Elena, H. Benavides, R. Guerrero, G. Blanco, C. Marchetti, and R. Piñero.
2000. JAMARC-INIDEP joint research cruise on Argentine short-finned squid (*Illex argentinus*). January-March 1997. Argentine Final Report. INIDEP Inf. Tec. 34:1–36.

Dawe, E. G., P. C. Beck, H. S. Drew, and G. H. Winter.
1981. Long distance migration of a short-finned squid *Illex illecebrosus*. J. Northwest Atlantic Fish. Sci. 2:75-76.

Ehrhardt, N. M., P. S. Jacquemin, F. García B., G. González D., J. M. López B., J. Ortiz C. and A. Solís N.
1983. On the fishery and biology of the giant squid *Dosidicus gigas* in the Gulf of California, Mexico. *In* Advances in assessment of world cephalopod resources (J. F. Caddy, ed.), p. 306–339. FAO Fish. Tech. Pap. 231.

Hammann, M.G., T. R. Baumgartner, and A. Badan-Dangon.
1988. Coupling of the Pacific sardine (*Sardinops sagax caeruleus*) life cycle with the Gulf of California pelagic environment. CalCOFI Rep. 29:102–109.

Hurley, G. V., and E. G. Dawe.
1981. Tagging studies on squid (*Illex illecebrosus*) in the Newfoundland area. North Atlantic Fisheries Organization (NAFO) SCR Doc., No. 80/II/33, serial no. 072, 11 p. NAFO, Dartmouth, Nova Scotia, Canada.

Ichii, T., K. Mahapatra, T. Watanabe, A. Yatsu, D. Inagake, and Y. Okada.
2002. Occurrence of jumbo flying squid *Dosidicus gigas* aggregations associated with the countercurrent ridge off the Costa Rica Dome during 1997 El Niño and 1999 La Niña. Mar. Ecol. Prog. Ser. 231:151–166.

Klett, A.
1982. Jumbo squid fishery in the Gulf of California, Mexico. *In* Proceedings of the International Squid Symposium, August 9–12, 1981, Boston, Massachusetts (prepared by the New-England Fisheries Development Found., Inc.), p. 81–100. UNIPUB, New York, NY.

Lipinski, M. R., and L. G. Underhill.
1995. Sexual maturation in squid: Quantum or continuum? S. Afr. J. Mar. Sci. 15:207–223.

Mangold, K.
1976. La migration chez les Céphalopodes. Oceanis 2(8):381–389. [In French.]

Markaida, U., and O. Sosa-Nishizaki.
2001. Reproductive biology of jumbo squid *Dosidicus gigas* in the Gulf of California, 1995–1997. Fish. Res. 54(1):63–82.
2003. Food and feeding habits of jumbo squid *Dosidicus gigas* (Cephalopoda: Ommastrephidae) from the Gulf of California, Mexico. J. Mar. Biol. Assoc. U.K. 83:507–522.

Markaida, U., C. Quiñónez-Velázquez, and O. Sosa-Nishizaki.
2004. Age, growth and maturation of jumbo squid *Dosidicus gigas* (Cephalopoda: Ommastrephidae) from the Gulf of California, Mexico. Fish. Res. 66(1):31–47

Morales-Bojórquez, E., M. A. Cisneros-Mata, M. O. Nevárez-Martínez and A. Hernández-Herrera.
2001. Review of the stock assessment and fishery biology of *Dosidicus gigas* in the Gulf of California, México. Fish. Res. 54:83–94.

Moser, H. G., E. H. Ahlstrom, D. Kramer, and E. G. Stevens.
1974. Distribution and abundance of fish eggs and larvae in the Gulf of California. CalCOFI Rep. 17:112–128.

Murata, M., and Y. Nakamura.
1998. Seasonal migration and diel vertical migration of the neon flying squid, *Ommastrephes bartramii*, in the North Pacific. *In* Contributed papers to the international symposium on large pelagic squids, Tokyo, July 18–19, 1996 (T. Okutani, ed.), p. 13–30. Japan Marine Fishery Resources Research Center (JAMARC).

Nakamura, Y.
1993. Vertical and horizontal movements of mature females of *Ommastrephes bartramii* observed by ultrasonic telemetry. *In* Recent advances in cephalopod fisheries biology: contributed papers to 1991 CIAC international symposium and proceedings of the workshop on age, growth and population structure (T. Okutani, R. K. O'Dor, and T. Kubodera, eds.), p. 331–336. Tokay Univ. Press, Tokyo, Japan.

Nagasawa, K., S. Takayanagi, and T. Takami.
1993. Cephalopod tagging and marking in Japan: a review. *In* Recent advances in cephalopod fisheries

biology: contributed papers to the 1991 Cephalopod International Advisory Council (CIAC) international symposium and proceedings of the workshop on age, growth, and population structure (T. Okutani, R. K. O'Dor, and T. Kubodera, eds.), p. 313–329. Tokay Univ. Press, Tokyo, Japan.

Nesis, K. N.
1983. *Dosidicus gigas*. *In* Cephalopod life cycles, vol. I, species accounts (P. R. Boyle, ed), p. 215–231. Academic Press, London, UK.

Nigmatullin, Ch. M., K. N. Nesis, and A. I. Arkhipkin.
2001. A review of the biology of the jumbo squid *Dosidicus gigas* (Cephalopoda: Ommastrephidae). Fish. Res. 54:9–19.

O'Dor, R. K.
1988. The energetic limits on squid distributions. Malacologia 29(1):113-119.

Roden, G. I., and G. W. Groves.
1959. Recent oceanographic investigations in the Gulf of California. J. Mar. Res. 18:10–35.

Roper, F. E., M. J. Sweeney, and C. E. Nauen.
1984. FAO species catalogue: vol. 3, Cephalopods of the world, 272 p. FAO, Rome.

SAGARPA (Secretaría de agricultura, ganadería, desarrollo rural, pesca y alimentación).
2001. Anuario estadístico de pesca 2000. SAGARPA-CONAPESCA (Comisión Nacional de Acuacultura y Pesca), Mexico, 268 p. [In Spanish.]

Santamaría-del-Angel, E., S. Álvarez-Borrego, R. Millán-Núñez, and F. E. Müller-Karger.
1999. On the weak effect of summer upwelling on the phytoplankton biomass of the Gulf of California. Rev. Soc. Mex. Hist. Nat. 49:207–212. [In Spanish, English abstract.]

Sauer, W. H. H., M. R. Lipinski, and C. J. Augustyn.
2000. Tag recapture studies of the chokka squid *Loligo vulgaris reynaudii* d'Orbigny, 1845 on inshore spawning grounds on the south-east coast of South Africa. Fish. Res. 45:283–289.

SEMARNAP (Secretaria del medio ambiente, recursos naturales y pesca). Distributed by the Mexican Secretary on Natural Resources.
1996. Anuario estadístico de pesca 1995, 235 p. SEMARNAP, Mexico. [In Spanish.]
1997. Anuario estadístico de pesca 1996, 232 p. SEMARNAP, Mexico. [In Spanish.]
1998. Anuario estadístico de pesca 1997, 241 p. SEMARNAP, Mexico. [In Spanish.]
1999. Anuario estadístico de pesca 1998, 244 p. SEMARNAP, Mexico. [In Spanish.]
2000. Anuario estadístico de pesca 1999, 271 p. SEMARNAP, Mexico. [In Spanish.]

Taipe, A., C. Yamashiro, L. Mariategui, P. Rojas, and C. Roque.
2001. Distribution and concentrations of jumbo flying squid (*Dosidicus gigas*) off the Peruvian coast between 1991 and 1999. Fish. Res. 54:21–32.

Yatsu, A., S. Midorikawa, T. Shimada, and Y. Uozumi.
1997. Age and growth of the neon flying squid, *Ommastrephes bartrami*, in the North Pacific Ocean. Fish. Res. 29:257–270.

Yatsu, A., K. Yamanaka, and C. Yamashiro.
1999. Tracking experiments of the jumbo squid, *Dosidicus gigas*, with an ultrasonic telemetry system in the Eastern Pacific Ocean. Bull. Nat. Res. Inst. Far Seas Fish. 36:55–60.

Superintendent of Documents **Publications** Order Form

*5178

☐ YES, please send me the following publications:

____ Subscriptions to *Fishery Bulletin*
for $55.00 per year ($68.75 foreign)

The total cost of my order is $ _____ . Prices include regular domestic postage and handling and are subject to change.

_____
(Company or Personal Name) (Please type or print)

_____
(Additional address/attention line)

_____
(Street address)

_____
(City, State, ZIP Code)

_____
(Daytime phone including area code)

_____
(Purchase Order No.)

Charge your order.
IT'S EASY!

VISA

MasterCard

Please Choose Method of Payment:

☐ Check Payable to the Superintendent of Documents
☐ GPO Deposit Account ☐☐☐☐☐☐☐–☐
☐ VISA or MasterCard Account
☐☐☐☐☐☐☐☐☐☐☐☐☐☐☐☐
☐☐☐☐ (Credit card expiration date)

To fax your orders (202) 512-2250

_____
(Authorizing Signature)

Mail To: Superintendent of Documents
P.O. Box 371954, Pittsburgh, PA 15250-7954

Thank you for your order!

Fishery Bulletin

Guidelines for contributors

Content of papers

Articles

Articles are reports of 10 to 30 pages (double spaced) that describe original research in one or a combination of the following fields of marine science: taxonomy, biology, genetics, mathematics (including modeling), statistics, engineering, economics, and ecology.

Notes

Notes are reports of 5 to 10 pages without an abstract that describe methods and results not supported by a large body of data. Although all contributions are subject to peer review, responsibility for the contents of articles and notes rests upon the authors and not upon the editor or the publisher. It is therefore important that authors consider the contents of their manuscripts carefully. Submission of an article is un-derstood to imply that the article is original and is not being considered for publication elsewhere. Manuscripts must be written in English. Authors whose native language is not English are strongly advised to have their manuscripts checked for fluency by English-speaking colleagues prior to submission.

Preparation of papers

Text

Title page should include authors' full names and mailing addresses (street address required) and the senior author's telephone, fax number, e-mail address, as well as a list of key words to describe the contents of the manuscript. **Abstract** must be less than one typed page (double spaced) and must not contain any citations. It should state the main scope of the research but emphasize the author's conclusions and relevant findings. Because abstracts are circulated by abstracting agencies, it is important that they represent the research clearly and concisely. **General text** must be typed in double-spaced format. A brief introduction should state the broad significance of the paper; the remainder of the paper should be divided into the following sections: Materials and methods, Results, Discussion (or Conclusions), and Acknowledgments. Headings within each section must be short, reflect a logical sequence, and follow the rules of multiple subdivision (i.e. there can be no subdivision without at least two subheadings). The entire text should be intelligible to interdisciplinary readers; therefore, all acronyms and abbreviations should be written out and all lesser-known technical terms should be defined the first time they are mentioned. The scientific names of species must be written out the first time they are mentioned; subsequent mention of scientific names may be abbreviated. Follow *Scientific style and format: CBE manual for authors, editors, and publishers* (6th ed.) for editorial style and the most current issue of the *American Fisheries Society's common and scientific names of fishes from the United States and Canada* for fish nomenclature. Dates should be written as follows: 11 November 1991. Measurements should be expressed in metric units, e.g. metric tons (t). The numeral one (1) should be typed as a one, not as a lower-case el (l).

Footnotes

Use footnotes to add editorial comments regarding claims made in the text and to document unpublished works or works with local circulation. Footnotes should be numbered with Arabic numerals and inserted in 10-point font at the bottom of the first page on which they are cited. Footnotes should be formatted in the same manner as citations. If a manuscript is unpublished, in the process of review, or if the information provided in the footnote has been conveyed verbally, please state this information as "unpubl. data," "manuscript in review," and "personal commun.," respectively. Authors are advised wherever possible to avoid references to nonstandard literature (unpublished literature that is difficult to obtain, such as internal reports, processed reports, administrative reports, ICES council minutes, IWC minutes or working papers, any "research" or "working" documents, laboratory reports, contract reports, and manuscripts in review). If these references are used, please indicate whether they are available from NTIS (National Technical Information Service) or from some other public depository. Footnote format: author (last name, followed by first-name initials); year; title of report or manuscript; type of report and its administrative or serial number; name and address of agency or institution where the report is filed.

Literature cited

The literature cited section comprises works that have been published and those accepted for publication (works in press) in peer-reviewed journals and books. Follow the name and year system for citation format. In the text, write "Smith and Jones (1977) reported" but if the citation takes the form of parenthetical matter, write "(Smith and Jones, 1977)." In the literature cited section, list citations alphabetically by last name of senior author: For example, Alston, 1952; Mannly, 1988; Smith, 1932; Smith, 1947; Stalinsky and Jones, 1985. Abbreviations of journals should conform to the abbreviations given in the *Serial sources for the BIOSIS previews database*. Authors are responsible for the accuracy and completeness of all citations. Literature citation format: author (last name, followed by first-name initials); year; title of report or article; abbreviated title of the journal in which the article was published, volume number, page numbers. For books, please provide publisher, city, and state.

Tables

Tables should not be excessive in size and must be cited in numerical order in the text. Headings in tables should be short but ample enough to allow the table to be intelligible on its own. All unusual symbols must be explained in the table legend. Other incidental comments may be footnoted (use italic arabic numerals for footnote markers). Use asterisks only to indicate probability in statistical data. Place table legends on the same page as the table data. We accept tables saved in most spreadsheet software programs (e.g. Microsoft Excel). Please note the following:

- Use a comma in numbers of five digits or more (e.g. 13,000 but 3000).
- Use zeros before all decimal points for values less than one (e.g. 0.31).

Figures

Figures include line illustrations, computer-generated line graphs, and photographs (or slides). They must be cited in numerical order in the text. Line illustrations are best submitted as original drawings. Computer-generated line graphs should be printed on laser-quality paper. Photographs should be submitted on glossy paper with good contrast. All figures are to be labeled with senior author's name and the number of the figure (e.g. Smith, Fig. 4). Use Helvetica or Arial font to label anatomical parts (line drawings) or variables (graphs) within figures; use Times Roman bold font to label the different sections of a figure (e.g. **A**, **B**, **C**). Figure legends should explain all symbols and abbreviations seen within the figure and should be typed in double-spaced format on a separate page at the end of the manuscript. We advise authors to peruse a recent issue of *Fishery Bulletin* for standard formats. Please note the following:

- Capitalize the first letter of the first word of axis labels.
- Do not use overly large font sizes to label axes or parts within figures.
- Do not use boldface fonts within figures.
- Do not create outline rules around graphs.
- Do not use horizontal lines through graphs.
- Do not use large font sizes to label degrees of longitude and latitude on maps.
- Indicate direction of degrees longitude and latitude on maps (e.g. 170°E).
- Avoid placing labels on a vertical plane (except on *y* axis).
- Avoid odd (nonstandard) patterns to mark sections of bar graphs and pie charts.

Copyright law

Fishery Bulletin, a U.S. government publication, is not subject to copyright law. If an author wishes to reproduce any part of *Fishery Bulletin* in his or her work, he or she is obliged, however, to acknowledge the source of the extracted literature.

Submission of papers

Send four printed copies (one original plus three copies)—clipped, *not stapled*—to the Scientific Editor, at the address shown below. Send photocopies of figures with initial submission of manuscript. Original figures will be requested later when the manuscript has been accepted for publication. Do not send your manuscript on diskette until requested to do so.

Dr. Norman Bartoo
National Marine Fisheries Service, NOAA
8604 La Jolla Shores Drive
La Jolla, CA 92037

Once the manuscript has been accepted for publication, you will be asked to submit a software copy of your manuscript. The software copy should be submitted in WordPerfect or Word format (in Word, save as Rich Text Format). Please note that we do not accept ASCII text files. Color figures must be CMYK files.

Reprints
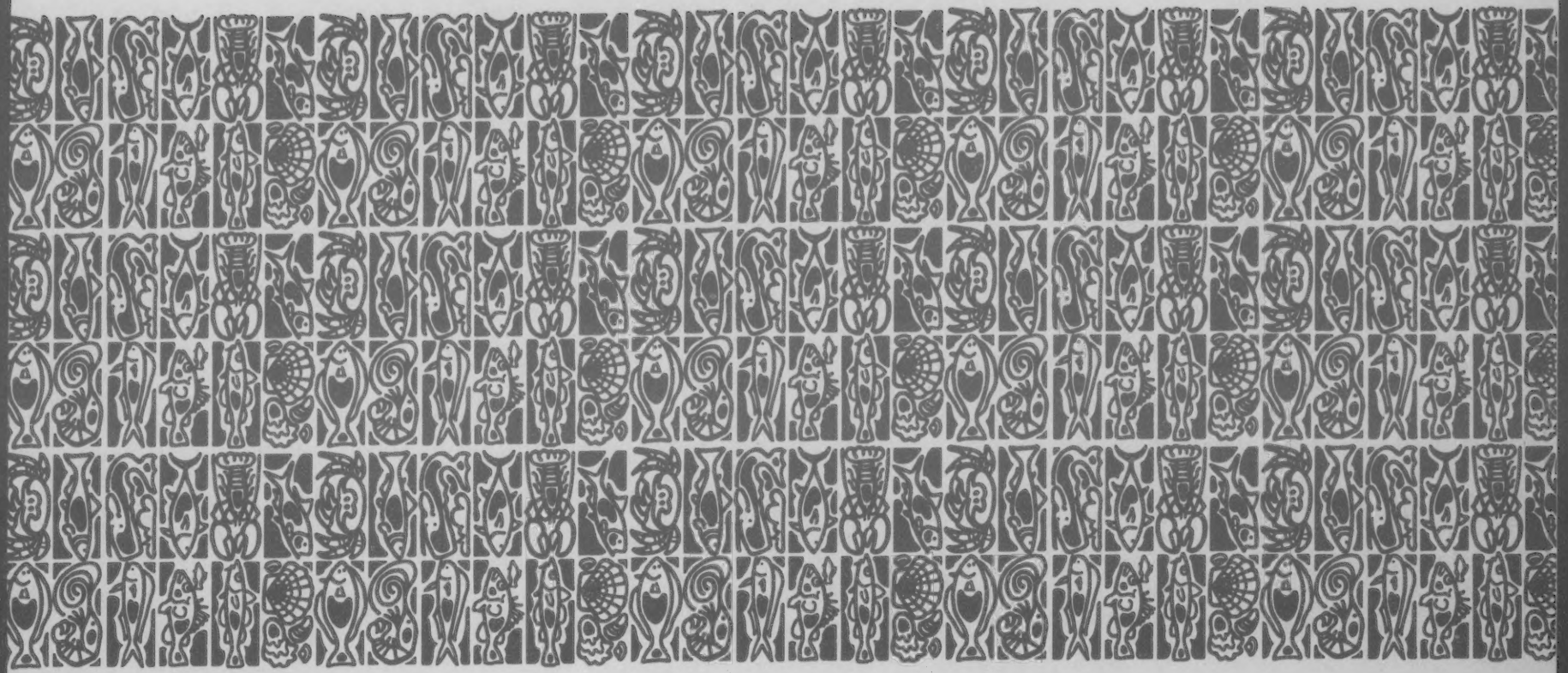
Copies of published articles and notes are available free of charge to the senior author (50 copies) and to his or her laboratory (50 copies). Additional copies may be purchased in lots of 100 when the author receives page proofs.